







PROCEEDINGS  
OF THE  
ROYAL SOCIETY OF LONDON

SERIES A—MATHEMATICAL AND PHYSICAL SCIENCES

VOL CLVII

LONDON

Printed and published for the Royal Society  
By Harnson & Sons, Ltd., 44–47, St. Martin's Lane  
Printers in Ordinary to His Majesty

2 December, 1936

LONDON:

HARRISON AND SONS, LTD , PRINTERS IN ORDINARY TO HIS MAJESTY  
ST. MARTIN'S LANE

## CONTENTS

### SERIES A VOL CLVII

No. A 890—1 October, 1936.

	PAGE
On Wave Matrices, and Some Properties of the Wave Equation. By S. R. Milner, F.R.S. ....	1
Spectra of $\text{SeO}$ and $\text{SeO}_2$ . By R. K. Asundi, M. Jan-Khan, and R. Samuel. Communicated by Sir C. V. Raman, F.R.S. ....	28
A New Method for Investigating Conduction Phenomena in Semi-Conductors. By J. A. V. Fairbrother. Communicated by F. W. Carter, F.R.S. ....	50
The Absorption of Light in Caesium Vapour in the Presence of Foreign Gases. By R. W. Ditchburn and J. Harding. Communicated by J. Chadwick, F.R.S. ....	66
The Structure of Resorcinol. A Quantitative X-Ray Investigation. By J. M. Robertson. Communicated by Sir William Bragg, O.M., F.R.S. ....	79
Absorption Spectra of Four Aldehydes in the Near Infra-Red. By L. Kellner. Communicated by A. O. Rankine, F.R.S. ....	100
The Crystal Structure of $\text{H}^4\text{PW}_{11}\text{O}_{40} \cdot 29\text{H}_2\text{O}$ . By A. J. Bradley and J. W. Illingworth. Communicated by W. L. Bragg, F.R.S. ....	113
Distribution of Magnetic Field Around Simply and Multiply Connected Supraconductors. By H. G. Smith and J. O. Wilhelm. Communicated by A. S. Eve, F.R.S. ....	132
Ionization, Excitation, and Chemical Reaction in Uniform Electric Fields. II—The Energy Balance and Energy Efficiencies for the Principal Electron Processes in Hydrogen. By R. W. Lunt and C. A. Meek. Communicated by F. G. Donnan, F.R.S. ....	146
The Lattice Spacings of Certain Primary Solid Solutions in Silver and Copper. By W. Hume-Rothery, G. F. Lewin, and P. W. Reynolds. Communicated by W. L. Bragg, O.M., F.R.S. ....	167
A Determination of the Absolute Velocity of the Alpha-Particles from Radium C. By G. H. Briggs. Communicated by Lord Rutherford, O.M., F.R.S. ....	183
Relations Between Optical Rotatory Power and Constitution in the Steroids. By R. K. Callow and F. G. Young. Communicated by O. Rosenheim, F.R.S. ....	194

	PAGE
The Atomic Rearrangement Process in the Copper-Gold Alloy Cu <sub>3</sub> Au. By C. Sykes and F. W. Jones. Communicated by W. L. Bragg, F.R.S. (Plate 3) .....	213
No. A 891—2 November, 1936.	
Some Influences of Dilution on the Explosive Combustion of Hydrocarbons. By W. A. Bone, F.R.S., and L. E. Outridge. (Plates 4-6) .....	234
Optical and Physical Effects of High Explosives. By R. W. Wood, For. Mem. R.S. (Plates 7 and 8) .....	249
The Zeros of the Riemann Zeta-Function. By E. C. Titchmarsh, F.R.S. ....	261
Viscosity of Liquid Sodium and Potassium. By Y. S. Chiong. Communicated by E. N. da C. Andrade, F.R.S. ....	264
The Effect of Pressure Upon Natural Convection in Air. By O. A. Saunders. Communicated by H. T. Tizard, F.R.S. ....	278
The Diffusion of Gases Through Metals. IV—The Diffusion of Oxygen and Hydrogen Through Nickel at Very High Pressures. By C. J. Smithells and C. E. Ranaley. Communicated by R. H. Fowler, F.R.S. (Plate 9) ..	292
The Anomalous Scattering of Protons in Light Elements. By E. G. Dymond. Communicated by C. G. Barkla, F.R.S. ....	302
The Electrical Conductivity of Thin Metallic Films. I—Rubidium on Pyrex Glass Surfaces. By A. C. B. Lovell. Communicated by A. M. Tyndall, F.R.S. ....	311
The Spectrum and Photochemistry of Carbon Suboxide. By H. W. Thompson and H. Healey. Communicated by C. N. Hinshelwood, F.R.S. ....	331
The Formation of Ethers by the Interaction of Primary Alcohols and Olefines at High Pressure. By D. M. Newitt and G. Semerano. Communicated by W. A. Bone, F.R.S. ....	348
A Critical Experimental Investigation of the "Force" Method of Determining the Dielectric Capacity of Conducting Liquids at Low Frequencies: Univalent Electrolytes in Aqueous Solution. By W. J. Shutt and H. Rogan. Communicated by W. C. McC. Lewis, F.R.S. ....	359
Transmutation of the Lithium Isotope of Mass Seven by Deuterons. By A. E. Kempton, B. C. Browne, and R. Maasdorp. Communicated by Lord Rutherford, O.M., F.R.S. ....	372
Angular Distributions of the Protons and Neutrons Emitted in Some Transmutations of Deuterium. By A. E. Kempton, B. C. Browne, and R. Maasdorp. Communicated by Lord Rutherford, O.M., F.R.S. ....	386
The Structure of Isatin—I. By E. G. Cox, T. H. Goodwin, and A. I. Wagstaff. Communicated by W. N. Haworth, F.R.S. (Plate 10). ....	399

	PAGE
Spectroscopic Identification and Manometric Measurement of Artificially Produced Helium. By F. A. Paneth, E. Glückauf, and H. Loleit. Communicated by J. C. Philip, F.R.S. ....	412
Hydrogen Overvoltage and the Reversible Hydrogen Electrode. By J. A. V. Butler. Communicated by J. Kendall, F.R.S. ....	423
Integral Electromagnetic Theorems in General Relativity. By J. L. Synge. Communicated by E. T. Whittaker, F.R.S. ....	434
The Elastic Constants and Specific Heats of the Alkali Metals. By K. Fuchs. Communicated by W. F. Mott, F.R.S. ....	444
The Electrical Properties of High Permeability Wires Carrying Alternating Current. By E. P. Harrison, G. L. Turney, H. Rowe, and H. Gollop. Communicated by Sir Frank Smith, Sec. R.S. ....	451

No. A 892—2 December, 1936.

Address of the President, Sir William Bragg, O.M., at the Anniversary Meeting, 30 November, 1936 . . . . .	697
Photochemical Reactions in the Fluorite Region. I—Photochemical Decomposition of Ethylene. By R. D. McDonald and R. G. W. Norrish, F.R.S. ....	480
Self-Consistent Field, with Exchange, for Cu <sup>+</sup> . By D. R. Hartree, F.R.S., and W. Hartree .....	490
The Kinetics of the Combustion of Methane. By R. G. W. Norrish, F.R.S., and S. G. Foord .....	503
The Forces of a Circular Cylinder Submerged in a Uniform Stream. By T. H. Havelock, F.R.S. ....	526
The Oscillations of the Atmosphere. By H. Jeffreys, F.R.S. With a Note by G. I. Taylor, F.R.S. ....	535
Correlation Measurements in a Turbulent Flow Through a Pipe. By G. I. Taylor, F.R.S. ....	537
Fluid Friction Between Rotating Cylinders. I—Torque Measurements. By G. I. Taylor, F.R.S. ....	546
Fluid Friction Between Rotating Cylinders. II—Distribution of Velocity Between Concentric Cylinders when Outer One is Rotating and Inner One is at Rest. By G. I. Taylor, F.R.S. ....	565
Further Work on Two Types of Diamond. By Sir Robert Robertson, F.R.S., J. J. Fox, and A. E. Martin. (Plate 11) ....	579
The Movement of Desert Sand. By R. A. Bagnold. Communicated by G. I. Taylor, F.R.S. (Plates 12-14) .....	594
A Note on the Quantum Yield of the Photosensitized Decomposition of Water and Ammonia. By H. W. Melville. Communicated by E. K. Rideal, F.R.S. ....	621

The Mercury Photosensitized Exchange Reactions of Deuterium with Ammonia, Methane, and Water. By A. Farkas and H. W. Melville. Communicated by E. K. Rideal, F.R.S. ....	625
The Formation of Radio-Phosphorus ( $P^{32}$ ). By J. R. S. Waring and W. Y. Chang. Communicated by C. D. Ellis, F.R.S. ....	652
Auger Effect for the L Level of Xenon and Krypton. By J. G. Bower. Com- municated by T. H. Laby, F.R.S. (Plate 15) ....	662
A Theory of Electro-Kinetic Effects in Solution ; Reactions between Ions and Polar Molecules. By E. A. Moelwyn-Hughes. Communicated by E. K. Rideal, F.R.S. ....	667
The Relativistic Interaction of Two Electrons in the Self-Consistent Field Method. By B. Swirles. Communicated by D. R. Hartree, F.R.S. ....	680
Index .....	729

---

*Contents*

v

No. A 914—7 December 1937

	PAGE
Address of the President, Sir William Bragg, O.M., at the Anniversary Meeting, 30 November 1937 . . . . .	455
A Discussion on Viscosity of Liquids. By G. I. Taylor, F.R.S. and others . . . . .	319
On the Torsion of Conical Shells. By R. V. Southwell, F.R.S. . . . .	337
Refractive Dispersion of Organic Compounds. IX—Optical Exaltation in Unsaturated Hydrocarbons containing Conjugated Double Bonds. By (the late) T. M. Lowry, F.R.S. and C. B. Allsopp . . . . .	356
Measurements of Range and Angle of Projection for the Protons produced in the Photo-Disintegration of Deuterium. By J. Chadwick, F.R.S., N. Feather and E. Bretscher . . . . .	366
An Attempt to Detect the Passage of Helium through a Crystal Lattice at High Temperatures. By Lord Rayleigh, F.R.S. . . . .	376
The Behaviour of an Osglim Lamp. III—Osglims in parallel, forming Models of Reciprocal Inhibition. By L. F. Richardson, F.R.S. . . . .	380
A Second-Order Focusing Mass Spectrograph and Isotopic Weights by the Doublet Method. By F. W. Aston, F.R.S. (Plate 17) . . . . .	391
Atomic Hydrogen. I—The Calorimetry of Hydrogen Atoms. By H. G. Poole. . . . .	404
Atomic Hydrogen. II—Surface Effects in the Discharge Tube. By H. G. Poole . . . . .	415
Atomic Hydrogen. III—The Energy Efficiency of Atom Production in a Glow Discharge. By H. G. Poole . . . . .	424

No. A 915—22 December 1937

Optical Activity in Ketones. The Rotatory Dispersion and Circular Dichroism of <i>m</i> -Methyl Cyclohexanone and of Pulegone in their Ketonic Absorption Bands. By the late T. M. Lowry, F.R.S., D. M. Simpson and C. B. Allsopp . . . . .	483
The Temperature Variation of the Work Function of Clean and of Thoriated Tungsten. By A. L. Reimann. . . . .	499

*Contents*

	PAGE
The Photochemical Polymerization of Methyl Methacrylate Vapour. By H. W. Melville . . . . .	511
Dissociation, Recombination and Attachment Processes in the Upper Atmosphere—I. By H. S. W. Massey . . . . .	542
A Transmutation Function for Deuterons. By P. L. Kapur . . . . .	553
A Study of Upper Carboniferous Coals from Western Australia. By C. R. Kent . . . . .	568
Explosion Waves and Shock Waves. V—The Shock Wave and Explosion Products from Detonating Solid Explosives. By W. Payman and D. W. Woodhead. (Plates 18–23) . . . . .	575
The Continuous Absorption Spectrum of Methyl Bromide and its Quantal Interpretation. By P. Fink and C. F. Goodeve . . . . .	592
Penetration into Potential Barriers in Several Dimensions. By P. L. Kapur and R. Peterls . . . . .	606
Index . . . . .	611

---

# On Wave Matrices, and Some Properties of the Wave Equation

By S. R. MILNER, F.R.S., The University, Sheffield

(Received 29 May, 1936)

1.—Wave matrices became important in wave theory as the result of the use of them made by Dirac<sup>†</sup> to express the operator of the second order wave equation as the square of a linear one, and hence obtain a first order equation. Thus,  $p^2$  representing the second order operator, the equation

$$p^2 \psi = 0,$$

may be factorized, and written

$$(\Sigma E_\alpha p_\alpha) (\Sigma E_\alpha p_\alpha) \psi = 0, \quad (\alpha = 1, 2, \dots, n),$$

giving the first order equation

$$\Sigma E_\alpha p_\alpha \psi = 0, \quad (1)$$

if the  $p_\alpha$  commute<sup>‡</sup> with themselves and with the  $E_\alpha$ , and if the  $E_\alpha$  are matrix roots of +1 or of -1, which satisfy

$$E_\alpha E_\beta = - E_\beta E_\alpha, \quad (\beta \neq \alpha). \quad (2)$$

This condition gives the standard definition of wave matrices. The number  $n$  of possible components  $p_\alpha$  is determined by the number of four square matrices which can be found mutually satisfying (2). Eddington<sup>§</sup> has shown that sets of five such matrices exist, in which each matrix is a square root of -1, so that there is a fifth component of  $p$  which gives the mass term in the equation (1).

† 'Proc. Roy. Soc.' A, vol. 117, p. 610 (1928).

‡ The conditions regarding the  $p_\alpha$  are satisfied when there is no electromagnetic field, which is the case dealt with initially by Dirac. The electromagnetic terms, which have the effect of making the  $p_\alpha$  non-commuting, are subsequent introductions made direct into the linear equation (1).

§ Eddington's notation for the matrices and choice of sign for their squares ('Proc. Roy. Soc.' A, vol. 133, p. 311 (1931)) has been followed here. Dirac and most other writers take the squares as +1. With the later definition (5) the choice of sign is immaterial.

Dirac's brilliant development is, I think, open to a minor criticism, the following up of which leads to a different definition of wave matrices. Relativity theory indicates that the two successive operations denoted by  $p^4$  are not identical in character, but one is a covariant and the other a contravariant differentiation. The point may be illustrated by the ordinary equation for the propagation of a potential with the velocity of light,

$$\nabla^4 \phi - \frac{1}{c^2} \frac{\partial^4 \phi}{\partial t^4} = 0.$$

This may be written in tensor form in flat space time as

$$\Sigma \frac{\partial}{\partial x_a} \frac{\partial}{\partial x^a} \phi = 0,$$

where the contravariant components  $x^a$  may stand for  $x, y, z, +ct$ , and the covariant  $x_a$  for  $x, y, z, -ct$ . The same distinction between the character of the differentiations is necessary also in the general theory,<sup>†</sup> and it evidently holds for any wave equation.

In matrix theory a covariant vector  $\psi$  is represented by a single *column* matrix of the components  $\psi_1 \dots \psi_4$ , and a contravariant vector  $\bar{\chi}$  by a single *row* matrix of its components  $\chi^1 \dots \chi^4$ . The rules of matrix multiplication then give

$$\bar{\chi} \psi = \chi^1 \psi_1 + \chi^2 \psi_2 + \chi^3 \psi_3 + \chi^4 \psi_4. \quad (3)$$

It lies at the basis of all geometry that this scalar product is invariant (the product may be regarded, indeed, as the real entity from which the vectors have been manufactured by a process of factorization). Since any linear transformation of  $\psi$  can be expressed as

$$\psi' = P \psi, \quad (4)$$

where  $P$  is a square matrix, it follows that the corresponding transformation for  $\bar{\chi}$  is

$$\bar{\chi}' = \bar{\chi} P^{-1}. \quad (4A)$$

With these ideas it seems logical to factorize the second order wave equation as follows. Writing it as

$$\bar{p} p \psi = 0,$$

we may put it into the equivalent form

$$(\Sigma p^a E_a^{-1}) (\Sigma E_a p_a) \psi = 0,$$

<sup>†</sup> Eddington, "Mathematical Theory of Relativity," p. 64.

which gives rise to the first order equation (1) when

$$E_{\alpha}^{-1}E_{\beta} = - E_{\beta}^{-1}E_{\alpha}, \quad (\beta \neq \alpha). \quad (5)$$

In this paper (5) will be taken as the defining condition of wave matrices. It is a more general definition than (2), allowing more latitude in the choice of them. The necessity for more latitude may be illustrated in a very simple way. The wave equation (1) clearly may be multiplied throughout by any matrix  $P$  without altering the value of its solution  $\psi$ . Hence  $(PE_{\alpha})$ ,  $(PE_{\beta})$  ought to be wave matrices, but they will not in general follow  $E_{\alpha}$  and  $E_{\beta}$  in satisfying (2). The anomaly disappears when (5) is the defining equation.

## 2—GROUP PROPERTIES OF WAVE MATRICES

A set of matrices, arranged in a definite order, and mutually satisfying (5) may be called a "wave set". There can be six matrices in such a set, as against the maximum of five in a set in standard theory. The simplest way of obtaining the six is to include the unit matrix along with a set of Eddington's five, as it is easily seen that (5) is then obeyed by them all, but wave sets of six which do not include unity also exist.

Their theory is very similar to that of Eddington's sets, which he has worked out extensively in several papers. His results have suggested much of what follows, but it is impossible to quote them in place of proof, because some apply and some do not to the matrices as here defined. In general the new definition makes both the matrices, and the wave sets, developable into closed groups, and the relations between them amenable to a complete classification, which is not possible on the earlier definition.

$E_{\alpha}$ ,  $E_{\beta}$ ,  $E_{\gamma}$ , etc., being different matrices which mutually satisfy equations similar to (5), if we use the notation

$$(\alpha\beta) \equiv E_{\alpha}^{-1}E_{\beta}, \quad (\alpha\gamma) \equiv E_{\alpha}^{-1}E_{\gamma}, \quad \text{etc.}, \quad (6)$$

then these derived matrices have the following properties:

$$\begin{aligned} (\alpha\alpha) &= 1, & (a) \\ (\alpha\beta)(\beta\gamma) &= E_{\alpha}^{-1}E_{\beta}E_{\beta}^{-1}E_{\gamma} = (\alpha\gamma), & (b) \\ (\alpha\beta) &= -(\beta\alpha), & (c) \\ (\alpha\beta)(\gamma\delta) &= (\alpha\beta)(\gamma\beta)(\beta\delta) \quad \text{by (b)}, \\ &= -(\alpha\beta)(\beta\gamma)(\beta\delta) \quad \text{by (c)}, \\ &= -(\alpha\gamma)(\beta\delta). & (d) \end{aligned} \quad \left. \right\} \quad (7)$$

Hence in developing products of the derived matrices, if two adjacent letters, whether they are in the same bracket or not, are the same, they can be omitted, or if they are different, they can be interchanged with change of sign. By using this rule any continued product can be reduced to a standard order of letters. A letter may be brought to any position desired by counting the number of letters different from itself required to be jumped over, and changing the sign when this number is odd. Also when a letter is brought up against itself the pair may be omitted.

We have further

$$\left. \begin{aligned} (\alpha\beta)^{-1} &= (E_a^{-1}E_\beta)^{-1} = E_\beta^{-1}E_a = (\beta\alpha), \\ (\alpha\beta)^{-1}(\alpha\gamma) &= (\beta\alpha)(\alpha\gamma) = -(\gamma\alpha)(\alpha\beta) \\ &= -(\alpha\gamma)^{-1}(\alpha\beta), \\ (\alpha\beta)^{-1}(\gamma\delta) &= (\beta\alpha)(\gamma\delta) = +(\delta\gamma)(\alpha\beta) \\ &= +(\gamma\delta)^{-1}(\alpha\beta). \end{aligned} \right\} \quad (8)$$

Thus all matrices which possess a common letter anticommute with each other's reciprocal, and so can form a wave set; those which have no common letter commute. On the other hand,  $(\alpha\beta)$  "reciprocally" anticommutes with  $i(\gamma\delta)$  (a matrix of Dirac's type whose square is  $+1$ ), and as will be seen later wave sets may be formed by combinations of this kind.

If we apply a transformation  $P \dots Q$  to each member  $E_a$  of the original set of matrices, the property (5) remains unchanged. This is readily proved by observing that  $(PE_aQ)^{-1} = Q^{-1}E_a^{-1}P^{-1}$ . The rules deduced above referring to the derived matrices are consequently unaffected by this transformation. It may be observed that the condition (2), on which wave matrices are based in the standard theory, is invariant only to the collineatory transformation  $P \dots P^{-1}$ ; the transformation  $P \dots Q$ , however, to which the properties of the present matrices are invariant, is the most general form possible of a linear transformation.

Using the multiplication rules we obtain

$$\begin{aligned} (\alpha\beta)^3 &= -1, \\ \{(\alpha\beta)(\gamma\delta)\}^3 &= +1, \\ \{(\alpha\beta)(\gamma\delta)(\epsilon\zeta)\}^3 &= -1. \end{aligned}$$

These products might be continued indefinitely but for the fact that, whatever set of  $E_a$  is taken as a starting point, the product  $(\alpha\beta)(\gamma\delta)(\epsilon\zeta)$  invariably reduces either to  $+i$  or to  $-i$ . This is true at any rate for all the sets derived as described above from Eddington's matrices, which are

all either wholly real or wholly imaginary. (Complex wave matrices, if they exist, have not been investigated.) The proof follows from the fact that, if each  $E_n$  of a given wave set is subjected to the general transformation

$$E'_n = PE_nQ, \quad (9)$$

the transformed value of the continued product  $(\alpha\beta)(\gamma\delta)(\epsilon\zeta)$  becomes reduced by intermediate cancelling to  $Q^{-1}(\alpha\beta)(\gamma\delta)(\epsilon\zeta)Q$  so that, if the product is originally a numeric, it remains unchanged by the transformation. It may readily be verified in a particular case that this product is either  $+i$  or  $-i$  (e.g., in Table I, (01)(23)(45) =  $-i$ ). Since (with one restriction) all wave sets can be obtained from a given one by the transformation (9) the property is general.

The result that

$$(\alpha\beta)(\gamma\delta)(\epsilon\zeta) = \text{either } +i, \text{ or } -i, \quad (10)$$

has the effect of closing the group of matrices obtained by continued multiplication; it also enables us to express them all by single pairs of symbols and so classify them. The set from which we start may be in certain respects chosen arbitrarily. For example, it may consist of any one of Eddington's sets of five with the addition of unity arranged in any order and with arbitrary signs. Once these have been chosen, however, let them be regarded as fixed, and the matrices be called  $+ E_0 \dots + E_8$  in order—it is convenient to distinguish a specified set by using numbers instead of letters for the suffixes. The set can now be reduced to a more standard form by applying the transformation  $E_0^{-1} \dots 1$  to each member. In this way we get a set (00), (01), ..., (05), of which the first member is unity.

Suppose for the sake of definiteness that the set thus chosen exhibits the  $-i$  property in (10), i.e.,

$$(01)(23)(45) = E_0^{-1}E_1E_8^{-1}E_3E_4^{-1}E_5 = -i. \quad (11)$$

Postmultiplying each side by (54) we get

$$(01)(23) = i(45), \quad (11A)$$

with all the permutations obtainable from it, subject to changing the sign of one side for each interchange of a pair of figures. By applying this and the multiplication rules to reduce the continued products of (01) ... (05), we arrive at a closed group of 64 members. In Table I is given an example of a group so formed from particular initial matrices along with the two-figure designation of each matrix. The 16 given form a sufficient repre-

sentation of the whole group, the remainder being  $-1$ ,  $+i$ , and  $-i$  times these.

To save space a simple contracted notation is used to specify the matrices, which is made possible by the fact that in them there is only one finite element in each row, and this is always reducible (by writing  $i$

TABLE I—A GROUP OF WAVE MATRICES

(00)	$+1 [= (1234)]$	(14)	$-i (4321)$
(01)	$i (\bar{2}14\bar{3})$	(15)	$(43\bar{2}\bar{1})$
(02)	$(\bar{2}14\bar{3})$	(23)	$i (2143)$
(03)	$i (\bar{1}23\bar{4})$	(24)	$(\bar{4}3\bar{2}\bar{1})$
(04)	$(\bar{3}412)$	(25)	$i (\bar{4}32\bar{1})$
(05)	$-i (3412)$	(34)	$i (\bar{3}4\bar{1}2)$
(12)	$i (\bar{1}2\bar{3}4)$	(35)	$(\bar{3}412)$
(13)	$(\bar{2}1\bar{4}3)$	(45)	$i (\bar{1}234)$

when necessary as a factor of the whole matrix) to either  $+1$  or  $-1$ . The four figures give the numbers of the columns in which the  $1$  comes in successive rows, and when it is  $-1$  the sign is indicated above the figure. Thus

$$(\bar{2}14\bar{3}) \text{ stands for } \begin{bmatrix} 0 & -1 & 0 & 0 \\ 1 & 0 & 0 & 0 \\ 0 & 0 & 0 & 1 \\ 0 & 0 & -1 & 0 \end{bmatrix}.$$

It is not difficult to verify that the matrices of Table I possess the various properties derived for them. Multiplications can be carried out on the contracted forms themselves by using a rule illustrated in the following example:

$$\begin{aligned} E_\mu E_\nu &= (\bar{2}14\bar{3}) \times (\bar{4}3\bar{2}\bar{1}) = (\bar{3}412), \\ \text{or} \\ (02)(24) &= (04). \end{aligned}$$

Since the first figure of  $E_\mu$  is  $\bar{2}$ , we take the second figure of  $E_\nu$  (3), and write it as the first figure of the product, putting a minus sign above it when the  $E_\mu$  and  $E_\nu$  figures have opposite signs; and so on.

With the exception of (00) the matrices in Table I are identical with those derived by Eddington. While their two figure designations are to a certain extent fixed arbitrarily, in the way explained above, they serve to make clear the relations which exist between them. Moreover, it will appear later that, with one important exception, similarly constructed tables starting from any other original wave set can be converted into

this by determinate transformations, so that this can serve to illustrate exhaustively the matrix properties.

The exception is produced by the fact that the equality of the continued product in (11) to  $-i$  is a group property of the originally chosen set, and is untransformable away. Although the product can easily be changed to  $+i$  (for example, by changing the sign of one member of the set), this cannot be done by transformation. It thus appears that wave sets are of two types, which have to be carefully distinguished from each other, one in which the product (01)(23)(45) is  $+i$  and the other in which it is  $-i$ . The distinction extends over the whole group of derived matrices. Table I could be changed from the " $-i$ " to the " $+i$ " group by changing the sign of  $i$  in it wherever it occurs. The two groups differ from each other in much the same way as do right- and left-handed axes in geometry, which can never be transformed into each other by a rotation. The two types of wave sets are only distinguishable from each other when the full number of six matrices is used to form the set; when five matrices only are employed, as in the standard treatment, this group property disappears.

### 3—ORDERING EQUATIONS

The equation

$$(\sum \bar{\chi} s_a E_a^{-1}) (\sum E_a s_a \psi) = 0, \quad (\alpha = 0, 1, \dots, 5), \quad (12)$$

is easily seen to be satisfied identically with arbitrary  $\bar{\chi}$  and  $\psi$  if (1)  $E_a$ ,  $E_b$  satisfy (5), and (2)  $s_0 \dots s_5$  are a set of algebraic quantities which obey the condition

$$\sum s_a^2 = 0. \quad (13)$$

The theorem indicates that a relation of a very general character between  $\psi$  and  $s_a$  may be specified by equating the second factor of (12) to zero. We thus reach the equation

$$\sum E_a s_a \psi = 0, \quad (\alpha = 0 \dots 5) \quad (14)$$

an important feature of which is that it states an always possible relation between  $\psi$  and  $s_a$  without restricting in any way the value of  $\bar{\chi}$ . Alternatively we might relate  $\bar{\chi}$  to  $s_a$  by equating the first factor of (12) to zero. It is shown below that both relations cannot hold simultaneously unless  $\bar{\chi}\psi$  is zero. We may, however, write

$$\sum \bar{\chi} s_a E_a^{-1} = 0, \quad (M4A)$$

where the  $s^*$  stand for another set of quantities such that  $\Sigma(s^*)^2 = 0$ . The relation between  $\bar{\chi}$  and  $\psi$  will then depend on that between  $s^*$  and  $s_*$ . These equations will be called here "ordering" equations (covariant (14) and contravariant (14A) forms) because (14) requires the  $\psi_*$  to be proportional to complex quantities formed by arranging the  $s_*$  in a certain order, and similarly for (14A).

While (14) is of the same general type as the wave equation (1), it has to be distinguished from it, since it is purely algebraic, the  $s_*$  being not operators but commuting quantities. It serves, nevertheless, to bring out certain features of wave matrices, which have useful applications to the wave equation. The four equations which it represents are homogeneous and it may readily be verified that (13) is their condition of consistency. Write

$$\psi = \Sigma E_*^{-1} s_* \lambda, \quad (\alpha = 0 \dots 5), \quad (15)$$

where  $\lambda$  is a single column matrix of four arbitrary terms. On substituting this in (14) we get

$$\Sigma(E_* s_*) (\Sigma E_*^{-1} s_* \lambda) = \Sigma(s_*)^2 \lambda = 0.$$

Thus this value of  $\psi$  always satisfies (14), and may be regarded as its general solution. The contravariant form (14A) has similarly the general solution

$$\bar{\chi} = \Sigma \bar{\lambda} s^* E_*, \quad (15A)$$

where  $\bar{\lambda}$  is an arbitrary row matrix of four terms. We see that

$$\bar{\chi} \psi = \bar{\lambda} (\Sigma s^* s_*) \lambda,$$

is an arbitrary scalar quantity, and also that, if the  $s^*$  are the same as the  $s_*$ , its value is zero.

The meaning of these solutions is brought out more clearly by considering the forms they take when the set of  $E_*$  to be used in them has been chosen. To illustrate this we shall use the set (00) ... (05) of Table I, i.e., let (14) take the form

$$\{s_0 + i(\bar{2}\bar{1}43) s_1 + (\bar{2}14\bar{3}) s_2 + i(\bar{1}23\bar{4}) s_3 + (\bar{3}\bar{4}12) s_4 - i(3412) s_5\} \psi = 0. \quad (16)$$

By (15) its solution is  $(E_*^{-1} = -E_*$  except for the (00) term)

$$\psi = \{s_0 - i(\bar{2}\bar{1}43) s_1 - (\bar{2}14\bar{3}) s_2 - i(\bar{1}23\bar{4}) s_3 - (\bar{3}\bar{4}12) s_4 + i(3412) s_5\} \lambda.$$

The contracted notation for the matrices has the useful feature of enabling the equation to be translated directly into column matrix form, giving

$$\begin{bmatrix} \psi_1 \\ \psi_2 \\ \psi_3 \\ \psi_4 \end{bmatrix} = s_0 \begin{bmatrix} \lambda_1 \\ \lambda_2 \\ \lambda_3 \\ \lambda_4 \end{bmatrix} - is_1 \begin{bmatrix} -\lambda_2 \\ -\lambda_1 \\ +\lambda_4 \\ +\lambda_3 \end{bmatrix} - s_3 \begin{bmatrix} -\lambda_2 \\ +\lambda_1 \\ +\lambda_4 \\ -\lambda_3 \end{bmatrix} - is_3 \begin{bmatrix} -\lambda_1 \\ +\lambda_2 \\ +\lambda_3 \\ -\lambda_4 \end{bmatrix} - s_4 \begin{bmatrix} -\lambda_3 \\ -\lambda_4 \\ +\lambda_1 \\ +\lambda_2 \end{bmatrix} + is_5 \begin{bmatrix} \lambda_3 \\ \lambda_4 \\ \lambda_1 \\ \lambda_2 \end{bmatrix}.$$

Rearranging the terms we get  $\psi$  expressed as the sum of four column matrices instead of six:

$$\begin{bmatrix} \psi_1 \\ \psi_2 \\ \psi_3 \\ \psi_4 \end{bmatrix} = \lambda_1 \begin{bmatrix} s_0 + is_3 \\ is_1 - s_2 \\ -s_4 + is_5 \\ 0 \end{bmatrix} + \lambda_2 \begin{bmatrix} is_1 + s_2 \\ s_0 - is_3 \\ 0 \\ -s_4 + is_5 \end{bmatrix} + \lambda_3 \begin{bmatrix} s_4 + is_5 \\ 0 \\ s_0 - is_3 \\ -is_1 + s_2 \end{bmatrix} + \lambda_4 \begin{bmatrix} 0 \\ s_4 + is_5 \\ -is_1 - s_2 \\ s_0 + is_3 \end{bmatrix}. \quad (17)$$

If we call the four terms on the right  $\psi(1), \psi(4)$  in order, we see that each  $\psi(\alpha)$  is a covariant vector (single column matrix) whose components are proportional to complex paired arrangements of the  $s_n$  made in a certain way. Since the  $\lambda_\alpha$  are arbitrary, each  $\psi(\alpha)$  forms by itself an elementary solution of (16). The complete solution is the resultant of the four vectors,

$$\psi = \sum_1^4 \psi(\alpha).$$

The elementary solutions are not independent. It may be proved from the theory of linear equations that only two independent solutions exist, and indeed it is easy algebraically to express any two  $\psi(\alpha)$  in terms of the other two. In order to describe the properties of the  $\psi(\alpha)$ , we shall use the notation already employed of  $\bar{\psi}$  to signify the row matrix which is the transposed of a column matrix  $\psi$ , and in addition an asterisk when we

wish to indicate that every  $i$  that occurs explicitly in  $\psi$  has been changed in sign.<sup>†</sup> For example, we write

$$\psi(1) = \lambda_1 \begin{bmatrix} s_0 + is_3 \\ is_1 - s_2 \\ -s_4 + is_5 \\ 0 \end{bmatrix}, \quad \bar{\psi}^*(1) = \lambda_1 [s_0 - is_3, -is_1 - s_2, -s_4 - is_5, 0]. \quad (18)$$

It is easy now to show that

$$\bar{\psi}^* = \sum_1^4 \bar{\psi}^*(\alpha)$$

is the solution of the contravariant ordering equation

$$\sum_0^5 \bar{\psi}^* s_a E_a^{-1} = 0,$$

formed from the same wave set and with the same  $s_a$ .

An examination of (17) now reveals that for all values of  $\alpha$  and  $\beta$ , including  $\beta = \alpha$ ,

$$\bar{\psi}^*(\alpha) \psi(\beta) = 0. \quad (19)$$

The four elementary vectors may consequently be described as being mutually perpendicular; also each is of zero scalar magnitude. They form a set of four complex perpendicular axes, constructed out of zero by factorizing it matrixwise.

Since the elementary solutions  $\psi(\alpha)$  of (16) are derived from  $s_0 \dots s_5$  by arranging complexes from them in a certain order, we may call an individual set of these complexes, such as that in the first equation of (18), an "ordering" of  $s_0 \dots s_5$  and  $\psi$  itself an "ordered complex". The function of the ordering equation (16) is then to determine a special set of four orderings which represent four mutually perpendicular  $\psi(\alpha)$ -vectors. Numerous other sets can be obtained from equations employing the same matrices as are used in (16). It makes no difference to the validity of an ordering equation, since the governing condition (5) is not affected, if any alteration in the order of the matrices is made, or if the sign of any term is changed. Each of these alterations will produce a different set of four orderings for the solution. There will thus be pro-

<sup>†</sup>  $\bar{\psi}^*$  has to be distinguished from the conjugate transposed of  $\psi$  as ordinarily defined, because, since  $\sum s_a^2 = 0$ , at least one of the  $s_a$  must be imaginary. The description of (19) as indicating perpendicularity is, of course, purely a formal one, though no more so than with any other complex vectors, since they cannot be pictured in Euclidian space.

duced altogether  $6! \times 2^6$  distinct sets. That the equation, treated in this way, gives a complete account of all the orderings possible of the type

$$s_0 + is_1, \quad s_2 + is_3, \quad s_4 + is_5, \quad 0,$$

is easily to be seen. For since the  $i$  in each term of the ordering distinguishes the two  $s_a$  from each other, there are  $6!$  different permutations of the  $s_a$  without altering the position of the zero term. Each  $s_a$  may be either  $+$  or  $-$ , giving a further factor of  $2^6$  when we include as distinct orderings those derivable from another by multiplying it throughout by  $-1$ ,  $+i$ , or  $-i$ . The result is finally to be multiplied by 4 since the 0 term may come in any position. The number of possible orderings is consequently  $6! \times 2^6 \times 4$ , and it is evident that there is a one to one correspondence between these and the elementary solutions  $\psi(\alpha)$  of the various modifications of (16). The feature of the ordering equations is, of course, that they select from the total number of orderings and join together those four which denote mutually perpendicular vectors.

#### 4—THE WAVE EQUATION

Dirac's equation for the  $\psi$ -waves of a single electron can be written

$$\left\{ \sum_1^4 E_a \left( -\frac{\hbar}{2\pi} \frac{\partial}{\partial x_a} - iV_a \right) + E_5 imc \right\} \psi = 0. \quad (20)$$

Here  $E_1 \dots E_5$  may be any five chosen from a set of six wave matrices as previously defined,  $x_4$  has been written for  $ict$ ,  $V_1 \dots V_3$  stand for  $e \times$  vector potential components, and  $V_4$  for  $ie \times$  the scalar potential, of the electromagnetic field, and  $e$  and  $m$  are the charge and rest-mass of the electron. In the present section it is proposed to discuss the general nature of this equation, in its mathematical aspect only, in the light of the results obtained in the previous section.

It has already been noted that while (20) bears a close resemblance to the ordering equation (14) there is a definite difference in that the co-factors of  $E_1 \dots E_4$  in the former are non-commuting operators as against the algebraic quantities  $s_1 \dots s_4$  in the latter. By an artifice, however, we can write the ordering equation in a form that approaches still more closely to that of (20). Suppose that  $s_1 \dots s_4$  in (14) represent the gradient of a scalar function of position,  $H(x_1 \dots x_4)$ , in a Euclidian fourfold and that  $\psi$  is an ordered complex satisfying the equation

$$\left\{ E_0 s_0 + \sum_1^4 E_a \frac{\partial H}{\partial x_a} + E_5 s_5 \right\} \psi = 0, \quad (21)$$

in which  $s_0$  and  $s_b$  may be any quantities chosen to satisfy the condition of consistency of (21), viz.,

$$s_0^2 + \sum_1^4 \left( \frac{\partial H}{\partial x_a} \right)^2 + s_b^2 = 0. \quad (22)$$

Now write

$$\psi = \phi e^{-2\pi H/\hbar}, \quad (23)$$

which can always be done, as it merely defines  $\phi$ , a similar column matrix to  $\psi$ . By differentiating (23) and rearranging we get

$$\frac{\partial H}{\partial x_a} \psi = \frac{\hbar}{2\pi} \left( -\frac{\partial \psi}{\partial x_a} + \frac{\partial \phi}{\partial x_a} e^{-2\pi H/\hbar} \right). \quad (24)$$

The exponential here can be expressed in terms of matrix products, for, if  $\bar{x}$  stands for *any* single row matrix of four terms (e.g., [1111]), and we premultiply both sides of (23) by it, we have

$$e^{-2\pi H/\hbar} = \frac{\bar{x} \psi}{\bar{x} \phi}.$$

Consequently (24) may be written

$$\frac{\partial H}{\partial x_a} \psi = \frac{\hbar}{2\pi} \left\{ -\frac{\partial}{\partial x_a} + \frac{1}{\bar{x} \phi} \left( \frac{\partial \phi}{\partial x_a} \bar{x} \right) \right\} \psi. \quad (25)$$

Substituting (25) in (21), we get

$$\left\{ E_0 s_0 + \sum_1^4 E_a \left( -\frac{\hbar}{2\pi} \frac{\partial}{\partial x_a} + \frac{\hbar}{2\pi \bar{x} \phi} \cdot \frac{\partial \phi}{\partial x_a} \bar{x} \right) + E_b s_b \right\} \psi = 0. \quad (26)$$

This very general equation requires for its satisfaction only that  $\psi$  should be an ordered complex derived from an arbitrary function  $H$ , which actually comes into the equation via  $\phi$  and (23). It is formally so similar in build to the wave equation that this might be derived from it by identifying symbols. If we write in (26), (1)  $s_0 = 0$ , (2)  $s_b = imc$ , and (3) assume that  $\frac{i\hbar}{2\pi \bar{x} \phi} \left( \frac{\partial \phi}{\partial x_a} \bar{x} \right)$  may be replaced by  $V_a$ , the equation reduces identically to (20). The first two conditions are straightforward, requiring only, by (22),

$$\sum_1^4 \left( \frac{\partial H}{\partial x_a} \right)^2 = (mc)^2, \quad (27)$$

which shows that  $H$  is a quantity of the nature of "action". The third assumption, however, is a considerable one, since  $\frac{\partial \phi}{\partial x_a} \bar{x}$  is a four square matrix, and  $V_a$  is an algebraic quantity. This last identification cannot

be true generally; it is clear it must involve a further limitation on the permissible values of  $\psi$ . Correspondingly it may be noted that, while (26) is satisfied by *any* ordered complex  $\psi$  (derived from H), finite and continuous solutions of the wave equation (20) are restricted to eigen functions.

For this reason one must not regard as more than formal the apparent identity of (20) and (26). It is justifiable, however, to consider that (26) constitutes the general mathematical form which, by specialization in the way described, gives rise to Dirac's equation.

Based on this conclusion, a useful inference may be made with regard to the mathematical form which the accurate solution of the wave equation should take. *In addition to  $\psi$  being an eigen function, we may expect it to be expressible in the form (23) and also as an ordered complex of imc and the derivatives of the function H, which themselves satisfy (27).*

In an earlier paper,<sup>†</sup> in which the formal identity of the wave and ordering equations was arrived at in a less complete way, I assumed (perhaps too hastily) the correctness of this inference, after verifying it in the case of a simple example. It has therefore seemed to be a useful piece of work to test it further by examining in detail a more comprehensive solution. Fortunately, accurate solutions of Dirac's equation, applicable to the hydrogen atom in all its quantum states, have been obtained by Darwin.<sup>‡</sup> So far as I know, these are the only accurate wave solutions extant, apart from the elementary case of no electromagnetic field. I have examined them in relation to the inference with the results given below.

The equations from which Darwin starts can be written in the form (20), with

$$\mathbf{V}_{1,2,3} = 0, \quad \mathbf{V}_4 = \frac{ie^2}{cr}, \quad r = (x_1^2 + x_2^2 + x_3^2)^{\frac{1}{2}},$$

and  $E_1 \dots E_5$  the matrices (01) ... (05) given in Table I. (This is, in fact, the reason why these particular matrices have been chosen to initiate the group and for illustration in equation (16).) He works out the values of  $\psi$  only so far as they depend on  $x_1 \dots x_3$ , i.e.,  $\partial/\partial x_4$  is treated as a constant multiplier instead of as an operator. The solutions fall into two types, of which only the first need be considered in detail. This is

$$\left. \begin{aligned} \psi_1 &= -i\mathbf{F}\mathbf{P}_{k+1}^u, & \psi_2 &= -i\mathbf{F}\mathbf{P}_{k+1}^{u+1}, \\ \psi_3 &= (k+u+1)\mathbf{G}\mathbf{P}_k^u, & \psi_4 &= (-k+u)\mathbf{G}\mathbf{P}_k^{u+1}. \end{aligned} \right\} \quad (28)$$

<sup>†</sup> 'Proc. Roy. Soc.,' A, vol. 139, p. 349 (1933).

<sup>‡</sup> 'Proc. Roy. Soc.,' A, vol. 118, p. 654 (1928).

Here  $k$  is any positive integer, including zero; and  $u$  is any integer from  $-k$  to  $+k$ , also including zero.  $P_k^u$  is the spherical harmonic function

$$P_k^u = \frac{(2k)!}{2^k k!} \sin^u \theta e^{iu\phi} \left[ \cos^{k-u} \theta + \sum (-1)^n \frac{(k-u)(k-u-1)\dots(k-u-2n+1)}{2 \cdot 4 \dots 2n(2k-1)(2k-3)\dots(2k-2n+1)} \cos^{k-u-2n} \theta \right], \quad (29)$$

the summation being taken over the integral values of  $n$  from 1 to  $(k-u)/2$  when this is integral, or to the next integer below it when it is not.  $F$  and  $G$  are functions of  $r$  and  $k$ , given later.

This solution not only does not represent  $\psi$  as an ordered complex, it does not even seem to represent a stationary system of waves. We should expect a particular solution describing a system of stationary vector waves to have the nodes of each of its components  $\psi_1 \dots \psi_4$  in the same places. The number of nodes in  $P_k^u$  forming circles of latitude is  $k-u$  (in addition to those at the poles); so that from (28) we shall have for  $\psi_1 \dots \psi_4$  respectively  $k-u+1, k-u, k-u, k-u-1$  nodes. There are similar variations in the numbers of longitudinal nodes, and, in fact, the various  $\psi_s$  do not at first sight seem to belong to the same wave system.

The discrepancy, both as regards nodes and the variation from the ordered complex form, can be resolved. In the first place we apply the following difference formula, provable from (29), to express the  $\psi_1$ - and  $\psi_2$ -harmonics in terms of those for  $\psi_3$  and  $\psi_4$ :

$$\begin{aligned} P_{k+1}^u &= (k+u+1) \cos \theta \cdot P_k^u - (k-u) \sin \theta e^{-iu\phi} \cdot P_{k+1}^{u+1}, \\ P_{k+1}^{u+1} &= (k+u+1) \sin \theta e^{iu\phi} \cdot P_k^u + (k-u) \cos \theta \cdot P_{k+1}^{u+1}. \end{aligned} \quad \left. \right\} \quad (30)$$

Secondly, examination of Darwin's rather complicated radial functions  $F$  and  $G$  reveals a connexion between them, which enables them to be written as follows:

$$F = (f-g) \frac{\gamma}{k'+n'+N} e^{-r/\alpha N}, \quad G = (f+g) e^{-r/\alpha N}, \quad (31)$$

where

$$\begin{aligned} f &= (N+k+1) r^{k'+n'-1} \left\{ 1 - \frac{aN}{r} \frac{n'(n'+2k')}{2} \right. \\ &\quad \left. + \frac{(aN)^2 n' (n'-1) (n'+2k') (n'+2k'-1)}{2 \cdot 4} - \dots \right\}, \end{aligned}$$

$$\begin{aligned} g &= r^{k'+n'-1} \left\{ \frac{aN}{r} \frac{n' (n'+2k')}{2} \right. \\ &\quad \left. - 2 \left( \frac{aN}{r} \right)^2 \frac{n' (n'-1) (n'+2k') (n'+2k'-1)}{2 \cdot 4} + \dots \right\}. \end{aligned}$$

Here  $n'$  is any positive integer, including zero, and

$$\left. \begin{aligned} \gamma &= \frac{2\pi e^3}{hc}, & a &= \frac{\hbar}{2\pi mc\gamma}, \\ k' &= ((k+1)^2 - \gamma^2)^{\frac{1}{2}}, & N &= (\gamma^2 + (k'+n')^2)^{\frac{1}{2}} \end{aligned} \right\} \quad (32)$$

( $\gamma$  is the fine structure constant, and  $a$  the radius of the first Bohr orbit).

Thirdly, for the purposes of the present discussion, we require a  $\psi$  which is a solution of the full equation, with  $\partial/\partial x_4$  not a constant multiplier, but a differentiator. Darwin's  $\psi_n$  are functions of  $x_1 \dots x_3$  only. The necessary modification giving them as four-dimensional solutions of the full equation is obtained (I find by trial) by multiplying each by

$$e^{-\frac{2\pi m c (k'+n') x_4}{\hbar N}}.$$

We apply these substitutions or modifications, replace in (30)  $\cos \theta$  by  $x_3/r$ ,  $\sin \theta e^{\pm i\phi}$  by  $(x_1 \pm ix_2)/r$ , and further, for simplification, multiply Darwin's solutions throughout by the common constant factor  $(k'+n'+N)$ . The solution of the full equation then becomes

$$\left. \begin{aligned} \psi_1 &= e^{-2\pi H/\hbar} (f-g) \gamma \left\{ \left( \frac{-ix_2}{r} \right) (k+u+1) P_k^u \right. \\ &\quad \left. + \left( \frac{ix_1+x_3}{r} \right) (k-u) P_k^{u+1} \right\}, \\ \psi_2 &= e^{-2\pi H/\hbar} (f-g) \gamma \left\{ \left( \frac{-ix_1+x_3}{r} \right) (k+u+1) P_k^u \right. \\ &\quad \left. + \left( \frac{-ix_3}{r} \right) (k-u) P_k^{u+1} \right\}, \\ \psi_3 &= e^{-2\pi H/\hbar} (f+g) (k'+n'+N) \{(k+u+1) P_k^u + 0\}, \\ \psi_4 &= e^{-2\pi H/\hbar} (f+g) (k'+n'+N) \{0 + (-1)(k-u) P_k^{u+1}\}, \end{aligned} \right\} \quad (33)$$

in which

$$H = \frac{mc}{N} \{ \gamma r + (k'+n') x_4 \}. \quad (34)$$

The various stationary states are fixed by the different integral values which may be given to  $u$ ,  $k$ , and  $n'$ ; the energy, however, depends on  $k$  and  $n'$  only, being

$$W = \frac{mc^3}{N} (k'+n').$$

The forecast that  $\psi$  will be expressible in the form

$$\psi = \phi e^{-2\pi H/h},$$

where

$$\sum_1^4 \left( \frac{\partial H}{\partial x_n} \right)^2 = (mc)^2,$$

is verified, the first part obviously, and the second readily, using (34) and (32). To make clear the extent to which  $\psi$  is an ordered complex in terms of  $\partial H / \partial x_n$  and  $imc$  we will substitute in (33)

$$\begin{aligned} s_4 &= + \frac{\partial H}{\partial x_4} = \frac{mcY}{N} \cdot \frac{x_n}{r}, \quad (\alpha = 1 \dots 3), \\ s_4 &= + \frac{\partial H}{\partial x_4} = \frac{mc}{N} (k' + n'), \\ s_5 &= + imc, \end{aligned} \quad \left. \right| \quad (35)$$

and put for shortness

$$\begin{aligned} X &= (N/mc) e^{-2\pi H/h} (k + u + 1) P_k^u, \\ Y &= (N/mc) e^{-2\pi H/h} (k - u) P_k^{u+1}. \end{aligned}$$

We then get

$$\begin{bmatrix} \psi_1 \\ \psi_2 \\ \psi_3 \\ \psi_4 \end{bmatrix} = -Xf \begin{bmatrix} is_3 \\ is_1 - s_2 \\ -s_4 + is_5 \\ 0 \end{bmatrix} + Yf \begin{bmatrix} is_1 + s_2 \\ -is_3 \\ 0 \\ -s_4 + is_5 \end{bmatrix} + Xg \begin{bmatrix} is_3 \\ is_1 - s_2 \\ s_4 - is_5 \\ 0 \end{bmatrix} - Yg \begin{bmatrix} is_1 + s_2 \\ -is_3 \\ 0 \\ s_4 - is_5 \end{bmatrix}. \quad (36)$$

Comparison with (17) which gives the solution of the ordering equation formed from the same wave matrices, while not disclosing the complete agreement inferred, reveals a definite extent of agreement described as follows. When allowance is made for  $s_6$  having been set zero in the wave equation, the first and second orderings of the  $s_n$  in (17) and in (36) are identical. The third and fourth orderings in (36), however, are not the same as in (17); they are repetitions of the first two with  $s_4$  and  $s_5$  changed in sign, and have no counterpart in (17).

The partial disagreement observed above appears to be due to a defect in the original forecast, which might perhaps have been, although in fact

it was not, anticipated. If we base an ordering equation on the quadratic equation (27) with nothing further given, there is an ambiguity in fixing the sign of each square root which forms an  $s_a$ . True, geometrical considerations might be called in for deciding to adopt the same signs for  $\partial H/\partial x_1 \dots \partial H/\partial x_3$ , but these fail when we come to the imaginary terms  $\partial H/\partial x_4$  and  $imc$ . The sign of an imaginary term is in geometry entirely conventional—whatever is achieved by  $+i$  is achieved equally well, alternatively, by  $-i$ . There is thus an essential indeterminateness as to whether we shall use  $+s_4$  and  $+s_5$  or  $-s_4$  and  $-s_5$  in constructing as has been done above an ordering equation for the purpose of identifying its terms with those of Dirac's equation.

The solution (36) appears to show that Dirac's equation disposes of this ambiguity by being equivalent in some way to two ordering equations (one in  $s_4$  and  $s_5$ , and one in  $-s_4$  and  $-s_5$ ) at the same time. Retracing on it the steps by which (17) was formed, we can write the solution (36)

$$\psi = \sum_1^5 E_a^{-1} s_a \lambda + \sum_1^5 E_a^{-1} s'_a \mu, \quad (36A)$$

where the  $s'_a$  are the same as the  $s_a$  of (35) with  $s_4$  and  $s_5$  changed in sign,  $\lambda$  is a column matrix of the terms,  $-Xf, Yf, 0, 0$ , and  $\mu$  of the terms  $Xg, -Yg, 0, 0$ .  $\psi$  is the sum of two ordered complexes, and each individually can be accounted for as the solution of an appropriate ordering equation. On the other hand, it does not appear feasible to write a single ordering which will be satisfied by the sum.

It may be asked what has become in the wave equation solution of the third and fourth orderings of (17), which are missing from (36). One answer is that, since only two of the four perpendicular orderings are independent, we could not expect to increase the generality of the solution by making use of more than two. Another answer may, however, be given. A second solution for the hydrogen atom, of another type, was discovered by Darwin, and investigation of this shows that it is expressible in a similar form to (36), but in this case in terms of the third and fourth orderings of (17), so that actually all the orderings are made use of.

In the more simple cases of Darwin's solution the duplicate orderings in terms of  $-s_4$  and  $-s_5$  disappear; for example, when  $n' = 0$  we have from (31)  $g = 0$ , and the second summation in (36A) vanishes. In such cases  $\psi$  accurately satisfies the ordering equation (21).

In the paper previously referred to, having found this result for the simplest case of all, the ground state ( $k = 0, n' = 0$ ), I virtually made the assumption that it was true in general in a calculation in which the five-term equation of Dirac was reduced to a simpler form possessing four terms

only. It appears from the present discussion, however, that the result is not true in the more complicated of the higher quantum states. I take the opportunity of observing here that the reduced equation referred to, although it certainly holds for some simple cases, consequently cannot claim to form a valid description of the *general* wave field.

Apart from the ambiguity mentioned, the analysis of this section brings out definitely the close connexion between the wave and ordering equations (20) and (21). The fact that the  $\psi$  of the wave equation is expressible as a sum of ordered complexes not only throws light on the mathematical properties of the function, but it may perhaps facilitate in other cases the accurate solution.

### 5—EXTENDED FORM OF WAVE EQUATION

Reference has already been made to the fact that the maximum number of terms in the wave equation (1) is settled by the possible number of matrices in a wave set, and when the defining condition of the set is taken to be (5) instead of (2) this number is six. In Dirac's equation five terms only are made use of—the four operators associated with the coordinates of a fourfold plus the mass term. It appears now that six possible terms exist in the most general form of a linear wave equation; indeed, the sixth term has to be introduced into Dirac's equation if its form is to remain invariant to all the possible mathematical transformations. As will be seen in the next section, the six  $s_a$  in an ordering equation, and equally terms which correspond to them in a wave equation are continuously interchangeable with each other by definite rotation transformations in a Euclidian sixfold. It is thus a straightforward operation apart from its physical meaning, to transform Dirac's equation into a six-term one; for we have only to write in it a zero sixth term and rotate the sixfold axes in the plane of this and one of the other terms, when the sixth term will become finite. The question naturally arises as to whether such an extended equation has any possibilities greater than those of the standard form for the purpose of a physical description of Nature, but it is too speculative for any attempt to be made to consider it here.

### 6—TRANSFORMATIONS

The equations

$$\sum_0^5 E_a s_a \psi = 0, \quad (14)$$

and

$$\Sigma P E_a Q s_a Q^{-1} \psi = 0,$$

$P$  and  $Q$  being matrices, will clearly be satisfied by the same value of  $\psi$ , so long as  $Q$  and  $s_a$  commute. The condition is fulfilled for any  $Q$  when the  $s_a$  are algebraics, as they are in the ordering equation. If they are operators, as in the wave equation, it will be fulfilled so long as  $Q$  is not a function of the coordinates. It follows that the equation

$$\sum_0^5 E'_a s_a \psi' = 0, \quad (37)$$

where

$$E'_a = PE_a Q, \quad (9)$$

will be satisfied by

$$\psi' = Q^{-1} \psi. \quad (38)$$

In this way (14) may be expressed in terms of any other wave set in the group, and the corresponding value of  $\psi$  determined. (The contravariant equation (14A), subject to the same transformation, is readily seen to be satisfied by  $\bar{\chi}' = \bar{\chi}Q$  so that the scalar  $\bar{\chi}\psi$  keeps its value unchanged.)

A particularly important transformation (9) for the purpose of classifying the group relations of wave sets is  $(\alpha\beta) \dots 1$ , where  $(\alpha\beta)$  is one of the matrices (00), (10) ... (54) of the group itself. If we apply these in succession to the wave set (00) ... (05), we get 16 sets, the equations constructed from which (since  $Q = 1$ ) are all satisfied by the same value of  $\psi$ . These may be called "equivalent" sets. As they will be useful in the next section, their two-figure designations are given here, the products being reduced, as explained earlier, on the basis of the " $-i$ " group multiplication rules. Table I exhibits a complete group of equivalent wave sets; any one of the transformations applied to any set merely gives rise to one of the other sets in the table. The sets are of two kinds, six of the general form, apart from the order,

$$(\alpha\alpha), (\alpha\beta), (\alpha\gamma), (\alpha\delta), (\alpha\varepsilon), (\alpha\zeta), \quad (39)$$

consisting of five anticommuting matrices and unity, and ten of the form

$$(\alpha\beta), (\beta\gamma), (\gamma\alpha), i(\delta\varepsilon), i(\varepsilon\zeta), i(\zeta\delta). \quad (40)$$

Here each set consists of two triads, the first three and the last three terms in (40); the matrices of each triad anticommute mutually, but commute with each matrix of the other triad. All six matrices nevertheless satisfy the condition (5) of "reciprocal" anticommutation.

In another important class ("rotation" transformations) it is found that the general result (37) can be converted into an alternative form

$$\sum_a^5 E_a s'_a \psi' = 0, \quad (41)$$

with  $\Sigma s_a^2 = 0$  and  $\psi' = Q^{-1} \psi$  as before. In this form the wave matrices are unchanged, and the axes of the  $s_a$  rotated. The theory as originally given by Eddington can be extended to apply to rotations in all the 15 coordinate planes of a sixfold in which the six  $s_a$  can be pictured geometrically. (Eddington developed it only for the 10 planes of a fivefold. His transformations were restricted to the form  $P \dots P^{-1}$  which covers the rotation theory of the five terms of the standard equation, but cannot be extended to cover a sixth. With the present definition of wave sets, however, the transformation possibilities are increased.)

TABLE II—EQUIVALENT WAVE SETS

(00)	(01)	(02)	(03)	(04)	(05)
(10)	(11)	(12)	(13)	(14)	(15)
(20)	(21)	(22)	(23)	(24)	(25)
(30)	(31)	(32)	(33)	(34)	(35)
(40)	(41)	(42)	(43)	(44)	(45)
(50)	(51)	(52)	(53)	(54)	(55)
(21)	(02)	(10)	<i>I</i> (54)	<i>I</i> (35)	<i>I</i> (43)
(31)	(03)	<i>I</i> (45)	(10)	<i>I</i> (52)	<i>I</i> (24)
(41)	(04)	<i>I</i> (53)	<i>I</i> (25)	(10)	<i>I</i> (32)
(51)	(05)	<i>I</i> (34)	<i>I</i> (42)	<i>I</i> (23)	(10)
(32)	<i>I</i> (54)	(03)	(20)	<i>I</i> (15)	<i>I</i> (41)
(42)	<i>I</i> (35)	(04)	<i>I</i> (51)	(20)	<i>I</i> (13)
(52)	<i>I</i> (43)	(05)	<i>I</i> (14)	<i>I</i> (31)	(20)
(43)	<i>I</i> (52)	<i>I</i> (15)	(04)	(30)	<i>I</i> (21)
(53)	<i>I</i> (24)	<i>I</i> (41)	(05)	<i>I</i> (12)	(30)
(54)	<i>I</i> (32)	<i>I</i> (13)	<i>I</i> (21)	(05)	(40)

The theory is based on the following proposition, easily proved by multiplying out the terms:

If  $A^2 = -1$ ,  $B$  being unrestricted, then

$$\begin{aligned}
 & \left( \cos \frac{\theta}{2} + A \sin \frac{\theta}{2} \right) B \left( \cos \frac{\theta}{2} \pm A \sin \frac{\theta}{2} \right), \\
 &= (\cos \theta + A \sin \theta) B, && \text{if } AB = \pm BA, \\
 &= B && \text{if } AB = \mp BA. \quad \} \quad (42)
 \end{aligned}$$

(The upper signs taken together express one result, and the lower signs a second.)

To apply this we let  $B$  be the sum of the  $E_a$ 's in (14), with the  $E_a$  expressed in either of the forms (39) or (40), and let  $A$  take any one of the 15 values  $(\alpha\beta) \dots (\epsilon\zeta)$ . In all cases  $A$  will either commute with two terms of  $B$  and anticommute with the remaining four, or anticommute

with two terms, commuting with the remainder. We apply the transformation denoted by the upper signs of (42) in the first-mentioned conditions, by the lower in the second; in each case the equation can be rewritten in the form (41), in which the  $s'_*$  are derivable from the  $s_*$  by a rotation through an angle  $\theta$  in the coordinate plane of the  $s_*$ -sixfold corresponding to the selected pair.

For example,  $(\alpha\beta)$  commutes with  $(\alpha\alpha)$  and  $(\alpha\beta)$  in (39), and anti-commutes with  $(\alpha\gamma) \dots (\alpha\zeta)$ . Using this for A and the upper signs of (42), we get for the transformed equation formed from the wave set (39)

$$\begin{aligned} & \left\{ \cos \frac{\theta}{2} + (\alpha\beta) \sin \frac{\theta}{2} \right\} \{(\alpha\alpha) s_0 + (\alpha\beta) s_1 + \text{etc.}\} \left\{ c - \frac{\theta}{2} + (\alpha\beta) \sin \frac{\theta}{2} \right\} \psi' \\ &= [\{(\alpha\alpha) \cos \theta + (\alpha\beta) \sin \theta\} s_0 + \{(\alpha\beta) \cos \theta - (\alpha\alpha) \sin \theta\} s_1 \\ &\quad + \text{unchanged terms}] \psi' = 0. \quad (43) \end{aligned}$$

This may be written

$$\{(\alpha\alpha) (s_0 \cos \theta - s_1 \sin \theta) + (\alpha\beta) (s_1 \cos \theta + s_0 \sin \theta) \\ + \text{unchanged terms}\} \psi' = 0, \quad (44)$$

where

$$\psi' = \left\{ \cos \frac{\theta}{2} + (\alpha\beta) \sin \frac{\theta}{2} \right\}^{-1} \psi. \quad (45)$$

In the first form we have the equation with a transformed set of matrices, in the second with the original matrices but with the  $s_*$  rotated in the plane  $s_1 s_0$ . Both forms are of interest.

If in (43)  $\theta = \pi/2$ , the equation becomes

$$\{(\alpha\beta) s_0 - (\alpha\alpha) s_1 + \text{unchanged terms}\} \psi' = 0,$$

and the matrices of  $s_0$  and  $s_1$  have been interchanged with a change of sign of one term. If  $\theta = \pi$ , we get

$$\{-(\alpha\alpha) s_0 - (\alpha\beta) s_1 + \text{unchanged terms}\} \psi' = 0,$$

and the signs of two terms have been changed without other modification of the set. By successive transformations the matrices of the wave set initially employed may be arranged in any order, and the corresponding effect on  $\psi$  determined. Only half, however, of the possible arrangements of the signs may be thus obtained. No transformation will change the sign of one term alone, or interchange the matrices of two terms without a change of sign. Such a modification would transfer the wave set into the alternative  $\pm i$  group of (10), which cannot be done by transformation.

7—RELATION BETWEEN THE  $s$ - AND  $\psi$ -ROTATIONS

By means of the ordering equation a general correspondence becomes established between  $s$ -vectors obeying Euclidian geometry in a sixfold and complex  $\psi$ -vectors in a fourfold.<sup>†</sup> Equations (44) and (45) show that, corresponding to each coordinate rotation through  $\theta$  of the  $s_a$ ,  $\psi$  undergoes a special complex rotation in its manifold through  $\theta/2$ . There are 15 coordinate planes of rotation in the sixfold, and 15 complex rotations in the fourfold to correspond with them.<sup>‡</sup>

This peculiar behaviour of the complex  $\psi$ , which is so different from that of ordinary vectors that a special name "spinor" has been accorded to  $\psi$ , deserves a closer examination. The transformation behaviour of  $\psi$  is actually determined by the way in which it is defined, and we have to distinguish between the different effects of two possible definitions.

(1) If we define  $\psi$  as a quantity satisfying the equation

$$\sum E_a s \psi_a = 0 \quad (14)$$

(or the equivalent wave equation), and undergoing the transformation

$$\psi' = Q^{-1} \psi \quad (38)$$

when the  $E_a$  undergo the transformation

$$E'_a = P E_a Q, \quad (9)$$

then we get the case discussed above.  $\psi$  always satisfies the transformed equation, and it undergoes the symbolic  $\theta/2$  rotation for each  $s$ -rotation  $\theta$ .

(2) On the other hand, we might define  $\psi$  as the solution of (14), viz.,

$$\psi = \sum E_a^{-1} s_a \lambda, \quad (15)$$

with fixed constants for the terms of the arbitrary matrix  $\lambda$ . We shall then have for its transformation law

$$\begin{aligned} \psi'' &= \sum (P E_a Q)^{-1} s_a \lambda \\ &= Q^{-1} \sum E_a^{-1} s_a (P^{-1} \lambda). \end{aligned} \quad (46)$$

This is not the same as the  $\psi'$  of (38)— $P^{-1}$  enters into its specification as well as  $Q^{-1}$ . If  $P \dots Q$  be the transformation illustrated in (43) which effects a rotation  $\theta$  in the  $s_1 s_2$  plane of the sixfold, we see that the  $\theta/2$  rotation,

$$Q^{-1} = P^{-1} = \cos \frac{\theta}{2} - (\alpha \beta) \sin \frac{\theta}{2},$$

comes twice into the expression for  $\psi''$ , giving effectively the full rotation of  $\theta$ . In fact, if  $\psi$  is to be a definite function of the  $s_a$  and fixed constants, the effect on it of a rotation  $\theta$  of the  $s_a$  must necessarily be that given by inserting the rotated values of the  $s_a$  in the expression.

<sup>†</sup> It is actually only a null cone of the sixfold that is contemplated, since  $\sum s_a^2 = 0$ .

<sup>‡</sup> Cf. Milner, 'Proc. Roy. Soc.' A, vol. 139, p. 356 (1933). There exists also a 16th possible rotation (got by putting in (42)  $A = I$ ) which has no application here.

We can now see more clearly what has implicitly been done in making the first definition. If in making the transformation (46) we do not regard  $\lambda$  as fixed, but modify it, giving it the value  $P\lambda$ , the result of the combined operation will be to give the  $\psi'$  of (38). This double operation is always possible, since  $\lambda$  is arbitrary, but it is not strictly a *transformation*.  $\psi$  is now no longer a definite function of the  $s_a$ , but a function the form of which undergoes change when the rotation transformation is applied.

In certain cases the distinction between the two definitions of  $\psi$  becomes important. For example, in § 3  $\psi$  in its simplest form is shown to be an ordered complex of the  $s_a$ , which is changed to another complex when a change is made in the order of the matrices in equation (14). Which transformation effects this change? The answer is the second form only (46)—ordered complexes may thus be regarded as definite functions of the  $s_a$ . The first form (38) gives a complicated expression for  $\psi'$  which, although of course it, too, satisfies the ordering equation, does not appear to be useful. On the other hand, in dealing with  $\psi$  considered purely as a solution of the wave equation (20), there is no guarantee that the transformation (46) is always definitely applicable to it. Trials have shown that it does apply in many cases of interchange of matrices between terms, but it fails when the interchange is between the mass-term matrix and another. This is a transformation the difficulty of interpretation of which has already been referred to (§ 5). The "transformation" (38), however, will in every case give a  $\psi'$  which is a solution of the transformed equation; it is usually a complicated expression, but is safe to use.

### 8—WAVE SET IDENTITIES

These are based on a discovery of Eddington's† which in our notation may be expressed as follows:

If  $A$  is any four-square matrix which is symmetrical about the leading diagonal ( $A_{ij} = A_{ji}$ ), and  $\bar{E}_a$  stands for the transposed of  $E_a$ , then, the sum being taken over the six terms formed from a wave set,

$$\sum_0^5 E_a A \bar{E}_a = 0. \quad (47)$$

This result may be verified readily for one of the sets in Table II, by using the special values for the matrices given in Table I; the following reasoning then proves it to be true generally.

Consider the matrix  $A' = QA\bar{Q}$ , where  $Q$  is any matrix and  $\bar{Q}$  its transposed. We have, using the summation convention,

$$\begin{aligned} A'_{ii} &= Q_{ii} A_{ii} Q_{ii}, \text{ by definitions of products and } \bar{Q}, \\ &= Q_{ii} A_{ji} Q_{ii}, \text{ interchanging } i \text{ and } j, \\ &= Q_{ii} A_{ii} Q_{ij}, \text{ since } A \text{ is symmetric,} \\ &= A'_{jj}. \end{aligned}$$

† 'Proc. Roy. Soc.,' A, vol. 133, p. 311 (1931).

Hence  $A'$  also is a symmetric matrix, and consequently, for the tested set,

$$\sum E_a (QA\bar{Q}) \bar{E}_a = 0.$$

This equation will still be valid after multiplication, before and behind, by any matrices, therefore

$$\Sigma PE_a Q \cdot A \cdot \bar{Q} \bar{E}_a \bar{P} = 0.$$

Remembering the inversion rule for the transposition of matrix products, we can write this equation

$$\Sigma E'_a A \bar{E}'_a = 0,$$

so that the result (47) is now proved to hold for any wave set obtained from the initial one by the general transformation

$$E'_a = PE_a Q. \quad (48)$$

It may be noted that the property of wave sets denoted by (47) is of a very comprehensive kind, for it implies the equation of 16 separate sums to zero, one for each term of the matrix. (47) may be given a more extended form by post-multiplying it by  $\bar{P}$  when it becomes

$$\sum_0^5 E_a A \bar{E}'_a = 0, \quad (48)$$

where

$$E'_a = PE_a. \quad (49)$$

The identity in this form may be applied to the group of equivalent wave sets (Table II), which are related to each other by transformations of the type (49). In the rest of this section we shall take the  $E_a$  to indicate any one of these sets, and the  $E'_a$  again any one, *i.e.*, it may be the same one as the  $E_a$  or one of the others. Then for every one of the 256 arrangements of an  $E_a$  with an  $E'_a$ , set taken from Table II an equation (48) will hold.

In addition to the scalar product  $\bar{\chi}\psi$  of two arbitrary vectors defined in (3), 15 other scalar products, of equal importance in general theory, can be defined by means of wave matrices. All 16 are given by the general form

$$\bar{\chi}(\alpha\beta)\psi,$$

where  $(\alpha\beta)$  is one of the 16 matrices (00) ... (45) of the group illustrated in Table I. The notation there given for special matrices enables their values to be written down easily, *e.g.*,

$$\begin{aligned} \bar{\chi}(01)\psi &= \bar{\chi}i(2\bar{1}43)\psi, \\ &= i\{-\chi^1\psi_2 - \chi^3\psi_1 + \chi^3\psi_4 + \chi^4\psi_3\}. \end{aligned}$$

These scalars are necessarily unchanged by transposition; thus

$$\bar{\chi} E_a \psi = \overline{E_a \chi}. \quad (50)$$

On the other hand,  $\psi E_a \bar{\chi}$  is not a scalar product but a four-square matrix. In particular  $\psi \bar{\psi}$  is a symmetrical matrix  $[\psi_i \psi_j]$ . We therefore have, for any vector  $\psi$ ,

$$\sum E_a \psi \bar{\psi} \overline{E'_a} = 0.$$

and, postmultiplying by any vector  $\chi$ ,

$$\sum \overline{E_a} \psi \bar{\psi} \overline{E'_a} \chi = 0.$$

By (50) this may be written

$$\sum_0^8 (\bar{\chi} E'_a \psi) \cdot E_a \psi = 0, \quad (51)$$

the quantity in brackets being a commuting scalar product.

The 256 relations, which are obtained by using for  $E_a$  and  $E'_a$  in (51) the various wave sets of Table II, are *identities*. This means that, when actual values (Table I) are inserted for the matrices, the left-hand sides reduce algebraically to zero for every  $\psi$  and  $\bar{\chi}$ . The relations thus state nothing about  $\psi$  or  $\bar{\chi}$ , but denote solely properties of wave sets. Eddington, who first derived the equation (51) (in a somewhat restricted form compared with the above), although he recognized it as an identity, refers to it as "the wave equation". Since the function of the latter is to determine *particular values* of  $\psi$  which satisfy it, I hardly think it can be sound to regard it as synonymous with an algebraical identity. On the other hand, it does appear that in (51) there has been discovered a remarkable set of solutions of the ordering equation (14), of a character inverse to those obtained in § 3. Suppose that in regard to the equations

$$\sum E_a s_a \psi = 0, \quad \sum s_a^2 = 0,$$

instead of solving them for  $\psi$ , we ask what values of the six  $s_a$  will satisfy them with arbitrary values of  $\psi$ . There are only five equations to determine the six unknowns, so that there must be many possible solutions. We see now from (51) that systematic sets of such solutions can be stated, viz.,

$$s_a \propto \bar{\chi} E'_a \psi,$$

where  $\bar{\chi}$  (as well as  $\psi$ ) is arbitrary, and the  $E'_a$  are any one of the 16 sets of Table II equivalent to that used in the equation.

Finally, we may multiply (51) by an arbitrary vector  $\bar{\phi}$ , and we get

$$\sum_0^5 (\bar{x}E'_*\psi)(\bar{\phi}E_*\psi) = 0, \quad (52)$$

in which each bracketed quantity is a scalar. (52) denotes relations between scalar products with arbitrary  $\psi$ ,  $\bar{x}$ , and  $\bar{\phi}$ , which will be satisfied identically on insertion of actual values for the matrices. There will be 136 identities of this type within the group of Table II—16 in which the  $E_*$  and  $E'_*$  are matrices of the same row, and  $16 \times 15/2 = 120$  where they are of different rows. (The factor 1/2 comes in here because  $\bar{x}$  and  $\bar{\phi}$ , being arbitrary, may be interchanged in (52) without altering its meaning.)

If we take  $\bar{\phi} = \bar{x}$ , (52) reduces to denoting relations (now much simplified) between one set only of scalar products  $\bar{x}E_*\psi$ . The 16 first-named identities become

$$\sum_0^5 (\bar{x}E_*\psi)^2 = 0,$$

and show that, out of the 16 scalar products, 6 may be chosen in 16 different ways (the  $E_*$  being given in the rows of Table II) so as to satisfy Euclidian geometry in the null-cone of a sixfold. The effect on the 120 other identities can be seen by considering an example. Take in (52)

$$E'_* = (00), \dots (05), \quad E_* = (54), \dots (40),$$

and write  $j_{\alpha\beta} = \bar{x}(\alpha\beta)\psi$ ; then

$$j_{00}j_{54} + j_{01}j_{53} + j_{02}j_{52} + j_{03}j_{51} + j_{04}j_{50} + j_{05}j_{40} = 0.$$

The last two terms cancel and the equation reduces to one of four terms only. Further the same reduced equation is obtained on using any one of the four pairs of  $E_*$ ,  $E'_*$  sets whose first terms are given by any of the paired suffixes of the equation, (00), (54), ..., (03), (21). This simplification occurs with them all and reduces the number of relations to 30.

The 46 identities expressing relations between the 16 scalar products can be classified as follows. Let  $\alpha\beta\gamma\delta\epsilon\zeta$  stand for the numbers 012345 arranged in any order. Then there are six equations of the form

10 of the form	$j_{\alpha\alpha}^2 + j_{\alpha\beta}^2 + j_{\alpha\gamma}^2 + j_{\alpha\delta}^2 + j_{\alpha\epsilon}^2 + j_{\alpha\zeta}^2 = 0,$	}
15 of the form	$j_{\alpha\beta}^2 + j_{\beta\gamma}^2 + j_{\gamma\alpha}^2 - j_{\alpha\delta}^2 - j_{\alpha\epsilon}^2 - j_{\alpha\zeta}^2 = 0,$	
and 15 of the form	$j_{\alpha\gamma}j_{\beta\gamma} + j_{\alpha\delta}j_{\beta\delta} + j_{\alpha\epsilon}j_{\beta\epsilon} + j_{\alpha\zeta}j_{\beta\zeta} = 0,$	
	$\pm j_{\alpha\alpha}j_{\beta\beta} + j_{\gamma\gamma}j_{\delta\delta} + j_{\epsilon\epsilon}j_{\zeta\zeta} + j_{\eta\eta}j_{\kappa\kappa} = 0.$	

(53)

In the last equations the + or - must be used for the first term according to whether the numbers used for  $\alpha \dots \zeta$  can be brought to the order 012345 by an odd or an even number of interchanges of figures—when the wave sets are in the “-i” group (and by an even or odd number for the “+i” group).

In place of the arbitrary  $\bar{\chi}$  in the scalar products we may write  $\bar{\psi}^*$ , the conjugate transposed of  $\psi$ , but, although the scope of the relations is narrowed down, no further mathematical simplification is obtained thereby. On the other hand, in wave theory the 16 scalars  $\bar{\psi}^*(\alpha\beta)\psi$  stand to some extent for quantities which have a physical significance. Four of them, for example, make their appearance in the conservation equation which every wave equation satisfies, and represent in four dimensions the flux of the probability distribution associated with the electron. Attempts have been made by some writers to express the whole set of products in terms of a four-dimensional geometrical scheme, but the general relations between them, (53), are not of a kind that can be fitted naturally into four dimensions—a much wider scheme is required for them. Such a scheme has been developed by Eddington, in his five-dimensional theory of the space-time of the world, in which sets of five scalar products are identified with space-time coordinates. We shall not, however, attempt to follow up this abstruse theory, the object here being purely to classify and systematize the mathematical results.

#### SUMMARY

There are reasons for believing that the “wave matrices” made use of in the first order wave equation should be defined by the condition

$$E_\alpha^{-1}E_\beta = -E_\beta^{-1}E_\alpha,$$

rather than by

$$E_\alpha E_\beta = -E_\beta E_\alpha,$$

the equation on which they are based in standard theory. It is shown that the new definition enables the matrices, and the “wave sets” formed from them, to be developed into closed groups, and the relations between them, such as the numerous “wave set identities”, to be classified and made amenable to a complete treatment, which cannot be done on the old definition. A further consequence is that the wave equation, in its general mathematical form, finds place in it for six terms, as against the five occurring in Dirac's equation. The properties of the matrices are applied also to draw certain inferences about the mathematical form of the accurate solution of the wave equation, which are tested by examining in detail the known solution for the hydrogen atom.

## Spectra of SeO and $\text{SeO}_2$

By R. K. ASUNDI, MOHD. JAN-KHAN, and R. SAMUEL

(Communicated by Sir C. V. Raman, F.R.S.—Received 28 April, 1936)

[PLATE 1]

An analysis of the near ultra-violet bands of  $\text{SO}_2$ , proposed recently\* has shown, that the energies of excitation are almost equal in  $\text{SO}$  and  $\text{SO}_2$  and that the frequency of the symmetric valence vibration of  $\text{SO}_2$  is about equal to the vibrational frequency of  $\text{SO}$  not only in the ground states of the two molecules, but also in their respective excited states. These results seem to be of considerable interest, particularly with regard to the theory of valency, since they indicate that the S=O bond is almost identical in both molecules. It seemed necessary, therefore, to investigate the spectra of  $\text{SeO}$  and  $\text{SeO}_2$ , in order to see whether such results are fortuitous or whether they are confirmed by the analysis of similar molecules. Such an investigation appeared desirable also, from the point of view that the method of analysis of the spectra of polyatomic molecules has not made so much progress as could be wished for and the bands of formaldehyde† and sulphur dioxide are indeed the only ones, for which a complete vibrational analysis has been offered at the present moment. An extension to polyatomic molecules of the clearer insight into the constitution of diatomic molecules, afforded by band spectroscopy, seems to us essential in the present state of knowledge.

### EMISSION SPECTRUM OF $\text{SeO}$

*Experimental*—The spectrum of  $\text{SeO}$  has not been described in literature. Various methods of producing bands of  $\text{SeO}$ , however, suggest themselves. In analogy with  $\text{SO}$  the best method probably would be one of a discharge through a vacuum tube in running vapour of  $\text{SeO}_2$ , or with high pressure  $\text{SeO}_2$  vapour.  $\text{SeO}_2$ , being a solid with rather a high melting point ( $340^\circ \text{C}$ ), such a method could not be adopted because of the want of a suitable quartz discharge tube and a suitable furnace. A glass discharge tube, with a quartz window for observation, containing

\* Asundi and Samuel, 'Proc. Ind. Acad. Sci.', vol. 2, p. 30 (1935).

† Dieke and Kistiakowsky, 'Phys. Rev.', vol. 45, p. 4 (1934); Herzberg, 'Trans. Faraday Soc.', vol. 27, p. 378 (1931).

SeO<sub>2</sub> was heated locally by a Bunsen burner, but the spectrum obtained showed only bands due to Se<sub>2</sub>. An arc on 110 volts D.C., with a current of 2.5 amps, between carbon or metal electrodes filled with SeO<sub>2</sub>, produced again the bands of Se<sub>2</sub> or the lines of Se as did also the arc on 220 volts D.C. with a current of 2 to 5 amps. The substance was then introduced in a solid state and in aqueous solution into the Bunsen flame. The flame of the solid substance gave only Se<sub>2</sub> bands, but the spectrum of the flame of the solution showed an unmistakable progression of bands, different from those of Se<sub>2</sub> between 4500 and 3200 Å. In the hope of exciting more vibrational levels of the emitter of these bands and thus extending the system, the oxy-coalgas flame giving a higher temperature was used. Under this condition the spectrum showed a further set of bands towards the ultra-violet until about 2400 Å. The bands are all degraded towards longer waves; they are diffuse and in some cases a close double head can be distinguished. The intensity of the bands is not at all high; and increased exposure only resulted in a more pronounced overlap of the bands with the strong continuum of the flame itself. The best plates were obtained, in the blue and near ultra-violet regions, with an exposure of 45 minutes, and in the ultra-violet region, of about two hours, using a Hilger medium quartz spectrograph as the resolving instrument.

That the bands in the blue and near ultra-violet are due to the SeO molecule is fairly certain. They belong decidedly to a diatomic molecule. They appear in the flame of SeO<sub>2</sub> solution and are similar to SO bands. The final plates were measured on the Abbe comparator. On account of the diffuse character of the bands and the accompanying continuum microphotograms on a recording microphotometer were also taken and the band heads measured with the same comparator. The final values of wave-lengths of the band heads were obtained from readings taken on two directly measured plates and three photometer plates. The agreement among various values of the same band heads was not as satisfactory as one would desire. This is due to the inherent diffuseness of the bands and in some cases also to the overlap of OH bands which made it difficult to spot bands lying in that region. The values accepted are therefore correct only to about 1 or 2 Å, i.e., to about 10 or 20 wave-numbers. We have reasons to believe that the weak bands in the further ultra-violet, however, belong rather to the SeO<sub>2</sub> molecule.

*Analysis*—Table I gives the wave-numbers *in vacuo* of the band heads as obtained from the weighted mean of the five measured values. Figs. 1 and 2, Plate 1, are reproductions of the bands from one of the original

plates and its microphotometer plate respectively. The starting point for the analysis was the obvious set of bands beginning from the band at  $30,433 \text{ cm}^{-1}$  towards longer waves. These bands fall into a progression with vibrational differences, 873, 866, 849, 835, 848, and  $823 \text{ cm}^{-1}$ . These differences are slightly irregular, as can be seen from Table II, which displays the analysis of the bands. The second progression from  $30,941 \text{ cm}^{-1}$  also fits into the scheme fairly well.

TABLE I—LIST OF OBSERVED BANDS

$\nu$ vac. $\text{cm}^{-1}$ SeO bands	$\nu$ vac. $\text{cm}^{-1}$ Further ultra-violet bands
25341	33948
26164	35765
27012	36777
27847	37252
27909	37681
28694	38228
28760	38575
(29223)	39075
29274	39498
29560	39972
30076	
30139	
30433	
30941	

The first progression is evidently  $v' = 0$  and therefore the second is  $v' = 1$ . But it is doubtful whether the band at  $30,433 \text{ cm}^{-1}$  is the  $(0, 0)$  band. Most probably it is not; because the molecule SeO should resemble SO, the intensity distribution here should be characterized by a wide Condon parabola whose apex would certainly not be at  $(0, 0)$  but would lie at a band with a higher value of  $v''$ . From this point of view we think that in Table II,  $x$  will have a value of 3. This would place the origin at about  $33,102$  and  $33,167 \text{ cm}^{-1}$  respectively for the two heads and the first vibrational difference of the final state will be about  $910 \text{ cm}^{-1}$ . The  $v' = 0$  progression in Table II as it is, can be expressed by the following formula:

$$\nu = 30433 - \frac{1}{(882v'' - 6v'^2)}.$$

The existence of apparent double heads in this band system which is probably due to a transition  ${}^3\Sigma \rightarrow {}^3\Sigma$  in analogy with O<sub>2</sub> and SO, is to be regarded as accidental. The head at the shorter wave-length is the weaker one, and there is a difference of roughly  $6.5 \text{ cm}^{-1}$  between the two

TABLE II

	$x$	$x + 1$	$x + 2$	$x + 3$	$x + 4$	$x + 5$	$x + 6$
0	$\overline{30433}$	$(873)$	$29560$	$(866)$	$28694$	$(851)$	$27909$
	$\overline{308}$	$(516)$	$(514)$	$(847)$	$27847$	$(835)$	$27012$
1	$\overline{30941}$	$(865)$	$30076$	$(853)$	$29223?$		

 $\times^{a'}$ 

0

1

heads. This distance appears to be the average distance between the origin and the head of the individual bands, the apparent strong head being due to the unresolved lines of the three P branches which should be strong and the two P-form Q branches and the two R-form Q branches, which all should be weak and which start roughly near about the origin.

The vibrational function of the initial state cannot be evaluated for want of more progressions, but the first frequency difference is  $\omega' = 513 \text{ cm}^{-1}$ .

The set of weak bands in the further ultra-violet does not seem to belong to this system at all. It was by no means possible to arrange them as an extension of the present system. Comparison of these bands with the absorption bands of  $\text{SeO}_3$  shows that they are really due to the  $\text{SeO}_3$  molecule, as can be seen by comparing Table I with Table III. They are identical inside the experimental error, with the bands due to a few transitions arising mostly from the vibrationless ground state of the molecule  $\text{SeO}_3$ .

#### ENERGY OF DISSOCIATION

Linear extrapolation of the vibrational levels gives a value of 4.17 volts for the energy of dissociation (D) of the ground level of  $\text{SeO}$ . This value agrees very well with what one would expect from the dissociation energies of  $\text{O}_2$  and  $\text{SO}$ .<sup>\*</sup> It is a general feature throughout the periodic system that the dissociation energy runs parallel to the strength of the nuclear fields, regardless of the polarity of the molecule.<sup>†</sup> In a series of oxides, in which the field of the O atom remains unchanged throughout, D should therefore follow roughly the ionization potential of the other atom, and this is true in each individual group of the periodic system, as may be seen from the following few examples.

Since for  $\text{SO}$  and  $\text{SeO}$  we have to use the value obtained from linear extrapolation, we have given in Table III besides the actual value of  $D(\text{O}_2) = 5.09$  directly deduced from the convergence point of the

TABLE III

CO	$\text{SiO}$	$\text{GeO}$
$D = 10.45$	7.8	7.3      volts
$\text{O}_2$	$\text{SO}$	$\text{SeO}$
6.56	5.1	4.17      volts
$D = 5.09$		

Schumann-Runge bands,\* also the value 6.56 which follows from linear

\* Herzberg, 'Z. phys. Chem.', B, vol. 10, p. 189 (1930); Frerichs, 'Phys. Rev.', vol. 36, p. 398 (1930); Martin, 'Phys. Rev.', vol. 41, p. 167 (1932).

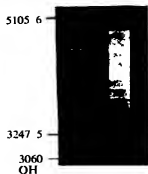


FIG. 1.

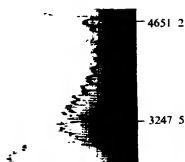


FIG. 2.



FIG. 3.



FIG. 4.



extrapolation. Furthermore, it has been shown\* that if we consider diatomic molecules built up of atoms of similar groups of the periodic system, so that the sum of the numbers expressing the periods of the two atoms remains the same, the dissociation energies of such similar molecules remains very often rather constant. This is clear from Table IV, which refers to their respective ground states.

TABLE IV

	CS	GeS	CP	PO	Br <sub>2</sub>
D =	7.75	5.7	6.9	6.47	2.0    volts
	SiO	SnO	SiN	NS	ICl
D =	7.8	5.8	6.2	5.93	2.1    volts

According to this, the dissociation of SeO should be about the same as that of S<sub>2</sub>, which on considerations of predissociation and linear extrapolation has been estimated as 4.45 volts.† In reality even this value is slightly too high. The direct observation of the point of convergence yields naturally a more exact value; this has been observed in the absorption spectrum of S<sub>2</sub> vapour by Rosen‡ as  $40,000 \pm 1000 \text{ cm}^{-1} = 4.94 \pm 0.12$  volts. If we subtract from this, the energy of excitation of the <sup>1</sup>D term, which is 1.14 volts,§ we obtain  $3.8 \pm 0.12$  volts as the energy of dissociation of S<sub>2</sub> in the normal state. The extrapolated value for SeO is 4.17 volts, in good agreement with the above rule.

The fact that the extrapolated value of SeO agrees with that value of S<sub>2</sub>, which is taken from the convergence limit, is an indication of the absence in the SeO bands of such perturbations as destroy the application of the linear extrapolation for the calculation of the energy of dissociation of S<sub>2</sub>. This is in agreement with the view of Heil,|| according to whom the repulsive curve arising from the combination of two unexcited atoms of the sixth group intersects the potential curve of the excited state of the molecule at lower vibrational levels and finally not at all, with increasing atomic numbers. The case of SeO seems already to be near to that of Se<sub>2</sub>, where the repulsive curve does not intersect at all.

#### ABSORPTION SPECTRUM OF SeO<sub>2</sub>

*Experimental*—The absorption spectrum of SeO<sub>2</sub> was obtained in the usual way, the substance being introduced in an evacuated silica tube,

\* Lessheim and Samuel, 'Proc. Ind. Acad. Sci.', vol. 1, p. 623 (1935), Sect. x, ff.

† Christy and Naude, 'Phys. Rev.', vol. 37, p. 903 (1931).

‡ 'Z. Physik,' vol. 43, p. 69 (1927).

§ Ruedy, 'Phys. Rev.', vol. 43, p. 1045 (1933).

|| 'Z. Physik,' vol. 74, p. 18 (1932).

heated by an electric furnace to various temperatures. As source of light the continuous spectrum of hydrogen was used, and as resolving instrument a Hilger medium quartz spectrograph; copper arc lines were utilized as standards. The plates obtained in this way were again run through the recording microphotometer and these microphotograms measured directly. Figs. 3 and 4, Plate 1, are reproductions of an original plate and a microphotogram.

The wave-lengths ultimately adopted are the weighted means of four values obtained by direct measurement of spectrograms and of two of the microphotograms. Of the subsidiary maxima observed in the microphotograms, only such as are obtained on both the plates and which do not differ in wave-length by more than  $0\cdot2\text{ \AA}$  have been accepted. The wave-lengths obtained from each of these six measurements did not differ by more than  $0\cdot5\text{ \AA}$  and therefore the accuracy of the accepted mean wave-length is believed to be not less than  $0\cdot2\text{ \AA}$  or  $2$  to  $6\text{ cm}^{-1}$  in the region covered by the bands. A few of the bands, however, on the extreme long and short wave sides respectively, of the system could be measured on some of the plates taken at higher temperatures only. The accuracy obtained for such bands only is not greater than  $1\text{ \AA}$  in each case, i.e.,  $10$  to  $15\text{ cm}^{-1}$ . Table V gives the wave-lengths in air, wave-numbers *in vacuo*, and their classification with the observed minus calculated values, the latter being based on the mean values of the spacings of the vibrational levels (Table VII).

TABLE V—LIST OF  $\text{SeO}_3$  BANDS

Bands	$\lambda \text{ \AA (in air)}$	$\nu \text{ cm}^{-1} (\text{in vacuo})$	Classification	$\text{O - C}$
a	3158.1	31655	$(010)'' \rightarrow (000)'$	-4
b	3116.0	32083	$(020)'' \rightarrow (020)'$	-1
b 1	3107.5	32171	$(001)'' \rightarrow (001)'$	+10
c	3092.0	32332	$\{(010)'' \rightarrow (010)', (020)'' \rightarrow (002)'\}$	+10 -10
d	3070.4	32560	$(000)'' \rightarrow (000)'$	0
e	3044.4	32838	$\{(001)'' \rightarrow (011)', (011)'' \rightarrow (003)'\}$	+14 -4
f	3032.8	32963*	$(010)'' \rightarrow (020)'$	-11
A 1	3008.9	33225*	$(000)'' \rightarrow (010)'$	+2
A 2	3007.8	33237	$(010)'' \rightarrow (002)'$	+5
B	2986.5	33474*	$(001)'' \rightarrow (021)'$	-2
C 1	2972.8	33629*	$(010)'' \rightarrow (030)'$	+8
C 2	2963.6	33733*	$(001)'' \rightarrow (003)'$	-2
D	2950.9	33878*	$(000)'' \rightarrow (020)'$	+3
E	2928.6	34136	$\{(000)'' \rightarrow (002)', (001)'' \rightarrow (031)'\}$	+3 +13
F 1	2917.2	34269*	$(010)'' \rightarrow (040)'$	+9

TABLE V—(continued)

Bands	$\lambda \text{ Å (in air)}$	$\nu \text{ cm}^{-1} (\text{in vacuo})$	Classification	$O - C$
F 2	2915·7	34287*	(020)'' → (032)'	-17
G	2906·6	34394	{ (001)'' → (013)' (011)'' → (005)'	-4 -2
H 1	2895·6	34525*	(000)'' → (030)'	+3
H 2	2894·3	34541*	(010)'' → (022)'	-6
I 1	2884·5	34658	(020)'' → (060)'	+6
I 2	2872·7	34800	{ (000)'' → (012)' (010)'' → (004)'	+4 -2
K	2860·8	34945	(020)'' → (042)'	+2
L 1	2851·4	35060*	(001)'' → (023)'	+10
L 2	2843·4	35159	(000)'' → (040)'	-2
L 3	2841·3	35185*	(010)'' → (032)'	-9
L 4	2839·1	35212	(020)'' → (024)'	-15
L 5	2831·4	35308	{ (001)'' → (005)' (020)'' → (070)'	+11 -3
M	2819·8	35453	{ (020)'' → (006)' (010)'' → (014)'	-11 -12
N	2800·6	35696	{ (000)'' → (004)' (001)'' → (033)'	-7 -3
O 1	2790·7	35823	{ (000)'' → (050)' (010)'' → (042)'	+13 -10
O 2	2788·3	35854*	(020)'' → (034)'	-20
O 3	2783·0	35922	(011)'' → (007)'	-4
O 4	2781·9	35936	(020)'' → (080)'	-12
O 5	2780·4	35955	(001)'' → (015)'	-5
P 1	2772·7	36053	(001)'' → (061)'	+9
P 2	2769·5	36097*	(000)'' → (032)'	-2
P 3	2768·0	36117	{ (010)'' → (024)' (020)'' → (016)'	0 -10
Q 1	2750·3	36349	{ (001)'' → (043)' (010)'' → (006)'	+13 -5
Q 2	2748·6	36371*	(000)'' → (014)'	+5
R 1	2739·6	36491	(010)'' → (052)'	+9
R 2	2738·3	36508*	(020)'' → (044)'	-5
S	2731·1	36606*	(001)'' → (025)'	-6
T 1	2721·0	36740*	(000)'' → (042)'	-16
T 2	2719·4	36762*	(010)'' → (034)'	-2
T 3	2713·9	36836	(001)'' → (007)'	+9
U 1	2700·8	37015	{ (000)'' → (024)' (020)'' → (008)'	-3 +12
U 2	2700·2	37023	(010)'' → (016)'	+6
V 1	2694·0	37109	{ (000)'' → (070)' (010)'' → (062)'	+7 +6
V 2	2690·0	37164*	(020)'' → (054)'	+2
W	2683·3	37256	{ (000)'' → (006)' (001)'' → (035)'	+1 -3

TABLE V—(continued)

Bands	$\gamma$ A (in air)	$\nu$ cm <sup>-1</sup> ( <i>in vacuo</i> )	Classification	O - C
X 1	2673.8	37389*	(000)'' → (052)'	+6
X 2	2671.1	37427	(020)'' → (036)'	+1
Y 1	2665.8	37501*	(001)'' → (017)'	+11
Y 2	2653.7	37672	{ (000)'' → (034)' (010)'' → (026)' (020)'' → (018)'	+7 +3 +6
Y 3	2649.6	37730	(000)'' → (080)'	-9
Y 4	2644.7	37800*	(020)'' → (064)'	+5
Z 1	2638.4	37890	(010)'' → (008)'	-3
Z 2	2636.7	37901*	(001)'' → (045)'	+3
Z 3	2635.9	37926	(000)'' → (016)'	+8
A' 1	2629.3	38022*	(000)'' → (062)'	+6
A' 2	2625.9	38071	(020)'' → (046)'	+6
A' 3	2620.4	38151	(001)'' → (027)'	+9
B' 1	2609.2	38314	{ (000)'' → (044)' (010)'' → (036)'	+10 -2
B' 2	2600.4	38444*	(020)'' → (074)'	-10
C' 1	2593.3	38549*	(001)'' → (055)'	+2
C' 2	2592.9	38555	{ (000)'' → (026)' (010)'' → (018)'	-15 -1
D' 1	2584.5	38681*	(000)'' → (072)'	+6
D' 2	2583.5	38697	(020)'' → (056)'	-17
D' 3	2577.6	38784	{ (000)'' → (008)' (001)'' → (037)'	-10 -5
E' 1	2569.1	38912*	{ (001)'' → (083)' (010)'' → (046)'	-2 +9
E' 2	2565.7	38964	{ (000)'' → (054)' (020)'' → (038)'	-11 -1
E' 3	2557.0	39097*	(020)'' → (084)'	+6
F' 1	2549.6	39210	{ (000)'' → (036)' (010)'' → (028)'	-7 +2
F' 2	2542.6	39318*	(000)'' → (082)'	+6
F' 3	2536.4	39414*	(001)'' → (047)'	-14
F' 4	2533.9	39453*	(000)'' → (018)'	-4
G'	2524.6	39598	{ (010)'' → (056)' (000)'' → (064)' (020)'' → (048)'	-6 +12 -6
H'	2508.5	39852	{ (000)'' → (046)' (001)'' → (075)' (010)'' → (038)'	-4 +13 -3
I' 1	2495.3	40063*	(001)'' → (057)'	-14
I' 2	2493.2	40097*	(000)'' → (028)'	-12
K'	2470.1	40472	(001)'' → (085)'	-4
L'	2459.7	40643	(020)'' → (086)'	0
M'	2455.3	40716	(001)'' → (067)'	+6
O'	2430.4	41133	(000)'' → (066)'	-5
P'	2417.0	41361	(001)'' → (077)'	-8

## ANALYSIS

The analysis of a band system due to a triatomic molecule is necessarily difficult. For a diatomic molecule, on account of a single vibrational frequency being involved in either state, the disposition of the bands in the spectrogram is rather regular, so that by a mere glance at the plate one can often pick out sequences or progressions with a great deal of certainty. Even here for molecules for which the intensity distribution of the band system arises out of a transition involving a considerable change in inter-nuclear distance and frequency of vibration, such a regularity of appearance is absent, thus rendering the analysis rather difficult. This difficulty is further enhanced in a triatomic molecule, where the same type of intensity distribution may occur for one or all of the frequencies concerned. Therefore, an attempt to seek a regularity in appearance is often misleading. On account of the large number of bands and on account of constant differences which may arise in altogether different ways, e.g., from a difference between two entirely different modes of vibrations of the same electronic state, it is nearly always possible to find a few bands with a constant difference of wave-numbers among the large number of bands observed. Such a frequency difference is therefore no definite indication of the magnitude of the difference of frequencies of the same mode of vibration in the initial and final state.

Another, and to our mind, preferable method of attack would be to select the  $(0, 0, 0)'' \rightarrow (0, 0, 0)'$  transition first and then try to find an analysis which obtains for the ground state such vibrational frequencies as are known already from considerations of Raman and infra-red spectra. An approximate selection of the vibrationless transition is rendered possible from two considerations. First, a comparison of the relative intensities of the  $(0, 0, 0)'' \rightarrow (0, 0, 0)'$  band and another one, involving a higher vibrational level of the ground state, should show that at higher temperatures the latter gains in relative intensity since then the number of molecules is increased in the excited vibrational levels of the ground state at the expense of the population in the  $(0, 0, 0)''$  level. Secondly, the  $(0, 0, 0)'' \rightarrow (0, 0, 0)'$  transition may be singled out approximately by considerations of the energy of excitation of the molecule. We know from a good deal of experimental evidence of the spectra of diatomic molecules as well as the absorption spectra of polyatomic molecules in the vapour or liquid state and in solution, that in a series of homologous molecules the energies of excitation together with the bond energies decrease with increasing mass of the molecule, e.g., in  $\text{SeO}_2$ , the origin of the band system is expected to be shifted slightly towards longer wave-

lengths than for  $\text{SO}_3$ . The latter being at  $3001\cdot9 \text{ \AA}$  the origin of the  $\text{SeO}_3$  bands might be expected to be slightly higher than this. On the other hand, assuming a similar relation for  $\text{SeO}$  and  $\text{SeO}_3$  as has been found for  $\text{SO}$  and  $\text{SO}_3$ , we may expect the origin of the  $\text{SeO}_3$  band system to be nearly at the same wave-length as that of  $\text{SeO}$ . A slight shift towards longer wave-length is, however, to be expected on account of the additional repulsive force between the two oxygen atoms, which tend slightly to weaken the bond energies. This force, however, should be considerably less than in  $\text{SO}_3$ , because of the increased internuclear distances due to the increased radius of the central atom. From the above figures of the origin of the  $\text{SeO}$  bands we obtain, therefore, a wave-length of about  $3020 \text{ \AA}$  as the lower limit.

The vibrational frequencies of the ground state of  $\text{SeO}_3$  are not known either from the infra-red or the Raman spectra. A comparison of the known frequencies of  $\text{SO}_3$  with those of the sulphates from Raman effect shows that the values from the sulphates give only a lower limit. In the same way, the known frequencies of the selenates give a lower limit for those of selenium dioxide. On the other hand, the frequencies of  $\text{SO}_3$  will give us an upper limit on account of the increased mass of  $\text{SeO}_3$ . The de-forming, the symmetric, and antisymmetric valence vibrations of  $\text{SO}_3$  have the values  $\omega_1 = 525$ ,  $\omega_2 = 1150$ , and  $\omega_3 = 1360 \text{ cm}^{-1}$  respectively. The Raman frequencies of the selenates\* are 875, 835, 415, and  $342 \text{ cm}^{-1}$  and the corresponding figures of  $\text{SeO}_3$  should be between these two sets.

With this preliminary knowledge about the approximate position of the origin and the approximate magnitude of the three fundamental frequencies, an attempt was made to analyse the bands observed in  $\text{SeO}_3$ . After several unsuccessful attempts with various possible values for the  $(0, 0, 0)'' \rightarrow (0, 0, 0)'$  band, it was ultimately found that starting from the band at  $32,560 \text{ cm}^{-1}$  as the origin, it was possible to assign the bands observed to transitions connected with the frequencies  $\omega'_2$ ,  $\omega''_2$ ,  $\omega'_3$ , and  $\omega''_3$ .

The analysis is displayed in Tables VA to VG. It will be seen that for the same vibrational spacings from different transitions different values are obtained which slightly disagree among themselves. This, we believe, is due to the fact that we do not measure the origin of the bands nor even their heads but the point of maximum intensity in each band, and the distance of this point from the true origin of the band cannot be supposed to remain constant in the different transitions in different modes of vibration. Such discrepancies are quite well known even in diatomic

\* Ganesan, ' Proc. Ind. Acad. Sci.,' vol. 1, p. 156 (1934).

TABLE VA—BANDS DUE TO THE SIMPLE TRANSITIONS  
 $(0, v_3, 0)'' \rightarrow (0, v_3 0)'$ 

$\cancel{(0v0)}''$	0	1	2
0	32560 (665)	31655 (677)	—
1	33225* (653)	32332 (631)	—
2	33878 (647)	32963* (666)	32083
3	34525* (634)	33629* (640)	—
4	35159 (664)	34269*	—
5	35823	—	—
6	—	—	34658 (650)
7	37109 (621)	—	35308 (628)
8	37730	—	35936*

TABLE VB—BANDS DUE TO THE SIMPLE TRANSITIONS  
 $(0, 0, v_3)'' \rightarrow (0, 0, v_3)'$ 

$\cancel{(00v)}''$	0	1	*
0	32560	—	
1	—	32171	
2	34136	—	
3	—	33733*	
4	35696	—	
5	—	35308	
6	37256	—	
7	—	36836	
8	38784	—	

TABLE VC—BANDS DUE TO THE CROSS TRANSITIONS  
 $(0, v_3, 0)'' \rightarrow (0, 0, v_3)'$ 

$\cancel{(00v)}''$	1	2
0	31655 (1582)	—
2	33237 (1563)	(905) 32332
4	34800 (1549)	—
6	36349 (1541)	35453 (1562)
8	37890 (875)	37015

TABLE VD—BANDS DUE TO COMPOSITE TRANSITIONS FROM GROUND STATE (0, 0, 0)''

		(0, 0, 0)'' → (0, v <sub>2</sub> , v <sub>3</sub> )'			
		2	4	6	8
v' <sub>2</sub>	v' <sub>3</sub>				
0		34136 (664)	35696 (675)	37256 (670)	38784 (669)
1		34800 (653)	36371* (644)	37926 (629)	39453* (644)
2		35453 (644)	37015 (657)	38555 (655)	40097
3		36097* (643)	37672 (642)	39210 (642)	—
4		36740* (649)	38314 (650)	39852	—
5		37389* (633)	38964 (634)	—	—
6		38022* (659)	39598	41133	—
7		38681* (637)	—	—	—
8	*	39318*	—	—	—

TABLE VE—BANDS DUE TO COMPOSITE TRANSITIONS FROM (0, 1, 0)''

		(0, 1, 0)'' → (0, v <sub>2</sub> , v <sub>3</sub> )'			
		2	4	6	8
v' <sub>2</sub>	v' <sub>3</sub>				
0		33237	34800 (653)	36349 (674)	37890 (665)
1		—	35453 (664)	37023 (649)	38555 (655)
2		34541* (644)	36117 (645)	37672 (642)	39210 (642)
3		35185 (638)	36762* (645)	38314 (650)	39852 (650)
4		35823 (668)	—	38964 (634)	—
5		36491 (624)	—	39598	—
6		37115	—	—	--

TABLE VF—BANDS DUE TO COMPOSITE TRANSITIONS FROM (0, 2, 0)''

		(0, 2, 0)'' → (0, v <sub>a</sub> , v <sub>b</sub> )'			
$\begin{array}{c} \diagup \\ v' \\ \diagdown \\ v_a \end{array}$		2	4	6	8
0	32332	—	35453 (664)	37015 (657)	
1	—	—	36117	37672	
2	—	35212 (642)	—	—	
3	34287* (658)	35854* (654)	37427 (644)	38964 (634)	
4	34945	36508* (656)	38071 (626)	39598	
5	—	37164* (636)	38697	—	
6	—	37800* (644)	—	—	
7	—	38444* (653)	—	—	
8	—	39097*	40643	—	

TABLE VG—BANDS DUE TO COMPOSITE TRANSITIONS FROM (0, 0, 1)''

		(0, 0, 1)'' → (0, v <sub>a</sub> , v <sub>b</sub> )'			
$\begin{array}{c} \diagup \\ v' \\ \diagdown \\ v_a \end{array}$		1	3	5	7
0	32171 (667)	33733 (661)	35308 (647)	36836 (665)	
1	32838 (636)	34394 (666)	35955 (651)	37501* (650)	
2	32474* (662)	35060* (636)	36606* (650)	38151 (633)	
3	34136	36696 (653)	37256 (645)	38784 (630)	
4	—	36349	37901* (648)	39414* (649)	
5	—	—	38549*	40063* (653)	
6	36053	—	—	40716 (645)	
7	—	—	39852 (620)	41361	
8	—	38912*	40472	—	

molecules, and we have to expect them to a greater degree here. The increased accuracy of measurement brings out this discrepancy, which by its existence we would rather take as an indication of the essential correctness and not otherwise of the analysis.

This choice of the origin is corroborated by intensity measurements at different temperatures. That the population of the higher vibrational levels will increase with higher temperature as mentioned above, is shown in Table VI which gives the relative intensities of a number of bands together with their classification, which follows from this choice of the origin of the band system.

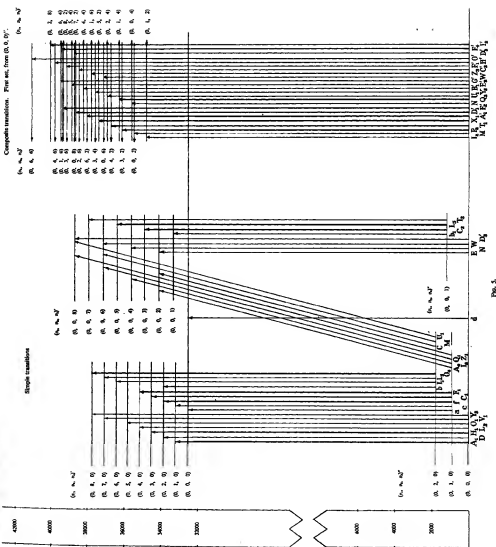
TABLE VI—RELATIVE INTENSITIES OF SOME BANDS AT DIFFERENT TEMPERATURES

Bands	Relative intensity at 290° C, 2 mm pressure	360° C, 6 mm pressure
$(0, 0, 0)'' \rightarrow (0, 0, 0)'$	1: 7 1	1: 20 0
$(0, 0, 1)'' \rightarrow (0, 0, 7)'$		
$(0, 0, 0)'' \rightarrow (0, 0, 0)'$	1: 6.9	1: 20 3
$(0, 0, 1)'' \rightarrow (0, 6, 1)'$		
$(0, 0, 0)'' \rightarrow (0, 0, 0)'$	1. 7.2	1. 20.9
$(0, 1, 0)'' \rightarrow (0, 1, 6)'$		
$(0, 0, 0)'' \rightarrow (0, 0, 0)'$	1: 5.9	1: 18.3
$(0, 2, 0)'' \rightarrow (0, 6, 0)'$		

Fig. 5 is a graphical representation of the simple transitions and one typical set of composite transitions, involved in the production of the bands of  $\text{SeO}_2$ , whose classification is also shown in Table V. As in  $\text{SO}_2$ , we again obtain only two frequencies, i.e.,  $\omega_1$  and  $\omega_2$ , in the ground state and the same two frequencies in the excited state. For each of these frequencies in the excited state, eight vibrational levels and in the normal state two and one respectively of each mode of vibration are obtained. Table VII gives the mean spacings of these levels as obtained by the analysis.

The spacings in the excited state are not regular, but we cannot definitely say that they are irregular. Some of the bands can be classified in more than one way, as shown in Table V, within the limits of accuracy of measurement and considering the fact that, far from measuring the origin of each band, we do not measure even its head but only the point of maximum intensity, which is affected by the overlap of neighbouring bands, we can generally say that the progressions are regular and there is no indication of pronounced perturbations.







## INTENSITY DISTRIBUTION

There are a few points of interest regarding the intensity distribution in the band system. Of course, it is not possible to come to very definite conclusions because in the first place the intensities estimated are relative and are deduced directly from the heights of the peaks in the microphotograms. Secondly, in estimating this intensity the influence of

TABLE VII—SPACINGS OF VIBRATIONAL LEVELS

Mode of vibration	Level	$\text{cm}^{-1}$	Difference
$\omega''_{\text{g}}$	0	0	—
	1	901	901
	2	1791	890
$\omega'_{\text{g}}$	0	0	—
	1	663	663
	2	1312	649
	3	1959	647
	4	2602	643
	5	3351	649
	6	3987	636
	7	4637	650
	8	5272	635
$\omega''_{\text{s}}$	0	0	—
	1	1189	1189
$\omega'_{\text{s}}$	0	0	—
	1	790	790
	2	1573	783
	3	2364	791
	4	3143	779
	5	3926	783
	6	4695	769
	7	5456	761
	8	6234	778

superposed bands cannot be eliminated. Thirdly, we take only the point of maximum intensity of each band and not its integrated value. Therefore considerations of intensity distribution which are offered here are only qualitative, but it is believed that even such a qualitative description of the intensity distribution will give us some idea as to the relative positions of the three dimensional potential troughs of the two electronic states.

In fig. 5 we have marked by thick lines those bands, which have got a

high intensity and possess at the same time only a single classification, which excludes to a certain extent the possibility of superposition. Also in Tables V to VG, such bands are marked by an asterisk. It will be seen that in the simple transitions  $\omega''_z \rightarrow \omega'_z$ , the strongest bands are those from  $v''_z = 0$  to  $v'_z = 1, 2$ , and 3, and from  $v''_z = 1$  to  $v'_z = 2, 3, 4$ . In the transitions of  $\omega''_z \rightarrow \omega'_z$ , no strong bands occur which have only one classification; but the general trend is that the stronger bands have a slightly larger  $\Delta\nu$  value. The transitions of  $\omega''_z \rightarrow \omega'_z$  are definitely weak. Among the composite transitions, those which arise from the unexcited vibrational state  $(0, 0, 0)''$  (Table VD) are strongest in combination with  $(0, v_z, 2)'$  and weaker in combination with  $(0, v_z, 4)'$ . The composite bands which arise from  $(0, 1, 0)''$  are also weak (Table VE). Among them the transitions  $(0, 1, 0)'' \rightarrow (0, v_z, 2)'$  are the most favoured, while  $(0, 1, 0)'' \rightarrow (0, v_z, 6)'$ , and  $(0, v_z, 8)'$  are rather fragmentary. Among the transitions from  $(0, 2, 0)''$  (Table VF), however, those which go to  $(0, v_z, 4)'$  are stronger than those to  $(0, v_z, 2)'$ , or  $(0, v_z, 6)'$ , or  $(0, v_z, 8)'$ . On the other hand, in transitions from  $(0, 0, 1)''$  (Table VG) the intensity appears to decrease in the following order:— $(0, 0, 1)'' \rightarrow (0, v_z, 5)' > (0, 0, 1)'' \rightarrow (0, v_z, 7)' > (0, 0, 1)'' \rightarrow (0, v_z, 3)'$ . The transition  $(0, 0, 1)'' \rightarrow (0, v_z, 1)'$  is definitely weak.

These peculiarities indicate that, if we consider the cross-section in such a plane of the three dimensional potential troughs, as gives us the Franck-Condon curves with respect to  $\omega''_z$  and  $\omega'_z$ , we can say that here we have the normal behaviour as in a diatomic molecule for which  $r'_0 > r''_0$  and  $\omega'_0 < \omega''_0$ ; particularly the turning points of the vibrational level  $v''_z = 0$  will be rather perpendicularly below those of  $v'_z = 2$  (the combinations with 1 and 3 occurring also) and those of  $v''_z = 1$  perpendicularly below those of  $v'_z = 3$  (the combinations with 2 and 4 occurring also). Similar considerations indicate that in a plane representing mainly a cross-section with respect to  $\omega_z$  we find again  $r'_0 > r''_0$  and  $\omega'_0 < \omega''_0$ , but the difference  $r'_0 - r''_0$  is enhanced as compared to that in the  $\omega_z$  plane. This view explains also the above peculiarities of intensity distribution among the composite transitions.

#### SELECTION RULES

Recently Herzberg and Teller\* have deduced selection rules for transitions between the vibrational levels of the electronic terms of polyatomic molecules from considerations of a generalized Franck-Condon principle and of the symmetry properties of a molecule. According to

\* Z. phys. Chem., B, vol. 21, p. 410 (1933).

this theory, transitions involving an antisymmetric frequency should occur, if at all, with low intensity and only if  $\Delta v_{(\text{antisym})}$  is an even number. This rule is rigorously valid so long as the change of internuclear distance between normal and excited state is not too big; in case  $r'_0 - r''_0$  is considerable also odd changes of  $v_{(\text{antisym})}$  may occur, the corresponding transitions leading with low intensity either to a forbidden electronic level or to one which involves a forbidden component of electric moment. The spectrum of selenium dioxide shows one peculiarity which is not accounted for by Herzberg and Teller's theory, *i.e.*, that the deforming vibration  $\omega_1$  does not occur at all. The deforming vibration is also a symmetric one and should therefore appear with greater intensity than the antisymmetric valence vibration  $\omega_3$ . Naturally we have tried to find progressions with distances of about 300 cm<sup>-1</sup> to 400 cm<sup>-1</sup>, which we believe will be the order of magnitude of the deforming vibrations. But an analysis on such a basis, appears to be impossible. In this respect the band system of SeO<sub>2</sub> resembles that of SO<sub>2</sub> completely, and therefore it seems likely that the complete absence of the deforming vibration rather indicates a principal deficiency of the theory. With respect to the selection rule for the antisymmetric mode of vibration  $\omega_3$ , however, the result of the analysis is an even better confirmation of Herzberg and Teller's theory than that of SO<sub>2</sub> bands. In sulphur dioxide the  $\Delta v_3$  selection rule for the antisymmetric mode of vibration was not rigorously valid since a few isolated transitions occurred involving an odd change in  $v_3$ . A glance at fig. 5 shows, however, that here, in the case of SeO<sub>2</sub>, the said selection rule is valid in its rigorous form. Thus, among the simple transitions there occur only those between  $v''_3 = 0$  to  $v'_3 = 0, 2, 4, 6$ , and 8, and from  $v''_3 = 1$  to  $v'_3 = 1, 3, 5$ , and 7. Among the composite bands we find transitions from (0,  $v_3, 0$ )'' to (0,  $v_3, v_3$ )' in which  $v''_3$  and  $v'_3$  have various odd and even values,  $v'_3$ , however, having only the even values 0, 2, 4, 6, and 8. Again transitions occur from (0, 0, 1)'' to the (0,  $v_3, v_3$ )' levels, in which again  $v'_3$  possess odd and even values,  $v'_3$ , however, is always odd. Whenever  $v''_3$  has an even value,  $v'_3$  has only even values, the odd ones being absent and whenever  $v''_3$  is odd,  $v'_3$  is odd too, the even values being absent. This is indeed a surprisingly good agreement with the theoretical predictions of Herzberg and Teller, and confirms our view that the present method of attack is indeed better suited for an analysis of the complicated band systems of polyatomic molecules.

## CHARACTER OF THE BONDS AND BOND ENERGY

As is well known, there exist two different conceptions as regards the theory of valency.\* It is possible to describe covalent linkage as due to an effect of single, non-localized electrons, and such a description assumes that the bonding effect due to the degeneracy of the nuclear fields predominates compared with that due to the degeneracy owing to the equality of the electrons. The other view holds, that such an approximation is sufficient only for the description of the term system and electronic configuration of the completed and undisturbed molecule, but is not a sufficient basis for the theory of valency. According to this conception, true covalent linkage in normal molecules of the first order (as distinct from genuine complex salts and organic ring structures) is due to the formation of pairs of electrons, one from each atom; the bonding effect is mainly due to the degeneracy owing to the equality of the electrons and the bonds are strongly localized between two atoms. Various arguments of theoretical and experimental nature have been recently put forward in support of the latter view, and the present work was originally undertaken also in the hope of contributing to the evidence which ultimately will bring about a decision between these two concepts.

TABLE VIII

Molecule	Origin	Ground state			Excited state			Remarks
SO	$v_0$ 39109	$\omega''_1$ —	$\omega''_2$ 1118	$\omega''_3$ —	$\omega'_1$ —	$\omega'_2$ 623	$\omega'_3$ —	—
SO <sub>2</sub>	—	525	1150	1360	—	—	—	Raman and infrared spectra
	33303	—	1128	1365	—	662	876	Band spectrum
SeO	33167	--	910	—	—	513	—	—
SeO <sub>2</sub>	32560	—	901	1189	—	663	790	—

From this point of view the most interesting result is that the vibrational frequencies of the normal and the excited states of SeO occur again almost unchanged in the symmetric valence vibration of SeO<sub>2</sub> in its normal and its excited states. Also the  $v_0$  of the diatomic and the corresponding triatomic molecules are similar. This is exactly the same behaviour as observed earlier in the case of SO and SO<sub>2</sub>, and we are now able to combine the results of both analyses in Table VIII (all figures in cm<sup>-1</sup>).

\* Cf. literature mentioned by Lessheim and Samuel, *loc. cit.*, and Samuel, 'Current Sci.', vol. 4, April (1936).

The values of  $\omega''$  and  $\omega'$  of the diatomic molecule agree, indeed, very well with those of  $\omega''_2$  and  $\omega'_2$  of the corresponding dioxide. The slight increase of the values has to be expected since the repulsive force between the two O atoms of the dioxide slightly weakens the bond energy and therefore probably slightly increases the internuclear distance. With SO<sub>2</sub> it was possible to show that the molecule undergoes a considerable change of form on excitation and cannot be considered any longer isosceles. That the agreement between the vibrational frequencies of the diatomic and the corresponding triatomic molecule is not quite so good in the excited state will be due to this change. The value of the anharmonic constant for the symmetric valence vibration of SeO<sub>2</sub> in the unexcited state is also very close to that of SeO. A definite value cannot be given because only three vibrational levels are observed. The value, however, obtained from these levels being 5.5 cm<sup>-1</sup>, in fair agreement with  $\omega_x = 6$  cm<sup>-1</sup> of SeO, we may conclude that the order of magnitude will be the same.

These considerations are corroborated by thermochemical measurements. The heat of formation of solid SeO<sub>2</sub> from solid Se + gaseous O<sub>2</sub> is 57.1 k cal/mol. The atomic heat of formation is obtained according to Born's cycle by adding to this value the energy of dissociation of O<sub>2</sub> (117 k cal/mol), the heat of sublimation of solid Se (24 k cal/gm atom), one-half of the energy of dissociation of Se<sub>2</sub> (the vapour consisting of Se<sub>2</sub> molecules until above 1000° C), and finally deducting the energy of sublimation of solid SeO<sub>2</sub>. The latter not being known we roughly measured the point of sublimation as about 470° C. According to Forcrand's rule,\* this corresponds to a value for the latent heat of vaporization of about 22 k cal. The dissociation energy of Se<sub>2</sub> is 2.63 volts = 59.3 k cal/mol obtained in exactly the same way as mentioned above for S<sub>2</sub> from the convergence point of the absorption spectrum of Se<sub>2</sub> (30874 cm<sup>-1</sup> = 3.81 volts) and the measured value of the <sup>1</sup>D term of Se (1.18 volts).† From these figures we obtain 205 k cal/mol as the atomic heat of formation of SeO<sub>2</sub> or 102.5 k cal/mol = 4.45 volts for each Se - O double bond. This value is as near to the dissociation energy of the SeO molecule, measured spectroscopically to 4.2 volts, as the estimated energy of sublimation of SeO<sub>2</sub> permits. This result is not surprising, since it has been shown recently‡ from the absorption spectra of the vapours of the chlorides and oxychlorides of sulphur, that the bond energy of the

\* Forcrand, 'C.R. Acad. Sci. Paris,' vol. 133, pp. 268, 513 (1901).

† Rao and Krishnamurti, 'Proc. Roy. Soc.,' A, vol. 145, p. 694 (1934).

‡ Asundi and Samuel, 'Proc. phys. Soc. Lond.,' vol. 48, p. 28 (1936).

S—Cl, the S = 0 and the S=S bond remains practically unchanged in such widely different molecules as S<sub>2</sub>, SO, SCl<sub>2</sub>, SOCl<sub>2</sub>, S<sub>2</sub>Cl<sub>2</sub>, and SO<sub>2</sub>.

The above thermochemical calculations also show that the bond energy of the Se = O bond remains the same in the molecules SeO and SeO<sub>2</sub>, and we may therefore take this as characteristic for molecules formed by atoms of the sixth group as long as they remain di- or tetravalent, *i.e.*, as long as the  $s^2$  group of electrons remains on atomic orbitals. The linkage is brought about, then, by the four *p*-electrons only and the ground state of the triatomic molecule arises probably directly from the ground state of the diatomic one.

To our mind these spectroscopical results, supported by thermochemical considerations, indicate clearly a strong localization of the bonds. This conclusion could not be drawn with any certainty, if we would consider the corresponding vibrations of the unexcited molecules only. Indeed, the fact that empirical rules, like Morse's  $\omega r^3 = \text{constant}$  for a large group of diatomic molecules exist in band spectroscopy shows already that  $\omega$  is more sensitive to the moment of inertia and less sensitive to the bond energy. We know, indeed, that  $\omega'$  is almost the same for the radical OH and the OH<sup>-</sup> ion with different electronic configurations or for N<sub>2</sub> and CO in spite of the fact that the energy dissociation of N<sub>2</sub> is much smaller than that of CO.

Therefore, conclusions on the number of valencies or the nearly related bond energies based on Raman and infra-red spectra alone, should be drawn with great caution only, as the factor of anharmonicity is of equal importance. In our case, however, there is correspondence between the harmonic frequencies not only of the ground state but also of the excited state and furthermore between the energies of excitation and for the ground state; even between the anharmonic constants. Even after the excitation of the molecule, *i.e.*, after one electron is transferred to a higher quantum group, the two  $\omega'$  values remain almost equal. Finally, the determination of the energy of dissociation of SeO makes it possible to compare it with the bond energies of SeO<sub>2</sub>. This shows, indeed, that only one of the two double bonds between Se and O or between S and O seems to take part in the process of excitation, that only one of the corresponding internuclear distances is increased in this process, and that the energy of excitation seems to be accumulated in only one of the two double bonds. The two double bonds seem to act quite independently of each other. Described from the view point of the concept of the single-electron-bond interpretation of the method of molecular orbitals, the linkage of two atoms of the sixth group is characterized (Herzberg, Mulliken) by eight electrons, forming three pairs of bonding and one pair of anti-bonding electrons, thus giving two valencies. The same number of

valencies is obtained in the electron pair bond interpretation of the method of molecular orbitals in quite a different way. Here only those pairs are counted whose electrons originate in different atoms and therefore two pairs are obtained irrespective of the presence of the two other pairs, one of which originates in our case from Se atoms only and the other from the O atom alone (Hund's method of counting). That pair of *p*-electrons which does not take part in the linkage of SeO, because both electrons are originally Se-electrons, will form again two bonding pairs together with two electrons of the second O atom in SeO<sub>2</sub>, and therefore this theory describes indeed the linkage of the Se = O bond in SeO and SeO<sub>2</sub> in a completely identical manner. In the single-electron bond interpretation, however, the linkage of SeO<sub>2</sub> is entirely different from that of SeO. Firstly, the antibonding electrons of SeO most probably become bonding electrons in SeO<sub>2</sub> and the linkage between each of the O atoms and the central atom is now made up of three bonding pairs and resembles the linkage of CO, which is indeed described as a triple bond in this theory. This distinction between the two SeO bonds in SeO<sub>2</sub> is, however, already an approach to the conception of localized bonds, and we shall not consider this as an argument. But if all non-localized electrons on molecular orbitals contribute towards the linkage, the bond of SeO is brought about by eight electrons in the field of two nuclei, and that of SeO<sub>2</sub> by twelve electrons in the field of three nuclei. These are two completely different cases. Why the bond energies, the energy of excitation, the anharmonic constant of the ground states, and the frequency of the symmetric valence vibration remain almost unchanged in SeO and SeO<sub>2</sub>, cannot, therefore, be explained on the basis of non-localized bonds without great difficulties, whereas it is almost the natural outcome of the conception of localized bonds.

#### SUMMARY

The emission spectrum of SeO and the absorption spectrum of SeO<sub>2</sub> are analysed. The energy of excitation and the energy of the Se = O bond are almost identical in SeO and SeO<sub>2</sub>, and the vibrational frequencies of SeO have almost the same values as the frequencies of the symmetric valence vibration of SeO<sub>2</sub>, both in the normal and the excited state. The same is true about the corresponding anharmonic constants of the two unexcited molecules; that of excited SeO could not be measured.

The results indicate strong localization of the two Se = O bonds in SeO<sub>2</sub>.

The analysis of the band system of SeO<sub>2</sub> is in complete agreement with Herzberg and Teller's theoretical selection rule for  $\Delta\nu_{\text{antib}}^{\text{(sym)}}$  for polyatomic molecules.

## A New Method for Investigating Conduction Phenomena in Semi-Conductors

By J. A. V. FAIRBROTHER, Ph.D., F.Inst.P., Research Laboratory of the British Thomson-Houston Co., Ltd., Rugby

(Communicated by F. W. Carter, F.R.S.—Received 28 April, 1936)

[PLATE 2]

Langmuir\* has shown that in low pressure gas discharges, that part of the discharge usually referred to as the positive column consists of equal numbers of positive ions and electrons per unit volume, and to this portion he has given the name "plasma". He has shown, moreover, that the current passing between cathode and anode is proportional only to the difference between the number of electrons passing in the direction of cathode to anode across 1 sq cm placed normally to the tube axis and the number of electrons passing across the same area in the opposite direction. The random electron current density is usually many times the anode current density. The electrons in the plasma have been shown by Langmuir to have a Maxwellian distribution of velocities and that they can therefore have ascribed to them a mean energy,  $V_e$ , corresponding to a temperature  $T$  where, as in the kinetic theory of gases

$$V_e = \frac{3}{2} kT \quad (1)$$

or

$$T = \frac{2}{3} \times \frac{1.59 \times 10^{-20}}{1.37 \times 10^{-16}} \times 10^6 \text{ Kelvin degrees per volt}$$

$$= 7730^\circ \text{ K per volt.}$$

In low pressure gas discharges  $T$  varies from  $5000^\circ$  K to  $30,000^\circ$  K or the mean energy of electrons expressed in electron volts varies from about 0.5 to 4 volts.

In a field-free plasma of infinite extent the positive ions acquire a Maxwellian velocity distribution. The ratio of random positive ion current density to random electron current density is then equal to the square root of the ratio of the electronic to the ionic mass. For mercury

\* 'Gen. Elect. Rev.', vol. 26, p. 731 (1923). Langmuir and Mott-Smith, jr., *ibid.*, vol. 27, pp. 449, 538, 616, 762, 810 (1924). Tonks and Langmuir, 'Phys. Rev.', vol. 34, p. 876 (1929).

vapour  $\sqrt{(m_e/m_{H_2})} = 1/608$ . In practice the positives do not have a chance to acquire a Maxwellian distribution of velocities by energy exchanges and  $I_s/I_e$  is more nearly equal to 400 than 600. Their velocities are mainly acquired as a result of the fields existing in the plasma.

If a plane probe, for instance, a mica-backed metal disk, is placed in the plasma and the probe current-probe voltage characteristic is plotted, voltages being measured with respect to anode potential, the resultant curve may be divided into three parts. Starting with the probe highly negative with respect to the anode and decreasing this voltage difference by making the probe more positive, a straight line is obtained below and parallel to the voltage axis. This current is the positive ion current density in the arc multiplied by the probe area. As Langmuir has shown, there is built up at the surface of the probe a positive ion sheath of such a thickness that the space charge limited current carried across the sheath under the voltage difference between the probe surface and the sheath outer edge is equal to the number of ions arriving at this edge on account of their proper motions in the plasma. The positive ion current per square centimetre across the sheath is related to its thickness and the voltage drop across it by the relation

$$I = 2 \cdot 33 \times 10^{-6} \frac{V_r}{d^2} \sqrt{\frac{m_e}{m_{H_2}}} . \quad (2)$$

The outer edge of the sheath is at a small negative potential with respect to the plasma (1 or 2 volts), sufficient to repel the majority of the electrons which likewise reach the sheath on account of their proper motions. The characteristics of the type of discharge used by the author in the work about to be described is shown in fig. 1, in which the line AB is an extrapolation of the straight portion of the positive ion current-voltage curve obtained at high negative voltages.

At about -40 volts, not shown in the figure, the curve begins to bend sharply upwards, and it is at this point that the fastest electrons in the plasma are no longer prevented from reaching the probe. As the negative voltage is still further decreased the electron current more than counteracts the positive ion current to it. This is the part CD. It is to be noted that the electron temperature at the surface of the probe and hence the mean velocity is still the same as in the plasma. The effect of the negative voltage on the probe, measured with respect to the plasma, is simply to decrease the electron density at its surface in accordance with the Boltzmann equation

$$\frac{n_{\text{probe}}}{n_0} = e^{-\frac{V_r}{kT}} . \quad (3)$$

The curve CD rises so steeply that its complete course is represented by the curve EF in which the current is represented on a scale reduced a thousand fold. When the potential of the probe rises to a value such that

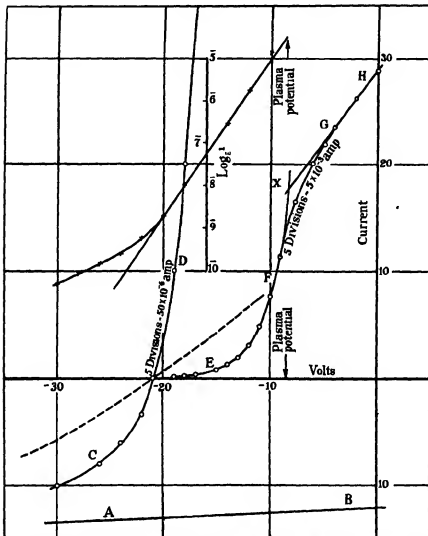


FIG. 1—Cylindrical probe characteristic in a mercury vapour arc. Vapour pressure corresponding to room temperature of 21° C. Cylindrical tungsten probe: length 2.55 cm, diameter 0.016 inch. Arc current 0.45 amp; arc voltage 23 volts; electron temperature 32,000° K.

electrons are no longer repelled but are accelerated towards it, there tends to be built up an electron sheath around it. Were it not for factors of which no account is taken in the elementary theory, such as ionization due

to collision in the sheath and of an alteration in the condition of the plasma itself due to the electron current drain upon it the curve for a plane probe would again become horizontal to the voltage axis.

In practice the curve EF becomes less steep and for a cylindrical probe is represented by the portion GH, fig. 1. The point of intersection X of this straight portion GH with the extrapolated portion EF according to the Boltzmann relation gives approximately the plasma potential. The plasma potential is about 8.5 volts negative with respect to the anode. The potential of -21 volts at the zero current point is the potential taken up by an insulating surface placed in the plasma, the glass walls of the discharge vessel, for example, and is about 2 volts above cathode potential.

Consider now Boltzmann's equation (3), we have, by taking the logarithms of both sides

$$\log n_{\text{probe}} - \log n_{\text{plasma}} = -\frac{e}{kT} V.$$

Since  $n_{\text{plasma}}$  is a constant and  $n_{\text{probe}}$  is proportional to the probe current

$$\log i - \text{const.} = -\frac{e}{kT} V,$$

or the slope  $e/kT$  of the  $\log i$  voltage curve enables the electron temperature to be determined since  $e/k$  is known. From the slope of the  $\log i$  voltage curve shown in fig. 1 the electron temperature is calculated to be about 32,000° K. The theory as applied to plane probes can only be applied to the use of a cylindrical probe, such as was used in obtaining the data shown in fig. 1, with strict limitations. With cylindrical probes the probe current is dependent upon the sheath thickness which in turn depends upon probe voltage. On this account the positive ion current part of the curve, of which AB is the prolongation, is not horizontal, neither is it to be expected that GH will become horizontal. For the range EF it is permissible for obtaining a rough estimation of the electron temperature to neglect the dependence of probe current on sheath thickness. The fact that the slope of the logarithmic plot decreases at the higher negative voltages is an effect already observed and reported upon by Kovalenko, Rozansky, and Sena\* and is due possibly to the inadmissibility of obtaining the positive ion currents by extrapolation. Uncertainty of the value of the positive ion current over the range EF does not appreciably affect the logarithmic plot since its value, although uncertain, is so small compared with the electron currents to the probe.

\* Tech. Phys. U.S.S.R., vol. 1, p. 9 (1934).

The electron current density cannot be deduced with any accuracy from the measurements shown in fig. 1 on account of the uncertainty in the height of the point X. A straightforward extrapolation of the fairly straight portion GH allows a fair estimate to be made of the plasma potential, but this is inadmissible for determining the electron current density at plasma potential. Nevertheless, taking the ordinate of the point X in the figure as a very rough measure of the electron current, this is about  $18 \times 10^{-8}$  amps or about 35 mA/sq cm. The diameter of the tube used for obtaining these characteristics was about 5 cm, and the anode current 450 mA or 23 mA/sq cm. The random current density is thus of the same order as the anode current density.

#### VOLTAGE CURRENT CHARACTERISTICS OF PROBES COATED WITH A LAYER OF INSULATING MATERIAL

If a cylindrical metal probe or wire coated with insulating material is inserted into the plasma its surface will take up a potential such that no current will flow to it regardless of the potential of the metal base. If the insulating coating is partly conducting, its outer face will take up a potential with respect to the plasma such that it can draw from it a current equal to the conduction current which is made to flow on account of the potential difference between the inner and outer surface of the material. If the wire is made negative with respect to the zero current voltage, electrons will flow from core wire outwards, and the outer surface will assume a sufficiently negative potential to draw from the plasma an equal number of positive ions. If the core wire is made positive, electrons will flow from the outer surface to the inner, if the conduction across the insulating material is electronic and not electrolytic. Assuming the outer diameter of the coated probe to be 0.016 inch and the current voltage characteristic of the insulating material to be ohmic a current voltage curve such as that shown by the broken line of fig. 1 is obtained. For any given current the potential of the outer surface of the insulating material must be equal to the potential of a bare metal probe taking the same current. For any given current, therefore, the voltage drop across the insulating coating is given by the horizontal separation of the broken curve and curve CD. It is in this manner that the dependence of electrical conductivity of alumina on temperature is investigated in this paper. For high positive or negative probe core voltages and for small probe currents the curve CD can be regarded as a vertical line without introducing any significant error into the results. In this case if the insulating coating has an ohmic resistance the broken curve becomes a straight

line through the zero current point. The temperature dependence of electrical conductivity was measured by heating the core wire electrically and the temperatures deduced from the known temperature coefficient of resistance of the core wire.\*

#### DESCRIPTION OF PROBE AND APPARATUS

The probe used was a tungsten wire 0·010 inch diameter, fig. 2, bent into the form of a U of height 38 mm and 5 mm width. This was welded vertically to support leads 1 and 2, passing through a glass stem 7. A potential lead 3 was welded to one limb of the U, 16 mm below the tip. This position was sufficiently far from the extremities to be out of the region of end cooling when the loop was heated by the passage of a current. The whole was enclosed in a nickel cylinder 4, open at the base and held in position by means of the dummy lead 8. The cylinder was closed at its top end by means of a lid pierced with two square holes 1·5 mm square placed on a diameter with their centres distant 5 mm, so that the limbs of the probe passed through them without touching the sides.

Before enclosing the probe in the nickel case, it was sprayed by means of a de Vilbiss spray gun with a suspension of pure alumina powder in a solution of cellulose nitrate in amyl acetate. After a layer about 0·002–0·003 inches thick had been formed the probe was placed in an atmosphere of hydrogen and raised to about 1300° C for 5 minutes. The effect of this process was to drive off the volatile constituents of the spraying solution and gently to sinter the alumina. Subsequent inspection under the microscope revealed a snow-like surface of alumina crystals completely free from cracks. It was then sprayed again and this time raised to 1500° C for 5 minutes in a hydrogen atmosphere. After this treatment the alumina was in the form of a hard, solid, continuous coating devoid of cracks, and in a state such that its diameter could no longer be reduced appreciably by glowing at the temperature to be used in the experiments. Such porosity as it possessed

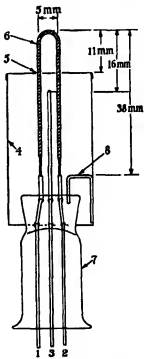


FIG. 2—Scale drawing of probe structure.

\* Jones and Langmuir, 'Gen. Elect. Rev.', pp. 310, 354, 408 (1927).

was due to the manner in which the individual crystals were packed together. The diameter of the coated probe was 0·020 inch. The thickness of the alumina was thus 0·005 inch.

The nickel case was then fixed in position. Its function was to limit the effective area of the coated probe and to prevent the plasma reaching any of the supporting wires. Throughout the experiments this shield was allowed to float so that it assumed the same potential with respect to the plasma as the glass walls. The effect was therefore the same as if the effective probe length shown in fig. 2 as 11 mm high stood out from the glass wall.

The probe was heated when required by means of a battery connected to leads 1 and 2. For a constant heating current the voltage drop was measured between leads 3 and 2, and leads 3 and 1. The difference gave the voltage drop across that portion of the U of height 16 mm, from which its resistance was deduced. The calculated resistance of the part 16 mm high (developed length 34·5 mm) at room temperature was 0·0385 ohms and that measured was 0·038 ohms. As the specific resistance of tungsten is changed by impurity contents, such as carbon, check tests were made with the object of determining if any change was produced in the cold resistance of the alumina coated tungsten probe after sintering on the alumina. As no change was observed, the resistance of the wire was used throughout the experiments as a measure of its temperature.

The alumina used was taken from a batch prepared according to the processes described by Navias.\* It was a dense white powder forming with cellulose nitrate and amyl acetate solution a smooth paste completely free from lumps. According to Navias, chemically pure alumina is fired in a muffle furnace at 1000° C to remove water vapour and carbon dioxide and is then fired in a hydrogen furnace at 1600° C. At this temperature silica and alkali are vapourized out, and the resultant charge after crushing and grinding is a dense white powder of a high degree of purity.

Throughout this work the temperature of the coating material was taken to be that of the tungsten core, since calculations of the temperature drop due to thermal conductivity across the coating, employing the formula

$$\theta_1 - \theta_s = \frac{Q}{2\pi K 4 \cdot 2} \log \frac{r_1}{r_s},$$

showed this to be small. Q is the watts liberated per centimetre length of the probe,  $\theta_1$ ,  $\theta_s$ , and  $r_1$ ,  $r_s$  being the temperatures and radii of the

\* 'J. Amer. Ceram. Soc.', vol. 15, p. 234 (1931).

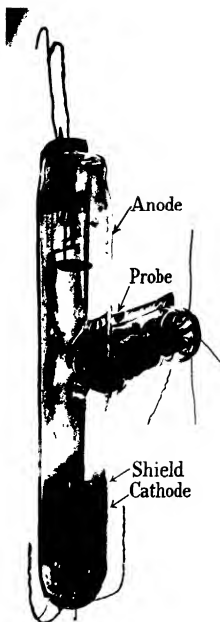


FIG. 3—Mercury vapour discharge tube used, showing probe.

(Facing p. 56)



inner and outer insulator surfaces respectively. Assuming a value for K equal to 0.004 cal/degree/ccm, the temperature drop at 1500° C is about 20° C.

The tube used in these measurements is shown in fig. 3, Plate 2, in which the cathode is a heated barium oxide coated nickel strip. A shield is mounted above the cathode in order to prevent evaporated active material from settling on the probe. This tube, into which a small quantity of mercury was introduced, was given a thorough bake out, all metal parts being outgassed by high frequency and the probe by raising it to incandescence. The tube was sealed off from the pumps, shielded from draughts so as to avoid variations due to changes in mercury vapour pressure, and was then ready for use.

#### MEASUREMENTS BETWEEN 0 AND 1000° C—ELECTRON DIFFUSION CURRENTS THROUGH ALUMINA

The first group of curves taken were numbers, 4, 5, and 6, fig. 4, for temperatures 1250° K, 920° K, and 300° K, and for an anode current of 0.15 amps. No. 6 is the volt-ampere characteristic of the probe for zero heating current. Except for low voltages near the zero current point, the current in the positive quadrant, that is, for the condition in which electrons pass from the outer to the inner surface of the probe, is about six times greater than that in the negative quadrant. The parts of the curves lying in the negative quadrant are drawn to two scales. The full line group is on the same scale as those in the positive quadrant. The broken line group represents the same curves on a current scale magnified five times.

For convenience, when electrons flow through the insulator from the outer surface to the inner, this is referred to as an electron flow from plasma to probe. The currents involved in these measurements are so small compared with those that would flow to a bare metal probe of the same size that the characteristic of such a probe can be drawn as a vertical line through the zero current point without introducing appreciable error into the results. If the curves were true conduction characteristics of the insulator they should be independent of the electron density in the plasma. To test this the set of curves 7, 8, and 9, were taken corresponding to temperatures 300° K, 1200° K, 1320° K for an anode current of 0.30 amps, that is, double the electron current density. In the negative quadrant curves 6 and 7 for a cold probe are almost coincident, whilst in the positive quadrant curve 7 is almost exactly twice as high as curve 6 for any voltage.

The part of the curve in the negative quadrant represents the case in which positive ions are arriving at the insulator surface at a greater rate than electrons, and these have to be neutralized by an electron current from the core to the surface. In the positive quadrant electrons are arriving in greater numbers and pass through the coating to the core. In view of the fact that the number passing through is proportional to the electron density, it seems to the author that the phenomenon presented here is that of the diffusion of electrons through the pores of the material or along the crystal faces. At the highest positive probe voltage, namely 150 volts, the electron current for curve 7 is about  $14 \times 10^{-6}$  amps or  $36 \times 10^{-6}$  amps per sq cm. For an all-metal probe of the same dimensions the total electron current to the probe at the zero current point is equal to the positive ion current. This was about  $80 \times 10^{-6}$  amps. Neglecting the slight conduction current, the outer surface of the probe takes up a potential slightly positive to the zero current point such that it can draw from the plasma an electron current exceeding in magnitude the positive ion current by the amount of the electron transmission current. The ratio of the number of electrons diffusing through the insulating coating to the number impinging upon it is thus about 14/94 or 15%. The alumina coating is composed of small crystals, its structure being not unlike that of a pile of shot. It seems, therefore, that the diffusing electrons are those plasma electrons which shoot through the surface spaces between the crystals and are drawn through the interstices under the potential gradient along them. The postulate of electron diffusion is supported by the fact that the current tends to saturate. If the field is sufficient to drag across all the electrons which enter, the current is no longer determined by the field but by the plasma density. Careful measurements show that for voltages very near the zero current point the current is proportional to a power of the voltage greater than unity, that is, it is concave upwards, a shape to be expected if the current within this range is limited by space charge within the holes.

The magnitude of the currents observed is seen by inspection of fig. 4 to be independent of temperature, a fact also to be expected if the effects observed are due to electron diffusion.

More information could have been gained about this phenomenon by measuring the electron diffusion current at higher plasma densities. It was not possible to do this on account of the limited current which the cathode of the tube could supply.

Fig. 5 gives the shape of curve 7 (fig. 4) for 20 volts on either side of the zero current point. The thickness of the insulating coating is 0.0125 cm, hence at 10 volts the field across the layer is about 800 volts per cm. The

real conduction currents are represented by those portions of the curves in the negative quadrant.

This result throws some light on results recently obtained by Reimann and Treloar\* on the electrical conductivity of a mixture of barium and

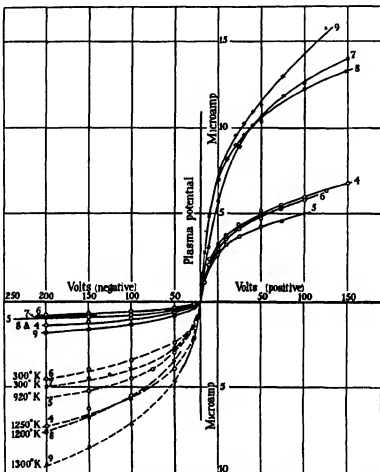


FIG. 4.—Electron diffusion currents through alumina.  $\times$  Anode current 0.300 amp;  $\circ$  anode current 0.150 amp. The same curves on a current scale five times larger are drawn in dotted lines.

strontium oxides at low temperatures. These authors obtained distinct types of current voltage curves. At high temperatures the current voltage curves were linear at low voltages, whilst at higher voltages they bent over towards the voltage axis. At low temperatures the slope of the

\* Phil. Mag., vol. 12, p. 1073 (1931).

current voltage curves increased with increase in voltage. In this paper the shapes of even the lowest temperature curves were of the type observed by Reimann and Treloar at high temperatures, except that the linearity of the part at the origin was not so marked. It seems probable, however, that the low temperature curves of Reimann and Treloar for voltages above a few volts represent electron diffusion currents through the oxide. The deductions of the values of the electrical conductivity made by these authors are not necessarily affected as for this purpose they measure the current flowing at 0.1 volts. Assuming the thickness of their oxide layer to be 0.0125 cm, 0.1 volts corresponds to a field strength of 8 volts

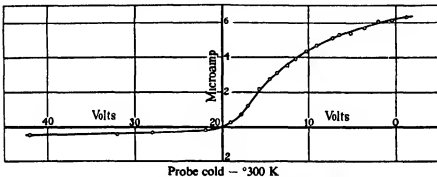


FIG. 5—Electron diffusion current versus voltage.

per cm at which value in these experiments the electron diffusion current is very small.

The phenomenon of electron diffusion observed in this work lends some support to the theory advanced by Lowry\* to explain the mechanism of the thermionic emission from oxide coated filaments. This author suggests that "the source of emission is on the composite layer formed by occlusion of alkaline earth metal on the surface of the core and that the electrons emitted diffuse through the interstices in the oxide coating into the vacuum space". On this theory Lowry states that "non-saturation may be due to a pseudo-space charge formed by occlusion of electrons on the surface of the coating particles". The shape of the curve in fig. 5 is certainly remarkably similar to the anode voltage-current characteristic obtained from an oxide coated cathode. If proportionality between electron diffusion current and the electron current density persists at current densities of the order of 100 milliamps per sq cm, then Lowry's explanation of electron emission from barium oxide coated cathodes would appear to be strongly substantiated. These suggestions could be

\* Phys. Rev., vol. 35, p. 1367 (1930).

tested by taking measurements on a cold barium-strontium oxide coated probe in a discharge of high random electron current density.

Reimann and Treloar in criticizing Lowry's theory of electron diffusion consider as evidence against it the fact that the "conduction" current-voltage curves measured by them show a marked variation with temperature. They argue that "one would naturally expect a current carried by electrons diffusing through the spaces between the crystals of a coating to depend as little on the temperature as do ordinary space charge limited thermionic currents". Now in the author's experiments the electron diffusion current is indeed seen to be independent of temperature, but it is proportional to the electron current density in the plasma. The same results are to be expected if the plasma is replaced by a bariated surface. The very close proportionality between the thermionic and "conduction" currents observed by Reimann and Treloar are thus explained if their conduction currents are electron diffusion currents, since these and the thermionic currents are proportional to the state of activation of the bariated nickel surface.

#### VARIATION OF ELECTRICAL CONDUCTIVITY AT THE ZERO CURRENT POINT WITH TEMPERATURE FROM 300° K TO 1800° K

The voltage applied to the probe was adjusted by means of a potentiometer until the current flowing to it was zero. This voltage was then made several tenths of a volt more negative and the electron current noted. By making the voltage more negative the electron flow was from the inner to the outer surface and errors due to electron diffusion through the coating, such as might occur if the probe were made more positive, were avoided. The probe was heated by means of a battery and the conduction current measured at points within the range 300° K to 1800° K. There was a voltage drop along the probe due to the heating current which at the highest temperature amounted to as much as 1.8 volts. On this account the probe heating battery was reversed and the conduction current measured again for a small increase in the negative potential of the probe. The mean of the readings gave the conduction current for an equipotential probe at various temperatures.

According to A. H. Wilson's theory\* of electronic semi-conductors, electrons only become available for conduction when they occupy certain allowed energy bands. For insulators at room temperatures the electrons occupy levels in a low energy band, the highest energy level of which is

\* 'Proc. Roy. Soc.,' A, vol. 133, p. 458 (1931); vol. 134, p. 277 (1931); vol. 136, p. 487 (1932).

separated from the lowest of the first allowed band by the width of a forbidden band. Those electrons which by thermal excitation are raised into the first allowed band across the gap function as conduction electrons. On this theory the conductivity varies with the temperature according to the formula

$$\sigma = \sigma_0 e^{-\frac{\theta_u}{T}}.$$

where  $\sigma_0$  is a constant. If  $W_2 - W_1$  is the energy difference between the lowest level of the unoccupied allowed band and the highest filled level of the occupied band then  $\theta_u = \frac{W_0 - W_1}{k}$  where for very small values of T,

$$W_0 = \frac{1}{2}(W_1 + W_2)$$

and

$$\sigma = \sigma_0 e^{-\frac{W_1 - W_0}{2kT}}.$$

This formula is valid only for  $T \ll \theta_u$ .

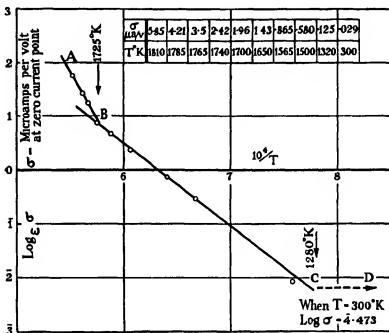
The curve obtained by plotting  $\log \sigma$ , where  $\sigma$  is measured in microamperes per volt, against the inverse of the temperature between the range 300° K to 1800° K is shown in fig. 6.

The curve is divided into three sections AB, BC, and CD. The experiments did not determine the actual shape of the part CD. Since the next point on the curve at 300° K is  $10^4/T = 33.3$ , and  $\log \sigma = 4.473$ , it is obvious that between 300° K and 1200° K the curve is practically horizontal with a slope which makes the energy difference  $\frac{1}{2}(W_2 - W_1)$  at the most a few tenths, and probably only a few hundredths of an electron volt. In this range T is no longer much less than  $\theta_u$  and the Wilson formula does not apply. Over this region, and compared with the magnitude of the increase at higher temperatures, the conduction remained practically independent of temperature.

From about 1280° to 1725° K, the section CD, the value of  $W_2 - W_1$  deduced from the slope is 2.9 e-volts. Above 1725° K the slope of the curve increases abruptly, and for this portion the value of  $W_2 - W_1$  is 6.6 e-volts. The change is marked by a decrease in the rate of increase of conductivity with temperature. It is significant that the change takes place at 1725° K or about 1450° C. This is the sintering temperature for alumina, a point at which the crystals in a hitherto loosely bound mass not yet raised above 1450° C unite with considerable shrinkage, to form a rigid body. This change is a reversible one so that the parts BC, CD are again obtained when the temperature is reduced.

**VOLTAGE-CURRENT CURVES FOR AVERAGE FIELD STRENGTHS OF  
0 TO 20,000 VOLTS PER CM**

A set of voltage current curves at different temperatures for an arc current of 0.15 amps is shown in fig. 7. Since for any voltage the conduction increases almost exponentially with increase of temperature the curves shown have each been plotted to a different scale. The curves represent the conduction currents obtained for the range in which the



A — B ( $W_2 - W_1$ ) = 6.6 e-volts, B — C ( $W_2 - W_1$ ) = 2.9 e-volts.

FIG. 6—Logarithm of the conductivity plotted against the inverse of the absolute temperature. A — B ( $W_2 - W_1$ ) = 6.6 e-volts; B — C ( $W_2 - W_1$ ) = 2.9 e-volts.

probe voltage is decreased from a value which is negative with respect to the plasma, that is, when electrons flow from the probe wire through the oxide coating to the plasma, to a value which is positive. When the probe is positive electrons flow through the oxide from the plasma. The parts of the curves lying in the positive right-hand quadrant are deduced from those shown in the positive left-hand quadrant by correcting for the electron diffusion current. This was effected on the assumption that the electron diffusion current is proportional to the number of electrons arriving at the surface of the probe.

Suppose the total number of electrons arriving is  $N$ , the diffusion current passing through at a given voltage is  $\alpha N$ , where  $\alpha$  is a constant.

If the conduction current is  $c$  and the positive ion current  $p$ , then  $I$ , the current measured, is

$$I = c + \alpha N,$$

and since

$$N = c + p + \alpha N$$

we have

$$c = I(1 - \alpha) - \alpha p$$

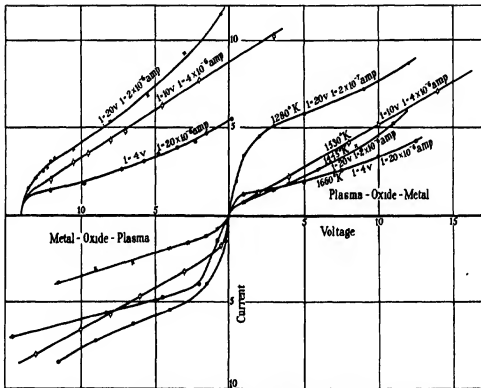


FIG. 7—Current voltage characteristics for a range of temperatures, corrected for electron diffusion currents.

$\alpha$  was 0.15, and  $p$  the positive ion current to the probe was about  $80 \times 10^{-6}$  amps. Thus the conduction current  $c$  can be deduced from the measured current  $I$ .

The shape of these curves is the same as that to be expected from Wilson's theory of electronic semi-conductors. The slope of the curves becomes rapidly smaller, a few volts from the origin. For a considerable range of voltage they are almost straight after which the slope increases

again. The final increase in slope is not very marked in fig. 7, but the experiments indicate that for higher voltages than those shown the slope increases rapidly. For low temperatures the curves are symmetrical about the origin, and for higher temperatures the conduction is greater in the negative quadrant, where the electron flow is in the direction metal—oxide—plasma. The linear portions of each curve are parallel. On any one curve the voltage corresponding to a given current is the sum of the barrier voltage between metal core and oxide, the voltage drop across the oxide and the barrier voltage from just inside the oxide to its surface. It has not been attempted in these experiments to separate the three voltage components. It is deduced, however, that if the greater portion of the voltage measured is that dropped across the oxide, then the specific resistance of the alumina used is some thousand times the normally accepted values. If the normally accepted values for alumina are correct then the curves shown in fig. 7 represent the sum of the voltage-current characteristics for the two barriers. It is of interest to note that the plasma has no work function. The electrical behaviour of semi-conductors and semi-conducting surfaces could therefore be investigated without the complications introduced by the presence of metal surfaces, by placing them between two plasmas and measuring the conduction currents passing when the plasmas are raised to a difference of potential.

The author wishes to express his thanks to the Directors of the B.T.H. Co. and to the Chief of the Research Laboratory for permission to carry out and publish these observations. He also makes grateful acknowledgment to his colleague Dr. Gábor for originally suggesting the possibility of investigating the electrical conductivity of insulators by probe methods, and for his helpful collaboration throughout the experiments.

#### SUMMARY

Using a tungsten wire coated with a layer of insulating material, a method is described whereby Langmuir probe methods of measurement in a low pressure mercury discharge can be made to yield information on the electrical behaviour of the insulating material.

For pure aluminium oxide the electrical conductivity is found to vary with temperature in accordance with A. H. Wilson's theory of electronic semi-conductors. The Wilson energy differences  $W_3 - W_1$  is found to be 2.9 e-volts between  $1280^\circ\text{ K}$  and  $1725^\circ\text{ K}$  and 6.6 e-volts at higher temperatures. The critical temperature  $1725^\circ\text{ K}$  is approximately the sintering point of alumina.

Experimental evidence is given in support of the discovery of electron diffusion through alumina. Mention is made of the bearing of this phenomenon on the experiments of Reimann, Treloar, and E. F. Lowry relating to the thermionic emission from oxide coated cathodes.

The conduction currents flowing across an alumina layer 0.005 inch thick between tungsten and plasma in the forward and reverse direction are given at different temperatures for voltages up to 250 volts. At high temperatures the conductivity is greater in the direction of electron flow from metal to oxide to plasma.

---

### The Absorption of Light in Caesium Vapour in the Presence of Foreign Gases

By R. W. DITCHBURN, Ph.D., Professor of Experimental Philosophy, and J. HARDING, B.A., FitzGerald Research Scholar, Trinity College, Dublin.

(Communicated by J. Chadwick, F.R.S.—Received 30 April, 1936)

#### INTRODUCTION

The absorption of caesium vapour on the short wave-length side of the series-limit, alone, and in the presence of helium, has been described in earlier papers.\* It was shown that helium, at a pressure of a few centimetres of mercury, greatly reduced the absorption at all wave-lengths and also produced significant changes in the shape of the absorption curve. No theoretical explanation of these results has been given. At this stage of the investigation it appeared more desirable to obtain measurements of moderate accuracy on a number of gases, rather than to attempt very detailed and accurate measurements on one other gas. The present paper contains results on the absorption of caesium in the presence of the following gases:—neon, argon, krypton, xenon, nitrogen, hydrogen, deuterium, and benzene. All these gases give effects qualitatively similar to those produced by helium. It is still not possible to give a detailed theory of the results, but some empirical generalizations emerge from the extensive data now available.

\* Braddick and Ditchburn, ' Proc. Roy. Soc.,' A, vol. 143, p. 472 (1934); vol. 150, p. 478 (1935), quoted below as I and II respectively.

**EXPERIMENTAL**

The methods used for the control of temperature were similar to those previously described. The photometric technique was the same except for one small alteration. In the experiments on the absorption of caesium in the presence of helium, the absorption was measured by comparison with certain grids. The reduction of light produced by these grids had previously been measured and they were used in the experiments on the absorption of caesium in vacuum. Some of the present experiments were carried out in this way, but in the later experiments the absorption of caesium in the presence of the foreign gas was compared more directly with the absorption of caesium in vacuum, by recording both kinds of absorption spectra on the same plate. Suitable calibration spectra were also included. This direct comparison eliminated the possibility of systematic errors due to imperfect temperature control, etc. It also reduced the effect of random errors.

In the experiments with helium it was necessary to wait, after admitting the gas and heating the side tube, for periods of from half an hour up to two hours, in order to allow the vapour to diffuse through the gas and to establish an equilibrium. The gases used in the present experiments all produced larger effects on the absorption than helium at corresponding pressures. It was thus possible to work at lower pressures and it was sufficient to wait a few minutes to establish equilibrium. This gave less time for changes in the experimental conditions and thus increased the accuracy of the results.

On the other hand, a source of error previously of negligible magnitude gave serious trouble towards the end of the present experiments. The quartz tube is continually being attacked by the caesium vapour, but in earlier experiments the effect on the transparency of the end windows during one experiment was very small. Comparison spectra taken before the absorption spectra usually agreed closely with similar spectra taken after the absorption spectra. As the experiments progressed, the attack gradually became more rapid, so that the two sets of comparison spectra no longer agreed, especially in the ultra-violet end of the spectrum. It appeared that the end windows had become slightly etched and that a semi-permanent action was taking place. This effect was much more marked during the experiments with hydrogen and deuterium than during the experiments with the rare gases. It was possible to apply a correction and determine the absorption near the series limit, when the effect was not too large. The correction was estimated, using the fact that near the series-limit the absorption of the vapour varies rapidly with wave-length.

whereas the spurious absorption, due to the change in the transmission of the windows, varies slowly with wave-length. This correction did not enable the absorption in the ultra-violet end of the spectrum to be measured, nor were we able to obtain really accurate results for hydrogen and deuterium.

#### GAS TECHNIQUE

The results show that the effects produced by different gases are all of the same order and therefore it is not necessary to take very elaborate precautions to purify the gases. Usually up to 5% of any likely impurity could be tolerated. The following notes indicate the purity of the different gases:—

- 1—Argon was oxygen free and contained 2% of nitrogen.
- 2—Neon was spectroscopically pure.
- 3—Krypton was stated by Messrs. Hilger, from whom it was obtained, to be 99.9% pure. The only likely impurities are the other rare gases.
- 4—Xenon contained 2% of krypton.
- 5—Nitrogen was prepared from sodium azide.
- 6—Hydrogen was prepared by the electrolytic method and was thoroughly dried.
- 7—Deuterium was prepared by passing deuterium oxide (99.9% pure) over heated copper gauze which has been previously outgassed.
- 8—Benzene was obtained from British Drug Houses. It was found to have a good melting point. It was tested and found to be free from thiophene. It was redistilled over a drying agent immediately before use.

The gases were admitted to the absorption tube through a trap containing copper turnings. This trap was cooled with ice-salt mixture when benzene was being admitted, with solid carbon-dioxide for xenon and krypton, and with liquid air for other gases. In view of the possibility of contaminating the apparatus with mercury when the benzene was admitted, this gas was used last, but no absorption due to mercury could be observed. Since the  $\lambda 2536$  absorption forms a sensitive test for mercury we conclude that there was probably no effective contamination. The spectrum of the gas was observed visually before and after each experiment. It was always found satisfactory except in two or three experiments, which were rejected.

The possibility of chemical reaction between the caesium and the foreign gas must be considered. The pressure of the foreign gas was measured from time to time during the experiment and except in the experiments with hydrogen and deuterium it remained constant. It has been shown

that the line absorption of caesium in the presence of nitrogen is not appreciably reduced, and this gives indirect evidence that the amount of caesium present is not reduced by reaction with this gas. With hydrogen and deuterium a definite quantity of gas disappeared when the caesium was heated, after which the pressure remained constant. Presumably a compound was formed and an equilibrium reached. No absorption could be attributed to this compound, though possibly some of the decrease in the transparency of the windows may have been due to a solid compound deposited on them. When corrected for the change in the transparency of the windows, the form of the absorption curve was similar to that obtained with caesium in vacuum except for small changes similar to those produced by the inert gases. Any absorption due to the formation of a gaseous compound might be expected to increase with the pressure of the foreign gas. It was found that the absorption always decreased when the pressure of the foreign gas was increased. Thus we conclude that the reaction, if any, did not influence our results.

After the conclusion of the other experiments, we attempted to measure the absorption in the presence of di-ethyl ether, a substance usually believed to be inert towards the metals and their vapours at the temperature of the present experiments. Change of pressure and the disappearance of the caesium line absorption indicated that a fairly rapid reaction was taking place. No results could be obtained. The pressure of the foreign gas was read on a McLeod gauge during each experiment. All pressures so read were reduced by the vapour pressure of the caesium (0.3 mm.) in order to obtain the true pressure of the foreign gas. After this correction the pressures were reduced to 0° C. by multiplying by  $273/T$  where T is the average absolute temperature of absorption tube. T was usually very near to 574° absolute.

#### RESULTS

(a) *General Reduction of Absorption*—Previous work\* had shown that the most important effect of helium was a reduction of the absorption at all wave-lengths. The ratio in which the absorption was reduced varied only slowly with wave-length and the reduction of the absorption near the series-limit was taken as a measure of this effect. This reduction could be expressed by the equation:

$$\frac{\alpha_p}{\alpha} = \frac{p + p_0}{p_0}$$

where  $\alpha$  is the maximum absorption in the presence of the foreign gas at

\* See paper II.

pressure  $p$ , and  $\alpha_0$  is the maximum absorption for caesium alone. Obviously  $p_0$  is equal to the pressure required to reduce the absorption to half the value obtained with caesium alone. It will therefore be called the half-value pressure, though it should be remembered that the reduction

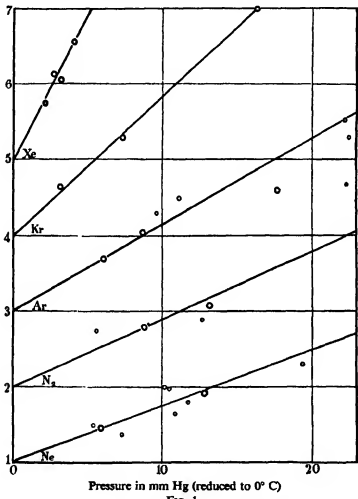


FIG. 1.—The ordinates give the values of  $\alpha_0/\alpha$ . The numbers are correct for successive gas.

FIG. 1.

Figs. 1 and 2—The ordinates give the values of  $\alpha_0/\alpha$ . The numbers are correct for successive gas. The symbol for the gas is written immediately above its own experiments from which a greater accuracy is to be expected.

does not follow an exponential law and thus a pressure of  $2p_0$  gives a reduction to one-third of the original value and not to one-quarter.

The determination of the half-value pressures for the different gases was the principal object of the present series of experiments. The results

of the measurements are shown in figs. 1 and 2.  $\alpha_0/\alpha$  is plotted against the pressure of the foreign gas. From the graphs it may be seen that the above law is satisfied within the accuracy of the experiments and the value of  $p_0$  may be obtained by reading off the pressure corresponding to  $\alpha_0/\alpha = 2$ .

The following values were obtained:—Helium,  $32 \pm 2$  mm.\*; neon,  $13.4 \pm 1$  mm.; argon,  $8.7 \pm 0.3$  mm.; krypton,  $5.5 \pm 0.2$  mm.; xenon,  $2.7 \pm 0.2$  mm.; nitrogen,  $11.4 \pm 1$  mm.; hydrogen,  $3.7 \pm 0.5$  mm.; deuterium,  $2.6 \pm 0.4$  mm.; benzene,  $0.9 \pm 0.4$  mm. These pressures have been reduced to  $0^\circ\text{ C}.$ , as explained above (see p. 69).

It is very difficult to estimate all the sources of error and to be sure that systematic errors have been eliminated, but it is very unlikely that

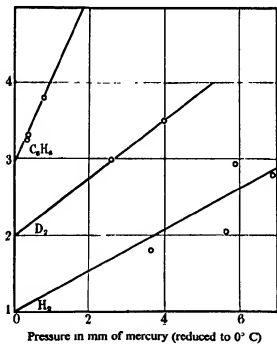


Fig. 2.

neon. For the other gases the zero line has been shifted one unit for each zero line and against its curve. The larger circles give the results of the later

any of the above results is incorrect by more than twice the errors given. The internal agreement would suggest a greater accuracy than that claimed. It was thought to be more important to obtain a reliable value

\* Included from II.

for the ratio of the half-value pressure for hydrogen to that for deuterium than to measure either accurately. For this reason a number of experiments was done in which spectra of absorption in the presence of hydrogen were recorded on the same plate as spectra in the presence of deuterium. The value of the ratio  $p_0(H_2)/p_0(D_2)$  was found to be  $1.4 \pm 0.15$ .

Since the above experiments were completed a new series of experiments on the absorption of caesium vapour at higher pressures has been commenced. Preliminary measurements show clearly that at pressures above 1 mm. the absorption does not increase in proportion to the vapour pressure. This indicates that the absorption is reduced by the interaction of caesium with caesium. A rough preliminary calculation indicates that the half-value pressure for this interaction is about 3.5 mm. This is of the same order as the value for the interaction of caesium with xenon.

Considering the results of the measurements for the inert gases and nitrogen, we see that the half-value pressure decreases steadily as the molecular-weight increases. The half-value pressure is approximately (but not exactly) proportional to the reciprocal of the square-root of the molecular weight. The rule takes a simple, and perhaps significant, form if we consider the number of collisions per second for the different gases. We may define a cross-section ( $\sigma$ ) by the assumption that the number of effective collisions is the same for all gases at the half-value pressure. This cross-section will contain an undetermined constant, but this does not matter as we shall not be concerned with absolute values. For the gases helium, neon, argon, krypton, and nitrogen we find that the cross-section is directly proportional to the molecular weight. This result is shown in fig. 3 where the function  $\sigma = \frac{1}{p_0 \cdot \sqrt{\frac{1}{m_e} + \frac{1}{m_f}}}$  is plotted against

the molecular weight; ( $m_e$  = molecular weight of caesium and  $m_f$  = molecular weight of the foreign gas). This fraction is proportional to the cross-section defined above. Hydrogen and deuterium, considered together, obey the same rule.

Thus it appears that when other factors are unchanged this rule gives the effect of changes of molecular weight. The cross-section for benzene is larger than we should expect if we only considered its molecular weight, but this is not surprising in view of the ring structure and the large kinetic theory radius of this molecule. We should also expect the cross-section for hydrogen to be large because of its large external field. The cross-section for xenon is also larger than would be expected from its molecular weight. This departure cannot be explained by experimental error unless there is some unsuspected error affecting all the experiments

on this gas. The effect may be due to some kind of resonance interaction between the caesium core and the xenon atom.

(b) *Changes in the Shape of the Absorption Curve*—Apart from the general reduction in the amount of absorption, three important changes in the shape of the curve of absorption vs. wave-length were observed with caesium in the presence of helium.

1—The absorption at the far ultra-violet end of the spectrum was reduced more than in the region near the series-limit.

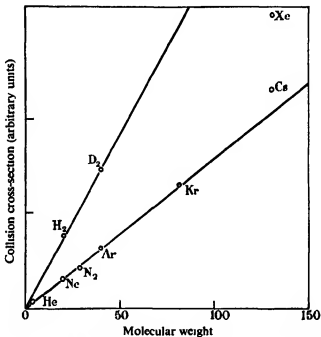


FIG. 3—Note that the scale for hydrogen and deuterium is different from that for the other gases.

2—The maximum in the curve near the series-limit was shifted towards the ultra-violet.

3—The steepness of the absorption curve on the long wave-length side of the series limit was reduced.

Experimentally it is difficult to investigate these effects unless they are sufficiently large in relation to the main effect (*i.e.*, the general reduction of absorption). Helium was much the most favourable gas for this part of the work and was the only one for which quantitative results of accuracy could be obtained. The following results show in a qualitative way how these effects differ in other gases.

1—It was found that for nitrogen, argon, and hydrogen there was no large change in the shape of the curve in the ultra-violet region. Changes were certainly not larger than those found for helium, though they might have been smaller. No results are available for other gases.

2—The shift of the maximum absorption was measured for argon. A curve of shift against pressure was obtained. Like the more accurate curve previously obtained for helium,\* it showed a shift which increased with pressure a little more rapidly than the first power of the pressure. The argon pressure for a given shift appeared to be about half the helium pressure for the same shift. Thus this effect is larger in argon than in helium, but not so large in proportion to the main reduction effect. A few rough measurements on neon indicated a result intermediate between those obtained for helium and for argon. No measurable shift could be obtained with the other gases at the rather low pressures employed. Thus the shift must be still smaller in proportion to the main reduction effect.

3—On the long wave-length side of the series-limit the absorption falls approximately linearly until it has reached about 60% of the maximum value. The quantity  $S = \frac{1}{\alpha} \frac{d\alpha}{d\lambda}$ , averaged over the approximately linear region, was taken as a measure of the steepness. Measurements for caesium with argon at different pressures were compared with previous (unpublished) measurements for caesium alone and for caesium with helium. It was found that the variation of  $S$  was given by the equation

$$S = \frac{1}{A + Bp},$$

where  $p$  is the pressure of the foreign gas.  $A$  and  $B$  are constants. If  $p$  is in centimetres of mercury (reduced to 0° C.) and  $\lambda$  is in Angstrom units, the value of  $A$  is 21 and the values of  $B$  are 17 for helium and 28 for argon. These results need correcting for the finite resolving power of the spectrograph. This correction was estimated from photometric measurements of the shape of a narrow line in this region of the spectrum. The correction so estimated takes account of finite width of slit and also makes some allowance for halation. Its effect is to reduce the value of  $A$  to 14. The values of  $A$  and  $B$  are probably correct within 25%.

#### DISCUSSION

It will be convenient to discuss the changes of shape of the absorption curve before considering the general problem. We shall discuss only

\* See paper II, fig. 3.

the changes near the series-limit because the other changes are small and the experimental data are far from complete. We have, firstly, a change in the position of the absorption maximum and, secondly, a change in the steepness of the curve on the long wave-length side of the series-limit. Both these effects are larger in argon than in helium, in about the same ratio. It is not difficult to see that they are both probably aspects of the same phenomenon. Let us suppose that in the absence of a foreign gas the absorption increases discontinuously at the series-limit. In the presence of the foreign gas the atoms are subject to a variable perturbation so that the limit is not in exactly the same place for the different atoms. We obtain an effect similar to the broadening of an absorption line. In an absorption line symmetrical broadening does not lead to a shift of the absorption maximum, because the original absorption is symmetrical

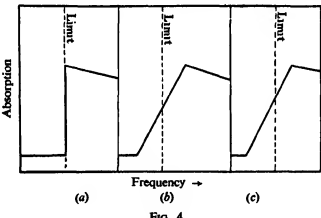


FIG. 4.

about the maximum. At the series limit the absorption is not symmetrically distributed, so we expect that a symmetrical broadening will lead to a shift of the maximum. This is illustrated in fig. 4, where 4a represents the original absorption curve and 4b represents the effect of symmetrical broadening. The form of the experimental curve, which is shown in fig. 4c, suggests a slightly asymmetrical broadening.

We thus regard the sudden change in absorption near the series-limit as analogous to the sudden change in absorption inside an absorption line. The reciprocal of the function  $S$ , which we have defined above, is thus analogous to the breadth of an absorption line. Consequently, we should expect it to be made up of four parts: (1) a "natural" width, (2) a part due to the Doppler effect, (3) a part due to interactions between caesium and caesium (Holtzmark effect), and (4) a part due to interaction between caesium and the foreign gas (Lorentz effect). We should expect

(1) and (2) to be negligible under the conditions of our experiments and we should therefore expect  $1/S$  to be approximately proportional to  $CP + Bp$ , where  $P$  is the pressure of the caesium and  $p$  is that of the foreign gas.  $B$  and  $C$  are constants. When  $P$  is constant we should expect  $1/S = A + Bp$  which is the result found experimentally. Since the vapour pressure of the caesium (when reduced to  $0^\circ\text{C}$ ) is only  $0.016\text{ cm.}$ , we require  $C$  to be of the order 100 to explain the observed value of  $A$ . This is considerably larger than the values of  $B$  found for helium and argon, but this would be expected from the analogy with the Lorentz and Holtzman effects.\* This explanation is confined by a few results of experiments on caesium at higher pressures.

Thus the above picture seems to give an adequate qualitative account of the results. It appears that with the unperturbed caesium atom a sharp change in absorption takes place near the series-limit. This is in agreement with the results of Trumpp† on sodium and also with the results of Waible.\* The latter calculated the limiting value of the absorption for the higher members of the series and found it to be only about a fourth of the absorption observed just on the short wave-length side of the series-limit, thus indicating a sharp change in the absorption. The experimental results are here in conflict with the theoretical calculations of Suigura.‡

We now turn to the discussion of the general problem. Our experiments clearly indicate a change of transition probability due to the presence of the foreign gas. It is of interest to seek evidence of analogous effects with other substances. Iodine has a region of continuous absorption on the short wave-length side of  $\lambda 4995$ , corresponding to photo-dissociation of the molecule. One of us (J. H.)§ has sought for a change in absorption due to the presence of helium, but no effect could be detected. The experiments of Kuhn and Oldenburg,|| Krefft and Rompe,¶ and Preston\*\* on emission bands produced by metals in the presence of the rare gases may indicate changes of transition probability at certain stages of the collision process, though the interpretation of these experiments is difficult. As previously suggested, the experiments of Mrozowski†† on the

\* 'Z. Physik,' vol. 53, p. 459 (1929).

† *Ibid.*, vol. 71, p. 720 (1932).

‡ 'J. Phys. Rad.,' vol. 8, p. 113 (1927).

§ 'Phil. Mag.,' vol. 21, p. 773 (1936).

|| 'Phys. Rev.,' vol. 41, p. 72 (1932).

¶ 'Z. Physik,' vol. 73, p. 681 (1932).

\*\* 'Phys. Rev.,' vol. 49, p. 140 (1936).

†† 'Z. Physik,' vol. 91, p. 600 (1934). See also Frank, 'Phys. Zeits.,' Sowjet Union, vol. 4, p. 637 (1933).

continuous absorption of mercury may be explained by a similar effect. All these experiments refer to continuous absorption. Direct experiments of Fuchtbauer, Joos, and Dinckelacker\* on the line absorption of mercury give similar effects to those we have observed but of a lower order of magnitude. In these experiments a pressure of 50 atmospheres produces a reduction of absorption by only 25%, a broadening of about 1 Å, and a shift of about 0.5 Å. The photoelectric absorption which we have investigated differs from the line-absorption in that one of the states concerned is continuous. Even when we remember that the changes in the absorption line are due to the difference of the perturbation of two quantized states, our experiments must indicate that the continuous state is very much more sensitive to perturbation than the normal state of the atom. Although we may expect the continuous state to be very easily perturbed, the magnitude of our effects is still surprisingly large.

The transition probability† depends on the function  $\int r P_{41} P_x dr$ , where

$\frac{1}{r} P_{41}$  is the eigenfunction for the normal state and  $\frac{1}{r} P_x$  is that for the continuous state. Now the value‡ of  $P_{41}$  is very small at distances (from the centre of the atom) greater than  $3 \times 10^{-8}$  cm. Thus, in order to affect the value of the integral by a change in  $P_x$ , it is necessary that the value of the  $P_x$  at distances less than  $3 \times 10^{-8}$  cm. from the centre of the atom should be altered. At the half-value pressure for helium (whose effect is smallest) the concentration is only  $10^{18}$  atoms per cc. The mean distance from a given caesium atom of the nearest helium atom is  $6 \times 10^{-7}$  cm. It does not appear likely that interactions of the ordinary van der Waals type could produce any appreciable alteration of the atomic field at this distance.

If we remember that the function  $P_x$  has to be normalized we may consider the matter from a slightly different point of view. If as a result of interaction with atoms of the foreign gas the electron in the continuous state is made to spend a greater time at large distances from the atom, there will be a change in the normalizing factor. This will act so as to reduce the value of  $P_x$  in the region where  $P_{41}$  is large. Whether this effect is sufficient to explain our results can be seen only by a detailed calculation. It appears to be capable of explaining qualitatively some of the features of our results. An elementary argument shows that if the additional time spent at large distances from the centre of the atom is

\* 'Ann. Physik,' vol. 71, p. 204 (1923).

† 'Proc. Cam. Phil. Soc.,' vol. 25, p. 75 (1929).

‡ See diagram, 'Phys. Rev.,' vol. 39, p. 908 (1932).

proportional to the pressure of the foreign gas the variation of absorption with pressure will be of the form found experimentally. Also on this view we should not expect any effect on the absorption of iodine, where there is no free electron. We should also expect that when the wave-length of the free electron is of the same order as the distance between the atoms, there might be irregularities in the shape of the absorption curves due to diffraction effects. Such effects have been found in X-ray spectra and explained by Kronig\* and Petersen.† In our experiments we should expect these effects to be small and to be confined to the region near the series-limit. As mentioned in paper II, such irregularities have been observed. The wave-length of the corresponding electrons is of the right order but the irregularities are too small for quantitative measurement.

On the other hand, it does not appear probable that this type of calculation would show the correct variation in the effect for different gases. In particular, it would appear to give no difference between hydrogen and deuterium. Also, we have to consider the variation of the effect with wave-length. Our measurements extend from the series-limit to about  $\lambda 2000$ . The velocities of the corresponding free electrons vary from zero to about 2.5 volts. We should expect that at some velocities the electrons would be scattered more than at others (Ramsauer effect). The reduction of absorption should show a corresponding variation with wave-length. This variation is not found. Despite these difficulties, the calculation of the change in the normalization factor seems at present to offer the best approach to the theory of our results.

[*Note added in proof*, 20 July, 1936.—Since the above was written Dr. Hans Motz has made approximate calculations based on an extension of the theory of Kronig and Petersen (*loc. cit.*). A reduction of absorption of the right order of magnitude is obtained. The law of variation with pressure and the difference between the effects of the different rare gases are correctly predicted. More complete calculations are now in progress.]

We are glad to take this opportunity to express our thanks to Professor Werner for the gift of deuterium oxide and for advice on chemical problems and to Dr. Massey and Mr. Broderick for helpful discussions of the theory.

#### SUMMARY

The continuous absorption of caesium vapour in the presence of several foreign gases has been measured.

\* 'Z. Physik,' vol. 75, p. 468 (1932).

† 'Z. Physik,' vol. 76, p. 768 (1932); vol. 80, p. 258 (1933).

All gases cause a reduction in the amount of absorption. The pressures required to reduce the absorption to half-value vary from 32 mm. for helium to 0·9 mm. for benzene. For the rare gases the half-value pressures decrease with increasing atomic weight.

The absorption curve near the series-limit is changed in shape, the slope of the curve becoming smaller and the maximum absorption being shifted to shorter wave-lengths.

No complete theory is available, but certain simple generalizations are given.

---

## The Structure of Resorcinol A Quantitative X-Ray Investigation

By J. MONTEATH ROBERTSON, M.A., D.Sc.

(Communicated by Sir William Bragg, O.M., P.R.S.—Received 1 May, 1936)

Previous investigations of organic crystals\* have served to determine the dimensions and structure of the aromatic carbon ring and of certain simple substituent groups. The hydroxyl group is particularly interesting, both in relation to chemistry and in the physical explanation of its associating properties. A considerable number of metallic hydroxides has been studied by X-ray analysis,† and the results show that the occurrence of the —OH group is generally characterized in the solid state by unusually small intermolecular distances. It is obviously of the greatest importance to study the dimensional properties of these groups in organic acids, phenols, and alcohols, but until now few really quantitative investigations along these lines have been carried out.

The properties of the phenols, intermediate as they are between those of the acids and the alcohols, would lead us to expect the characteristic hydroxyl or hydrogen bond distances (2·5 to 2·8 Å) between the reactive groups on adjoining molecules; but the question arises whether this can be achieved in the crystal structure without sacrificing the usual minimum van der Waals distance of about 3·5 Å, between some of the aromatic

\* Robertson, 'Proc. Roy. Soc.,' A, vol. 140, p. 79 (1933); vol. 142, p. 659 (1933); vol. 150, p. 106 (1935), etc.

† Summarized by Bernal and Megaw, 'Proc. Roy. Soc.,' A, vol. 151, p. 384 (1935).

carbon atoms of the molecules. The solution of the present structure shows that these two distinct sets of intermolecular distances are, in fact, retained without bringing in any intermediate values.

The simplest member of the series, phenol itself, is difficult to study quantitatively owing to its low melting point. Resorcinol has been chosen in this investigation because it forms good and comparatively stable crystals, which have the added interest of exhibiting in a high degree the well-known pyro-electric and piezo-electric properties. Indeed, one principal object of this work was to provide the data by which a correlation of the physical properties of the crystal with those of the individual molecules might be made.

#### CRYSTAL DATA, SPACE GROUP, FORMULAE

Resorcinol,  $C_6H_4O_2$ , melting point  $116^\circ C$ , belongs to the pyramidal class of the orthorhombic system, and the axial ratios are recorded by Groth\* as

$$a:b:c = 0.9105:1:0.5404.$$

The crystal has been examined by means of the ionization spectrometer by Sir William Bragg,† who first determined the axial lengths and the general disposition of the molecules in the unit cell. Preliminary data from further photographic investigations have been given by the writer.‡ In the descriptions of the structure in the present paper, the  $a$  and  $b$  axes referred to by Groth have been interchanged to secure uniformity in comparisons with other structures. We then find that the  $(h0l)$  reflexions are halved when  $h$  is odd, and the  $(0kl)$  reflexions when  $(h+l)$  is odd. The space group is thus  $C_{2h}^0(Pna)$ . The axial lengths are

$$a = 10.53 \pm 0.03, \quad b = 9.53 \pm 0.03, \quad c = 5.66 \pm 0.02 \text{ \AA}.$$

The four molecules of  $C_6H_4O_2$  in the unit cell contribute no symmetry of their own to the crystal, which is polar, and exhibits the strong pyroelectric and piezo-electric properties noted above. The volume of the unit cell is  $568 \text{ \AA}^3$ , and the density of the crystal calculated from this figure is  $1.278$ , which compares with a measured value of  $1.272$ . The total number of electrons in the unit cell,  $F(000)$ , is  $232$ .

There is no centre of symmetry in the space group  $C_{2h}^0(Pna)$ . The symmetry elements are twofold screw axes parallel to the  $c$  axis; glide

\* 'Chem. Krystallog.', vol. 4, p. 85 (1917).

† 'J. Chem. Soc.', p. 2766 (1922); "X-Rays and Crystal Structure," p. 247 (1925).

‡ 'Z. Krystallog.', vol. 89, p. 518 (1934); 'Nature,' vol. 136, p. 755 (1935).

planes parallel to the (100) place with glides of  $\frac{1}{2}(b+c)$ ; and glide planes parallel to (010) with glides of  $a/2$ . Thus if we fix attention on one molecule in the unit cell of the crystal, which we may arbitrarily term "molecule (1)", the operation of these symmetry elements will give rise to three other molecules of different orientations. Let  $x, y, z$  be the coordinates (expressed as fractions of the axial lengths  $a, b$ , and  $c$ ) of a representative point, or atom, on molecule (1). The origin of the  $x$  and  $y$  coordinates is taken on a twofold screw axis, while that of the  $z$  coordinate is arbitrary. Then the coordinates of equivalent points on the four molecules are

- $$(1) \quad x, y, z; \quad (2) \quad -x, -y, \frac{1}{2} + z;$$
- $$(3) \quad \frac{1}{2} - x, \frac{1}{2} + y, \frac{1}{2} + z; \quad (4) \quad \frac{1}{2} + x, \frac{1}{2} - y, z.$$

In the present analysis we have to discover the orientation and structure of molecule (1); the relative arrangement of all the molecules in the crystal is then easily obtained from the above relations. Diagrams showing the arrangement of the symmetry elements, and expressions for the structure factor of the general plane ( $hkl$ ),\* summed over the above coordinates, will be found in the "International Tables for the Determination of Crystal Structures," vol. I, p. 108. For the axial zones of reflexions, which are discussed in this paper, the structure factor simplifies to the following expressions, A and B representing the real and imaginary parts. These expressions have now to be summed over all the atoms in one molecule.

( $hk0$ ) reflexions:

$$A = 4 \cos 2\pi hx \cos 2\pi ky \quad \text{when } (h+k) \text{ is even}$$

$$A = -4 \sin 2\pi hx \sin 2\pi ky \quad \text{when } (h+k) \text{ is odd}$$

$$B = 0$$

( $h0l$ ) and ( $0kl$ ) reflexions:

$$A = 4 \cos 2\pi \frac{hx}{ky} \cos 2\pi lz \quad \left. \right\} \quad \text{when } l \text{ is even}$$

$$B = 4 \cos 2\pi \frac{hx}{ky} \sin 2\pi lz \quad \left. \right\} \quad \text{when } l \text{ is odd.}$$

$$A = -4 \sin 2\pi \frac{hx}{ky} \sin 2\pi lz \quad \left. \right\} \quad \text{when } l \text{ is odd.}$$

$$B = 4 \sin 2\pi \frac{hx}{ky} \cos 2\pi lz \quad \left. \right\} \quad \text{when } l \text{ is even.}$$

\*  $F(hkl) = \sum f_i e^{2\pi i(hx+ky+lz)}$ .

The twofold axis is equivalent to a centre of symmetry in the projection of the structure along the *c* axis. Hence in making a two-dimensional Fourier synthesis for the (*hk0*) zone of reflexions, the ordinary series for the electron density applies

$$\rho(x, y) = \frac{1}{ab} \sum_{-\infty}^{+\infty} \sum_{-\infty}^{+\infty} F(hk0) \cos 2\pi(hx + ky),$$

the sign of  $F(hk0)$  for each term being given by the sign of  $A$  in the preceding formulae; *i.e.*, the phase constant can only be  $0^\circ$  or  $180^\circ$ . But in the projections along the *a* and *b* axes, the phase constants may have any value. Thus for the *b* axis projection the series is

$$\rho(x, z) = \frac{1}{ac} \sum_{-\infty}^{+\infty} \sum_{-\infty}^{+\infty} F(h0l) \cos(2\pi hx + 2\pi lz - \alpha(h0l)).$$

The value of the phase constant,  $\alpha(h0l)$ , is here  $\tan^{-1} \frac{B}{A}$ , due regard being paid to the signs of  $A$  and  $B$  in determining the quadrant in which  $\alpha$  lies.

### EXPERIMENTAL

Large crystals of resorcinol are easily obtained from aqueous solutions, but these are not very suitable for photographic purposes. Some very fine prisms, elongated along the *c* axis, were obtained by crystallization from benzene, and these were employed throughout this work. One such prism, 1.25 mm long, and of nearly square cross-section, side about 0.40 mm, weighing 0.229 mg, was set for rotations about the *c* axis. A large number of rotation and moving film photographs was made, the crystal being completely immersed in a beam of Cu K $\alpha$  radiation. Direct comparisons between the very strong and very weak reflexions were carried out by means of automatic shutters, while for the absolute values of the intensities comparisons with a known standard were made by interchange on the two-crystal moving film spectrometer.\* All the films were calibrated with a continuous wedge giving linear increments of X-ray intensity, and measured on the integrating photometer.† The calculated absorption coefficient of resorcinol,  $\mu = 9.34$  per cm for  $\lambda = 1.54$ , was used in correcting the absolute values of the intensities of the principal reflexions.

Similar exposures were made on other crystal specimens mounted for rotations about the *a* and *b* crystal axes. Care was taken to trim the

\* Robertson, 'Phil. Mag.', vol. 18, p. 729 (1934).

† Robinson, 'J. Sci. Instr.', vol. 10, p. 233 (1933).

specimens so that they presented nearly square cross-sections to the rotation axis. The average path of the X-ray beam through the crystal was thus nearly the same for all the reflexions in a given zone, and sufficient accuracy was attained by applying a single correction factor to allow for the absorption of the X-ray beam.

In order to check the absolute measurements another smaller crystal of resorcinol (0.090 mg) was measured directly on the ionization spectrometer with monochromatic Mo K $\alpha$  rays. The values obtained were somewhat higher for the very strong reflexions, and corrections were accordingly made.

The values of the structure factor F were derived from the intensity measurements by the usual formulae for the mosaic crystal, and the results are given in Table I under "F measured" (last column). The calculated values of F, and the phase constant  $\alpha$ , are derived from the results of the analysis given in the next section.

TABLE I—MEASURED AND CALCULATED VALUES OF THE STRUCTURE FACTOR

<i>hkl</i>	$\sin \theta$ $\lambda = 1.54$	$\alpha^\circ$ calc.	F calc.	F measured
200	0.146	0	12.5	13
400	0.292	0	13	16
600	0.438	0	11.5	12.5
800	0.584	180	10.5	13.5
10,00	0.730	180	6	7.5
020	0.162	0	7	5.5
040	0.323	0	14.5	16
060	0.484	0	12.5	12
080	0.646	0	2	<4.5
0,10,0	0.807	0	1	<5.5
002	0.272	195	32	36.5
004	0.544	211	9	11
011	0.158	46	45	45.5
013	0.416	206	12	12.5
015	0.684	217	4.5	<9.5
022	0.316	297	9	16
024	0.567	230	14.5	12.5
031	0.278	177	16	18.5
033	0.474	6	10.5	8
042	0.422	308	20.5	25.5
044	0.632	151	20.5	19
051	0.426	129	22.5	27
053	0.574	322	14	11

TABLE I—(continued)

<i>hkl</i>	sin θ $\lambda = 1 \cdot 54$	$\alpha^\circ$ calc.	F calc.	F measured
062	0.555	169	10.5	9.5
071	0.581	12	6	<9
201	0.200	134	11.5	11
401	0.322	20	13	17.5
601	0.459	41	17	20
801	0.600	232	8	11
10,01	0.743	351	5	<6.5
202	0.309	114	27	31.5
402	0.399	63	15.5	20
602	0.516	96	8	6
802	0.645	352	14	17
203	0.433	209	10	13.5
403	0.502	352	8.5	7.5
603	0.598	213	5	<6
803	0.713	141	14.5	14.5
204	0.562	3	6	<6
404	0.617	324	10	7
604	0.698	121	7.5	7
205	0.695	34	5.5	<6.5
405	0.739	200	14.5	11
110	0.109	0	1	3
210	0.167	180	46.5	50.5
310	0.234	180	3.5	5
410	0.303	180	19	20
510	0.374	0	6.5	11.5
610	0.446	180	23.5	27
710	0.518	180	15.5	18.5
810	0.590	180	5	4
910	0.663	0	2	6
10,10	0.735	0	0.5	<5.5
11,10	0.808	0	4.5	<5.5
120	0.177	180	32	37.5
220	0.218	180	45.5	52
320	0.272	0	9.5	11
420	0.334	180	15.5	19.5
520	0.400	180	1.5	<2.5
620	0.467	0	7.5	12
720	0.536	0	2	<4
820	0.606	0	1.5	<4.5
920	0.677	0	7.5	7.5
10,20	0.748	180	8	8.5
11,20	0.820	0	4	<5.5

TABLE I—(continued)

<i>hkl</i>	sin θ $\lambda = 1.54$	α° calc.	F calc.	F measured
130	0.253	180	7	9
230	0.283	180	5	9
330	0.327	0	19.5	26
430	0.380	0	7.5	10.5
530	0.439	—	0	<3
630	0.501	180	4.5	6.5
730	0.566	180	4.5	6
830	0.633	—	0	<4.5
930	0.701	0	1.5	<4.5
10,30	0.769	0	0.5	<5
11,30	0.839	180	3	<5
140	0.331	180	10	8
240	0.355	180	11	12.5
340	0.390	0	0.5	<2.5
440	0.436	180	13.5	16
540	0.488	180	11.5	11.5
640	0.544	0	9	11
740	0.605	0	1.5	<4.5
840	0.668	0	1.5	<4.5
940	0.733	180	4.5	6.5
10,40	0.799	180	0.5	<5
150	0.410	180	3	6
250	0.429	180	4	4
350	0.459	0	5	7
450	0.498	0	2.5	6
550	0.544	0	9	6.5
650	0.596	0	5	7
750	0.657	—	0	<4.5
850	0.711	0	6	7
950	0.772	0	5	<5
10,50	0.835	180	4	<5.5
160	0.490	180	10	11.5
260	0.506	180	3	5
360	0.532	0	3.5	<3.5
460	0.566	180	2.5	3.5
560	0.606	180	3.5	3.5
660	0.653	0	19.5	20.5
760	0.704	180	4	<4
860	0.760	180	2	<5
960	0.817	180	2.5	<5.5
170	0.570	180	17	17.5
270	0.584	180	2.5	<4.5
370	0.606	180	4.5	<4.5
470	0.637	0	13	15
570	0.673	180	3.5	<4.5

TABLE I—(continued)

<i>hkl</i>	$\sin \theta$ $\lambda = 1.54$	$\alpha^\circ$ calc.	F calc.	F measured
670	0.715	180	4.5	6
770	0.762	180	3.5	<5
870	0.813	180	5.5	7
180	0.650	180	2	<4.5
280	0.662	0	3.5	8.5
380	0.682	0	11	11.5
480	0.709	180	10	12
580	0.742	0	10.5	12
680	0.781	0	0.5	<5
780	0.824	0	1	<5.5
190	0.730	0	6	6
290	0.741	180	3.5	4
390	0.759	0	13.5	15.5
490	0.784	0	1	<5
590	0.814	180	2.5	<5.5
690	0.848	180	0.5	<5
1,10,0	0.811	0	1.5	<5.5
2,10,0	0.820	0	1	<5.5
3,10,0	0.836	180	4.5	<5.5

## ANALYSIS OF THE STRUCTURE

The strongest reflexions are given by the (220), (210), (120), (011), and the (002) planes, which have structure factors ranging from 52 to 37 absolute units. But none of these values exceeds about 40% of the possible maximum which would apply if all the atoms were in phase, or nearly in phase, for any of these large spacing planes. This fact, supported by the comparatively small variation in the refractive indices of the crystal (Groth, *loc. cit.*), shows conclusively that no simple parallel arrangement of the molecular planes is possible, but that they must be inclined at considerable angles to the symmetry planes of the crystal.

In testing various possible structures it is convenient to refer the atoms to two molecular axes L and M (compare fig. 7) passing through the centre of the benzene ring and lying in the plane of the ring. The centre of the ring itself may have any position relative to the symmetry elements. Let the coordinates of the ring centre be  $x_0, y_0, z_0$ , and let the angles which L and M make with the  $a, b$ , and  $c$  crystal axes be  $\chi_L, \psi_L, \omega_L$ , and  $\chi_M, \psi_M, \omega_M$ . The crystal coordinates of an atom A are then given by

$$L_A \cos \chi_L + M_A \cos \chi_M + x_0 = x_A$$

$$L_A \cos \psi_L + M_A \cos \psi_M + y_0 = y_A$$

$$L_A \cos \omega_L + M_A \cos \omega_M + z_0 = z_A$$

where  $L_A$  and  $M_M$  are the coordinates of the atom relative to the molecular axes. We have already mentioned that the crystal coordinates,  $x$  and  $y$ , are referred to an origin on a twofold screw axis. The coordinate  $z$ , measured along this twofold axis, is still undetermined, so we may now fix the origin by making  $z_0 = 0$ , i.e., we choose the origin on the level of the centre of the benzene ring.

Any suggested structure involving a planar molecule can now be tested. We may assume a regular benzene ring of the usual dimensions, radius about 1.4 Å. The distance of the —OH group from the ring is unknown, but this may be taken as roughly of the same order, 1.4 Å. (These assumptions will first be tested, and later the true values ascertained by means of a Fourier analysis.) We can now test certain orientations by varying  $\chi$ ,  $\psi$ , and  $\omega$  and try various positions for the molecule by changing  $x_0$  and  $y_0$ . The simultaneous evaluation of these parameters is, of course, a rather formidable task, but a consideration of some outstanding features of the spectra serves to narrow down the search.

For example, in the  $(hk0)$  zone, the  $(110)$ ,  $(020)$ , and  $(200)$  planes all give very weak reflexions compared with the strong  $(220)$  and  $(210)$ . These results suggest that the parameters  $x_0$  and  $y_0$  are nearly equal and probably of the order of 1.5 Å, an arrangement which places the molecules diagonally about the twofold axis of origin. It was at first thought the pairs of —OH groups on adjoining molecules (1) and (2) might be directed towards each other across this twofold axis ( $\psi_M$  about 45°) while the structure factors for the basal reflexions,  $F(002) = 36$ ,  $F(004) = 11$ , suggested that the molecular planes might be inclined at about 33° to the  $c$  axis ( $\omega_L = 147^\circ$ ); but tests of these positions revealed no general agreement with the observed intensities. However, the general position and orientation of the molecules seemed plausible. The positions found for the benzene rings were therefore retained, but the —OH groups were now attached to the opposite sides of the rings, so that on adjoining molecules across the twofold axis through the origin they were directed away from each other (compare fig. 8). This arrangement, at first sight rather unlikely when attention was confined to one pair of molecules, proved correct, and a good general agreement with the observed intensities was immediately obtained.

Further movements gradually refined the results, and finally the structure factors for the whole  $(hk0)$  zone were calculated. From the values of the phase constants obtained (+ or -  $F$ ), a two-dimensional Fourier synthesis was made, which gave a projection of the structure along the  $c$  axis. Careful measurement of this projection led to new and fairly accurate values for the interatomic distances and orientation angles. With

jection, consequently two pairs of carbon atoms (AF and CD) overlap so much that they are not separately resolved, but form oval concentrations of density. The long axes of these ovals, however, are obviously parallel to the line joining the resolved pair of carbon atoms, B and E. The whole diagram, in fact, corresponds accurately to the projection of a regular plane hexagon, with oxygen atoms attached to the 1:3-positions. The

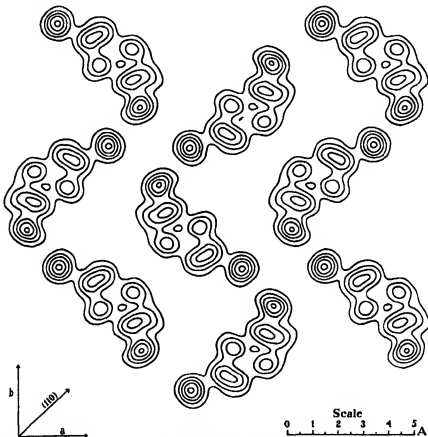


FIG. 2.—The *c* axis projection on a smaller scale showing the relations of a group of nine molecules. Each line represents two electrons per  $\text{Å}^2$ .

greatest inclination of the molecule is nearly along the axis L, joining B and E, but the other axis M, parallel to the line through the oxygen atoms, is also inclined slightly to the plane of the projection. Consequently, the oxygen atom H, when seen in this projection of the structure, appears to be at a greater distance from the benzene ring, and is much more clearly resolved than the other oxygen atom G. But when the actual dimensions of the molecule are worked out, these distances are found to be the same.

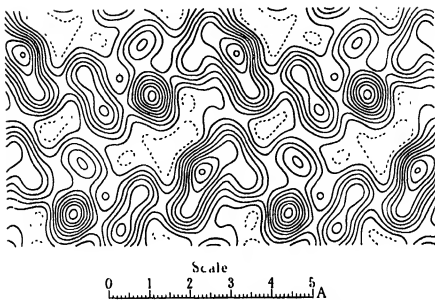


FIG. 3—Projection along the *b* axis. Each line represents one electron per  $\text{Å}^3$  (first line dotted). The positive direction of the *z* coordinate (*c* axis) is directed downwards.

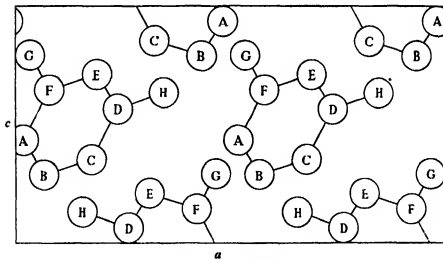


FIG. 4—Showing how the molecules are arranged in the *b*-axis projection.

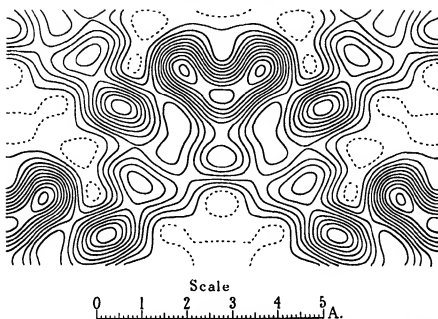


FIG. 5—Projection along the  $\alpha$  axis. Each line represents one electron per  $\text{A}^3$  (first line dotted). Positive  $z$  coordinate directed downwards.

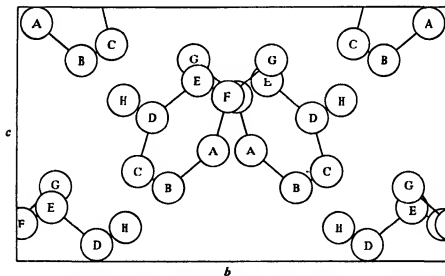


FIG. 6—Showing how the molecules are grouped in pairs in the  $\alpha$  axis projection, but the component molecules are actually widely separated *along* the  $\alpha$  axis. Compare fig. 2.

In the projection along the *b* axis (fig. 3) the positions of all the atoms in the molecule can be observed. But owing to the close approach of the surrounding molecules, the average definition of the atoms is not nearly so good as in fig. 1. In fig. 5, which gives the projection along the *a* axis, the molecules overlap in pairs, with the result that the individual atoms are not resolved at all.

By putting together the results of figs. 1 and 3, the actual dimensions of the molecule and its orientation in the crystal can be ascertained. But owing to the better definition of fig. 1, the most accurate results are probably obtained by taking coordinates and directions from this diagram alone, using the other diagrams merely as a general check on the regularity of the structure. Thus it is found that the benzene ring is a regular plane hexagon and that the distance between the carbon atoms which best accounts for all the results is  $1.39 \pm 0.01$  Å. The oxygen atoms are essentially equivalent and appear to be symmetrically placed with respect to the ring, although a slight uncertainty affects the position of the less perfectly resolved atom G.

With these regularities in the structure we can obtain the complete orientation and dimensions of the molecule from the *c* axis projection (fig. 1). The angles which the axis L (BE) makes with the *a*, *b*, and *c* crystal axes are denoted by  $\chi_L$ ,  $\psi_L$ ,  $\omega_L$ , while the corresponding inclinations of M (GH) are  $\chi_M$ ,  $\psi_M$ ,  $\omega_M$ .

The measured distance between the carbon atoms B and E is 1.466 Å. Taking the real distance here to be  $2 \times 1.39$  Å, we obtain  $\omega_L$ . Further, the observed angle between L (BE) and the *a* axis is  $\theta_L = 26.5^\circ$ . Thus we have

$$\sin \omega_L = 0.5201$$

$$\cos \psi_L = \cos \chi_L \tan \theta_L$$

$$\cos^2 \chi_L + \cos^2 \psi_L + \cos^2 \omega_L = 1$$

which gives the orientation of L as

$$\chi_L = 62.25^\circ \quad \cos \chi_L = 0.4656$$

$$\psi_L = 76.6^\circ \quad \cos \psi_L = 0.2321$$

$$\omega_L = 148.65^\circ \quad \cos \omega_L = -0.8540.$$

The observed angle between M (GH) and the *a* axis is  $\theta_M = 135.1^\circ$ , and

$$\cos \psi_M = \cos \chi_M \tan \theta_M$$

$$\cos \chi_L \cos \chi_M + \cos \psi_L \cos \psi_M + \cos \omega_L \cos \omega_M = 0$$

$$\cos^2 \chi_M + \cos^2 \psi_M + \cos^2 \omega_M = 1$$

which gives the orientation of M as

$$\begin{aligned}\chi_M &= 134.05^\circ & \cos \chi_M &= -0.6953 \\ \psi_M &= 46.15^\circ & \cos \psi_M &= 0.6929 \\ \omega_M &= 101.0^\circ & \cos \omega_M &= -0.1908.\end{aligned}$$

The measured distance between the oxygen atoms G and H is 4.636 Å. When this figure is corrected for the orientation given above, the real distance between G and H is found to be 4.722 Å. In a similar way, all the dimensions of the molecule can be reconstructed, and the results are shown in fig. 7.

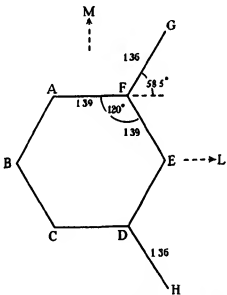


FIG. 7—Dimensions of resorcinol molecule.

The centres of the hydroxyl groups are thus seen to lie at 1.36 Å from the centres of the ring carbon atoms. These groups appear to be slightly displaced towards each other, out of the symmetrical position, but the amount of the displacement, 1.5°, is very small. We have already noted a small uncertainty in the position of the group G. From the results of the *b* axis projection (fig. 3), this group would appear to be displaced slightly more, by from 0.04 to 0.08 Å, towards the axis L, and perhaps also slightly out of the plane of the ring. This effect, if real, would make the model slightly unsymmetrical about the axis L; the evidence on this point, however, is not conclusive, owing to the poor resolution achieved in the *b* axis projection.

The molecular dimensions are summarized in Table III, which gives the coordinates of the atoms, in Angstrom units, with respect to the molecular axes and the centre of the ring as origin. The coordinates of the centre of the ring itself,  $x_0$ ,  $y_0$ , with respect to the twofold symmetry axis, are obtained by direct measurement from the  $c$  axis projection.

TABLE III—COORDINATES REFERRED TO MOLECULAR AXES  
(Compare fig. 7)

Coordinates of origin:  $x_0 = 1.342 \text{ \AA}$ ,  $y_0 = 1.288 \text{ \AA}$

Atom	A	B	C	D	E	F	G	H
L coordinate (A)	-0.695	-1.39	-0.695	0.695	1.39	0.695	1.404	1.404
M coordinate (A)	1.20	0	-1.20	1.20	0	1.20	2.36	-2.36

When these figures are combined with the orientation angles given above, we obtain the coordinates of the atoms referred to the crystal axes,  $a$ ,  $b$ , and  $c$ , and the twofold symmetry axis as origin (Table IV). All the explanatory diagrams accompanying the contour maps are prepared from these figures, atoms being drawn as circles, half-size. The accuracy of the coordinates is in general from 0.01 to 0.02 Å, but atoms A, F, and G are a little less certain. Alternative values are given for the  $x$  and  $z$  coordinates of G, based upon a slightly different interpretation of the projections.

TABLE IV—COORDINATES REFERRED TO CRYSTAL AXES, ORIGIN ON  
TWOFOLD SCREW AXIS

Atom	$x\text{\AA}$	$2\pi x/a$	$y\text{\AA}$	$2\pi y/b$	$z\text{\AA}$	$2\pi z/c$
A CH	0.18	° 6 2	1.96	74.1	0.365	° 23 1
B CH	0.695	23.8	0.965	36.5	1.185	75.5
C CH	1.185	63.4	0.29	11.1	0.825	52.4
D C	2.50	85.5	0.615	23.2	-0.365	-23.1
E CH	1.99	68.0	1.61	60.9	-1.185	-75.5
F C	0.83	28.4	2.28	86.3	-0.825	-52.4
G OH	0.355 (0.38)	12.1 (13.0)	3.25	122.8	-1.65 (-1.70)	-104.9 (-108.1)
H OH	3.64	124.4	-0.02	-0.8	-0.75	-47.6

#### INTERMOLECULAR DISTANCES AND ARRANGEMENT OF MOLECULES IN THE CRYSTAL

The dominant feature in this structure is the grouping of the molecules in spiral arrays about alternate twofold screw axes, the hydroxyl groups of successive pairs of molecules approaching each other to within the

remarkably short distances of 2.66 and 2.75 Å respectively. Owing to the slight uncertainty in the position of the hydroxyl group G, the difference in these distances is perhaps not significant. The alternative values for the coordinates of G, given in Table IV, make these distances of equal value, viz., 2.70 Å. The arrangement is best seen from fig. 8, which represents the c axis projection, and corresponds to the contoured map of fig. 2. The dotted lines indicate the short distances between the hydroxyl groups. The origin of the coordinates given in Table IV is at P, and these coordinates refer to molecule (1). The coordinates of the atoms in the other molecules (2), (3), and (4) can be obtained from the relations on p. 81. From these figures all the distances below 4 Å between the atoms of molecule (1) and the atoms of the surrounding molecules have been calculated and are given in Table V. Letters indicate the atoms, suffixes the molecule, and an accent indicates a molecule one translation along the c axis, which cannot be shown in the projection of fig. 8.

TABLE V—INTERMOLECULAR DISTANCES

Oxygen-oxygen:	H <sub>1</sub> G <sub>4</sub>	2.66 Å	Carbon-carbon:	E <sub>1</sub> B' <sub>1</sub>	3.59 Å
	G <sub>1</sub> H' <sub>2</sub>	2.75		B <sub>1</sub> A <sub>2</sub>	3.66
Oxygen-carbon:	D <sub>1</sub> G <sub>4</sub>	3.49		B <sub>1</sub> F <sub>2</sub>	3.68
	H <sub>1</sub> F <sub>4</sub>	3.51		B <sub>1</sub> B <sub>2</sub>	3.70
	H <sub>1</sub> A <sub>4</sub>	3.53		D <sub>1</sub> A <sub>4</sub>	3.75
	G <sub>1</sub> D' <sub>2</sub>	3.56		B <sub>1</sub> E <sub>2</sub>	3.75
	A <sub>1</sub> H <sub>2</sub>	3.57		B <sub>1</sub> C <sub>2</sub>	3.76
	G <sub>1</sub> C' <sub>2</sub>	3.57		B <sub>1</sub> D <sub>2</sub>	3.79
	G <sub>1</sub> B' <sub>1</sub>	3.65		E <sub>1</sub> C' <sub>2</sub>	3.82
	E <sub>1</sub> G <sub>4</sub>	3.66		C <sub>1</sub> A <sub>2</sub>	3.85
	F <sub>1</sub> H' <sub>2</sub>	3.78		F <sub>1</sub> B' <sub>1</sub>	3.88
	G <sub>1</sub> A' <sub>1</sub>	3.87		E <sub>1</sub> C' <sub>1</sub>	3.88
	F <sub>1</sub> H <sub>2</sub>	3.89		C <sub>1</sub> F <sub>2</sub>	3.90
	E <sub>1</sub> H' <sub>2</sub>	3.96		F <sub>1</sub> C' <sub>2</sub>	3.97
	B <sub>1</sub> H <sub>2</sub>	3.99		E <sub>1</sub> A <sub>4</sub>	3.97

There are clearly two distinct types of intermolecular approach. Between the hydroxyl groups the distance is about 2.7 Å. Then there is a gap, and the next minimum occurs between oxygen and carbon where there are several distances of about 3.5 Å, and then between carbon and carbon, where the distances range from 3.6 Å. These latter distances of 3.5 and 3.6 Å are characteristic of structures where only van der Waals forces are operative between adjacent atoms. But the distances between the oxygen atoms indicate hydroxyl bonds of the type recently discussed by Bernal and Megaw,\* each oxygen atom being closely connected to

\* Proc. Roy. Soc., A, vol. 151, p. 384 (1935).

two others on adjacent molecules. This view is confirmed by calculating the angles between the hydroxyl bonds indicated by the dotted lines in figs. 8 and 9. From the coordinates we obtain the values of the angles as

$$\begin{array}{ll} G_3H_1D_1 = 116\cdot3^\circ & H'_3G_4H_1 = 105\cdot5^\circ \\ D_1H_1G_4 = 116\cdot6^\circ & H_1G_4F_4 = 117\cdot8^\circ \\ G_4H_1G_3 = 101\cdot9^\circ & F_4G_4H'_3 = 130\cdot6^\circ \end{array}$$

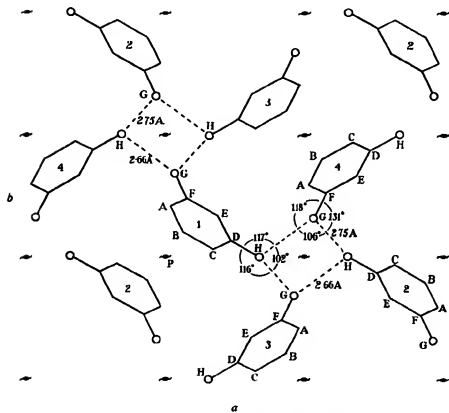


FIG. 8—*c* axis projection on the (001) plane.

It will be noted that all the angles except the last are fairly near the tetrahedral value of  $109\cdot5^\circ$ .

It should be especially noted that the dotted lines connecting the hydroxyl groups of molecules (1), (4), (2), (3), (1), in fig. 8, do not form a closed circuit connecting these four molecules, but are the projection of a spiral array ascending throughout the crystal. The return connexion  $G_3H_1$  leads to a molecule one translation along the *c* axis. The operation of

the glide plane of symmetry gives rise to a descending spiral (when taken in the same sense of rotation) about the other screw axis, shown in the upper left-hand part of the diagram. The arrangement will be clear from fig. 9, which gives the same array of molecules projected along the *b* axis.

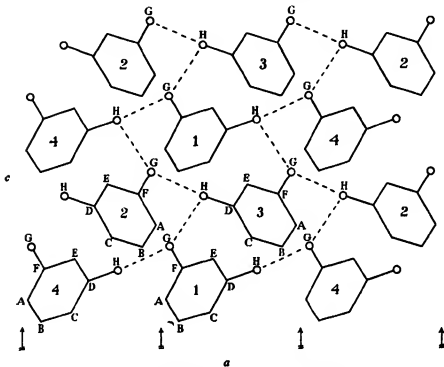


FIG. 9—*b* axis projection on the (010) plane

#### OTHER PHYSICAL PROPERTIES

The optical properties of the crystal recorded by Groth (*loc. cit.*) are consistent with the structure described above. The magnetic susceptibilities have recently been measured by Mrs. Lonsdale,\* and they are found to agree remarkably well with the orientation of the aromatic rings deduced in this analysis. Further work on the electrical properties of the crystal is proceeding.

In conclusion, I wish to thank Sir William Bragg, O.M., Pres. R.S., for his interest in this work, and the Managers of the Royal Institution for the facilities afforded at the Davy Faraday Laboratory. I am also much

\* 'Nature,' vol. 137, p. 826 (1936).

indebted to Miss Woodward for assistance in preparing the diagrams of this paper.

### SUMMARY

Resorcinol forms strongly polar crystals, space group  $C_{2h}^0$ (Pna), with four asymmetric molecules to the unit cell. A quantitative X-ray investigation based on absolute intensity measurements of about 100 reflexions from the axial zones has led to a complete determination of the structure, and the results have been refined by means of three double Fourier syntheses giving projections of the molecules along the crystal axes. The benzene rings are regular plane hexagons, the distance between the carbon atoms being  $1.39 \pm 0.01 \text{ \AA}$ . The centres of the hydroxyl groups (oxygen atoms) lie at  $1.36 \text{ \AA}$  from the centres of the ring carbon atoms. The orientation of the molecule and the coordinates of all the atoms are given.

In the crystal the molecules are grouped in spiral arrays about the two-fold screw axes, the hydroxyl groups of successive pairs of molecules approaching each other to within about  $2.7 \text{ \AA}$ , an intermolecular distance which indicates the presence of hydroxyl bonds. The minimum distances of approach between the other atoms on adjoining molecules (carbon to oxygen, and carbon to carbon) are all  $3.5 \text{ \AA}$  or more.

---

## Absorption Spectra of Four Aldehydes in the Near Infra-Red

By LOTTE KELLNER

(Communicated by A. O. Rankine, F.R.S.—Received 1 May, 1936)

### INTRODUCTION

It has been common knowledge for a considerable time that the infra-red spectra of organic molecules show a close resemblance to each other. It has been possible to attribute some of the bands in these spectra to inner vibrations of certain constituents of the molecules (O—H, C—H, C=O, etc.), and in recent years the analysis of the fundamental vibrations of relatively simple molecules has been accomplished. In the present paper an investigation of the absorption spectra of four aldehydes in the near infra-red is described. Hitherto, no attention has been given to the intensity of the absorption, the investigators have only been concerned with the determination of the positions of the bands. In this paper the absorption coefficient of each of the substances under investigation has been determined, in addition to the wave-lengths of the bands. Furthermore, an attempt is made to interpret the absorption frequencies as overtones and combination frequencies of some fundamental vibrations.

### DESCRIPTION OF APPARATUS

The spectrometer employed in the present investigation was a prism spectrometer of the type ordinarily used in infra-red spectroscopy. The silvered mirrors had a focal length of 69 cm and an aperture of 6.5 cm. The prism was of quartz of the Cornu type with a refracting angle of 59° 59' 0" and a base of 8.8 cm. A Wadsworth mirror served to maintain the minimum deviation of the light-beam. The light-sources employed were a gas-filled tungsten filament lamp of 1000 watts for wave-lengths between 1 and 2  $\mu$ , and a Nernst filament for wave-lengths greater than 2  $\mu$ . An iron-hydrogen resistance kept the current flowing through the Nernst filament constant. The light was focussed on the first slit of the spectrometer by a silvered mirror of 53 cm focal length and 9.6 cm aperture. The first slit was 0.15 mm wide, the second 0.14 mm. The range of wave-length entering the second slit then corresponded to a rotation of the prism through an angle of 20".

A Moll-thermopile in connexion with a Moll-galvanometer\* served as receiving apparatus. The slit of the thermopile was used as the second slit of the spectrometer. As the galvanometer was placed on a niche in the tiled wall of a basement room, no disturbances occurred. A 6-volt battery of large capacity furnished the current (*ca.* 0.9 amp) necessary for the electromagnet of the galvanometer. Readings of the deflexions of the galvanometer-mirror were taken by means of a scale and a telescope. The distance between the scale and the galvanometer was 2 metres.

The slit of the thermopile was covered by a quartz window and the whole thermopile kept air-tight. This precaution was necessary as the open thermopile was affected by the adiabatic fluctuations of the atmospheric pressure, which gave rise to deflexions of the galvanometer corresponding to several millimetres of scale reading. In order to protect the thermopile from extraneous changes of temperature, it was enclosed in a case which was stuffed with cotton wool, and cotton wool was wound round the wires which connected thermopile and galvanometer.

The whole spectrometer, including the thermopile, was enclosed in a wooden box to protect it from stray radiation. A brass shutter, which could be opened and shut from the seat of the observer, gave the light access to the spectrometer. If the lamp was left burning for at least three hours before the beginning of observations, the deflexions of the galvanometer-mirror were found to be constant to 0.1–0.2 mm of scale reading.

#### EXPERIMENTAL PROCEDURE

The prism was adjusted to give minimum deviation for the light of the yellow sodium lines and fixed in this position. A divided circle rotated together with the prism, and a vernier allowed the angle of rotation to be read with an accuracy of 20''. The observations of this angle were made from outside the box with the help of a totally reflecting prism mounted on the vernier, and a telescope. The angles were measured relative to the position of the prism when the unresolved yellow sodium lines coincided with the middle of the thermopile-slit. This position was noted before and after each set of measurements. The wave-lengths corresponding to the measured angles were determined in the following way. If  $\delta$  is the angle through which the light is deflected and  $\phi$  the refracting angle of the prism, we have for the refractive index  $n$ :

$$n(\lambda) = \frac{\sin \frac{1}{2}(\phi + \delta)}{\sin \frac{1}{2}\phi}. \quad (1)$$

\* 'Proc. phys. Soc.,' vol. 35, p. 253 (1923).

Taking the position of the yellow sodium lines as zero point, the value of  $\delta$  for any other line is obtained by adding twice the angle through which the prism must be turned to bring that line to the second slit. According to Schónrock,\* the refractive index of quartz is given by the formula (where  $\lambda$  is measured in  $\mu$ ):

$$n^2 = 3.5968913 + \frac{0.01064379}{\lambda^2 - 0.0106291} - \frac{138.20519}{111.45202 - \lambda^2}. \quad (2)$$

This formula is valid over the range of  $\lambda$  here investigated ( $\lambda = 0.71 - 2.4 \mu$ ). Using the equations (1) and (2), the values of  $\delta$  were plotted against the values of  $\lambda$  at intervals of  $0.001 \mu$ . In Table I the refractive indices of quartz are given together with the dispersive power, resolving power, and purity of the prism. If  $R^\dagger$  is the resolving power for an infinitely narrow slit,  $P$  is the resolving power for a finite slit-width (the purity), and  $D$  is the dispersive power, then

$$R = -p \frac{dn}{d\lambda}, \quad (3)$$

$$P = \frac{\lambda}{d\lambda} = \frac{\lambda}{\lambda + \psi d} R, \quad (4)$$

$$D = \frac{d\delta}{d\lambda} = \frac{R}{a}, \quad (5)$$

where  $p$  is the length of the base of the prism ( $= 8.8 \text{ cm}$ ),  $\psi$  is the angle subtended by the diameter of the collimating mirror at the slit,  $d$  is the width of the slit, and  $a$  is the breadth of the beam leaving the prism.

TABLE I

$\lambda$ in $\mu$	$n$	$R$	$P$	$D$ (in $\mu$ per $20'$ )
1.0973	1.53 366	1186	91	0.0053
1.3070	1.53 090	1140	105	0.0053
1.4972	1.52 842	1184	121	0.0053
1.9000	1.52 263	1394	200	0.0045
2.1000	1.51 927	1534	211	0.0041

In order to verify the method of calibration mentioned above, an observation of the absorption curve of water was made. The following values were found for the positions of the maxima of absorption (Table II).

\* "Z. InstrumKde," vol. 48, p. 275 (1928).

† Baly, "Spectroscopy," vol. 1.

The agreement of the present observations with those of other authors is satisfactory. The values given in Table II lie between the greatest and smallest wave-lengths which have been hitherto recorded.

TABLE II

Values found	Previous observations	Mean values of previous observations
$\lambda$ in $\mu$	$\lambda$ in $\mu$	$\lambda$ in $\mu$
0.988	0.97 Collins* 0.99 Ellis† 0.995 Dreisch‡	0.985
1.200	1.20 Collins 1.185 Ellis 1.21 Dreisch	1.198
1.470	1.44 Collins 1.44 Ellis 1.475 Dreisch 1.48 Grantham§ 1.48 Coblenz	1.463
1.957	2.00 Collins 1.96 Ellis 1.97 Dreisch 1.98 Grantham 1.95 Coblenz	1.972

\* "Phys. Rev.", vol. 36, p. 305 (1930).

† "J. opt. Soc. Amer.", vol. 8, p. 1 (1924).

‡ "Z. Physik," vol. 30, p. 200 (1924).

§ "Phys. Rev.", vol. 18, p. 339 (1921).

|| "Investigation of Infra-Red Spectra," Washington (1905-10).

The absorption of four aldehydes in the liquid state was investigated, viz., propionic aldehyde, butyric aldehyde, valeric aldehyde, iso-valeric aldehyde. The absorption cells were rectangular frames of brass,  $2 \times 4$  cm and of varying thickness. Two quartz windows, which were twice as long as the frame, were sealed to the two sides of a cell, so as to enclose the liquid. The cell was mounted in a holder, which was placed inside the box immediately before the first slit. This holder was free to slide on two rails so that either the cell containing the liquid or the projecting empty ends of the windows was before the slit: two stops kept it in position. Using a micrometer, the thickness of the quartz windows was measured first and the thickness of the whole filled cell determined after each set of

readings. The difference between these two widths gave the thickness of the absorbing liquid.

The aldehydes under investigation were obtained from the British Drug Houses, Ltd., with the exception of the *iso*-valeric aldehyde which came from the Eastman Kodak Company, Rochester, U.S.A.

The procedure of observation was as follows. After the prism had been set for the desired wave-length, several readings of the deflexions of the galvanometer-mirror were taken alternately with the absorption cell before the slit and then with the quartz windows in the same position. In this way, error due to the loss of radiation through reflexion in the quartz was eliminated, as the light passed both times through the windows. If the average deflexion is  $D_1$  for the cell before the slit and  $D_2$  for the windows before the slit, the transmission  $T$  of the absorbing layer is defined as:

$$T = \frac{D_1}{D_2}, \quad (6)$$

$T$  defined in this way is independent of the intensity of the incident light for the values obtained in this investigation.

The absorption of the aldehydes was investigated between 1.1 and 2.1  $\mu$ . Each spectrum was taken with three cells of different thicknesses (10, 7, and 5 mm up to 1.6  $\mu$  and 3, 2, and 1 mm from 1.6 to 2.1  $\mu$ ). The maxima of absorption, as indicated by the agreement of the results with different thicknesses of liquids, could be determined with an accuracy of  $\pm 0.005 \mu$ . From the values for the transmission  $T$ , the molecular absorption coefficient  $\alpha$  was calculated according to the formula:

$$T = e^{-\frac{\alpha}{M} d}, \quad (7)$$

where  $d$  is the thickness of the absorbing layer in cm and  $M$  the molecular weight of the substance under investigation. Since the densities of the liquids examined were almost identical, the molecular absorption coefficient gives the absorption per equal number of molecules. No correction was made for the losses through reflexion at the surfaces of the liquid as no data are available for the refractive indices of the aldehydes in this spectral region. The limits of accuracy of the absorption coefficient were  $\pm 7\%$  for the maxima of absorption and  $\pm 10\%$  for the minima. It follows that the determinations of the shapes of the bands are not very exact.

#### EXPERIMENTAL RESULTS

In Table III the positions in wave-numbers  $\nu$  of the maxima of the bands are given, together with the data of previous investigations and also the corresponding absorption coefficients.

TABLE III—DATA FOR ABSORPTION OF ALDEHYDES

Propionic aldehyde	Absorption maxima		Butyric aldehyde		Valeric aldehyde		Absorption maxima		Iso-valeric aldehyde		
			Absorption maxima		Absorption coefficient		maxima coefficient		Absorption maxima		
	I	II	I	II	x	y	x	y	I	a	
Ellis*	v	v	v	v	Ellis*	Sappenfield†	x	y	v	v	
8643	8621	36	—	8621	8370	—	8636	65	—	—	
8051	8064	17	8137	8000	7855	61	8137	20	8104	81	
7036	(6849)	70	7117	'7143,	'6944,	7052	68	7067	97	7008	83
5942	—	232	5956	—	—	95	6035	36	6024	75	
5740	—	292	5754	—	5741	351	5701	455	5714	518	
—	—	—	5647	—	—	440	5593	402	5593	470	
5197	5236	282	5249	5236	5261	345	5258	264	5280	320	
5155	5102	358	5149	5102	5147	348	5131	241	5149	325	
4888	—	241	4798	—	4808	267	4822	320	4796	320	
4748	—	431	4762	—	—	304	4764	334	4713	397	

\* J. Amer. Chem. Soc., vol. 51, p. 1384 (1929).

† Phys. Rev., vol. 33, p. 37 (1929).

For the first two aldehydes the figures in column I represent the results of the present paper, and those in column II the results obtained by other authors. Valeric and *iso*-valeric aldehydes have not been investigated before. The data given by Ellis and Sappenfield on propionic and butyric aldehyde agree satisfactorily with the present results. The only serious discrepancy occurs with butyric aldehyde in the region 8000–9000. Here Ellis and Sappenfield found two bands, while one only could be found in the present investigation, though the region has been gone over nine times with two different samples of butyric aldehyde. Sappenfield found

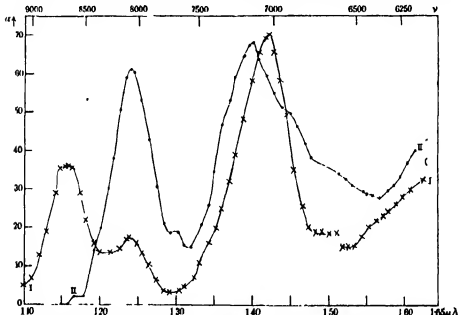


FIG. 1.—Molecular absorption of propionic and butyric aldehydes between 110 and 165  $\mu$ .  $\alpha$  propionic aldehyde, curve I  $\bullet$  butyric aldehyde, curve II.

that the band at 8370 is far stronger than the band at 7855, as occurs with propionic and valeric aldehyde (Table III). However, in the present investigation the band of butyric and *iso*-valeric aldehyde in the region 8000–8100 presumably corresponding to Sappenfield's 7855, was found to be much more intense than the corresponding band of propionic and valeric aldehyde and of the same order of intensity as the band 8600. It is not possible to give an explanation for this dissimilarity.

Ellis was able to resolve the broad band in the region 7200 to 6800 into two components for butyric aldehyde. In the present investigation only *iso*-valeric aldehyde showed a (probably incomplete) separation of this band, but it is very likely that with higher resolving power it would be

separated into several components. A glance at figs. 1 and 2 shows indications that this band is complex.

The very broad and intense band at  $1\cdot74\mu$  (between  $\nu$  6000 and  $\nu$  5600) has been resolved into three components, though the resolution is by no means complete. Sappenfield gives here only one broad band, though his spectrometer had a resolving power approximately three times as great. But as his apparatus was provided with an automatically registering device, it is possible that the spectrum was moved too quickly

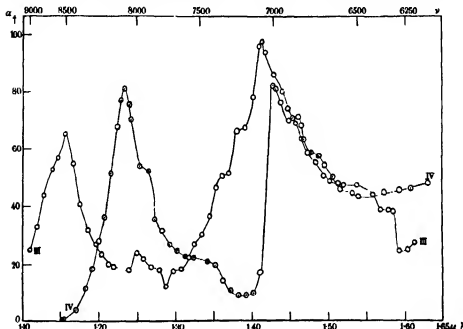


FIG. 2—Molecular absorption of valeric and iso-valeric aldehydes between  $1\cdot10$  and  $1\cdot65\mu$ . O valeric aldehyde, curve III.  $\odot$  iso-valeric aldehyde, curve IV.

across the slit of the thermopile, so that the components could not be properly separated.

In figs. 1-4 the absorption coefficients have been plotted against the wave-lengths for the various aldehydes. On the upper axes of the diagrams the wave-numbers  $\nu$  are given.

Fig. 1 shows the absorption of propionic aldehyde ( $\text{CH}_3\cdot\text{CH}_2\cdot\text{CHO}$ ) and butyric aldehyde ( $\text{CH}_3\cdot\text{CH}_2\cdot\text{CH}_2\cdot\text{CHO}$ ) between  $1\cdot1$  and  $1\cdot6\mu$ , and fig. 2 that of valeric aldehyde ( $\text{CH}_3\cdot\text{CH}_2\cdot\text{CH}_2\cdot\text{CH}_2\cdot\text{CHO}$ ) and iso-valeric aldehyde ( $\text{CH}_3\cdot\text{CH}_2\cdot\text{CH}\cdot\text{CH}_2\cdot\text{CHO}$ ) in the same region. The absorption curve of butyric aldehyde shows a stronger background than that of propionic aldehyde, while the peak at  $1\cdot4\mu$  reaches nearly

the same height. Comparison of the absorption below  $1\cdot3\mu$  would lead to no definite conclusions in consequence of the differences mentioned above. From a comparison of curve II, fig. 1, and curve III, fig. 2, it will be seen that valeric aldehyde shows the same background as butyric aldehyde, but that the maximum absorption at  $1\cdot4\mu$  is greater. *Iso*-valeric aldehyde (curve IV, fig. 2) has on the whole a weaker absorption than the normal compound, with the exception of the band at  $1\cdot23\mu$ .

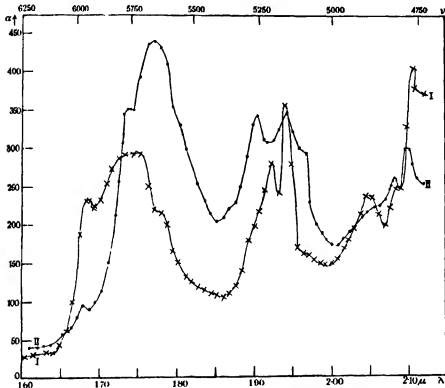


FIG. 3—Molecular absorption of propionic and butyric aldehydes between  $1\cdot60$  and  $2\cdot15\mu$ .  $\times$  propionic aldehyde, curve I.  $\bullet$  butyric aldehyde, curve II.

The intensity of the  $1\cdot4\mu$  band decreases very rapidly towards larger frequencies.

In figs. 3 and 4 similar curves are given for the region between  $1\cdot6$  and  $2\cdot1\mu$ . Butyric aldehyde has a greater absorption coefficient than propionic aldehyde below  $2\cdot07\mu$  (fig. 3). The intensity of the bands at  $1\cdot7\mu$  is nearly the same for butyric aldehyde as for valeric aldehyde, but the latter shows smaller absorption for the region between  $1\cdot8$  and  $2\cdot0\mu$  and greater intensity above this wave-length. It follows from a comparison of curves III and IV, figs. 2 and 4, that an alteration in the molecular

configuration has no influence on the positions of the bands in this spectral region. Except for the doubtful region below  $1\cdot 3 \mu$ , the curve for *iso*-valeric aldehyde runs almost parallel to that for valeric aldehyde (fig. 4), and the shapes of the corresponding bands are very similar to each other. From  $1\cdot 6$  to  $2 \mu$  the *iso*-compound has a stronger absorption than the normal compound. The shifts which occur in the positions of the bands are mostly within the limits of experimental error. Where they are greater, they do not show any marked regularities (Table III).

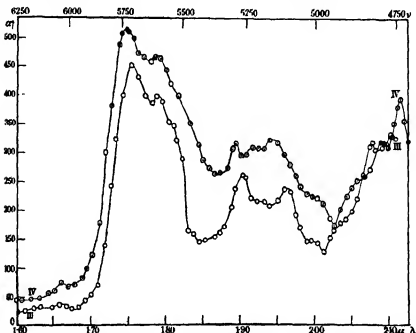


FIG. 4—Molecular absorption of valeric and *iso*-valeric aldehydes between  $1\cdot 60$  and  $2\cdot 15 \mu$ . O valeric aldehyde, curve III.  $\odot$  *iso*-valeric aldehyde, curve IV.

#### DISCUSSION

The striking feature of the band spectra of the four aldehydes is the great similarity in the numbers and positions of the bands. This similarity suggests a corresponding similarity of the oscillating centre. The vibrations,\* which are independent of the configuration of the molecule, are the oscillations lying outside the upper and lower limits of the C—C valence frequencies, i.e.,  $\nu\nu$  836–1185. For the aldehydes, these independent oscillations are the inner vibrations of the  $\text{CH}_3$  and  $\text{CH}_2$  groups respec-

\* Bartholomé and Teller, 'Z. phys. Chem.', B, vol. 19, p. 366 (1932).

tively, and the valence vibration of the C=O bond. In the region between 1 and 2  $\mu$  we are dealing with the overtones and combination tones of these fundamentals. As the chain frequencies are very far off and of relatively low intensity, their overtones will not appear in our spectra. In Table IV the wave-numbers of the fundamentals are given which are necessary for the analysis of the observed spectra.

TABLE IV—WAVE-NUMBERS OF FUNDAMENTALS OF C=O AND CH VIBRATIONS

Propionic aldehyde	Butyric aldehyde	Valeric aldehyde	<i>Iso</i> -valeric aldehyde	Mode of vibration
1377 L↑	1366 L↑	(1390) K‡	1361 L↑	$\delta(\pi)_{\text{CH}}$
1439	1445	(1448)	1445	* $\delta(\sigma)_{\text{CH}}$
1695	1695	(1717)	1695	$\nu_{\text{C}=\text{O}}$
2841	2882	(2874)	2865	$\nu_{\text{C}\text{H}}$

The data in the first, second, and fourth columns, which are marked with "L", are taken from Lecomte's\* investigation. As no measurements of the infra-red spectrum of valeric aldehyde have been made, the data of the Raman lines are given in brackets in the third column.† In the last column the bands are assigned to different modes of vibration. The symbols  $\delta$ ,  $\nu$  refer to bending and valence frequencies respectively. The index C=O or CH indicates which group is oscillating. The change of the dipole moment, whether perpendicular ( $\sigma$ ) or parallel ( $\pi$ ) to the axis of the molecule, is also shown. The fundamental of the C=O valence vibration at 1695 is well known from the infra-red and Raman spectra of aldehydes, ketones, and fatty acids. In assigning 1360 to  $\delta(\pi)_{\text{CH}}$  and 1440 to \* $\delta(\sigma)_{\text{CH}}$  (the index \* at the left side of  $\delta$  means that the vibration is doubly degenerate), I have followed Bartholomé and Sachsse‡ in their interpretation of the fundamentals of  $\text{CH}_3\cdot\text{OH}$  and  $\text{C}_2\text{H}_6$ . In formic aldehyde (H·CHO) we have a parallel band at 1500 and a perpendicular band at 1340.§ As, however, the molecule H·CHO must be considered as a whole for the interpretation of its vibrational spectrum, while in more complicated molecules the CH groups may vibrate independently of the rest, it seemed justifiable to assume that the oscillations in an aldehyde molecule resembled the oscillations of the same group in other compounds. In any case, the assignment can only be a preliminary

\* 'C R. Acad. Sci. Paris,' vol. 180, p. 1481 (1925).

† Kohlrausch and Koppl, 'Z. phys. Chem.,' B, vol. 24, p. 370 (1934).

‡ 'Z. phys. Chem.,' B, vol. 30, p. 40 (1935).

§ Nielsen, 'Phys. Rev.,' vol. 46, p. 117 (1934).

one.  $^{1\delta}(\sigma)_{\text{CH}}$  and  $\nu_{\text{CH}}$  are common to the  $\text{CH}_3$  group and the  $\text{CH}_2$  group.\* In the Raman spectrum there is a second  $\text{CH}$  valence vibration at 2960 besides the one at 2880 given above (Table IV). As this vibration is not infra-red active, it has not been taken into account here. Table V represents an attempt at interpreting the bands between 1 and 2  $\mu$  as overtones and combination tones of the fundamentals given in Table IV. The interpretation of the bands at 5150, 6800, and 8100 as overtones of  $\nu_{\text{C}-\text{O}}$  has been previously proposed by Ellis.†

TABLE V—INTERPRETATION OF OBSERVED BAND SPECTRA

Assignment	Propionic		Butyric		Valeric		<i>Iso</i> -valeric	
	aldehyde		aldehyde		aldehyde		aldehyde	
$2\nu_{\text{C}-\text{O}} + \delta(\pi)_{\text{CH}}$	4748	4767	4762	4696	4764	(4824)	4713	4751
$2\nu_{\text{C}-\text{O}} + ^{1\delta}(\sigma)_{\text{CH}}$	4888	4829	4798	4775	4822	(4882)	4796	4833
$3\nu_{\text{C}-\text{O}}$	5155	5085	5149	5085	5131	(5151)	5149	5085
$4\delta(\pi)_{\text{CH}}$ (?)	5197	5508	5249	5464	5258	(5560)	5280	5444
$2\nu_{\text{H}}$	—	5682	5647	5764	(5593	(5748)	5593	5730
$\nu_{\text{H}} + 2^{1\delta}(\sigma)_{\text{CH}}$	5740	5729	5754	5772	5701	(5770)	5714	5755
$4^{1\delta}(\sigma)_{\text{CH}}$	5942	5756	5956	5780	6035	(5792)	6024	5780
$4\nu_{\text{C}-\text{O}}$	6780		6780			(6868)	6863	6780
$2\nu_{\text{H}} + \delta(\pi)_{\text{CH}}$	7036	7059	7117	7130	7067	(7138)	7091	
$2\nu_{\text{H}} + ^{1\delta}(\sigma)_{\text{CH}}$		7121		7209		(7196)	7008	7175
$5^{1\delta}(\sigma)_{\text{CH}}$		7195		7225		(7240)		7225
$6\delta(\pi)_{\text{CH}}$ (?)	8051	8262	8137	8196	8137	(8340)	8104	8166
$5\nu_{\text{C}-\text{O}}$ (?)		8475		8475		(8585)		8475
$3\nu_{\text{CH}}$		8523		8646		(8622)		8595
$2\nu_{\text{H}} + 2^{1\delta}(\sigma)_{\text{CH}}$	8643	8560	—	8654	8636	(8644)	—	8620
$6^{1\delta}(\sigma)_{\text{CH}}$		8634		8670		(8688)		8670

The overtones of  $\nu_{\text{CH}}$  show resonance degeneracy with the overtones of  $^{1\delta}(\sigma)_{\text{CH}}$  and the combination tones of both. That accounts for the fact that the band at 7000 has approximately the same intensity as the band at 8600, though the latter should be weaker, belonging to a higher quantum number. The assignment of 5250 to  $4\delta(\pi)_{\text{CH}}$  is somewhat doubtful as the agreement between calculated and observed values is not good. Besides, the band does not appear in the spectra of molecules containing only carbon and hydrogen atoms.

Ellis† tried to arrange the  $\text{CH}$  bands in a series of overtones of  $\nu_{\text{CH}}$  only. This interpretation did not explain the presence of the band at 7000. As

\* Dennison and Sutherland, ' Proc. Roy. Soc.,' A, vol 148, p. 250 (1935).

† 'J. Amer. Chem. Soc.,' vol. 51, p. 1384 (1929).

‡ 'Phys. Rev.,' vol. 33, p. 27 (1929).

this band appears in the spectra of molecules containing carbon and hydrogen atoms only, it follows that it must be due to vibrations of these constituents.

In view of the fact, however, that the separation of the bands into their components is by no means complete, any assignment can only be regarded as tentative.

The aldehydes under investigation, with the exception of *iso*-valeric aldehyde, differ from one another by the number of CH<sub>3</sub> groups. If the CH<sub>3</sub> groups are the oscillating centres, we might expect an increase in the absorption coefficient of the bands with increasing number of CH<sub>3</sub> groups, while a frequency caused by the vibrations of the C=O group should not be affected. This assumption would mean that the molecular absorption coefficient, as it determines the absorption for equal numbers of molecules, should increase from propionic to valeric aldehyde for vibrations in which the CH groups take part. If we look at the C=O frequencies (Tables III and V), we find that the intensity of 3v<sub>C=O</sub> ( $\nu = 5150$ ) remains of the same order with the exception of valeric aldehyde. It is not possible to compare the intensities of 4v<sub>C=O</sub> as this band has not been separated from the neighbouring CH vibrations.

If we now proceed to the CH vibrations, we find that the overtones and combination tones of  $^{28}(\sigma)_{\text{CH}}$  and v<sub>CH</sub> are so near to each other that disturbances by resonance between the different vibrational levels are very likely to occur (Table V). The only bands which show a regular increase in intensity are 5700 and 4800 (Tables III and V). However, the increase continues to *iso*-valeric aldehyde, though *iso*-valeric aldehyde contains one CH<sub>3</sub> group less than valeric aldehyde.

I wish to express my gratitude to Professor G. P. Thomson and Dr. Herbert Dingle for placing the laboratory facilities of the Imperial College at my disposal. Furthermore, I am very much indebted to the Central British Fund for German Jewry for a grant awarded to me which enabled me to carry out these investigations.

#### SUMMARY

An investigation has been made of the infra-red absorption spectra of propionic, butyric, valeric, and *iso*-valeric aldehydes in the liquid state between 1.1 and 2.1  $\mu$ . The wave-numbers and absorption coefficients are tabulated and compared with previous observations.

An attempt is made to interpret the observed bands as overtones and

combination tones of the inner vibrations of the CH<sub>3</sub> and CH<sub>2</sub> groups respectively and the C=O valence vibration. It is suggested that four fundamentals are sufficient to explain all observed bands.

It is not possible to find a relation between the intensity of the bands and the number of oscillating centres, as most of the vibrational levels lie so close together that resonance occurs.

---

## The Crystal Structure of H<sub>3</sub>PW<sub>12</sub>O<sub>40</sub> · 29H<sub>2</sub>O

By A. J. BRADLEY, D Sc., Royal Society Warren Research Fellow, and  
J. W. ILLINGWORTH, M.Sc.

(Communicated by W. L. Bragg, F.R.S—Received 1 May, 1936)

The special interest of this structure lies in the peculiar manner in which the anions (PW<sub>12</sub>O<sub>40</sub>)<sup>-3</sup> are linked together by the water molecules. The remarkable number (29) of water molecules associated with each anion is accounted for by symmetry considerations. Alternating with the anions on a body-centred cubic lattice, seventeen molecules of water are linked together in tetrahedral symmetry. These comprise a central molecule in contact with four molecules at the corners of a tetrahedron, and twelve molecules strung out in pairs along fourfold cube axes, to link together six anions. Midway between two blocks of seventeen waters and independent of them, six water molecules form a puckered hexagonal ring, which links together six anions, lying symmetrically about a threefold axis. For each anion there are two hexagonal rings and one block of seventeen molecules. This accounts for the total of 29 molecules per anion.

The environment of the water molecules is in striking contrast with that of the oxygen atoms in the anions. The latter are close-packed, being held together by the phosphorus and tungsten atoms. The water molecules are more open, and only six of the 29 have more than four nearest neighbours. The interatomic distances of the water molecules are very consistent, all lying between 2.8 Å and 2.9 Å.

In conformity with the space-group O<sup>7</sup>h, the structure is composed of two interpenetrating diamond lattice-complexes. The one consists of eight anions (PW<sub>12</sub>O<sub>40</sub>)<sup>-3</sup>; the other consists of eight clusters of water

molecules together with the acidic hydrogen ( $H_3 \cdot 29H_2O$ )<sup>+3</sup>. The structure may therefore be regarded as a regular alternation of anions and cations. Each anion is identical with the anion found by Keggin in the 5-hydrate.

A unique feature of the investigation is that the structure was determined entirely from one powder photograph. This was taken by Keggin in a camera 19 cm in diameter, using special methods in order to attain high accuracy. We have based the structure on intensity measurements from this photograph, and the correctness of the structure rests on the extremely close agreement between the observed and calculated intensity. Alternative arrangements were unable to give such close agreement.

#### PREVIOUS WORK

(a) *The Anion (PW<sub>12</sub>O<sub>40</sub>)<sup>-3</sup>*—The first 3-dimensional structural formula for the 12 heteropoly acids was suggested by Pauling\* on theoretical grounds. Then Hoard† investigated the structure of the higher hydrate of phosphomolybolic acid and some of its rare earth salts. Laue and oscillation photographs showed that the acid was cubic, the cell dimensions being in each case about 23 Å, and the symmetry probably O<sup>7</sup>h. He could not obtain even an approximate agreement between the observed intensities and those calculated using Pauling's model anion.

With the help of the X-ray powder method, Keggin‡ determined the structure of the anion (PW<sub>12</sub>O<sub>40</sub>)<sup>-3</sup> in the very stable, partially dehydrated acid H<sub>3</sub>PW<sub>12</sub>O<sub>40</sub> · 5H<sub>2</sub>O. This substance is produced in powder form by a partial dehydration of the higher hydrate, which crystallizes from aqueous solution in beautiful octahedral crystals. Since approximately 24 molecules of water are lost in the process of drying, the formula of the higher hydrate is most probably H<sub>3</sub>PW<sub>12</sub>O<sub>40</sub> · 29H<sub>2</sub>O. A powder photograph of this hydrate indicates a diamond-like pattern. From intensity measurements Keggin concluded that the anion (PW<sub>12</sub>O<sub>40</sub>)<sup>-3</sup>, first identified by him in the 5-hydrate, was also present in the 29-hydrate, the centre of each anion corresponding to each point of the diamond-like pattern. The object of the present investigation is to fix the mutual orientations of the anions and to determine the positions of the 29 water molecules.

The anion (PW<sub>12</sub>O<sub>40</sub>)<sup>-3</sup> is a coordinated structure of point group symmetry T<sub>d</sub>; it consists of a central PO<sub>4</sub> tetrahedron, surrounded by

\* 'J. Amer. Chem. Soc.', vol. 51, p. 2868 (1929).

† 'Z. Kristallog.', vol. 84, p. 217 (1933).

‡ 'Proc. Roy. Soc.,' A, vol. 144, p. 75 (1934); 'Nature,' vol. 132, p. 351 (1933).

twelve slightly distorted  $WO_6$  octahedra, linked together by shared oxygen atoms. The twelve tungsten atoms are situated on the twelve edges of a cube, at the centre of which lies the phosphorus atom. In conformity with  $T_d$  symmetry, the tungsten atoms are slightly displaced from the most symmetrical positions at the midpoints of the cube edges, but the extent of the displacement is difficult to determine in the lower hydrate, as it has little effect on the intensities of the lines in the powder photograph. The arrangement of the oxygen atoms can be seen in fig. 1, which represents a schematic picture of an anion. Signer and Gros,\* and Illingworth and Keggin† showed that the 5-hydrates of other acids contained similar anions.

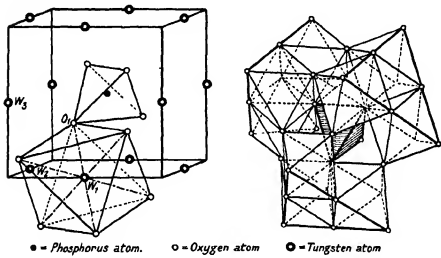


FIG. 1.

(b) *The 5-Hydrate Packing*—In the partially dehydrated acids, with the 5-hydrate structure, the packing is cubic with two molecules per unit cube and space group  $O^h$ . The relative position of the anions is such that the central phosphorus atoms lie on a body-centred cubic lattice as shown in fig. 2. The structure is, however, inconsistent with a body-centred cubic space-group, because the anions are not spherical but tetrahedral, and they do not all point the same way. The surface of the anion may be considered to be made up of six cube faces and eight octahedral faces. The latter consist of four approximately flat faces (heavily outlined in fig. 1) and four re-entrant faces. The anions are

\* 'Helv. Chim. Acta,' vol. 17, p. 1076 (1934).

† 'J. Chem. Soc.,' p. 575 (1935).

linked together diagonally by adjacent octahedral faces. Each of the four flat faces is directly linked to a flat face of a neighbouring anion; each of the four re-entrant faces is linked to a water molecule lying on a threefold axis. These water molecules therefore serve to bind together the re-entrant octahedral faces of adjacent anions. In addition the unit cube contains six water molecules lying at the centres of faces and edges. These occupy the spaces between neighbouring anions. To sum up, each anion has fourteen neighbours. Four are linked directly, flat to flat, four indirectly through water molecules; six are unattached leaving holes big enough for water molecules.

It is possible to imagine a modified structure in which all the anions face the same way so that they are joined flat to re-entrant. The structure would belong to the body-centred space-group  $T_d^3$  which is distinguished from  $O^3h$  by the absence of reflexions for which  $h + k + l$  is odd. In fact, faint lines 441 and 621 may be observed on the powder photographs of all the 5-hydrate compounds. Keggin's\* powder photographs from a specimen of  $H_3PW_{12}O_{40} \cdot 5H_2O$  dehydrated over  $P_2O_5$  has fuzzy doublets and 441 and 621 were scarcely visible. Santos† showed that by heating for a few hours at  $120^\circ C$ , the doublets became sharp and the odd lines strengthened. These intensity changes suggest that heating helps to turn all the anions into the correct directions, whereas in the unheated material some have an incorrect orientation. Santos also examined the caesium salts of the 12 acids and found essentially the same structures as for the acids. The caesium ions replace water molecules in cube faces. The water molecules on threefold axes are absent and the volume of the unit cell is correspondingly smaller.

(c) *The 29-Hydrate Packing*—From measurements of a powder photograph taken in a camera of 19 cm diameter Keggin found a cubic structure of unit cell  $23\cdot28$  Å. This cell contains eight molecules of composition  $H_3PW_{12}O_{40} \cdot 29H_2O$ . The powder photograph gives only reflexions from planes with  $h + k + l = 4n$  or  $h^* + k^* + l^* = 8n + 3$ . This indicates a diamond lattice complex ( $O^3h$ ). The combination of eight anions ( $PW_{12}O_{40}$ )<sup>-3</sup>, of point symmetry  $T_d$ , on the diamond lattice complex ( $O^3h$ ) gives a structure belonging to the space group  $O^3h$ . The special missing spectra for this space group are  $0kl$ , where  $k = 2n$ ,  $l = 2n$ , and  $k + l = 4n + 2$ , e.g., 020, 042, 640, etc. These are special cases of reflexions of the type  $h + k + l = 4n + 2$ , none of which can be observed on the powder photograph. The conditions for the space-group  $O^3h$  are therefore fulfilled.

\* Proc. Roy. Soc., A, vol. 144, p. 75 (1934).

† Proc. Roy. Soc., A, vol. 150, p. 309 (1935).

The missing spectra of the type  $0kl$  where  $k = 2n$ ,  $l = 2n$ , and  $k + l = 4n + 2$ , cannot be used as a definite criterion, because the photograph does not register very weak reflexions. The special parameter values of the tungsten atoms reduce all reflexions of the type  $k + l = 4n + 2$  below the visibility limit, both for space-groups  $T_d^3$  and  $O^7h$ . The choice of space-group can, however, be made from intensity measurements.

Being kindly provided with intensity measurements from Keggin's powder photograph, we have tested various possible arrangements for the anions and water of crystallization. Our calculations prove the identity of the anions in the 5- and 29-hydrates, and show how they are



FIG. 2.

attached to one another by the water molecules. They further enable us to predict possible positions for metal radicles in salts of analogous structure, which are the subject of further investigation.

#### A GENERAL ACCOUNT OF THE 29-HYDRATE STRUCTURE

The presence of reflexions of only two types  $h^2 + k^2 + l^2 = 8n$  and  $h^2 + k^2 + l^2 = 8n + 3$ , indicates that the eight molecules in the unit cube follow a diamond-like arrangement, such as is indicated by the white or black circles in fig. 3. This figure shows two interpenetrating diamond lattice complexes which together form an eightfold body-centred cubic structure. In the 5-hydrate *every point* of this structure corresponds to the centre of an anion, whereas in the 29-hydrate only *alternate points* (white circles) correspond to anions, the remainder (black circles) being allotted to groups of water molecules. If we may include among the latter the three protons, which must balance the negative charges on the anions, the 29-hydrate structure may be regarded as built up of equal numbers of oppositely charged ions  $(\text{PW}_{12}\text{O}_{40})^{-3}$  and  $(\text{H}_3 \cdot 29\text{H}_2\text{O})^{+3}$ , lying on two interpenetrating diamond lattices.

Every point on a body-centred cubic lattice has fourteen neighbours, eight diagonally along threefold axes and six along fourfold axes. In the structure of fig. 3, ten neighbours are of opposite type and four neighbours of the same type. Quite apart from the relation between the water molecules and the anions, it is necessary to fix the relative orientation of each anion to its four neighbouring anions. This may be done from a comparison of the intensities of reflexion with  $h^2 + k^2 + l^2 = 8n + 3$ . Once this relationship has been settled, it is possible to find the grouping of the water molecules from spatial considerations. Here

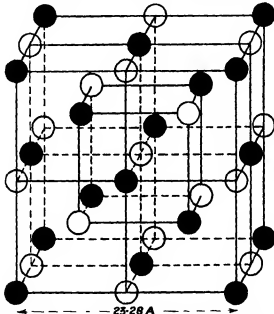


FIG. 3—Anions ( $\text{PW}_{12}\text{O}_{40}$ ) $^{4-}$  and cations ( $\text{H}_3\cdot 29\text{H}_2\text{O}$ ) $^{+3}$  shown as black and white circles.

the intensity measurements are used to decide between two alternative arrangements and finally help to fix the atomic coordinates.

#### THE RELATIVE ORIENTATION OF THE ANIONS IN $\text{H}_3\text{PW}_{12}\text{O}_{40} \cdot 29\text{H}_2\text{O}$

In consequence of the tetrahedral character (point symmetry  $T_d$ ) of the anions (see fig. 2), they may be fitted together in three different ways. If the space-group is  $T_d^2$ , they may all point the same way and the flat octahedral surface of one anion faces the re-entrant octahedral surface of the neighbouring anion. To agree with the holohedral space-group  $O\bar{h}$ , either a re-entrant faces a re-entrant or a flat faces a flat. Table I

shows the intensity data for the lines with  $h^2 + k^2 + l^2 = 8n + 3$ .<sup>\*</sup> The observed values corrected for absorption<sup>†</sup> and temperature factors<sup>‡</sup> are compared with calculated values for the three types of orientation. The values cannot be expected to agree very well since no allowance is made at this stage for the water of crystallization. However, it is clear that the arrangement of re-entrant to re-entrant gives the best general

TABLE I—INTENSITIES COMPARED FOR THREE ORIENTATIONS OF THE ANIONS

$hkl$	$\Sigma h^2$	Observed intensity	Calculated intensities		
			Re-entrant to re-entrant	Re-entrant to flat	Flat to flat
331	19	5	8	6	4
333 511}	27	12	17	12	8
531	35	7	9	12	15
533	43	14	12	18	24
711 551}	51	7	11	10	10
731 553}	59	32	29	29	29
733	67	3	1	4	6
751 555}	75	51	46	40	33
911 753}	83	29	31	40	50
Total differences, observed - calculated (without regard to sign)		.	28	39	71

agreement, as may be seen by adding all the arithmetic differences between observed and calculated values. These differences are much less for the re-entrant to re-entrant solution. It may be noted that the scale of values is chosen to correspond to an experimental accuracy of about one unit.

\* Only those reflexions are compared which give different calculated intensities for the three orientations of the anions.

† Bradley, 'Proc. Phys. Soc.', vol. 47, p. 879 (1935).

‡ Debye, 'Ann. Physik,' vol. 43, p. 49 (1914).

## THE WATER OF CRYSTALLIZATION

The number 29 for the molecules of water of crystallization associated with the anion  $(PW_{12}O_{40})^{-2}$ , deduced by Keggin, is in agreement with the mass of chemical evidence, which gives either 29 or 30. We therefore tried to find a way of arranging 29 molecules, in accordance with the point symmetry of the anions ( $T_d$ ), to fill a space roughly equivalent to that occupied by an anion. We may regard the problem in the following way: Suppose that the volume of the unit cell is divided symmetrically into sixteen equal units of volume or polyhedra, each corresponding to a

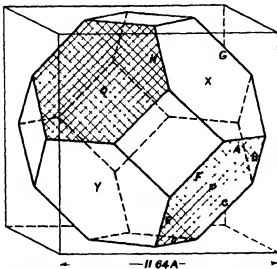


FIG. 4—Volume allotted to a single anion or cation shown as a polyhedron.

point of a body-centred cubic lattice (compare fig. 3). Each polyhedron is bounded by six cube faces and eight octahedral faces, as shown in fig. 4. An anion (fig. 2) fits comfortably into such a polyhedron, and the surfaces of the anion lie roughly parallel to the surfaces of the polyhedron, cube face to cube face, and octahedral face to octahedral face. It is required to fit a group of 29 water molecules into a similar polyhedron.

The problem is extraordinarily like that of  $\alpha$ -manganese when a cluster of 29 atoms takes exactly this shape.\* There the atoms fall into the following groups: two groups of 12 lie on planes of symmetry, a group of four lies on threefold axes, and a single atom lies at the very centre of the polyhedron. Other arrangements are theoretically possible, and these are discussed in the  $\alpha$ -manganese paper. All but one other arrangement

\* Bradley and Thewlis, 'Proc. Roy. Soc.,' A, vol. 115, p. 456 (1927).

of 29 atoms demand an excessive concentration of atoms on threefold and fourfold axes. There are, in fact, only two practical possibilities for water molecules. The groups of water molecules must be divided in one of the following ways:—

- (a) 12 + 12 + 4 + 1
- (b) 12 + 6 + 6 + 4 + 1.

In arrangement (b) the two groups of six molecules lie on the fourfold axes. This arrangement is possible without overcrowding, only because the anion does not completely fill its allotted polyhedron. As will be seen, one group of six water molecules extends into the neighbouring polyhedra occupied by anions.

Some of the parameters need to be fixed prior to deciding between arrangement (a) and (b). One molecule lies at the intersection of the threefold and fourfold axes, and is therefore invariant. The remainder may be approximately fixed from spatial requirements. Since the anions do not by any means fill their own polyhedra, it is clear that the 29 water molecules should occupy more space than the 40 oxygens in the anion. The parameters of the water molecules must therefore conform to an open packing with few neighbours per atom. In the anion each oxygen atom of the central tetrahedron has twelve oxygen neighbours, and the structure of the anion in general is a type of oxygen close-packing. The average volume per oxygen atom in the anion is 19 Å<sup>3</sup>, whereas that allowed for each water molecule is 28 Å<sup>3</sup>. The ratio is consistent with a change from 12 coordination in the anion to either 4 or 6 coordination for the water molecules depending on the interatomic distances of the water molecules.

Thus the central water molecule may be in contact with a 4 group or a 6 group but not with a 12 group. Arrangement (a) would require a central molecule in contact with a tetrahedral group surrounded by an outer zone of 24 molecules. This gives very reasonable interatomic distances. There are, however, two objections. It leaves big holes near the cube surfaces of each anion and it does not explain the observed intensity, whatever parameter changes are made (see Table II).

Table II gives the observed intensities for the complete series of reflexions measured by Keggin and us. These are to be compared with the calculated values (1) without allowing for the water; (2) after allowing for the water in (a) grouping; (3) after allowing for the water in (b) grouping. It is clear that arrangement (a) gives worse agreement than without the water, although the most favourable parameters have been chosen.

TABLE II—COMPARISON OF OBSERVED INTENSITIES WITH CALCULATED  
VALUES FOR  $H_3PW_{19}O_{40} \cdot 29H_2O$

<i>hkl</i>	$\Sigma h^2$	Calculated intensities				Observed intensities	
		No allowance for water	(a) Water arranged		Complete structure		
			12 + 12 + 4 + 1	(b) Water arranged	12 + 6 + 4 + 1		
311	11	0	0	0	0	—	
222	12	0	0	0	0	—	
400	16	5	5	3	4		
331	19	8	4	6	5		
420	20	0	0	0	—		
422	24	3	3	3	3		
511, 333	27	17	17	14	12		
440	32	14	15	12	10		
531	35	9	8	8	7		
600, 442	36	0	0	0	—		
620	40	6	5	5	4		
533	43	12	12	14	12		
622	44	0	0	0	—		
444	48	50	64	58	60		
711, 551	51	11	14	7	7		
640	52	0	0	0	—		
642	56	3	3	1	2		
731, 553	59	29	18	32	32		
800	64	20	20	26	24		
733	67	1	3	2	3		
820	68	0	0	0	—		
822, 660	72	10	9	6	8		
751, 555	75	46	40	52	51		
662	76	2	2	2	—		
840	80	9	13	6	6		
911, 753	83	31	34	31	29		
842	84	0	0	0	—		
664	88	48	47	45	45		
931	91	0	0	0	—		
844	96	0	0	0	—		
Differences between observed and calculated intensities..		58	74	19			

Arrangement (b), on the other hand, gives an excellent agreement with experiment. Arrangement (b) is therefore correct and the 29 water molecules are divided in the following groups:—

$$12 + 6 + 6 + 4 + 1.$$

## THE ATOMIC COORDINATES AND INTERATOMIC DISTANCES

The unit cell contains eight phosphorus, 96 tungsten, 552 oxygen, and 256 hydrogen atoms. The positions of all the phosphorus, tungsten, and oxygen atoms have been found, but it is impossible to say anything at all concerning the positions of the hydrogen atoms. Instead of giving the coordinates of all the atoms, it is sufficient to give those of a typical anion ( $\text{PW}_{12}\text{O}_{40}$ )<sup>3-</sup> and of a typical cation ( $\text{H}_3\cdot 29\text{H}_2\text{O}$ )<sup>+2</sup>, referred to the central P atom and the central water molecule respectively. Let  $xyz$  be the coordinates of any atom in the anion,  $mnp$  those of any atom in the cation. Then the coordinates of the corresponding atoms in each anion in the unit cell are given in the following table.

TABLE III

Coordinates of atoms in anions		Coordinates of atoms in cations ( $\text{H}_3\text{O}$ molecules)	
Central phosphorus	Typical atoms	Central water	Typical waters
0 0 0	xyz	$\frac{1}{2} \frac{1}{2} \frac{1}{2}$	$\frac{1}{2} + m, \frac{1}{2} + n, \frac{1}{2} + p$
$\frac{1}{2} \frac{1}{2} 0$	$\frac{1}{2} + x, \frac{1}{2} + y, z$	0 0 $\frac{1}{2}$	$m, n, \frac{1}{2} + p$
$\frac{1}{2} 0 \frac{1}{2}$	$\frac{1}{2} + x, y, \frac{1}{2} + z$	0 $\frac{1}{2} 0$	$m, \frac{1}{2} + n, p$
$0 \frac{1}{2} \frac{1}{2}$	$x, \frac{1}{2} + y, \frac{1}{2} + z$	$\frac{1}{2} 0 0$	$\frac{1}{2} + m, n, p$
$\frac{1}{2} \frac{1}{2} \frac{1}{2}$	$\frac{1}{2} - x, \frac{1}{2} - y, \frac{1}{2} - z$	$\frac{1}{2} \frac{1}{2} \frac{1}{2}$	$\frac{1}{2} - m, \frac{1}{2} - n, \frac{1}{2} - p$
$\frac{1}{2} \frac{1}{2} \frac{1}{2}$	$\frac{1}{2} - x, \frac{1}{2} - y, \frac{1}{2} - z$	$\frac{1}{2} \frac{1}{2} \frac{1}{2}$	$\frac{1}{2} - m, \frac{1}{2} - n, \frac{1}{2} - p$
$\frac{1}{2} \frac{1}{2} \frac{1}{2}$	$\frac{1}{2} - x, \frac{1}{2} - y, \frac{1}{2} - z$	$\frac{1}{2} \frac{1}{2} \frac{1}{2}$	$\frac{1}{2} - m, \frac{1}{2} - n, \frac{1}{2} - p$
$\frac{1}{2} \frac{1}{2} \frac{1}{2}$	$\frac{1}{2} - x, \frac{1}{2} - y, \frac{1}{2} - z$	$\frac{1}{2} \frac{1}{2} \frac{1}{2}$	$\frac{1}{2} - m, \frac{1}{2} - n, \frac{1}{2} - p$

The atomic coordinates of a typical anion are given in Angstrom units in Keggin's first paper, but there is some slight and unavoidable inaccuracy in the tungsten coordinates, which was corrected by Santos. This is due to insufficient data from reflexions with  $h + k + l$  odd, a point to which reference was made in the introductory section of the present paper. The difficulty is inherent in the 5-hydrate structure, but does not arise in the 29-hydrate structure. Here the tungsten coordinates are fixed chiefly by reflexions from planes with  $h^2 + k^2 + l^2 = 8n + 3$ , many of which are capable of giving accurate measurements. Conse-

quently we can claim to have established the tungsten coordinates on a firmer basis. Our results confirm the values given by Santos, and for convenience of reference the coordinates of the anion are given below.

TABLE IV—THE ATOMIC COORDINATES IN THE  $(PW_{12}O_{40})^{-2}$  ANION

1 P atom at	$(0, 0, 0)$ .		
4 O <sub>1</sub> atoms at	$(a, a, a)$	$(\bar{a}, \bar{a}, a)$	$(\bar{a}, a, \bar{a})$
where $a = 0.99 \text{ \AA}$ .			
12 O <sub>2</sub> atoms at	$(b, b, c)$	$(\bar{b}, \bar{b}, \bar{c})$	$(b, b, \bar{c})$
	$(\bar{b}, c, b)$	$(\bar{b}, \bar{c}, b)$	$(b, \bar{c}, b)$
	$(\bar{c}, b, b)$	$(\bar{c}, \bar{b}, \bar{b})$	$(c, b, \bar{b})$
where $b = 0.97 \text{ \AA}; c = 2.84 \text{ \AA}$ .			
12 O <sub>3</sub> atoms at	$(d, d, e)$	$(d, d, \bar{e})$	$(\bar{d}, d, e)$
	$(d, e, d)$	$(d, \bar{e}, \bar{d})$	$(\bar{d}, e, \bar{d})$
	$(e, d, d)$	$(e, \bar{d}, \bar{d})$	$(\bar{e}, d, \bar{d})$
where $d = 1.49 \text{ \AA}; e = 3.54 \text{ \AA}$ .			
12 O <sub>4</sub> atoms at	$(f, g, g)$	$(\bar{f}, \bar{g}, g)$	$(f, g, \bar{g})$
	$(g, f, g)$	$(g, \bar{f}, g)$	$(g, f, \bar{g})$
	$(g, g, f)$	$(g, g, \bar{f})$	$(g, \bar{g}, f)$
where $f = 0.1 \text{ \AA}, g = 3.79 \text{ \AA}$ .			
12 W atoms at	$(h, k, k)$	$(h, \bar{k}, \bar{k})$	$(\bar{h}, k, \bar{k})$
	$(k, h, k)$	$(k, \bar{h}, \bar{k})$	$(\bar{k}, h, k)$
	$(k, k, h)$	$(k, h, \bar{k})$	$(\bar{k}, k, \bar{k})$
where $h = 0.15 \text{ \AA}; k = 2.495 \text{ \AA}$			

TABLE V—ATOMIC COORDINATES OF A GROUP OF 29 MOLECULES OF WATER OF CRYSTALLIZATION

1 O <sub>6</sub> water molecule at	$(0, 0, 0)$ .		
4 O <sub>4</sub> water molecules at	$(b, b, b)$	$(\bar{b}, \bar{b}, \bar{b})$	$(\bar{b}, b, \bar{b})$
where $b = 1.68 \text{ \AA}$ .			
12 O <sub>2</sub> water molecules at	$(\bar{e}, d, d)$	$(\bar{e}, \bar{d}, \bar{d})$	$(e, d, \bar{d})$
	$(d, e, d)$	$(d, \bar{e}, \bar{d})$	$(d, e, \bar{d})$
	$(\bar{d}, d, e)$	$(\bar{d}, \bar{d}, \bar{e})$	$(d, d, e)$
where $d = 3.64 \text{ \AA}; e = 0.39 \text{ \AA}$ .			
6 O <sub>3</sub> water molecules at	$(f, 0, 0)$	$(0, f, 0)$	$(0, 0, f)$
	$(\bar{f}, 0, 0)$	$(0, \bar{f}, 0)$	$(0, 0, \bar{f})$
where $f = 3.36 \text{ \AA}$ .			
6 O <sub>1</sub> water molecules at	$(g, 0, 0)$	$(0, g, 0)$	$(0, 0, g)$
	$(\bar{g}, 0, 0)$	$(0, \bar{g}, 0)$	$(0, 0, \bar{g})$
where $g = 6.31 \text{ \AA}$ .			

Tables VI and VII give the nearest neighbours and interatomic distances for the atoms of the anion and the water molecules respectively. The close-packed character of the anionic oxygen ( $O_1 - O_4$ ) may be contrasted with the open character of the water molecules ( $O_5 - O_9$ ). The

TABLE VI—THE INTERATOMIC DISTANCES OF THE ATOMS IN THE ANIONS

Atom	No of neighbours	Type of neighbour	Distance in Å
P	4	$O_1$	1.71
$O_1$	1	P	1.71
	3	W	2.29
	3	$O_1$	2.65
	6	$O_2$	2.70
	3	$O_1$	2.80
W	1	$O_4$	1.84
	2	$O_2$	1.93
	2	$O_3$	1.97
	1	$O_1$	2.29
$O_2$	2	W	1.93
	2	$O_1$	2.61
	2	$O_1$	2.70
	1	$O_3$	2.75
	2	$O_4$	3.10
	1	$O_3$	2.90
$O_3$	2	W	1.97
	2	$O_1$	2.61
	1	$O_1$	2.65
	2	$O_4$	2.80
	1	$O_3$	2.80
	1	$O_7$	2.86
$O_4$	1	W	1.84
	2	$O_1$	2.80
	2	$O_2$	3.10
	1	$O_3$	2.89

number of nearest neighbours is much more in the anion, though the  $O_4$  and  $O_9$  groups suggest the possibility of an intermediate state ( $OH?$ ).

#### DISCUSSION OF THE STRUCTURE

The structure of the higher hydrate of phosphotungstic acid,  $H_3PW_{12}O_{40} \cdot 29H_2O$  is shown in the six figures (figs. 3-8). It is most

TABLE VII—INTERATOMIC DISTANCES OF WATER MOLECULES

Type of water	No. of neighbours	Type of neighbours	Distances in Å
O <sub>5</sub>	4	O <sub>6</sub>	2.84
O <sub>4</sub>	1	O <sub>5</sub>	2.84
	3	O <sub>6</sub>	2.84
O <sub>7</sub>	1	O <sub>2</sub>	2.86
	2	O <sub>7</sub>	2.89
O <sub>8</sub>	2	O <sub>6</sub>	2.84
	1	O <sub>9</sub>	2.89
O <sub>9</sub>	2	O <sub>3</sub>	2.80
	2	O <sub>4</sub>	2.89
	1	O <sub>8</sub>	2.89
	2	O <sub>1</sub>	2.90

The next smallest distances all exceed 3.2 Å

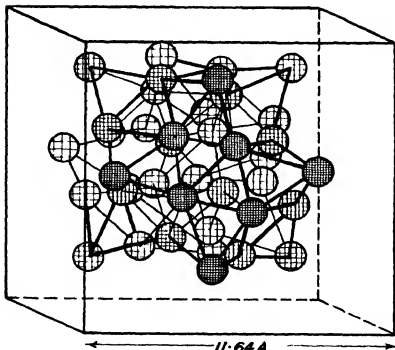


FIG. 5.—The anion-oxygen atoms only.

simply regarded as a combination of anions ( $\text{PW}_{12}\text{O}_{40}^{3-}$ ) and cations ( $\text{H}_3 \cdot 29\text{H}_2\text{O}^{13}$ ) situated on two interpenetrating diamond lattice complexes (fig. 3). Anions and cations have each point symmetry  $T_d$ , and are shown to scale in figs. 5 and 6 respectively. These figures are shaded to show contours, the darkest shading being nearest the observer and the lightest farthest away. The anion and cation are each shown as lying at the centre of a cube, the volume of which is one-eighth of the volume of the whole unit cell. The same small cube is indicated in fig. 4, where

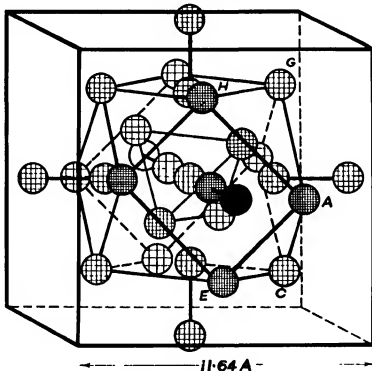


FIG. 6.—The 29 water molecules—showing symmetry

the volume allotted to one anion or cation is shown as a polyhedron bounded by six cube faces and eight octahedral faces. The whole unit cell is then composed of sixteen polyhedra, eight occupied by anions and eight by cations. The anions fit easily into alternate polyhedra. Each anion is linked through cube faces to six water molecules and through octahedral faces to twelve water molecules, but there is no direct linkage between anion and anion.

The grouping of the 29 molecules of water of crystallization is shown in fig. 6. This is drawn primarily to show the conformity with  $T_d$  sym-

metry. The lines joining certain molecules are not bonds, but are inserted in order to show the positions of the molecules in space, and to serve for comparison with fig. 4. One molecule at the centre is surrounded by a tetrahedron and outside this is a further group of twelve water

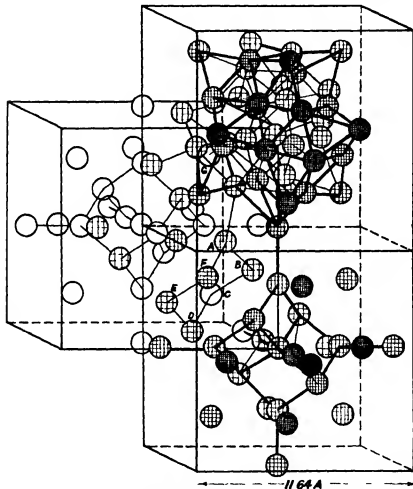


FIG. 7—The bonding of the anions and water molecules.

molecules. The cluster of 29 is completed by six pairs of atoms lying on fourfold axes.

The bonding is shown in figs. 7 and 8. Fig. 7 shows a cluster of 29 molecules of water of crystallization in juxtaposition with a neighbouring anion and a second cluster of 29 water molecules. The bonding of the water molecules is in two distinct sets. Seventeen water molecules are

grouped around the central molecule in  $(1 + 4 + 6 + 6)$  symmetrical sets. The other twelve molecules at the periphery of the cluster are quite separate. The seventeen central molecules are linked together through the centre itself. This is joined directly to four neighbours in tetrahedral formation, and these in turn are in contact with six atoms on

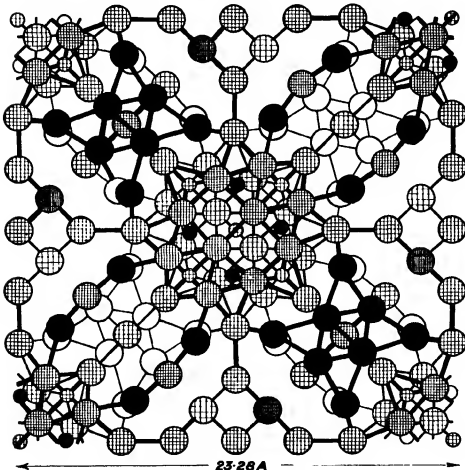


FIG. 8—A section of the unit cell.

fourfold axes. Through a second set of six atoms the whole unit is linked on to the cube faces of six neighbouring anions. In this way the seventeen water molecules serve to bind together six anions, corresponding to six cube faces.

The remaining twelve water molecules, forming the cube-octahedron in

fig. 6, are entirely unconnected with the central seventeen. Neither do they make any contact with one another in the same cluster of 29. Each has two neighbours belonging to an adjacent cluster, and together with these it helps to form hexagonal rings, at the junction of two clusters. Three molecules, A, C, E, from one cluster and three from a neighbouring cluster, B, D, F, form a puckered ring such as A, B, C, D, E, F, in fig. 7. This hexagon lies almost in an octahedral boundary face of the polyhedron occupied by the water. In fig. 4 there are eight such planes, and the positions A, B, C, D, E, F, correspond roughly with the centres of the hexagonal edges of the polygons. In accordance with tetrahedral symmetry, the molecules are somewhat displaced into the shaded faces PQ and away from the unshaded faces XY. The shaded faces PQ are planes of contact between neighbouring clusters of water molecules. The unshaded faces XY are planes of contact between neighbouring anions and the water molecules, which are linked together at A, G, and H (cf. figs. 4 and 7). In this way each hexagonal ring of water molecules serves to link together a ring of six anions.

Fig. 8 shows a section through the unit cell parallel to a cube face. For the sake of clarity, only one-quarter of the depth of the cell is shown. The central phosphorus atom is shown as a small circle at the centre of the unit cell (000) and on the vertical edges ( $\frac{1}{2}\frac{1}{2}0$ ). These points are taken as ground level; heights above are indicated by darker shading, and depths below by lighter shading. The greatest height and greatest depth are approximately one-eighth of the cell dimensions. Oxygen atoms, whether as part of the anion or as water molecules, are indicated by large circles; tungsten and phosphorus atoms are indicated by small circles. Table VIII gives a key to the heights and depths of the atoms.

Portions of anions are shown near  $0\ 0\ 0$ ,  $\frac{1}{2}\frac{1}{2}\ 0$ ,  $\frac{1}{2}\frac{1}{2}\frac{1}{2}$ ,  $\frac{1}{2}\frac{1}{2}\frac{1}{2}$ ,  $\frac{1}{2}\frac{1}{2}\frac{1}{2}$ , and  $\frac{1}{2}\frac{1}{2}\frac{1}{2}$ . Within the limits of the diagram it is only possible to show the centre levels near  $0\ 0\ 0$ ,  $\frac{1}{2}\frac{1}{2}\ 0$ , the lower levels near  $\frac{1}{2}\frac{1}{2}\frac{1}{2}$ ,  $\frac{1}{2}\frac{1}{2}\frac{1}{2}$ , and the upper levels near  $\frac{1}{2}\frac{1}{2}\frac{1}{2}$ ,  $\frac{1}{2}\frac{1}{2}\frac{1}{2}$ . Sufficient water molecules are shown to indicate the contrast between the more open packing of the water and the close packing of the oxygen in the anions, where they are linked together by tungsten and phosphorus atoms.

Bonds are indicated by lines. Thin lines join atoms below ground level and thick lines join atoms above ground level. Every bond on this diagram, as in fig. 7, corresponds to an interatomic distance given in Tables VI and VII.

In conclusion, the authors wish to thank Professor W. L. Bragg, F.R.S., for his kind interest in the work. One of us (J. W. Illingworth) is indebted

to Messrs. Tootal, Broadhurst, Lee Co., Ltd., for a grant which enabled him to carry out the work. Our thanks are also due to Dr. J. F. Keggin for kindly providing us with a powder photograph of  $H_5PW_{12}O_{40} \cdot 29H_2O$ .

### SUMMARY

The higher hydrate of phosphotungstic acid,  $H_5PW_{12}O_{40} \cdot 29H_2O$ , is cubic. The unit cell contains eight molecules and the length of the edge of the cell is 23.28 Å. The anion  $(PW_{12}O_{40})^{3-}$  is identical with the one found by Keggin in the lower hydrate  $H_5PW_{12}O_{40} \cdot 5H_2O$ .

TABLE VIII

Type of atom		Height or depth in Å	Indication above ground level	Indication below ground level
P; O <sub>6</sub> ; O <sub>5</sub> O <sub>4</sub> W	(water)	0	Medium shading	Medium shading
	(anion)	0.10		
		0.15		
O <sub>7</sub> O <sub>8</sub>	(water)	0.39	Medium-heavy shading	Medium-light shading
	(water)	0.49		
O <sub>2</sub> O <sub>1</sub> O <sub>3</sub>	(anion)	0.97	Heavy shading	Light shading
	(anion)	0.99		
	(anion)	1.49		
O <sub>4</sub>	(water)	1.68	Very heavy	Very light
O <sub>4</sub> O <sub>7</sub> O <sub>8</sub> O <sub>5</sub> W O <sub>3</sub>	(anion)	2.03	Black shading	Open circles
	(water)	2.18		
	(anion)	2.28		
	(water)	2.46		
		2.495		
	(anion)	2.99		

The structure consists of two interpenetrating diamond lattices, the one of  $(PW_{12}O_{40})^{3-}$  anions and the other of groups of 29 molecules of water of crystallization. The positions of all the atoms, with the exception of the hydrogens, have been found. A feature of the work is that the structure was entirely determined from one powder photograph taken by Keggin.

The remarkable number (29) of water molecules associated with each anion is accounted for by symmetry considerations. The 29 waters are divided up into six groups, viz.,  $12 + 6 + 6 + 4 + 1$ . It is interesting to note that the interatomic distances of the water molecules all lie between 2.8 and 2.9 Å. The packing of these molecules is quite open, in contrast to the oxygen atoms in the anion, which are very closely packed.

## Distribution of Magnetic Field Around Simply and Multiply Connected Supraconductors

By H. GRAYSON SMITH and J. O. WILHELM, McLennan Laboratory,  
University of Toronto

(Communicated by A. S. Eve, F.R.S.—Received 14 May, 1936)

### INTRODUCTION

The experiments to be described in this paper arose from a suggestion by M. von Laue that it would be of interest to examine more closely the behaviour of simply and multiply connected supraconducting bodies in an external magnetic field. If a closed circuit be taken wholly within a supraconducting body, sufficiently far from the surface, the magnetic flux through the circuit should be constant as long as no part of the body is subjected to a magnetic field greater than the critical field strength. For a simply connected body, if the spontaneous ejection of flux on cooling through the transition point, the so-called Meissner effect, is complete, the constant flux through any circuit should be zero. For a multiply connected body, it should be equal to the value immediately after the body became supraconducting.\*

Only in the case of a multiply connected body, that is, a closed circuit, can there be a resultant current through any cross-section in the steady state. This may be taken as a definition of the current  $I$  in the circuit, the so-called persistent current. Let  $L$  be the self-inductance of the circuit, calculated for the supraconducting state on the assumption that the current flows entirely in a layer very close to the surface. Let  $\phi$  be the calculated magnetic flux through the circuit due to external magnetic field, allowing for the distortion of the field by the presence of supraconducting material. Then, if it can be assumed that the maintenance of the constant flux through the closed circuit is due to a persistent current in the above sense, the law of constant flux can be written in the form

$$LI + \phi = \phi_0. \quad (1)$$

Most previous measurements of persistent currents have been made by observing the magnetic moment of the circuit in which they are presumed to be flowing. However, in certain experiments a large magnetic moment

\* F. and H. London, 'Physica,' vol. 2, p. 341 (1935).

has been observed when the circuit is broken by a narrow gap.\* There is, therefore, still some doubt whether the magnetic moment gives a true measure of the resultant current  $I$ , and a definite test of the law of constant flux, with its possible limitations, seemed worth while. The success obtained by applying relation (1) to the supraconducting galvanometer of the authors and Tarr† indicates that it is correct for a coil of fine supraconducting wire in small external fields. It has now been definitely confirmed for a simple circuit consisting of comparatively heavy bars, as long as the current is less than a certain saturation value. The saturation current is apparently determined by the mean magnetic field around the smallest cross-section of the circuit.

#### APPARATUS

The body upon which the experiments were performed consisted of two parallel cylinders of cast tin, of a high degree of purity, but polycrystalline. The cylinders (AA, fig. 1) were 13.3 cm. in length, 0.8 cm. in diameter, and placed with their centres 2.8 cm. apart. They were connected at top and bottom by cross-bars of the same tin. In order to make room for the rods operating the search coils, the upper cross-bar was bent into the form of a semicircle, and the diameter of this part of the circuit reduced to 0.496 cm. Around the upper bar was wound a coil S consisting of 360 turns of fine copper wire, described below as the switch magnet. By passing a current through this coil, supraconductivity could be interrupted in this part of the circuit, and any resultant persistent current could be stopped. This coil therefore acted as a switch, by means of which the circuit could be opened or closed at will, without disturbing the rest of the apparatus. The field caused by the switch magnet had no appreciable effect on the test coils used for exploring the field distribution between the cylinders.

Four small test coils, of dimensions approximately 4 cm. by 0.5 cm., were placed in the positions marked 1, 2, 3, 4 in fig. 1. These were arranged so that they could be rotated through 180° from an initial position at right angles to the external field. Coil 1 was further arranged so that its initial position could be turned through 90°, in order to measure both components of the magnetic field at this point. All the magnetic fields were determined from the deflexions of a Grassot fluxmeter equipped with a mirror and a scale, when the coils were rapidly rotated. The flux-

\* Kammerlingh-Onnes, 'Comm. Phys. Lab. Leiden,' No. 141b; Steiner and Grassmann, 'Phys. Z.,' vol. 36, p. 520 (1935).

† Grayson Smith and Tarr, 'Trans. Roy. Soc. Canada,' vol. 29/III, p. 1 (1935).

meter was found to give consistent readings over the small range of deflexions covered in the experiments, and for steadiness and reproducibility it was superior to a ballistic galvanometer. The external magnetic field was supplied by an air-cored electromagnet, located outside the cryostat. This gave a mean field over the area occupied by the test coils of 12.2 gauss per ampere.

#### THEORETICAL DISTRIBUTION OF MAGNETIC FIELD

**A—Simply Connected Bodies**—The lines of force of a magnetic field applied at right angles to the plane of the supraconducting cylinders

coincide with the equipotentials of an external electrostatic field applied parallel to the plane of the cylinders. The two-dimensional problem can be readily solved by transforming to coordinates  $\xi$ ,  $\eta$ , where

$$x + iy = c \coth(\xi + i\eta).$$

The calculated distribution of field is shown in fig. 2, and the calculated mean fields at the four test coils are:

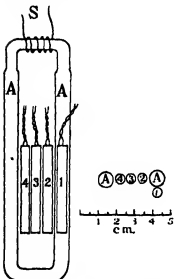


FIG. 1.—Arrangement of test coils around the supraconducting circuit.

The maximum field at the surface of the cylinders is very nearly  $2H_0$ , as for a single cylinder. This type of field is to be expected when the supraconducting circuit is broken by passing a current through the switch coil.

In this case the effect of the cross-bar on the field can be neglected in comparison with the effect of non-uniformity of the field.

**B—Current in Cylinders Without External Field**—The lines of force of the magnetic field due to current in supraconducting cylinders agree with the equipotentials of the electrostatic field due to oppositely charged cylinders, and the problem is solved by the same transformation as for A.

The magnetic field at any point can be most simply derived by considering the current to flow in two filaments separated by a distance

$$2c = (a^2 - b^2)^{\frac{1}{2}}$$

where  $b$  is the diameter of either cylinder, and  $a$  is the distance between their centres. The distribution of magnetic field in this case is shown in fig. 3, for infinite cylinders. The crosses indicate the positions of the equivalent current filaments. The mean field strengths at the test coils, due to a current  $I$  amperes, have been calculated for the actual circuit

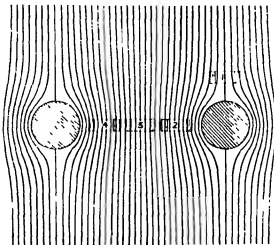


FIG. 2—A, supraconducting cylinders in an external magnetic field.

used, allowing for the current in the cross-bars, and are given below. The upper cross-bar was assumed straight, as the contribution from this part of the circuit is small

	Coil 1 (L)	I (II)	2 and 4	3
Field strength ..	0.056 I	-0.265 I	0.380 I	0.306 I
Ratio to coil 3 ..	0.19	-0.87	1.24	1

A case of persistent current can be clearly recognized in the experiments by the characteristic ratio between the fields at the different test coils, and the resultant current can be calculated. The calculated field at the surface of the cylinders varies from 0.677 I inside to 0.510 I outside.

C—*Multiply Connected Body in an External Field*—The theoretical distribution for infinite cylinders, joined at the ends, can be found by superposing on a field of A one of B, in such a way that the flux between

the cylinders is zero. This field is shown in fig. 4, where the broken lines indicate fractional values. However, this field cannot be realized experimentally, since it is not possible to obtain a uniform magnetic field over

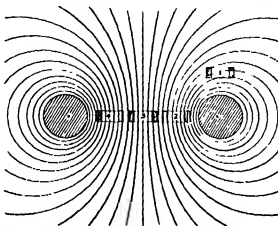


FIG. 3—B, magnetic field due to a current in supraconducting cylinders.

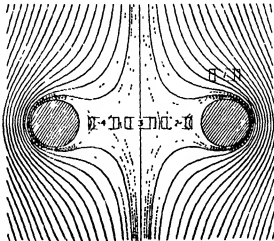


FIG. 4—C, closed supraconducting circuit in an external magnetic field.

cylinders of sufficient length that the calculations are valid. The only experimental test for this case is to show that the relation

$$LI = -\phi$$

is satisfied.

#### THE EXPERIMENTS

*Permanent Magnetization*—Most of the experiments were carried out in one continuous series at a temperature of 2.96° K. At this temperature

the ordinary threshold magnetic field for the restoration of electrical resistance in pure tin is 104 gauss (transverse field, half resistance restored).\* The cylinders were cooled without an external field, and the readings for small fields were taken first. At frequent intervals the external field was removed, the switch magnet turned on in order to stop any persistent current, and the field explored in order to test the possibility of permanent magnetization caused by "locked-in flux". The field due to this cause was appreciable as soon as an external field of about 70 gauss had been once applied. It increased with further experimenting, and finally reached a steady value when 104 gauss had been once applied. In another series of experiments the cylinders were cooled to 2.61° K in an external field of 79 gauss, and then the permanent magnetization was sensibly constant throughout. The permanent field strengths observed are given in Table I, the negative sign indicating a direction opposite to that of the

TABLE I—FIELD DUE TO PERMANENT MAGNETIZATION

Temp ° K.	Coil				
	1 (I)	1 (II)	2	3	4
2.96	6	½	6	-3	-7
2.61	8	1	-·†	-3	9

† Coil 2 became frozen, and was not in use at the lower temperature.

applied fields. The field strengths are too small for numerical discussion, but the distribution is plainly compatible with the assumption of a small permanent magnetization in both cylinders. In the tables below, except where indicated for large external fields, the results have been corrected for this permanent magnetization.

*Disconnected Cylinders*.—The field of case A was obtained by applying an external field while a current was passing through the switch magnet. Table II gives the ratio of observed to applied field for the four test coils. In this case the departure of the observed ratios from the theoretical in small fields is probably due to lack of uniformity of the external field. Coil 1, which was not symmetrically placed with respect to the external magnet, showed a field in the parallel position at all times.

In order to show the gradual penetration of the field into the cylinders, the above ratios for coil 1 and for the mean of coils 2 and 4 have been plotted against the external field strength in fig. 5, together with similar values from the last columns of Table IV. Since the maximum field

\* Tuyn and Kammerlingh-Onnes, 'Comm Phys. Lab Leiden,' No. 174a (1926)

TABLE II—FIELD ABOUT PARALLEL CYLINDERS

Temp. °K	External field gauss	Ratio of observed to external field				
		Coil 1 (I)	Coil 1 (II)	Coil 2	Coil 3	Coil 4
2.96 $H_0 = 104$ gauss	52	0.63	0.16	1.32	1.16	1.34
	61	0.72	0.17	1.30	1.16	1.35
	70	0.76	0.16	1.29	1.15	1.33
	76	0.79	0.16	1.24	1.09	1.31
	85	0.81	0.16	1.24	1.10	1.29
2.61 $H_0 = 145$	73	0.70	0.17	—	1.18	1.43
	124	0.80	0.15	—	1.13	1.27
Not corrected for permanent magnetization						
2.96	85	0.89	0.16	1.18	1.10	1.18
	104	0.92	0.14	1.11	1.06	1.12
	122	0.88	0.12	1.04	1.02	1.04
Theoretical ratios						
	0.81	0	1.37	1.25	1.37	

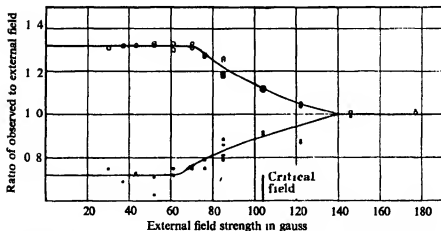


FIG. 5.—Penetration of magnetic field into the supraconducting cylinders. ○ mean of coils 2 and 4; ● coil 1.

strength at the surface of the cylinders is  $2H_0$ , penetration should commence under an external field of  $\frac{1}{2}H_0$ . This is approximately confirmed, but penetration is by no means complete when  $H_0 = H_s$ .

**Persistent Current**—The field due to a persistent current, case B, was definitely obtained in three ways. (1) A large field was applied to the closed circuit and removed, which produced a current even for field

strengths less than  $H_c$ . (2) A field was applied to the cylinders with the switch magnet on (case A), the switch magnet was turned off, and finally the external field was removed. (3) In one case only the connected cylinders were cooled in an external field, and then the field removed. That a true resultant current is produced by each of these processes is shown, first by the characteristic field distribution, when corrected for permanent magnetization, and secondly by the fact that the field was immediately reduced to that caused by the permanent magnetization when a current was passed through the switch magnet.

In Table III are given, first the ratios of the observed fields at the four test coils (taking coil 3 as unity), in order to show that the field distribution is that characteristic of a resultant current, then the mean field strength for coils 2, 3, 4, and finally the current strength calculated from the latter. All values are corrected for permanent magnetization. From the results it is evident that the greatest current which could be obtained in this circuit was approximately 120 amperes at 2.96° K. The current is apparently limited by the upper cross-bar, which had a diameter of 0.496 cm. The magnetic field at the surface of this part of the circuit, due to a current in it of 120 amperes, would be given by

$$H = 2I/10r = 97 \text{ gauss},$$

somewhat smaller than the threshold field at this temperature, and probably equal to the field at which the first traces of resistance appear.

*Closed Circuit in an External Field*—In order to study case C, a field was applied to the closed circuit and the readings of the test coils taken. A current was then passed through the switch magnet and the readings taken again. The ratios after the circuit was broken agree satisfactorily with the ratios of Table II.

From this it is evident that the persistent current is actually stopped by the use of the switch magnet. Further, it will be seen from Table IV that there was no difference between the simply and multiply connected cases in external fields greater than about 75 gauss at 2.96° K.

The difference between the fields before and after using the switch should represent the field of the persistent current induced when the external field is applied. This difference was calculated in each case, and the ratios between the fields at the different test coils were found to be those characteristic of persistent current. These ratios and the calculated currents are given in Table V.

The current  $I$  induced is plotted against the external field in fig. 6 (solid curve) for the series of measurements at 2.96° K. As long as the

current was less than the saturation value it was proportional to the external field,

$$I = -2.26 H_0.$$

Then for larger external fields the induced current fell off very rapidly, although the field distribution showed that the cylinders were still very

TABLE III—FIELD CAUSED BY A PERSISTENT CURRENT

Temp. ° K.	External field gauss	Ratio of field to that at coil 3				Mean field at 2, 3, 4	Resultant current amp.
		I (I)	I (II)	2	4		
<b>External field applied and removed with circuit closed</b>							
2.96	52	—	—	—	—	0	0
	61	0.21	-0.86	1.14	1.21	23.5	66
	70	0.23	-0.91	1.25	1.32	41.0	115
	76	0.21	-0.94	1.28	1.42	41.3	116
	85	0.18	-0.89	1.27	1.37	40.7	114
	104	0.19	-0.89	1.25	1.31	42.7	120
	122	0.21	0.96	1.31	1.31	42.3	119
	146	0.20	-0.90	1.27	1.34	42.3	119
	177	0.20	-0.96	1.30	1.39	42.5	119
2.61	122	0.15	-0.90	—	1.34	59.3	167
	183	0.17	-0.86	—	1.30	57.7	162
<b>Field applied to open circuit, circuit closed, and field removed</b>							
2.96	61	0.16	-0.90	1.26	1.38	43.0	121
	70	0.20	-0.89	1.28	1.30	41.7	117
	85	0.23	-0.96	1.20	1.33	41.2	116
	122	0.19	-0.93	1.28	1.34	43.3	122
<b>Closed circuit cooled in field and field removed</b>							
2.61	79	0.20	-0.90	—	1.32	61.8	174
<b>Mean ratios</b>							
	0.19	-0.91	1.25	1.34			
<b>Theoretical ratios</b>							
	0.19	-0.87	1.24	1.24			

largely in the supraconducting state. This is in qualitative agreement with some experiments on persistent currents performed by McLennan,\* in which the current was deduced from the magnetic moment.

It remains to be shown that the relation (1) is satisfied over the straight portion of the curve in fig. 6. For this purpose the self-inductance of the supraconducting circuit was calculated, and found to be

$$L = 121 \text{ cm.}$$

\* McLennan, Allen, and Wilhelm, 'Phil. Mag.', vol. 14, p. 168 (1932).

TABLE IV—CLOSED CIRCUIT IN AN EXTERNAL FIELD

Temp. ° K.	External field gauss	Ratios to applied field for closed circuit						Ratios after breaking circuit			
		1 (I)	1 (II)	2	3	4	1 (I)	1 (II)	2	3	4
2.96	30½	0.62	0.74	0.48	0.48	0.44	0.75	0.20	1.28	1.15	1.34
	37	0.59	0.73	0.46	0.46	0.46	0.69	0.19	1.28	1.13	1.35
	43	0.63	0.78	0.44	0.49	0.43	0.73	0.16	1.28	1.15	1.36
	52	0.78	0.77	0.44	0.49	0.44	0.71	0.16	1.29	1.16	1.36
	61	0.69	0.45	0.87	0.82	0.90	0.75	0.17	1.28	1.15	1.31
	70	0.76	0.26	1.18	1.06	1.20	0.74	0.16	1.31	1.15	1.35
	76	0.76	0.21	1.26	1.13	1.32	0.75	0.16	1.24	1.12	1.30
	85	0.80	0.15	1.24	1.13	1.28	0.79	0.15	1.23	1.13	1.27
2.61	67	0.60	0.75	—	0.54	0.52	0.73	0.17	—	1.18	1.36
	125	0.89	0.14	—	1.10	1.19	—	—	No change	—	—
Not corrected for permanent magnetization											
2.96	85	0.86	0.15	1.18	1.10	1.20	—	—	—	—	—
	104	0.91	0.13	1.11	1.07	1.13	—	—	—	—	—
	122	0.87	0.13	1.05	1.03	1.05	—	—	—	—	—
	146	0.99	0.13	1.01	1.02	1.01	—	—	—	—	—
	177	1.02	0.13	1.01	1.02	—	—	—	—	—	—

TABLE V—CURRENT INDUCED IN CASE C

Temp. ° K.	External field gauss	Ratio of field to that at coil 3				Mean field at 2, 3, 4 gauss	Persistent current amp
		1 (I)	1 (II)	2	4		
2.96	30½	0.22	-0.80	1.19	1.34	24.2	68
	37	0.14	-0.80	1.22	1.32	29.5	83
	43	0.16	-0.93	1.26	1.40	34.8	98
	52	0.10	0.90	1.29	1.36	42.2	119
	61	0.18	0.85	1.25	1.25	23.3	66
	70	0.14	0.9	1.3	1.5	8.8	25
	76	—	—	—	—	5 (?)	14 (?)
2.61	67	0.20	0.91	—	1.32	50.2	141

The calculation of L for infinite parallel supraconducting cylinders is simple, and leads to an exact formula, since it can be taken to be the magnetic flux between the cylinders due to unit current in the equivalent current filaments of the theoretical case B. The value given above, however, was corrected for the finite length of the cylinders, for the current in the connecting bars, and for the change in diameter in the upper part of the circuit, these various corrections amounting to about 15% of the

whole. There is an uncertainty in the calculated value of  $L$  of perhaps 2%, due mainly to uncertainty in the effective length of the cylinders. In order to indicate the effect of supraconductivity on the self-inductance, the inductance per unit length for infinite cylinders was also estimated for the normal state, and found to be 9.4 as compared with 7.70 for the supraconducting state.

The total flux  $\phi$  due to an external field of mean strength  $H_0$  near the centre was found by means of a test coil of five turns connected to the fluxmeter, with dimensions as nearly as possible the same as the mean

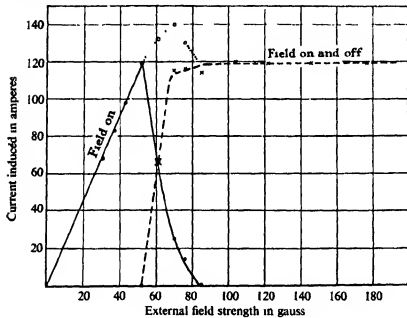


FIG. 6—Current induced in the supraconducting circuit.

dimensions of the supraconducting loop. By this means the flux was found to be

$$\phi = 27.9 H_0$$

with an uncertainty of about 3%.

Then in order to satisfy

$$LI = -\phi$$

we should have

$$121 I/10 = -27.9 H_0$$

or

$$I = -2.30 H_0$$

in very satisfactory agreement with the experimental value.

Whenever the current induced on applying the field is less than the value given by the law of constant flux, a current in the opposite direction must be left in the circuit after the field is removed. The currents set up by the first method of Table III belong to this category, and the current so produced is plotted against the external field strength in the broken curve of fig. 6. If the relation (1) were accurately obeyed on removing the field, the sum of the currents induced on application of the field and after removal should give points on an extension of the straight line. These points are indicated by circles in fig. 6, but the result is inconclusive, since only for the first point are both the currents smaller than the saturation value.

*The Maximum Current*—When there is no external field present, the maximum persistent current is determined by the magnetic field produced around the smallest cross-section of the circuit, in agreement with Silsbee's hypothesis. When the current flows in the presence of an external field, so that the field strength is not constant around a cross-section, practically the same maximum current was found (fig. 6). The experiment shows clearly that the field surrounding the cylinders in case C is simply the resultant of the distorted external field and the field of the persistent current. Therefore the maximum field strength at the surface of the metal occurs in the diametral plane on the outside surface (fig. 4), and amounts to

$$H_{\max} = 2H_0 + 0.510 I = 3.2 H_0.$$

There was, however, no indication of any discontinuity in the relation between external field and current induced until  $H_0$  was considerably greater than  $H_s/3.2$  (32 gauss).

On the other hand, in an experiment to examine the action of the switch magnet, the presence of an external field, smaller than the critical field strength, did affect the persistent current. In this case the field was applied over a portion of the circuit, in a direction parallel to the surface of the supraconductor, and therefore approximately uniform around a cross-section. When the current through the switch magnet was increased in steps, the following results were obtained (temperature  $2.61^\circ$  K.):

Current in switch magnet amp.	Persistent current amp.
0	162
0.5	136
0.7	102
1.0	0

The field produced by the switch magnet is not accurately known. However, remembering that the fields produced by these two currents are at right angles, the figures are consistent with a rule that the resultant magnetic field remains constant as the current through the switch is increased.

*Cooling in an External Field*—Only one partial set of readings was obtained for this case, but this was sufficient to give a qualitative result. The closed circuit was cooled to  $2.61^\circ\text{K}$  in an external field of 79 gauss, and the following readings were obtained:

	Coil				
	1 (I)	1 (II)	2	3	4
Ratio to applied field as measured . . .	0.91	0.12	—	1.11	—
Corrected for permanent magnetization	0.81	0.12	—	1.16	—

The spontaneous expulsion of flux on cooling was evidently not complete, and probably still not quite complete when allowance is made for the "locked-in flux" which causes the permanent magnetization. Apart from partial penetration, however, the magnetic field after cooling was definitely that of case A, as might be expected, with no evidence of resultant current.

#### CONCLUSION

It has been definitely shown by these experiments that the persistent current in a closed supraconducting circuit is a true resultant current, not to be confused with the local circulation of current which causes magnetic effects in a simply connected body. It has been shown that the resultant current is caused entirely by changes in the magnetic field which takes place after the body has passed into the supraconducting state. For sufficiently small magnetic fields and currents, the law that the magnetic flux through a closed supraconducting circuit should be constant is accurately obeyed. Therefore towards changes of magnetic field which take place when a metal is definitely in the supraconducting state, it behaves like a conductor without resistance. But towards a steady external magnetic field applied while the metal is cooling it behaves like a material of high diamagnetic susceptibility.

The distribution of magnetic field around the closed circuit when carrying a persistent current probably agrees within experimental error with that calculated on the assumption that the current flows entirely in a layer near the surface. This is confirmed by the very satisfactory agree-

ment found when the total flux instead of the distribution is considered, the self-inductance of the circuit being calculated on the assumption of surface currents.

For a given supraconducting circuit at a given temperature there is a maximum persistent current which can be induced. In the present experiment this maximum current agreed with the current which, according to Silsbee's hypothesis, would commence to restore resistance in the smallest part of the circuit. In a recent experiment with the supraconducting galvanometer, performed by the authors and Mann,\* the current which would have been induced by a magnetic field equal to the threshold field was not sufficient to disturb supraconductivity in any part of the circuit. The maximum current obtainable then corresponded to an external field somewhat smaller than the threshold value. In both experiments, when a current was induced by removing a field greater than the threshold value, the maximum current was always obtained. However, when the current was induced by applying a field, the current increased with the field strength up to its maximum, and then fell rapidly to zero, even though the distribution of magnetic field showed that the supraconducting state was not completely destroyed.

Again, when a magnetic field was applied to a circuit in which the maximum persistent current was already flowing, the current decreased gradually as the external field was increased, apparently in such a way that the field at the surface of the supraconductor remained equal to a value somewhat smaller than the ordinary threshold field strength. These results are apparently in qualitative agreement with the recent theoretical work of F. London.† However, further investigation, using a single crystal, will be necessary in order to draw definite conclusions concerning the interruption of the persistent current by a magnetic field.

The authors wish to acknowledge their indebtedness to Professor M. von Laue for the correspondence and suggestions which led to their undertaking the work, to Professor E. F. Burton for his continued encouragement and advice, and to Mr K. C. Mann for his assistance in making the experimental measurements.

#### SUMMARY

By means of small test coils, the magnetic field has been explored in the neighbourhood of two parallel supraconducting cylinders of pure tin,

\* Grayson Smith, Mann, and Wilhelm, 'Trans. Roy. Soc. Canada,' vol. 30/III, p. 13 (1936).

† 'Physica,' vol. 3, p. 450 (1936).

both when they are connected at the ends to form a closed circuit and when one connexion is broken. The circuit was broken by interrupting supraconductivity in one cross-bar by means of a small magnet coil wound round it. By observing the change in distribution when this magnet was turned on, the field due to current circulating in the closed circuit could be distinguished from the distorted external field, and the current strength could be measured. The success of this method of breaking the circuit shows that the so-called persistent currents are in truth circulating currents. A definite saturation value was found for the persistent current which could be induced. The closed supraconducting circuit in an external field obeyed the law that the magnetic flux through it should be constant as long as the circulating current was less than the saturation value. As the field was increased beyond this point, the current induced fell rapidly to zero, although the cylinders were still partly supraconducting.

---

## Ionization, Excitation, and Chemical Reaction in Uniform Electric Fields

### II—The Energy Balance and Energy Efficiencies for the Principal Electron Processes in Hydrogen

By R. WINSTANLEY LUNT and C. A. MEEK (The Sir William Ramsay Laboratories of Inorganic and Physical Chemistry, University College, London, W.C.1, and Imperial Chemical Industries, Ltd.)

(Communicated by F. G. Donnan, F.R.S. -Received 16 May, 1936)

#### I—INTRODUCTION

In a previous communication, Part I, Emeléus, Lunt, and Meek\* have discussed the rate of an electron collision process, ionization, in a uniform electrical field. In this paper we elaborate their analysis and extend it to five other types of electron collision processes. The discharge conditions now postulated are those of a swarm of electrons moving through a gas under the influence of a uniform electric field so that the system is in a steady state, the current density being sufficiently low so that the stationary concentration of all products of electron collisions (ions and

\* Proc. Roy. Soc., A, vol. 156, p. 394 (1936).

excited particles) is negligible compared with that of the gas molecules in the ground state. Such conditions are realized with considerable exactitude in the uniform positive column. This is of particular importance because in such a discharge the rates of the various types of electron collisions contemplated in the present theory are sufficiently large to enable comparisons to be made between experiment and the predictions of the theory.

There are many experiments, notably those of Townsend\* and Langmuir,† relating to the conditions now postulated which show the velocities of the electrons in the swarm are distributed at random about a mean, and that the mean velocity greatly exceeds that of the gas molecules (or atoms) in which the swarm moves; in a given gas the average electron energy,  $V$  electron-volts, has been shown by Townsend and his collaborators‡ to be a function of  $Xp^{-1}$ , the ratio of the electric field to the gas pressure. In addition to this random motion, there is a relatively small drift motion of the swarm in the direction of the uniform field  $X$ ; the drift velocity,  $W$  cm. sec<sup>-1</sup>, in a given gas is also a function of  $Xp^{-1}$ ,‡ and its magnitude determines the rate at which electrons gain energy from the field, and also the magnitude of the (drift) current carried by the ionized gas §.

In moving under the influence of the uniform field the electrons lose energy mainly in "inelastic" collisions resulting in the ionization or excitation of the gas molecules; in addition they lose energy in "elastic" collisions in which there is a small transfer of kinetic energy only. These energy losses give rise to the distribution of electron energies about the mean, and this distribution is not necessarily Maxwellian.

The general expression for the rate  $R$  of a collision process effected by an electron swarm moving through a gas has been discussed by Fowler,|| and contains terms which are known to depend only on the electron energy distribution function and the probability cross-section (or effective target area) for the given process. The form of the electron energy distribution function is the one quantity with which we shall be concerned on which it is difficult to obtain direct evidence from experiment.

\* "Electricity in Gases," Oxford, 1915, "The Motion of Electrons in Gases," Oxford, 1925.

† J. Franklin Inst., vol. 196, p. 751 (1923).

‡ "Electricity in Gases," Oxford, 1915, "The Motion of Electrons in Gases," Oxford, 1925.

§ On account of the relatively low mobility of the positive ions, the gain and loss of energy by these may be neglected.

|| "Statistical Mechanics," Cambridge, 1928, § 17.

In this paper we shall be concerned with the particular form taken by the general expression for  $R$  when the concentration of electrons in the swarm is expressed in terms of the drift current density, and the drift velocity; this is the form considered in the recent work of the Townsend school,\* in which, however, what we believe to be unsatisfactory approximations for the cross-sections have also been introduced. Quite recently Llewellyn Jones† has discussed an expression for  $R$  which conforms to the general expression considered here. When  $R$  is known it is a simple matter to derive the average rate per electron per second  $S$ ; this is a quantity frequently convenient to discuss in relation to experimental data.

Following the formal analysis of Part I, we shall consider two other characteristics of a collision process due to an electron swarm, both of which are related to  $R$ ; these are the fractional energy loss  $F$ , and the energy efficiency  $\eta$ , the latter being defined as the number of molecules (or atoms) suffering some specified type of collision per electron-volt of energy supplied to maintain the discharge, that is gained by the electrons from the field in which they move. For electronic transitions, there are the following possibilities for the excited state:

- (a) it may react with some other species present;
- (b) it may change to some lower state by the emission of radiation;
- (c) it may be metastable and give out no radiation;
- (d) it may dissociate spontaneously, and the resulting fragments be the final result, or react with themselves or other species present.

In these cases it is clear that the  $\eta$  for the production of the excited state will determine the  $\eta$  for the resulting light emission or for the final product whether this be molecular fragments or some product of chemical reaction. The analysis developed in this paper predicts that  $\eta$  for any specified electron collision process will be a function of  $Xp^{-1}$ , and therefore that the same will be true for any resulting process, light emission, or the production of a new chemical species. The recent experiments of the Townsend school‡ have demonstrated that, for positive column discharge in the rare gases,  $\eta$  for the light emission is a function of  $Xp^{-1}$ ,§ and a similar deduction§ for the hydrogen continuous spectrum may be

\* Townsend and Llewellyn Jones, 'Phil. Mag.', vol. 11, p. 679 (1931), *ibid.*, vol. 12, p. 815 (1931); Townsend and Pakkala, *ibid.*, vol. 14, p. 418 (1932), Keyston, *ibid.*, vol. 16, p. 625 (1933).

† 'Proc. Phys. Soc.' vol. 48, p. 513 (1936).

‡ Townsend and others, *loc. cit.*

§ The data are not presented in this form in the original papers (for hydrogen, cf. § IV).

made from the data of Chalonge.\* On the other hand, despite the many researches dealing with chemical reaction in the positive column, the dependence of  $\eta$  for the final reaction product on  $Xp^{-1}$  does not seem to have been suspected until recently; it is, however, implicit in a fuller analysis of the early experiments of Kirkby† on the formation of water from electrolytic gas, and this conclusion is supported by a review of the more recent data. When the form of the electron energy distribution function is the only unknown quantity in the calculation of  $\eta$  for some specified process, a comparison over a range of  $Xp^{-1}$  of the experimental values and those calculated for an assumed form of the distribution function provides a criterion for the validity of the form assumed.‡

The remaining characteristic property of an electron collision process effected by an electron swarm, to be considered here, is the quantity  $F$  which is defined as the fraction of the energy gained per electron per second (from the field) which is absorbed in the specified collision process. The postulated condition of the steady state then requires that the sum of the  $F$  terms for all the possible electron collision processes shall be unity.

This condition provides a quantitative criterion for the validity of theoretically calculated values of  $F$  (which are closely related to the corresponding values of  $\eta$ , and  $S$ ), and is conveniently termed the energy balance criterion. When the electron energy distribution function is the only unknown quantity in the expressions for  $S$ ,  $\eta$ , and  $F$ , this criterion may be used to test the validity of any assumed form for this distribution function. This is the procedure adopted in this paper.

We believe that the energy balance criterion provides a more exacting test of the validity of any assumed form of the distribution function than is afforded by the comparison between the calculated and observed energy efficiencies for any single type of process due to electron impact. Essentially this criterion demands the simultaneous quantitative fulfilment of the predictions based on the assumed form of the distribution function for all the collision processes that can occur. Moreover, in its simplest form this criterion is independent of restrictions on the current density provided that the postulated condition is fulfilled, that the stationary concentration of all products of electron impacts shall be negligible com-

\* 'Ann. Physique,' ser. 11, vol. 1, p. 123 (1934).

† 'Proc. Roy. Soc., A, vol. 85, p. 151 (1911).

‡ This procedure is formally identical with that adopted in Part I for ionization by electron impact, it is immaterial whether the results are discussed in terms of Townsend's coefficient  $\alpha p^{-1}$  or the derived quantity (cf. Appendix (6)) the energy efficiency of ionization,  $\eta_i$ .

pared with that of the gas molecules in the ground state. The main weakness of this criterion, admittedly, is that even if it is fulfilled by some assumed form for the distribution function, this fulfilment is no guarantee that the solution is a unique one; considered broadly, we believe, however, that such a fulfilment constitutes very strong evidence that the assumed distribution is essentially that corresponding to the actual experimental conditions for which the fulfilment is found.

Concerning the form of the electron energy distribution function, we have assumed in this paper that this is Maxwellian because the calculations given in Part I for the Townsend coefficient of ionization demonstrated that, in hydrogen especially, the experimentally measured ionization could be interpreted as that due to this distribution over a very wide range of  $Xp^{-1}$ .

Believing that great weight may be attached to the fulfilment of the energy balance criterion, we have applied it in this paper to hydrogen in order to obtain confirmation of the results gained in Part I. For this purpose the relative importance of the many possible types of collision processes is determined by the magnitude of their F values; from an inspection of the expressions (4) and (4.1) it can be seen that, for a given value of  $Xp^{-1}$ , these are mainly determined by the values of the cross-section ( $Q_r(V)$ ) and the loss in a single collision ( $V_L$ ), the values of the latter being largest for electronic transitions. Guided by the predictions of theory\* and the comparisons that may be drawn with analogous atomic collisions (for which the experimental and theoretical data on cross-sections is much more abundant than for molecules),† we have selected for consideration here the excitation of the  $^1\Pi_u$ ,  $^3\Sigma_u^+$ ,  $^3\Sigma_g^+$  states and also the ionization of the molecule. In addition, we have dealt with the excitation of the first vibrational level and elastic collisions, which latter give rise to relatively large F values at the lower values of  $Xp^{-1}$ . For all these processes we have therefore calculated the values of  $\eta$  and F for an assumed Maxwellian electron energy distribution over the same wide range of  $Xp^{-1}$  in which this distribution was found in Part I to account for the Townsend coefficient  $\alpha p^{-1}$ . These calculations enable not merely the energy balance to be examined, but they also enable comparisons to be made between the calculated and experimental data for two other pro-

\* Mott and Massey, "The Theory of Atomic Collisions," Oxford, 1933, Massey and Mohr, "Proc. Roy. Soc., A," vol. 132, p. 605 (1931); vol. 135, p. 258 (1932), vol. 140, p. 613 (1933).

† Hanié and Larche, "Ergebn. Exakt. Wiss., vol. 10, p. 283 (1931); Lees, "Proc. Roy. Soc., A," vol. 137, p. 173 (1932); Langstroth, "Proc. Roy. Soc., A," vol. 146, p. 166 (1934).

cesses: the emission of the hydrogen continuous spectrum (from  $^3\Sigma_g^+$ ) and the formation of hydrogen atoms (from both triplet states), the latter affording an absolute comparison. The main conclusion of this paper is again that the Maxwellian distribution represents the actual distribution to a close approximation.

## II—GENERAL EXPRESSIONS FOR COLLISION PROCESSES EFFECTED BY AN ELECTRON SWARM MOVING IN A UNIFORM ELECTRIC FIELD

1—*Statement of Quantities Concerned*—In addition to the average electron energy,  $\bar{V}$  electron volts, the electron drift velocity,  $W \text{ cm sec}^{-1}$ , and the Townsend coefficient of ionization,  $\alpha p^{-1}$ , all of which have been defined in Part I, we shall be concerned here with the following average properties of collision processes effected by an electron swarm moving under a uniform electric field, of intensity  $X \text{ volts cm}^{-1}$ , through a gas at a pressure  $p \text{ mm. Hg}$

- (1)  $R_r$ , the number of molecules suffering some specified type of collision process per  $\text{cm}^3$  per second.\*
- (2)  $S_r$ , the average number of molecules suffering some specified type of collision process per second per electron; if  $n_e$  is the concentration of electrons per  $\text{cm}^3$ ,

$$S_r = R_r/n_e.$$

- (3)  $\eta_r$ , the energy efficiency for the specified collision process, that is, the number of molecules suffering the specified type of collision per electron-volt of energy gained by the electron swarm by moving in the field  $X$ . If  $E$  is the rate of gain of energy from the field in electron-volts per  $\text{cm}^3$  per second,

$$\eta_r = R_r/E$$

- (4)  $F_r$ , the fraction of the energy gained by the electron swarm in unit time which is absorbed in effecting the specified type of collision. If  $V_r$  is the energy in electron-volts absorbed in effecting a single collision of the specified type,

$$F_r = V_r / E$$

\* Most of the collision processes with which we shall be concerned involve excitation, to denote which we have added the suffix “e” to the symbols concerned; in order to differentiate between different processes appropriate suffixes will be introduced as required.

From the work of Townsend and his collaborators,\*  $\bar{V}$  and  $W$  are known to be determined in a given gas by the ratio  $Xp^{-1}$ ; the theory now developed predicts that  $S_r$ ,  $\eta_r$ , and  $F_r$  are likewise determined. The remaining characteristic of an electron swarm which is required is the electron energy distribution function.

- (5)  $f(V) \cdot dV$ , the probability that an electron selected at random from the swarm shall have energy lying between  $\bar{V}$  and  $V + dV$  electron-volts.

Lastly, we require the following quantities relating to single impacts:—

- (6)  $V_c$ , the least, or critical, electron energy necessary to effect the specified type of collision process
- (7)  $Q_r(V)$ , the probability cross-section for the specified type of collision process for an electron of energy  $V$  electron-volts. For this quantity we shall adopt the conventional unit of  $\pi a_0^2$ ;† it then follows from the definition of this cross-section‡ that the number of collisions of the specified kind per cm. of track of an electron of energy  $V$  is  $3.15 \times p Q_r(V)$ . For  $V$  less than  $V_c$ ,  $Q_r(V)$  is zero.

For values of  $Xp^{-1}$  greater than about 1 it is known from the work of Townsend\* that in many gases including hydrogen the velocity of the electrons greatly exceeds that of the charged particles of molecular mass; for these conditions the drift current density,  $I$ , electrons  $\text{cm}^{-2} \text{ sec.}^{-1}$  may be expressed to a close approximation by

$$I_r = n_r \cdot W$$

Since the swarm moves in a field  $X$  volts  $\text{cm.}^{-1}$ , it follows that the gain of energy from the field by the swarm per unit volume,  $E$  electron-volts  $\text{cm.}^{-3} \text{ sec.}^{-1}$ , is given by

$$E = n_r \cdot W \cdot X.$$

When  $E$  takes this particular form, we have, from the foregoing definitions,

$$\eta_r = S_r / (W \cdot X)$$

and

$$F_r = V_L \cdot S_r / (W \cdot X).$$

In the particular case that  $V_L$  is sensibly independent of the energy of the colliding electron, and equal to the critical energy,  $V_c$ , which is the case for

\* Townsend, "The Motion of Electrons in Gases," Oxford, 1925.

†  $a_0$  is the radius of the first Bohr orbit in the hydrogen atom,  $0.53 \times 10^{-8}$  cm.

‡ Mott and Massey, "Theory of Atomic Collisions," Oxford, 1933, chap. 2 and 9.

all the processes to be considered in this paper except elastic collisions, we find the simple expression

$$F_e = \eta_e \cdot V_e.$$

As in Part I, we shall consider the case of a swarm moving through a gas with an isotropic distribution in velocity, an assumption which, as pointed out there, is in any case a close approximation to the true conditions for the lower range of  $Xp^{-1}$  considered in that and in this paper; for the higher values of  $Xp^{-1}$  we have applied the approximate correction\* derived in Part I (Table X).

**2—Expressions for  $R_e$ ,  $S_e$ ,  $\eta_e$ , and  $F_e$ .**—The derivation of  $R_e$  for any specified collision process is strictly analogous to that for the rate of ionizing collisions per  $\text{cm}^3$  per second,  $R_i$ , given in Part I. When the number of ionizing collisions per  $\text{cm}$  of electron track is replaced by the corresponding number of collisions of the specified kind, that is, when  $p \cdot P(V)$  is replaced by  $3.15 \times p \cdot Q_e(V)$  in the expression for  $R_i$ , we find

$$R_e = k_0 \cdot n_e \cdot p \int Q_e(V) \cdot V^{0.5} \cdot f(V) \cdot dV \quad (1)$$

and hence

$$S_e = k_0 \cdot p \int Q_e(V) \cdot V^{0.5} \cdot f(V) \cdot dV, \quad (2)$$

where  $k_0 = 1.87 \cdot 10^6$ . When  $E$  takes the particular form  $E = n_e \cdot W \cdot X$ , it then follows from the definitions of  $\eta_e$  and  $F_e$ , that

$$\eta_e = k_0 \cdot (W \cdot Xp^{-1})^{-1} \int Q_e(V) \cdot V^{0.5} \cdot f(V) \cdot dV \quad (3)$$

and

$$F_e = k_0 \cdot (W \cdot Xp^{-1})^{-1} \int Q_e(V) \cdot V_L \cdot V^{0.5} \cdot f(V) \cdot dV. \quad (4)$$

In all these expressions the integration must be performed for that range of  $V$  in which  $Q_e(V)$  has a significant magnitude.

For a given gas, the energy distribution function,  $f(V) \cdot dV$ , whatever its form, must be a function of the average electron energy  $\bar{V}$ ; for a given type of collision process  $Q_e(V)$  is a function of  $V$  only, and  $V_L$  is a function of  $V$  or is a constant. It therefore follows that the integrals in (1), (2), (3), and (4) are functions of  $\bar{V}$  only. Moreover,  $\bar{V}$  and  $W$  are known from experiment to be functions of  $Xp^{-1}$ ; it then follows that  $S_e$  is a function of  $p$  and  $Xp^{-1}$ , and that  $\eta_e$  and  $F_e$  are functions of  $Xp^{-1}$  only. This is of

\* Cf. Appendix (I)

particular importance experimentally because, for an electron swarm moving in a uniform electric field,  $X$  and  $p$  are two of the characteristic properties most easy to measure.

**3—The Energy Balance Expression**—In considering the energy balance in the gas it is necessary to take into account, in addition to the fractional energy loss for collisions involving excitation of the molecules (for which we shall continue to use the symbol  $F_e$ ), the fractional energy loss associated with elastic collisions and those resulting in ionization; these two quantities are conveniently denoted by  $F_d$  and  $F_i$  respectively, and they may be derived from (5) by using the appropriate values of  $Q_e(V)$  and  $V_L$ . The postulated condition of the steady state then requires that

$$F_i + F_d + \Sigma F_e = 1,$$

where the summation extends over all the possible excitation processes. Since in practice the summation is restricted to the principal excitation processes only, the form of the energy balance expression which is of practical importance is

$$F_i + F_d + \Sigma F_e \approx 1.$$

**4—Particular Forms for  $\eta_e$  and  $F_e$  Corresponding to a Maxwellian Electron Energy Distribution**—For a Maxwellian distribution we have\*

$$f(V) \cdot dV = (27/2\pi)^{0.5} V^{-1.5} V^{0.5} e^{-1.5V/\bar{V}} \cdot dV.$$

On inserting this expression for  $f(V) \cdot dV$  in (3) and (4) we find, after evaluating the numerical terms,

$$\eta_e = k_1 \cdot (W \cdot Xp^{-1})^{-1} V^{-1.5} \int Q_e(V) \cdot V \cdot e^{-1.5V/\bar{V}} \cdot dV \quad (3.1)$$

and

$$F_e = k_1 \cdot (W \cdot Xp^{-1})^{-1} \bar{V}^{-1.5} \int Q_e(V) \cdot V \cdot V \cdot e^{-1.5V/\bar{V}} \cdot dV, \quad (4.1)$$

where

$$k_1 = 3.87 \cdot 10^8.$$

\* This may be derived from the more usual form involving the r.m.s. velocity,  $\bar{v}$ , by the relation

$$0.5mv^2 = 1.5kT_e = e\bar{V}/300,$$

where  $k$  is Boltzmann's constant,  $T_e$  the electron temperature in °K., and  $e$  the electronic charge in e.s.u.

III—THE NUMERICAL RESULTS FOR THE FRACTIONAL ENERGY LOSSES  
AND THE ENERGY BALANCE

The calculations of the F terms (and also of the  $\gamma$  terms discussed in the next section) have been carried out for the range of  $Xp^{-1}$  for which it was found in Part I that the assumption of a Maxwellian electron energy distribution led to absolute values of the Townsend coefficient  $\alpha p^{-1}$ , in good agreement with experiment. The details of the procedure adopted in carrying out these calculations, and the sources of the relevant auxiliary, are described in the Appendix. The results for the F terms are given in Table I.

TABLE I—THE FRACTIONAL ENERGY LOSS F IN ELECTRON COLLISION PROCESSES IN HYDROGEN, AND THE TOTAL ENERGY LOSS  $\Sigma F$  FOR AN ASSUMED MAXWELLIAN ELECTRON ENERGY DISTRIBUTION

V	$Xp^{-1}$	F values						$\Sigma F$
		Ionization	$^1\text{H}_u$	$^3\Sigma_u^+$	$^3\Sigma_g^+$	Vibration	Elastic	
2	13	0.02	0.02	0.04	0.00	0.05	0.67	0.80
3	21	0.02	0.12	0.15	0.02	0.03	0.44	0.78
4	31	0.05	0.27	0.18	0.04	0.01	0.24	0.79
5	42	0.09	0.39	0.16	0.04	0.01	0.14	0.83
6	55	0.13	0.45	0.12	0.04	0.00	0.10	0.84
7	68	0.18	0.48	0.10	0.04	—	0.06	0.86
8	80	0.19	0.50	0.08	0.03	—	0.05	0.85
9	93	0.21	0.50	0.07	0.03	—	0.04	0.85
10	105	0.22	0.48	0.05	0.02	—	0.03	0.80

An interesting result of the calculations for the three electronic transitions is that F<sub>i</sub> (and  $\gamma_i$ ) passes through a maximum value, and that although the critical energies do not differ widely amongst themselves, the value of  $Xp^{-1}$  at which the maximum occurs is much greater for the singlet state than for the triplet states. The maximum for F<sub>t\*</sub> also occurs at a high value of  $Xp^{-1}$ ; this similarity to the singlet state is to be expected because the transitions are optically allowed and may therefore be expected to be characterized by similar curves for the dependence of the Q's on the electron energy.

The values of the total fractional energy loss  $\Sigma F$  given in column 9 are approximately constant, the mean is 0.82 with an average deviation of 3%. It is now necessary to review briefly to what extent the values of  $\Sigma F$

\* The results in Part I were expressed in terms of the Townsend coefficient of ionization,  $\alpha p^{-1}$ ; the conversion of such values into F<sub>i</sub>'s is given in the Appendix.

depend upon adjustable constants, arbitrary assumptions, or approximations, described in the Appendix. Experimental data have been used for  $F_e$ ; calculation would have given values about 10% lower, but this would lead to a diminution in  $\Sigma F$  of only 3% at the higher end of the range of  $Xp^{-1}$ , and the difference is thus not significant. There is some uncertainty about the constant  $A^*$  which determines the  $F_e$  values for the  ${}^1\Pi_u$  state, but the experimental data for the total and ionizing cross-sections greatly restrict the possible values for  $A$ : an increase in  $A$  of 33% produces a slight maximum in  $\Sigma F$  in the middle of the range, and alters the mean to 0.94 with an average deviation of 6%; a diminution in  $A$  of the same amount causes a downward drift of  $\Sigma F$ , and alters the mean to 0.70 with an average deviation of 4%. The factor 1.3† has been used in estimating the amplitude of the cross-sections of the upper triplet state from those of the lower: the true factor probably lies between 1/2 and 1/5, and the use of either of these would neither disturb the steadiness nor the mean value of  $\Sigma F$  as given in Table I by more than 2%. A small error has been introduced in the values of  $F_e$  for vibrational excitation by neglecting the cross-section for  $V > 6$ , this is only appreciable at the higher values of  $Xp^{-1}$ , but is unimportant for the energy balance because the values of  $F_e$  are then less than 1% of  $\Sigma F$ .‡ Possibly the least certainty attached to the values for the elastic loss  $F_{el}$ , since the factor  $f$  giving the excess over the classical loss in a single collision§ was derived for one value of  $V$  and assumed valid over a wide range, on the other hand, there appears to be little doubt that  $f$  is appreciably greater than unity.

The foregoing examination of the  $\Sigma F$  values shows that neither their mean value nor their constancy in the range of  $Xp^{-1}$  concerned is significantly sensitive to the adjustable constants and approximations involved in calculating the component  $F_e$  terms; moreover, the mean value of  $\Sigma F$  does not lie far from unity.

#### IV—THE COMPARISON OF THE CALCULATED ENERGY EFFICIENCIES WITH EXPERIMENT FOR THE ELECTRONIC TRANSITIONS

There are two sets of experimental investigations which provide data which may be compared with the calculated values of the  $\eta_e$ 's for the excitation of the two triplet states; unfortunately, in neither case have the conditions postulated by the theory been completely fulfilled. The values

\* Appendix, (2).

† Appendix, (4).

‡ Appendix, (5).

§ Appendix, (6).

of  $\eta_e$  for the intensity of the continuous spectrum (emitted by  $^3\Sigma_g^+$  molecules) in arbitrary units may be derived from the data of Chalange;\* and the energy efficiency for the production of atoms  $\eta_H$  in direct current positive column discharges in streaming hydrogen has been investigated by Poole (private communication) in these laboratories.

Since the comparison of the calculated and experimental values of  $\eta_e$  for the triplet states in Table I presupposes the validity of the values of V and W for discharges of much higher current density than those in which these quantities were determined, it is pertinent to point out that Harris's† data on the Hall effect in positive column discharges through hydrogen show that the values of W are still valid under these conditions. For the continued validity of the values of  $\bar{V}$  at such high current densities there appears to be no experimental evidence, but the fact that the values for one component of the total motion, W, continue to be valid is at least a very strong indication that the same is true for the values of the mean energy of the total motion V; further support for this view is afforded by the recent theoretical analysis of the relation between V and W by Bradbury and Nielsen.‡

(1) *The Continuous Spectrum*—Chalange§ has examined the dependence of the intensity of the continuous spectrum I on the pressure in the range 1·15 to 70 mm. for a positive column discharge of 50 ma in a tube 6 mm. diameter and 10 cm. long; it was found to pass through a well-defined maximum for  $p = 3$ . When the potential V across the tube is known, it is a simple matter to evaluate  $Xp^{-1}$  and also the energy efficiency for the excitation process, the latter being given in *arbitrary units* by  $\eta_e = I/V$ . Dr. Chalange in a private communication has kindly furnished us with the data from which his published curve was drawn and with the corresponding values of the electrode potential; from the latter, values of V have been obtained by deducting the normal cathode fall for aluminium electrodes, 200 volts.||

The resulting values of  $Xp^{-1}$ , V, and  $\eta_e$ , are, however, somewhat uncertain averages because low frequency alternating potentials were used to maintain the discharge. These experimental values for the dependence of  $\eta_e$  on  $Xp^{-1}$  for the excitation of the  $^3\Sigma_g^+$  state are shown in fig. 1, the calculated values being represented by the full line; since the experimental

\* Ann. Physique, ser. 11, vol. 1, p. 123 (1934).

† Phil. Mag., vol. 17, p. 131 (1934).

‡ Phys. Rev., vol. 49, p. 388 (1936).

§ Ann. Physique, ser. 11, vol. 1, p. 123 (1934).

|| Knoll-Ollendorf-Rompe, 'Gasentladungstabellen,' Leipzig, 1934.

values are in arbitrary units their values have been adjusted to agree with the calculated one at  $Xp^{-1} = 31$ . It is seen from fig. 1 that the experimental values follow the general trend of the calculated values surprisingly well.

This result must be regarded to some extent as fortuitous in view of the uncertainties already mentioned in deriving the experimental values for  $\eta_e$  and  $Xp^{-1}$ , and because it is not certain that the dependence of  $\bar{V}$  and  $W$  on  $Xp^{-1}$  in low frequency alternating fields is the same as that measured for steady fields.

Quite recently experiments have been commenced in these laboratories to repeat Chalange's work under conditions more closely approximating to those required by the theory by using direct current uniform positive

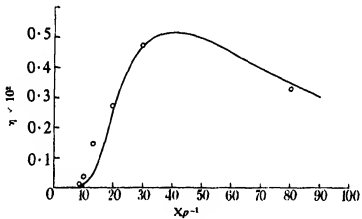


FIG. 1

column discharges through streaming hydrogen. Whilst no quantitative data are yet available, the results show that  $\eta_e$  falls off as  $Xp^{-1}$  is increased from 50 to 200 in much the same way as is predicted by the calculated data represented by the curve in fig. 1; the experiments also indicate that the position of the maximum is about  $Xp^{-1} = 45 \pm 7$ , whilst the theoretical value is  $Xp^{-1} = 42$ . Considered in conjunction with Chalange's data there remains, therefore, little doubt that the calculated values of  $\eta_e$  predict satisfactorily the observed trend of the dependence of the intensity of the continuous spectrum on  $Xp^{-1}$ .

**2—The Production of Hydrogen Atoms**—The importance of Poole's determinations of the efficiency of the production of hydrogen atoms  $\eta_{H^+}$  is that they afford a quantitative test of the theoretical calculations. Since the excitation of the  ${}^3\Sigma_u^+$  and  ${}^3\Sigma_g^+$  states leads in each case to the

ultimate production of two hydrogen atoms, for any given value of  $Xp^{-1}$ , the calculated energy efficiency for the production of atoms  $\eta_H$  is given by twice the sum of the  $\eta_e$ 's for these two states. For the atoms actually measured, Poole has obtained a mean value of  $\eta_H$  about  $8.6 \times 10^{-2}$  atoms per electron-volt, the corresponding values of  $Xp^{-1}$  ranging from about 17 to 29. The true values of  $\eta_H$  must have been considerably higher because of the loss of atoms by recombination; the difficult corrections for this and for the effect of the streaming velocity have been attempted by Poole and lead to the values given in Table II, column 3. Now, the maximum calculated value of  $\eta_H$  is  $4.40 \times 10^{-2}$  at  $Xp^{-1} = 31$ . It will be observed that the maximum value derived from these experiments on the formation of hydrogen atoms in a *striated* positive column dis-

TABLE II—THE ENERGY EFFICIENCY OF ATOM FORMATION

$Xp^{-1}$	$\eta_H, \text{ calc.} \dagger$	$\eta_H, \text{ expt.}$
13	2.8 $\times 10^{-2}$	—
17	7.2	$10.6 \times 10^{-2}$
18	8.2	7.6
20	10.0	11.8
25	12.2	12.6
26	12.4	14.4
30	13.0	10.0
42	12.0	—
80	6.6	—
105	4.4	—

† For purposes of comparison the values in column 2 have been calculated, using cross-sections for the triplet states three times greater than those used for the  $F_e$  values in Table I.

charge is larger by a factor of about 3 than this calculated maximum, which is based on Massey and Mohr's\* cross-section calculated by wave mechanics. Dr. Massey, in a private communication, has pointed out that although these values of the cross-section probably represent correctly the form of the dependence of the cross-section on the electron energy, there may be some uncertainty in their absolute magnitudes.

Whilst Poole's data are not strictly comparable with the theoretical values because the postulated condition of an electron swarm moving in a uniform electric field is not fulfilled, the trend of the experimental values is approximately that predicted by the  $F_e$  values in Table I, and the concordance becomes approximately quantitative (*cf.* Table II) if it is assumed that Massey and Mohr's cross-sections for the lower triplet

\* Proc. Roy. Soc., A, vol. 135, p. 258 (1932); these published values require to be corrected by the factor 1/30, *cf.* Appendix, (3).

state are too small by a factor of 3. This suggests that a striated discharge may differ little in effect from a uniform one. It is therefore interesting to consider what would be the effect on the  $\Sigma F$  values if it were assumed that the true cross-sections for the two triplet states were three times larger than those used in compiling Table I. The  $\Sigma F$  values then rise from 0.87 to a maximum of 1.23 at  $Xp^{-1} = 42$  and then slowly fall to 0.95 at the upper end of the range, the mean being 1.09. Whilst the trend of these  $\Sigma F$  values is less satisfactory than those in Table I, it is still true that the energy balance is approximately fulfilled. It would not be profitable to carry this discussion of the triplet cross-sections further until experimental data are available for atom formation in a *uniform* positive column.

**3—The Excitation of the  $^1\Pi_u$  State**—The only experimental observations bearing on the calculated  $\eta_e$  values for the singlet state are that the intensity of the  $^1\Pi_u - ^1\Sigma_g^+$  bands emitted from a positive column discharge is markedly increased both by roughening the interior surface of the discharge tube\* and by diminishing the pressure;† at the same time it was found that the intensity of the continuous spectrum is decreased. The effect of roughening is probably to increase the effective surface for recombination of ions and therefore to increase the value of  $Xp^{-1}$ , and the same effect would almost certainly result from decreasing the pressure. It can be seen from the trend of the  $F$  values in Table I that for  $Xp^{-1} > 40$  an increase in  $Xp^{-1}$  would account for the observed changes in intensity.

**4—The Stationary Concentration of Normal Hydrogen Molecules**—In deriving the calculated values of  $F$ , in Table I, it has been assumed in accordance with the conditions postulated in § 1 that the stationary concentration of all products of electron collision processes are negligible compared with that of hydrogen molecules in the ground state. Whilst this is easily demonstrated for such very low current densities as, for example, are used in Townsend's experiments to measure  $\bar{V}$ ,  $W$ , and  $\alpha p^{-1}$ , it is important to point out that the rate of destruction of molecules, for example, by the excitation of the triplet states, is very considerable for the current densities in positive column discharges. In order to illustrate this, it will suffice to consider the rate,  $R_e$ , of destruction of molecules by the excitation of the  $^3\Sigma_u^+$  state for the conditions when the calculated value of  $\eta_e$  is a maximum,  $Xp^{-1} = 31$ , and for a current density of 1 ma. cm.<sup>-2</sup> or  $6.3 \times 10^{19}$  electrons cm.<sup>-2</sup> sec.<sup>-1</sup>. From the definition of  $\eta_e$  and  $R$ , we have  $R_e = n_e \cdot W \cdot X \cdot \eta_e$ , and since the current density

\* Hymann, 'Phys. Rev.', vol. 36, p. 187 (1930).

† Jepperson, 'Phys. Rev.', vol. 44, p. 165 (1934).

$n, W$  is known and  $\tau_r = F_r V$ .<sup>1</sup> (Table I), we may evaluate  $R_r$  for any specified pressure, for  $p = 1$ , and therefore  $X = 31$ , we find  $R_r \approx 3.7 \times 10^{15}$ . But the total number of molecules present is only  $3.5 \times 10^{16}$ , or about 11% of the molecules initially in the ground state would be destroyed in 1 second. In order to maintain the concentration of ground state molecules greater than, say, 99% of the whole, it would therefore be necessary to maintain a stream of (ground state) hydrogen molecules through the electron swarm such that the gas is replaced at least eleven times a second.

### CONCLUSIONS

The results given in Table I show that, over a wide range of  $Xp^{-1}$ , there is a satisfactory agreement with experiment for the calculated energy efficiencies for the excitation of the triplet states, and that the energy balance condition is approximately fulfilled for six types of collision processes, which, on general grounds, are likely to include all the important ones. The only assumption involved in the calculations not based on experiment or theory is that the form of the electron energy distribution is Maxwellian.

In considering the results for the energy balance it must be remembered that there are uncertainties in the magnitudes of the cross-section of all the processes considered except ionization; whilst it has been shown that the results calculated are but slightly sensitive to the estimated uncertainty in the cross-sections, no exact fulfilment of the energy balance condition (apart from the discrepancy due to the neglect of the higher electronic transitions) is therefore to be expected while these uncertainties remain. The sensible fulfilment of the energy balance condition leads to the conclusion that the Maxwellian distribution represents the actual distribution to a close approximation, and, moreover, by including elastic losses, removes any restriction on the range of electron energies concerned; it thus confirms and extends the conclusion reached in Part I by considering ionizing collisions only. Strictly speaking, this deduction is valid only for the low range of current density to which the values of  $V$  relate. As pointed out in Part I, there are no theoretical reasons for supposing that the Maxwellian distribution might be anything more than an approximation to the true one.

An alternative way of regarding the matter is to consider that the cross-sections for all the possible processes determine the possible electron energy distribution. The results for the energy balance may then be interpreted to signify that, on account of the particular values of the cross-sections for the various possible collision processes in hydrogen, the

distribution does not change greatly over the range of  $Xp^{-1}$  examined, and that its form is close to the Maxwellian. It is interesting to consider what perturbation of the Maxwellian distribution would be necessary to increase the values of  $\Sigma F$  as given in Table I to unity. This could be effected by increasing the fractional concentration of fast electrons capable of effecting electronic excitation and ionization. The necessary increase would be less than 0.05% of the total electrons at the lowest value of  $Xp^{-1}$  in Table I, and only 8% at the highest. Such increases would have little effect on the elastic loss values as given in Table I.

Despite the fact that in the experiments of Chalonge and Poole the conditions postulated by the theory have not been exactly fulfilled, the agreement now presented (fig. 1 and Table II) between the calculated and experimental data for the energy efficiencies for the excitation of the triplet states is very satisfactory. This agreement is given added weight by the more recent experiments on the continuous spectrum in which the conditions postulated by the theory have been more closely fulfilled. Admittedly the significance of this agreement rests in part on the supposition that the measured dependence of  $V$  on  $Xp^{-1}$  is still valid at the higher current densities in positive column discharges; but reasons have been given previously believing this to be so.

Since these calculated values of  $\eta$  (and  $F$ ) are independent of any further assumption concerning the current density, it then follows that the Maxwellian distribution is probably also a close approximation to the true one at these high current densities found in positive column discharges; it is interesting to recall that Langmuir probe data for such discharges frequently lead to the same conclusion.

From the point of view of the use of discharges either as a source of light or for the production of chemical change, the results for the energy efficiencies are particularly interesting, for they illustrate that in the positive column it is to be expected that these quantities will depend greatly on the value of  $Xp^{-1}$ , and, moreover, that there will be well-defined conditions where they attain a maximum value and which are mainly determined in a given gas by the form of the curves for the dependence of the cross-section on the electron energy.

#### SUMMARY

This paper makes an attempt to calculate the absolute values of the energy efficiencies and fractional energy losses for the principal collision processes effected by an electron swarm moving through molecular hydrogen in a uniform electric field. The data used in calculating these

quantities are the absolute probabilities in single collisions derived partly from experimental and partly from theoretical data, and the dependence of the mean electron energy and drift velocity on  $Xp^{-1}$  as determined by Townsend. The assumption made is that the form of the electron energy distribution is Maxwellian.

Satisfactory agreement with experimental data is obtained for the energy efficiencies for the excitation of the two lowest triplet states. The total fractional energy loss is approximately constant over a wide range of  $Xp^{-1}$  and is close to unity; this result is shown to be insensitive to the adjustable constants and approximations involved. These results confirm the conclusions reached in Part I, and establish that, over a wide range of  $Xp^{-1}$  the actual rates of electron collision processes are, to a close approximation, those arising from a Maxwellian distribution; they also indicate that this is probably the case over a wide range of current density.

The authors wish to express their cordial thanks to Dr H S W Massey for many suggestions and helpful discussions, and to Mr H G Poole for his kindness in supplying unpublished information.

## APPENDIX

### *The Data and Procedure used in Calculating and F for the Principal Collision Processes*

(1)  $V$  and  $W$ —The dependence of these quantities on  $Xp^{-1}$  has been determined by Townsend, and his data are given in Part I, Table I. At the higher values of  $Xp^{-1}$  it was pointed out in Part I that the energy associated with the drift motion is appreciable in comparison with that of the random motion to which latter the measurements of  $V$  relate; it was also shown there that, to a first approximation, allowance may be made for the drift energy by considering the total motion to be sensibly isotropic but with the mean energy  $\bar{V} + V_w$ , where  $V_w = 2.84 \times 10^{-16} W^2$  is the energy associated with the drift motion. This procedure was found to lead to calculated values of the Townsend coefficient  $\alpha p^{-1}$  in very good agreement with experiment (Part I, Table X) and has therefore been adopted here [except for the excitation of the  ${}^3\text{H}_u$  state, cf (2)]. Concerning the actual values of  $W$  it may be noted that the recent determinations by Bradbury and Nielsen (*loc. cit.*), using a new method for  $Xp^{-1} < 20$ , confirm those of Townsend.

(2) *The Excitation of the  ${}^3\text{H}_u$  State*—The value of  $V$ , is known from

spectroscopic data,\* 12·6 electron-volts. There are no data for  $Q_e(V)$ , but since this is an extreme case of an optically allowed transition, estimates may be derived in the following way. By analogy with similar atomic† and molecular‡ transitions, and from the predictions of theory,§ it is to be expected that  $Q_e(V)$  will rise approximately linearly with  $V$  passing through a broad maximum for  $V = 3 - 5V_c$ , and that in this latter region it will form the main contribution to the total cross-section,  $Q_T(V)$ , apart from the ionizing cross-section,  $Q_i(V)$ , or  $Q_e(V) \approx Q_T(V) - Q_i(V)$ . For  $V = 64$ , using the data of Normand||  $Q_T(V)$  and of Tate and Smith for  $Q_i(V)$ ,¶ we find  $Q_e(64) \approx 2.06 \pi a_0^2$ . For the initial "linear" region,  $V < 3V_c$ , we may use the approximate expression  $Q_e(V) = A \cdot (V - V_c)$ , and the mean gradient of  $Q_e(V)$  between  $V = V_c$  and  $V = 64$  then sets a lower limit to the value of the constant  $A$ , 0.04. Again by analogy with similar transitions, it appears that a reasonable value to take for  $A$  is the somewhat greater value, 0.10 which we adopt here. Whilst it is obviously difficult to assess the error in this estimate, we believe that it is probably correct within a factor of 2.

This approximate expression for  $Q_e(V)$  has been introduced into (3.1) and (4.1) in order to derive the values of  $\eta_e$  and  $F_e$ , using for the latter  $V_t = V_c$ . This procedure is strictly analogous to that adopted in Part I (*c.f.*, for example, the derivation of  $a_0 p^{-1}$  in Table I of that paper), where it was found to give satisfactory agreement with experiment (for ionization) if no correction for the energy of drift motion were applied to the mean energy. Since the two cases are closely similar, we have performed the calculations for the  ${}^1\Pi_u$  state likewise without applying this correction. By comparison with the data for ionization (Part I, Table I) it may be estimated that the error in the resulting values of  $\eta_e$  and  $F_e$  does not exceed 25% apart from the uncertainty in the value of the constant  $A$ .

**3—The Excitation of the  ${}^3\Sigma_u^+$  State**—The values of  $Q_e(V)$  have been calculated by Massey and Mohr\*\* assuming  $V_c = 11.5$ . Dr. Massey has informed us in a private communication that the appropriate correction for the value  $V_c = 9.5$  derived from spectroscopic data†† is effected by

\* Mulliken, 'Rev. Mod. Phys.', vol. 4, p. 1 (1932); Richardson, "The Molecular Spectrum of Hydrogen," London, 1934.

† Hanlé and Larche, Lees, *loc. cit.*

‡ Langstroth, *loc. cit.*

§ Mott and Massey, *op. cit.*; Massey and Mohr, *loc. cit.*

|| Normand, 'Phys. Rev.', vol. 35, p. 1217 (1930).

¶ Tate and Smith, 'Phys. Rev.', vol. 39, p. 270 (1932).

\*\* Mott and Massey, *op. cit.*; Massey and Mohr, *loc. cit.*

†† Winans and Stueckelberg, 'Proc. Nat. Acad. Sci., Wash.', vol. 4, p. 867 (1928); Finkelnberg and Weizel, 'Z. Physik,' vol. 68, p. 577 (1931).

reducing the scale of  $V$  by the factor  $9.5/11.5$ . He has also informed us that a recent check of the calculations leading to the  $Q_e(V)$  values has shown that the published data require to be corrected by the factor  $1/30$ .\* The values of  $\eta_e$  and  $F_e$  have been calculated according to (3.1) and (4.1) using for the latter  $V_L = V_e$ .

The shape of the curve for the dependence of  $Q_e(V)$  on  $V$  suggested that a simple approximation for this is to take  $Q_e(V)$  equal to the mean value,  $0.16 \pi a_0^2$ , in the range  $V_e$  to  $2V_e$ , and zero elsewhere; the advantage of this approximation is that the integrals in (3.1) and (4.1) can then be evaluated algebraically. On comparing the values of  $\eta_e$  derived from this approximation for  $Q_e(V)$  with the true ones it was found that, for the range of  $Xp^{-1}$  in Table I, they were low by 14% on the average; the error introduced by the approximate expression for  $Q_e(V)$  is thus small, a result we shall make use of in considering the excitation of the  ${}^3\Sigma_e^+$  state.

**4—The Excitation of the  ${}^3\Sigma_e^+$  State**—From spectroscopic data it is known that  $V_e = 12$  electron-volts.† Since there are no data for  $Q_e(V)$  it is necessary, as for the  ${}^1\Pi$  state (*q.v.*), to fall back on the predictions of theory and the analogies that may be drawn from the data for atomic transitions; these indicate that the variation of  $Q_e(V)$  with  $V$  will closely resemble that for the lower triplet state previously considered, and the amplitudes will be about a third smaller. In the absence of more precise data we have therefore felt justified in using the type of approximation which was found satisfactory for lower triplet state, and which, from the foregoing considerations, now takes the form  $Q_e(V) = 0.055 \pi a_0^2$  from  $V_e$  to  $2V_e$ . The values of  $\eta_e$  and  $F_e$  have therefore been derived by introducing this approximation in (3.1) and (4.1) using for the latter  $V_L = V_e$ .

**5—The Excitation of the First Vibrational State**—From spectroscopic data it is known that  $V_e = 0.53$  electron-volt.‡ For  $V = 7$ , Massey has calculated  $Q_e(V)$ ,  $0.07 \pi a_0^2$ ;§ this value is probably valid down to  $V = 3$ ,|| for which there is experimental support in Ramien's|| determinations of the energy loss suffered by slow electrons. For simplicity in performing

\* These corrected values are given in the following table, the original ones from which the published curve was drawn being kindly supplied by Dr. Massey:—

$V$	9.5	10.3	12.4	14.5	16.5	18.6
$Q_e(V)$	0	0.16	0.22	0.22	0.16	0.10

† See footnote ††, p. 164.

‡ Mulliken, Richardson, *loc. cit.*

§ Massey, 'Trans. Faraday Soc.', vol. 31, p. 556 (1934).

|| Massey, private communication.

¶ Ramien, 'Z. Physik,' vol. 70, p. 353 (1931).

the calculations of  $\eta_e$  and  $F_e$  according to (3.1) and (4.1), using for the latter  $V_L = V_e$ , we have assumed that  $Q_a(V)$  has the constant value 0.07 over the slightly shorter range from  $V = 3$  to  $V = 6$ , and zero elsewhere. This procedure does not introduce an error significant for the purposes of this paper because the values of  $\eta_e$  and  $F_e$  are in any case very small except at the lower values of  $Xp^{-1}$  where the fractional concentration of electrons having  $V > 6$  is also small.

**6—Elastic Collisions**—For  $V < 9.5$  the cross-section,  $Q_{el}(V)$  is approximately equal to  $Q_T(V)$  because  $Q_a(V)$  is negligible compared with the latter, and because, as Massey has pointed out,\* the cross-section for the only other possible process, rotational excitation, must be much less than  $Q_a(V)$ . For  $V > 9.5$  we have taken  $Q_{el}(V)$  to be equal to  $Q_T(V)$  diminished by the sum of the  $Q$ 's for ionization† and for the three electronic transitions considered previously. Bradbury and Nielsen have pointed out‡ that Ramien's data§ indicate that the energy loss average in a single collision,  $V_{L,el}$ , must exceed the classical value,  $(2m/M) \cdot V$ , by the factor  $f$ . For  $V = 4.2$  Ramien found  $V_{L,el} = 0.02 V$ , hence, following Bradbury and Nielsen but making allowance for the loss in vibrational excitation,  $V_{L,el}$ , we have, for the energy loss per cm. of electron track,  $-dT/dx$ ,§

$$\begin{aligned}-dT/dx &= (3.15 \cdot p) \cdot 0.02 \cdot V \cdot Q_T(V) \\ &= (3.15 \cdot p) \cdot [V_{L,el} \cdot Q_{el}(V) + V_{L,v} \cdot Q_v(V)];\end{aligned}$$

from this we find, for  $V = 4.2$ , that  $f = 7.8$  using as before Normand's data for  $Q_T(V)$ || and Massey's for  $Q_v(V)$ .\* In the absence of other data we have assumed that this value of  $f$  is valid over the whole range of  $V$  concerned in our calculations; values of  $F_{el}$  have then been calculated from (4.1) using values of  $Q_a(V)$  derived as indicated above from Normand's data for  $Q_T(V)$ .||

**7—Ionization**—From the definition of the Townsend coefficient of ionization,¶  $\alpha$ , and from that of the energy efficiency of a collision process (p. 15), it follows that  $\eta_i = \alpha X^{-1} = \alpha p^{-1} \cdot (Xp^{-1})^{-1}$ ; since, for this process,  $V_L = V_e = 15.8$  electron-volts, the values of  $F_i$  follow immediately. We have used the experimental data for  $\alpha p^{-1}$  as a function of  $Xp^{-1}$ .\*\*

\* Massey, *loc. cit.*

† Tate and Smith, *loc. cit.*

‡ Bradbury and Nielsen, *loc. cit.*

§ Mott and Massey, *op. cit.*, chap. ix.

|| Normand, *loc. cit.*

¶ Townsend, *op. cit.*

\*\* Handb. Exp. Physik, vol. 13, part 3, p. 112.

# The Lattice Spacings of Certain Primary Solid Solutions in Silver and Copper

By WILLIAM HUME-ROTHERY, Warren Research Fellow of the Royal Society, GEORGE FARLEY LEWIN, and PETER WILLIAM REYNOLDS, The Old Chemistry Department, Oxford

(Communicated by W. L. Bragg, O.M., F.R.S.—Received 20 May, 1936)

## I—INTRODUCTION

In continuation of previous work† on valency effects in alloys, the present paper describes an investigation of the mean lattice spacings of primary solid solutions of cadmium, indium, tin, and antimony in silver, and of zinc, gallium, and germanium in copper. From these measurements the mean lattice distortions at equiatomic compositions are compared. The term "mean lattice distortion" is used here to denote the difference between the lattice constants of the solid solution and the solvent metal, as measured by the ordinary powder method of X-ray crystal analysis. It is well known that in solid solutions the X-ray methods give the mean lattice distortions, while more or less intensely localized regions of distortion may occur without preventing the formation of sharp diffraction lines. The present experimental data refer to the mean values only.

## 2—EXPERIMENTAL

*X-ray Technique*—The lattice constants were determined from Debye-Scherrer photographs obtained with a 9 cm. diameter camera of the type used by Bradley and Jay,‡ in conjunction with a demountable X-ray tube made by the Metropolitan Vickers Electrical Co., Ltd., to whom the authors must express their thanks for instruction in manipulation. The powder specimens were made from filings which had passed through a 380 mesh sieve, and were mounted on a hair with Canada balsam. The camera contained a sliding window through which a thermocouple was inserted with its hot junction near to the specimen, and the temperature was controlled accurately by blowing a current of air round the camera.

† Hume-Rothery, Mabbott, and Channel-Evans, 'Phil. Trans.', A, vol. 233, p. 1 (1934).

‡ Bradley and Jay, 'Proc. Phys. Soc.', vol. 44, p. 563 (1932).

The camera was standardized against quartz as recommended by Bradley and Jay,<sup>†</sup> whose  $\cos^2 \theta$  extrapolation method<sup>‡</sup> was used throughout the work in order to eliminate errors due to absorption, film shrinkage, eccentricity of the specimen, etc. The effective height of the specimen was limited by the size of the aperture admitting the X-rays, and was thus a constant throughout the whole series of experiments. The films were measured on a travelling microscope kindly lent by Professor F. Soddy, F.R.S., which read accurately to 0·01 mm., and allowed estimation to 0·002 mm. The centre of darkening of each line was measured four times,<sup>§</sup> and duplicate measurements of the same film showed that the measuring technique gave results reproducible to 0·0001 Å. The lattice constant determinations have been reduced to standard temperatures of 24° C. for the silver alloys and 23° C. for the copper alloys, since, although constant in any one experiment, the actual temperature varied with that of the room. For this correction it was assumed that the coefficients of expansion of the alloys were the same as those of the solvent metals; data for other alloys suggest that, since the temperature corrections were rarely as much as 3° C., the error introduced by this assumption is negligible. When the correction was made, duplicate photographs from the same specimen gave results agreeing within 0·0001 Å. In the course of the work, slight alterations were made to the slit system controlling the width and divergence of the X-ray beam, but duplicate experiments suggested that any errors introduced were within the above limits. The accuracy was increased as the work proceeded, and it is considered that nearly all the results given for silver alloys and the later results for copper alloys were reproducible to 0·0001 Å. The earlier results were reproducible to 0·0002 Å., and are distinguished in the tables by the mark \*.

The standard angle of the camera, as given by shadows of the fixed knife edges, corresponded with an angle of 84·989° in the Bragg equation. Cobalt radiation was used for all the alloy diffraction photographs. With silver alloys this gave strong well-defined K<sub>a</sub> doublets for the 024 and 133 lines at approximately 78° and 72° respectively, and the lattice spacings depended entirely on extrapolation from the points calculated for these lines. The 400 line was also measured, and was clearly resolved in the majority of the alloys (*see* p. 170). With the copper alloys cobalt radiation gave (*see* p. 173) high angle 400 lines at approximately 82°, with 222 and 113 lines at 59° and 55° approximately, which were distinctly resolved.

As in the work of Bradley and Jay,<sup>†</sup> values obtained from the K<sub>a1</sub> and

<sup>†</sup> Bradley and Jay, 'Proc. Phys. Soc.' vol. 45, p. 507 (1933).

<sup>‡</sup> *Ibid.*, vol. 44, p. 573 (1932).

<sup>§</sup> With faint lines six measurements were made.

$K_{\alpha 2}$  doublets were averaged in the ratio  $2_{\alpha 1} : 1_{\alpha 2}$ , and the fundamental constants on which the results depend are as follows:

*for the calibration of camera*

$$\begin{aligned}\text{Copper radiation} \dots & \quad \lambda K_{\alpha 1} = 1537.395 \text{ X.U} \\ & \quad \lambda K_{\alpha 2} = 1541.232 \text{ X.U}\end{aligned}$$

$$\text{Quartz at } 27^\circ \text{ C. } a = 4246.53 \text{ X.U}$$

$$c/a = 1.09996 (5)$$

*for the experimental values*

$$\begin{aligned}\text{Cobalt radiation} \dots & \quad \lambda K_{\alpha 1} = 1785.29 \text{ X.U} \\ & \quad \lambda K_{\alpha 2} = 1789.19 \text{ X.U}\end{aligned}$$

The wave-lengths are taken from the 2nd edition of Siegbahn's "Spektroskopie der Röntgenstrahlen".

*b—Preparation of the Specimens*—Great difficulty was found in determining the composition of the filings in the specimen with an accuracy equivalent to that of the lattice constant measurements. The technique finally employed is being published elsewhere.† The alloy was always annealed to equilibrium in lump form, after which 0.5 to 1.0 gm. of filings was prepared with precautions to avoid contamination or errors due to segregation effects. The filings were annealed in evacuated tubes to relieve mechanical strain, and rapidly cooled in air. The whole sample was then sieved and a small portion of the well-mixed fine filings removed for the preparation of the X-ray specimen. The remainder of the filings was analysed, both metals being determined, so that all figures given are based on the analysis of filings, and not of lump-alloy. These methods were found to be essential in order to obtain strictly reproducible results, and the details of the technique should be consulted.

### 3—RESULTS

#### *a—Pure Silver and Copper*

The lattice constant of chemically pure silver was determined as  $4.0778, \pm 0.0001$  Å. at  $24^\circ$  ( $= 4.0773$ , at  $18^\circ$  C.),‡ which is in good agreement with the values of  $4.0770$ , and  $4.0771$ , at  $18^\circ$  obtained by Owen

† Paper to appear in 'J. Inst. Met.'

‡ All experimental values have been corrected for the deviation from the Bragg Law.

and Yates<sup>†</sup> for less pure silver<sup>‡</sup> with cobalt radiation, and with the value of 4.0774<sub>s</sub> at 18° obtained by Jay<sup>§</sup> with copper radiation.

Some specially pure copper was kindly provided by the British Non-Ferrous Metals Research Association, and for this the lattice constant was determined as 3.6073<sub>s</sub> at 23°, which corresponds with 3.6070<sub>s</sub> at 18°. This is distinctly lower than the values of most other workers,<sup>||</sup> who give values from 3.6077 to 3.6079 Å. with copper radiation, although Owen and Yates give a lower value of 3.6076 Å. with cobalt radiation. Part of this difference may be due to the use of copper radiation for the standardization of the camera, and cobalt radiation for the parameter determinations, since the work of Owen and Yates showed that cobalt radiation frequently gave results lower than those obtained by the use of other radiations.

#### *b—Silver-Cadmium*

The silver-rich alloys were supplied by Messrs. Johnson, Matthey & Co., Ltd., in the form of rods, whilst three other specimens (Nos. 6, 7, and 8) were kindly prepared in the form of  $\frac{1}{4}$ -in. sand castings by the British Non-Ferrous Metals Research Association. The results are shown in Table I, and plotted graphically in fig. 1. The films were all of the highest quality except for alloys Nos. 3 and 5, where the 400 lines were not so clearly resolved. The mean lattice spacing-composition curve is definitely not linear, the mean lattice distortion in the concentrated solid solutions being greater than that required by a linear relation. The points lie on a smooth curve from which no point differs by more than 0.0002 Å. except that for alloy No. 6, which is 0.0006 Å. too high. The figures agree well with the data of Westgren and Astrand,<sup>¶</sup> who gave the value 4.140 Å. for an alloy containing 28.5 atomic per cent of cadmium.

#### *c—Silver-Indium*

Alloys Nos. 2, 4, 6, and 8 were prepared by remelting cooling curve ingots used by one of us<sup>\*\*</sup> with 99.99% silver grain. The indium in the

<sup>†</sup> 'Phil. Mag.', vol. 15, p. 472 (1933).

<sup>‡</sup> The silver used by Owen and Yates is described as being of 99.9% purity, and we are informed by Messrs. Johnson, Matthey & Co., Ltd., that silver of this class is usually not less than 99.96% pure, the chief impurity being copper which decreases the lattice spacing; a detailed comparison cannot therefore be made.

<sup>§</sup> 'Z. Kristallog.', vol. 86, p. 106 (1933).

<sup>||</sup> Owen and Yates, 'Phil. Mag.', vol. 15, p. 472 (1933); Obinata and Wassermann, 'Naturwiss.', vol. 21, p. 382 (1933); Barrett and Kaiser, 'Phys. Rev.', vol. 37, p. 1695 (1931).

<sup>¶</sup> 'Z. anorg. Chem.', vol. 175, p. 90 (1928).

<sup>\*\*</sup> Hume-Rothery and others, 'Phil. Trans.', A, vol. 233, p. 1 (1934).

original ingots was from a specially pure sample of 99.98% material supplied by Messrs. Adam Hilger, Ltd. The remaining alloys were prepared from chemically pure silver and the purest indium supplied by the Indium Corporation of America.<sup>†</sup> The metals were melted under charcoal in small Salamander crucibles, and were cast in the form of  $\frac{1}{4}$ -in.

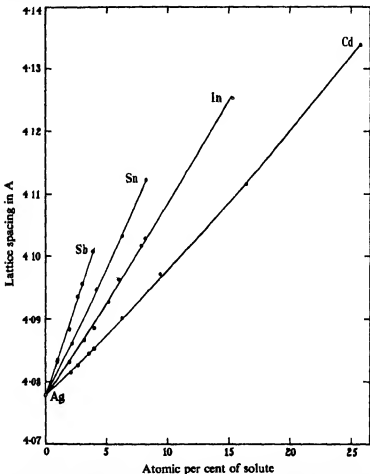


FIG. 1—Lattice spacings of primary solid solutions of cadmium, indium, tin, and antimony in silver.

cylindrical rods in sand moulds in order to reduce inverse segregation effects. The results are recorded in Table II. The lattice-spacing composition curve (fig. 1) is again not a straight line, but shows an increased gradient at the higher concentrations. A smooth curve can be drawn

<sup>†</sup> This metal was found to contain less than 0.02% of lead.

TABLE I

Alloy No	Wt. % Cd	At. % Cd	Lattice constant at 24°
1	2.15	2.07	4.0814 <sub>3</sub>
2	2.75	2.64	4.0826 <sub>1</sub>
3	3.66	3.52	4.0844 <sub>3</sub>
4	4.10	3.94	4.0852 <sub>4</sub>
5	6.50	6.25	4.0901 <sub>3</sub>
6	9.72	9.37	4.0971 <sub>3</sub>
7	16.97	16.40	*4.1116 <sub>4</sub>
8	26.55	25.76	*4.1338 <sub>3</sub>

Lump anneals—Nos. 1, 2, and 4, 120 hr. at 600°; Nos. 3 and 5, 2½ hr. at 910°; No. 6, 5 hr. at 850°, Nos. 7 and 8, 4 hr. at 800°.

Filing anneals—Nos. 1, 2, 4, and 6, 15 hr. at 450°; the rest for 15 hr. at 400°.

Analyses—Made by the Midland Laboratory Guild. Weight percentages totalling from 99.87 to 100.00.

TABLE II

Alloy No.	Wt. % In	At. % In	Lattice constant at 24°
1	2.06	1.94	4.0831 <sub>1</sub>
2	3.30	3.11	4.0866 <sub>1</sub>
3	4.21	3.97	4.0885 <sub>1</sub>
4	5.45	5.14	*4.0926 <sub>4</sub>
5	6.35	5.99	4.0962 <sub>4</sub>
6	8.27	7.81	*4.1017 <sub>1</sub>
7a	8.64	8.16	4.1028 <sub>1</sub>
7b	8.65	8.17	4.1028 <sub>3</sub>
8	16.09	15.27	*4.1253 <sub>3</sub>

Lump anneals—Nos. 1 and 3, 2 hr. at 890°; Nos. 2 and 4, 3 hr. at 800–850°; Nos. 5, 7a, and 7b, 2 hr. at 845°; No. 6, 6 hr. at 800–850°; No. 8, 3 hr. at 750° and 6 hr. at 850°.

Filing anneals—15–20 hr. at 400° in all cases.

Analyses—Made by the Midland Laboratory Guild, the weight percentages totalling from 99.98 to 100.00 for Nos. 5, 7a, and 7b, and from 99.90 to 99.94 in the other cases.

through the points from which no point differs by more than 0.0005 Å. (which is equivalent to 0.2% on the composition scale). The values of the lattice spacings obtained in the present work are lower than those given by Weibke† for silver-indium alloys, the difference being about 0.003 Å. at 5.0 atomic per cent indium. The values given by Weibke are stated to involve errors of  $\pm 0.001$  Å., but the difference between the results of the two investigations is clearly greater than this.

† Weibke and Eggers, 'Z. anorg. Chem.', vol. 222, p. 145 (1935).

*d—Silver-Tin*

The alloys used were supplied by Messrs. Johnson, Matthey & Co., Ltd., in the form of drawn rods prepared from chemically pure silver and Chempur tin. The preliminary lump anneals of alloys Nos. 2a, 3a, and 4a were not quite sufficient, the 400 lines in the photographs from these samples being rather indistinct. In the other cases these lines were very clearly resolved and the exact correspondence of the results in the two series indicates that, for these alloys, the slight fuzziness of lines due to insufficient preliminary annealing introduces no appreciable error. The results are recorded in Table III and fig. 1, and are in agreement with the value 4·108 Å. given by Nial, Almin, and Westgren† for an alloy containing 7·3 atomic per cent of tin. The lattice distortion in the more concentrated alloys is again slightly greater than that required by a linear relation, although the difference is very small.

TABLE III

Alloy No.	Wt. % Sn	At. % Sn	Lattice constant at 24°
1	2·38	2·17	4·0860 <sub>3</sub>
2a	4·53	4·13	4·0945 <sub>3</sub>
2b	4·53	4·13	4·0945 <sub>3</sub>
3a	6·82	6·24	4·1032 <sub>3</sub>
3b	6·84	6·26	4·1032 <sub>3</sub>
4a	8·92	8·17	4·1122 <sub>3</sub>
4b	8·95	8·20	4·1122 <sub>4</sub>

Lump anneals—Nos. 1 and 2a, 20 hr. at 650°, 40 hr. at 780°, and 11 hr. at 860°; Nos. 3a and 4a, 20 hr. at 650° and 4 hr. at 780°; Nos. 2b, 3b, and 4b, 5 days at 725°.

Filing anneals—15 hr. at 520° for all.

Analyses—Made by Messrs. Johnson, Matthey & Co., Ltd., the weight percentages totalling from 99·97 to 99·99.

*e—Silver-Antimony*

Alloys Nos. 1 and 4 were prepared by Messrs. Johnson, Matthey & Co., Ltd., from chemically pure silver and some specially pure antimony (99·917%) kindly presented by the Cookson Lead and Antimony Co., Ltd. Alloys Nos. 2, 3, and 6 were prepared from slightly less pure silver and contained from 0·04 to 0·09% copper. The effect of this upon the lattice spacing has been allowed for (as shown in fig. 2) by assuming an additive

† Nial, Almin, and Westgren, 'Z. phys. Chem.', B, vol. 14, p. 81 (1931).

relation, using the data of Megaw<sup>†</sup> which show that 0·1 atomic per cent of copper reduces the lattice spacing of silver by 0·0003 Å. The validity of this method of correction was tested by means of alloy No. 5 which contained 0·46% by weight of copper, the corrected parameter for this

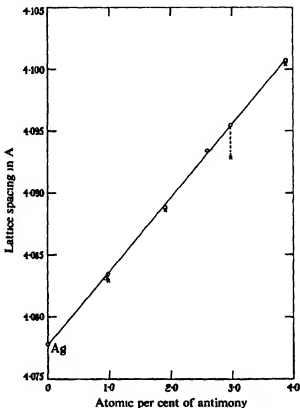


FIG. 2.—Lattice spacings of primary solid solutions of antimony in silver. For the alloys containing slight traces of copper the points marked  $\times$  are the measured lattice spacings, and those marked  $\circ$  the points corrected as described on p. 173 to allow for the effect of the copper. The validity of this method of correction is shown by the fact that the point for alloy No. 5, which contained as much as 0·46% of copper by weight, agrees well with the remainder. Where only the  $\circ$  point is shown, it implies that the alloy was completely free from copper.

alloy lying very closely on the straight line drawn through the remaining points. The results are recorded in Table IV and fig. 2, and, as shown in fig. 2, a straight line can be drawn from which no point differs by more than 0·0003 Å., which is equivalent to 0·05 atomic per cent on the composition axis.

<sup>†</sup> 'Phil. Mag.', vol. 14, p. 130 (1932).

TABLE IV

Alloy No.	Wt. % Sb	At. % Sb	Wt. % Cu	At. % Cu	Lattice spacing at 24°	
					Measured	Corrected to 0% Cu
1	1.06	0.94	0	0	4.0830,	4.0830,
2	1.10	0.98	0.09	0.15	4.0829,	4.0834,
3	2.15	1.91	0.04	0.07	4.0886,	4.0888,
4	2.93	2.60	0	0	4.0934,	4.0934,
5	3.35	2.98	0.46	0.78	4.0928,	4.0955,
6	4.36	3.88	0.05	0.08	4.1004,	4.1007,

Lump anneals—No. 1, 16 hr. at 650° and 3 hr. at 860°; Nos. 2 and 5, 3 days at 470° and 14 days at 590°; Nos. 3 and 6, 14 days at 550°, No. 4, 16 hr. at 650° and 5 hr. at 750°.

Filing anneals—15 hr. at 420° in all cases.

Analyses—Made by Messrs. Johnson, Matthey & Co., Ltd., the weight percentages totalling from 99.97 to 100.00.

#### f—Copper-Zinc

These alloys were kindly presented by the British Non-Ferrous Metals Research Association, and were prepared from the purest metals. The results are recorded in Table V and fig. 3. In alloys Nos. 2 and 4 the filings contained charcoal or carbonaceous matter, and the sum of the percentages of the two metals as determined by analysis was only 99.62

TABLE V

Alloy No.	Wt. % Zn	At. % Zn	Lattice constant at 23°
1	5.20	5.06	*3.6178
2	9.85	9.60	*3.6273
3	14.68	14.33	*3.6377
4	24.63	24.11	*3.6600

Lump anneals—Nos. 1 and 2, 1 hr. at 800°; No. 3, 1 hr. at 850°; No. 4, 2 hr. at 800°.

Filing anneals—6 hr. at 600° for all.

Analyses—Made by the Midland Laboratory Guild.

and 99.68 respectively. The charcoal did not, however, appear to affect the ratios of the two metals as determined by the analyses, and these two and the remaining points lie accurately on a smooth curve which agrees excellently with the results of Owen and Pickup† when allowance is made for the difference in the values obtained for the lattice constant of copper.

† 'Proc. Roy. Soc.,' A, vol. 137, p. 397 (1932).

*g—Copper-Gallium*

These alloys were prepared by melting pure electrolytic copper with gallium obtained from the Vereinigte Chemische Fabriken zu Leopolds-hall, and were cast into  $\frac{1}{4}$ -in. diameter chill moulds. The purity of the gallium varied from 99.85 to 99.95% in different batches. In the early

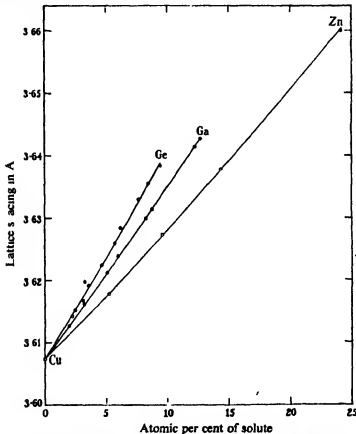


Fig. 3—Lattice spacings of primary solid solutions of zinc, gallium, and germanium in copper.

stages of the work difficulty was encountered in the analytical separation owing to the presence of carbonaceous matter in the filings.<sup>†</sup> All results in which the sum of the percentages was less than 99.80 were

<sup>†</sup> In some of the early work filings were annealed with charcoal as a further precaution against oxidation, but this was later found to be unnecessary and disadvantageous. In the later work the greatest care was taken to ensure the complete absence of carbonaceous matter from filings, the total metallic content of which was then not less than 99.97%.

rejected, and the final data are summarized in Table VI. The points for alloys Nos. 4 and 9 lie completely off the smooth curve given by the remainder. The difference is of the order 1% by weight, and is so great that it is clear that some large accidental error has occurred. It is significant that in each case the percentage of gallium by analysis was

TABLE VI

Alloy No.	Wt. % Ga	At. % Ga	Lattice constant at 23°	Lump anneal	Filing anneal
1	2.11	1.93	*3.6126	12 hr. at 700° 5 hr. at 800°	6 hr. at 600°
2	2.71	2.48	*3.6151	17 hr. at 700° 6 hr. at 850°	12 hr. ,
3	3.41	3.12	3.6161,	1 hr. at 990°	15 hr. ,
4	5.50	5.04	*3.6191,	33 hr. at 700° 3½ hr. at 900°	23 hr. ,
5	5.54	5.08	3.6212,	1½ hr. at 975°	15 hr. ,
6	6.51	5.97	*3.6238	13 hr. at 700° 5½ hr. at 800°	5 hr. ,
7	8.93	8.21	3.6298,	1½ hr. at 975°	15 hr. ,
8	9.55	8.78	*3.6314	23 hr. at 700° 4½ hr. at 800°	5 hr. ,
9	9.70	8.92	*3.6304	34 hr. at 700° 4 hr. at 900°	5 hr. ,
10	13.25	12.22	*3.6412,	33 hr. at 700° 12 hr. at 800°	29 hr. ,
11	13.70	12.64	*3.6426	10 hr. at 700° 9 hr. at 800°	5 hr. ,

Analyses—Nos. 3, 5, and 7 were analysed by Messrs. Johnson, Matthey & Co., Ltd., the remainder by the Midland Laboratory Guild, Ltd.

considerably greater than that calculated from the weights of metals melted together, which suggests that either some mistake occurred in the analysis, or that the filings were accidentally mixed with those of higher gallium content. These results are therefore omitted from fig. 3. The remaining points lie accurately on a smooth curve from which only one point differs by more than 0.0005 Å.; this one point was obtained in the

early stages of the work. The lattice distortion in the more concentrated alloys is slightly greater than would be expected from a linear relation. The results agree with those of Weibke† which were stated to be accurate to  $\pm 0.001$  or  $\pm 0.002$  Å.

TABLE VII

Alloy No.	Wt. % Ge	At. % Ge	Lattice constant at 23°	Lump anneal	Filing anneal
1	2.51	2.20	3.6141 <sub>s</sub>	36 hr. at 750–800°	5 hr. at 600°
2	3.49	3.07	*3.6166	5 hr. at 700° 5 hr. at 800°	"
3	3.67	3.23	*3.6197	15 hr. at 700° 6 hr. at 850°	"
4	4.01	3.53	3.6191 <sub>s</sub>	36 hr. at 750–800°	"
5	5.26	4.64	*3.6223 <sub>s</sub>	5 hr. at 700° 5 hr. at 800°	"
6	6.46	5.70	3.6258 <sub>s</sub>	36 hr. at 750–800°	"
7	6.97	6.16	*3.6284	6½ hr. at 800°	"
8	8.60	7.61	*3.6329	15 hr. at 700° 6 hr. at 850°	"
9	9.55	8.46	*3.6355	6 hr. at 800°	"
10	10.64	9.44	*3.6382 <sub>s</sub>	6 hr. at 800°	"

Analyses—Performed by the Midland Laboratory Guild, Ltd., the weight percentages totalling from 99.86 to 100.05.

#### *h—Copper-Germanium*

These alloys were prepared in the form of small chill castings by melting pure electrolytic copper with specially pure germanium kindly presented by Professor Dennis of Cornell University, U.S.A., to whom the authors must express their gratitude. The results are recorded in Table VII and fig. 3. A smooth curve may be drawn from which no point differs by more than 0.0005 Å. with the exception of the point for alloy No. 3. This point appears to be inaccurate, since a redetermination of the lattice constant near this composition by means of alloy No. 4 gave a value lying near to the smooth curve. The apparent slight decrease in slope of

† 'Z. anorg. Chem.', vol. 220, p. 293 (1934).

the curve at the higher concentrations may be due to the nearness of approach to the 2-phase region.

### DISCUSSION

The curves in figs. 1 and 3 show clearly that a definite valency effect exists for the distortions of the lattices of silver and copper by the elements

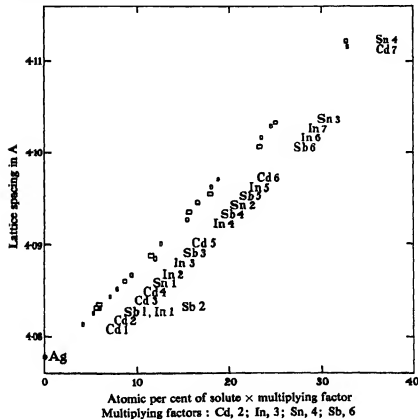


FIG. 4.—In this figure the lattice spacings of dilute solid solutions of cadmium, indium, tin, and antimony in silver are plotted against the atomic percentages of the solute elements multiplied by the following factors: Cd, 2; In, 3; Sn, 4; Sb, 6. Each point is represented by a rectangle of height equivalent to 0.0004 Å, and width equivalent to 0.05 atomic per cent of solute.

which immediately follow them in the Periodic Table. In each series increasing valency of the solute produces an increased lattice distortion at equiatomic compositions.

Examination now shows that in the silver series, the atomic percentages of cadmium, indium, tin, and antimony in alloys of equal lattice distortion vary as  $\frac{1}{2} : \frac{1}{3} : \frac{1}{4} : \frac{1}{6}$ . In dilute solid solutions where the lattice spacing-composition curves are straight lines this implies that the lattice distortions per atom of cadmium, indium, tin, and antimony vary as 2:3:4:6.<sup>†</sup> This relation indicates that if the lattice spacings of the different alloys are plotted against the atomic percentages of the solutes multiplied by the above factors, the points lie on a single curve, as shown in fig. 4. The above method of plotting naturally makes the results for the elements of higher valency much more sensitive to errors in composition, since a given error is multiplied by 2 for cadmium, and by 6 for antimony. Each point is therefore represented by a rectangle the height of which is equivalent to 0.0004 Å., and the width to 0.1 atomic per cent. These limits represent errors of roughly  $\pm 1$  part in 20,000 for the lattice spacings, and  $\pm 0.05$  atomic per cent on the composition axis. The agreement with the above whole number relation is therefore very exact, and in general the deviations from a single curve in fig. 4 correspond with the deviations from the curves for the individual systems in fig. 1. Thus the lowest point in fig. 4 is that for the silver-indium alloy No. 3, and this is slightly below the smooth curve for the silver-indium series in fig. 1. Similarly the two points which are slightly high in fig. 4 are those for the silver-indium alloy No. 5, and the silver-cadmium alloy No. 6, and these are again the points which are high in their respective systems.

The accuracy within which a whole number relation can be claimed is difficult to estimate, but if the multiplying factor for cadmium is assumed to be 2.0, the factor for tin cannot lie outside the limits 3.9 and 4.2 without producing a definite separation of the points for the silver-cadmium and silver-tin series. With indium, if allowance is made for the slight deviation of the two points from a smooth curve, the corresponding factor is within the limits 2.85 and 3.15. The small solid solubility of antimony in silver prevents a very critical test, but a factor outside the limits 5.8 and 6.2 appears improbable.

For the copper alloys a similar examination shows that the relative factors for zinc and gallium are as 3:4. This is shown in fig. 5 where the points are plotted with the same convention as in fig. 4, the atomic percentages of zinc being multiplied by 3, and those of gallium by 4. The agreement with a whole number relation is very exact, and if the factor

<sup>†</sup> The previous statement (Hume-Rothery, 'Nature,' vol. 135, p. 1038 (1935)) that the distortions varied as 2:3:4:5 was due to results from silver-antimony alloys which were accidentally contaminated.

for gallium is taken to be 4·0, that for zinc cannot lie outside the limits 2·93 and 3·13. The points for the copper-germanium alloys do not, however, agree with a factor of 5·0. The factor which produces the best agreement of the copper-germanium results with those of the other series is 4·8, and although this is very near to the value 5·0 required to give a regular increase 3:4:5, the difference appears to be outside the limits of experimental error.

The above results show, therefore, that the relative lattice distortions produced by one atomic per cent of cadmium, indium, tin, and antimony

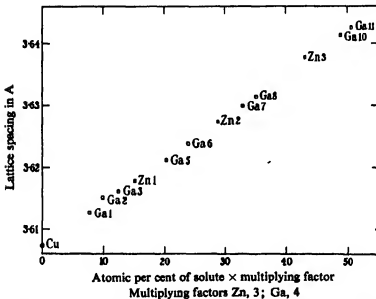


FIG. 5—In this figure the lattice spacings of dilute primary solid solutions of zinc and gallium in copper are plotted against the atomic percentages of the solute elements multiplied by the following factors: Zn, 3; Ga, 4. Each point is represented by a rectangle of height equivalent to 0·0004 Å, and width equivalent to 0·05 atomic per cent of solute.

in solid solution in silver follow a different law from that existing for the corresponding solid solutions of zinc, gallium, and germanium in copper. In both series of alloys the lattice distortions at equiatomic compositions increase with the valency of the solute, but the effect of change of valency is less marked for the copper series, and this difference appears in two distinct ways. In the first place the relative increase in passing from solutes of Group II to Group III is less marked in the copper series, where the ratio is 3:4, than in the silver series, where it is 2:3. In the second place the increase on passing to Group IV is no longer regular for the

copper alloys where the factors are as 3:4:4·8, in contrast to the regular series 2:3:4 in the silver alloys. These facts suggest that the effect of increasing valency tends to expand the lattice but is opposed by some factor which is more effective in the series of elements following copper than in those following silver. This opposing factor may be an atomic effect due to the gradual closing up of the electron shells with increasing atomic number, which may be expected to be more important for the copper series, since the *relative* change in atomic number between each successive element is here greater than in the silver series. Alternatively the effect may be due to the more electronegative nature of germanium (compared with that of tin) resulting in a more closely bound structure. Possibly both factors may act together, the suggested atomic effect being responsible for the difference between the fundamental ratios of 2:3:4 and 3:4:5, and the electronegative valency effect causing the change from a fundamental ratio of 3:4:5 to one of 3:4:4·8.

We must express our thanks to Professor F. Soddy, F.R.S., for his kindness in providing laboratory accommodation, and many other facilities which have greatly assisted the present work. One of us (W. H.-R.) must thank the Council of the Royal Society for election to a Warren Research Fellowship, and for generous financial assistance. Thanks are also due to the Department of Scientific and Industrial Research, the British Non-Ferrous Metals Association, and the Fellows of Brasenose College, Oxford, for grants made to us individually, and to the Aeronautical Research Committee for defraying the cost of some of the apparatus used in this and other research work. We must thank Mr. R. G. Johnstone and Miss U. Willis of the Midland Laboratory Guild, Ltd., and Mr. A. R. Powell of Messrs. Johnson, Matthey & Co., Ltd., for their care and skill in connexion with the analytical work. We must also acknowledge our indebtedness to Professor W. L. Bragg, F.R.S., for criticizing this paper and submitting it for publication.

#### SUMMARY

Accurate measurements have been made of the lattice spacings of the primary solid solutions of cadmium, indium, tin, and antimony in silver, and of zinc, gallium, and germanium in copper. In each series of alloys increasing valency results in increased lattice distortion at equal atomic percentages of the solute elements. In dilute solid solutions in silver equal atomic percentages of cadmium, indium, tin, and antimony expand the lattice of silver by amounts proportional to 2:3:4:6 respectively; this whole number relation holds to an accuracy equivalent to 1 part in

20,000 in the measurements of the lattice spacings, and  $\pm 0.05\%$  in the compositions of the alloys. In the dilute alloys of the copper series, equal atomic percentages of zinc and gallium expand the lattice of copper by amounts proportional to the factors 3:4. The corresponding factor for germanium is, however, 4.8 and not 5. The general conclusion is, therefore, that, whilst whole number relations exist in both series, the effect of increasing valency is less marked in the copper series. It is suggested that in both series increasing valency tends to expand the lattice, but that this expansion is opposed by some factor which is relatively more important in the copper series. This opposing factor may be due to a contraction of the atom with increasing atomic number, since the change in atomic number resulting from one step in the Periodic Table is relatively less for the elements following silver of atomic number 47 than for those following copper of atomic number 29.

---

## A Determination of the Absolute Velocity of the Alpha-Particles from Radium C'

By G. H. BRIGGS, Ph.D., The University of Sydney

(Communicated by Lord Rutherford, O.M., F.R.S.--Received 21 May, 1936)

### 1—INTRODUCTION

The first accurate determination of the velocity of expulsion of the  $\alpha$ -particles from radioactive substances was made by Rutherford and Robinson,\* who, by measuring magnetic and electric deflexions, found for the  $\alpha$ -particles from radium C'  $H_p = 3.983 \times 10^6$  E.M.U. and  $V = 1.922 \times 10^9$  cm./sec., the accuracy being 1 in 400. In 1926 the writer† measured  $H_p$  for the same group of  $\alpha$ -particles and found the value  $3.993 \times 10^6$  E.M.U. to 1 in 1000. This result, together with the value of the faraday and Aston's determination of the atomic weight of helium, gave  $V = 1.922 \times 10^9$  cm./sec. Absolute velocity determinations have been made for polonium by I. Curie,‡ and for several groups by

\* 'Phil. Mag.', vol. 28, p. 552 (1914).

† Briggs, 'Proc. Roy. Soc.,' A, vol. 118, p. 549 (1928).

‡ 'Ann. Physique,' vol. 3, p. 299 (1925).

Rosenblum and Dupouy,\* who found for the radium C' group  $V = 1.9218 \times 10^9$  cm./sec. with an accuracy greater than 1 in 1000.

The velocities of over fifty  $\alpha$ -particle groups have now been measured relative to the main radium C' group; these measurements have been summarized in a paper by Lewis and Bowden.† The present paper describes a new determination of  $H_p$  for this group. Using for E/M for the  $\alpha$ -particle a value calculated from the faraday and the atomic weight of helium the velocity and energy have been calculated. The maximum error in  $H_p$  is estimated to be of the order of 1 in  $10^4$ .

## 2—THE EXPERIMENTAL ARRANGEMENT

The experiments described below were made with the electromagnet which was used in the measurement of the relative velocities of the  $\alpha$ -particles from radon, radium A, and radium C',‡ and the fields, which were of the order of 10,000 gauss, have been measured with a form of magnetic balance capable of a high precision which has recently been described by Briggs and Harper.§ Except for the poles, the faces of which measured 33 cm. by 13 cm., the magnet was immersed in a tank of oil which was cooled by circulating water and stirred by bubbling air through it; the poles also were water cooled. Before an experiment the magnet current, observed by a potentiometer system, was kept constant to about 1 in 50,000.

The radius of curvature  $\rho$  of the path of the particle is given by the well-known equation:

$$\frac{1}{\rho^2} = \frac{1}{4d^2} (l_1^2 + d^2) [(l_1 + l_2)^2 + d^2], \quad (1)$$

where  $2d$  is the double deflexion obtained on the photographic plate by reversing the frame carrying the source, slits, and plate, and  $l_1$  and  $l_2$  are the distances from source to slit and from slit to plate respectively.

The frame which carries the photographic plate, the slits, and the source of  $\alpha$ -particles is shown in fig. 1. It consists of a rigid brass casting designed so that the distances  $l_1$  and  $l_2$  could be measured by precision methods. These two distances were each about 12.5 cm. Slots indicated by dotted lines permit the passage of the  $\alpha$ -particles. These slots are 3 mm. wide at A and D and 6 mm. wide at the source. The photographic plate A

\* 'J. Phys. Rad.' vol. 4, p. 262 (1933).

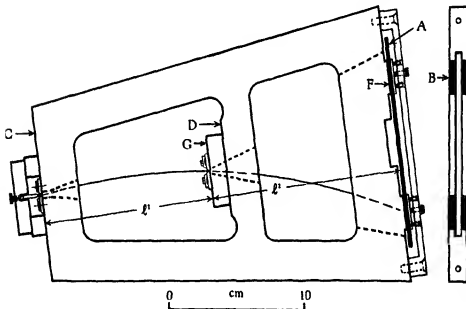
† 'Proc. Roy. Soc., A', vol. 145, p. 235 (1934).

‡ Briggs, 'Proc. Roy. Soc., A', vol. 143, p. 604 (1934).

§ 'J. Sci. Inst.', vol. 13, p. 119 (1936).

is pressed firmly against four flat projections B, each 2 cm. by 0·4 cm. The plane of these four projections, the end surface C and the surface D of the cross bar were lapped accurately flat and parallel to one another; the surfaces of the detachable brass block G were treated similarly.

The source of  $\alpha$ -particles was a flattened platinum wire activated by exposure to about 100 millicuries of radon at atmospheric pressure contained in a glass capillary tube sealed with mercury. This exposure usually lasted for about 30 minutes; the wire was then heated in vacuum for about 1 minute and mounted behind a slit as shown in fig. 2. The jaws



of this slit consisted of two pieces of hard gold alloy, the lower surfaces of which were lapped optically flat so that the plane of the slit coincided with the surface C;  $l_1$  is therefore the distance between the surfaces C and G and can be measured accurately. The slit on the block G was constructed similarly, so that, except for a correction due to the finite thickness of the emulsion of the photographic plate, the distance  $l_2$  is the distance between the planes F and G. A flat source reduces to a minimum the retardation of the  $\alpha$ -particles due to recoil of active deposit into the source wire during activation. To avoid errors due to non-uniform distribution of activity over the surface the same wire served for the two exposures necessary to obtain the double deflexion  $2d$ .

The relative positions of the poles, the field measuring coil, and the path of the  $\alpha$ -particles are indicated in fig. 3. The first series of experiments was made with a brass vacuum box of very rigid construction having sides of half-inch mild steel and an air gap of 1.2 cm. With this arrangement fields of 11,000 gauss were readily obtained. On evacuation of the box, however, there was a change in field of about 7 gauss which varied over the poles and which was probably chiefly due to the change in susceptibility of the sides of the box under strain. The effect was so difficult to measure that it was necessary to replace this box with one entirely of brass. The maximum field which could be conveniently obtained with the consequently larger gap was 9400 gauss. The double deflexions obtained by reversing the frame carrying the source, slits, and plate holder were about 10 cm. with the former box and 8 cm. with the brass box.

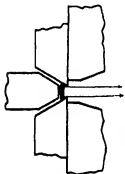


FIG. 2.—Section normal to the length of the activated platinum wire, and the slit; 30 times actual size.

Fig. 2—Section normal to the length of the activated platinum wire, and the slit; 30 times actual size.

The best-known form of instrument by which strong magnetic fields are measured by determining the pull on a current carrying conductor in the field is the Cotton magnetic balance. Scott\* has described a modification of this which is somewhat similar to that developed for the present experiments. The magnetic balance used here consists essentially of an ordinary good quality physical balance with a 10-inch beam, from one side of which a flat rectangular coil is suspended. This coil consists of 10 turns of No. 18 bare copper wire about 85 cm. long and mean width about 15.7 cm. and is mounted on a rectangular sheet of glass. The balance is set up on a movable platform so that the lower end of the coil can be lowered into the gap between the poles when a field measurement is to be made, as indicated in fig. 3. The current  $i_1$ , which produces equilibrium of the balance when the direction of this current is such that the force on the coil is downward, is first observed. Then an appropriate mass  $M$ , which in these experiments was about 300 gm., is added to the coil, the equilibrium again established by adjusting the current to a new value  $i_2$ . The field is given by the equation

$$(H - H') Ln(i_1 + i_2) = 2Mg, \quad (2)$$

\* 'Phys. Rev.', vol. 46, p. 633 (1934).

where  $L$  is the effective mean width of the rectangular coil,  $H$  is the mean value of the field over the trapezium-shaped area occupied by the  $n$  horizontal wires forming the base of the coil, and  $H'$  is a quantity approximately equal to the stray field at the top of the coil. The sensitivity of the arrangement is such that the setting of the current for balance can be made to about 2 in  $10^6$ . Full details of this apparatus have been published elsewhere.\*

The currents  $i_1$  and  $i_2$  were measured in terms of a standard resistance, and one of a group of six acid cadmium cells. The resistance was kept

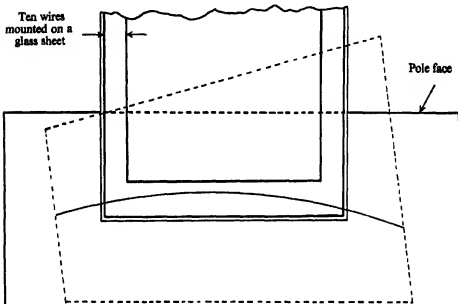


Fig. 3

under observation at the National Physical Laboratory for six months during 1932 and was recently remeasured there. From these results the curve of its secular change was well established and no error on that account should be present.

The six cadmium cells were measured to 1 in  $10^6$  by the National Physical Laboratory in terms of the international volt as maintained at that laboratory. They were set up in an oil bath in the basement, where temperature changes are small, and the standard resistances were kept in an air-stirred oil bath. After the experiments were completed, three of the cadmium cells were remeasured by the National Physical Laboratory,

\* Briggs and Harper, *loc. cit.*

and were found to be identical in E.M.F. and in agreement with the original mean of the six. It was arranged that the currents  $I_1$  and  $I_2$  were each very approximately 1.018 amperes, so that errors in the Wolff potentiometer with which the observations were made were eliminated. It is considered that for both the E.M.F. and the resistance measurements the systematic errors were not greater than  $2 \text{ in } 10^4$ .

The value of gravity at Sydney is established as a result of measurements by five competent observers. These observations have been discussed by Love,\* who considers that the value of  $g$  at Sydney in the Potsdam system is 979.680 with a probable error of 0.002. Corrected for height this gives 979.683 at the Physical Laboratory. Including the possibility of error in the Potsdam value, it is unlikely that the maximum error in  $g$  is greater than 2 in  $10^6$ .

In determining the value of the magnetic field, corrections are required for the stray field at the top of the coil, for the effect of the inhomogeneity of the field over the area occupied by the horizontal wires at the bottom of the coil and for the inhomogeneity along the track of the  $\alpha$ -particles. The inhomogeneity of the field was determined several times during the series of experiments by the usual method of exploration with a small search coil. The maximum variation along the track of the  $\alpha$ -particle was 2.5 gauss. The corrections applied were:—

$$\begin{aligned}
 & + 18.73 \pm 0.06 \text{ gauss for stray field} \\
 - & 0.39 \pm 0.04 \quad \text{,, inhomogeneity over base of coil} \\
 - & 0.07 \pm 0.01 \quad \text{,, along track of } \alpha\text{-particle} \\
 \hline
 & + 18.27 \pm 0.11 \text{ gauss}
 \end{aligned}$$

Uncertainty in the height of the measuring coil may introduce errors due to the vertical variation of the stray field at the top of the coil and of the field between the poles. These two effects amount to  $0.5$  in  $10^5$  and  $0.65$  in  $10^5$  for a change of 1 mm. in the height of the coil. They are of opposite sign and are therefore practically eliminated. The setting of the coil parallel to the poles involves an uncertainty of  $0.5$  in  $10^5$ .

The field was measured immediately before the first exposure, again when the vacuum box was opened to reverse the plate carrier for the second exposure, and finally at the end of the second exposure. The exposures were generally about 30 to 45 minutes long, and although in a complete experiment  $H$  might change by amounts up to 1 in 7000 the

\* \* Proc. Roy. Soc. Victoria, vol. 35, p. 90 (1922).

three measurements of the field made it possible practically to eliminate uncertainties in H due to this.

#### 4.—THE MEASUREMENTS OF LENGTH

The microphotometer previously used to measure the separation of lines on photographic plates has been reconstructed and fitted with a new screw with a travel of 20 cm. which was prepared, according to the method used by Grayson\* for the screw of his ruling engine, by lapping with a semi-split nut 20 cm. long. The screw has a diameter of 2.5 cm. and a pitch of 1 mm. Variations in pitch along the screw are too small to be of any significance.

This apparatus has been adapted so that it can also be used as a measuring machine with travelling microscope and all the length measurements, i.e.,  $l_1$ ,  $l_2$ , L, and  $2d$ , have been made in terms of the pitch of this screw. Under these conditions it can be shown from equations (1) and (2) that a knowledge of the absolute pitch of the screw is unnecessary. The measurement of the velocity of a group of  $\beta$ -particles has been treated similarly by Scott.† The lengths  $l_1$  and  $l_2$  of the brass frame which carries the photographic plate and slits could have been determined by precision end measurements, but to conform with the condition indicated above and measure them in terms of the microphotometer screw it was necessary to have recourse to line measurements. This was done with a specially prepared plane to take the place of the photographic plate and two small blocks each carefully lapped flat on one face and inscribed on another face with a group of reference lines. By a simple process of interchange of the blocks, the required distances are each given as the mean of two, or, if the brass frame is reversed, of four measurements. These measurements gave  $l_1 = 12.72668$  cm. and  $l_2 = 12.65458$  cm. at  $16.7^\circ$  C., the maximum error being 0.00010 cm. This contributes a systematic maximum error of  $1.3 \times 10^{-5}$  in  $\rho$ . These measurements agreed to 0.0001 cm. with precision end measurements of  $l_1$  and  $l_2$  made by the metrology section of the Commonwealth Munitions Supply Laboratory when corrected for the small error in the absolute pitch of the screw of the measuring machine.

The effective mean width L of the field measuring coil was found to be 15.74435 cm. at  $16.7^\circ$  C. with a maximum error of 0.00010 cm.

The lines on the photographic plates were not so satisfactory as in the measurements of the relative velocities of the  $\alpha$ -particles from radon and its products owing to the difficulty of obtaining sources strong enough

\* 'Proc. Roy. Soc. Victoria,' vol. 30, p. 44 (1917).

† *Loc. cit.*

to give strong lines with the narrow slits used. It was found that if the source wire was exposed to the radon for longer than three-quarters of an hour it was likely to become coated with mercury beads and somewhat tarnished, while exposures of half an hour gave perfectly clean wires. The lines were 3 mm. long and the separation  $2d$ , which was about 8 cm., was measured in three places. It was concluded that the maximum error in  $2d$  was about  $0.0003$  cm., so that a considerable part of the spread of the individual determination of  $H_p$  can be attributed to errors in this measurement.

The finite thickness of the emulsion of the photographic plates necessitates a small correction to the length  $l_1$ . The development was carried out at  $12^\circ\text{C}$ . in dilute developer for about 45 minutes and therefore should be uniform throughout the thickness of the emulsion. Microscope sections of some of the lines showed that the photographic density in a line was constant throughout the thickness of the emulsion so that the correction to  $l_1$  is half the thickness of the emulsion. This thickness, which was about  $0.002$  cm., was measured to about 5% close to the lines on each plate. This correction produces an uncertainty of  $0.6$  in  $10^6$  in the final result for  $H_p$ .

One of the largest corrections arises from temperature expansion of the plate holder, the photographic plate and the glass support of the field measuring coil. The cooling system kept the temperature of the vacuum box fairly constant, but its average temperature was often 7 or 8 degrees above the temperature at which the dimensions of the plate carrier and coil were measured. The correction was evaluated for each experiment and amounted to about 1 in  $10^4$  in  $H_p$ , but may involve a systematic error of one-tenth of that amount.

### 5—THE RESULTS

Besides the corrections to the field and length measurements already discussed, there is a general correction for the effect of recoil of the radium C' into the source wire during activation. Taking the mean range of recoil of radium B from radium A to be  $4.0 \times 10^{-6}$  mm. in platinum,\* there would be a reduction in velocity of  $3.9$  in  $10^6$  if the radium C' were uniformly distributed throughout this depth. However, some of the active material will reach the wire as radium B, which will give rise to radium C' on the surface. From such considerations it was estimated that the correction to the velocity is  $2.6$  in  $10^6$  with a maximum uncertainty of 1 in  $10^6$ . There is also a correction for obliquity due to the

\* Briggs, 'Proc. Roy. Soc.,' A, vol. 139, p. 646 (1933).

finite length of the source which amounts to  $2 \cdot 4$  in  $10^6$ . These corrections have been applied to the results which are given in Table I.

To the above probable error of  $1 \cdot 9$  in  $10^6$ , which may be taken as a measure of the accidental error of the experiments, must be added the effect of the systematic errors already described. These were expressed as maximum errors, and, assuming that a maximum error is three times the corresponding probable error, they contribute a further probable error of  $1 \cdot 5$  in  $10^6$  giving a total probable error of  $2 \cdot 5$  in  $10^6$ .

TABLE I

Experiment	$H_P$	Weight
1	$3 \cdot 992207 \times 10^6$ E.M.U.	2
2	1848	2
3	2304	3
4	2508	4
5	2421	4
6	2898	4
7	2560	2
8	2051	3
9	2180	4
10	2343	4
11	2098	4
12	1532	4
13	1668	3

Weighted mean,  $3 \cdot 992214 \times 10^6$  E.M.U. Probable error,  $0 \cdot 000076 \times 10^6$  E.M.U.

To deduce the velocity and the energy we require  $E/M$  for the  $\alpha$ -particle. This involves the faraday which is accurately known in *international* electrical units. The final results for  $H_P$  and for the energy will be given in absolute electrical units in which, as will be seen below, they can be more accurately expressed than in international units. The magnetic fields involved in the results for  $H_P$  of Table I were calculated from the equation of the magnetic balance, *i.e.*, equation (2), the current being measured in international amperes. However, since the product of  $H$  and  $i$  appears in this equation the  $H$  so calculated is not in international (nor in absolute) gauss, but if  $H_P$  is the value in absolute E.M.U. then

$$H_P = \frac{H}{q},$$

where  $q$  is the ratio of the international ampere to the absolute ampere.

The velocity  $V$  and the energy  $T$ , the latter expressed in absolute

electron volts, are given by the following equations in which the directly measured  $H\rho$  of Table I is retained and E/M is in international E.M.U.:—

$$\begin{aligned} V &= \frac{H\rho E}{M} (1 - \beta^2)^{\frac{1}{2}} \\ T &= \frac{(H\rho)^2 E}{10^6 q M} \frac{(1 - \beta^2)^{\frac{1}{2}}}{\beta^2} \left\{ (1 - \beta^2)^{-\frac{1}{2}} - 1 \right\} \\ &= \frac{(H\rho)^2 E}{10^6 q M} \left( 1 - \frac{\beta^2}{4} - \frac{\beta^4}{8} \dots \right) \end{aligned}$$

It is of interest to note that the expression for the velocity involves no ratios of the international to the absolute electrical units and that for the energy involves  $q$  to only the first power. Had the fields been measured with a search coil  $q$  would have appeared in the expression for  $V$  and  $q^2$  in that for  $T$ .

The value of the faraday is here taken to be 96498 international coulombs, p.e. 3 in  $10^6$ . This is deduced from the definition of the international ampere and the atomic weight of silver, allowing 4 in  $10^6$  for inclusions in the silver deposits. Recent determinations of the atomic weight of iodine reduce considerably the discrepancy in the important researches of Vinal and Bates\* on the silver and iodine voltameters; hence the possibility of unknown systematic errors in silver voltameter measurements suggested by Birge† is now much reduced.

The mass of the helium atom is now known very precisely both from nuclear disintegration experiments,‡ and also from Aston's§ more direct determination with the mass-spectrograph. Taking his value  $\text{He} = 4.00391$ , on the  $O_{16} = 16$  scale, and using a revised conversion factor,|| namely 1.000271 instead of the old value 1.00022, for the ratio of the physical to the chemical atomic weight scales we obtain  $M = 4.00173$  for the mass of the helium nucleus in the latter scale. The probable error in  $M$  is taken to be 2 in  $10^6$ .

\* 'Bull. U.S. Bur. Stand.', No. 10, p. 425 (1914).

† 'Rev. Mod. Phys.' vol. 1, p. 1 (1929).

‡ Bethe, 'Phys. Rev.', vol. 47, p. 633 (1935); Oliphant, Kempton, and Rutherford, 'Proc. Roy. Soc.,' A, vol. 150, p. 241 (1935); Cockcroft and Lewis, 'Proc. Roy. Soc.,' A, vol. 154, p. 278 (1936).

§ 'Nature,' vol. 137, p. 357 (1936).

|| This is deduced from  $O_{16}:O_{18} = 508 \pm 10:1$  which is the mean of the results of Smythe ('Phys. Rev.', vol. 45, p. 299 (1934)), and Manian, Urey, and Bleakney ('J. Amer. Chem. Soc.', vol. 56, p. 2601 (1935)), and  $O_{16}:O_1 = 5:1$  found by Mecke and Childs ('Z. Physik,' vol. 68, p. 362 (1931)).

There is at present a discrepancy\* of 8 or 9 in  $10^6$  between recent determinations of  $q$  by the standardizing laboratories. I am indebted to members of the National Bureau of Standards and of the National Physical Laboratory for discussion of this matter. For the present calculation 1 N.P.L. international ampere is taken to be 0.99986 absolute ampere, and, in view of the existing discrepancy, the probable error has been taken as 3 in  $10^6$ .

With the above data the following values for the main group of  $\alpha$ -particles from radium C' are obtained:—

		p.e. parts in $10^6$
$H_p$ .....	$3.99277 \times 10^5$ abs. E.M.U. . . .	4
Velocity .....	$1.92148 \times 10^6$ cm./sec. . . . .	4.5
Energy of $\alpha$ -particle .....	7.6802 abs. e-volt . . . . .	7
Disintegration energy .....	7.8268 abs. e-volt . . . . .	7

In these results the experimental errors of the present measurements contribute probable errors of 2.5 in  $10^6$  in  $H_p$ , 2.5 in  $10^6$  in V, and 5.0 in  $10^6$  in T, and the probable errors given above include the errors assumed

TABLE II

Velocity in cm./sec. $\times 10^6$	p.e. parts in $10^6$	Energy of $\alpha$ -particle in e-volts $\times 10^{-6}$	"Disint- egration" . . . . . energy in e-volts $\times 10^{-6}$	p.e. parts in $10^6$
Radon .....	1.62467	5	5.4860	5.5868
Radium A .....	1.69865	5	5.9981	6.1104
Radium C' .....	1.92148	4.5	7.6802	7.8268
Thorium X .....	1.65327	7	5.6813	5.7845
Thoron .....	1.73825	7	6.2818	6.3981
Thorium A .....	1.80484	7	6.7744	6.9025
Thorium C (mean)	1.70649	7	6.0537	6.1704
Thorium C' .....	2.05352	5.5	8.7759	8.9451

in the values of M,  $q$ , and the faraday, calculated as the root of the sum of the squares. Table II summarizes data for certain main groups whose velocities relative to the radium C' group have been measured by the author.

I wish to express my thanks to the members of the mechanical engineering department of the Sydney Technical College for their assistance in

\* "Rept. National Physical Laboratory," 1932. Curtis and Curtis, "Bur. Stand. J. Res., vol. 12, p. 665 (1934); "Fourth Report (1935) of the Electrical Committee to the Internat. Committee of Weights and Measures."

preparing the screw for the measuring machine. I am also indebted to the Department of Cancer Research of the University of Sydney for the supplies of radon and to the Commonwealth Oxygen Company for liquid air.

#### SUMMARY

Precision measurements of  $H_p$  for the  $\alpha$ -particles from radium C' are described in which the probable experimental error is estimated to be  $2 \cdot 5$  in  $10^5$ ; uncertainty in the ratio of the international to the absolute ampere increases the probable error to 4 in  $10^5$ . From this result and the value of the faraday and the atomic weight of the helium nucleus the velocity and energy are calculated.

## Relations Between Optical Rotatory Power and Constitution in the Steroids

By R. K. CALLOW and F. G. YOUNG\*

(From the National Institute for Medical Research, London, and the Department of Physiology, Pharmacology, and Biochemistry, University College, London)

(Communicated by O. Rosenheim, F.R.S.—Received 21 May, 1936)

### I—VALIDITY OF RULES OF ISOROTATION FOR CERTAIN CARBON ATOMS

The group of biologically important compounds containing the reduced cyclopentenophenanthrene ring system (the "steroids" †) provides a field for the exploration of relations between optical rotatory power and constitution which has hitherto received little attention. In the present paper a preliminary survey has been made of the scattered data in the literature with the object of finding in the first place whether constant partial rotations can be assigned to certain carbon atoms and groups. Even with compounds of established constitution the results are not by any means so concordant as those obtained by Hudson‡ with many of the

\* Beit Memorial Fellow.

† The term "steroids" is proposed as generic name for the group of compounds comprising the sterols, bile acids, heart poisons, saponins, and sex hormones.

‡ Hudson, 'Sci. Pap. U.S. Bur. Stand.', No. 533 (1926), and subsequent papers in 'J. Amer. Chem. Soc.'

series of carbohydrates, but there is indubitable evidence of regularity, in spite of the fact that many of the determinations recorded are of a low order of accuracy, have been made with impure specimens of materials notoriously difficult to purify, or are discordant among themselves. For numerous substances determinations of optical activity under conditions which allow comparison with related compounds are lacking, and it is to be hoped that such evidence of regularity as is brought forward in this communication will lead to the filling of some of these gaps.

The steroid skeleton, with an indication of the system of numeration adopted, is shown in fig. 1. A number of pairs of compounds are known

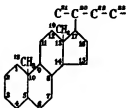


FIG. 1.

in which there are opposite configurations of carbon atoms 3, 4, 5, and 17, and we have investigated whether it is possible to apply to these a rule analogous to Hudson's "first rule of isorotation", *i.e.*, whether the partial rotations of carbon atoms 3, 4, 5, and 17, as measured by the effect of reversing the configuration, are affected by changes in the structure of the remainder of the molecule. In Tables I-IV are summarized the data collected, with three exceptions, from the literature for the specific rotations of these diastereoisomeric pairs of compounds, determined for the D line and, as far as possible, the same solvents. Where more than one determination exists, the values of  $[\alpha]_D$  are, in general, the means of the recorded figures for presumably pure compounds, and no attempt has been made to select them critically. The last two columns show the differences of  $[\alpha]_D$  and the differences of  $[M]_D$  ( $[M]_D$  being defined as  $[\alpha]_D \times (\text{mol. wt.})/100$ );  $\Delta[M]_D$  corresponding to twice the partial rotation of the carbon atom concerned.

It is generally accepted that the configuration of the 3-hydroxyl group in sterols is indicated by their behaviour with digitonin, the compounds in which the 3-hydroxyl group is *cis* to the 10-methyl group forming sparingly soluble digitonides. The figures in Table I show that in fifteen cases out of eighteen an increase in dextrorotatory power is entailed by inversion of the 3-hydroxyl group from the *cis* to the *trans* position relative to the 10-methyl group. (It should be noted that in the table the usual

TABLE I—INVERSION OF 3-HYDROXYL GROUP

Substance	Substituents	Solvent	$[\alpha]_D$	$\Delta[\alpha]$ (B - A)	$\Delta[M]$
<i>(a) Saturated sterols</i>					
A. Cholestanol	3-OH, 17-C <sub>6</sub> H <sub>5</sub>	CHCl <sub>3</sub>	+29.7	°	°
B. <i>epi</i> Cholestanol	3-OH, 17-C <sub>6</sub> H <sub>5</sub>	"	+33.9	+4.2	+16.3
A. Coprostanol	3-OH, 17-C <sub>6</sub> H <sub>5</sub>	"	+24.7	°	°
B. <i>epi</i> Coprostanol	3-OH, 17-C <sub>6</sub> H <sub>5</sub>	"	+31.5	+6.8	+26.4
A. Dihydroocinol	3-OH, 17-C <sub>6</sub> H <sub>5</sub>	"	+22	°	°
B. <i>epi</i> Dihydroocinol	3-OH, 17-C <sub>6</sub> H <sub>5</sub>	"	+26	+4	+17.5
A. Ergostanol	3-OH, 17-C <sub>6</sub> H <sub>5</sub>	"	+15.5	°	°
B. <i>epi</i> Ergostanol	3-OH, 17-C <sub>6</sub> H <sub>5</sub>	"	+14	-1.5	-6.3
A. Sitostanol*	3-OH, 17-C <sub>6</sub> H <sub>5</sub>	"	+26.1	°	°
B. <i>epi</i> Sitostanol	3-OH, 17-C <sub>6</sub> H <sub>5</sub>	"	+26	-0.1	-0.4
A. Stigmastanol*	3-OH, 17-C <sub>6</sub> H <sub>5</sub>	"	+24.8	°	°
B. <i>epi</i> Stigmastanol	3-OH, 17-C <sub>6</sub> H <sub>5</sub>	"	+25	+0.2	+0.8
<i>(b) Unsaturated sterols</i>					
A. Dihydrocholesterol	Δ <sub>8</sub> 14-22 23, 3-OH, 17-C <sub>6</sub> H <sub>5</sub>	"	-19	°	°
B. <i>epi</i> Dihydrocholesterol	Δ <sub>8</sub> 14-22 23, 3-OH, 17-C <sub>6</sub> H <sub>5</sub>	"	-4.4	+14.6	+58.2
A. Ergosterol-D	Δ <sub>9</sub> 8-14 16-22 23, 3-OH, 17-C <sub>6</sub> H <sub>5</sub>	"	+19.8	°	°
B. <i>epi</i> Ergosterol-D	Δ <sub>9</sub> 8-14 16-22 23, 3-OH, 17-C <sub>6</sub> H <sub>5</sub>	"	+33.2	+13.4	+53.2
A. [ <i>trans</i> -Δ <sub>4</sub> -Cholestenol (" <i>allo</i> Cholesterol")]	Δ <sub>4</sub> , 3-OH, 17-C <sub>6</sub> H <sub>5</sub>	"	+11.2	°	°
B. [ <i>cis</i> -Δ <sub>4</sub> -Cholestenol (" <i>epi</i> - <i>allo</i> Cholesterol")]	Δ <sub>4</sub> , 3-OH, 17-C <sub>6</sub> H <sub>5</sub>	C <sub>6</sub> H <sub>6</sub>	+120.8	+109.6	+4231
A. β-Dihydrofucosterol	Δ <sub>7</sub> , 3-OH, 17-C <sub>6</sub> H <sub>5</sub>	CHCl <sub>3</sub>	-38.7	°	°
B. <i>epi</i> -β-Dihydrofucosterol	Δ <sub>7</sub> , 3-OH, 17-C <sub>6</sub> H <sub>5</sub>	"	+12.2	+50.9	+208

\* Sitostanol and stigmastanol may be identical, cf. Bergson, 'Z. physiol. Chem.', vol. 237, p. 46 (1935).

(c) <i>Bile acids</i>					
A. <i>trans</i> -3-Hydroxyallocholic acid	.....	3-OH, 17-C <sub>6</sub> H <sub>5</sub> CO <sub>2</sub> H	.....	CHCl <sub>3</sub>	+17.2
B. <i>cis</i> -3-Hydroxyallocholic acid	.....	.....	.....	"	+23.3
		+6.1			+22.9
(d) <i>Androstan derivatives</i>					
A. <i>trans</i> -Androsterone	.....	3-OH, 17-O	.....	EtOH	+91
B. " "	.....	.....	.....	MeOH	+88.3
C. <i>cis</i> -Androsterone	.....	.....	.....	EtOH	+94
D. " "	.....	.....	.....	MeOH	+103.5
E. <i>trans</i> -Androstan-3:17-diol	.....	3-OH, 17-OH	.....	EtOH	+4.2
F. <i>cis</i> -Androstan-3:17-diol	.....	.....	.....	EtOH	+4.2
		"	"	"	+12.6
					+8.4
					+24.5
(e) <i>Reduced irradiation products of ergosterol</i>					
A. <i>epi</i> Dihydrolumisterol	.....	.....	.....	CHCl <sub>3</sub>	+43.3
B. Dihydrolumisterol	.....	.....	.....	"	+50.4
A. <i>epi</i> Dihydroxyrocalciferol	.....	.....	.....	"	+54.3
B. Dihydroxyrocalciferol	.....	.....	.....	"	+70.3
A. <i>epi</i> Hexahydrovolumisterol	.....	.....	.....	"	+10.3
B. Hexahydrovolumisterol	.....	.....	.....	"	+9.5
A. <i>epi</i> Hexahydroxyrocalciferol	.....	.....	.....	"	+30.2
B. Hexahydroxyrocalciferol	.....	.....	.....	"	+34.4
					+4.2
					+16.8

method of nomenclature, referring to the 5-hydrogen atom, is employed.) In thirteen of these cases, excluding the  $\Delta^4$ -cholestenois and  $\beta$ -dihydrofucosterols, the contribution of carbon atom 3 to the molecular rotation varies between the fairly narrow limits of  $\pm 0.4^\circ$  and  $\pm 32^\circ$ , with a mean value of  $\pm 11.5^\circ$ . This may be compared with the figure of  $\pm 80^\circ$  for C-1 in glucose. In the three cases in which a decrease in dextrorotation is observed, the differences are very small, and these are cases where doubts may legitimately be raised as to the purity of one or other of the pair of compounds. In the case of the  $\Delta^4$ -cholestenois ("allocholesterol" and "*epi-allocholesterol*"), where there is a comparatively very large increase in dextrorotation, a difference of solvent must be taken into account, but there is also some doubt as to the homogeneity and true constants of *trans*- $\Delta^4$ -cholestenol.\* On the other hand, the ethylenic linkage adjacent to two asymmetric carbon atoms, C-3 and C-10, may have an effect on the rotatory powers. The anomaly of the two  $\beta$ -dihydrofucosterols is almost as striking. It may be pointed out that although one compound is assumed to be the epimeride of the other, no statement of the behaviour of either with digitonin is made by Coffey *et al.*†

It is of particular interest that three of the four pairs of compounds derived from irradiated ergosterol show an increase in dextrorotation in passing from the isomeride precipitable by digitonin (called the "*epi*"-form in these cases only) to the other. Both lines of evidence are, therefore, concordant in indicating that an inversion of the hydroxyl group occurs in the first stage of the irradiation of ergosterol.

The two cases available for consideration of the 4-hydroxyl group (Table II) hardly provide evidence for or against the existence of a rule, since the configuration of cholestan-4-ol is undetermined, and the figure for the 3:4-diol may be affected by the *cis*-configuration of the hydroxyl groups relative to each other in compound A.

The effect of inversion of the 5-hydrogen (Table III) is small, but irregular, being a decrease of dextrorotation in three cases of change from *trans* to *cis* (relative to the 10-methyl group) and an increase in the other three cases.

The two examples available of inversion of the 17-acetyl group (Table IV) show changes of rotation which are in the same direction, although of somewhat different magnitude.

\* Gottberg, 'Dissert.,' Göttingen (1932).

† 'J. Chem. Soc.,' p. 1207 (1935).

TABLE II—INVERSION OF 4-HYDROXYL GROUP

Substance	Substituents	Solvent	$[\alpha]_D$	$\Delta[\alpha]$ (B - A)	$\Delta[M]$
A. Cholestan-4-ol	.....	4-OH, 17-C <sub>2</sub> H <sub>5</sub> , .....	CHCl <sub>3</sub>	+3.9°	°
B. <i>epi</i> Cholestan-4-ol	.....	.....	"	+29.0°	+25.1°
A.	Δ <sup>5</sup> - <i>trans</i> -Cholestene-3 : 4-diol	Δ <sup>5</sup> -O, 3-OH, 4-OH, 17-C <sub>2</sub> H <sub>5</sub> , .....	"	-58°	+96.9°
B.	<i>trans</i> - <i>cis</i> -Cholestene-3 : 4-diol	.....	"	+7°	+65°

TABLE III—INVERSION OF S-HYDROGEN

Substance	Substituents	Solvent	$[\alpha]_D$	$\Delta[\alpha]$ (B - A)	$\Delta[M]$
A. Cholestan	17-C <sub>6</sub> H <sub>5</sub>	CHCl <sub>3</sub>	+24°	°	°
B. Coprostan	.....	"	+25.3	+1.3	+4.8
A. Cholestanol	3-OH, 17-C <sub>6</sub> H <sub>5</sub>	"	+29.7	°	°
B. Coprostanol	.....	"	+24.7	-5.0	-19.4
A. <i>epi</i> Cholestanol	3-OH, 17-C <sub>6</sub> H <sub>5</sub>	"	+33.9	°	°
B. <i>epi</i> Coprostanol	.....	"	+31.5	-2.4	-9.3
A. <i>allo</i> Cholanic acid	17-C <sub>6</sub> H <sub>5</sub> CO <sub>2</sub> H	"	+22.2	°	°
B. Cholanic acid	.....	"	+21	-1.2	-4.3
A. Androsterone	3-OH, 17-O	EtOH	+94	°	°
B. <i>epi</i> -3-Hydroxyacetocholestan-17-one	Ring I pentatomic, 17-C <sub>6</sub> H <sub>5</sub>	CHCl <sub>3</sub>	+104	+10	+29
A. <i>trans</i> -Hydrocarbon C <sub>28</sub> H <sub>46</sub>	.....	"	+25.1	°	°
B. <i>cis</i> -Hydrocarbon C <sub>28</sub> H <sub>46</sub>	.....	"	+33.2	+8.1	+29

TABLE IV—INVERSION OF 17-COMB<sub>3</sub> GROUP

Substance	Substituents	Solvent	[α] <sub>D</sub>	$\Delta[\alpha]$ (B - A)	$\Delta[M]$
A. <i>allo</i> Pregnandione .....	3-O, 17-COMe .....	EtOH	+126.9	◦	◦
B. <i>Iso-allo</i> Pregnandione .....	.....	"	-14.56	-141.5	-446
A. <i>allo</i> Pregnan-3-ol-20-one .....	3-OH, 17-COMe .....	"	+90.8		
B. <i>Iso-allo</i> Pregnan-3-ol-20-one .....	.....	"	+6.05	-84.7	-269

## II—INDUCED DISSYMMETRY IN UNSATURATED COMPOUNDS

With the principal object of evaluating the effect of ethylenic linkages on optical activity, the application of the principle of optical superposition has been extended to the unsaturated steroids with results which are more striking than those obtained with the inversion of intrinsically active, "fixed" centres of asymmetry. The presence of unsaturated linkages is generally associated with the development of high optical activity, particularly when they are close to an asymmetric carbon atom, and the steroids afford some notable examples of this effect. Lowry and his co-workers\* have called this effect "induced dissymmetry", putting forward the theory that the unsaturated group in an asymmetric molecule itself acquires asymmetry and itself becomes optically active.

By comparison of unsaturated compounds with the corresponding saturated compounds, one can obtain a value for the partial rotation of the centre of induced dissymmetry, and consideration of a number of such pairs of compounds will indicate to what extent this partial rotation is affected by changes in the rest of the molecule. The possibilities are then opened of comparing the inductive power of a particular asymmetric atom on different, adjacent parts of the molecule, or of comparing the inductive power of different atoms on a particular unsaturated linkage.

The unsaturated compounds which have been considered are those with ethylenic linkages in positions 1:2, 4:5, 5:6, 7:8, 8:14, 14:15, and 22:23, which have been compared with the corresponding compounds in which these linkages are saturated (Tables V-X), and those with a 17-keto-group, which have been compared with the corresponding secondary alcohols (Table XI) on the assumption that the configuration of the 17-hydroxyl group is the same in all cases.

There are only two pairs of compounds available for evaluation of the rotatory power of the 1:2-ethylenic linkage induced by C-10 (Table V). In each case, the effect is a large decrease in dextrorotation, although the values of  $\Delta [M]$  do not correspond very closely, possibly owing to a difference of solvent in one case.

The effect of a 4:5-ethylenic linkage under the influence of C-10 (Table VI) is to cause generally a marked increase in dextrorotation. One of the exceptions to this is the decrease from cholestanol to  $\Delta^4$ -cholestenol.†

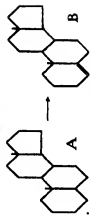
\* Lowry and Walker, 'Nature,' vol. 113, p. 565 (1924); Lowry, *ibid.*, vol. 131, p. 563 (1933); Lowry and Cutter, 'J. Chem. Soc.,' vol. 127, p. 604 (1925); Lowry, "Optical Rotatory Power," Longmans, Green & Co., 1935.

† [Footnote added in proof, 17 July, 1936.—*Cf.*, however, Evans, E. A., Jr., 'J. Biol. Chem.,' vol. 114, 'Sci. Proc.,' vol. 30, p. xxxiii (1936), who gives  $[\alpha] = +43.6^\circ$  for "allo-cholesterol".]

TABLE V—INFLUENCE OF ETHYLENIC LINKAGE AT 1:2

Substance	Substituents	Solvent	$[\alpha]_D^0$	$\Delta[\alpha]_{(B-A)}$
A. Cholestanone .....	3:O, 17-C <sub>4</sub> H <sub>9</sub> .....	CHCl <sub>3</sub>	+41°	°
B. Δ <sup>1</sup> -Δ <sup>2</sup> -Cholestanone .....	.....	EtOH	-32.1	-73.1 -231
A. <i>allo</i> Pregnenedione .....	3:O, 17-COMe .....	"	+126.9	
B. Δ <sup>1</sup> - <i>allo</i> Pregnenedione .....	.....	"	+68.6	-58.3 -184

TABLE VI—INFLUENCE OF ETHYLENIC LINKAGE AT 4:5

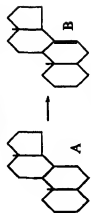


Substance	Substituents	Solvent	$[\alpha]_D$	$\Delta[\alpha]_{(B-A)}$
A. Cholestanone .....	17-C <sub>6</sub> H <sub>5</sub>	CHCl <sub>3</sub>	+24°	°
B. $\Delta^4$ -Cholestenone .....	"	"	+62.8	+38.8
A. Cholestanol .....	3-OH, 17-C <sub>6</sub> H <sub>5</sub>	"	+29.7	+144
B. <i>trans</i> - $\Delta^4$ -Cholestanol " <i>allo</i> Cholestanol "	"	"	+11.2	-18.5
A. <i>epi</i> Cholestanol .....	3-OH, 17-C <sub>6</sub> H <sub>5</sub>	"	+24.7	-72
B. <i>cis</i> - $\Delta^4$ -Cholestanol " <i>epi</i> - <i>allo</i> Cholestanol "	"	C <sub>6</sub> H <sub>6</sub>	+120.8	+96.1
A. Cholestanone .....	3-O, 17-C <sub>6</sub> H <sub>5</sub>	CHCl <sub>3</sub>	+41	+373
B. Cholestanone .....	"	"	+87.6	+46.6
A. 3-Ketobisnorcholanic acid .....	3-O, 17-CHMe <sub>2</sub> CO <sub>2</sub> H	"	+4.6	+178
B. $\Delta^{4:5}$ -3-Ketobisnorcholanic acid .....	"	"	+60	+55.4
A. <i>allo</i> Pregnandione .....	3-O, 17-COMe	EtOH	+126.9	+203
B. $\Delta^{4:5}$ -Pregnandione (Progesterone) .....	"	"	+192	+66.9
A. Androstone-17-ol-3-one .....	3-O, 17-OH	"	+32.4	+210
B. $\Delta^{4:5}$ -Androstone-17-ol-3-one (Testosterone) .....	"	"	+106.5	+74.1

TABLE VII—INFLUENCE OF ETHYLENIC LINKAGE AT 5:6

		Substituents	Solvent	$[\alpha]_D$	$\Delta[\alpha]_{(B-A)}$
A.	Cholestan	17-C <sub>4</sub> H <sub>9</sub>	CHCl <sub>3</sub>	+24°	°
B.	Cholestene	"	"	-54.9	-78.9
A.	Sitostane	17-C <sub>4</sub> H <sub>9</sub>	"	+25.2	-294
B.	Sitostene	"	"	-59.3	-338
A.	Cholestanol	"	"	+29.7	-
B.	Cholesterol	3-OH, 17-C <sub>4</sub> H <sub>9</sub>	"	-37.5	-67.2
A.	$\beta$ -Ergostenol	"	"	+20.3	-260
B.	Ergostadienol	"	"	-28.5	-48.8
A.	$\gamma$ -Ergostenol	"	"	0	-195
B.	22:23-Dihydroergosterol	Δ <sup>7</sup> , 3-OH, 17-C <sub>4</sub> H <sub>9</sub>	"	-109	-109
A.	Dihydrocinehol	3-OH, 17-C <sub>4</sub> H <sub>9</sub>	"	+22	-436
B.	Cinchol	"	"	-33.5	-
A.	Sitostanol	3-OH, 17-C <sub>4</sub> H <sub>9</sub>	"	+26.1	-230
B.	Sitosterol	"	"	-33.1	-59.2
A.	Cholestanone	3-O, 17-C <sub>4</sub> H <sub>9</sub>	"	+41	-245
B.	$\Delta^5,4$ -Cholestanone	"	"	-4.2	-45.2
A.	<i>allo</i> Pregn-3-ol-20-one	3-OH, 17-OMe	EtOH	+90.8	-173
B.	<i>allo</i> Pregn-3-ol-20-one	"	"	+30	-60.8
A.	<i>trans</i> -Androstanone	3-OH, 17-O	"	+91	-192
B.	<i>trans</i> - $\Delta^5,4$ -Androstanone	"	"	+10.9	-80.1
A.	<i>trans</i> -Androstan-3:17-diol	"	"	+4.2	-232
B.	<i>trans</i> - $\Delta^5,4$ -Androstan-3:17-diol	"	PrOH	-55.5	-59.7
A.	<i>allo</i> Pregnadiene	3-O, 17-OMe	EtOH	+126.9	-174
B.	<i>allo</i> Pregnene-3:20-diene	"	CHCl <sub>3</sub>	+65.5	-71.4
					-224

TABLE VIII—INFLUENCE OF ETHYLENIC LINKAGE AT 7:8



Substance	Substituents	Solvent	$[\eta]_D$	$\Delta[\eta]_{(B-A)}$
A. Ergostanol	.....	3-OH, 17-C <sub>4</sub> H <sub>9</sub>	+15.5	°
B. $\gamma$ -Ergostenol	.....	CHCl <sub>3</sub>	0	-15.5
A. $\Delta^5$ - $\alpha$ -Cholestanone	.....	"	-54.9	-62
B. $\Delta^5$ - $\alpha$ -Cholestadiene	.....	"	-127	-72.1
A. Cholesterol	.....	"	-37.5	-267
B. $\Delta^5$ - $\beta$ -Cholestadienol	.....	"	-113.6	-293
A. Dihydroxycholestanic acid	.....	EtOH	+60.1	°
B. $\alpha$ -Dihydroxycholestanic acid	.....	"	-62	-122.1
A. Oestrone	.....	Dioxane	+163	-476
B. Equilin	.....	"	+308	+392
A. Oestradiol	.....	"	+80.5	°
B. Dihydroequilin	.....	[No 10-Me]	+220	+139.5
		[No 10-Me]	"	+381

The unfortunate uncertainty about the true physical constants of  $\Delta^4$ -cholestenol renders entirely speculative any suggestion of a combined effect of C-3 and C-10 in *cis*- and *trans*- $\Delta^4$ -cholestenol. The mean value of  $\Delta [M]$  for the five other pairs of compounds is +190°.

The effect of a 5:6-ethylenic linkage, also under the influence of C-10 (Table VII), is to cause a marked decrease in dextrorotation, opposite and nearly equal numerically to the effect of the 4:5-ethylenic linkage. Omitting 22:23-dihydroergosterol, the mean value of  $\Delta [M]$  for eleven pairs of compounds is -230°. There is no evidence of the actual electronic configuration, but it seems possible that 4:5- and 5:6-unsaturated compounds are diastereoisomeric as regards the configuration of the atoms adjacent to carbon atom 5. It is particularly remarkable that differences of this order should occur in the unsaturated compounds when the configuration of C-5 has so little effect on rotatory power in the saturated compounds (Table III). The high value of the difference  $\gamma$ -ergostenol-22:23-dihydroergosterol,  $\Delta [M] = -436^\circ$ , may be an effect of mutual reinforcement of the 5:6- and 7:8-ethylenic linkages.

The influence of the 7:8-ethylenic linkage, as shown in Table VIII, is irregular. The value of  $\Delta [M]$  for ergostanol- $\gamma$ -ergostenol is -62°. When a 5:6-ethylenic linkage is present the value of  $\Delta [M]$  is from -267° to -476°, possibly as a result of enhancement by conjugation, but in the oestratriene derivatives it is of opposite sign, +387°, an anomaly for which there is no obvious explanation if the constitution assigned to equilin is correct (unless the absence of asymmetry at C-10 is responsible). On the other hand, the rotation of the isomeric hippulin,  $[\alpha]_D + 128^\circ$ , is not inconsistent with its being the  $\Delta$  7:8-derivative.

The figures showing the effects of the 8:14- and 14:15-ethylenic linkages have been grouped together in Table IX because of the existence of a number of pairs of compounds, particularly ergosterol derivatives, to which these constitutions have been assigned. These are characterized chemically by the resistance to catalytic hydrogenation of the assumed 8:14-unsaturated compound, which may, however, be isomerized by acid to the reducible 14:15-unsaturated compound. The typical behaviour is a small decrease in dextrorotation in the 8:14-unsaturated compounds, and a small increase in the 14:15-unsaturated compounds, but  $\alpha$ -ergostenone shows a small, and *apo*cholanic acid a larger, increase in dextrorotation. The grounds for the inclusion of spinastanol and zymostanol derivatives in this group are speculative, but, with the exception of  $\alpha$ -dihydrozymosterol, the figures are concordant with the rest. The isomeric anhydrodigoxigenins and anhydrodigitoxigenins, to which, it should be noted, the respective positions of the ethylenic linkage have not

TABLE IX.—INFLUENCE OF ETHYLENIC LINKAGES AT 8:14 AND 14:15

Substance	Substituents	Solvent	$\Delta[\alpha]$		$\frac{\Delta[M]}{(C - A)}$	
			(B - A)	(C - A)	(B - A)	(C - A)
A.	Ergostane .....	17-C <sub>4</sub> H <sub>9</sub> .....	CHCl <sub>3</sub> .....	+19°	•	•
B.	$\alpha$ -Ergostenone .....	.....	"	+11.0	-8.9	-34.3
C.	$\beta$ -Ergostenone .....	.....	"	+21.3	+1.4	+5
A.	Ergostanol .....	3-OH, 17-C <sub>4</sub> H <sub>9</sub> .....	"	+15.5	-	-
B.	$\alpha$ -Ergostenol .....	.....	"	+13.1	-2.4	-9.6
C.	$\beta$ -Ergostenol .....	.....	"	+20.3	+4.8	+19.2
A.	Ergostane .....	3-O, 17-C <sub>4</sub> H <sub>9</sub> .....	"	+34.9	-	-
B.	$\alpha$ -Ergostenone .....	.....	"	+38.8	+3.9	+15.6
C.	$\beta$ -Ergostenone .....	.....	"	+36.8	+1.9	+7.6
A.	Spinasterol .....	3-OH, 17-C <sub>4</sub> H <sub>9</sub> .....	"	+27.8 ( $\lambda = 5461$ )	-	-
B.	$\alpha$ -Spinasterol .....	.....	"	+24.2 ( $\lambda = 5461$ )	-3.6	-14.5
C.	$\beta$ -Spinasterol .....	.....	"	+36.5 ( $\lambda = 5461$ )	+8.7	+33.9

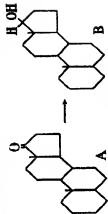
A.	Zymosanol .....	3-OH, 17-C <sub>4</sub> H <sub>9</sub>	.....	"	+20.6 ( $\lambda = 546\text{l}$ )	+6.6	+25.6
B.	$\alpha$ -Dihydrozymosterol .....	.....	.....	"	+27.2 ( $\lambda = 546\text{l}$ )	+11.5	+43.1
C.	$\beta$ -Dihydrozymosterol .....	.....	.....	"	+32.1 ( $\lambda = 546\text{l}$ )		
A.	Deoxycholic acid .....	3-OH, 12-OH,	.....	EtOH	+57.1		
B.	<i>apo</i> Cholic acid .....	17-C <sub>4</sub> H <sub>9</sub> CO <sub>3</sub> H	.....	"	+49.9	-7.2	-28.1
C.	Dihydroxycholestanic acid .....	.....	.....	"	+60.1	+3.0	+11.8
A.	Cholanic acid .....	17-C <sub>4</sub> H <sub>9</sub> CO <sub>2</sub> H	.....	CHCl <sub>3</sub>	+21		
B.	<i>apo</i> Cholanic acid .....	.....	.....	"	+37.0	+16.0	+57
C.	—	—	—	—	—	—	—
A.	—	—	—	—	—	—	—
B.	$\alpha$ -Anhydrodigoxigenin ..	3-OH, 17-C <sub>4</sub> H <sub>9</sub> O <sub>3</sub>	.....	MeOH	+39.0 (D line)		
C.	$\beta$ -Anhydrodigoxigenin ..	.....	.....	(+43.7 ( $\lambda = 546\text{l}$ ))	$\Delta[M]_D^{\text{D}} (C - B) = -186$		
A.	—	—	—	(-13.3 (D line))	$\Delta[M]_{\text{IR}}^{\text{D}} (C - B) = -217$		
B.	$\alpha$ -Anhydrodigoxigenin ..	3-OH, 7-OH, 17-C <sub>4</sub> H <sub>9</sub> O <sub>3</sub> ..	.....	"	(-17.3 ( $\lambda = 546\text{l}$ ))		
C.	$\beta$ -Anhydrodigoxigenin ..	.....	.....	"	+46.0 ( $\lambda = 546\text{l}$ )	$\Delta[M]_{\text{IR}} (C - B) = -231$	
				"	-16.3 ( $\lambda = 546\text{l}$ )		

TABLE X—INFLUENCE OF ETHYLENIC LINKAGE AT 22:23

Substance	Substituents	Solvent	$[\alpha]_D$	$\Delta[\alpha]_{(B-A)}$	$\Delta[M]$
A. 22:23-Dihydroergosterol.	CH(Me)CH <sub>2</sub>	CHCl <sub>3</sub>	-109°	°	°
B. Ergosterol	CH <sub>2</sub> s	"	-135	-26	-103
A. $\alpha$ -Ergostenol	CHMe	"	+13.1		
B. Dihydroergosterol-I	CHMe	"	-19	-32.1	-128
A. 22:23-Dihydroergosterol peroxide	CH <sub>2</sub> s	"	+5.4		
B. Ergosterol peroxide	CH <sub>2</sub> s	"	-35.7	-41.1	-174
A. Ergostenetriol	O <sub>2</sub>	Pyridine	0		
B. 22:23-Dihydroergosterylacetate-maleic anhydride	[5:8: C <sub>4</sub> H <sub>9</sub> O <sub>4</sub> ]	"	-13.7	-13.7	-59
A. Ergostenetriol acetate-maleic anhydride	"	CHCl <sub>3</sub>	-9.1		
B. 22:23-Dihydroergosteryl acetate	"	"	-19	-9.9	-53
A. 22:23-Dihydroergosterol	CH(Me)CH <sub>2</sub>	"	-3.1		
B. Neogesterol	CH <sub>2</sub> s	"	-12	-8.9	-36

TABLE XI.—INFLUENCE OF REDUCTION OF 17-KETO-GROUP TO SECONDARY CARBINOL

Substance	Substituents	Solvent	[α] <sub>D</sub>	$\Delta[\alpha]$
			(B - A)	$\Delta[M]$
A. <i>cis</i> -Androsterone	...	...	3-OH, 17:O	+
B. <i>cis</i> -Androstan-3:17-diol	...	?	EtOH	+94°
A. <i>trans</i> -Androsterone	...	?	EtOH	+12.6
B. <i>trans</i> -Androstan-3:17-diol	...	?	EtOH	-81.4
A. $\Delta^4$ <i>3</i> ,Androstone-3:17-dione	...	...	"	+91
B. $\Delta^4$ <i>5</i> ,Androstone-17-ol-3-one	...	...	"	+4.2
A. <i>trans</i> - $\Delta^5$ <i>6</i> -Androsten-3-ol-17-one	...	...	"	+190
B. <i>trans</i> - $\Delta^5$ <i>6</i> -Androstone-3:17-diol	...	...	"	+106.5
A. Oestrone	...	...	"	-83.5
B. Oestradiol	...	...	"	-82.5
A. Equilin	...	...	"	-82.5
B. Dihydroequilin	...	...	"	-223
P. B.	...	...	"	-88
			[No 10-Me]	-236
			[No 10-Me]	-220
			[No 10-Me]	-88
			[No 10-Me]	-220



yet been assigned,\* show a considerable difference in rotation, and there is a discrepancy between chemical and physical evidence here, which further work on ergosterol or the heart poisons may clear up.

The data for the influence of an ethylenic linkage at 22:23 (Table X) are drawn from ergosterol derivatives. The simpler compounds give moderately concordant values of  $\Delta[M]$ , but the remaining values are much lower, though of the same sign.

The figures in Table XI show a high degree of uniformity in the decrease of dextrorotatory power when the 17-keto-group, which is under the inductive influence of C-13, is reduced to the carbinol. The one discordant figure may be attributed to a difference in solvent.

In assuming that simple relations should exist between the optical activities of different substances for an arbitrary wave-length and in an arbitrary solvent, no account is taken of the occurrence of anomalous rotatory dispersion or of solvent effects, which await detailed examination in this group, and some of the discrepancies may be due to these causes. It is known that the nature of the solvent has a great influence on the rotation, and that the influence is sometimes in different directions in different substances in this group. In a number of compounds selective absorption in the near ultra-violet region may be expected to affect rotatory power, whilst in other cases unrecognized constitutional influences may be operative.† However, it seems that a useful basis of criticism of constitutional formulae proposed on chemical grounds may be provided in the steroid group by the obedience to, or divergence from, simple empirical rules derived from van't Hoff's principle of optical superposition. If relations in the steroid group should, in fact, prove to be too complicated for optical activity to serve as a guide and stimulus to further investigation in the same way that Hudson's classical work has acted in the carbohydrate group, further exact study of optical rotations and investigation of the cause of deviations from simple rules may be expected to lead to a closer knowledge of the structural and physico-chemical factors involved.

\* Smith, S., 'J. Chem. Soc.', p. 1050 (1935); p. 354 (1936).

† For a discussion of these factors in the carbohydrate group see Lowry (*loc. cit.*) and the series of papers by Hirst and co-workers, 'J. Chem. Soc.', 1932-35, also Hirst, 'Rep. Brit. Ass. Adv. Sci.', p. 358 (1935).

---

# The Atomic Rearrangement Process in the Copper-Gold Alloy Cu<sub>3</sub>Au

By C. SYKES, Ph.D., F.Inst.P., and F. W. JONES, B.Sc.

(Communicated by W. L. Bragg, F.R.S.—Received 25 May, 1936)

[PLATE 3]

## I—INTRODUCTION

When certain single-phase alloys are cooled from high temperatures they undergo transformations consisting of a change from a random distribution of atoms amongst the atomic sites to an ordered one. The thermodynamics of such transformations have been considered by Bragg and Williams\*† and also by Bethe‡ and Peierls;§ the former assume that the energy involved in any atomic interchange is directly proportional to the statistical degree of order (superlattice order) throughout the whole alloy crystal, whilst the latter consider that it depends only on the relative number of like and unlike atoms immediately surrounding the atoms concerned in the interchange (order of nearest neighbours).|| Both assumptions enable relations to be derived for the change in degree of order (as separately defined) with temperature under equilibrium conditions. These relations are then used to calculate the change in energy content produced as a result of the atomic rearrangement.

According to the theory of Bragg and Williams, the superlattice order disappears entirely on heating the alloy through the critical temperature and the energy content is affected only by the ordering process below the critical temperature. The theory of Bethe predicts that, although superlattice order disappears at the critical temperature, a high degree of local order persists, which vanishes only at very high temperatures; an abnormally high specific heat is to be expected, therefore, even above the critical temperature. In the case of  $\beta$  brass (CuZn) both theories give practically the same result for the total change in internal energy below the critical temperature, which is in reasonable agreement with experimental measure-

\* Bragg and Williams, ' Proc. Roy. Soc.,' A, vol. 145, p. 699 (1934).

† ' Proc. Roy. Soc.,' A, vol. 151, p. 540 (1935).

‡ Bethe, ' Proc. Roy. Soc.,' A, vol. 150, p. 552 (1935).

§ Peierls, ' Proc. Roy. Soc.,' A (1936) (*in print*).

|| Bethe originally proposed the theory for CuZn; Peierls extended it for the case of Cu<sub>3</sub>Au.

ment.\* Neither theory gives the correct rate of release of energy in the neighbourhood of the critical temperature, and it would appear that the final disappearance of superlattice order is more sudden than theory indicates. The specific heat is abnormally high above the critical temperature owing presumably to the presence of local order.

$\beta$  brass may be considered as typical of binary alloys of equiatomic composition XY: both theories suggest considerable modifications in the form of the transformation for an alloy having the composition  $X_3Y$  and in particular the appearance of latent heat is predicted at the critical temperature as distinct from an increase of specific heat of about 70% for alloys of the type XY. The present paper describes the results of an investigation of the thermal effects of the transformation in  $Cu_3Au$  which enable the theoretical predictions to be compared with experiment for the alloy type  $X_3Y$ .

In a recent investigation into the effects of the ordering process on the electrical resistivity and X-ray crystal structure of  $Cu_3Au$ ,† it was demonstrated that the mechanism of the process was complicated by the formation of antiphase nuclei. The face-centred lattice of  $Cu_3Au$  may be considered in terms of the four interpenetrating simple cubic lattices to which it is equivalent. When completely ordered, one lattice contains nothing but gold atoms and the other three, copper atoms. As the alloy cools through the critical temperature, gold atoms may segregate on any of the four lattices, consequently any individual crystal in the alloy will contain a large number of small volumes or nuclei, each of which is ordered throughout on the same simple cubic lattice, but different nuclei will be out of phase with one another. By annealing the alloy just below the critical temperature for about 50 hours, certain nuclei grow at the expense of others, until finally the remaining nuclei become comparable in size with the crystal, the superlattice lines become quite sharp, and the resistance attains a steady value. The alloy may then be cooled to lower temperatures without any further appearance of antiphase nuclei (as far as may be judged from the sharpness of superlattice lines). If the alloy is cooled continuously from the critical temperature, before a consistent scheme of order has been achieved, the electrical resistance is affected in two ways, one by the increase of order inside each nucleus produced by lowering the temperature, the other by the decrease in disordered material consequent on the growth of nuclei. The growth of nuclei is a function not only of the temperature but also of the size of the nuclei—the larger the nuclei the slower the rate of growth.

\* Sykes, 'Proc. Roy. Soc.,' A, vol. 148, p. 422 (1935).

† Sykes and Evans, 'J. Inst. Met.,' vol. 58 (1936).

By eliminating these nuclei the alloy is in a condition when it could reasonably be expected to behave as the theories predict. Measurements of the total energy released by the transformation under such conditions are in reasonable agreement with the predicted values, although, as with CuZn, the rate of release of energy near the critical temperature is not correctly given by either theory. The presence of latent heat or, at any rate, an extremely high specific heat has been confirmed.

The ability of the alloy to produce nuclei, coupled with an inherently slow rate of diffusion, enables a variety of metastable states to be examined. The information obtained from such experiments definitely suggests that the energy of any atomic interchange is fixed primarily by its near neighbours and not by the superlattice order; for example, it is possible to release upwards of 40% of the total energy involved in the transformation without producing any appreciable change in the electrical resistance or any suggestion of superlattice lines, and 95% of the energy may be released whilst the electrical resistivity is still 70% higher than the equilibrium value and the superlattice lines are still diffuse.

## 2—EXPERIMENTAL

A detailed account of the methods used to measure the thermal effects of the ordering process in Cu<sub>3</sub>Au has already been published.\* The following outline of the experimental work will assist in the interpretation of the results.

(a) *Specific Heat Measurements*—A specific heat-temperature (S.T.) curve of an alloy undergoing an order-disorder transformation consists of the normal S.T. curve with the thermal effects of the transformation superimposed. The method used for the determination of such curves is as follows. The specimen in the form of a closed hollow cylinder is mounted inside a hollow cylinder of copper. The copper cylinder is heated at a uniform rate by means of a furnace, whilst the specimen is heated independently from a small internal heating coil. By suitable manipulation of the power input to the heating coil, the temperature difference between specimen and copper cylinder may be kept very small, so that no heat is lost by the specimen to its surroundings. The instantaneous specific heat may then be calculated from the known input to the heating coil and the measured heating rate of the specimen. Since determinations of specific heat can be made at any stage in the experiment, a complete S.T. curve is obtained whilst the temperature of the specimen is continuously

\* Sykes and Jones, 'J. Inst. Met.', (1936) (*In print*).

changing. Figs. 2 and 4 have been obtained in this way. The method is only applicable to the measurement of specific heat on heating; the heating rate of the specimen was roughly the same in each experiment; it varied within the range  $1\cdot5^\circ\text{ C./min.} \pm 20\%$ .

(b) *Equilibrium Energy Content Measurements*—Whilst the qualitative effect of the ordering process on the energy content may be deduced from the specific heat temperature curve by integration, the results obtained in this way are not of much quantitative value since the specimen is, in general, not in equilibrium, and the precise relation between the actual state and equilibrium state of the specimen at each temperature is unknown. Direct measurements of the equilibrium energy content are made as follows.

It has been found that all S.T. curves are identical from  $420^\circ\text{ C.}$  upwards, no matter what the initial state of the specimen at room temperature. From this it is inferred that the alloy is always in equilibrium in this region under the experimental conditions used. The effect of temperature on the energy content is, therefore, obtained by measuring the energy necessary to heat the alloy from temperature  $T$  to  $420^\circ\text{ C.}$ , and plotting this energy against  $T$ . The same apparatus is used as for the specific heat determinations. The specimen is first annealed *in situ* at the temperature  $T$  until it is in equilibrium. The heating coil is then supplied with constant current well in excess of that required to heat the specimen at  $1\cdot5^\circ\text{ C./min.}$ , and the copper cylinder is simultaneously heated from  $T$  to  $420^\circ\text{ C.}$  The temperature of the specimen is held within  $\pm 0\cdot1^\circ\text{ C.}$  of the temperature of the copper cylinder by switching off the current to the coil at appropriate intervals. The current is simultaneously passed through a voltameter which enables the total time the coil was energized to be calculated. Since the specimen is in equilibrium both at the beginning and end of the experiment, the energy input to the coil is equal to the difference in equilibrium energy content corresponding to the initial and final temperatures although at intermediate temperatures the alloy is not in equilibrium.

(c) *The Specimens*—An ingot of copper gold alloy was kindly prepared by Mr. A. R. Raper of the Mond Nickel Co., Ltd., Acton. This was annealed for 2 hours at  $825^\circ\text{ C.}$  The specimen was machined from the ingot and then reannealed. An X-ray "powder" photograph was taken, using the back reflexion method, and the sharpness of the reflexions showed that the specimen was then free from coring and cold working effects. The chemical composition was 24.9% Au by atoms. All the heat measurements were made on this sample.

An alloy of slightly different composition, 25·05% Au by atoms, was used for the resistance measurements and X-ray structure investigation quoted later in this paper. The specimens were wires which had been specially heat-treated to remove coring and cold-working effects. The crystal size in the resistivity specimens (1 mm. diameter wires) was of the same order as that in the specific heat specimens—1 mm. The specimens used for structure investigation were 0·4 mm. diameter and had a crystal size of the order  $10^{-3}$  cm. Monochromatic radiation (Cu K<sub>α</sub>) was used for the determination of lattice structure by X-ray diffraction.

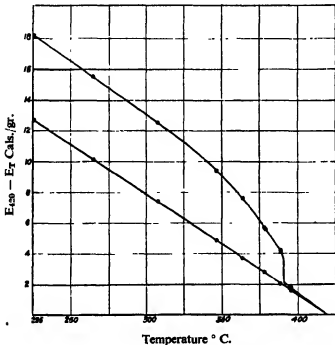


FIG. 1—○ Actual energy difference; ● normal energy difference.

### 3—ALLOY IN EQUILIBRIUM

(a) *Energy Content*—Fig. 1 shows the effect of temperature on the equilibrium energy content of the alloy, the reference temperature being 420° C. The annealing treatments, used to bring the specimen into equilibrium at the various points, were based on the results of an investigation of the effect of the ordering process on the electrical resistivity of the alloy. In each case the alloy was first annealed for at least 50 hours just below the critical temperature to ensure the rapid growth of

nuclei, and thus produce a consistent scheme of order throughout each crystal. The specimen was then cooled to the final temperature in stages, the cooling period was 50 hours for temperatures above 350° C., increasing to 500 hours for the measurement made at 226° C.

The normal energy content of the alloy in the absence of any transformation may be estimated from specific-heat temperature curves. Fig. 2 is an S.T. curve obtained after cooling at 30° C./hour from 450° C. Disordering commences at about 220° C., whilst up to this temperature

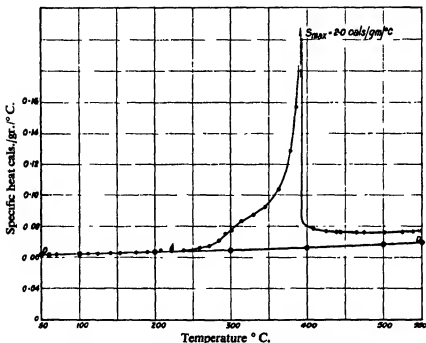


FIG. 2—Specific heat-temperature curve (specimen cooled at 30° C./hr.).

part OA the specific heat curve is quite normal. We shall assume that the curve would traverse OAD if no transformation occurred. The specific heats of both copper and gold are known accurately from the work of Jaeger\* and his associates; using their results we have calculated the specific heat of Cu<sub>3</sub>Au assuming it to be a pure mixture and obtained the points marked ⊕. These are in good agreement with the specific heat measurements for the alloy in the range 40° C.-220° C., so that there is some justification for the extrapolation to 420° C.

\* Jaeger, Rosenbohm, and Bottema, 'Proc. acad. Sci. Amst.', vol. 35, p. 772 (1932).

Fig. 3a gives the extra energy content due to the transformation as a function of temperature. In both theoretical treatments of the transformation the energy is calculated in terms of the energy per atomic interchange, and this bears a definite relation to the critical temperature. We have taken the experimental value  $T_c = 391^\circ\text{ C.} = 664^\circ\text{ K.}$  found in this investigation, and calculated figs. 3b and 3c. The experimental curve lies between the two theoretical curves and the agreement is reasonable.

It is unlikely that the experimental measurements recorded in fig. 1 are in error by more than 1%. Moreover, it is found that the energy released by the transformation in the specimen, as cooled at  $30^\circ\text{ C./hour}$ , is in the

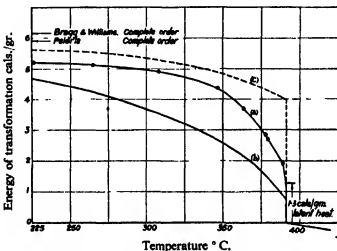


FIG. 3—(a) Experimental curve; (b) Bragg and Williams; (c) Peierls.

region  $226^\circ\text{ C.}-420^\circ\text{ C.}$ , the same to within 2% as that obtained corresponding to equilibrium (cooled in 500 hours) at  $226^\circ\text{ C.}$  There can be little doubt, therefore, that the heat treatments given were entirely adequate. Although the energy content curve is still rising at  $220^\circ\text{ C.}$ , the effect is very slight, indicating that the alloy is almost completely ordered, and very little extra energy may be expected at lower temperatures. We conclude that the maximum energy available below the critical temperature is not more than  $5.5\text{ cals./gm.}$

Both theories, therefore, give results for the total amount of heat involved in the transformation which are about 10% too high. Neither gives a correct representation of the release of energy near the critical temperature. The Bragg-Williams theory gives a curve rising too slowly with decreasing temperature and Peierls's theory gives much too high a latent heat. Fig. 2 indicates that the specific heat of the alloy is still

abnormally high above the critical temperature, viz., 0.076 cals./gr./° C. as against 0.066 as determined from Jaeger's results. Beyond the critical temperature the specific heat remains practically constant up to 500° C. and then rises slowly. (The accuracy of the specific heat measurements is of the order of  $\pm 1\%$ .) We have estimated the abnormal specific heat due to the disordering of nearest neighbours according to the theory of Peierls and an increase of 0.004–0.005 cals./gm./° C. is to be expected. This is about half the observed difference. In view of the difficulty of determining the normal specific heat this result must be regarded as reasonable.

(b) *Behaviour of the Alloy at the Critical Temperature*—Referring to fig. 1, it will be seen that two determinations of energy content were made just below the critical temperature (389.5° C.  $T_c = 391$ ° C.) after soaking at this temperature for 100 hours, and one determination just above at 396° C. The energy difference is 2.4 cals. and if it is assumed the average normal specific heat in this region is 0.066 then the upper limit to the latent heat is 1.9 cals./gm.

The detailed experimental results forming the basis for the statement that latent heat is absorbed at the critical temperature have been given in a prior publication.\* It was found that provided the specimen had a consistent scheme of order throughout each crystal at a temperature just below the critical temperature, then, although energy was continuously supplied to the specimen, its temperature-time curve in the neighbourhood of the critical temperature showed first a maximum and then a minimum; in brief, an effect exactly opposite to the "undercooling" phenomena observed on cooling curves and generally produced by a change of phase. The fact that the temperature of the specimen falls, although heat energy is continuously supplied, proves that latent heat is absorbed at the critical temperature on heating. If antiphase nuclei are present then only a large specific heat is observed, cf. fig. 2 where the specific heat rises to 2 cals./gm./°C., but no latent heat is observed. The figure of 1.9 cals./gm./ mentioned above is undoubtedly too high; since no allowance is made either for the heat released below the critical temperature or for the abnormal specific heat contributed by the change in local order above the critical temperature. If these factors are taken into account, a value of 1.26 cals./gm./° C. is obtained, as a lower limit. The true value for the specimen concerned is considered to be within the limits 1.26 cals.  $\pm 10\%$ . Peierls's result of 4.0 cals./gm. appears, therefore, to be much too high.

\* Sykes and Jones, 'J. Inst. Met.' (in print).

Differences in the behaviour of the alloy Cu<sub>3</sub>Au at the critical temperature have been observed by various investigators\* and attributed to the presence of traces of impurities, in particular oxygen. These raise the critical temperature on heating and render the transformation more sluggish than it would normally be. Experimental results obtained under such circumstances would be too small. It is extremely unlikely that any appreciable effect of this sort has occurred in this work. To obtain a latent heat of 4.0 cals./gm. the *true* critical temperature would have to be as low as 350° C., whereas it is quite certain that the alloy transforms from the disordered phase at normal rates of cooling (30° C./hour) at 370° C. On the other hand, it is possible that the precise shape of the energy content curve in the neighbourhood of the critical temperature may be affected appreciably by small traces of impurities and slight divergences from the exact composition Cu<sub>3</sub>Au. Further experiments on specimens of compositions near to the theoretical composition and melted in various atmospheres are contemplated in order to determine whether these factors do affect the shape of the curve near the critical temperature.

(c) *The Change in Entropy*—The difference in entropy between the ordered and the disordered state has been calculated by Williams† on the assumption (a) that the transformation results solely due to atomic rearrangement, and (b) that the entropy of the ordinary vibrations is independent of the degree of order. He obtains the result of 0.0116 cals./gm./°C. for Cu<sub>3</sub>Au and this should be quite independent of the nature of the forces governing the transformation. Since, according to Bragg and Williams, order disappears entirely above the critical temperature, the whole of the entropy change should be located below this temperature. On the other hand, according to Peierls, a part of the entropy change, viz., that resulting from the alteration in local order, should take place above the critical temperature.

The experimental result for the change in entropy for the temperature range 226° C.–391° C. is 0.0081 cals./gm./°C., which is much smaller than the Bragg-Williams result. Assuming that the normal specific heat curve (fig. 2) is correct, the change in entropy from 550° C. to 390° C. produced, as a result of the increase in local order, is 0.0017 giving a final figure of 0.0098 cals./gm./°C. This is still appreciably smaller than the theoretical result, indicating that the contribution made by the local order is still incomplete.

\* See Haughton and Payne, 'J. Inst. Met.', vol. 46, p. 481 (1931).

† Williams, 'Proc. Roy. Soc.,' A, vol. 152, p. 231 (1935).

#### 4—METASTABLE STATES

The experimental method described in brief in § 2 (*a*) enables a variety of metastable states to be examined and the mechanism of the ordering process traced through its various stages.

(*a*) *Specific Heat-Temperature Curves*—Fig. 4 shows a number of S.T. curves taken whilst the temperature of the specimen was raised continuously at  $1\cdot 5^\circ$  C./minute from room temperature to  $450^\circ$  C. The previous heat-treatments given to the specimen were:—

Fig. 4*a*—water quenched from  $395^\circ$  C (just above the critical temperature);

Fig. 4*b*—water quenched from  $550^\circ$  C.;

Fig. 4*c*—water quenched from  $450^\circ$  C., annealed for 2 hours at  $130^\circ$  C., then cooled to room temperature;

Fig. 4*d*—annealed at  $380^\circ$  C. for 60 hours and then water quenched;

Fig. 4*e*—cooled at  $1500^\circ$  C./hour from  $450^\circ$  C. to  $300^\circ$  C. and then cooled to room temperature in 1 hour.

In order to prevent oxidation, the specimen was sealed in an evacuated glass bulb whilst being heat-treated. This shattered on entering water and a satisfactory quench was obtained. Two sets of points are shown in fig. 4*b*; these refer to two different experiments and demonstrate that the metastable states can be accurately reproduced. The curves are not continued to the critical temperature as this would complicate the diagram; above the critical temperature they were all the same as fig. 2, within the limits of experimental error. Through each curve a line is drawn which represents the S.T. curve for the normal alloy, assuming no atomic rearrangement (*cf.* fig. 2, line OAD), and this forms a convenient zero line.

(*b*) *Interpretation of fig. 4*a**—When the alloy Cu<sub>3</sub>Au is quenched from above the critical temperature the structure, which contains no superlattice order, is preserved down to room temperature.

An X-ray photograph, typical of the alloy as quenched from above the critical temperature is shown in fig. 6, Plate 3. The structure is a normal face-centred one. No superlattice lines are present, from which it can be deduced that any small volumes in the specimen, throughout which there is a coherent scheme of order, must be appreciably smaller than  $5 \times 10^{-7}$  cm. linear dimensions.\* We shall assume that, in the specimen

\* We shall subsequently describe measurements which indicate that superlattice lines become visible when the ordered volumes attain a linear dimension of  $5\cdot 5 \times 10^{-7}$  cm. The lattice spacing for Cu<sub>3</sub>Au is 3.75 Å, so that this distance corresponds to about 14 atomic distances.

as quenched from 395° C., only local order exists, but that owing to fluctuations there is a large number of places where a small number of adjacent atoms has a high degree of order of nearest neighbours. These places act as nuclei, and as soon as the speed of atomic interchange becomes appreciable (60° C.) growth commences and energy is released. From

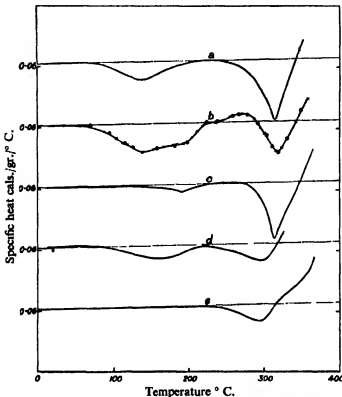


FIG. 4—Specific heat-temperature curves. *a*, Specimen quenched in water from 395° C. ( $T_c = 391^\circ$  C.). *b*, Specimen as water-quenched from 550° C. *c*, Specimen water-quenched from 450° C. annealed for 2 hours at 130° C. and then cooled to room temperature. *d*, Specimen annealed at 380° C. for 50 hours then quenched in water. *e*, Specimen as cooled at 1500° C./hour through the critical temperature to 300° C. cooled to room temperature in 1 hour.

130° C. the rate of evolution of energy diminishes, and finally at about 230° C. the specific heat becomes normal once more, showing that any rearrangement process going on in the alloy produces no net effect. The alloy is not in true equilibrium at 230° C., since, if the temperature is raised still further, more energy is evolved. It is necessary, therefore, to explain why the ordering process takes place in two stages and two hypotheses are suggested.

In the first place, as we have already mentioned in the introduction to this paper, adjoining nuclei are probably antiphase, otherwise they would coalesce. Once they touch at certain points ( $130^{\circ}$  C.) further growth should very rapidly diminish, and when the nuclei touch at all points growth can only occur due to the absorption of certain nuclei by others. This is likely to be a very slow process indeed. Apart, however, from the fact that the various adjoining nuclei are antiphase, there is also the possibility that variations in chemical composition\* occur in the alloy over such small distances. As the nuclei grow they will absorb gold and copper atoms in the proportion of 1 : 3, and any excess atoms of either kind will be finally concentrated at the boundaries. Further growth can then take place only by moving atoms around the boundaries which will again be a very slow process.

Both the above hypotheses lead us to expect a rapid falling off in the rate of energy release once the nuclei touch, from  $130^{\circ}$  C. onwards. As the temperature is raised the number of atomic interchanges per second increases and tends to counteract the retardation. At  $230^{\circ}$  C. growth recommences, and by reducing the amount of disordered material in the boundaries, produces a second dip in the S.T. curve. This growth continues until the nuclei dissolve at the critical temperature. At  $314^{\circ}$  C. a sharp minimum is observed and thereafter the specific heat rises rapidly until the critical temperature is reached. From  $230^{\circ}$  C. upwards, two effects are superimposed: the reduction of the amount of boundary material leads to an evolution of heat; the degree of order inside the nuclei decreases and leads to an absorption of heat. As the temperature rises the first effect decreases since the proportion of disordered material becomes smaller, the second effect increases rapidly (*cf.* fig. 2, which is a near approximation to the equilibrium S.T. curve), hence the very sharp minimum. At  $342^{\circ}$  C. the two effects are equal and opposite; beyond this temperature the small heat evolution due to growth of nuclei is entirely masked by disordering inside the nuclei.

(c) *Size and Structure of Nuclei*—Before proceeding to the interpretation of the other curves in fig. 4, some idea of the size and constitution of the nuclei in the various stages of the curve in fig. 4a will be given. A number of wires was quenched in water from  $450^{\circ}$  C. and then heated at  $2^{\circ}$  C./minute; a wire was quenched at approximately  $25^{\circ}$  C. intervals from  $150^{\circ}$  C.– $350^{\circ}$  C. Figs. 7 and 8, Plate 3, give the structure of the

\* We shall show later that the size of the nuclei under consideration at this stage is about 6–8 atoms across, so that fluctuations in chemical composition are not excluded.

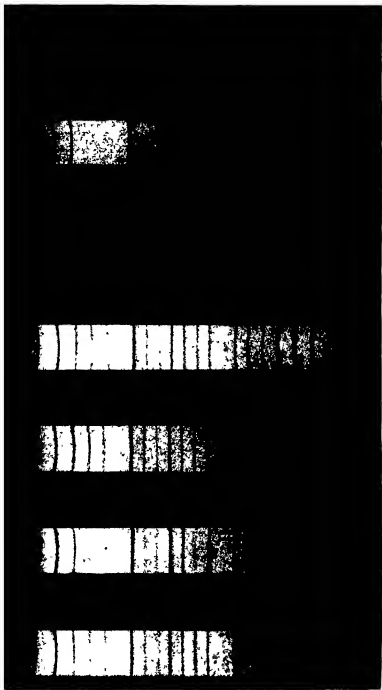


FIG. 6.

FIG. 7

FIG. 8

FIG. 9.

FIG. 10.

FIG. 11.

FIG. 12.



two specimens quenched from 320° C. and 344° C. respectively. Super-lattice lines are visible only on fig. 8, Plate 3.

It is known that the breadth of the X-ray reflexions is inversely proportional to the size of the particles producing the reflexions, and Scherrer\* has given the following relation

$$B = \frac{0.94 \lambda}{t \cos \theta} + b.$$

B is the angular width of the reflected beam between the two points where the intensity falls to half value;

*b* is the angular width the line would have owing to the finite slit width and other experimental features even if the optical resolution were perfect;  $\lambda$  is the wave-length of the radiation used (1.54 Å. for Cu K);

$\theta$  is the Bragg angle for the particular reflexion under consideration; and

*t* is the thickness of the crystal.

The breadth B of the superlattice lines on fig. 8, Plate 3, was obtained, using the well-known photometric methods. The corresponding value of *b* was obtained by extrapolation of the breadth of the normal lattice lines against the Bragg reflexion angle. Six sets of measurements were made to reduce errors produced by grain size in the photographic emulsion and by any slight preferential orientation existing in the specimen. The final result for the average size (*t*) of the nuclei using the above formula was  $5.5 \times 10^{-7}$  cm., i.e., 14 atomic distances. Experimental determinations of this type are liable to errors of  $\pm 30\%$ , and it is doubtful whether the formula itself is strictly accurate, consequently such results can only be regarded as estimates from which the approximate constitution of the nuclei may be deduced.

The energy released by the formation of nuclei existing at 340° C. is given by the area between the S.T. curve, fig. 4a, and the normal S.T. line in the temperature range 20° C.-340° C. This energy is 2.5 cals./gm. and, since the total energy available is 5.2 cals./gm., cf. fig. 3, a fraction of 0.45-0.5 of the total energy has been released at this stage. Let us suppose the nuclei are cubic in shape with an edge *d* atomic distances long. If the atoms forming the surface layer are arranged at random whilst the remainder are completely ordered, then to a first approximation the energy released will be the fraction  $(1 - 6/d)$  of the total energy provided the energy of any atom is fixed only by the identity of its immediate neighbours. In order to get the experimental value of 0.5, the above

\* Bragg, "The Crystalline State," p. 190.

hypothesis leads to nuclei 12 atomic diameters long as compared with the value of 14 actually measured. Bearing in mind the uncertainties involved in the measurement of particle size and that there will be a certain amount of disorder in the interior of the nuclei at 340° C., it is reasonable to conclude that the energy of any atom is fixed only by the identity of its neighbours within, at the most, two atomic distances, *i.e.*, all the atoms in the nuclei may be considered to have the energy associated with the equilibrium degree of order at the particular temperature concerned, with the exception of those in the two boundary layers.

In the case of the specimen as cooled at 30° C. per hour the nuclei have an average length of  $2.8 \times 10^{-6}$  cm., *i.e.*, 75 atomic distances, so the experimental result already mentioned: that the energy content of such a specimen at 226° C. is almost the same as that of the alloy in true equilibrium at that temperature, is to be expected if the suggested constitution of the nuclei is correct.

It is estimated that the first dip in the S.T. curve, fig. 4a, is produced by the formation of nuclei of linear dimensions of from 6–8 atomic distances.

(d) *Further Effects of Nuclei on the Specific-Heat Temperature Curve*—The first dip in the S.T. curve has been eliminated by annealing at 130° C. for 2 hours. On the other hand, the second dip is just as prominent, and extends over the same range of temperature. By annealing at 130° C. the nuclei are allowed to grow until they touch; since this growth gives rise to the first dip observed in the quenched alloy we should not expect to observe it in fig. 4c. Further, once the nuclei are touching at all points, a state of affairs likely after 2 hours at 130° C., further growth will only take place at a much higher temperature where the rate of atomic interchange is correspondingly larger; this is in agreement with the result on fig. 4c where the second dip commences at about 260° C. A back-reflexion X-ray photograph taken from the actual specific heat specimen after annealing at 130° C. for 2 hours (*i.e.*, immediately prior to the experiment recorded in fig. 4c) showed no trace of superlattice lines. This is in agreement with the deduction that the first dip is to be associated with the formation of nuclei of about 6–8 atomic distances in length, since the intensity of reflexion from such small volumes will be extremely weak. It further disposes of the possibility that the behaviour of the specific heat specimen might be essentially different from that of the wire (measurements of nuclei size were made from films of wire specimens).

Fig. 4b—It is of interest to compare fig. 4b with fig. 4a. The initial dip in fig. 4b is much larger, and it was at first thought that a certain amount of local disorder had been frozen in the alloy by quenching from

550° C. (at 395° C. the local order is a maximum since the alloy is on the point of changing over to superlattice order). Further investigation showed that the total energy absorbed to raise the alloy from 25° C. to 420° C. was the same in both cases, within the limits of experimental error. Moreover, it will be noticed that both curves cut the normal specific heat line at the same temperature: 341° C., and integration of the S.T. curves from this point to 420° C. gives the same result for the energy content. At 341° C. then, the alloy has arrived at the same structure in both experiments, *i.e.*, the nuclei are the same size. It is suggested that the number of centres for growth is smaller in the alloy as quenched from 550° C. than as quenched from 395° C.; the nuclei reach an appreciably larger size before they touch so that the initial dip is bigger, and consequently the second dip must be correspondingly smaller. The ratio of the amounts of energy involved in the first dip suggests that the number of nuclei as quenched from 395° C. is about 30% more than in the alloy as quenched from 550° C. At 230° C. (fig. 4b) disordering takes place inside the nuclei, so that the apparent specific heat rises above the normal value. The reason for the difference in the number of nuclei in the two cases is not entirely clear; 395° C. is very near to the temperature at which superlattice order sets in and possibly a large number of minute nuclei exist in the alloy at the high temperature and are frozen by the quenching operation. At 550° C. this effect will not be so marked. On the other hand, the fact that the energy of the specimen in the two conditions is the same, suggests that no appreciable amount of local disorder is preserved in the alloy as quenched at 550° C.

Fig. 4d—The structure of the alloy after this treatment may be deduced from fig. 9, Plate 3. The superlattice lines are sharp and the high reflexions show the K<sub>s</sub> doublet completely resolved. This forms a convenient index to the particle size,\* since if  $\lambda$  and  $\lambda + \partial\lambda$  are the wave-lengths of the doublet, and  $t$  the size of the crystals, for resolution

$$\frac{2t}{\lambda} > \frac{\lambda}{\partial\lambda} > 40 \text{ For Cu K. } \frac{\lambda}{\partial\lambda} = 400; \lambda = 1.5 \text{ A.}$$

*i.e.*,

$$t > 200 \lambda > 300 \text{ A} > 80 \text{ atomic distances.}$$

The superlattice lines are practically as sharp as the main lattice lines, consequently, we may conclude that there is a coherent scheme of order over distances comparable in size with the individual crystals  $10^{-8}$  cm. According to fig. 3, 2.7 cals./gm. is released by the alloy in passing from

\* Bragg, "The Crystalline State," p. 190.

disorder to equilibrium at 380° C. If  $S^*$  is the superlattice order at this temperature

$$S^* = \frac{2.7}{5.2} = 0.52,$$

i.e.,  $S \equiv 0.7$  to a first approximation. So that at the commencement of the experiment the extremely large nuclei have a high degree of order.

On heating, two dips again are observed, although appreciably smaller than in the case of figs. 4a and 4b. If the lattice ordered as a whole, one dip only would be expected. (Growth of nuclei of the size present in the quenched alloy cannot be responsible for either dip since, (a) the boundary material is of negligible proportions, and (b) a very high temperature ( $> 380^\circ$  C.) would be necessary for growth to proceed.) Regions of high local order must form, lock, and then coalesce at the high temperatures. It is unlikely that antiphase volumes even of, say, 6 atomic distances in dimensions can form in a single phase pattern having a basic degree of order throughout of 70%, and the second hypothesis of variation in chemical composition, which has already been put forward, appears to be the more likely explanation of the locking action in this case. If the specimen is annealed for 2 hours at 130° C. after the treatment at 382° C. the superlattice lines are still quite sharp, see fig. 10, Plate 3, indicating that antiphase volumes larger than 14 atomic distances are not produced. The minimum of the second dip occurs at an appreciably lower temperature than in the disordered alloy and is much flatter. The energy available from the boundary material is smaller and is soon counterbalanced by the disordering effect.

Fig. 4e—This S.T. curve shows a combination of effects not emphasized by the other curves. There is no initial dip at 130° C., and the first effects due to atomic rearrangement start at 230° C. A flat minimum, similar to that in fig. 4d, follows and the curve crosses the normal S.T. line at 314° C.

Fig. 11, Plate 3, is an X-ray photograph of a wire heat-treated in a similar manner to the specimen. The superlattice lines are very similar to those in fig. 8, Plate 3; the nuclei present in the specimen at the beginning of the specific heat measurement are roughly the same size as those present in the quenched alloy, fig. 4a, by the time it reaches 340° C. This fact may be deduced from the S.T. curves, figs. 4e and 4a.

In fig. 4a the specific heat curve intersects the normal specific heat line at 340° C., in fig. 4e, on the other hand, the intersection occurs at 314° C.

\* Bragg and Williams, 'Proc. Roy. Soc.,' A, Vol. 145, p. 713 (1934).

At an intersection of this type the atomic rearrangement process produces no net effect, therefore the energy released due to the growth of the nuclei is equal to the energy absorbed by the disordering of the material inside the nuclei. If  $d$  is the linear dimension of the nuclei and if  $S$  is the abnormal equilibrium specific heat, *i.e.*, that part of the specific heat above the line OAD in fig. 2, then to a first approximation

$$\frac{6}{d} \propto \left(1 - \frac{6}{d}\right) S.$$

Since the abnormal specific heat at 340° C. is higher than that at 314° C., it follows that the nuclei at 340° C. in the experiment given by fig. 4a are smaller than those at 314° C. in fig. 4e. If our interpretation of previous curves is correct, such nuclei are too large to grow appreciably in the temperature range up to 314° C. and must have existed in the specimen at the start.

There are, therefore, two peculiarities in fig. 4e: the absence of the initial dip, and the appearance of the second dip, if the nuclei at the commencement are too large to affect the energy content by growth in the temperature range 230° C.-310° C.

The relatively large nuclei formed during cooling from 450° C. will cease to grow at about 320° C. and thereafter local regions of high order will be produced inside them in the subsequent cooling to room temperature. (The equilibrium degree of order at 320° C. is lower than the equilibrium degree of order at room temperature.) According to fig. 4d, we expect these regions of high order (nuclei within nuclei) to lock, so that on heating very little energy should be released until a temperature of 230° C. is reached, when they can begin to coalesce. The dip in fig. 4e is therefore strictly comparable to the second dip on fig. 4d.

### 5—EFFECT OF SIZE OF NUCLEI ON ELECTRICAL RESISTANCE

The ordering process, as we have already mentioned, affects the electrical resistance of the alloy.

Fig. 5 gives certain curves of resistivity as a function of temperature, which may be compared with S.T. curves in figs. 2 and 4.

According to fig. 5a, the electrical resistance begins to fall at 310° C. on heating, the general shape of the curve is, however, quite different from the S.T. curve, fig. 4a. The type of order responsible for the first dip on fig. 4a has no effect on the electrical resistance. This was confirmed by annealing a wire, quenched from 450° C., for 2 hours at 130° C. The change in resistance (if any) was less than  $\frac{1}{2}\%$ . It is clear, then, that

a considerable amount of energy (upwards of 40% of the total energy of the transformation) corresponding to formation of nuclei (8–10 atoms long) may be released before the resistance is affected at all.

From fig. 5b we see that the electrical resistance of a specimen cooled at 30° C./hour is about 30% higher at 250° C. than the equilibrium value: yet according to energy measurements practically the whole of the energy has been released.

Fig. 12, Plate 3, gives the structure of the alloy as cooled at 30° C./hour, the superlattice lines of large reflexion angle are still not resolved. From

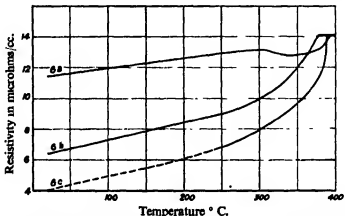


FIG. 5—Resistivity temperature curves. (a) Heating rate 2° C./minute. Specimen as quenched from 450° C. (b) Specimen cooled at 30° C./hour. (c) Equilibrium curve obtained after long annealing.

the measured width of the lines it is estimated that the average size of the nuclei is 75 atomic distances. Such nuclei are still sufficiently small to affect the electrical resistance and other experiments carried out at constant temperature have shown that the electrical resistance only reaches a steady value when the superlattice lines are completely resolved, when the nuclei are considerably greater than 300 Å.

The recent wave-theory of the metallic state leads to the following formula for the mean-free path  $\lambda$  of the electron in a metal of resistivity  $\rho$

$$\lambda = \frac{h}{\rho e^2} \times \left( \frac{\pi}{3N^3} \right)^{\frac{1}{2}},$$

where  $e$  is the electronic charge,  $N$  is the number of atoms per cc., and  $h$  is Plank's constant. The disordered alloy at 350° C. has a resistivity of  $14 \times 10^{-6}$  ohms/cc. and the ordered alloy in equilibrium a resistivity of  $10 \times 10^{-6}$  ohms/cc., the corresponding mean-free path being 30 atomic

distances and 40 atomic distances,  $1.1 \times 10^{-6}$  and  $1.5 \times 10^{-6}$  cm. According to our experiments, then, the size of the nuclei affects the resistance when it lies between  $4 \times 10^{-7}$  and  $3 \times 10^{-6}$  from  $\lambda/3$  to  $2\lambda$ , a result which would be expected if the electron had particle properties.

The electrical resistance is affected, not only by the size of nuclei (presumably due to reflexions of electrons at the boundaries) but also by the degree of order inside the nuclei, and it is possible to produce a variety of different structures, all having the same electrical resistance at the same temperature.\* The general relations between degree of order, size of nuclei, and resistance are now being determined experimentally.

Hitherto, much of the experimental work on the Cu<sub>3</sub>Au transformation has been concerned with the measurement of resistance, very little attention being given to X-ray structure and energy measurements. This is unfortunate, since the electrical resistance bears no simple relation to either the temperature or structure of the alloy. Bragg and Williams,† in an investigation of the relaxation to the equilibrium state, assumed that the electrical resistance was a linear function of the superlattice order in the alloy and calculated that atomic interchange should cease at 270° C. for Cu<sub>3</sub>Au. They pointed out that the diffusion coefficient necessitated by this result was much smaller than the recognized value. Nevertheless, resistance-temperature curves showed the first effects of the transformation in the temperature range 250° C.-310° C. (the slower the heating rate, the lower the temperature). Actually, rearrangement occurs at temperatures as low as 60° C.; but before the nuclei have attained the minimum size necessary to affect the resistance, they lock. Thereafter growth becomes so slow that at normal heating rates a temperature in excess of 250° C. is reached before the nuclei attain the requisite minimum size.

## 6—CONCLUSIONS

The experimental work on the equilibrium state indicates that both theories of the ordering process are in error to about the same extent. The facts that an abnormally high specific heat is observed above the critical temperature, and that the change in entropy below the critical temperature is much smaller than the calculated change from complete disorder to complete order, are, however, in favour of the theory of Bethe and Peierls. Neither theory purports to consider the metastable state containing nuclei, but the evidence from this work is conclusive in sug-

\* Sykes and Evans, 'J. Inst. Met.', vol. 58, p. 255 (1936).

† Bragg and Williams, 'Proc. Roy. Soc.,' A, vol. 145, pp. 723, 729 (1934).

gesting that the basic assumption of Bethe, that the energy of any atom is determined by the identity of its immediate neighbours, is a good approximation.

The alloy passes from a state of disorder to the state of order at a given temperature by rearrangement around small atomic configurations having a high degree of order of nearest neighbours at the temperature concerned. The nuclei thus formed have very narrow boundaries, and the equilibrium degree of order practically up to the surface, so that a large decrease in energy content can occur before the nuclei are large enough to produce superlattice lines. The formation of nuclei within nuclei appears to take place under suitable conditions. The growth of nuclei is affected not only by the temperature but also by the size of the nuclei themselves.

Since a considerable amount of atomic rearrangement can take place before either the lattice structure or electrical resistance is affected, interpretation of experimental results in the absence of energy measurements must be made with caution.

Further experimental work is desirable to test the two hypotheses put forward to explain the interlocking effect of the nuclei. Investigation of suitable alloys of the type XY are likely to assist in this direction, since interlocking in such alloys due to the antiphase character of the nuclei must be very much smaller than in the case of alloys of the type X<sub>3</sub>Y.

The authors are indebted to Major C. Johnson, Refinery Manager of the Mond Nickel Co., for his kindness in arranging a loan of the specific heat specimen from his Company. Their thanks are also due to the Metropolitan-Vickers Electrical Co., Ltd., for kindly providing the necessary facilities for this work, and in particular they are indebted to Mr. A. P. M. Fleming, C.B.E., Director of the Metropolitan-Vickers Electrical Co., Ltd., and Manager of the Research Department, for his personal interest in the investigations.

The authors thank Professor W. L. Bragg, F.R.S., for his kind and continued interest.

#### SUMMARY

The effect of the atomic rearrangement process on the energy content of the alloy Cu<sub>3</sub>Au has been determined experimentally. The results are compared with those predicted by the theories of Bragg and Williams, and Bethe and Peierls, and it is shown that the latter theory gives the best approximation. From an examination of the behaviour of the alloy in certain metastable states, it has been deduced that the energy of any atom

is fixed only by the identity of its neighbours within two atomic distances. Consequently a large proportion of the energy of the ordering process is released by the time the regions of consistent order attain a length of  $5 \times 10^{-7}$  cm.

The electrical resistance of the alloy, on the other hand, starts to diminish when the ordered regions are about  $5 \times 10^{-7}$  cm. long, and has not reached the equilibrium value even when these regions are  $3 \times 10^{-6}$  cm. long.

---



is fixed only by the identity of its neighbours within two atomic distances. Consequently a large proportion of the energy of the ordering process is released by the time the regions of consistent order attain a length of  $5 \times 10^{-7}$  cm.

The electrical resistance of the alloy, on the other hand, starts to diminish when the ordered regions are about  $5 \times 10^{-7}$  cm. long, and has not reached the equilibrium value even when these regions are  $3 \times 10^{-6}$  cm. long.

---

## Some Influences of Dilution on the Explosive Combustion of Hydrocarbons

By WILLIAM A. BONE, F.R.S., and L. E. OUTRIDGE, Ph.D.

(Received 23 May, 1936)

[PLATES 4, 5, 6]

At the Bakerian Lecture of 1932,\* experiments were shown for the purpose of demonstrating (1) that on exploding either ethylene or acetylene with its own volume of oxygen there is neither the slightest separation of carbon nor appreciable condensation of steam on cooling, the end products being in accordance with the empirical equations:—



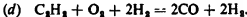
and



respectively; and (2) that the end result is unaffected by considerable dilutions of the media with hydrogen, e.g., as in the following cases,



and



A year later, in experiments made during a lecture to the Chemical Society at the Royal Institution† for the purpose of showing how little (if any) the last-named result (d) is affected by dilution with an inert gas (He, Ar, or N<sub>2</sub>), it was noticed that, while the colour of the explosion flame varied with the diluent and there was neither carbon separation nor any visible steam condensation during a helium- or argon-diluted explosion (*i.e.*, of C<sub>2</sub>H<sub>2</sub> + O<sub>2</sub> + 2H<sub>2</sub> + 4He or Ar), both were just discernible during a nitrogen-diluted explosion (*i.e.*, of C<sub>2</sub>H<sub>2</sub> + O<sub>2</sub> + 2H<sub>2</sub> + 4N<sub>2</sub>), a result indicating, as had been previously mentioned in a paper by Bone, Fraser, and Lake,‡ that the course of events might be "slightly affected by nitrogen", the matter being reserved for further investigation.

The possible significance of such observations in regard to the explosive combustion of hydrocarbons induced us to study systematically how explosions of equimolecular mixtures of ethylene or acetylene and oxygen

\* 'Proc. Roy. Soc.,' A, vol. 137, p. 243 (1932).

† 'J. Chem. Soc.,' p. 1599 (1933).

‡ 'Proc. Roy. Soc.,' A, vol. 131, p. 11 (1931).

may be affected by progressive dilutions with helium, argon, and nitrogen, respectively, and in the present paper are summarized the results of our further experiments in such direction.

## EXPERIMENTAL

### 1—CHEMICAL INVESTIGATIONS

**Procedure**—The experimental mixtures  $C_2H_4 + O_2 + xR$  or  $C_3H_8 + O_2 + xR$  (where R = He, Ar, or N<sub>2</sub>) were all accurately made up in glass holders over mercury from their highly purified constituents, and were subsequently exploded at some convenient initial pressure, e.g., between *circa* 130 mm. for an undiluted and 760 mm for a well-diluted medium, in a sealed cylindrical bulb of 'red-line' Jena glass of about 100 cc. capacity fitted with capillary ends and platinum electrodes (fig. 1). In each case the mixture fired was "moist", i.e., just saturated with water vapour at the room temperature. Special precautions were always taken to ensure both the initial firing pressure ( $p_1$ ) and the final pressure of the cold end-products ( $p_2$ ) at the room temperature being accurately ascertained, and in each case both the original mixture and the end gaseous products were fully analysed. Careful notes were always made of the colour of the explosion flame, or of any discernible separation of carbon or condensation of steam during the cooling period.

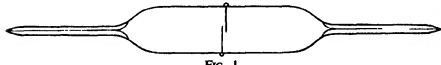


FIG. 1.

In the tabulated results, the initial and final pressures ( $p_1$  and  $p_2$ ) are always expressed in terms of the *dry* media at the initial firing- (i.e., room-) temperature, adjustment having been made for any slight temperature change between the instant of firing and the final pressure-reading of the cold products. From the combined pressure and analytical results, C—H<sub>2</sub>—O<sub>2</sub> "balances" were drawn up from which the proportionate amount of any carbon-deposition and/or steam-condensation during or after each explosion could be ascertained. To assist in the interpretation of results, the main experiments were supplemented by photographic and spectrographic investigations of the explosion flames.

**General Results**—The analytical results of the main series of experiments, as summarized in Tables I and II for acetylene- and ethylene-

mixtures, respectively, show that while in each case up to a certain limit "dilution" had no appreciable influence on the course of events during explosions of  $C_2H_2 + O_2$  or  $C_2H_4 + O_2$  media, beyond it there was a progressive tendency to cause both carbon deposition and formation of steam, such being much more marked in  $C_2H_4 + O_2$  than in  $C_2H_2 + O_2$  explosions, and with nitrogen than with either argon or helium as diluents.

Except where incipient or actual carbon deposition intervened, the explosion flames were blue, and the eye could detect no change in the appearance of the explosion vessel either during or after the cooling period. Incipient carbon-deposition was always heralded by a whitish tinge in the flame, and (maybe) by a slight "mistiness" afterwards, and any pronounced carbon-deposition was marked by a yellowish smoky flame. The surest criterion of any appreciable  $H_2O$ -formation during an explosion was a  $CO_2$ -content exceeding 1% in the final gaseous products, because of the operation of the secondary reversible  $CO + OH \rightleftharpoons CO_2 + H_2$  reaction during the cooling period. Also, it would be indicated by an observed  $p_2/p_1$  ratio below that calculated for the hydrocarbon being burnt to  $CO$  and  $H_2$  only, after allowing for any small  $CH_4$ -formation during the explosion.

(1)  $C_2H_2 + O_2 + xR$  Explosions (Table I)—With Ar or He as diluent, the limit of inflammability at atmospheric pressure was reached with  $x$  slightly over 7.5. Thus with He as diluent, the medium exploded when  $x = 7.7$  but not when  $x = 8$ , and not the slightest sign of any carbon-deposition or  $H_2O$ -formation could be detected until  $x$  exceeded 7.5, nor with Ar-diluted media until it approached that ratio. Hence in neither case had the dilution any appreciable effect upon carbon-deposition or  $H_2O$ -formation until near the limit of inflammability.

With nitrogen as diluent, however, incipient C-deposition and  $H_2O$ -condensation were observable with  $x$  slightly greater than 4.0. For while when  $x = 3.96$  neither was detectable, with  $x = 4.7$  both were in evidence and progressively increased on further dilution. Hence while neither carbon-deposition nor  $H_2O$ -formation was detectable during the explosion of an undiluted  $C_2H_2 + O_2$  mixture, or even during that of the corresponding air-mixture (*i.e.*, of  $C_2H_2 + O_2 + 3.77 N_2$ ), a little further dilution of the medium sufficed to bring both in evidence, though even at extreme dilution the principal reaction still remained



Moreover, except at extreme  $N_2$ -dilutions, where a trace of aldehyde could be detected, no appreciable aldehyde, cyanide, or nitrite was present in the cold explosion products.

TABLE I— $C_3H_8 + O_2 + x(H_2, Ar, or N_2)$  EXPLOSIONS

$x$	% composition before explosion			% composition of gaseous products						% unaccounted for in gaseous products			Visual observations regarding			
	$C_3H_8$	$O_2$	Dil.	$P_i$ mm.	$P_i$ Obs.	$P_i/P_i$ *Calc.	$CO_2$	$CO$	$H_2$	$C_3H_8\ddagger$	$CH_4$	Dil.	$C$	$H_2$	$O_2$	Flame colour C and/or $H_2O$ formed
<b>Unfilled medium</b>																
0	50.0	50.0	—	332	508	1.44	1.48	0.75	67.1	30.6	—	1.55	—	—	None	
0	50.0	50.0	—	331	487	1.47	1.48	1.05	66.15	31.1	—	1.7	—	—	Blue	
<b><math>x = \text{helium}</math></b>																
4.2	16.0	16.1	67.9	474	544	1.15	1.154	0.9	26.5	12.9	0.1	0.55	58.9	—	None	
6.4	11.9	12.0	76.1	728	797	1.095	1.110	0.7	19.9	9.15	0.1	0.7	69.25	—	Blue	
7.5	10.4	10.5	79.1	741.5	803	1.082	1.100	0.4	17.9	8.2	0.2	0.5	72.9	—	None	
7.7†	10.35	10.4	79.25	742.5	790.5	1.104	1.095	1.0	16.5	7.2	0.2	0.8	74.2	3.9	Whiteash	
<b><math>x = \text{argon}</math></b>																
4.2	16.1	16.2	67.7	480.1	548	1.14	1.152	0.5	26.6	12.6	0.1	0.75	59.25	—	None	
6.7†	11.6	11.5	76.9	731.3	804	1.10	1.112	0.45	19.8	9.4	0.1	0.5	69.65	—	Blue	
7.5	10.4	10.4	79.2	730.2	761	1.04	1.104	1.1	15.9	6.7	0.1	0.4	75.6	12	Yellowish	
<b><math>x = \text{nitrogen}</math></b>																
3.2	19.2	19.3	61.5	418.6	475.3	1.14	1.186	0.4	30.8	13.0	0.4	1.3	54.0	—	Blue	
4.0†	16.8	16.7	66.5	513.0	581.3	1.13	1.163	—	26.0	11.3	0.25	—	60.25	—	Mist	
4.7	14.85	14.65	70.8	518.0	555.0	1.07	1.140	0.35	23.6	9.05	—	0.3	66.0	11	Yellowish	
5.8	12.8	13.1	74.1	609.8	642.1	1.05	1.120	0.6	20.7	7.7	0.2	0.35	69.6	11	Both	
6.8	11.4	11.4	77.2	734.5	734.0	0.998	1.110	1.8	13.3	4.15	1.0	0.3	78.2	24	Yellow	

\* Calculated on the basis of the hydrocarbon having burnt thus,  $C_3H_8 + O_2 + xR = 2CO + H_2 + xR$ , without either carbon deposition or water formation, but allowing for any small methane formation during explosion.

† Indicates a dilution beyond which carbon deposition and water formation became visually evident.

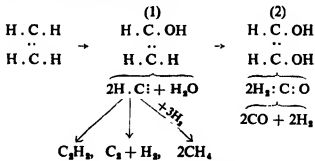
‡ In this and subsequent Tables  $C_3H_8$  = unsaturated hydrocarbons.

(2)  $C_2H_4 + O_2 + xR$  Explosions (Table II)—While neither carbon deposition nor  $H_2O$ -formation was observable with an undiluted  $C_2H_4 + O_2$  medium, both became *slightly* evident when  $xR = 1$  He, or Ar, or  $0.5 N_2$ . But whereas even when  $xR = 3$  (He or Ar) such effect remained slight, with nitrogen-dilution beyond  $x = 2$  it sufficed to produce a yellow smoky flame, although the reaction  $C_2H_4 + O_2 = 2CO + 2H_2$ , still greatly predominated. It should be noted also that a  $C_2H_4 + O_2 + 4N_2$  mixture was found not to explode at atmospheric pressure, and that neither aldehyde, cyanide, nor nitrite could be detected in the cold products.

(3)  $C_2H_2 + O_2 + xH_2$  and  $C_2H_4 + O_2 + xH_2$  Explosions (Table III)—At this point it is important to compare the foregoing results with those of similar experiments upon hydrogen-diluted  $C_2H_2 + O_2$  and  $C_2H_4 + O_2$  media. Accordingly in Table III are summarized the results of experiments with such mixtures. It will be seen that while dilution of a  $C_2H_2 + O_2$  medium with even as much as  $4H_2$  did not cause any appreciable carbon-deposition or  $H_2O$ -formation on explosion, progressive dilution of a  $C_2H_4 + O_2$  medium with hydrogen soon resulted in some  $H_2O$ -formation on explosion without any perceptible carbon-deposition.

Comparing now the  $C_2H_4 + O_2 + xH_2$  with the corresponding  $C_2H_4 + O_2 + xN_2$  explosions, it will be seen how effective was the substitution of hydrogen for nitrogen in suppressing any carbon-deposition without, however, much increasing the percentage of oxygen appearing as steam in the final products.

According to the hydroxylation theory, the explosive combustion of ethylene may be represented as involving:—



Now as on exploding an undiluted equimolecular  $C_2H_4 + O_2$  mixture there is a "non-stop" run through (1) to (2), without any appreciable thermal decomposition occurring at (1), progressive dilutions of the medium with hydrogen should have two distinct effects on its explosion.

TABLE II— $C_4H_4 + O_2 + x(H_2, Ar \text{ or } N_2)$  EXPLOSIONS

$x$	% composition of medium before explosion	$p_1$ mm.	$p_2$ mm.	% composition of gaseous products				Dil.	% unaccounted for in gaseous products	Visual observations regarding	
				Obs.	*Calc.	$CO_2$	$H_2$			Flame colour	C and/or $H_2O$ formed
$C_4H_4 \quad O_2 \quad$ Dil. Undiluted medium											
0	50.0	50.0	—	280.3	546.5	1.95	1.96	0.45	50.0	47.55	2.0
				545.3	1053	1.93	1.96	0.3	50.0	48.0	1.7
$x = \text{helium}$											
1.0	33.3	32.8	33.9	460.3	724.5	1.57	1.62	0.7	37.0	34.5	0.65
†	19.9	19.9	60.2	736.5	886.0	1.204	1.38	1.85	23.4	20.4	1.7
3.0	19.9	19.4	60.7	710.2	845.0	1.19	1.393	2.0	22.9	18.75	1.85
$x = \text{argon}$											
1.0	34.0	33.8	32.2	472.0	742.5	1.57	1.658	1.05	38.5	36.9	0.7
†	19.9	19.4	60.7	710.2	845.0	1.19	1.393	2.0	22.9	18.75	1.85
$x = \text{nitrogen}$											
0.5	39.9	39.7	20.4	510.5	843.5	1.65	1.764	0.6	43.5	40.6	0.6
0.75	36.3	36.0	27.7	604.7	960.0	1.59	1.698	0.6	41.0	39.2	0.7
1.0†	34.2	31.7	31.7	728.0	1092	1.50	1.648	0.8	39.3	34.9	0.8
2.2	23.5	23.4	53.1	582.0	671.0	1.15	1.437	3.95	23.8	20.9	2.25
2.9	20.4	20.3	59.3	733.0	809.7	1.05	1.375	3.20	20.9	16.05	2.0

\* Calculated on the basis of the hydrocarbon having been burnt thus,  $C_4H_4 + O_2 + xR = 2CO + 2H_2 + xR$ , without either carbon deposition or water formation, but after allowing for any small methane formation.

† Indicates the dilution beyond which carbon deposition and water formation become visually evident.

TABLE III— $C_4H_8 + O_2 + xH_2$  AND  $C_4H_4 + O_2 + xH_2$  EXPLOSIONS

Medium	% composition of medium before explosion			$\frac{P_2}{P_1}$			% composition of gaseous products			% unaccounted for in gaseous products			Visual observations regarding			
	$C_4H_8$ or $C_4H_4$	$O_2$	$H_2$	mm.	min.	Obs. *Calc.	$CO_2$	$CO$	$C_4H_8$	$CH_4$	$H_2$	$C$	$H_2$	$O_2$	Flame colour	$C$ and/or $H_2O$ formed
$C_4H_8 + O_2 + 2H_2$	25.0	50.0	50.0	534.5	653.6	1.22	1.248	0.2	39.8	—	0.2	59.8	—	None	Blue	None
$C_4H_8 + O_2 + 4H_2$	16.15	16.05	67.8	753.0	850.0	1.13	1.144	0.2	28.1	—	1.5	70.2	—	None	Blue	None
$C_2H_4 + O_2 + H_2$	33.45	32.65	628.2	927.8	1.476	1.610	0.65	38.95	1.3	3.9	55.2	Nil	5.7	11	No C	
$C_2H_4 + O_2 + 2H_2$	25.0	23.0	50.0	385.0	737.0	1.259	1.44	0.8	31.3	1.4	3.9	61.6	1.7	9	14	Some $H_2O$
$C_2H_4 + O_2 + 3H_2$	20.1	19.8	60.1	717.8	783.5	1.092	1.323	1.5	23.8	3.3	5.5	65.7	Nil	10.8	25	

\* Calculated on the basis of the hydrocarbon having been burnt thus,  $C_4H_8 + O_2 = 2CO + \frac{H_2}{2} + xH_2$ , without carbon deposition or water formation, but after allowing for any small methane formation during explosion.

By participating more and more, in proportion to its active mass, in the initial oxygen-distribution, the hydrogen should (a) prevent some of the hydrocarbon being oxidized to the di-hydroxy stage, and thus bring about some C-deposition and H<sub>2</sub>O-formation by thermal decomposition at the mono-hydroxy stage, and (b) hydrogenize the :CH residues so produced, and so counteract or even altogether suppress carbon-deposition. And such indeed is what actually happened.

The potency of hydrogen-dilution in thus suppressing carbon-deposition in such hydrocarbon explosions is well illustrated by the results of a series of C<sub>2</sub>H<sub>4</sub> + O<sub>2</sub> + xH<sub>2</sub> explosions under pressure in which, while the partial pressure of the ethylene was kept constant at 10 atm., that of the hydrogen was increased in successive stages from 10 to about 40 atm. In no case was there any carbon deposition or acetylene formation; and from Table IV, in which P<sub>i</sub> = the initial pressure of the explosive medium, and P<sub>f</sub>, the final pressure of the cold gaseous products (in each case corrected for deviations from Boyle's Law) it will be seen that while increasing excess of hydrogen participated progressively in the oxygen-distribution, it also prevented any carbon-deposition by converting :CH residues into methane.

TABLE IV—C<sub>2</sub>H<sub>4</sub> + O<sub>2</sub> + xH<sub>2</sub> EXPLOSIONS

X in C <sub>2</sub> H <sub>4</sub> + O <sub>2</sub> + X H <sub>2</sub>	2	4	6	8
P <sub>i</sub> atm. .... . . . .	20.84	26.00	40.67	49.0
P <sub>f</sub> atm. .... . . . .	29.41	29.43	46.20	45.0
P <sub>f</sub> /P <sub>i</sub> .... . . . .	1.41	1.132	1.135	0.918
% of—				
(i) Original carbon as CH <sub>4</sub> .... . . . .	7.65	22.4	26.9	43.5
(ii) Original O <sub>2</sub> as H <sub>2</sub> O .... . . . .	5	18	34	40

(4) C<sub>2</sub>H<sub>4</sub> + 2N<sub>2</sub>O and C<sub>2</sub>H<sub>4</sub> + 2N<sub>2</sub>O + 2N<sub>2</sub> Explosions—By this time it was becoming evident that carbon-deposition and steam-formation during *diluted* C<sub>2</sub>H<sub>4</sub> + O<sub>2</sub> + xR and C<sub>2</sub>H<sub>4</sub> + O<sub>2</sub> + xR explosions are probably connected with the mean maximum flame temperature. For on calculating the latter, on certain reasonable assumptions regarding specific heats of products and the effects of radiation, dissociation, etc., it appeared that both the features referred to first became perceptible when dilution had depressed the flame-temperature below a certain point somewhere between 1500 and 1900°, according as combustion may be deemed to have occurred under "constant pressure" or "constant volume" con-

ditions (or, as would appear more likely, intermediately\*), and that they both increased *pari passu* with further reduction thereof.

Thus, for example, if for comparative purposes an arbitrary temperature scale 10 to 30 be constructed such that each division is equivalent to some near fraction or multiple of 100°, according to the degree of approximation of the underlying assumptions to actuality, and if the calculated mean maximum temperatures attained in the explosions are set out thereon, as in fig. 2, it would be found that the points at which progressive dilution of either the  $C_2H_2 + O_2$  or the  $C_2H_4 + O_2$  medium caused perceptible carbon-deposition or  $H_2O$ -formation during the various explosions, as indicated by an asterisk in each case, would all fall between 18 and 21, thus:—

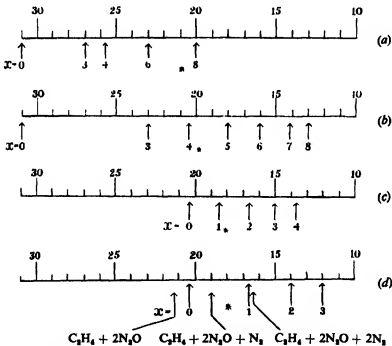


FIG. 2.—Temperature scale: (a)  $C_2H_2 + O_2 + x$  (Ar or He); (b)  $C_2H_2 + O_2 + xN_2$ ; (c)  $C_2H_4 + O_2 + x$  (Ar or He); (d)  $C_2H_4 + O_2 + xN_2$ .

This being so, further calculation showed that whereas the mean temperature attained in a  $C_2H_4 + 2N_2O$  explosion would be just over 20, that

\* Although the actual point cannot be calculated, because of its depending on certain unverifiable assumptions, it must lie somewhere between the limits indicated, and probably nearer the higher than the lower, because of the combustion probably occurring more under "constant volume" than "constant pressure" conditions.

in a  $C_2H_4 + 2N_2O + 2N_2$ , would fall well below 17, on the scale. Hence, if flame-temperature is the chief factor, it might be predicted that whereas neither carbon-deposition nor  $H_2O$ -formation would be perceptible in the former, both would be observable in the latter explosion. And on putting the matter to an experimental test, such prediction was fulfilled, as will be seen from the results recorded in Table V. For whereas the former explosion yielded substantially carbonic oxide, hydrogen, and nitrogen only, in accordance with the equation:—



the latter yielded also material proportions of both carbon and steam. Hence it would appear that the chief factor in causing or promoting carbon-deposition or  $H_2O$ -formation in such explosions is a lowering of the flame temperature by the diluent present.

## 2—PHOTOGRAPHIC AND SPECTROGRAPHIC EXPERIMENTS

(1)—*Flame Speeds and Photographs*—By means of a revolving drum camera, photographs were taken on a vertically moving film of explosion flames traversing horizontally some of the moist experimental mixtures in a closed cylindrical tube of Jena glass, 34 cm. long and 2·5 cm. in diameter, after ignition by a condenser spark passed between platinum electrodes situated midway along the tube (fig. 3).

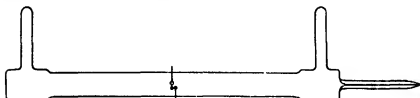


FIG. 3.

Although, owing to the feebleness of their luminosities, difficulty was experienced in obtaining good photographs of some of the more diluted explosion flames, more especially with argon as the diluent, sufficiently readable records resulted to enable conclusions being drawn as to the relative speeds and other features of the flames. Again, owing to the violence of the undiluted, and the feeble luminosities of the most diluted, explosions, it was not possible to obtain  $C_2H_2 + O_2 + xR$  flame-photographs all at the same pressure; seeing, however, that the relative flame-speeds are not greatly affected by considerable pressure changes,

this would scarcely invalidate the general conclusion. On the other hand, the moist  $C_2H_4 + O_2 + xR$  mixtures were all fired at just below atmospheric pressure.

The flame-speeds and total durations of luminosity (T.D.) deduced from the resulting photographs are shown in Table VI, and the flame-

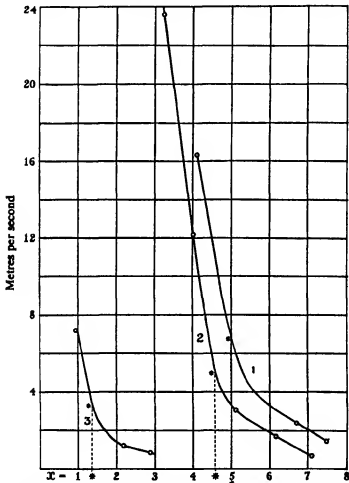


FIG. 4—Mean flame speeds: (1)  $C_2H_4 + O_2 + xAr$ ; (2)  $C_2H_4 + O_2 + xN_2$ ; (3)  $C_2H_4 + O_2 + xN_2$ .

speeds are plotted against "dilutions" in fig. 4. From the last named it will be observed that in each case there was a marked break in the flame-deceleration by dilution at a point, indicated by an asterisk, which other features of the photographs associated with incipient aggregated carbon-separation. Indeed, we incline to consider such break in each flame-

TABLE V— $C_4H_4 + 2N_2O + xN_2$  EXPLOSIONS

$x$	% composition of medium before explosions			$\frac{P_1}{P_0}$			$\frac{P_1}{P_0} / P_1$			% composition of gaseous products			% unaccounted for in gaseous products			Visual observations regarding				
	$C_4H_4$	$N_2O$	$N_2$	mm.	mm.	Obs.	Calc.	$CO_2$	$CO$	$H_2$	$C_2H_6$	$CH_4$	$N_2$	$C$	$H_2$	$O_2$	Flame	C and/or $H_2O$ formed	colour	Bright yellowish
Undiluted medium																				
0	31.2	68.8	—	589.4	1083	1.84	1.92	0.3	31.6	30.9	0.4	0.9	35.5	None						None
†																				
2	20.8	39.6	39.6	742.4	1058	1.425	1.608	1.4	22.1	19.0	0.3	1.0	55.95	14	26.5	9	Smoky	Both formed	yellow	

\* Calculated on the basis of the hydrocarbon having been burnt thus,  $C_4H_4 + 2N_2O + xN_2 = 2CO + 2H_2 + (x+2)N_2$ , without either carbon deposition or water formation, but after allowing for any small methane formation during explosion.

† Indicates the dilution beyond which carbon deposition and water formation become visually evident.

speed curve as probably a surer criterion of incipient aggregated carbon-separation during explosions than any purely chemical data.

Neither of the photographs of the undiluted  $C_3H_8 + O_2$  and  $C_2H_4 + O_2$  explosion flames\* showed any sign of solid carbon separation in the flame front, nor yet of carbon-steam reaction behind it. And the same applies also to those of the  $C_3H_8 + O_2 + 4\cdot1Ar$ , the  $C_3H_8 + O_2 + 3\cdot2N_2$ , and the  $C_2H_4 + O_2 + N_2$  explosions (figs. 5, 7, and 9, Plates 4, 5, respectively).

TABLE VI—MEAN FLAME SPEEDS AND TOTAL DURATIONS OF  
LUMINOSITY

Explosion	Initial pressure mm.	Mean flame speed		Total duration T.D. milliseconds
		Over 1st 5 cm. metres/sec.	Overall metres/sec.	
* $C_3H_8 + O_2$ . . . . .	370	333	585	—
$C_3H_8 + O_2 + 4\cdot1Ar$ . . . . .	572	19·2	16·3	20
$C_3H_8 + O_2 + 6\cdot7Ar$ . . . . .	747	4·1	2·35	113·5
† $C_3H_8 + O_2 + 7\cdot5Ar$ . . . . .	725	2·9	1·36	167·5
$C_3H_8 + O_2 + 3\cdot2N_2$ . . . . .	435	28·3	23·6	10·5
† $C_3H_8 + O_2 + 5\cdot1N_2$ . . . . .	540	7·0	3·0	80
$C_3H_8 + O_2 + 6\cdot2N_2$ . . . . .	624	4·0	1·8	137
$C_3H_8 + O_2 + 7\cdot1N_2$ . . . . .	733	1·1	0·7	331
* $C_2H_4 + O_2$ . . . . .	735	55	55	7·7
† $C_2H_4 + O_2 + N_2$ . . . . .	740	9·5	7·1	34·5
$C_2H_4 + O_2 + 2\cdot2N_2$ . . . . .	746	2·15	1·25	168·0
$C_2H_4 + O_2 + 2\cdot9N_2$ . . . . .	759	1·67	0·75	286

\* Already published, cf. Bone and Bell, 'Proc. Roy. Soc.,' A, vol. 144, p. 264 (1934).

† Indicates the dilution beyond which carbon deposition and water formation became visually evident.

But at higher dilutions than those indicated by the asterisk in fig. 4 there were always signs of a uniformly diffused carbon-separation, both in the flame front and behind it, progressively increasing with the dilution, as shown in the photographs reproduced in fig. 6, 8, 10, and 11, Plates 4, 5, which need no further comment.

\* These having been already published in 'Proc. Roy. Soc.,' A, vol. 131, p. 11 (1931), are not reproduced here.

**Spectrographic Evidence**—Spectrograms of  $C_2H_4 + O_2$ ,  $C_2H_4 + O_2 + \frac{1}{2}N_2$ , and  $C_2H_4 + O_2 + 3N_2$  explosion flames, respectively, were obtained by exploding from 30 to 36 litres of each mixture at atmospheric pressure in a cylindrical nickel-steel bomb (explosion chamber 1 metre long, 5 cm. diameter, capacity = 1 litre) fitted at one end with a quartz window, and at the other with a blank plug and firing piece. The spectrum of each explosion flame travelling towards the quartz window was recorded by means of a Hilger E2 quartz-spectrograph fitted with a Cornu prism, and having a dispersion of 20 Å. per mm. at 3110 Å. the image of the flame being focussed by means of a quartz lens on the slit of the spectrograph.

In considering the resulting spectrograms, it should be kept in mind that whereas neither chemical nor photographic tests had revealed any carbon-separation during either the  $C_2H_4 + O_2$  or the  $C_2H_4 + O_2 + \frac{1}{2}N_2$  explosions, it had been proved in the  $C_2H_4 + O_2 + 3N_2$  explosions.

(1) Although in a first series of experiments, in which "Ilford Special Rapid Panchromatic" plates, highly sensitive in the red region, were used, the resulting spectrograms (figs. 12, *a*, *b*, and *c*, Plate 6, in which an iron arc *e* is also included for reference purposes) showed well-marked  $C_2$ -bands at 5630, 6190, and 6500 Å. in the  $C_2H_4 + O_2$  and  $C_2H_4 + O_2 + \frac{1}{2}N_2$  explosion flames, and a continuous spectrum only, extending between 3800 Å. and 6600 Å., in the  $C_2H_4 + O_2 + 3N_2$  explosion flames, no HO—bands were observable in any of them. In (*b*) there was also a faint line at 4315 Å., scarcely visible in the reproduction, possibly attributable to an incipient —CH band. From all this it is clear that, whereas some  $C_2$ -emitters had been formed in the  $C_2H_4 + O_2$  and  $C_2H_4 + O_2 + \frac{1}{2}N_2$  explosions, no aggregated solid carbon particles had separated out until the dilution of the explosive medium had reached the  $C_2H_4 + O_2 + 3N_2$  ratio, thus confirming both the analytical and photographic evidence.

(2) In a further experiment with an undiluted  $C_2H_4 + O_2$  mixture, the flame-temperature of which would exceed 2000° C., where, if any steam were primarily formed on explosion, HO—bands should be discernible, "Ilford Zenith 650" plates, highly sensitive in the 2300 to 4300 Å. ultra-violet region, were employed. Yet although no fewer than 36 litres of the  $C_2H_4 + O_2$  mixture were exploded, no HO—bands appeared in the resulting spectrogram (*d*) which showed nothing more than the aforesaid line at 4315 Å., again possibly attributable to an incipient —CH band. Hence the spectrographic confirms the chemical evidence regarding the non-formation of steam during the primary oxidation involved in an undiluted  $C_2H_4 + O_2$  explosion.

### CONCLUSIONS

(1) From the combined chemical, photographic, and spectrographic evidence obtained during the investigation, it would appear that whereas there is neither H<sub>2</sub>O-formation nor aggregated carbon-separation during undiluted C<sub>2</sub>H<sub>2</sub> + O<sub>2</sub> or C<sub>2</sub>H<sub>4</sub> + O<sub>2</sub> explosions, progressive dilution of the media by an inert gas beyond a point at which the mean flame-temperature falls well below 2000° C. may induce both, the more so in C<sub>2</sub>H<sub>4</sub> + O<sub>2</sub> than in C<sub>2</sub>H<sub>2</sub> + O<sub>2</sub> explosions, and with nitrogen than with either argon or helium as diluent.

(2) Although there is no evidence of any primary H<sub>2</sub>O-formation, some "C<sub>2</sub>-emitters" are undoubtedly formed during an undiluted C<sub>2</sub>H<sub>4</sub> + O<sub>2</sub> explosion, but not in quantities sufficient to allow of any solid carbon-aggregation in the explosion flame, which indeed is only observable after considerable dilution of the medium with inert gas.

(3) Any carbon separation or steam formation discernible in a sufficiently diluted C<sub>2</sub>H<sub>2</sub> + O<sub>2</sub> or C<sub>2</sub>H<sub>4</sub> + O<sub>2</sub> explosion is a secondary effect probably induced by the mean flame temperature having been reduced to well below 2000°.

### SUMMARY

The paper deals with certain effects of dilution with inert gases (Ar, He, and N<sub>2</sub>) upon explosions of equimolecular mixtures of ethylene or acetylene and oxygen, i.e., C<sub>2</sub>H<sub>4</sub> + O<sub>2</sub> and C<sub>2</sub>H<sub>2</sub> + O<sub>2</sub> which normally give rise to carbonic oxide and hydrogen, without any separation of carbon or steam-formation, in accordance with the equations:—



and



It is now shown by chemical, photographic, and spectrographic tests that sufficient dilution of such media, while not much affecting the main result, may induce some secondary carbon deposition and steam-formation on explosion when the mean flame temperature is thereby reduced to a point well below 2000° C., such result being probably due to the fall in flame temperature induced by dilution.

---

$\text{C}_2\text{H}_2 + \text{O}_2 + x(\text{Ar or N}_2)$  explosions

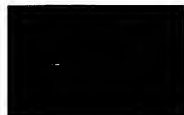


FIG. 5— $\text{C}_2\text{H}_2 + \text{O}_2 + 4$  Ar



FIG. 6— $\text{C}_2\text{H}_2 + \text{O}_2 + 6.7$  Ar

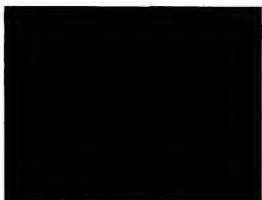


FIG. 7— $\text{C}_2\text{H}_2 + \text{O}_2 + 3.2$  N<sub>2</sub>



FIG. 8— $\text{C}_2\text{H}_2 + \text{O}_2 + 5.8$  N<sub>2</sub>

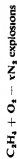


FIG. 10— $\text{C}_2\text{H}_2 + \text{O}_2 \rightarrow \text{vN}_2$

150

100

50

10



FIG. 11— $\text{C}_2\text{H}_2 + \text{O}_2 \rightarrow 2 \text{ N}_2$

200

msec



FIG. 9— $\text{C}_2\text{H}_2 + \text{O}_2 \rightarrow \text{O}_2 - 2 \text{ N}_2$

30

-

20

10

msec



Fig. 12.—Spectrograms of  $C_2H_4 - O_2 - N_2$  explosions

- (a) and (d)  $C_2H_4 - O_2$
- (b)  $C_2H_4 - O_2 - \frac{1}{2} N_2$
- (c)  $C_2H_4 + O_2 - 3 N_2$



## Optical and Physical Effects of High Explosives

By R. W. WOOD, For. Mem. R.S., Professor of Experimental Physics,  
Johns Hopkins University

(Received 25 June, 1936)

[PLATES 7 AND 8]

### I—PLASTIC FLOW OF METALS

My interest in the study of the effects produced by high explosives originated in the investigation of "evidence" in a number of murders by bomb, and more especially in connexion with a most unfortunate and unusual accident which resulted in the almost instant death of a young woman who, on opening the door of the house furnace to see if the fire was burning properly, was struck by a small particle of metal which flew out of the fire and penetrated the breast bone, slitting a large artery and causing death in 2 or 3 minutes from internal haemorrhage. The particle, which was not much larger than a pin-head, was submitted to me for identification, and though its form resembled nothing with which I was familiar, I surmised that it was probably a part of a dynamite-cap or "detonator" used for exploding the dynamite charges in the mines, which, by some carelessness on the part of a miner, had been delivered intact with the coal.

These detonators are spun from very thin sheet copper and consist of a tube about 5 mm. in diameter and 40 mm. in length. The head is formed into a shallow cup, as shown in cross-section in fig. 1, and the tube is charged with mercury fulminate and fired by an electrically heated wire. It seemed probable that the solid pellet of copper, recovered during the autopsy, had been formed in some way from the concave head of the detonator by the enormous instantaneous pressure developed by the detonation of the fulminate.

I accordingly suspended one about 2 feet above a large earthenware jar holding about five gallons of water, pointing the head downwards. On firing the detonator the jar was shattered into a dozen or more pieces by the pressure wave exerted in the water by the passage of the small copper fragment (the head of the detonator) entering the water with three times the velocity of a rifle bullet, just as a milk can filled with water is burst open when the bullet of a high powered rifle is fired through it. The minute fragment of copper which was found in the ruins of the jar matched perfectly the fragment found during the autopsy but bore

no resemblance to the original head of the detonator which is about the size of, and resembles closely the cap of, a shot-gun shell after it has been indented by the firing pin. It was a pear-shaped pellet of copper, surrounded at the middle by a skirt of thin copper of a diameter considerably less than that of the original head of the detonator. This looked interesting, and a study of exploding detonators was commenced with a view of finding out how the forces operate to mould this solid pellet.

A stereoscopic photograph, made with a low power binocular microscope, of one of these pellets is reproduced on fig. 4, Plate 7. This one was arrested by firing the head of the detonator along the axis of a cylindrical paste-board tube filled with cotton, diaphragmed with thin paper disks every two inches, the pellet being searched for in the cotton lying

between the last disk perforated and the next intact disk. As the pellet, which starts off with an initial velocity of about 6000 feet per second, penetrates the cotton it gathers a tightly wadded ball of cotton around it as it advances, spinning its own cocoon, so to speak, and is thus protected from friction against the matter through which it is passing.

A photograph of this wad of cotton, protruding through the paper disk, is reproduced on fig. 5, Plate 7, with one of the copper pellets lying on its



FIG. 1.

summit to show the comparative size. The neck of the pear-shaped pellet was in part covered with the thin film of red lacquer, which had originally covered the exterior of the detonator, proving that the base of the pear had formed itself on the *inside*. My first theory was that the cup-shaped hollow had been squeezed around, forming a hollow ball, but the pellet was found to be solid by slow solution in nitric acid with frequent examinations. Further examination of the pellets indicated that the base of the pear had been built up by a plastic flow of the surface layers of metal on the inside of the detonator, the radial lines of flow on the inside of the skirt being closely visible with the microscope, which showed also that the thickness of the skirt was much less than that of the original shell of the detonator. It was less easy to see how the neck of the "pear" had been formed, since it had been pushed out forwards at the centre of the head of the detonator where the cup-shaped cavity was deepest. In some cases the neck of the "pear" tapered to a sharp point as shown at *a* in fig. 8, Plate 7, in which case the neck and skirt had been

bent sharply downwards, probably by some small obstruction in the cotton (a shred of copper, perhaps, from a previous shot). The base of the pear, formed by plastic flow, is marked *b* in this figure. I formed the hypothesis that the formation took place as follows: the horizontal components of the pressure (normal pressure indicated by arrows in fig. 1) caused a radial contraction of the cup as it flattened out, resulting in an extrusion at the centre on both the inside and outside as shown at *b*, fig. 1. Piled up on this came the plastic flow on the inside, which gradually covered up the extruded knob at the centre, as shown by *c*, *d*, and *e*. This hypothesis was proved by experiment as follows.

Through the courtesy of Dr. W. E. Lawson of the Du Pont Experiment Station, detonators were prepared with reduced charges of varying amount. In this way I obtained pellets in the various stages of formation shown in fig. 1. A stereoscopic photograph of the stage shown at *c*, fig. 1, is reproduced in fig. 6, Plate 7, in which the plastic flow has about half covered the central extrusion.

The radial contraction was proved as follows. I had a number of detonators prepared with circular grooves engraved on the head, as shown in fig. 9, Plate 7. With a light charge of fulminate the fragment shown in fig. 10, Plate 7, was recovered showing a marked contraction of the rings. A heavier charge gave the fragment shown by fig. 11, Plate 7. Here the extruded neck of the pellet appears at the centre, its height being indicated by the length of the shadow, while the inner ring has contracted to half its original diameter, and is wrapped closely around the base of the "peak".

So far as I have been able to find, from conversations with the technical staff of four large Explosive factories, the formation of the solid pellet of copper has not been noticed, and this transformation is the probable explanation of why the dent in the head of the detonator increases its efficiency, as was found by the increased penetration in the lead plate test, which has been generally accepted as the test of efficiency. So far as I have been able to find, no comparison test between dented- and flat-headed detonators has been made, in regard to their ability completely to detonate a dynamite stick. The deeper penetration of the lead is due obviously to the impact of a solid copper projectile instead of a thin disk of sheet copper.

Detonators were fired from various distances against various obstacles, and it was found that the pellet of soft copper penetrated a block of steel to a depth of  $\frac{1}{2}$  in. Fired against a sheet of paper it was shown that the solid pellet was accompanied by some 60 or 70 smaller fragments all travelling in the same general direction, each one of which moving with

such a velocity that its impact on a brass block caused a "crater" with a raised rim, as though the metal had actually been melted by the heat generated by the impact. Subsequent experiments showed, however, that we are probably dealing with a plastic flow of the metal under a high instantaneous pressure.\*

In lateral directions the shower was made up of some 800 minute copper fragments, as was shown by surrounding the detonator with a large paper cylinder. Each one of these was capable of producing a "nick" on a glass surface, while the larger fragments caused white spots half an inch in diameter made up of hundreds of intersecting cracks which extended half-way through the sheet of plate glass, which had been mounted at a distance of two feet from the detonator to protect the lens of the camera used in photographing the flash of the explosion.

Fired against a brass block, the "crater" made by the pellet of copper was much larger than the pellet and about one-quarter of an inch in depth, and the walls were smooth and highly polished. Around the rim of the crater were three concentric circular ridges of raised metal (fig. 7, Plate 7), the wave pattern resembling the one described by Dr. Charles E. Monroe in 1888 for a gun-cotton cylinder exploded under water on a block of steel.

In his case there were some six or eight concentric ripples in the steel around the edge of the circular depression made in the metal by the exploding cylinder. Dr. Monroe was unable to account for the formation of these ripples, and no explanation has ever been offered so far as I know. In one case the pellet was found attached to the brass block, one side of the "skirt" quite firmly welded to the brass with the "pear" lying within the crater. On prying off the "skirt" concentric ripple marks were found on both surfaces, those on the copper being casts of the ones on the brass. In the photograph, fig. 7, they appear only on one side, and frequently they are not present at all. It appears to me that they form only at the interface between the two metals where they are pressed together by the force of the detonation.

Surrounding the main crater were many small craterlets made by minute shreds of copper, each one resembling the mark left by throwing a small pebble into very soft mud, one of which appears at the bottom of fig. 7. The metal appears to flow like a liquid under the terrific impact, without having its temperature raised to the fusion point. Another detonator was fired against a large flat file of hard steel and the copper pellet penetrated to a depth of  $\frac{1}{16}$  in. breaking the file in two. Fired

\* No trace of luminosity was seen or photographed at the point of impact of the pellet on a brass block.

against an old telephone directory, the pellet from a mercury fulminate detonator penetrated 500 pages, while two superposed directories were required to stop one from a detonator charged with lead azide and tetryl, the pellet going through 1200 pages.

## II—THE SECONDARY FLASH OF DETONATION

One of the most astonishing effects exhibited by all high explosives is the enormous velocity with which the reaction which we call "detonation" is propagated, over four miles per second for the case of nitroglycerine in a glass tube.

Experiments on the velocity of detonation were made in this country by Perrot and Gauthrop,\* photographs being taken of the flash of the detonation of bars of explosives on a photographic film in rapid motion. The velocity of detonation was deduced from the obliquity of the image on the film. One interesting effect noted was the increased luminosity of the flash at the centre of the bar when the explosion was started simultaneously at both ends. More accurate results were obtained in the following year in England with an improved apparatus by E. Jones,† who published in the Proceedings of the Royal Society a remarkable set of photographs obtained by detonating long cylinders of various high explosives behind a very narrow slit in a steel plate, reinforced by a backing of armour plates in step-wise formation. The duration of the actual "flash" of detonation was extremely brief, of the order of 1/400,000 of a second, but the most remarkable effect was the apparent circumstance that after the first brief flash there was a period of darkness, followed by a second much brighter flash of much longer duration. This secondary flash was usually recorded as three flashes occurring in rapid succession and the photographs indicated that it was formed by gaseous products of the detonation which had passed through the narrow slit and impinged on the steps of the armour plate which were three in number.

More recently Payman and Woodhead photographed the explosion of detonators, taken by the "Schlieren-methode"‡ of Töpler, in which instantaneous photographs are taken, by the flash of an electric spark, of the flying debris, expanding gases, and the sound waves which accompany the larger particles of copper, similar in form to that of the waves accompanying bullets in flight, or the bow wave of a rapidly moving ship. From the angle made by the two branches of the wave generated by the "head" of the detonator, they calculated that its velocity varied from

\* *J. Franklin Inst.*, vol. 203, pp. 103, 387 (1927).

† *Proc. Roy. Soc., A*, vol. 120, p. 603 (1928).

‡ *Proc. Roy. Soc., A*, vol. 132, p. 200 (1931).

3000 to 6000 feet per second, depending on the nature of the explosive.

Other observations of the secondary flash have been recorded; for example, a very brilliant burst of luminosity half-way between two parallel cylinders of high explosive detonated simultaneously, and a brilliant flash on the surface of a metal plate facing the muzzle of a steel tube at the centre of which a detonator was exploded.

The cause of this secondary flash is somewhat obscure, various theories having been advanced such as heat of compression, dust in the air, undecomposed portions of the explosive projected against the obstacle, etc.

It seemed probable that some light might be thrown on the phenomenon by a spectroscopic study of the primary flash of detonation and the secondary flash which followed it.

Experiments were commenced with fulminate of mercury, placed at my disposal through the kindness of Dr. Lawson. This substance, like most high explosives, can disintegrate in two quite different ways. Ignited in the open air, if the quantity is not too large, it goes off in a flash of yellow flame making no sound save a dull "thud". This type of explosion is called deflagration. If, however, the substance is confined, "detonation" occurs as soon as the pressure reaches a certain critical value, and we have a shattering explosion which pulverizes everything in its vicinity. Placed in a vacuum tube and heated well above the ignition temperature, nothing happens save a slow decomposition unattended by either light or noise. Lead azide, however, detonates readily in a vacuum tube, shattering the glass in its immediate vicinity, but not breaking the rest of the tube, a phenomenon which dispels the old idea that the so-called "downward" effect of high explosives was due to the fact that the atmosphere acted as "tamping". Photographs made of exploding fulminate of mercury detonators showed that little light was emitted during detonation in comparison to the brilliant flash of deflagration, but it seemed possible that the flash was over before the copper tube gave way, and as a suitable source of the light of *detonating* fulminate was required. For the spectroscopic work the material was packed in a thick-walled capillary glass tube (7 mm. diameter, 1 mm. bore) closed at the bottom and fired at the top by an electrically heated wire. A photograph of the explosion showed that detonation commenced at a distance of about 6 mm. from the top of the tube, the material near the open end deflagrating. This is clear from fig. 18, Plate 8. The extensive and very brilliant flash above the tube is due to the deflagration of the comparatively small amount of fulminate in the first few millimetres of the tube. The remainder of the tube is seen to be filled with light and the thick walls are in the act of breaking up, for they are traversed by fine cracks.

It is evident that the intensity of the light given out when detonation occurs is very much less than for deflagration; this circumstance was more clearly evident in a photograph of an exploding detonator in which case the amount of material is perhaps twenty times as great as that in the glass tube. The photograph showed only a very feeble luminosity of the products of the detonation, though of course the luminosity of the material before the copper shell burst was undoubtedly greater.

As it seemed possible that the luminosity in the glass tube might have been due to the reflexion, from the cracks, of the light of the deflagrating material at the top, imprisoned within the glass by total internal reflexion, a tube was prepared with the top and upper half painted with black shellac.

No difference appeared in the photograph of the detonation except that the upper portion of the tube was not recorded. It is to be noticed that, in the glass tube, no luminosity appeared outside of the wall, which shows that the radiation of light is practically over by the time the pulverization of the tube is complete.

The very uneven distribution of the luminosity of the detonating fulminate appeared to be due to the opacity of totally reflecting cracks in the glass wall of the tube, but to make sure of this I prepared a tube in such a way that a cylinder of fulminate in air could be detonated. A capillary tube open at both ends was filled to a depth of 1 cm. with fulminate crystals, rammed down lightly with a thin glass rod, the bottom being temporarily closed with the finger. A drop of water containing a trace of gelatine (hardly enough to cause it to "jel" when cold) was applied to the bottom of the tube, and renewed until the fulminate was completely moistened. The glass rod was then pushed down until an 8 mm. rod of wet fulminate had been extruded. The tube was then placed over a steam radiator for an hour to dry. It was then filled to the top with dry fulminate rammed down as before. A very remarkable phenomenon appeared in the photograph made when the tube, supported by a stiff wire over a glass plate 15 mm. below the end of the cylinder, was fired by an electrically heated wire at the top. The protruding cylinder was sharply outlined by the light of its detonation, and faint wisps of luminosity were seen projecting from it. Immediately below the cylinder, resting on the plate, there appeared a self-luminous phantom in the form of an urn or vase with a very brilliant cover. It was supported on a nebulous patch of luminosity but was itself as sharply outlined as if made of glass. It was repeatedly obtained, the ratio of its height to its diameter depending on the distance between the plate and the end of the fulminate cylinder: as the latter was diminished the vase flattened finally becoming

more like a saucer. Fig. 13, Plate 8, is a reproduction of an especially good photograph of the phenomenon, and the one which finally gave me the explanation of the apparent "cover" of the vase, which here is clearly seen to be the rim of the urn turned over into what appears to be a vortex ring, which seen edge-on appears more luminous than the rest of the structure.

The structure of the urn, as it appears in the print, is as shown by fig. 2, though the vortex may not come out clearly in the reproduction. That such a sharply outlined structure of luminous gas could form and record itself photographically *by its own light* in the commotion of a shattering explosion seems very surprising. If there was no protruding cylinder of fulminate, no trace of the urn appeared, only a shallow pool of luminosity on the plate. With a cylinder of greater length the turned-over rim appeared fragmented, as shown by fig. 15, Plate 8. A short cylinder of fulminate, prepared as before described by pushing it out of a tube, was supported by a fine wire (attached by a droplet of glue) immediately above the plate. This was to ascertain whether the production of the urn required the detonation of the glass tube in addition to that of the protruding cylinder. Since the electrically heated wire would merely deflagrate the fulminate under these conditions, the cylinder was capped



FIG. 2.

with a small drop of lead azide made into a soft paste with water. The wire was brought into contact with the azide which was dried rapidly by hot air rising from a lamp bulb placed below it. The room was then darkened, the camera lens opened, and the cylinder fired. The photograph, reproduced in fig. 16, Plate 8, shows that perfect detonation of the fulminate cylinder took place. The urn formed but no trace of the cover appeared; in other words, the rim does not turn over into a vortex in the absence of the simultaneous explosion of the glass tube. This experiment was also repeatedly performed, always with the same result.

Fig. 17, Plate 8, was made by placing a thin wafer of lead azide on the glass plate immediately below the cylinder of fulminate, its detonation by the impact of the explosion changing the form of the urn, abolishing the turned-over rim, and giving it a filamentous structure.

It must be clearly understood that all of these photographs were made in a totally dark room by the light of the detonation.

Experiments, which I shall describe presently, showed that the spectrum of the "urn" was the bright line spectrum of *deflagrating* fulminate, while that of the cylinder was the continuous spectrum of *detonation*.

I then decided to try to capture some trace of the material shot down onto the plate, which appeared to be instrumental in forming the urn.

The rim of a wide-mouthed bottle was greased and the bottle filled with water, heaped up above the edge so that the level surface could be photographed edge-on. This was substituted for the glass plate below the fulminate cylinder, and the tube detonated. The resulting photograph is reproduced in fig. 15, Plate 8. Though not so brilliant as with the glass plate, the "urn" is there with its cover, which shows that matter moving with the velocity of the products of detonation does not know whether it is striking glass or water. The water showed no trace of any solid matter suspended in it, even with a beam of concentrated sunlight. Not much of the water was scattered, but it is of course possible that only a thin surface layer contained trapped material and that this layer was blown away. This experiment should be repeated under conditions providing for the capture of all of the water.

Most of these experiments were repeated with lead azide, which is much more treacherous than the properly prepared fulminate. I made my first samples in very small quantities by the usually described method of precipitating it from a solution of sodium azide in warm water (slightly acidified with nitric acid) by means of lead acetate, washing the precipitate in a large volume of water, filtering and allowing the semi-fluid mass on the filter paper to fall a drop at a time on blotting paper, each drop splashing out to a disk about a centimetre in diameter. After drying, the blotting paper was cut up, with a thin wafer of the azide on each piece. These wafers could be detached intact if handled carefully with a slip of stiff paper. It is well to keep the fingers always at a distance of several inches from even these small quantities, as the detonation pressure in their *immediate vicinity* is terrific. The wafers were about as thick as writing paper, but one of them laid on a plate of glass and detonated blew a round hole through the glass without, however, breaking up the plate. A small pile of the material the size of a match head on a piece of rather thick glass blew a circular hole through it of the same diameter as the pile of explosive, exactly similar in appearance to the hole made by a small high velocity bullet: clean cut on one side, spread out into a crater on the other side, with not a single radiating crack. Prepared in this way and handled carefully, I do not believe there is much danger, though the explosive experts all say that "home-made" azide is very risky material, as sometimes large crystals form, which detonate on the slightest provocation. Most of my experiments were made with material supplied by Dr. Lawson, though for some experiments I found the thin wafers more suitable than the fine powder, which was, of course, kept under water. It is usually stated in books on explosives that lead azide never deflagrates, but always detonates. I have found, however, that

this is not so. If one puts the slightest trace of gelatine in the water, to act as a binder, detonation does not occur when the material is fired in the open. Deflagration also occurs, even in the absence of gelatine, if the powder is not bone dry. The pasty material supplied to me, on drying fell into a fine powder. This powder had to be exposed to the air for ten or fifteen minutes longer before detonation would occur, the material burning like gunpowder. Even after thorough drying, an exposure of several days to the air brought it into the condition in which only deflagration occurred. Apparently the chain reaction which is supposed to account for detonation, is blocked by the slightest surface film, gelatine, water, or some decomposition product. I found also that freshly dried material, which invariably detonated when touched by the flame of burning paper, merely deflagrated when the flame came from deflagrating azide. In this case it seems probable that lead vapour from the latter forms a protective coating on the crystals of the former before the temperature reaches the point necessary for decomposition.

### III—SPECTRA OF DEFLAGRATION AND DETONATION

The spectroscopic investigation of these exploding materials is attended with unusual difficulties, as many of them will not detonate except when confined, in which case we have a shower of flying fragments.

The deflagration spectrum of mercury fulminate was obtained by firing a number of small charges in succession on a brass block mounted at such a distance from the spectroscope that the image of the entire flash was projected on the slit. In this way the character of the spectrum from the point of ignition to the top of the flame was recorded. The spectrum, reproduced on fig. 19, Plate 8, shows that the mercury lines and cyanogen bands appear only at the base of the flame, while the calcium lines originate a little higher up (*see especially the lines at the left of Hg 4358*), and extend to a much greater height, while the D lines of sodium extend upwards to the tip of the flame. The calcium probably got into the fulminate from the tap water during the process of manufacture. It could not be removed by repeated washing with distilled water.

The spectrum of the 3883 band of cyanogen was obtained with our large 3 metre concave grating by firing about 20 shots of fulminate in front of the slit in the same manner. It is reproduced in fig. 12, Plate 7, in coincidence with photographs of the same band from a vacuum tube and the carbon arc.

It was not easy to get the spectrum of detonating fulminate on account of the small amount of light.

It was secured by employing a prism spectrograph equipped with a F2 photographic objective and focussing the image of the charged capillary glass tube on the slit before detonating it, protecting the lens from the shower of minute glass fragments by a sheet of plate glass, the surface of which was found to be covered with hundreds of minute pits after the explosion.

A single shot gave a considerably under-exposed continuous spectrum with the two mercury lines, but no trace of the very strong cyanogen bands which were present in deflagration.

Lead azide was next prepared and investigated. Work with this substance is very hazardous as it is liable to crystallize after preparation and detonate on the slightest provocation. A comparatively safe type is prepared for detonators by a special technique. A "wafer" of the substance, prepared as previously described, was broken up into small fragments which were detonated in succession by bringing them into contact with an inverted  $\Lambda$  of platinum wire heated to just below a dull red by an electric current. The sharp fork of the  $\Lambda$  was focussed on the slit by a lens and the small fragments of azides detonated by lifting them on the tip of a slightly moistened wire and touching them to the top of the  $\Lambda$ .

Before adopting this method, I tried a small metal plate heated by a flame, but the detonation extinguished the flame and bent the plate out of the correct position.

A very satisfactory spectrum was obtained with 30 shots. As with the fulminate, the spectrum is continuous with two very bright lines, one of lead, the other of calcium, fig. 20, Plate 8.

The deflagration of lead azide was obtained in the same manner as that of the fulminate, employing material which had been brought into the proper condition as before described. The spectrum, in coincidence with that of iron, is reproduced in fig. 23, Plate 8.

It consists of the lead line 4058 and the bands of lead oxide. An attempt was now made to gather some information about the "secondary flash" by means of the spectroscope. A short cylinder of mercury fulminate, capped by lead azide as previously described, was sharply focussed on the slit of the F2 spectrograph and detonated. A camera had been placed at such a distance as to give an image of the detonating cylinder of the same size as its spectral image. The two photographs (enlarged sixfold) are reproduced as negatives side by side in fig. 21, Plate 8, and show that the detonating cylinder gives a continuous spectrum, while the fainter flames which issue from its lower end give the bright line spectrum of deflagration. Fig. 16, Plate 8, gives a better idea

of the appearance of the detonating cylinder than the black smudge of fig. 23.

The inference from this photograph is that either undecomposed fulminate is thrown off from the detonating cylinder and immediately deflagrates, or that we have a two stage reaction, the products of detonation subsequently deflagrating. The comparatively small amount of light given off, however, inclines one to adopt the first hypothesis. It seems possible that some of the crystals may be in such a state (surface layer of some impurity, for example) that they cannot take part in the chain reaction of detonation.

A second spectrogram was taken of the detonation of the glass capillary with its protruding cylinder of fulminate, and the luminous "vase" which appears below it when the detonation products strike a glass plate. The spectrum of the "vase" and the luminous mass on which it rested was similar to that of the flame jets which issued from the detonating cylinder, namely the deflagration spectrum. The secondary flash of lead azide was next investigated.

A drop of very soft azide paste was allowed to dry on the top of a brass cylinder, giving a smooth hemispherical pile of the crystals. The detonation flash was photographed with a camera so placed as to view the surface of the cylinder foreshortened to a line, and the resulting picture showed the azide hemisphere brilliantly luminous and very sharply outlined, but with no trace of any luminous jets such as appear with fulminate. The upper surface of the cylinder, however, appeared to be covered with a very shallow layer of luminous vapour, which, I imagine, can be considered as the secondary flash, and seems to show that the detonation products shoot out radially from the centre of the explosion as indicated in fig. 3.

The diagram illustrates a rectangular gap cut into a piece of thick sheet brass. A small pile of azide crystals is shown resting on a polished aluminium base positioned directly beneath the brass sheet, indicating the experimental setup for the detonation test.  
The azide was detonated by an electrically heated wire applied at the top of the hemisphere, and it seems possible that the minute crystals in the lower layers may have been shot out laterally over the surface. It seems more probable, however, that the light can be considered as the secondary flash produced by the impact of the detonation products on the solid surface. No luminosity appeared in the region over the heap of azide. The spectrum of the detonation and secondary flash was secured by sawing out a rectangular gap in a piece of thick sheet brass, as indicated by the small diagram at the right of fig. 22, Plate 8. The azide crystals were piled on a small piece of very clean and highly polished aluminium on the lower surface as indicated. An image of the gap and the region immediately below it was formed on the slit of the F2 spectrograph and the azide detonated.

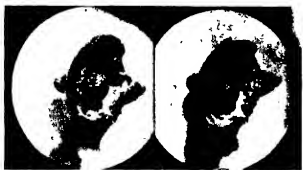


FIG. 4



FIG. 5



FIG. 6



FIG. 7



FIG. 8



FIG. 9



FIG. 10



FIG. 11



FIG. 12.

(CN)  $\lambda = 3883 \text{ } \uparrow$



FIG. 13.



FIG. 14.



FIG. 15.



FIG. 16.



FIG. 17.



FIG. 18.

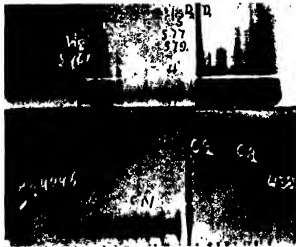


FIG. 19.



FIG. 20.



FIG. 21.



FIG. 22.



FIG. 23.

Fig. 22, Plate 8, is a reproduction of the resulting spectrogram, in point-to-point coincidence with the diagram of the gap. The detonating pile of azide crystals gives a continuous spectrum similar to fig. 20, the lead and calcium lines traversing the gap in the brass plate. The lead line is enormously broadened by the density of the vapour and pressure. The spectrum of the secondary flash is the continuous band at the top, interrupted just over the lead line by the absorption of the vapour. This is not very striking in the enlargement, but it was verified by numerous repetitions of the experiment and was very clear on the original negatives. The spectrum below the surface on which the azide detonated is that of the vapour which was blown down over the front surface of the brass block, and is chiefly that of aluminium, the lines 3944 and 3961 and the oxide bands being very conspicuous. It will be of interest to repeat the experiment of the lead azide hemisphere on the brass block in a high vacuum, as the "tamping" action of the atmosphere will be eliminated.

---

## The Zeros of the Riemann Zeta-Function

By E. C. TITCHMARSH, F.R.S.

(Received 20 July, 1936)

In my previous paper\* I described calculations which show that all the zeros of  $\zeta(s)$ , where  $s = \sigma + it$ , between  $t = 0$  and  $t = 390$  lie on the line  $\sigma = \frac{1}{2}$ . With the help of a Government Grant, these calculations have now been carried as far as  $t = 1468$ . The number of zeros up to this point is 1041, and they all lie on the line  $\sigma = \frac{1}{2}$ .

I have to thank Dr. L. J. Comrie for planning and supervising the calculations, which were carried out with Brunsviga, National, and Hollerith machines.

The main results of the calculations are contained in a table giving the values of the function  $\frac{1}{2} f(\tau) = \frac{1}{2} e^{it} \zeta(\frac{1}{2} + 2\pi i\tau)$ , where  $\tau = t/(2\pi)$ , defined in the previous paper, for  $\kappa = 90, 90.5, 91, \dots$  to  $\kappa = 520.5$ . The corresponding range of  $\tau$  is roughly 58.6 to 233.7. There is also a table giving  $\tau$ , to five decimals, as a function of  $\kappa$ , for the above values of

\* Proc. Roy. Soc., A, vol. 151, p. 234 (1935).

$\kappa$ ; a table of five-figure values of the function  $h(\xi)$  (see paper I, p. 235), and a table of four-figure values of  $\cos 2\pi x$  at intervals 0.0001.

The following is a specimen of the main table :—

v	x = 434	434.5	435	435.5	436
1	0.9259	8.9270	0.9281	8.9292	0.9302
2	9.9360	9.5284	0.7070	9.5074	9.9649
3	9.4294	0.2370	0.4441	9.5257	9.8095
4	9.5082	0.0553	0.4996	0.0148	9.5025
5	9.5698	9.9741	0.4132	0.2971	9.7815
6	0.0985	0.3891	0.3086	9.9335	9.6218
7	9.9122	0.2144	0.3748	0.2870	0.0088
8	0.0950	0.2879	0.3529	0.2609	0.0525
9	0.3178	0.2209	0.0611	9.8836	9.7393
10	0.1135	0.2230	0.2945	0.3159	0.2832
11	9.7499	9.8114	9.8902	9.9791	0.0701
12	0.2727	0.2485	0.2144	0.1716	0.1218
13	0.2405	0.2536	0.2640	0.2715	0.2760
14	0.2645	0.2652	0.2657	0.2662	0.2666
—	0.4339	0.6358	5.0182	9.6435	0.4287

The entries in the first fourteen rows are the values of the numbers.

$$\alpha_v = v^{-\frac{1}{2}} \cos 2\pi (\kappa - \tau \log v);$$

but  $\frac{1}{2}g(\tau)$ , the first remainder term in the Riemann-Siegel asymptotic formula, has been added to the first row (which would otherwise be  $\pm 1$ ). Negative numbers are shown with 10 added to them. Since the  $\alpha_v$  all lie between  $-1$  and  $1$ , this does not lead to any ambiguity. The last row, which may be taken as accurate to three decimals, is the resulting value of  $\frac{1}{2}f(\tau)$ . The values of  $\tau$  corresponding to the above  $\kappa$  are 201.59583, 201.78427, 201.97267, 202.16105, 202.34939.

In the great majority of cases it is found that  $\frac{1}{2}f(\tau)$  has the same sign as  $(-1)^\kappa$ , and hence that  $\zeta(\frac{1}{2} + 2\pi i\tau)$  has a zero between values of  $\tau$  corresponding to successive values of  $\kappa$ .

In the above specimen, the signs of  $f(\tau)$  are  $+, +, +, -, +$ . It follows that  $f(\tau)$  has a zero in each of the last two intervals. For the first two intervals the calculations are so far inconclusive. However, the large positive value at  $\kappa = 435$  suggests that  $f(\tau)$  may be increasing at  $\kappa = 434.5$ , and so may become negative just to the left of this point. And, in fact, by an independent calculation I find that at  $\tau = 201.72$ , i.e.,  $\kappa = 434.32948$ , we have  $\frac{1}{2}f(\tau) = -0.09$ . Hence there are two zeros between 434 and 434.5.

Of the values of  $\frac{1}{2}f(\tau)$  given in the table, all but forty-three have the same sign as  $(-1)^\kappa$ . In each of the exceptional cases the value of  $\frac{1}{2}f(\tau)$

at an additional point has been calculated. In each case it is found that the absence of zeros in one interval is compensated for by the occurrence of two zeros in one of the adjacent intervals. The departure from Gram's law (see paper 1, § 7) is therefore still very slight.

The successive maxima and minima of  $\frac{1}{2} f(\tau)$  vary considerably in absolute value. The greatest value of  $\frac{1}{2} f(\tau)$  so far noticed is 5·2, at  $\kappa = 481\cdot5$ . In the neighbourhood of  $\kappa = 497\cdot5$  there is a minimum value of about -0·01. In this case Theorem 2 of paper 1 is not sufficiently accurate to determine the sign, and the next term in the Riemann-Siegel asymptotic formula has to be used.

The encouragement which these calculations must give to believers in the Riemann hypothesis is obvious. But there are still some features of the table with which believers in the contrary hypothesis might console themselves. In the main, the results are dominated by the first term  $\alpha_1$ , and later terms more or less cancel out. Occasionally, as at  $\kappa = 435$ , all, or nearly all, the  $\alpha_i$  have the same sign, and  $f(\tau)$  has a large maximum or minimum. As we pass from this to neighbouring values of  $\kappa$ , the first few  $\alpha_i$  undergo violent changes, while the later ones remain comparatively constant. It is conceivable that if  $\tau$ , and so the number of terms, were large enough, there might be places where the smaller slowly varying terms would combine to overpower the few quickly varying ones, and so prevent the graph from crossing the zero line between successive maxima. The fourteen or fifteen terms occurring in the table are hardly enough to test this possibility.

There are, of course, relations between the  $\alpha_i$  which destroy any too simple argument of this kind. The Riemann hypothesis may be said to be that there is some relation, at present hidden, which prevents the suggested possibility from ever occurring at all.

#### SUMMARY

Calculations are described which show that the Riemann Zeta-function has 1041 zeros between  $t = 0$  and  $t = 1468$ , all on the line  $\sigma = \frac{1}{2}$ .

---

## Viscosity of Liquid Sodium and Potassium

By Y. S. CHIONG, Ph.D., China Foundation Research Fellow

(Communicated by E. N. da C. Andrade, F.R.S.—Received 11 March, 1936)

### 1—INTRODUCTION

According to the theory of liquid viscosity put forward by Professor Andrade,\* the viscosity of a liquid is closely connected with the characteristic frequency of vibration, and the temperature coefficient of viscosity obeys an exponential formula involving an internal energy coefficient. It appears that, for comparison with theory, viscosity data for elementary substances like liquid metals are specially desirable. Hitherto, viscosity measurements have been largely confined to organic liquids, while for liquid metals, with certain notable exceptions,† viscosity data have been scanty and discrepant. The work described below was undertaken with the view of supplying some of the data which are needed. Sodium and potassium were chosen for the measurement on account of the simplicity of both their atomic structures and of their crystal form. They also have the advantage that the viscosities of the other three alkali metals—lithium, rubidium, and caesium—are also accessible to measurement, the melting points lying within an easily-realized temperature range.‡

Owing to the fact that these metals oxidize very quickly in the presence of even a slight trace of air, the sphere§ method, in which the liquid is enclosed in a sphere and its viscosity found by observing the damping of the oscillations about a vertical axis, is specially suitable for the purpose. This method, as lately developed by Professor Andrade and the author, has proved capable of an accuracy probably as great as that of the standard methods. It is simple in manipulation, renders temperature control easy, and does not involve the corrections involved in capillary tube methods.

### 2—APPARATUS

The suspension§ was a bifilar one, and, in order to obtain a pure rotation free from any swing, a special mechanical arrangement for starting the oscillation was adopted.

\* 'Phil. Mag.', vol. 17, p. 497; p. 698 (1934).

† E.g., mercury (Koch, 'Ann Physik,' vol. 14, p. 1 (1881); Plüss, 'Z. anorg. Chem.', vol. 93, p. 1 (1915)); tin (Stott, 'Proc. Phys. Soc.', vol. 45, p. 530; Lewis, 'Proc. Phys. Soc.', vol. 48, p. 102); and gallium (Spells, 'Proc. Phys. Soc.', vol. 48, p. 299 (1936)).

‡ Measurements on these metals are now being carried out in the Physics Laboratory of University College, London.

§ Andrade and Chiong, 'Proc. Phys. Soc.', vol. 48, p. 247 (1936).

The bifilar suspension is made of a single wire, the loop of which carries a wheel W pivoted on a frame. The wire is fixed to the frame in the method described in the earlier publication. This frame is joined through

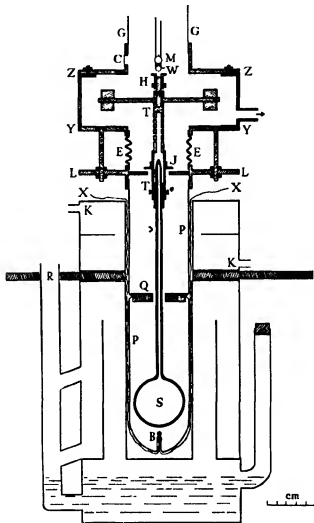


Fig. 1

its lower tube H to the connecting rod TT, which carries the inertia pieces (fig. 1). The lower part of the rod is a hollow tube, into which the stem of the glass sphere S is fitted by means of a metal sleeve. The tube is perforated along its length with holes, firstly to reduce the weight of the

rod, and secondly, to provide an outlet for air when we wish to work with the bulb exhausted, in order to find the external damping. The whole suspension is in a vacuum-tight enclosure, as shown in fig. 1. This consists of a glass tube GG, a metal box ZZYY inside which hangs the connecting rod TT, together with the inertia pieces, and the pyrex tube PP which encloses the sphere. The metal tube on top of the box is provided with two small glass windows standing at right angles to each other. Light entering the side window C after being reflected by the mirror M comes out at the front window, where observation is made. The tombac bellows EE are used to take the weight off the suspension wire when desired, by raising up the lower plate LL to meet the flange J. Long metal screws, shown in the diagram, prevent the bellows from collapsing when the system is evacuated. The evacuation was carried out with a mercury vapour pump, suitably backed, and the vacuum produced was estimated to be about  $10^{-5}$  mm. of mercury, or less.

The sphere hangs inside the pyrex tube PP, leaving a clearance of about 3 mm between its equator and the tube. Q is a thick copper disk, blackened all over except its upper surface, upon which a piece of chromium-plated copper foil is placed. The disk rests upon small projections from the glass tube. In order to lessen the time taken for temperature equilibrium to be reached, the sphere and the pyrex tube below the disk are all blackened outside.

The thermocouple B is very close to the sphere, the leads XX being fastened on to the tube and covered with strips of mica. The potential was measured by a Crompton potentiometer, which enables the temperature to be read to  $0.1^\circ\text{C}$ .

About 8 inches of the tube PP is inside a well-lagged vapour jacket, made of copper. The jacket is of the ordinary hydrometer type, in which the vapour, after being condensed inside a water-cooled condenser attached at R, is led back again into the boiler. The condenser is connected to a large reservoir provided with a manometer gauge, so that the liquid may be made to boil at different pressures. It may be mentioned that a special jacket made of steel was used for the case when mercury was used as the boiling liquid.

KK is a jacket, made in two halves, used to protect the waxed joints. It is kept cool by running water. The cooling was found to be effective, since no appreciable increase of temperature was noticed even when the lower part of the tube was at the highest temperature used.

## 3—PURIFICATION OF METALS

To obtain the metals pure and free from gas, they were distilled in vacuo at about 300° C., in an apparatus made of pyrex glass. The use of pyrex glass for the work was quite satisfactory, since it was found that vapours of the metals did not begin to attack the glass until the temperature exceeded 300° C.

Freshly-cut small lumps of the metal were introduced into the filtering tube L (fig. 2) and heated by a cylindrical furnace enclosing the tube. The molten metal flowed through a capillary tube C, dust particles and oxides being left behind, so that the liquid collected in the flask D was quite bright. The metal was then slowly distilled over into the reservoir R, and finally allowed to stream into the sphere. With potassium, which was supplied in the form of sticks and preserved in benzene, special care was taken to drive away traces of benzene as completely as possible before the metal was introduced into the filtering tube.

The distilled sodium, kindly analysed for me by Mr. Terrey, senior lecturer in the Chemistry Department of University College, was found to contain 99.8% of pure metal, while a separate analysis, also done by Mr. Terrey, showed that the sample did not contain potassium to the extent of more than 0.02%. The potassium used was supplied by Schering-Kahlbaum as specially pure, and was said to contain only a slight trace of iron. Probably the trace of iron was reduced after the distillation. Thus, from the point of view of viscosity measurement, where small contaminations produce only a small effect, these metals may be said to be satisfactorily pure.

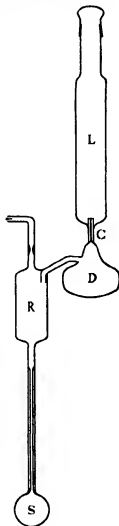


FIG 2.

## 4—EXPERIMENTAL

(a)—*The Spheres and the Calibration*—Spheres D, E, used in the present work, were two of the five spheres used in the previous work on the determination of the viscosity of water. The result obtained with these

spheres, over a temperature range from 13° to 60° C., showed satisfactory agreement with the standard values given in the International Critical Tables.\*

Values of the diameter of the sphere at various temperatures were calculated by taking the linear coefficient of expansion of pyrex as  $3 \times 10^{-6}$ . Correction due to this at the highest temperature employed was less than 1 part in 1000 on the diameter, involving a correction of about 1% in the viscosity, for which allowance was made.

(b)—*The Moment of Inertia*—The moment of inertia of the system was determined within 1 part in 2000. This accuracy was made possible by a special design of the inertia bar, the moment of inertia of which can be calculated accurately from its geometrical form, and by arranging for the unknown part of the moment of inertia to be only a small fraction of the total \*

As the inertia pieces together with other attachments, to which about 97% of the total moment of inertia was due, were inside the metal box ZZYY, where the temperature was kept practically constant, the moment of inertia of the system may be safely regarded as constant in all the measurements.

(c)—*The Effect of Thermal Expansion of the Liquid Metal*—In filling the sphere it was not possible to distil over from the flask D exactly the amount of pure metal needed to fill the sphere. The sphere was therefore filled a little more than was required, and the excess removed in the following way. The stem was first sealed near the top by allowing a pellet P of the molten metal to solidify there, so that the sphere can be removed from the distillation apparatus, and fused on to the reservoir R without air entering (fig. 3). The apparatus was evacuated before communication was established by melting the metal pellet. The molten metal was allowed to flow into the reservoir R carrying away the slight amount of oxide formed on the top of the pellet during the opening of the stem. The bulb was then put in an oil bath having a temperature a few degrees above the melting point of the metal. Unwanted liquid appearing inside the stem was removed by shaking it into the reservoir R, and the stem was then sealed.

At the higher temperatures, owing to thermal expansion, the liquid would occupy a considerable part of the stem if the sphere were full at a temperature in the neighbourhood of the melting point. Before the viscosities were measured, the sphere was therefore raised to a temperature

\* See Andrade and Chiong, ' Proc. Phys. Soc.,' vol. 48, p. 247 (1936).

in the neighbourhood of the range contemplated, and excess liquid metal removed until the sphere was full at the temperature in question. This was done for every increase of  $50^{\circ}$  or so, leaving, in the maximum case, a metal column about 4 cm. in the stem. The damping effect due to this was negligibly small—less than 0·04% as calculated according to Mützel's\* work on the determination of viscosity by an oscillating cylinder filled with the liquid. As the metal column was only 3·7 mm. in diameter, its effect on the moment of inertia was also negligible.

In the earlier experiments, the tube was opened and the metal actually removed; later on a simpler method was devised for regulating the content of liquid inside the bulb. The stem was fused directly to a wider tube which was about 4 cm. long, and of a capacity sufficient to hold the total excess of liquid for the whole temperature range used. Unwanted liquid was made to flow into the reservoir tube and solidify there. As this tube was in the cooled part of the apparatus, the metal remained in a solid state. The increase of moment of inertia due to this was negligibly small. Another advantage of this arrangement was that it was possible, by shaking down the required amount of metal into the bulb, to repeat readings at lower temperatures after measurements had been done at the highest temperature used.

(d)—*The Damping*—The logarithmic decrement was calculated from photographic records taken for the amplitude of swing, by the method described by Andrade and Chong. Successive experiments at the same temperature gave differences in the decrement of not more than 1 part in 2000, which means a difference in viscosity of not more than 1 part in 1000.

The correction for external damping due to imperfect elasticity of the suspension wires and residual gas on the enclosure surrounding the sphere was made by taking the logarithmic decrement with the sphere evacuated. The values taken at different times (over a period of six months) showed a difference of at most 3%. The agreement is satisfactory, since the external damping never amounted to more than 1% of the total damping, and at low temperatures was much less than this.

The effect of the earth's field on the oscillating sphere full of metal has been investigated by means of a pair of Helmholtz coils placed with the sphere suspended in the centre. The value of the current in the coils was adjusted to give a magnetic field about 10 times as strong as the earth's



FIG. 3.

\* Mützel, 'Ann. Physik,' vol. 43, p. 15 (1891).

field. The external damping was found to increase by 15%, which means that the earth's field alone did not contribute to the total damping by more than 3 parts in 20,000, and so was completely negligible.

(e)—*The Temperature*—Owing to possible complications from the strong magnetic field inside an ordinary electric furnace, a vapour jacket was used instead. Other advantages of a vapour jacket are : the temperature is steadier than it is in an electric furnace, and there is no temperature gradient. The temperature was kept steady within a tenth of a degree for more than five hours before the first reading was taken. A second value for the logarithmic decrement, taken about an hour after the first determination, showed satisfactory agreement, so that it was certain that the liquid inside the sphere had reached a steady state. To find if the temperature that the metal finally attained was equal to that of the enclosure as recorded by the thermocouple B, the following separate experiment was done.

A new thermocouple, which had been calibrated side by side with the thermocouple B, was inserted into the sphere filled with pure sodium, so that the junction was central. The pyrex tube PP was removed from the apparatus, and, by means of a special metal cover, the sphere was cemented so as to be fixed centrally in the tube, in the same position as it occupied during the actual experiment. The tube PP was evacuated, and temperature measurements taken at intervals, under conditions exactly similar to those prevailing during the viscosity measurements. The experiment was done at two temperatures, namely, at 100° C. and 357° C. In both cases the temperature of the metal, as recorded by the inner thermocouple, was found to follow readily the temperature of the enclosure with a slight lag. The temperatures indicated by the two thermocouples finally approached each other. In the experiment done at 100° C., the difference in temperature was less than 0·1° C. after 4 hours, while at the higher temperature it took only 2 hours to reach this degree of agreement. The actual interval of 5 hours allowed was therefore amply sufficient.

### 5—THE CALCULATION OF VISCOSITY\*

The viscosity is given by the following formulae :

$$\eta = \frac{a^2 R^2 \pi \rho}{4 q^{1/2} T} \{1 - (1 - \mu)^2\}^2, \quad (1)$$

and

$$\eta = \frac{9}{16\pi} \frac{I^2 (T^2 - T_0^2)^2}{T T_0^4 R^4 \rho}, \quad (2)$$

\* Andrade and Chiong, 'Proc. Phys. Soc.', vol. 48, p. 247 (1936).

where

$$\mu = \frac{3q'I\delta}{2\pi^2 a^2 R^5 \rho} \left( \frac{T^2}{T_0^2} + 1 \right),$$

$$q' = 2 - \frac{gR - 1}{(gR - 1)^2 + hR^2},$$

$$a = 1 - \frac{1}{2} \left( \frac{\delta}{2\pi} \right) + \frac{1}{8} \left( \frac{\delta}{2\pi} \right)^2,$$

$$g = h = \sqrt{\frac{\pi\rho}{T\eta}} \quad \text{roughly,}$$

and  $R$  is the radius of the sphere,  $I$  moment of inertia of the oscillating system,  $T$  period of oscillation when the sphere is filled with liquid,  $T_0$  when it is empty,  $\delta$  the logarithmic decrement, and  $\rho$  density of the liquid.

The process of calculation is first to get a rough value of  $\eta$  from (2), with which we compute  $q'$ . By using this value of  $q'$  and by working through the equation (1), a second approximation is obtained. The third approximation is carried out in the same manner. In the actual series of experiments it is generally possible to guess the first value of  $\eta$  to within a few per cent, instead of using (2); if so, the second approximation gives the required accuracy.

## 6—ON THE DENSITY OF LIQUID SODIUM AND POTASSIUM

The values of the densities of liquid sodium and potassium given by different workers show certain discrepancies. Hagen's\* values agree tolerably with those given by Griffiths and Griffiths† and those by Hackspill,‡ while values by Bernini and Cantonis§ appear a little too high. In all cases the data cover only a small range of temperature, the highest temperature being 155° C. in Hagen's work, and about 230° C. in the measurement of Bernini and Cantonis. Recent work of Rink supplies density data for these metals to a higher temperature, 600° C. These measurements, however, started from above 360° C. Thus there still exists a gap between 155° and 360° C., inside which there might be a little uncertainty with regard to the densities. Fortunately, for these metals, Rink's values lie fairly close to the extension of the straight line plotted by Hagen's values. As Hagen's values appear more consistent, they were

\* 'Ann Physik,' vol. 19, p. 437 (1883).

† 'Proc. Phys. Soc.,' vol. 27, p. 477 (1915).

‡ 'C.R. Acad. Sci. Paris,' vol. 152, p. 259 (1911).

§ 'Nuovo Cim.,' vol. 8, p. 241 (1914).

|| 'C.R. Acad. Sci. Paris,' vol. 189, pp. 39 and 135 (1929).

adopted in the present work. Densities at temperatures higher than those at which Hagen's measurement was done were calculated from the values given by him for the coefficients of expansion of the metals.

Experiments are now in progress in the University College laboratory on the densities of the liquid alkali metals, which are designed to remove the discrepancies, but the values here adopted are hardly likely to be in error by an amount sufficient to affect the value of the viscosity within the experimental limits.

### 7—VISCOSITY DATA

TABLE I—SODIUM

Constants used in formula (3) for calculating  $\eta$ :  $K = 1.183 \times 10^{-3}$ .  
 $c = 716.5$ .

Temperature °C.	$\eta$ experimental (c g.s. units)	$\eta$ calculated	$\eta$ exp.— $\eta$ cal.
98.0	0.007264	—	—
99.6	0.007142	—	—
102.4	0.006856	—	—
120.4	0.006170	0.006188	+ 0.29%
154.5	0.005314	0.005336	+ 0.41%
155.0	0.005322	0.005308	+ 0.26%
159.1	0.005225	0.005221	+ 0.07%
173.7	0.004942	0.004933	+ 0.19%
183.4	0.004760	0.004761	- 0.02%
206.7	0.004431	0.004399	+ 0.72%
218.0	0.004239	0.004240	- 0.02%
289.0	0.003506	0.003495	+ 0.31%
355.0	0.003015	0.003035	- 0.66%

TABLE II—POTASSIUM

$K = 1.293 \times 10^{-3}$ .  $c = 600.0$

Temperature °C.	$\eta$ experimental (c.g.s.)	$\eta$ calculated (c.g.s.)	$\eta$ exp.— $\eta$ cal.
64.2	0.005535	—	—
67.0	0.005256	0.005242	+ 0.27%
67.9	0.005230	0.005216	+ 0.26%
79.4	0.004930	0.004945	- 0.31%
99.5	0.004540	0.004539	+ 0.02%
119.6	0.004188	0.004203	- 0.36%
155.5	0.003707	0.003729	- 0.59%
175.5	0.003530	0.003515	+ 0.43%
207.7	0.003249	0.003231	+ 0.56%
282.5	0.002750	0.002756	- 0.22%
352.5	0.002457	0.002458	- 0.04%

## 8—RESULTS AND DISCUSSION

Results of the experiments are given in tables I and II, together with values of  $\eta$  calculated by Andrade's formula\*—

$$\eta v^{\frac{1}{2}} = K e^{\frac{c}{T}} \quad (3)$$

where  $v$  is the specific volume,  $T$  the absolute temperature, and  $K$  and  $c$  are constants, their values being found from the experimental data by the method of least squares. Points very near the melting point of the metal have not been taken for the fitting, for reasons to be given later. In the tables, percentages of difference between theoretical and experimental values are also given, the maximum deviation being a little over a half per cent. It is to be noted that there is no indication of any systematic trend.

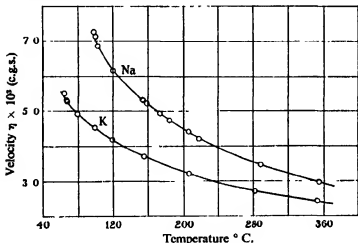


FIG. 4.

In fig. 4 values of the viscosity of sodium and potassium are plotted against temperature, while fig. 5 shows the result of plotting  $\log \eta v^{\frac{1}{2}}$  against  $1/vT$ . All the points except those very close to the melting point lie very well on a straight line. It is to be noted that for sodium the lowest temperature at which viscosity was measured was less than half a degree above the melting point, and that for potassium it was about 2° C. above the melting point.

Theoretical values of the viscosity of sodium and potassium at the melting point are given by Andrade's formula

$$\eta_m = 5.1 \times 10^{-4} \frac{(A T_m)^{\frac{1}{2}}}{V^{\frac{1}{2}}} \quad (4)$$

\* 'Phil. Mag.', vol. 17, p. 698 (1934).

where  $A$  is the atomic weight,  $V$  the atomic volume, and  $T_m$  the melting point in absolute temperature. The formula gives for the viscosities 0.0056 and 0.0045 respectively. The constant  $5.1 \times 10^{-4}$  is not arbitrary, but is obtained by taking  $C = 2.8 \times 10^{12}$  in Lindemann's frequency formula. These values compare with the experimental values 0.00695 and 0.00537 extrapolated from the linear relation.\*

If the values of  $\eta_m$  are calculated directly by the formula\*

$$\eta_m = \frac{4}{3} \frac{\nu m}{\sigma}, \quad (5)$$

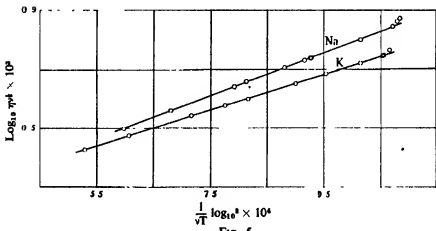


FIG. 5.

where  $m$  is the mass of a molecule,  $\sigma$  the average distance between the molecules, and  $\nu$  the characteristic frequency of vibration, we get  $\eta_m = 0.63$  and  $0.52$  c.p. for sodium and potassium respectively upon taking  $\nu_{Na} = 4.3 \times 10^{12}$  and  $\nu_K = 2.6 \times 10^{12}$ , as given by Lindemann.† The experimental value  $\eta_m$  of sodium then differs from its theoretical value only by 9%, and in the case of potassium the difference is only 3%. The agreement between experimental and theoretical values is therefore very satisfactory in this case. The large difference obtained in the first calculation is due to the smaller value of  $C$  taken. In fact, the value  $C = 3.4 \times 10^{12}$  as calculated from Andrade's formula by using viscosity data of sodium, gives  $\eta_m$  of potassium a value only 4% higher than the experimental value.

As seen in fig. 5, the viscosities of sodium and potassium at temperatures very close to the melting point behave abnormally, departing markedly from the straight line given by values of viscosity at higher temperatures.

\* Andrade, 'Phil. Mag.', vol. 17, p. 497 (1934).

† See Blom, 'Ann. Physik,' vol. 42, p. 1402 (1913).

The abnormality probably suggests that a crystal structure of these metals persists to some extent for a few degrees above the melting point. The phenomenon is clearly exhibited by sodium. In the case of potassium it is not so obvious, probably owing to the fact that the measurement was not taken so close to the melting point (about 2° above).

Stott\* and Lewis† in their works on the viscosity of tin, which also showed satisfactory agreement with Andrade's formula, failed to observe any abnormality in viscosity near the melting point, but it is to be noted that the lowest temperature measured in their works was about 6° C. above the melting point, which is likely to be too high to show the effect. Dobinski's‡ work on phosphorus is interesting, since he has measured the viscosity far into the super-cooled region. The viscosity shows an appreciably larger slope in this region than it does at higher temperatures when we plot  $\log \eta v^{\frac{1}{2}}$  against  $1/vT$ .

The constant  $c$  in the formula (3) is found to be 716.5 for sodium and 600.0 for potassium. The small difference in the values of  $c$  for these metals seems to indicate the familiar fact that their external molecular fields are more or less similar. These values of  $c$  appear large when compared with that for mercury, 22. This is probably due to the great difference existing both in the densitics and in the coefficients of thermal expansion of mercury and the alkali metals.

The characteristic frequency of vibration of molecules has been calculated in various ways from the specific heat and elastic constants of a substance. As summarized by Blom,§ there are more than seven formulae in existence. It will be seen that no two of them give results that agree moderately. Blom's investigation shows that it is impossible to say which of them is best. Some of the formulae have apparently a better theoretical basis than others, but they give bad results owing to the fact that they involve constants that have not been, or cannot be, measured with precision.

Andrade's formula for viscosity of a substance at its melting point having proved successful in representing experimental fact, it can clearly be used as an approximate frequency formula for a simple solid, when the viscosity at the melting point is known.

Formula (5) can be written as follows :

$$\nu = \frac{1}{2} \left( \frac{N^2}{\rho A^3} \right)^{\frac{1}{2}} \eta_m \quad (6)$$

\* 'Proc. Phys. Soc.', vol. 45, p. 530 (1933).

† 'Proc. Phys. Soc.', vol. 48, p. 102 (1936).

‡ 'Bull. int. Acad. Cracovie.', 3-4A, p. 103 (1934).

§ 'Ann. Physik', vol. 42, p. 1397 (1913).

where  $N$  is Avogadro's number,  $A$  the atomic weight,  $\rho$  the density and  $\eta_m$  the viscosity at the melting point. It is to be noted that Andrade's frequency formula, unlike the others, does not contain any arbitrary constant. In addition to a theoretical basis, the formula has the advantage that in general the only constant unknown is  $\eta_m$ , which can be easily determined within a half per cent.

In the following table, the characteristic frequencies of a number of elements, as calculated by Andrade's formula, are given together with the values calculated from formulae\* by (1) Nerst-Lindemann, (2) Einstein, (3) Lindemann, (4) Alterthum, (5) Benedicks, (6) Grüneisen, and (7) Debye. The agreement between the values given by Andrade's formula and those given by Lindemann's formula, in column 3, is striking. Andrade's formula, as used for calculating  $v$ , is quite independent of Lindemann's, but this good agreement means that if we substitute Lindemann's formula for  $v$  in the above formula (6), we can calculate  $\eta_m$  without invoking an arbitrary constant, as was done in Andrade's original paper. Gallium, for which the discrepancy is largest, has a particularly complicated crystal structure.

TABLE III

Element	$v \times 10^{18}$						
		Andrade	1	2	3	4	5
L	1.38	2.02	1.8	1.4	2.2	2.06	—
K	2.66	2.1	1.7	2.6	2.1	—	—
Na	4.62	3.0	2.9	4.3	3.6	—	—
Sn	2.33	3.8	3.5	2.5	3.3	3.1	—
Bi	1.63	3.2	2.2	1.8	2.8	2.5	—
Pb	1.96	1.98	2.2	2.0	2.1	1.96	2.2
Sb	2.80	5.0	3.1	3.2	4.4	4.0	—
Cu	6.37	6.7	6.6	7.4	6.7	7.2	6.7
Ga	3.54	7.3	—	2.8	—	5.6	—

After the work was completed, a short paper by Sauerwald† came to my notice, in which experiments are described which he carried out with liquid sodium and potassium, for the purpose of checking Andrade's melting point formula. The method, that of a simple capillary viscometer, in which surface tension introduces considerable uncertainties, is clearly not designed to give accurate values, nor was Sauerwald attempting to find anything but a rough approximation. The values, given by the author to two figures only, for melting point viscosities are 0.0077 and 0.0056 for sodium and potassium respectively, which are, according to this work, a

\* See Blom, 'Ann. Physik,' vol. 42, p. 1397 (1913).

† 'Z. Metallk.', vol. 26, p. 259 (1934).

few per cent. too high. For sodium he gives only the melting point value ; for potassium, values at two higher temperatures, viz., 100° C. and 183° C. The value at the latter temperature, viz., 0·00346, agrees exactly with the value here given. It may be noted that with Sauerwald's method the values are likely to be more accurate at high temperatures, on account of the decrease of surface tension.

#### ACKNOWLEDGMENT

It gives me great pleasure to express my thanks to Professor Andrade, F.R.S., for introducing me to the subject, and for the constant help and guidance given to me during the carrying out of the work and in the preparation of this paper. I am also indebted to the Provincial Government of Anhui, China, for giving me the opportunity of studying abroad.

#### SUMMARY

The viscosity of liquid sodium and potassium has been measured by the oscillating sphere method, in which the liquid is enclosed in a glass sphere, and its viscosity calculated from the damping of the oscillation. The alkali metals have been chosen because their simple crystal structure has advantages for comparison with theory. The measurement was done from the immediate neighbourhood of the melting point up to about 360° C. Results obtained for both sodium and potassium are found to obey satisfactorily the two viscosity formulae of Andrade.

---

## The Effect of Pressure Upon Natural Convection in Air

By O. A. SAUNDERS, M.A., M.Sc.

(Communicated by H. T. Tizard, F.R.S.—Received 15 April, 1936)

### INTRODUCTION

Dimensional considerations show, on certain assumptions, that natural convection depends upon the dimensionless numbers

$$M = \frac{ag\theta l^3 s p^2}{\mu k}, \quad \text{and} \quad N = -\frac{\mu s}{k},$$

where  $l$  is a representative linear dimension,  $\theta$  a representative temperature difference,  $a$  the coefficient of expansion of the fluid,  $s$  the specific heat per unit mass at constant pressure,  $\rho$  the density,  $\mu$  the viscosity, and  $k$  the conductivity. If  $H$  denotes the rate of heat flow across unit area of any given surface within the fluid, it also follows that  $P = Hl/k\theta$ , is a function of  $M$  and  $N$ . The assumptions made are discussed in an Appendix.

For gases  $N$  varies little between wide limits of pressure and temperature, and may in general be omitted,  $P$  therefore depending only upon  $M$ . For a given gas,  $M$  is proportional to  $\theta/l^3$ , and increases with the pressure  $p$ , being nearly proportional to  $p^2$ . The variation of  $P$  with  $M$  can be found by experiments in which either  $\theta$ ,  $l$ , or  $p$  is varied, but the range of  $M$  to be got by varying  $\theta$  is relatively small, not only because of the different indices in  $M$ , but also because for large values of  $\theta$  the assumption made in the dimensional analysis, that the constants of the gas do not vary with temperature, is inadmissible. By varying the pressure,  $M$  can be varied over a wide range for a single value of  $l$ ; thus only one experimental apparatus need be constructed, and it may be of reasonable size, large surfaces being difficult to heat uniformly and the surrounding conditions difficult to control.

The object of the present work was to find accurate values of  $P$  over a wide range of  $M$  for vertical plane surfaces in a relatively large volume of air, by experiments in a specially constructed enclosure at pressures from 0.001 to 65 atmospheres. It is proposed to extend the work to some other shapes.

## PREVIOUS EXPERIMENTAL RESULTS

Measurements of the heat loss from vertical planes in atmospheric air have been made by Nusselt, Jurges, Griffiths and Davis, Schad, King, and Carpenter and Wassell. Their results are compared in fig. 3 with those of the author. The effect of pressure upon natural convection has not previously been studied, except by Petavel, who in 1901 made some accurate measurements with a horizontal wire in a cylindrical enclosure filled with various gases up to pressures of 170 atmospheres. The author has expressed Petavel's results in dimensionless coordinates and, later in the paper, they are discussed with some more recent values obtained with a similar apparatus at higher pressures, and are compared with other results for horizontal cylinders in atmospheric air.

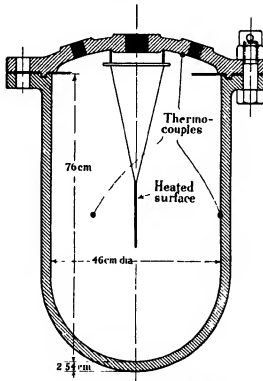


FIG. 1—Experimental enclosure.

## APPARATUS

The experimental surfaces were suspended from the lid of a cylindrical cast steel pressure chamber of internal diameter 46 cm. and height 76 cm., designed to withstand 70 atmospheres (see fig. 1). The axis of the chamber

was vertical, the lower end being hemispherical, and resting in a steel cradle. The detachable lid was held on by twenty steel bolts, the joint being made with a ring of gutta percha cord. Tightening the bolts flattened out the cord, and the joint could be re-made many times with the same cord.

Electrical leads, not shown in fig. 1, were taken from the experimental surfaces to a junction board, and thence to terminals passing through plugs screwed into the lid, the terminals being insulated by ebonite sleeves. The pressure could be maintained for some days without appreciable leakage. The chamber was immersed in a tank of water to keep its temperature steady. The air inside the chamber was kept dry by calcium chloride. The pressure was measured with Bourdon gauges, which were calibrated before and after use. At low pressures mercury manometers were used.

The experimental surfaces consisted of three platinum strips and a copper heater plate. The platinum strips were stretched horizontally with their surfaces in a vertical plane; they were 0.0025 cm. thick, 23 cm. long, and of three heights, 0.325, 2.50, and 7.60 cm. The copper plate was hung vertically and was 22.9 cm. high by 15.25 cm. wide, and 0.55 cm. thick. The heights were chosen to give overlapping ranges of  $M$ , corresponding to the ranges of pressures investigated.

The platinum strips were the more satisfactory type for accurate measurements, but greater heights than 7.6 cm. could not conveniently be used owing to the heavy heating currents required. The ends of the strips were gripped between pairs of copper bars connected by flexible links to copper leads of 0.1 cm. diameter supported in a light wooden frame. Potential leads of fine platinum wire were led away at right angles to the surfaces from points 7.6 cm. apart and equidistant from the middle of each strip. The copper bars used to grip each strip were of sufficient cross-section for the horizontal potential gradient to be uniform from top to bottom. The energy dissipated from the part of a strip between the potential leads was found from the potential difference and the total current flowing along the strip. The temperature of the same part was derived from its resistance, as found by dividing the potential difference by the total current, using a calibration obtained as described below.

The vertical distribution of temperature in each strip is a function of the distribution of convective cooling, and the thickness and thermal conductivity of the strip. The temperature is uniform only if the convective cooling is uniform. Assuming the cooling to be given by the results of the present experiments (see fig. 4), the temperature distribution can be calculated by a simple approximate method. It is found that the

temperature difference between the top and bottom of a strip increases with the pressure. For the 0.325 cm. strip the difference in temperature is negligible at all pressures. For the 2.5 cm. and 7.6 cm. strips it becomes appreciable at pressures above a few atmospheres, reaching about 25° C. for a temperature excess of 55° C. in the extreme case considered. In no case, however, does the measured temperature of the strip differ from its true mean temperature by more than 0.5° C. The total convection heat loss may, however, depend upon the distribution of temperature as well as upon the mean temperature. The overlapping in fig. 2 of the points for the 2.50 cm. strip at the higher pressures with those for the 22.9 cm. plate (which was known to have a uniform temperature) at the lower pressures, indicates that the effect of non-uniformity of temperature upon the results may be neglected; the results may thus be taken as applicable to a surface at a uniform temperature.

The relation between resistance and temperature was found for each strip by calibration in a special air-tight tin box, which was totally immersed in an electrically heated oil bath, with a propeller for circulation. Four thermocouples soldered to the top, bottom, and two side faces of the tin box read the same within 0.5° C., and their mean was taken as the strip temperature, the current through the strip being too small to raise its temperature appreciably above that of the box.

The copper heater plate was made of two copper sheets held together by screws and enclosing a heater of nichrome strip wound on a thin sheet of asbestos and insulated from the plates by thin mica sheets. In some preliminary experiments with the heater wound on mica, air circulation between the plates caused unduly large heat losses at the higher pressures, at which convection in narrow spaces takes place more readily, but this trouble was overcome when asbestos was used. Sealing the gap around the edges of the plates had no appreciable effect on the results. The temperatures of the copper surfaces were measured by thermocouples tightly embedded in grooves cut in the inside faces of the copper sheets. Each surface had three thermojunctions at points along the centre line parallel to the longer edges, respectively at the middle, 2.5 cm. from the top, and 2.5 cm. from the bottom, the mean being taken as the surface temperature. Tests with additional thermocouples showed that the temperature was uniform up to 1.0 cm. from the edge along any horizontal line, while in the vertical direction, differences up to 3° C. were found between positions 1.0 cm. from the top and 1.0 cm. from the bottom, for a temperature excess of 55° C.

In all cases the air temperature was measured by a fine thermocouple midway between the top and bottom of the heated surface, and about

midway between the surface and the enclosure walls. The temperatures of the walls and lid of the enclosure were measured by embedded thermocouples.

#### CORRECTIONS APPLIED TO RESULTS

*Edge Losses from Copper Plate*—The heat loss given for the copper plate is for unit area of total surface, including the edges. To find the effect of the vertical edges, a similar plate of half the width was tested; the results for the narrower plate were less consistent, but were within  $\pm 2\frac{1}{2}\%$  of those for the wider plate, showing that the mean heat loss per unit area from the wider plate is not appreciably affected by including the vertical edges. The horizontal edges were included without investigation.

*Radiation Loss*—The radiation to the enclosure walls was calculated and subtracted from the measured heat loss to give the convection. The emissivities of the platinum and copper surfaces were measured, using a thermopile with a suitable reflecting cone, and comparing the radiation with that from a similar plate coated with camphor black, taking care that the coating was thick enough to give maximum emissivity. The thermopile and plate were surrounded by a metal screen, bright on the outside, and black on the inside, to prevent radiation from relatively cold walls, or any other surfaces not at air temperature, from being reflected by the plates into the thermopile cone. The emissivity of the copper plate was between 0.03 and 0.045, according to its condition. The emissivity of the platinum was 0.05. The radiation heat loss is independent of the pressure; it amounted for the copper plate to 6% of the loss at atmospheric pressure, and less than  $\frac{1}{2}\%$  at 65 atmospheres. For the platinum strips, the radiation was below 4% at atmospheric pressure, but for the 7.6 cm. strip rose to 20% at the lowest pressure.

*Loss Along Suspending Wires and Leads*—For the copper plate this was proved negligible by attaching an additional set of dummy wires and leads. With the platinum strips, both the loss along the potential leads and any loss along the strip from the middle experimental section were neglected.

#### RESULTS

Readings were taken for surface temperatures from about 60° C. to 80° C. in air at about 15° C. with each of the four experimental surfaces of different height ( $l$ ), at pressure ( $p$ ) between 0.043 and 65 atmospheres. Table I gives the results for a surface temperature of 70° C., in terms of  $H/\theta$ , where  $H$  is the convection heat loss from unit area in unit time, and

0 the temperature difference between surface and air, i.e., 55° C. It was found that the variation of H with 0, for any given size and pressure, could be expressed by the relation  $H = C0^n$ , where C and n are constants, n increasing from about 1.15 at M = 10 to a constant value of 1.33 beyond M = 10.

TABLE I—CONVECTION HEAT LOSS H/0 IN CALS./CM<sup>2</sup>. SEC. ° C

P	H/0 × 10 <sup>4</sup>	P	H/0 × 10 <sup>4</sup>	P	H/0 × 10 <sup>4</sup>
<i>l</i> = 0 325 cm.		<i>l</i> = 2.5 cm.		<i>l</i> = 22.9 cm.	
0.043	2.25	0.043	0.657	3.31	2.52
0.064	2.58	0.064	0.78	4.38	2.92
0.194	3.27	0.108	0.93	5.94	3.38
0.38	4.96	0.19	1.18	7.00	3.75
0.97	5.10	0.475	1.71	7.47	3.95
5.29	9.75	0.97	2.33	9.81	4.98
10.7	13.4	2.20	3.48	13.2	6.45
18.0	17.4	2.84	3.95	17.3	7.75
23.9	19.8	5.29	5.15	19.0	8.35
41.1	26.7	10.7	7.51	20.3	8.75
45.0	27.8	18.0	10.1	25.4	10.2
67.7	35.8	23.9	11.8	29.6	11.4
		41.1	16.1	35.2	13.1
<i>l</i> = 7.60 cm.		56.3	20.4	35.7	13.4
				45.7	16.0
0.035	0.40	<i>l</i> = 22.9 cm		53.5	18.0
0.145	0.72			54.8	18.5
0.375	1.12	1.0	1.49	64.3	21.0
1.01	1.81	1.68	1.84		
3.07	3.16	2.53	2.22		

In fig. 2 the results are plotted in dimensionless coordinates, the constants taken being given in Table II. It will be seen that the points for different height (*l*) agree well, their deviation from the mean curve being less than 6%.

Fig. 3 shows results by other experimenters for surfaces in atmospheric air, together with the mean curve from fig. 2. For the higher values of M there is fairly good agreement, the points tending to be above the curve, probably because many of the experiments were carried out under conditions in which draughts were not entirely excluded. For the lower values of M, King's results are in close agreement with the curve, but Griffiths and Davis's results for vertical cylinders with heavily insulated ends depart more and more from it as *l* decreases, probably on account of the increasing difficulty of allowing correctly for the end losses.

The results between  $M = 10^8$  and  $M = 10^{11}$  are of special interest, and are shown in fig. 4, using  $P$  and  $M^{\frac{1}{4}}$  as coordinates. The curve has points of inflection at about  $M = 1.7 \times 10^9$  and  $M = 7.0 \times 10^9$ , and becomes

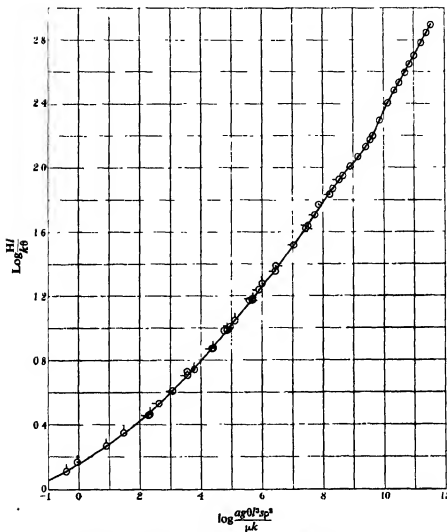


FIG. 2—Experimental results for vertical plane surface.  $\circ$   $l = 22.9$  cm.;  $\odot$   $l = 7.6$  cm.;  $\times$   $l = 2.5$  cm.;  $\bullet$   $l = 0.325$  cm.

a straight line above about  $M = 15 \times 10^9$ . If the heat loss per unit area  $h$ , at a distance  $l$  from the bottom of the vertical plane, be assumed independent of the height of plane above it, then  $h$  is equal to  $\frac{d}{dl}(Hl)$  and

is therefore proportional to the slope of the curve in fig. 4. Thus  $h$  appears to have minimum and maximum values at the two points of inflection, equal respectively to about 0.65 and 1.1 times its value when  $M$  is greater than  $15 \times 10^6$ . Griffiths and Davis† in their experiments with vertical cylinders, and also with a vertical wall built up in separately heated sections, found  $h$  a minimum at a height between 1 and 2 feet, which corresponds to a value of  $M$  between  $0.12 \times 10^6$  and  $1.0 \times 10^6$ .

TABLE II—CONSTANTS FOR AIR AT 43° C.

Pressure (atmospheres)	Viscosity ( $\frac{\text{gm.}}{\text{cm. sec.}}$ )	Coefficient of expansion ( ${}^\circ\text{C}^{-1}$ )	Density ( $\frac{\text{gm.}}{\text{cm.}^3}$ )	Thermal conductivity ( $\frac{\text{cal.}}{\text{cm. sec.} {}^\circ\text{C.}}$ )	Specific heat cal ( $\frac{\text{gm.}}{\text{gm.} {}^\circ\text{C.}}$ )
$P$	$\mu$	$a$	$\rho$	$k$	$s$
1	$185 \times 10^{-6}$	$367 \times 10^{-8}$	1.12	$10^{-3} 5.7$	$10^{-6}$
10	187	375	11.2	5.8	0.24
20	189	383	22.5	6.0	0.25
30	191	392	33.7	6.1	0.25
40	193	402	45.1	6.2	0.25
50	195	410	56.5	6.4	0.26
60	197	418	68.0	6.5	0.26
70	199	425	79.5	6.7	0.26

Values of  $a$ ,  $\rho$ ,  $s$ , are from the International Critical Tables. Values of  $\mu$  are from Michels and Gibson ('Proc. Roy. Soc., A, vol. 134, p. 288 (1932)) (for nitrogen). In obtaining  $k$ ,  $\mu s/k$  has been taken equal to 0.78 at all pressures. At pressures below 1 atmosphere,  $a$ ,  $s$ ,  $\mu$ , and  $k$  were taken the same as at 1 atmosphere, and  $\rho$  was assumed to follow Boyle's law.

and a constant value of  $h$  above about 4 feet, corresponding to  $M = 8.0 \times 10^6$ , but they did not observe an intermediate maximum value. They suggested, in explanation of their results, that the motion of the rising air changes from streamline to turbulent at a certain distance up the plate, and that finally, beyond a certain distance, the mean temperature and the mean upward velocity become constant. Thus the heat loss decreases with increasing distance up the plate where the motion is streamline, owing to the air becoming warmed, but increases when turbulence starts, and finally reaches a constant value. The author, using the refraction of a grazing ray of light to measure the air temperature gradient near, and normal to, the surface, found that the point of initial turbulence was very sensitive to draughts, which caused it to occur at a lower height than in undisturbed conditions. The somewhat higher critical values of  $M$  found in the present experiments, compared with those of Griffiths and

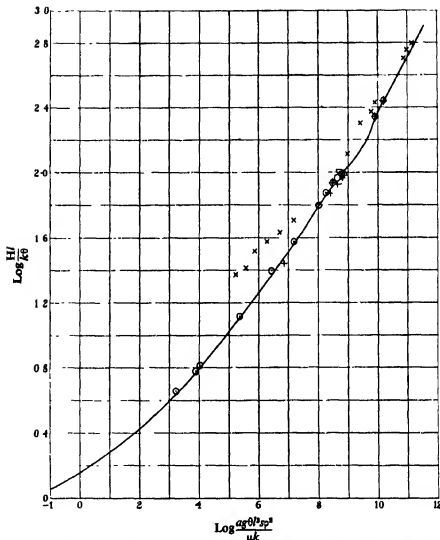


FIG. 3—Comparison of results with those of other experimenters.  $\times$  Griffiths and Davis;\*  $\odot$  King;†  $+$  Schmidt and Beckman;‡  $\oplus$  Carpenter and Wassell;§  $\nabla$  Nusselt and Jurgens;||  $\Delta$  Schad.|| Curve taken from author's results, fig. 2.

\* 'Spec. Rep. Food Invest. Bd.,' No. 9 (1922), revised ad., 1931.

† 'Mech. Engr.,' vol. 54, p. 347 (1932).

‡ 'Tech. Mech. Thermo-Dynam.,' vol. 1, pp. 341 and 391 (1930).

§ 'Proc. Instn. Mech. Eng.,' vol. 128, p. 439 (1934).

|| 'Z. Ver. deuts. Ing.,' vol. 72, p. 597 (1928).

¶ 'Heat. Pip. Air Condit.,' vol. 2, p. 957 (1930).

Davis,\* are probably to be explained by the steadier conditions inside the enclosure.

*Effect of Size of Enclosure*—For the higher values of M the air temperature falls sharply from the surface to a practically uniform value, but as M

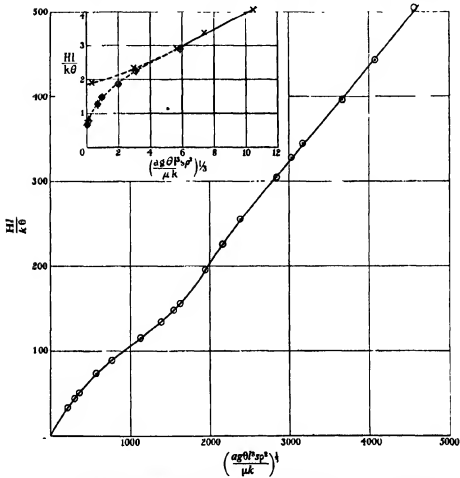


FIG. 4—Results in region of points of inflection.  $\oplus$   $l = 0.325$  cm.;  $\times$   $l = 2.5$  cm.;  $\odot$   $l = 22.9$  cm.

decreases the temperature gradient flattens out, until ultimately the uniform value is not reached at the position of the thermocouple midway between the surface and the enclosure walls. When this happens, the experimental results for  $H/\theta$  would be expected to cease to be independent

\* Special Rep. Food Invest. Bd., No. 9 (1922), revised ed., 1931.

of the size of the enclosure. The critical value of  $M$  must depend upon the ratio of the sizes of the hot surface and enclosure. The agreement between the points in fig. 2 for surfaces of different size shows that the enclosure is large enough for its effect to be neglected, within the limits of experimental accuracy, and that the results are applicable to conditions in which the volume of air is unlimited. In the small graph of fig. 4, results at pressures down to 0.001 atmospheres (lower than in fig. 2) are given, and there is agreement for the two sizes above  $M^{\frac{1}{2}} = 6$ , but below this value the larger surfaces give higher results. When  $M = 0$ , the heat flow is by pure conduction between the surface and the enclosure, and  $P$  is therefore greater for the larger surface; if the enclosure were infinitely large,  $P$  would have a definite value depending only on the shape of the hot surface.

*Experiments with Wires in Gases at High Pressures*—Many experimenters have measured the heat loss from horizontal cylinders of different diameters and temperatures in atmospheric air. A mean curve of the results, including some by the author for a cylinder of 2.5 cm. diameter at pressures from 1 to 65 atmospheres, is given in fig. 5. As already mentioned, values at high pressures were found by Petavel for a wire of diameter 0.0106 cm. in a horizontal enclosure of diameter 2.0 cm. containing various gases up to 170 atmospheres, and also recently, in some work not yet published, by the author's colleague, Mr. J. W. James, who used a wire and enclosure of the same size as Petavel's,\* and experimented with nitrogen up to 1000 atmospheres. Difficulties arise in attempting to express these results by dimensionless coordinates because the constants are not all known at these high pressures. In particular, the conductivity of gases, although known to be constant within certain limits, has not been measured at the higher pressures. It is interesting to note, however, that if  $\mu s/k$  is assumed constant up to 1000 atmospheres the points from the experiments quoted fall fairly well on the mean curve from results for larger diameters at atmospheric pressure (see fig. 5, in which the points up to 150 atmospheres are from Petavel's, and those from 250 to 1000 atmospheres from James's, experiments). Alternatively, assuming  $k$  to be constant up to 1000 atmospheres, the points from the same experiments fall on the branch marked 1. If the abscissa in fig. 5 is changed to  $MN = \frac{ag\theta^{\frac{1}{2}}s^{\frac{3}{2}}c^{\frac{1}{2}}}{k^{\frac{1}{2}}}$  (see Appendix) and  $k$  is assumed constant, the same values fall on the branch marked 2. Thus, whichever coordinate is taken, these results appear to afford evidence that  $\mu s/k$  is not far from

\* 'Phil. Trans.,' A, vol. 197, p. 229 (1901).

constant up to 1000 atmospheres, from which it follows that  $k$  increases considerably at the higher pressures. It is to be noted from fig. 5 that the range covered by results between 250 and 1000 atmospheres is comparatively small; hence results above about 200 atmospheres are of little value in defining the curve.

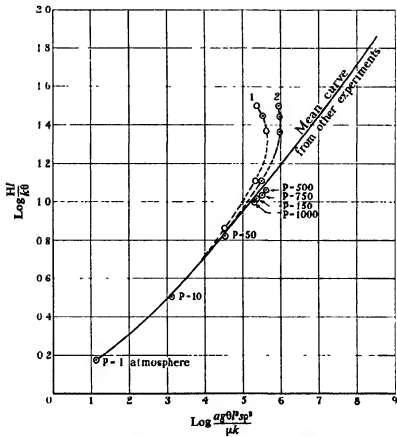


FIG. 5.—Experimental results for horizontal wire in nitrogen at high pressures.

#### SUMMARY

Dimensional considerations suggest that natural convection in air should depend upon the dimensionless number  $ag\theta^3sp^3/\mu k$ , the effect of which can be found experimentally by varying either the representative linear dimension  $l$ , the representative temperature difference  $\theta$ , or the pressure of the air. Many experimenters have determined the effect of  $l$  and  $\theta$  upon the heat loss from surfaces to the surrounding atmosphere,

but the effect of pressure has not been investigated systematically except in one particular case.

The present paper describes measurements with vertical plane surfaces of four different heights in air at pressures from 0·001 to 65 atmospheres. It is shown that the results can be expressed satisfactorily in terms of the dimensionless number, and values are given over a wide range. These are compared with, and are believed to be more accurate than, previous results of other experimenters obtained by varying the height at atmospheric pressure.

Natural convection at higher pressures, up to 1000 atmospheres, is also discussed, and results for a hot wire in nitrogen are mentioned. The values of some of the constants are uncertain at the higher pressures, but  $\alpha s \rho^3 / \mu k$  is not appreciably increased by raising the pressure above about 200 atmospheres. There is evidence from the results that  $\mu s/k$  is nearly independent of pressure up to 1000 atmospheres.

## APPENDIX

### *Note on the Dimensionless Numbers Associated with Natural Convection*

The association of the variables in the dimensionless numbers

$$M = \frac{\alpha g \theta l^3 s \rho^3}{\mu k} \quad \text{and} \quad N = \frac{\mu s}{k}$$

is based on the assumptions that the density is uniform and that the fluid at any point is acted on by an effective gravitational force —  $\rho ag(t - t_0)$  per unit mass, where  $t$  is the temperature, and  $t_0$  a fixed temperature. It may also be shown, on these assumptions, that if the momentum terms are omitted from the equations of motion, only  $M$  need be considered. If the viscosity terms are omitted, only the product  $MN$  need be considered.

In the general case of a viscous fluid whose density is a function of temperature the equations of motion may be written

$$\begin{aligned} & \left( u \cdot \frac{\partial}{\partial x} + v \cdot \frac{\partial}{\partial y} + w \cdot \frac{\partial}{\partial z} \right) (\rho u, \rho v, \rho w) - \nabla^2 (u, v, w) \\ & + \frac{g \rho_0^3 l^3}{\mu^3} \left( \frac{\partial}{\partial x}, \frac{\partial}{\partial y}, \frac{\partial}{\partial z} \right) P + \frac{g \rho_0^3 l^3}{\mu^3} (X, Y, Z) = 0, \quad (1) \end{aligned}$$

and the equation of conduction

$$\nabla^2 \theta = \frac{\mu s}{k} \rho \left( u \cdot \frac{\partial \theta}{\partial x} + v \cdot \frac{\partial \theta}{\partial y} + w \cdot \frac{\partial \theta}{\partial z} \right), \quad (2)$$

where  $x, y, z$  are dimensionless ratios of distances parallel to the axis to a fixed length ( $l$ ),  $u, v, w$  ratios of the velocity components to a fixed velocity  $u_0 = \frac{\mu}{\rho_0 l}$ ,  $\rho$  the ratio of the density to a fixed density  $\rho_0$ ,  $p$  the ratio of the pressure to a fixed pressure  $p_0 (= g\rho_0 l)$ ,  $\theta$  the ratio of the temperature to a fixed temperature  $\theta_0$ ,  $\mu$  the viscosity,  $s$  the specific heat per unit mass, and  $k$  the thermal conductivity. The axis of  $z$  is taken vertical.

For motion under gravity,  $X = Y = 0$  and  $Z = 1$ .

For a gas at constant pressure, using the dimensionless coordinates defined above,

$$\rho = (1 + a\theta_0)(1 + a\theta_0\theta)^{-1},$$

where  $a$  is the coefficient of expansion at  $\theta = 0$ .

Solutions of (1), (2), and (3) for any given boundary conditions of  $u$ ,  $v$ ,  $w$ ,  $\theta$ , and  $p$ , involve the three dimensionless numbers  $g\rho_0^2 l^3 / \mu^2$ ,  $\mu s/k$ ,  $a\theta_0$ . Thus the association of  $\rho_0$  and  $l$  in the number  $g\rho_0^2 l^3 / \mu^2$  is established without simplifying assumptions, except that the effect of local pressure differences upon the density is neglected in (3).

---

## The Diffusion of Gases Through Metals

### IV—The Diffusion of Oxygen and of Hydrogen Through Nickel at Very High Pressures

By C. J. SMITHILLS, D.Sc., and C. E. RANSLEY, B.Sc.

*(Communicated by R. H. Fowler, F.R.S.—Received 8 May, 1936)*

[PLATE 9]

The effect of pressure  $P$  on the rate of diffusion  $D$  has been measured for a large number of gas-metal systems. In a previous paper\* we have pointed out that the experimental results are more nearly represented by an equation

$$D = k \cdot \theta \cdot \sqrt{P} \quad (1)$$

than by the usual equation

$$D = k \cdot \sqrt{P}, \quad (2)$$

where  $\theta$  is the fraction of the surface covered by adsorbed gas atoms.<sup>†</sup>

Whilst equation (1) represented within the limits of experimental error all the systems so far investigated, its theoretical basis was obscure. The factor  $\theta$  was introduced on the hypothesis that the departure from the  $\sqrt{P}$  relation at very low pressures was due to the surface being incompletely covered with adsorbed gas. It has generally been assumed that the rate of diffusion is determined by three processes :—

- (i) Adsorption on the surface,
- (ii) Penetration of the surface,
- (iii) Diffusion through the metal,

each of which requires an activation energy.

\* Proc. Roy. Soc., A, vol. 150, p. 172 (1935).

† In that paper we substituted for  $\theta$  the Langmuir isotherm—

$$\theta = \frac{aP}{1 + aP},$$

but it has since been pointed out by Fowler (' Proc. Camb. Phil. Soc.,' vol. 31, p. 260 (1935)) that when the gas is dissociated, as it is in all cases of diffusion, the value of  $\theta$  is given by

$$\frac{aP^{1/2}}{1 + aP^{1/2}}.$$

Whilst at low pressures adsorption on the surface might well be the controlling process, when the surface becomes completely covered the rate should be independent of  $P$ , rather than proportional to  $\sqrt{P}$ . The rate of diffusion plotted against  $\sqrt{P}$  would then be like curve 2 in fig. 1 rather than curve 1, which represents equation 1.

There are no published data on the effects of pressures higher than about 1 atmosphere, and it seemed possible that the curves published in our previous paper might have shown a departure from the square root relation at sufficiently high pressures.

Two systems have therefore been studied. The rate of diffusion of hydrogen through nickel has been measured at pressures up to 112 atmospheres, at  $248^{\circ}\text{C}$ , and  $400^{\circ}\text{C}$ . This is a typical representative of those

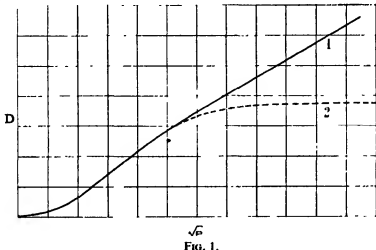


FIG. 1.

systems in which no definite metal-gas compound is formed. The diffusion of oxygen through nickel, which involves the presence of a definite oxide film at higher pressures, has also been studied. We may anticipate the results by saying that in the case of oxygen the rate of diffusion becomes independent of the pressure at quite low pressures, but with hydrogen the rate remains accurately proportional to  $\sqrt{P}$  even up to 112 atmospheres.

#### DIFFUSION OF HYDROGEN THROUGH NICKEL

*Apparatus*—The apparatus is illustrated in fig. 2. Diffusion was measured through a diaphragm A, 0.35 mm. thick, and of sufficiently small area ( $1.25\text{ cm.}^2$ ) to withstand high pressures. This was clamped rigidly between the accurately-faced ends of two thick-walled nickel tubes B, by

means of a screwed collar C. The outer edge of the diaphragm, and the collar, were copper brazed in hydrogen, as shown in detail in fig. 2b. This gave a perfectly tight joint, and the copper did not penetrate to the surface of the diaphragm.

A small electric furnace D enabled the diaphragm to be maintained at any desired temperature, registered by the thermocouple E inserted in a hole in the collar.

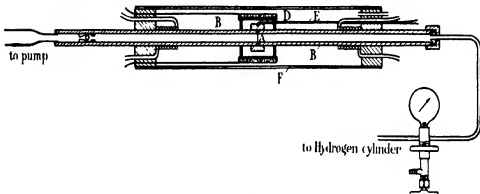


FIG. 2a.

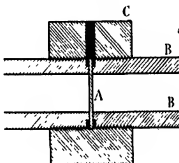


FIG. 2b.

The nickel tube, water-cooled at both ends, was surrounded by a metal jacket F, which was continuously evacuated to prevent indirect diffusion through the walls of the tube B. One end of the nickel tube was soldered to a copper thimble sealed directly to the glass diffusion pump and analytical system described previously.\* This enabled a vacuum of  $10^{-4}$  mm. of mercury to be maintained on one side of the diaphragm. The other end of the nickel tube was connected by thick-walled copper pipe to a hydrogen cylinder fitted with a fine adjustment tap, and to another tap opening

\* *Loc. cit.*

directly to the air or rough vacuum. The pressure was measured by a Bourdon tube gauge which had been calibrated by a deadweight method.

*Materials*—The nickel diaphragm was rolled sheet of the following analysis :—

	%
Manganese .....	0·13
Iron .....	0·12
Magnesium.....	0·09
Carbon .....	0·01

Electrolytic hydrogen, purified by bubbling at high pressure through molten sodium, was stored in cylinders previously dried by evacuation for two days.

*Experimental Results*—Since both sides of the diaphragm could not be subjected to high vacuum, the metal was degassed by heating in hydrogen, which was flushed out repeatedly. The efficiency of this method of removing other gases has been established in a previous paper.\* The tube was then run for some hours until the rate of diffusion was found to be constant.

The rate of diffusion was determined at various pressures between 10 and 112 atmospheres, both at 248° C., and at 400° C. Higher temperatures could not safely be used at these pressures. Under these conditions an accurate determination of the rate could be made in about 20 minutes. Measurements made with both increasing and decreasing pressures showed no signs of hysteresis. The results are recorded in figs. 3 and 4, where the rate of diffusion  $D$ , in cm.<sup>3</sup> per second per cm.<sup>2</sup> of surface 1 mm thick, is plotted against the square root of the pressure. The results leave no doubt that over this range of pressure the square root law is accurately obeyed. The temperature coefficient for the diffusion of hydrogen is high, and the spread of the individual readings would be almost entirely accounted for by a variation in temperature of  $\pm 2^\circ$  C.

The values of  $b$  and  $k$  in the diffusion equation

$$D = \frac{k}{d} \sqrt{P} e^{-b/T},$$

calculated from these results are compared in Table I with published data obtained at higher temperatures and lower pressures.

This order of agreement is satisfactory and indicates that these values are constants for the nickel-hydrogen system and are independent of the origin and structure of the metal.

\* 'Proc. Roy. Soc.,' A, vol. 155, p. 195 (1936).

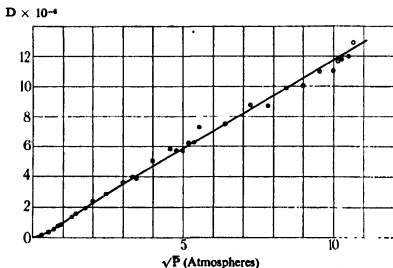


FIG. 3—Diffusion of hydrogen through nickel at 248° C.  $\circ$  High pressure measurements;  $\bullet$  low pressure measurements.

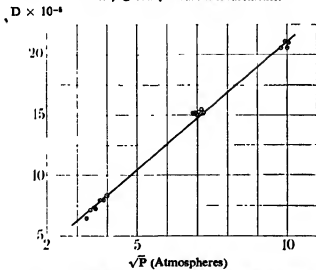


FIG. 4—Diffusion of hydrogen through nickel at 400° C.

TABLE I—DIFFUSION CONSTANTS FOR HYDROGEN-NICKEL

Author	$b$	$k$
Lombard (1923) .....	7,710	$2 \cdot 3 \times 10^{-8}$
Deming and Hendricks (1923) .....	6,930	0.85
Borelius and Lindblom (1927) .....	6,900	1.4
Ham (1933) .....	6,700	1.05
Smithells and Ransley .....	6,630	1.44



Section through wall of diffusion tube (200)



When the high pressure experiments had been completed, the rate of diffusion at 248° C. was determined at low pressures. For these measurements the high pressure system was disconnected, and the nickel tube connected to a high vacuum system. After prolonged degassing at 400° C., the rate of diffusion was measured with hydrogen pressures varying from one atmosphere pressure down to 3 mm. of mercury. The results are plotted in fig. 5, and show the same deviation from the square root relation that we have described in our earlier paper.

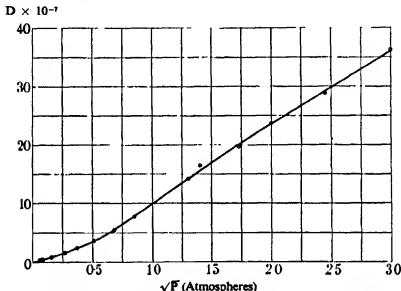


FIG. 5.—Diffusion of hydrogen through nickel at 248° C., and at low pressures.

*Diffusion of Oxygen Through Nickel*—The method of measuring the diffusion of oxygen through nickel was described in a previous paper\* which dealt only with the effect of temperature. The principle of the method was to maintain a pressure of oxygen on the outside of a nickel tube, the inner surface of which was carbonized, and to measure the rate of production of CO inside the tube. From this the rate of diffusion of oxygen can be calculated. The measurements were made at 900° C. on the same apparatus as previously described, and on three different nickel tubes having the following analysis :—

	%
Carbon .....	0.012
Iron .....	0.13
Magnesium.....	0.04

\* 'Proc. Roy. Soc.,' A, vol. 155, p. 195 (1936).

With pressures of oxygen below about 0.1 mm. the surface of the tube remained untarnished. With pressures above 0.25 mm. the surface was always covered with a visible layer of green nickel oxide. The measurements are given in detail in Table II and fig. 6. It will be seen that at pressures above 0.25 mm. the rate of diffusion is substantially constant, even up to 112 mm., but that below 0.25 mm. the rate of diffusion falls off. In the latter range the rate appears to be roughly proportional to the square root of the pressure, but the measurements are not of sufficient accuracy to establish this with certainty.

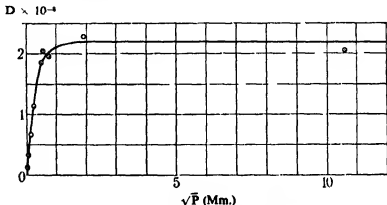


FIG. 6—Diffusion of oxygen through nickel at 900° C.

TABLE II—DIFFUSION OF OXYGEN THROUGH NICKEL AT 900° C.

Tube No	Oxygen pressure	Rate of evolution of CO	Rate of diffusion of
	P mm.	cc/sec./cm. <sup>2</sup> for 1 mm. thick	oxygen D
5	0.0012	$0.22 \times 10^{-8}$	$0.11 \times 10^{-4}$
5	0.0048	0.62	0.31
3	0.025	1.32	0.66
3	0.050	2.27	1.13
3	0.25	3.69	1.84
4	0.30	4.07	2.03
4	0.57	3.92	1.96
4	3.77	4.60	2.30
4	112.0	4.13	2.06

#### GENERAL DISCUSSION

The diffusion process includes two important steps:—

- (a) Passage of the gas into the metal.
- (b) Diffusion through the metal.

It is possible that either of these may be so slow compared to the other as virtually to control the rate of diffusion.

The diffusion of oxygen through nickel at 900° C. becomes independent of pressure at about 0·25 mm. Above this pressure a layer of nickel oxide is visible on the surface. Plate 9 shows a section through the wall of a tube that had been used for diffusion measurements. It will be seen that a zone rich in nickel oxide has formed to a depth of about  $2 \times 10^{-3}$  cm. below the surface of the metal. At 900° C. nickel dissolves about 1·1% NiO. The depth of this zone increases steadily because the rate of passage of oxygen through the surface is faster than the rate of diffusion through the metal. The rate of diffusion is simply determined by the difference in the oxygen concentration in this zone and at the inner surface of the tube, where it is substantially zero. Oxygen is supplied to the nickel from the oxide layer at a rate which is independent of the gas pressure. The gas pressure may influence the rate of oxidation (although even this is doubtful\*) but cannot influence the rate of diffusion. This explanation of the constancy of the rate of diffusion at pressures above the critical value of 0·25 mm. is independent of any assumptions regarding the nature of the reactions taking place at the gas-metal interface. At lower pressures, when no oxide is formed on the surface, we may assume that the rate of penetration through the surface is the limiting factor and that diffusion in the metal is comparatively rapid. In this range of pressure the rate of diffusion appears to be roughly proportional to  $\sqrt{P}$ , and is therefore similar to the diffusion of hydrogen.

Roberts† has recently given a theory of adsorption, which postulates an incomplete layer of adsorbed atoms the gaps in which are covered by adsorbed molecules. Melville and Rideal‡ have developed a formal equation for diffusion based on this conception of the nature of the adsorbed layers. If the concentration of adsorbed molecules is  $[H_s]$  and the concentration of hydrogen atoms just inside the metal is  $[H]$ , then at equilibrium

$$k_1 [H_s] - k_2 [H]^2 - k_3 [H] = 0, \quad (3)$$

the second term being due to evaporation from the surface of pairs of atoms, and the third term due to diffusion through the metal. They also point out that

$$[H_s] = k \frac{aP}{1 + aP} = k\theta. \quad (4)$$

\* See Wilkins, ' Proc. Roy. Soc.,' A, vol. 128, p. 407 (1930).

† ' Proc. Roy. Soc.,' A, vol. 152, p. 445 (1935).

‡ ' Proc. Roy. Soc.,' A, vol. 153, p. 89 (1935).

Equation (3) therefore implies that when  $\theta = 1$  the rate of diffusion will become independent of pressure. For the nickel-hydrogen system at 250° C.,  $\theta = 0.9$  at 200 mm. pressure,\* and therefore the rate of diffusion should show some indication of becoming independent of pressure above this value.

The theory given above is based on the assumption that the rate of supply of H atoms depends solely on the concentration of adsorbed molecules in the second layer.

It appears to us from the present experiments, however, that the gas phase may have a more direct effect on diffusion than that of merely maintaining an adsorbed layer, since all the experimental evidence indicates that adsorption, as measured in the usual way, is sensibly complete at pressures of the order of one atmosphere.

To explain the continued effect of pressure, it is suggested that the rate of diffusion at higher pressures depends mainly on the impact of molecules from the gas phase on the atoms adsorbed on the surface. If the impinging molecules have sufficient energy, the adsorbed atoms may acquire the energy necessary to penetrate the surface, and the rate of diffusion will continue to be a direct function of pressure even after adsorption is complete.

The activation energy necessary for penetration is not known exactly, but for the palladium hydrogen system it is 2500 cal./mol.† It is certainly small compared with the total activation energy of the diffusion process, which for hydrogen-nickel is 26,500 cal./mol. We may safely assume, therefore, that it is not greater than 5000 cal./mol. It may readily be shown that at 248° C., the number of hydrogen molecules  $N$ , striking 1 cm.<sup>2</sup> of surface per second with an energy exceeding this value is sufficiently large to account for the observed rate of diffusion. For example, at 10 atmospheres pressure, the value of  $N$  is  $1.3 \times 10^{38}$  molecules per second, whilst the observed rate of diffusion for a thickness of 1 mm. and 10 atmospheres pressure only corresponds to  $1.1 \times 10^{14}$  mols. cm.<sup>2</sup>/sec. It is therefore clear that the energy necessary for penetration of the surface can be derived from the kinetic energy of the gas molecules.

Assuming this mechanism, it is possible to derive a basic equation for diffusion of the form

$$D = A \{ \sqrt{1 + Kf(P)} - 1 \} \quad (5)$$

where  $D$  is the rate of diffusion,  $P$  the pressure, and  $A$  and  $K$  are terms

\* Gauger and Taylor, 'J. Amer. Chem. Soc.', vol. 45, p. 920 (1923); Smittenburg, 'Rec. Trav. Chim.', vol. 52, p. 112 (1926).

† Melville and Rideal, 'Proc. Roy. Soc.,' A, vol. 153, p. 89 (1935).

which include  $\theta$ , the fraction of surface covered. The exact form of the equation depends upon the particular collision mechanisms which are considered.

If all types of collision were effective, then as soon as the surface was completely covered (*i.e.*, above 1 atmosphere pressure) increasing the pressure by means of an inert gas should increase the rate of diffusion. We therefore measured the rate of diffusion at 248° C. when the pressure was increased from 4 atmospheres of hydrogen up to 100 atmospheres by the addition of argon. The rate of diffusion was entirely unaffected by increasing the pressure in this way. This indicates that of the possible types of collision, only those which involve the simultaneous adsorption of the impinging molecule are effective in causing diffusion.

A simple form of equation (5)

$$D = A \{ \sqrt{1 + K\theta P} - 1 \} \quad (6)$$

can be made to agree very closely with the experimental results for several systems, by selecting suitable values for  $a$  in the adsorption isotherm.

The validity of the equation cannot be checked conclusively, however, in the absence of exact knowledge of the form of the adsorption isotherm under the conditions of the diffusion measurements. Adsorption measurements made with powders, and at lower temperatures, cannot be assumed to apply to sheet metal surfaces at higher temperatures. Such measurements must be made before the mechanism of the diffusion process can be established, but the present experiments serve to indicate that some of the energy for diffusion is probably derived from the kinetic energy of the gas molecules.

In conclusion, the Authors desire to tender their acknowledgments to the General Electric Company and the Marconiphone Company, on whose behalf the work was done which has led to this publication.

#### SUMMARY

Recent theories of diffusion, in which adsorption at the gas-metal interface was assumed to be the controlling factor, indicate that the rate of diffusion should become independent of pressure at high pressures.

The rate of diffusion of oxygen through nickel at 900° C. has been measured and found to be independent of the oxygen pressure above 0.25 mm. This is shown to be due to equilibrium between the concentration of oxygen just inside the metal and the layer of nickel oxide formed on the surface, with which it is in contact.

The rate of diffusion of hydrogen through nickel has been measured at pressures up to 112 atmospheres, at 248° C. and at 400° C. The rate of diffusion is proportional to the square root of the pressure within the accuracy of measurement at the highest pressures. The rate of diffusion at 248° C. has also been determined at pressures down to 3 mm., and shows the usual deviation from the square root law at pressures below 4 atmospheres.

A tentative theory of the mechanism of diffusion is advanced, which accounts for the continued effect of pressure after adsorption is sensibly complete.

---

## The Anomalous Scattering of Protons in Light Elements

By E. G. DYMOND, Carnegie Teaching Fellow, University of Edinburgh

(Communicated by C. G. Barkla, F.R.S.—Received 15 May, 1936)

By a study of the scattering of protons by atomic nuclei we can gain information about the interactions of these particles. For sufficiently low velocities of the impinging protons, corresponding to 30 electron kilovolts, it has been shown by Gerthsen\* that they are scattered by celluloid according to the Rutherford law, and by hydrogen according to the Mott law of scattering of similar particles. At a distance of approach represented by this energy, the inverse square law of force still holds between the particles. Schneider† has investigated the scattering of protons of energies up to 300 e.-kv. in aluminium, carbon, and boron. He found a pronounced maximum in the scattering by boron, compared with that by aluminium, at 200 e.-kv. It is not possible to say whether this anomaly is due to a breakdown in the Coulomb law of force between the boron nucleus and a proton, as he used thick layers of scattering material, a fact which renders the interpretation of his results difficult.

The present work was undertaken with a view to checking these results, using sufficiently thin targets to ensure single scattering. Schneider's observations have not been confirmed, although other anomalies have presented themselves.

\* 'Ann. Physik,' vol. 86, p. 1025 (1928); vol. 9, p. 769 (1931).

† 'Naturwiss.,' vol. 21, p. 349 (1933).

## APPARATUS

The source of protons was a canal ray tube of the type developed by Oliphant.\* This type of tube provides a beam of high intensity. The main accelerating tube, also of type similar to Oliphant's, was fed from a voltage doubling circuit, providing steady potentials up to 200 kv. The accelerated protons traversed a magnetic field to separate them from the molecular ions and entered the scattering chamber (fig. 1) through two 1 mm. diameter holes spaced 25 mm. apart. The maximum intensity of

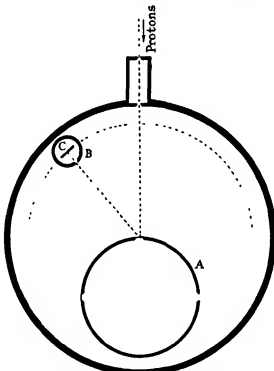


FIG. 1—Diagram of scattering chamber

the collimated beam entering the chamber was  $2 \times 10^{-7}$  amperes. The scattering material, in the form of a thin film, was mounted in the centre of the chamber, on an insulated cylinder A. The major part of the beam traversed the film and was trapped in A, which was connected to a galvanometer to measure the beam intensity. Other films were mounted on the periphery of A and could be brought into position by rotating A. One aperture, exactly similar to the others, had no film mounted on it. When

\* 'Proc. Roy. Soc.,' A, vol. 141, p. 259 (1933).

this aperture was in position a blank determination gave the amount of stray scattering from the rest of the apparatus. As the protons entered the chamber in a beam 1 mm. in diameter, and the apertures in A were 4 mm. diameter, this stray effect was small and never more than a few per cent. of the scattering from the films.

The scattered beam entered a slit in the earthed cylinder B and struck C, which was connected to the grid of an electrometer valve. B and C could be rotated about the centre of the chamber (and scattering film) so that angles of scattering from  $110^\circ$  to  $160^\circ$  could be used. Initially a Faraday cylinder was employed instead of the plate C, in order to give a true measure of the proton current. This current was, however, only just on the limits of measurement, with the thickness of films used, so that in the final arrangement the cylinder was replaced by a platinum plate. One proton liberated many electrons from C, so that the observed positive current to the grid of the valve was about twenty times the proton current. It was found that after suitable ageing of the platinum surface this multiplying factor, for a given proton energy, remained sensibly constant. It varied, however, with the energy in a manner which could be determined. This point will be discussed below, but it may be mentioned here that the method of taking observations eliminated the effect of the variation of this factor.

The main beam of protons also liberated copious secondary electrons in A, besides giving rise to soft X-rays, and photoelectrons throughout the chamber. It was necessary to cover the slit B with layers of aluminium foil of combined thickness  $10^{-6}$  cm. to exclude slow particles (protons and electrons) from the collector. Also A was charged to 240 volts positive to entrap the slow electrons. The necessity for these precautions will be appreciated when it is realized that the scattered current to C was  $10^{-14}$  amps., at most, while the electron emission from A when earthed amounted to about 1 milliamperc. The smallest hole in the aluminium foil protecting the collector admitted sufficient electrons to vitiate the results. It was possible to test whether the exclusion of electrons was complete by varying the potential on A. With two sound foils, prepared by the evaporative process, over the slit, no change in the current to C could be detected when this potential was increased from 120 to 240 volts. The latter value was accordingly used in all the measurements.

The collector C was connected to an electrometer valve (G.E.C. electrometer triode), as vibration from the neighbouring machinery rendered an electrometer unsuitable. The valve, together with earthing key and lead to the collector, were placed in an evacuated chamber to eliminate leaks due to X-rays. It was connected in the balanced bridge circuit described

by Turner and Siegelin\* and with the galvanometer employed gave a sensitivity of 11,000 mm./volt. It was used with the rate of drift (free grid) method of observation. In these conditions the limit of sensitivity is set by the natural drift with no proton current. This drift is compounded of two parts, that due to the grid current of the valve, and the drift of the bridge itself. The former, with due care, was reduced to  $1.5 \times 10^{-16}$  amps., and the latter, though variable, was equivalent to a current of about the same magnitude. The bridge drift was closely correlated with temperature fluctuations of the room and was traced to thermal expansion of the valve itself. The rest of the bridge was either thermally insensitive or could be maintained at a constant temperature. As the natural drift only varied slowly and could be accurately observed, the current sensitivity could be taken as  $1.0 \times 10^{-16}$  amps.

The proton energy was obtained from the magnetic field required to bend the beam into the scattering chamber. As the defining apertures were small, this field was quite critical. A sphere spark gap to measure the accelerating voltage enabled the magnetic field to be calibrated against proton energy. The absolute values of the energies may be in error by 5% or more, but their relative values should be correct to about 1%.

#### THE SCATTERING FILMS

Scattering was observed in Ag, Al, B, and Be. The films were always prepared by evaporating on to a cellulose nitrate base which was subsequently removed by solvents. The usual technique of evaporating from a bead placed on a coiled tungsten filament could not be applied, as special care had to be taken that the films were free from impurities, especially of heavy elements. Also it is not possible to evaporate boron by this method owing to the very high temperature required (2500° K.). All the elements used, with the exception of silver, dissolve tungsten and rapidly attack the filament, and under these conditions it is to be expected that traces of tungsten will be carried over with the vapour. In fact, Strong† has demonstrated the presence of tungsten lines in the spectrum of evaporating aluminium. As the scattered intensity varies as  $Z^2$ , 0.1% of tungsten in a beryllium film would contribute 40% of the total scattering.

Accordingly, a modification of the technique described by O'Bryant‡ was used. The material to be evaporated was heated in a very small crucible of pure graphite by electron bombardment. The base to receive

\* 'Rev. sci. Instrum.', vol. 4, p. 429 (1933).

† 'Phys. Rev.', vol. 48, p. 136 (1935).

‡ 'Rev. sci. Instrum.', vol. 5, p. 125 (1925).

the film was shielded from the filament, which was made of large size so that it could be run at a relatively low temperature. Tungsten contamination of the films should be very small under these conditions.

The silver films may have contained traces of copper, but as these films were used as standards, presumed to give only classical scattering, traces of such impurities were unimportant. The aluminium was commercial wire containing probably traces of iron, of which only a very small fraction should have been carried over on to the film, which may be assumed to have been of high purity. The source of beryllium was a spectroscopically pure specimen (H.S. brand) from Hilger. The boron films alone were of doubtful purity. Carbon (as carbide) and aluminium are common impurities, and carbide is formed by reaction with the graphite crucible. It is known, however, that the carbide is considerably more refractory than boron itself, and should not evaporate to any large extent. As its nuclear charge approximates to that of boron, carbon should not exert a serious influence on the results. The aluminium impurities cannot be so lightly dismissed. The cellulose nitrate base was protected by a shutter while the crucible was being heated up and was not exposed until evaporation of the boron had already started. As this does not occur till about 2500° K., most of the aluminium should have distilled off first; but it is not possible to be sure of this.

The thickness of the films was computed from their optical transmissions. The thicknesses were  $2 \cdot 3$  to  $3 \cdot 7 \times 10^{-6}$  cm. for silver,  $3 \cdot 8$  to  $6 \cdot 5 \times 10^{-6}$  cm. for aluminium, and  $10 \cdot 4 \times 10^{-6}$  cm. for beryllium. The optical constants of boron are not known, but from their mechanical properties the boron films seemed to be of the same order of thickness.

## RESULTS

For reasons to be discussed below, the results in the various elements were referred to those in silver as standard.

In fig. 2 are plotted the ratios of scattered intensities  $I/I_{\text{st}}$ , where  $I_{\text{st}}$  is the intensity from silver, which was assumed to behave classically. The results for two angles  $110^\circ$  and  $150^\circ$  are shown. The probable errors determined statistically from the individual readings are also indicated. All the curves have been fitted at the lowest proton energy, 130 e.-kv.

It will be seen that both aluminium and beryllium give an excess scattering for faster protons. In aluminium the excess is greater at the greater angle (closer distance of approach), while the reverse is true in beryllium. The maximum at about 170 e.-kv., for beryllium at  $150^\circ$ , may not be real, as may be seen from an inspection of the probable errors,

which are themselves liable to error owing to the limited number of readings.

For the same reason the deviations for boron, which are at most 3%, can be given little weight, and it would be safer to assume on the evidence here presented, that the scattering in boron is normal. There is no trace of the anomaly found by Schneider with thick layers of material.

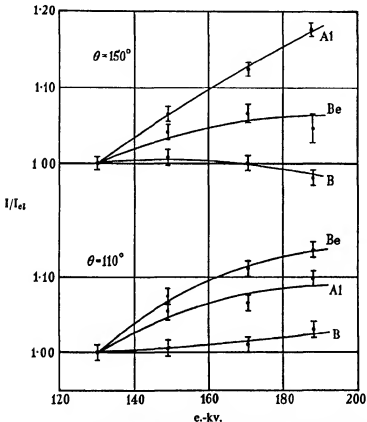


FIG. 2—Curves of scattering against proton energy in aluminium, boron, and beryllium, for two angles  $110^\circ$  and  $150^\circ$ . The ratio  $I/I_{el}$  of the scattering to that in silver is plotted.

#### DISCUSSION

Before discussing the deviations which have been observed, it is necessary to be sure that the measurements on the silver films really represent classical scattering. It was unfortunately impossible to measure absolutely the variation of scattering with proton energy. Before entering the collector the protons must first have penetrated a layer of aluminium

$10^{-6}$  cm. thick, which was required to exclude electrons and slow protons. This layer scattered and retarded the beam so that the number actually arriving at the collector was a function of the energy of the particles. Further, the current to the collector was increased by secondary electron emission, and this increase was also a function of energy. These two effects were measured and attempts were made to correct the results accordingly, but the corrections required amounted to 30% at the highest energy, and as they could not be made with any degree of precision they could not be regarded as reliable.

Accordingly, it was decided to treat the scattering from silver as classical and compare with it directly the scattering from other elements. The high atomic number (47) of silver makes anomalous scattering in the energy region explored extremely unlikely. Single scattering was assured by using sufficiently thin films. The thickest film was  $3.7 \times 10^{-6}$  cm., as calculated from its optical transmission. For this film the Wentzel criterion as modified by Rose, gives  $14^\circ$  as the minimum angle for single scattering for an energy of 160 e.-kv. The smallest angle used was  $110^\circ$ , so the criterion was fulfilled by a wide margin.

Another factor which must be taken into account is the loss of energy of the proton as it traverses the film; this renders the actual energy of the proton when it is scattered slightly uncertain. The loss, as calculated from the data of Blackett and Lees,\* amounts to 4.3 e.-kv. for a 140 e.-kv. proton traversing  $3.7 \times 10^{-6}$  cm. of aluminium. The loss in silver may be three or four times as great, the uncertainty arising from doubt of the mean ionization potential of silver. As, however, the range-energy curve for low velocity protons is sensibly straight, this loss of energy will be substantially the same throughout the energy region explored in this investigation. We may therefore correct the scattering curves, by shifting the energy scales by approximately half this loss, to arrive at the mean energy of scattering. The scale for silver should accordingly be shifted by about 5 e.-kv. in a downward direction with respect to aluminium.

If this is done the slopes of the aluminium curves in fig. 2 are slightly reduced, but by little more than the probable errors of the individual points. The energy loss in the beryllium films was almost the same as that in aluminium, the effect of lower atomic number being balanced by the greater thickness of film, so that the correction is the same as for aluminium. It is likely that the same is true for the boron films, although their thickness cannot be directly estimated.

\* 'Proc. Roy. Soc.,' A, vol. 135, p. 132 (1932).

The most conclusive evidence that these losses are not important, however, lies in the comparison of scattering from silver films of different thicknesses. In a range from  $2 \cdot 3$  to  $3 \cdot 7 \times 10^{-6}$  cm. no systematic variation in scattering was detected, the variation found being within the probable errors of the individual measurement.

It is justifiable, therefore, to regard the deviations from classical scattering found in aluminium and beryllium as real. Doubt arises, however, in the case of boron for which the evidence for any anomaly is not strong enough.

These deviations are to be interpreted on a classical picture as a breakdown in the inverse square law of force between proton and nucleus. The closest distances of approach for a 190 e.-kv. proton scattered at  $150^\circ$  are  $9 \cdot 0 \times 10^{-13}$  cm. in aluminium, and  $2 \cdot 9 \times 10^{-13}$  cm. in beryllium. These may be compared with the values found by Riezler\* to give anomalous scattering of  $\alpha$ -particles. He found distances of  $6 \times 10^{-13}$  cm. for aluminium and  $4 \cdot 8 \times 10^{-13}$  cm. for boron. The "radius" of the nucleus towards protons would seem to be much greater.

The more exact wave mechanical picture attributes the breakdown of the classical law to a penetration of the potential barrier by the impinging particle. The amount of this penetration can be calculated from the work of Gamow, using the modified formula given by Cockcroft.† It is found to be quite insignificant in aluminium. If we assume that the proton, after penetrating the barrier, is subsequently expelled in a random direction we can calculate the contribution of these protons to the scattering at  $180^\circ$ . It is found to be 1% of the classical scattering in beryllium and several times less in boron. Its influence would be more apparent in lithium, amounting to 6.5%. Comparison with the experimental curves shows, therefore, that this simple type of penetration is quite inadequate to account for them.

Resonance levels for the proton in the nucleus will allow of greatly increased penetration, and it is necessary to presume their existence to account for the results. The low values required for the energies of these levels, especially for aluminium, are surprising. Proton levels in light nuclei have been detected by Hafstad and Tuve,‡ who gave them energies of 450, 400, and 300 e.-kv. in Li, C, and F1 respectively.

No indication of levels of lower energy as required to explain the anomalous scattering were found, but this does not preclude their existence, as Hafstad and Tuve could only observe levels whose occupation leads to disintegration.

\* Proc. Roy. Soc., A, vol. 134, p. 154 (1931).

† Int. Conf. Phys. London, vol. 1, p. 126 (1934).

‡ Phys. Rev., vol. 47, p. 507 (1935).

The modification in the scattering brought about by resonance levels has been studied by Mott,\* who gives a curve showing the ratio of the scattering to the classical value in the neighbourhood of a resonance S level. The first effect of increasing the proton energy is a decrease in the ratio  $I/I_{cl}$ . This is the reverse of what the experimental results show so that we may conclude that an S level is not concerned either in aluminium or in beryllium. Calculations for other levels† show that for a P level  $I/I_{cl}$  initially behaves in the same way, but will rise for a D level. We may conclude, therefore, that the latter is responsible for the anomalous scattering. This is not unlikely when we consider the large number of units of angular momentum possessed by the proton. It is, however, quite possible that two or more neighbouring levels, one of which is a D, are concerned. The experimental curves do not extend to high enough energies to discuss more fully these possibilities. The only conclusion which we can at present draw is that proton levels at or a little above 200 e.-kv. exist both in the aluminium and the beryllium nuclei.

I am indebted to the Moray Fund of the University of Edinburgh for a grant to defray part of the cost of the new equipment, and to the Government Grants Committee of the Royal Society for the continued use of some of the high tension apparatus.

#### SUMMARY

Measurements have been made of the scattering of protons, 130 to 190 e.-kv. in energy, from thin films of silver, aluminium, boron, and beryllium. The results are given in terms of the ratio of the scattering in silver and in the other elements, as it may be assumed that silver scatters classically.

It is found that at 190 e.-kv. in aluminium there is an excess scattering of  $17.6 \pm 1.8\%$  at  $150^\circ$  and  $9.7 \pm 1.0\%$  at  $110^\circ$ , and in beryllium  $4.4 \pm 1.6\%$  at  $150^\circ$  and  $13.5 \pm 1.0\%$  at  $110^\circ$ . Within the limits of probable error the scattering in boron is normal.

To account for these results it is necessary to assume that existence of resonance D levels for the proton in aluminium and beryllium in the neighbourhood of 200 e.-kv. These levels are considerably lower in energy than any that have been previously found by other means.

\* Proc. Roy. Soc., A, vol. 133, p. 228 (1931).

† I am much indebted to Professor Mott for giving me the necessary data with which to make these calculations.

---

# The Electrical Conductivity of Thin Metallic Films

## I—Rubidium on Pyrex Glass Surfaces

By A. C. B. LOVELL, H. H. Wills Physical Laboratory, University of Bristol

(Communicated by A. M. Tyndall, F.R.S.—Received 16 May, 1936)

### 1.—INTRODUCTION

This paper describes measurements of the resistivity of thin films of rubidium, deposited on cooled pyrex surfaces by a method which allows the use of the conditions of purity and high vacuum possible with modern technique.\*

In this work, by vigorous heat treatment in high vacua, clean pyrex surfaces have been obtained on which stable and coherent films as thin as 40 Å. have been produced. Conductivities have been obtained with a number of atoms on the surface corresponding to less than the number contained in a monatomic layer of rubidium; moreover, the approach of thicker films to the resistivity of the bulk metal is in agreement with that calculated from a simple theory which takes account of the fact that the film thickness is less than the normal electronic mean free path in the bulk metal.

In contrast with this, it may be noted that the features of previous work on thin films have been the complete non-conductivity of films less than several atomic layers in thickness, and the failure of films of many hundred atomic layers to approach the resistivity of the bulk metal. For example, Braunbek† condensed mercury vapour on a cooled surface and obtained films of 1000 layers in thickness, having resistivities still three times in excess of the bulk metal.

In most of the previous work the films have been deposited by cathode sputtering which has prohibited the use of high vacuum conditions. The discrepancies which exist in the previously published work are undoubtedly due to the many uncontrollable effects which are unavoidably introduced by such methods of deposition (*cf.* Andrade and Martindale).‡

\* A preliminary announcement of these results appeared in 'Nature,' vol. 137, p. 493 (1936).

† 'Z. Phys.,' vol. 59, p. 191 (1930).

‡ 'Phil. Trans.,' A, vol. 235, p. 69 (1935).

For a bibliography of work prior to 1928 cf. Bartlett.\* In recent years work has been done principally by Reinders and Hamburger,† Perucca,‡ Braunbek,§ Braunsfurth,|| Zahn and Kramer,¶ Kramer,\*\* and Murnmann.††

An investigation of the effects of the substrate in the present work has given a probable explanation of the anomalous behaviour of thin films found by all previous workers. The nearest approach to the present low resistivities is in the work of Reinders and Hamburger,† who deposited films by evaporation from silver and tungsten wires *in vacuo*. Conductivities were observed with single layers of tungsten on the surface, but even at thicknesses of 400 atomic layers the resistivities were still 10 to 100 times in excess of that of the bulk metal, while in the case of films 40 Å. thick (where the author's resistivities have been only 10 times greater than that of the bulk metal), those of Reinders and Hamburger were as much as 10,000 times greater.

A theory of the increase of resistance in thin films in terms of the modification in the mean free path of the electrons was given by J. J. Thomson,†† but previously the experimental values have been much too high to be explained on any such simple theory, and authors have postulated various types of structure to account for their own results. The present results are accurately explained by a simple modification of J. J. Thomson's theory of the increase in resistance to be expected when the film thickness is very much less than the normal electronic mean free path in the bulk metal. Moreover, these results are reproducible to within 2 or 3%, which has not been the case in previous work.

This work on the alkali metals was suggested by the observation of Ives and Johnsrud,§§ that the invisible *spontaneously deposited* films of rubidium on glass were electrically conducting. Ives,||| using an optical method, estimated these deposits to be of the order of one atom thick.¶¶

\* 'Phil. Mag.', vol. 5, p. 848 (1928).

† 'Rec. Trav. chim. Pays-Bas.', vol. 50, p. 441 (1931).

‡ 'Ann. Physique,' vol. 4, p. 252 (1930); 'Z. Phys.', vol. 91, p. 660 (1934).

§ 'Z. Phys.', vol. 59, p. 191 (1930).

|| 'Ann. Physique,' vol. 9, p. 393 (1931).

¶ 'Z. Phys.', vol. 86, p. 413 (1933).

\*\* 'Ann. Physique,' vol. 19, p. 37 (1934).

†† 'Z. Phys.', vol. 89, p. 426 (1934).

†† 'Proc. Camb. Phil. Soc.', vol. 11 (2), p. 119 (1901).

§§ 'Astrophys. J.', vol. 62, p. 309 (1925).

||| 'J. Opt. Soc. Amer.', vol. 15, p. 374 (1927).

¶¶ An account of a full investigation on the conductivity of films of this type will be published separately.

## 2—EXPERIMENTAL TUBE

In fig. 1 a defined beam of rubidium atoms was condensed on the cooled pyrex surface K. The rubidium was contained in O and the beam defined by the pinhole P (punched in a thin glass partition G) and a square glass defining aperture S. S was cooled by liquid air in FF, which also stopped undesirable reflexion from the walls WW.

The method of making contacts to the films is shown in the plan view fig. 1a. The shaded part of the surface consisted of a layer of platinizing covered with colloidal graphite, baked in air at 400° C. for some hours. Connexion to this graphite was made by the platinum wires cc wrapped around glass projections on the side of J. The disposition of the pinhole, slit, and surface was arranged so that the edges of the atomic beam slightly overlapped the graphited edges of K, thus ensuring contact with the film. The efficiency of the contacts has been tested by employing different distances between the graphited edges. In all cases the experimental results and resistivities of the films have been identical.

The surfaces K were turned flat in the blowpipe flame only, in order to avoid contamination from a tool.

The estimation of the film thickness depends on a knowledge of the time of effusion of the beam through P, when the rubidium in O is at a constant temperature. While O was reaching temperature equilibrium the pinhole P was therefore closed by a steel ball D, externally controlled by a magnet. In no case has the leak through this shutter exceeded 2% of the total beam intensity.

The electric current through the oven O was maintained constant by a device due to Potter.\* In order to prevent condensation of the rubidium

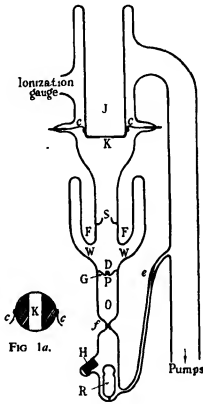


FIG. 1a.

FIG. 1.

\* 'J. sci. Instrum.,' vol. 11, (3), p. 95 (1934).

around the pinhole, this region was maintained at a few degrees' higher temperature than O by an additional series winding on the glass.

### 3—PREPARATION OF RUBIDIUM

The metallic rubidium was prepared by the reduction of rubidium chloride with calcium metal in a separate high vacuum apparatus. After repeated distillations the rubidium was introduced into glass ampoules, which could be sealed off and stored for use. When it was required to introduce rubidium into the oven O (fig. 1), one of these ampoules R was introduced into the extension tube shown there, broken by means of the magnetic slug H and the rubidium distilled into O. The by-pass pumping lead was then removed by drawing off at the constrictions e and f. In this way only carefully degassed rubidium ever entered the main apparatus.

Samples of this rubidium have been submitted for analysis to Messrs. Adam Hilger, Ltd., who report the following impurities: sodium 0·03%, potassium 0·8%, caesium 0·2%, boron 0·2%, with very slight traces of calcium and silicon. Of these impurities caesium is the only metal with a vapour pressure comparable with rubidium, and thus it can be predicted with confidence that the atomic beam effusing through P has contained not more than 0·3% of impurity atoms.

Prior to the breaking of the ampoule, the whole tube was baked-out at 500° C. for about 6 hours, and the pumping tubes thoroughly torched. The tube was continuously evacuated, the first stages of the bake-out being carried out without a liquid air trap in order to avoid condensation of excessive amounts of impurity. Once the bake-out is accomplished, the very greatest care has to be exercised to prevent the entry of mercury vapour into the tube. The vacuum in these tubes, measured by an ionization gauge, has been from  $5 \times 10^{-7}$  to  $5 \times 10^{-8}$  mm. of Hg.

### 4—THE INTENSITY OF THE ATOMIC BEAM

The intensity of the atomic beam has been determined directly by measuring the positive ion emission from a hot oxidized tungsten filament placed in the path of the beam. In principle the method is due to Langmuir and Kingdon\* and (in the case of rubidium) Killian.† The technique of using the oxidized filament method has been fully described by Powell and Mercer.‡

\* 'Phys. Rev.,' vol. 21, p. 380 (1923); 'Proc. Roy. Soc.,' A, vol. 107, p. 61 (1925).

† 'Phys. Rev.,' vol. 27, p. 578 (1926).

‡ 'Phil. Trans.,' A, vol. 235, p. 101 (1935).

Alternatively, the beam intensity can be calculated from the vapour pressure of rubidium and the dimensions of the apparatus. From the Kinetic Theory and the Cosine Law of Effusion the beam intensity  $I$  is given by

$$I = \frac{L}{\pi r^2} \cdot \frac{5.83 \times 10^{-2}}{\sqrt{MT}} \cdot p \cdot f \text{ atoms/cm.}^2/\text{sec.}, \quad (1)$$

where  $r$  is the distance between surface and pinhole,  $f$  the area of the pinhole,  $p$  the vapour pressure of the alkali,  $M$  its molecular weight,  $T$  the oven temperature, and  $L$  Avogadro's number.

A representative series of dimensions are  $r = 15.50$  cm.,  $f = 0.00525$  cm.<sup>2</sup>, for rubidium  $M = 85.44$  so that (1) becomes

$$I = 2.661 \times 10^{16} \cdot \frac{p}{\sqrt{T}} \text{ atoms/cm.}^2/\text{sec.} \quad (2)$$

Owing to a discrepancy in the published data, the vapour pressure of rubidium is uncertain to within a factor of 2 at 100° C \*. A value of vapour pressure within 20% of that obtained by Scott would bring the calculations by the two methods into agreement. But it should be pointed out that the direct calibration carried out by the tungsten filament method not only eliminates this uncertainty but avoids any systematic errors of measurement of temperature or of dimensions; and further it does not depend on the validity of formula (1). The errors in the stated number of atoms on the surface depend solely on the error in the calibration and are certainly not greater than 5%.

### 5—CALCULATION OF FILM THICKNESS FROM THE NUMBER OF ATOMS DEPOSITED

The above methods give the number  $n$  atoms per cm.<sup>2</sup> on the surface. The film thicknesses have been estimated by assuming that these films contain the same number of atoms per cm.<sup>3</sup> as the bulk metal.

For rubidium at liquid air temperatures we then obtain the thickness

$$t = \frac{n}{1.14} \times 10^{-22} \text{ cm.} \quad (3)$$

This assumption has been denied by various authors. However, there is no evidence for any variation in the case of rubidium; on the contrary, the experimental results to be described are inconsistent with any such

\* *Vide* Scott, 'Phil. Mag.', vol. 47, p. 32 (1924); Killian, *loc. cit.*, and Rowe, 'Phil. Mag.', vol. 3, p. 524 (1927).

variation. The thicknesses quoted in this paper are therefore probably a close approximation to the actual thickness.

It is frequently convenient to speak of the number of atomic layers in a film. Brady\* has defined the number of atoms per cm.<sup>2</sup> in a monatomic layer as  $N_0^{\frac{1}{2}}$  where  $N_0$  is the number of atoms per cm.<sup>3</sup> in the bulk metal. On this definition a monatomic layer at liquid air temperatures contains  $5.06 \times 10^{14}$  atoms per cm.<sup>2</sup>. The definition of a monatomic layer is quite arbitrary and we have preferred to define it as a layer of rubidium whose thickness is that of the normal crystal lattice. Thus a film of thickness  $t$  A. contains  $t/5.62$  atomic layers, each of which contains  $6.41 \times 10^{14}$  atoms per cm.<sup>2</sup>.

#### 6—MEASUREMENT OF RESISTANCE

Resistances greater than  $10^4$  ohm have been measured by a potentiometer and galvanometer. With 100 volts across the film it is possible to detect a resistance of  $10^{13}$  ohm. Resistances below  $10^4$  ohm have been measured on a dial P.O. box. Such arrangements enable resistances to be measured continuously with time.

#### 7—THE TEMPERATURE OF DEPOSITION

The temperature of the surface K at deposition has been determined by placing in J either liquid oxygen or liquid nitrogen boiling under known reduced or atmospheric pressures. With the pumps available the lowest temperature obtainable was 64° K., namely, oxygen boiling at 1.4 cm.

#### 8—ATTAINMENT OF REPRODUCIBLE RESULTS

When the oven O has reached a steady temperature with liquid oxygen in the containers FF and J, the shutter can be opened and the resistance measured continuously with time. We will first discuss the anomalies encountered and their explanation, in order to show the rigid conditions necessary to obtain reproducible results. The measurements which will be quoted were made on a film size of 1.55 cm. long with 1.35 cm. between the graphiting, but, as stated in § 2, the results are not in any way influenced by the size of this patch. The effects of contamination of the substrate will now be considered.

\* 'Phys. Rev.', vol. 41, p. 613 (1932).

(a) *Effect of Rubidium Remaining on the Surface*—Though the curves in fig. 2a actually relate to the effect of CO<sub>2</sub>, they may also be used to illustrate other effects giving curves of the same type. A curve such as A, fig. 2a, shows the formation of a film of 3·9 layers' (21·8 Å.) thickness, at 90° K. plotted as log resistance/time of deposition (which is proportional to the thickness) using a beam intensity of  $3 \cdot 18 \times 10^{12}$  atoms/cm.<sup>2</sup>/sec. Conductivity first became appreciable with about 0·5 layers on the surface and after 13 minutes the resistance had fallen to  $4 \cdot 6 \times 10^4$  ohm. The deposition was then stopped by closing the shutter at the point marked S on the graph, and although the surface was maintained at the temperature of deposition 90° K., the film showed a decay of conductivity with time represented by B. As a convenient though arbitrary measure of this decay the decay factor  $\Delta R/R$  will be taken, where  $\Delta R$  is the increase in resistance during the first 30 minutes' decay.

If now the liquid oxygen in J is evaporated, the surface warms to room temperature and the resistance rises to  $\infty$ . If, then, liquid oxygen is reinserted in J, and another distillation started, one might expect a repetition of the previous resistance curves. But this is not so; conductivity does not begin until a thicker layer, the resistance after 13 minutes is higher and the decay of conductivity is greater (curves such as A'', B''). Further repetitions of the process make matters successively worse. Although the resistance is infinite after the surface has warmed to room temperature, it can be shown that rubidium is still on it by the existence of a photo-resistance effect. In other words, when the surface is illuminated a conductivity is observed due to the liberation of photoelectrons which move under the potential gradient along the surface. When these nuclei of rubidium are present we may assume that incident atoms in a succeeding distillation tend to segregate around them, thus delaying the commencement of conductivity. This phenomenon in a less exaggerated form is considered again later in an explanation of the phenomenon of decay. These effects are disposed of if the surface is heated to drive off this rubidium between the distillations.

(b) *Effect of Rubidium Spontaneously Deposited on the Surface*—Effects similar to the above are encountered if a distillation is performed after the tube has stood for some time (e.g., over night). This is due to the rubidium which condenses around FF during a distillation, forming spontaneous deposits on the surface K. This effect is disposed of by placing a heater in J with liquid air in FF for some hours before commencing a distillation.

(c) *Effect of Surface Impurities*—With a new surface at K, even after

the baking out process already described, consistent results could never be obtained until after prolonged heating of the surface K. The initial distillations gave graphs of type A'', B'', fig. 2a, improving to a limiting condition AB, as the heating progressed. After 40 to 80 hours' baking at about 250° C., the results settled down to consistency, and after this point further heat treatment of the surface at this or any higher temperature up to 500° C. produced no change.

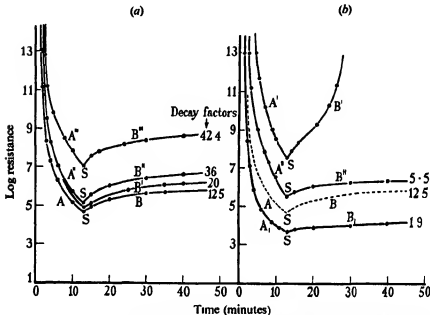


FIG. 2.—Influence of contaminated substrate on the formation and decay of conductivity for films 21.8 A. thick deposited at 90° K. with beam intensity  $3.18 \times 10^{18}$  atoms/cm<sup>2</sup>/sec. (a) Influence of varying amounts of CO<sub>2</sub> impurity. (b) Influence of varying amounts of H<sub>2</sub>O impurity. The decay factors are inserted at the right-hand side of all subsequent decay curves. S = shutter closed (cessation of deposition). - - - standard surface curve for comparison.

To obtain this final condition of the surface it was found convenient to heat at 250° C. for many hours, but the final state was entirely independent of the baking temperature. One may attribute the efficiency of this method of cleaning the surface to the fact that with the heater in J the surface is 250° C. hotter than the rest of the apparatus and at the same time a very high vacuum is maintained. Thus the removal of gaseous or volatile impurities from the surface to colder parts of the tube is facilitated in a way impossible during the general bake-out at 500° C. Extremely small quantities of gas and impurity are removed during this subsequent

heating as proved by the results of the following section, and also by the fact that this heating never impaired the vacuum. On this standard surface results are reproducible to about 2%, provided the precautions are observed respecting (a) and (b). The conditions are satisfied by always maintaining the surface at a high temperature until the distillation is commenced, and placing liquid air in FF at least one hour before the heater is removed from J.

(d) *Artificial Production of the Observed Anomalies*—Convincing explanations of the effects observed in (c) have been obtained by introducing foreign molecules on to the surface K. Tungsten filaments placed in a side tube were coated with  $\text{Ba}(\text{OH})_2$  and  $\text{BaCO}_3$ , so that on heating the filaments either  $\text{CO}_2$  or water vapour could be obtained, with the pressure fully under control

With the surface K in its standard condition, one of the filaments was heated until a vapour pressure of  $10^{-6}$  mm of either  $\text{CO}_2$  or water vapour was established. This pressure was maintained for some minutes with liquid air in J to ensure considerable condensation of the impurity on the surface K. The impurity was then pumped out until the previous vacuum conditions were obtained and a distillation commenced. The results of these experiments are shown in figs. 2(a) ( $\text{CO}_2$ ) and 2(b) (water).

In both cases the initial distillations gave no measurable conductivity. After heating for one hour at  $250^\circ\text{C}$ ., the surface contaminated with  $\text{CO}_2$  gave the curve A''', B''' (fig. 2a) after 20 hours A'', B''; after 40 hours A', B', and finally after about 80 hours the original standard surface condition AB was reached. Further heat treatment at any temperature gave no further change in the reproducibility of the curve.

The effects with water vapour are more complicated. After baking for one hour at  $250^\circ\text{ C}$ . a curve A', B' (fig. 2b) is obtained decaying to an infinite resistance, after 20 hours A'', B'', and after prolonged baking the surface conditions became permanently changed, giving curves A<sub>1</sub> B<sub>1</sub> of lower resistance and less decay than the standard surface AB (shown dotted). Such a change in the surface conditions had been previously observed when a film about 40 Å. thick held at  $90^\circ\text{ K}$ . was accidentally oxidized, the vacuum being ruined for a few seconds. On heat treatment of such a surface it settled down to a condition which gave films more stable than the standard pyrex surface. It is considered to be due to the formation of a stable rubidium compound which soaks into the surface on heating; standard conditions can then only be regained by changing the surface at K. Films decaying to  $\infty$  such as A' B' of fig. 2b had also

been observed in the earlier tubes before the necessity of stringent conditions of purity and vacuum were realized.

Every observed departure from the curves obtained on the standard surface has received an explanation in terms of the effects described above. A probable interpretation of these anomalies and of the effects of CO<sub>2</sub> and water vapour will be dealt with later.

### 9—MEASUREMENTS ON CLEAN STANDARD SURFACES

Under the conditions described above, a surface giving a standard result such as the curve AB for a given distillation reproduces with certainty. In four different tubes after the initial stages described in 8(c) above, the measured resistivities on a given film have not differed by more than about 2 or 3%, whatever subsequent heat treatment has been given to the surface.

After several distillations in a tube, visible quantities of rubidium collect around the inside of the container FF, and the possibility of stray effects from the rubidium already in the tube cannot be overlooked. However, it has been established by experiments over periods far exceeding the normal duration of a run, that provided the precautions outlined in (8) are observed, there is absolutely no contribution from any such stray rubidium.

Fig. 3 illustrates measurements at different temperatures of deposition, using a constant beam intensity of  $3 \cdot 18 \times 10^{12}$  atoms/cm.<sup>2</sup>/sec. At 90° K. conductivity first becomes appreciable at 0.5 layers, and at 64° K. at 0.4 layers. The broken curves emerging from the points marked S<sub>1</sub> show the decay of conductivity of films 4.4 Å. thick; the shutter being closed after 157 seconds' deposition. For films of this thickness the decay factor decreases from 21.5 at 90° K. to 0.22 at 64° K. At the instant of closing the shutter the resistivity is  $1 \cdot 79 \times 10^8$  ohm/cm. at 90° K. and decreases to  $3 \cdot 09 \times 10^{-3}$  ohm/cm. for the film deposited at 64° K.

The curves emerging from the points S<sub>2</sub> show the behaviour of films when the deposition is stopped after 26 minutes (43.6 Å. thickness). A summary of resistivities and decays for various thicknesses is given in § 10, for films deposited with this beam intensity. The effect of depositing a film of given thickness with a lower beam intensity is to increase the final film resistivity and the decay factor.

The 43.6 Å. film deposited at 64° K. (fig. 3) is completely stable and has a resistivity of  $1 \cdot 84 \times 10^{-5}$  ohm. cm., which according to Hackspill's measurements of the resistivity of the bulk metal\* is 10 times greater than

\* 'C.R. Acad. Sci. Paris,' vol. 151, p. 305 (1910).

the resistivity of the bulk metal at this temperature. Although this stable film is quite invisible, the resistance has fallen to a value as low as 30 ohm across the measured patch. With these stable films completely reproducible temperature/resistance graphs (fig. 8) have been obtained over the range to 90° K.

In the case of these low resistances the resistance of the end contacts and leads becomes of importance. This resistance has been determined by depositing thick layers of rubidium. It was 1·1 ohm in the tubes

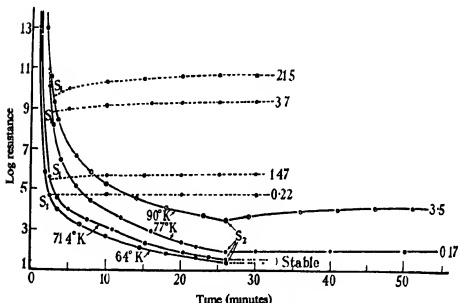


FIG. 3—Formation and decay of conductivity for films deposited at different temperatures of deposition with beam intensity  $3 \cdot 18 \times 10^{18}$  atoms/cm.<sup>2</sup>/sec. S = shutter closed (cessation of deposition). The curves are spread in the early stages for clarity, thus the points S<sub>1</sub> should all lie on the ordinate at 157 sec.

used. Data on rubidium films of greater thickness than those investigated in the present work would be of much interest, but the relatively high value of the resistance of the end contacts would have seriously limited the accuracy obtainable in the present apparatus.

The resistivity of films of the order of 90 Å. thick deposited at these lower temperatures approaches to 5 or 6 times that of the bulk metal. These films are still invisible but carry currents limited only by the heating of the end contacts (up to  $\frac{1}{2}$  amp.) and obey Ohm's law at these current densities ( $10^6$  amps. per cm.<sup>2</sup>).

10—SUMMARY OF THE EXPERIMENTAL DECAYS AND  
RESISTIVITIES

Fig. 4 collects the results of the measurements of the decay of conductivity given in § 9, showing the decay factor as a function of the

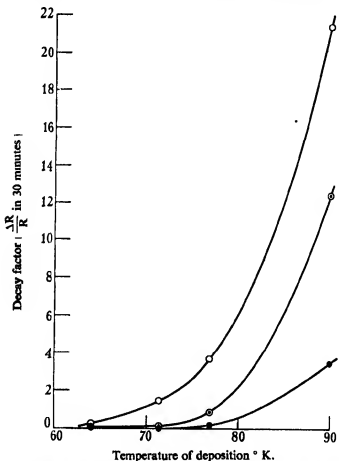


FIG. 4.—Decay factors as a function of the temperature of deposition for films of a given thickness deposited with beam intensity  $3 \cdot 18 \times 10^{18}$  atoms/cm.<sup>2</sup>/sec.  
 O 4.4 Å.; ○ 21.8 Å.; ● 43.6 Å.

temperature of deposition for a given number of layers. These curves show the large decrease in decay caused by lowering the temperature of deposition for a film of a given thickness. At the lowest temperature reached (64° K.) the film 43.6 Å. thick is completely stable, whereas this film deposited at 71.4° K. is stable at that temperature but begins to

decay at the rate 0.019 if it is raised to 90° K. A film of double this thickness deposited at 71.4° K. is completely stable. Films much thinner than these decay at all temperatures of deposition; thus the film 21.8 Å. decays at the rate 0.013 even at 64° K.

Fig. 5a is a curve of the film resistivities against film thickness (up to 40 Å.) for various temperatures of deposition. The large influence of the

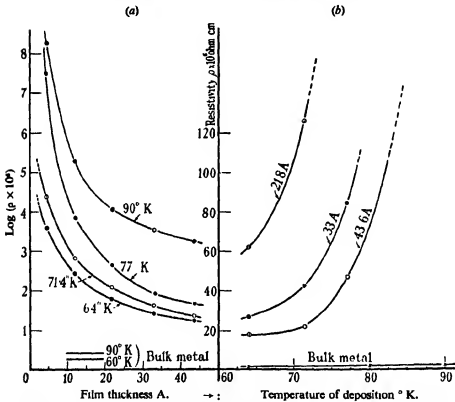


FIG. 5—(a) Film resistivities (log. scale) as a function of film thickness for different deposition temperatures. (b) Dependence of resistivity (linear scale), on the temperature of deposition for films of a given thickness.

temperature of deposition is illustrated in fig. 5b which shows the dependence of resistivity on this temperature for films of a given thickness. On this linear scale the ordinate would need to be extended for one mile to include the resistivity of a 4.4 Å. film deposited at 90° K. Hackspill's measurements of the bulk resistivity\* are drawn in for comparison.

It must be pointed out that only a very few of the experimental points, viz., on figs. 5a and 5b, are determinations from stable films, and in this

\* C.R. Acad. Sci. Paris, vol. 151, p. 305 (1910).

sense the curves are rather arbitrary, since the resistance plotted is that measured immediately after completing the deposition with a definite beam intensity.

#### 11—DISCUSSION. RESISTIVITIES OF THE STABLE FILMS

It seems possible to explain quantitatively the resistivities of the stable films by taking into account the shortening of the mean free path of the electrons through collisions with the film boundaries.

The normal mean free path  $\lambda_0$  for a rubidium atom in the bulk metal can be calculated from the relation

$$\frac{1}{\rho_s} = \frac{Ne^2}{2mv} \cdot \lambda_0, \quad (4)$$

where

$\rho_s$  is the resistivity at temperature 0° K.

$\lambda_0$  = the mean free path at 0°

$N$  = number of electrons per cm.<sup>3</sup> = ~1/atomic volume for the alkalis\*

$e$ ,  $m$ , and  $v$  = the electronic charge, mass, and velocity.

The relation (4) follows both from the classical and quantum mechanics, but whereas in the classical mechanics  $v$  varies with temperature, on the quantum mechanics  $v$  is obtained as a constant given by

$$\frac{1}{2} mv^2 = \frac{\hbar^2}{2m} \left[ \frac{3N}{8\pi} \right]^{\frac{1}{3}}. \quad (5)$$

Using Hackspill's measurements of the bulk resistivity, and calculating  $N$  from the density of rubidium at these temperatures, formulae (4) and (5) give mean free paths of from 1980 Å. at 90° K. to 2860 Å. at 60° K.

The films considered in this work were all less than 100 Å. thick, so that the consequent modification in the mean free path will contribute to the higher resistivity.

Two hypotheses may be considered:

(a) *Elastic Collisions*—If the electrons are reflected elastically from the boundaries of the film, and if the boundaries are parallel planes, the mean free path will not be directly affected through the thickness. The higher resistivity of the film compared with that of the bulk metal must then be considered as due to strain. This should give a residual resistance at

\* Evidence for this, *vide* R. W. Wood, 'Phys. Rev.', vol. 44, p. 353 (1933); Zener, 'Nature,' vol. 132, p. 968 (1933); Mott and Zener, 'Proc. Camb. Phil. Soc.', vol. 30, p. 249 (1934).

0° K., and the absolute change of resistivity between any two temperatures should be the same as that of the bulk metal.

From Hackspill's measurements the change in resistivity of bulk rubidium between 64° and 90° K. is  $0.57 \times 10^{-6}$  ohm cm., whereas we find the corresponding change for a film of 43.7 Å. thick is  $1.6 \times 10^{-6}$  ohm cm. The elastic collision theory must therefore be rejected.

(b) *Inelastic Collisions*—If the collision of the electrons with the film boundaries is inelastic, then the consequent shortening of the average mean free path may be calculated as follows.\* We make the assumption that the electron, after collision with the side of the film, is reflected in a direction independent of the angle of incidence. Since the thickness is very much less than the normal free path, it is unlikely that an electron will make two consecutive collisions without coming into contact with

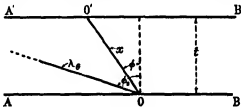


FIG. 6.

the film boundaries. In this case, every free path may be considered as beginning or ending on a side of the film.

Consider an electron suffering a collision at O (fig. 6) on a side of the film AB; then the next collision may occur at some such point O' on another side of the film A'B' after a free path  $x$ . Also those electrons reflected at an angle greater than  $\phi_0$  given by  $\cos \phi_0 = t/\lambda_s$  (where  $\lambda_s$  is the normal free path in the bulk metal), will be able to pursue the normal free path  $\lambda_s$ , without collision with the film boundaries.

If we assume that a large number  $q$  electron paths start from O, then since their directions are uniformly distributed throughout a hemisphere, the number between the two cones  $\phi$  and  $\phi + d\phi$  is  $q \sin \phi d\phi$ , so that the average path  $\lambda'$  is given by

$$\lambda' = \frac{1}{q} \left[ \int_0^{\phi_0} x \cdot q \sin \phi \cdot d\phi + \int_{\phi_0}^{\pi/2} \lambda_s \cdot q \sin \phi \cdot d\phi \right],$$

where for  $\phi = \phi_0$ ,  $x = \lambda_s$ ; and  $x = t/\cos \phi$ ,  $\cos \phi_0 = t/\lambda_s$ , so that

$$\lambda' = t \left[ 1 + \log \frac{\lambda_s}{t} \right].$$

\* The idea that the mean free path could be affected by the thickness of the film is due to J. J. Thomson, 'Proc. Camb. Phil. Soc.', vol. 11, p. 119 (1901).

Thus the final expression for the resistivity of a film of thickness  $t$  cm., at temperature  $0^\circ$  K., in terms of the normal free path  $\lambda_0$  at that temperature is

$$\rho = \frac{2mv}{Ne^2} \cdot \frac{1}{\lambda'} = \frac{2mv}{Ne^2} \cdot \frac{1}{t[1 + \log \lambda_0/t]} \quad (6)$$

Substituting now the value of  $v$  and  $\lambda_0$ , given by the quantum relations (4) and (5), one obtains the dotted curve in fig. 7 for the temperature  $70^\circ$  K.

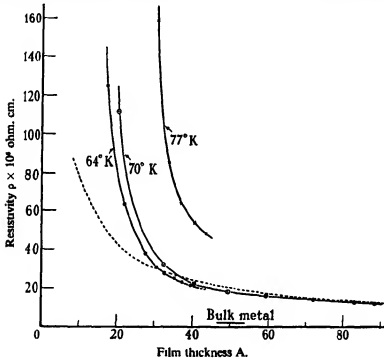


FIG. 7.—Theoretical (---) and experimental resistivity/thickness curves. —●—●— film deposited at  $64^\circ$  K.; —○—○— film deposited at  $70^\circ$  K.; —×—×— film deposited at  $77^\circ$  K.

The corresponding experimental results are shown as circles and full lines for deposition temperatures of  $64^\circ$  K. and  $70^\circ$  K. (The difference in the theoretical curves for these temperatures is too small to illustrate in the figure.) It will be seen that there is an excellent quantitative agreement between them above a certain film thickness. It is not necessary to assume that the agreement really breaks down for thinner films. The departure of the curves in the initial stages may be explained by the observed fact that the actual films are "decaying" to some slight extent at these thicknesses. This is supported by the curves running together

earlier for the lower temperature where these thinner films are more stable, as already discussed in the previous section. The curve shown by crosses in fig. 7 is the resistivity of a film deposited at 77° K. and shows the lack of agreement for the case when the film is known to decay at all thicknesses.

Fig. 8 shows the resistivity/temperature curves for the final state of the films whose formation is shown in fig. 7.

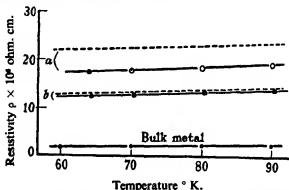


FIG. 8—Resistivity/temperature graphs for stable films. (a) For a film 43.7 Å. thick deposited at 64° K.; (b) for a film 87.4 Å. thick deposited at 70° K. —○—○— experimental; - - - - theoretical.

## 12—DISCUSSION OF THE PHENOMENON OF THE DECAY OF CONDUCTIVITY

The decay of conductivity is almost certainly not due to re-evaporation of rubidium atoms, since the vapour pressure of rubidium at 90° K. is of the order of  $10^{-30}$  mm. of Hg. Moreover, the variation in magnitude of the decay under different conditions has to be explained.

It appears possible to obtain a qualitative explanation of decay by taking account of the surface tension forces. In a rubidium drop with a radius of 10 Å. these forces are of the order of 30 tons/in.<sup>2</sup>, which is of the same order of magnitude as the ultimate tensile strength of carbon steel.

It follows that if any crack exists in the film it will tend to widen. The widening will be resisted by the force with which the rubidium adheres to the glass surface (*i.e.*, by the surface tension forces at the rubidium/glass interface), and the rate at which the crack widens depends upon the mobility of the rubidium atoms over their neighbours. This decreases as the temperature of the surface is lowered (*i.e.*, the mechanical rigidity of the material of the film increases).

Except at low temperatures and on very clean surfaces, the widening proceeds so rapidly that the film breaks up into little islands or aggregates of metal on the glass surface. With the best conditions, however, the gaps will be filled up before they widen too much. We assume that a uniform film once formed is stable, so that there is no tendency for a crack to form if there is not one there already. In fact, provided the film is continuous, the surface tension forces can only act so as to diminish any small inequalities of thickness if they exist initially. This explains the complete stability of films such as the film 43·6 A. thick (§ 9) deposited at 64° K., remaining stable at 90° K., although a film of this thickness deposited at 90° K. would decay considerably.

The high resistivity of the unstable films is then to be associated with cracks. According to modern theory, electrons can cross a crack of several A., though such a crack would have a high resistance.

If the deposition is in progress the decay is counterbalanced to some extent by the increasing size of the aggregates tending to bring them closer together. When the deposition ceases, the rate of decay is initially comparatively large, and then (except in the case of films decaying to infinity, see § 8 (d)), the rate of decay decreases with time. This is to be expected since as the aggregates increase in size, the surface tension forces are reduced, and are more equally opposed by the rigidity of the material of the film which exists at that temperature. At a given temperature of deposition the decay is greater for thinner films. This is to be expected on the above assumptions.

The effect of the condition of the substrate dealt with experimentally under 8 (in particular figs. 2a, 2b) is then to be explained in terms of the influence of impurities on the surface tension forces at the rubidium glass interface. It is seen that minute amounts of impurity on the substrate give rise to a large break up with consequent high resistivities. This is undoubtedly the cause of the anomalies which have been observed by previous workers on thin films. In these cases the importance of the cleanliness of the substrate has not been fully realized, and it seems possible that the substrate has always contained a certain amount of impurity of the type which causes a decay of great rapidity with consequent high resistivities, as reproduced artificially in the present work in § 8 (d). It appears that in the majority of this previous work, this decay may have been so rapid that the intermediate stages of decay have not been observed, and the final state of the decayed film has been taken as its true resistance value.

This hypothesis of decay leads to an explanation of the effect (described in § 8 (a)) of rubidium remaining on the surface although it is non-

conducting. At some temperature above 90° K. when the surface is warming to room temperature the films have been observed to jump quickly to an infinite resistance. In this case the forces tearing apart the film have full play since at these higher temperatures the rubidium atoms possess a large mobility (*i.e.*, the film is now non-rigid), and the rubidium remains on the surface in the form of completely isolated aggregates. Such aggregates would normally evaporate quickly at room temperature, but equilibrium is set up through the rubidium which has collected in the region of the aperture S during a distillation, and is then no longer held there at liquid air temperatures.

When the deposition is carried out with a lower beam intensity the supply of atoms to the aggregates is slower, so that the tendency for the aggregates to increase in size will have less counterbalancing effect on the break up. This results in higher resistances and greater decays.

In the case of the more stable layers the effect of the beam intensity becomes less, and for a temperature of deposition low enough for mobility over the surface to be completely arrested, the rate of deposition would be expected to have no influence on the film resistivity. Such a temperature has not yet been attained since even in the case of the lowest temperature 64° K., the earliest layers decay very slightly. In this case, however, the final effect of this early decay must be very small, since 3·9 layers are already stable at this temperature.

Somewhat similar phenomena of break up in thin films have been found by other investigators, *e.g.*, Andrade and Martindale\* in films of silver and gold when heated to several hundred °C. Moreover, the shrinking of the aggregates postulated here to explain the decay would give electron diffraction photographs corresponding to larger crystal sizes. These ideas receive strong support from the work which has been done on the structure of other thin films using electron diffraction methods. Kirchnert investigated various substances and found increasing crystal sizes on heating the films, on further deposition and, in some cases, spontaneously on cessation of the deposition. Gen, Zelmanoff, and Schalnikoff† found a growth in crystal size on heating the films. Cosslett‡ has also observed the same type of break up in thin films of indium.

The author is greatly indebted to Dr. E. T. S. Appleyard for suggesting the problem, and for his constant supervision and encouragement; and

\* 'Phil. Trans.,' A, vol. 235, p. 69 (1935).

† 'Z. Phys.,' vol. 76, p. 576 (1932).

‡ 'Phys. Z. Sowjet.,' vol. 4, p. 825 (1934).

§ Unpublished work in this laboratory.

to Professor N. F. Mott for help in the theoretical treatment. He also wishes to record his thanks to Professor A. M. Tyndall for his interest in the work, and to the D.S.I.R. for a Maintenance Grant.

### 13—SUMMARY

The paper describes measurements of the resistivity of thin films of rubidium deposited on cooled pyrex surfaces by a defined atomic beam. By employing high vacua and working under stringent conditions of purity with rigorous preheating of the surface, results consistent to within 2 or 3% have been obtained.

It is shown that minute amounts of impurity on the substrate give rise to anomalous results of the type obtained by all previous workers on thin films, and an explanation of these anomalies is suggested.

Conductivity has been observed with films of only 1 Å. in thickness. Normally, the films showed a decay of conductivity with time after cessation of the deposition; but this decay decreased with increasing film thickness and with a lowering of the temperature of deposition. At the lowest temperature so far used (64° K.), this decay was inappreciable at a thickness of 25 Å. Films of thickness greater than 40 Å. were so stable that their temperature coefficients have been determined. The thickest film investigated (90 Å.) was still invisible but obeyed Ohm's Law up to current densities of at least  $10^6$  amp./cm.<sup>2</sup>.

The resistivity of a 40 Å. film was 10 times greater than that of the bulk metal, whereas previously the lowest resistivity obtained in metallic films of this thickness has been 10,000 times greater.

The variation of resistivity with thickness and temperature for these stable films is in quantitative agreement with a formula derived by simple quantum mechanical treatment.

The phenomenon of the decay of conductivity is discussed in terms of a break up of the film under surface tension forces.

---

## The Spectrum and Photochemistry of Carbon Suboxide

By H. W. THOMPSON (Fellow of St. John's College, Oxford) and N. HEALEY  
 (Exhibitioner of St. John's College)

(Communicated by C. N. Hinshelwood, F.R.S.—Received 22 May, 1936)

Measurements of the spectra, fluorescence, and photochemical decomposition of aldehydes and ketones containing the chromophoric carbonyl group are already extensive and well known. There is, however, one compound of the same type, possessing a unique structure, which has so far received little attention. This substance, carbon suboxide, is according to the electron diffraction measurements of Pauling and Brockway,\* linear, and may be written  $O=C-C=C=O$ . It thus contains solely a combination of  $C=O$  and  $C=C$  linkages, the chromophoric and physical properties of each of which have already been investigated experimentally. In addition, the electronic structures and energy levels of these groupings have been studied recently by theoretical methods.<sup>†</sup>

We have therefore examined the absorption spectrum and photochemistry of this pentatomic molecule. Since it is gaseous at room temperatures, carbon suboxide has obvious experimental advantages; on the other hand, its tendency to polymerize thermally under ordinary conditions introduces complications into the photochemical measurements. The thermal decomposition of the substance was recently described by Klemenc, Wechsberg, and Wagner,<sup>‡</sup> which adds interest to the present work.

The present paper deals primarily with the spectrum and fluorescence data. After beginning our measurements, we noticed a paper by Badger and Barton<sup>§</sup> on the main features of the absorption spectrum. Since our results are not in agreement with theirs, it will be necessary to explain the differences more fully below.

\* Proc. Nat. Acad. Sci., Wash., vol. 19, p. 860 (1933).

† Mulliken, 'Phys. Rev.', vol. 40, pp. 49, 751 (1932); vol. 43, p. 279 (1933); 'J. Chem. Phys.', vol. 1, p. 492 (1933); vol. 3, pp. 375, 506, 514, 517, 573, 586, 645 (1935); and particularly 'J. Chem. Phys.', vol. 3, pp. 564, 720 (1935); Eastwood and Snow, 'Proc. Roy. Soc.' A, vol. 149, p. 446 (1935).

‡ 'Z. phys. Chem.', A, vol. 170, p. 97 (1934).

§ 'Proc. Nat. Acad. Sci., Wash.', vol. 20, p. 166 (1934).

## EXPERIMENTAL METHOD

The carbon suboxide was first prepared by dehydrating malonic acid with phosphorus pentoxide at high temperature. The yield was poor, and the product was subsequently obtained pyrogenically from diacetyl tartaric anhydride.\* Likely impurities in the latter method are carbon dioxide and acetic acid. The latter was removed fairly satisfactorily by means of water condensers and ice-traps, and the former by repeated fractional distillation. The presence of small traces of either of these two impurities in the final product would not materially affect the measurements, since neither compound absorbs in the spectral region involved.

The presence of small traces of sulphur dioxide in the final product is, however, more serious, especially since this substance has a very high extinction coefficient and may reveal itself in the absorption spectrum even though only present in small amount. Our earlier photographs showed bands remarkably like the well-known near ultra-violet bands of sulphur dioxide. Removal of all rubber connexions from the apparatus used for the preparation by using an all-pyrex glass arrangement decreased the intensity of these bands markedly, but did not completely remove them. The residual sulphur dioxide was found to arise from sulphuric acid used in the early stages of the preparation, namely, in the condensation of acetic anhydride with tartaric acid. The condensation was therefore carried out using a little concentrated hydrochloric acid as condensing agent. The fractionated product then obtained gave a spectrum free from the characteristic sulphur dioxide bands.

The purity of this product was tested by measurements of its vapour pressure, the experimental method being that described by Thompson and Linnett.† The data, which agree well with those of Stock,‡ are as follows:—

$t^{\circ}$ C. .....	-36.0	-7.0	0	4.9	13.0
$p$ mm. . . .	127.1	460.1	595.4	712.4	948.1

The interpolated b.p. is  $6.8^{\circ}$  C., and the Trouton Constant  $\lambda/T_b$  is 19.6. This may indicate slight, but not pronounced, association in the gaseous phase. The results can be represented by the equation:

$$\log_{10} p = - \frac{1190}{T} + 7.13.$$

\* Hurd and Pilgrim, 'J. Amer. Chem. Soc.', vol. 55, p. 757 (1933).

† 'Trans. Faraday Soc.', vol. 32, p. 681 (1936).

‡ 'Ber. deuts. chem. Ges.', vol. 50, p. 498 (1917).

For the spectral measurements three instruments were used: a Hilger E.315 quartz spectrograph covering the region 2000–7000 Å., and of dispersion ca. 12 Å./mm. at 3000 Å.; a quartz Littrow spectrograph giving 4 Å./mm. at 3000; and a concave grating with Eagle mounting giving 5 Å./mm.

The column of absorbing vapour was 20–100 cm. in length (glass tubes with quartz ends cemented on) and pressures 20–800 mm. were used. The continuous source was a hydrogen discharge tube.

The fluorescence was examined by the method previously described by Thompson and Linnett.\*

## RESULTS

1—*Preliminary Measurements*—In agreement with the results found for other compounds containing the carbonyl chromophore, carbon sub-oxide shows two regions of absorption in the ultra-violet. At low pressures the first region extends from 3300–2400 Å., with a maximum at ca. 2700 Å.; the second region extends from ca. 2200 Å. to shorter wave-lengths. At higher pressures this second region is developed to longer wave-lengths so as eventually to overlap the former, giving continuous absorption from ca. 3200 Å. to shorter wave-lengths. The second region of absorption is entirely continuous, but the former is composed of bands between 3300–2800 Å., with an overlapping continuum at the short-wave end.

This region of absorption between 3300–2400 Å. requires primary and more detailed consideration. It is well known that this characteristic region of carbonyl absorption is in general associated with a relatively low extinction coefficient. In agreement with this, our earlier experiments showed that in order to obtain satisfactory absorption it was necessary to use columns 50–100 cm. in length with pressures 200–800 mm. of vapour; even then the absorption was not strong. This appeared to be in partial disagreement with the work of Badger and Barton, who obtained convenient absorption in a 15-cm. column with pressures 100–600 mm., and it suggested the presence in the product used by Badger and Barton of a small amount of impurity of high extinction coefficient.

As already explained, our preliminary photographs showed the main features of the characteristic absorption of sulphur dioxide. This was traced to the causes given above. We then noticed that the wave-lengths of the strong bands given by Badger and Barton agreed very closely with the strong bands of sulphur dioxide. In Table I are given

\* 'J. Chem. Soc.', p. 1452 (1935).

(1) wave-lengths in Å. of the most intense sulphur dioxide bands given by Watson and Parker\*, (2) approximate wave-lengths of the most intense sulphur dioxide bands measured separately by us on a comparison spectrogram, (3) the values given by Badger and Barton for the strongest bands of carbon suboxide.

TABLE I

(1)	(2)	(3)
3131 5	3131	3130·3
3108	3107	3106·9
3087	3087	3086
3065	3064	3064 8
3042 5	3041	3042
3021	3022	3020 2
3001	3000	3000·2
2981·5	2981	2979 2
2961	2961	2959 4
2939	2939	2938·2
2923	2922	2921 7
2902	2903	—
2887 5	2886	2887·9
2867	2867	2865 5
2853	2852	2851·7

The agreement between these data is such that there seemed little doubt that the bands described by Badger and Barton were in reality due to traces of sulphur dioxide present as impurity, the high extinction coefficient of this substance causing them to be developed strongly. Moreover, the feebler bands described by Badger and Barton appearing between the main bands correspond closely with those described in the detailed analysis of Watson and Parker.

There are several additional independent arguments which substantiate this view, of which three may be given:

- (1) The vapour pressure of our product was measured and agreed closely with the accepted value, and gave a correct b.p.
- (2) At low pressures two regions of absorption are detected in the ultra-violet. Badger and Barton make no reference to the intermediate transparent region, which may have been masked by sulphur dioxide absorption.
- (3) The wave-lengths of the bands observed by us and given below, do not agree with those of Badger and Barton; in particular we have

\* 'Phys. Rev.', vol. 37, p. 1484 (1931).

observed bands to wave-lengths as long as 3300 Å., whereas the longest wave-length band of these authors was 3200 Å.

2—*The Spectrum*—The arrangement of bands observed with carbon suboxide is depicted in fig. 1.

The nature of the bands is such that the wave-lengths given may be in error by  $\pm 2$  Å. The intensities shown are not quantitatively accurate, and are only judged visually and shown in this way in order to make possible interval relationships more obvious. It is seen that in passing from longer to shorter wave-lengths there is first a series of about ten narrow bands between 3380–3250 Å. These are almost equidistantly spaced and are completely diffuse, showing no signs of rotational structure. Between 3250–2910 Å. there is a somewhat complicated arrangement of bands. The principal feature of this is the occurrence of intense pairs of diffuse bands (marked A, A', B, A'', C, etc.), each pair being separated by *ca.* 100 cm.<sup>-1</sup>. Interspersed among these strong band-pairs are feebler pairs with smaller separation (*ca.* 50–70 cm.<sup>-1</sup>). Some of the feebler bands show definite signs of structure. For a few bands (*e.g.*, at 3185 Å.) it is impossible to say whether there is a narrow doublet or a group of very close lines crowded together to give the appearance of a single band. At wave-lengths shorter than *ca.* 2910 Å. the bands become so crowded and overlap to such an extent that it has not been possible to measure them.

The nature of the pyrogenic method of preparing the carbon suboxide suggested that acetone or keten might be present as impurity, and give bands in the same region. In addition to considerable independent evidence against either of these possibilities, the bands given do not agree in wave-length with those of acetone,\* or of keten.†

3—*The Fluorescence*—Attempts were made to excite visible fluorescence of the carbon suboxide by irradiation with lines of the mercury lamp. No fluorescence could be detected. The addition of small amounts of carbon suboxide to fluorescing acetone quenched the fluorescence of the latter. This phenomenon is similar to that described earlier for acrylic aldehyde.‡ The absence of fluorescence may be thought to imply dissociation as a primary act associated with the electronic excitation, but this cannot be regarded as certain.

#### 4—*The Energy Levels of the Molecule and the Analysis of the Spectrum*—

\* Noyes, Duncan, and Manning, 'J. Chem. Phys.', vol. 2, p. 717 (1934).

† Norrish, Crone, and Saltmarsh, 'J. Chem. Soc.', p. 1533 (1933).

‡ Thompson and Linnett, *loc. cit.*

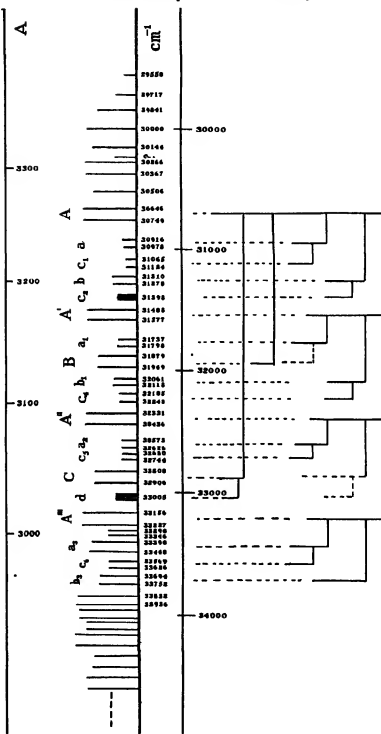


Fig. 1

The energy levels of the molecule may be conveniently discussed under three headings: (a) electronic, (b) rotational, and (c) vibrational.

(a) The nature of the spectrum of carbon suboxide does not provide conclusive evidence with regard to the excited electronic levels. The region of absorption at *ca.* 3000 Å. is common to all carbonyl compounds and the excited level associated with this region is presumably of the same type as is involved with aldehydes and ketones. The introduction of a system of conjugated double linkages into a ketone or aldehyde molecule has been found to displace this region somewhat towards the red. It is therefore interesting to find that in the present case of double linkages without conjugation the region of absorption is "normal". If the bands observed between 2800–3300 Å. are associated with the same electronic level as the overlapping continuum, it would be natural to infer an electronic level at *ca.* 2700 Å. (37000 cm.<sup>-1</sup> or 4.6 volts), the maximum of this continuum. The results, however, seem rather to suggest that there are two independent close electronic levels, one (A) associated with the band system at *ca.* 31000 cm.<sup>-1</sup> (3.8 volts), and another (B) with the continuum at *ca.* 4.6 volts. The double nature of most of the bands of level A probably arise from resonance between the various vibrations rather than from a doublet electronic level.

The continuous absorption which extends from *ca.* 2200 Å. to shorter wave-lengths may involve electronic excitation either in a C-O or C=C linkage, this level lying at *ca.* 47,000 cm.<sup>-1</sup> (5.8 volts).

It is probable that the ground state of carbon suboxide is a singlet level. In order to provide reasonably strong combination, the excited level A corresponding to the band system might therefore also be expected to be singlet.

Carbon suboxide appears to be a particularly suitable molecule for consideration by the theoretical method of molecular orbitals, developed by Mulliken and used by Eastwood and Snow.\* Predictions of the type and relative positions of the electronic levels in this way would be valuable.

(b) Some predictions about the rotation levels may be made from the known interatomic distances in the molecule. According to Pauling and Brockway (*loc. cit.*), the molecule is linear, and the C=C distances are 1.3 Å., and the C=O 1.2 Å. For the moments of inertia then,  $I_A = 0$  and  $I_B = I_C = 3.97 \times 10^{-48}$  gm. cm.<sup>2</sup>. The interval between successive rotation lines in a band will then be of the order  $\hbar/4\pi^2I$ , i.e., 0.15 cm.<sup>-1</sup>. The instruments used in the present work could hardly be expected, therefore, to resolve the rotational structure in the bands if it really existed.

\* See reference to Mulliken.

The diffuse nature of the bands cannot therefore in itself be taken to imply a process of predissociation.

(c) Considerably more can be said in regard to the vibration levels of the molecule. This linear pentatomic molecule possesses  $(3n - 5)$  internal degrees of freedom for vibration. The frequencies of these vibrations might best be derived from a study of the Raman and infra-red spectra. Unfortunately, neither of these has been measured. Considerable experimental difficulties might make a study of the Raman spectrum unprofitable, for illumination of the vapour with an intense source for the long period required would undoubtedly lead to rapid decomposition and polymerization. The heavier nature of the molecule than those containing lighter atoms such as hydrogen may, too, lead to a displacement of the infra-red spectrum to wave-lengths outside the photographable region. If, however, the third harmonic of the unsymmetrical vibration (say  $2500 \text{ cm}^{-1}$ , see below) could be excited, or if there were a coupling of this level with others, the absorption might be displaced to ca.  $11.000 \text{ A}$ . A search is being made in this region.

Theoretical considerations of the magnitude of the various frequencies are, however, both possible and useful. The  $(3n - 5) = 10$  vibrations are represented diagrammatically in fig. 2. There are four valency vibrations  $v_1(s)$ ,  $v_2(s)$ ,  $v_3(a)$ , and  $v_4(a)$ , and three deformation vibrations  $\delta_1(a)$ ,  $\delta_2(a)$ , and  $\delta_3(s)$ , each of the latter being doubly degenerate. The deformation vibrations would *a priori* be expected to have lower frequencies than the valency vibrations.

The vibrations depicted each satisfy the required conditions of normal vibrations, such as symmetrical or antisymmetrical character.\*

On the basis of the known force constants of the C=O and C=C linkages, it is now possible by regarding the molecule as a system of mass-points subject to simple harmonic motion and neglecting the forces between non-adjacent atoms, to calculate approximately the values of the valency vibration frequencies.

We require first to know the force constants of the C=C and C=O linkages. The former can be estimated by consideration of either the symmetrical or unsymmetrical carbon dioxide vibration. In the first case (fig. 3a) we have,

$$v_s = \frac{1}{2\pi} \sqrt{\frac{c}{\mu}} = \frac{1}{2\pi} \sqrt{\frac{2c_2}{2m_2}} = \frac{1}{2\pi} \sqrt{\frac{c_2}{m_2}},$$

therefore

$$c_2 = 4\pi^2 \cdot v_s^2 \cdot m_2.$$

\* See Dennison, 'Rev. Mod. Phys.', vol. 3, p. 280 (1931); Mecke, 'Leipziger Vorträge,' p. 23 (1931); Teller, 'Hand-u. Jahrb. chem. Phys.', vol. 9 (2), p. 98.

According to Sponer,\*

$$\nu_s = 1336 \text{ cm.}^{-1} = 4 \cdot 0 \times 10^{13} \text{ sec.}^{-1}$$

and

whence

$$m_2 = 2 \cdot 64 \times 10^{-22} \text{ gm.},$$

$$c_2 = 16 \cdot 7 \times 10^5 \text{ dynes/cm.}$$

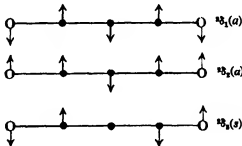


FIG. 2.

In the second case (fig. 3b),

$$\nu_a = \frac{1}{2\pi} \sqrt{\frac{2c}{\mu}}$$

where

$$\frac{1}{\mu} = \frac{1}{m_1} + \frac{1}{2m_2},$$

therefore

$$c_2 = 4\pi^2 \cdot \nu_a^2 \cdot \frac{m_1 m_2}{m_1 + 2m_2}.$$

\* Sponer, "Molekulspektren," vol. I. Springer, 1935, pp. 75, 89.

According to Sponer,

$$v_a = 2350 \text{ cm.}^{-1} = 7.05 \times 10^{13} \text{ sec.}^{-1}$$

and

$$m_1 = 1.98 \times 10^{-28} \text{ gm.}, \quad m_2 = 2.64 \times 10^{-28} \text{ gm.},$$

whence

$$c_s = 14.1 \times 10^6 \text{ dynes/cm.}$$

Sidgwick\* gives  $11.9 \times 10^6$  as the value of this force constant, but his value was determined from considerations of the vibration frequencies of formaldehyde and may be less accurate. Of the two values worked out above, it must be remarked that the symmetrical frequency may be

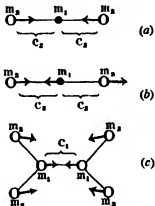


FIG. 3.

less accurately known than the unsymmetrical one. We shall therefore take  $c_s = 14.1 \times 10^6$ .

For C=C it is easiest to consider the totally symmetrical ethylene vibration of fig. 3c. Since C-H linkages may be regarded as remaining fairly rigid during the vibration, we can write approximately

$$\nu = \frac{1}{2\pi} \sqrt{\frac{c_1}{\mu}},$$

where

$$\frac{1}{\mu} = \frac{1}{(m_1 + 2m_2)} + \frac{1}{(m_1 + 2m_2)},$$

and

$$c_1 = 4\pi^2 \cdot v^2 \cdot \mu.$$

According to Sponer

$$\nu = 1623 \text{ cm.}^{-1} = 4.869 \times 10^{13} \text{ sec.}^{-1}$$

\* Sidgwick, "The Covalent Link," p. 123, Cornell, 1933.

and

$$\mu = 1 \cdot 155 \times 10^{-23} \text{ gm.},$$

whence

$$c_1 = 10 \cdot 8 \times 10^5.$$

Sidgwick gives  $9 \cdot 36 \times 10^5$  for this.

In order to simplify the problem it is now best to consider first frequencies  $v_1$  ( $s$ ) and  $v_2$  ( $s$ ) of fig. 2, shown in fig. 4. If the vibrations are symmetrical and fulfil the requirements of normal vibrations, the displacements of the particles will also be symmetrical as shown by  $+x$ ,  $-x$ ,  $+y$ ,  $-y$ , the convention being to measure displacements to the right as positive.

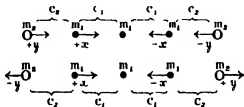


FIG. 4

Suppose that  $v = \frac{1}{2\pi} \sqrt{\beta}$ . There will be then two values of  $\beta$  to give the two required frequencies. We can then write equations for the restoring forces acting on each particle as follows:

$$F_x = -\beta m_1 x = -c_1 x - c_3 (x - y), \quad (1)$$

and

$$F_y = -\beta m_3 y = c_2 (x - y), \quad (2)$$

whence

$$x(c_1 + c_3 - \beta m_1) = c_2 y,$$

and

$$x(c_2) = y(c_2 - \beta m_3).$$

In order that these two equations be simultaneously true,

$$\left| \begin{array}{cc} (c_1 + c_3 - \beta m_1), & -c_2 \\ c_2, & (\beta m_3 - c_2) \end{array} \right| = 0,$$

that is,

$$\beta^2 - \beta \left\{ \frac{c_1}{m_1} + \frac{c_3}{m_3} + \frac{c_2}{m_2} \right\} + \frac{c_1 c_3}{m_1 m_3} = 0.$$

Introducing the above values for  $c_1$ ,  $c_3$ ,  $m_1$ ,  $m_3$ , and solving, we find that  $\beta = 16 \cdot 13 \times 10^{23}$  or  $1 \cdot 80 \times 10^{23}$ . This gives for the frequency  $v$  values  $2130 \text{ cm.}^{-1}$  and  $730 \text{ cm.}^{-1}$  respectively. It can be seen at once that

$\nu_1 = 730$  and  $\nu_2 = 2130$ . This can be checked by evaluating the  $x/y$  ratio for each value of  $\beta$ ; in one case the ratio is positive, and in the other it is negative. We may therefore take as approximate values  $\nu_1(s) = 750$  and  $\nu_2(s) = 2150$ .

Consider now the two vibrations  $\nu_3$  and  $\nu_4$  shown again in fig. 5.

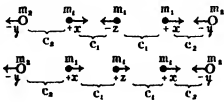


FIG. 5.

Let us suppose as before that  $v = \frac{1}{2\pi} \sqrt{\beta}$  and let the displacements of the three mass-points be  $z$ ,  $x$ , and  $y$ . Then considering the restoring forces in a vibration, and with the same sign conventions as before,

$$F_z = -\beta m_1 \cdot z = -2c_1(z - x) \quad (1)$$

$$F_x = -\beta m_1 \cdot x = c_1(z - x) - c_2(x - y), \quad (2)$$

and

$$F_y = -\beta m_2 \cdot y = c_2(x - y). \quad (3)$$

Rewriting, we have,

$$2c_1x + (\beta m_1 - 2c_1)z = 0$$

$$(c_1 + c_2 - \beta m_1)x - c_2y - c_1z = 0,$$

and

$$c_2x + (\beta m_2 - c_2)y = 0.$$

In order that all three equations may be simultaneously valid,

$$\text{whence } \begin{vmatrix} 2c_1 & , & 0 & , & (\beta m_1 - 2c_1) \\ (c_1 + c_2 - \beta m_1), & -c_2, & -c_1 & & \\ c_2, & (\beta m_2 - c_2), & 0 & & \end{vmatrix} = 0$$

$$\beta^3 - \beta^2 \left\{ \frac{c_1}{m_2} + \frac{c_2}{m_1} + \frac{3c_1}{m_1} \right\} + \beta \left\{ \frac{3c_1c_2}{m_1m_2} + \frac{2c_1c_2}{m_1^2} \right\} = 0.$$

There are three roots to this cubic, of which one is seen to be  $\beta = 0$ , and the other two given by the quadratic

$$\beta^2 - \beta \left\{ \frac{c_1}{m_2} + \frac{c_2}{m_1} + \frac{3c_1}{m_1} \right\} + \left\{ \frac{3c_1c_2}{m_1m_2} + \frac{2c_1c_2}{m_1^2} \right\} = 0. \quad (4)$$

The first root  $\beta = 0$  gives at once from (1), (2), and (3) that  $x = y = z$ , and  $v = 0$ , and implies simply a translational displacement of the entire molecule without vibration.

Substituting the above values for  $c_1$ ,  $c_2$ ,  $m_1$ , and  $m_2$  in (4) and solving as before, the roots are  $\beta = 20.95 \times 10^{18}$  and  $\beta = 7.8 \times 10^{18}$ , giving frequencies 2430 and 1450 respectively. These are respectively  $v_3(a)$  and  $v_4(a)$  of fig. 3. (Although  $x/y$  is negative in each case, for  $v_3$  we find  $x/z$  is negative, and for  $v_4$ ,  $x/z$  is positive.)

The same result is attained if we pre-suppose that the centre of gravity of the molecule remains fixed in space, since in this case,

$$2m_1x + 2m_2y + m_1z = 0,$$

that is,

$$z = -2 \left\{ x + \frac{m_2}{m_1} \cdot y \right\} \quad (5)$$

Combining equations (5), (1), and (3), equation (4) is obtained, the roots being as before.

To summarize then, we have, approximately,  $v_1 = 750$ ,  $v_2 = 2150$ ,  $v_3 = 2450$ , and  $v_4 = 1450$ . The frequencies of the deformation oscillations may be expected to be smaller in magnitude. By comparison with the data for other analogous compounds,\* and making allowances for the difference in the nuclear masses, we might expect to find values in the present case of 200–600 cm.<sup>-1</sup>. This falls into line with the values just given. We might, further, expect  $\delta_2 < \delta_3 < \delta_1$ .

For the present purpose of interpreting the ultra-violet absorption bands it is now necessary to consider how the above frequencies will be modified in the excited electronic state. Duncan† has recently summarized much of the existing data about this; in general, the excited state frequencies are somewhat smaller than those of the ground state, although frequently the difference is slight.

Even with the help of all the above data, both experimental and theoretical, no conclusive interpretation of the vibrational structure of the band system can be given. It is nevertheless reasonable to attempt to draw any likely correlations between the two respective sets of data.

The "origin" of the system is not obvious. Since at room temperatures very few higher vibrational levels in the ground state are excited, we should expect (provided that the 0–0 transition is observed at all) the origin to lie at the long-wave end of the band system. Owing to the ease of thermal decomposition and polymerization of carbon suboxide, it

\* See Mecke, "Hand-u. Jahrb. chem. Phys.", p. 319.

† J. Chem. Phys., vol. 3, p. 384 (1935).

is experimentally impracticable to raise the temperature sufficiently to cause any marked excitation of vibrational levels in the ground state, which might be revealed in the structure of the spectrum, and give a clue to the 0—0 band. At the long-wave end of the band system (3380–3250 Å.) appears, the series of narrow diffuse bands already referred to, on the longer wave side of the pair A. These bands are all fairly strong and do not appear to decrease in intensity towards longer wave-lengths in a pronounced manner.

Two features of the system are marked: (1) with one or two possible exceptions all the bands to shorter wave-lengths than A (3252 Å.) occur in pairs, and (2) there are two distinct sets of pairs, in one the pair separation being *ca.* 100 cm.<sup>-1</sup> and in the other 50–70 cm.<sup>-1</sup>. If the double bands were to be explained by a doublet electronic level, it seems likely that the separation of all pairs would be the same. We may therefore suppose that the pairs arise from some resonance phenomenon between the vibrations, which is not surprising in view either of the molecular structure of the molecule or of its many normal vibration frequencies. For the purpose of the following attempt at analysis we shall regard the centre of each pair as the wave number of the pair.

TABLE II

Designation	$\nu$ obs. cm <sup>-1</sup>	Interval between pairs	Suggested interpretation	$\nu$ calc.
	29558 ?			
	29717 ?			
	29841			
	30000			
	30148			
	(30220) ?			
	30266			
	30367			
	30506			
A	30646			
.	30749	30697	103	
a	30910			
	30978	30944	68	$\nu_e + \delta_1(s)$
c <sub>1</sub>	31065			
	31124	31095	59	$\nu_e + \delta_1(s) + \delta_1(a)$
b	31210			
	31278	31244	68	$\nu_e + \delta_1(a)$
c <sub>2</sub>	~ 31398		—	$\nu_e + \delta_1(a) + \delta_2(a)$
A'	31488			31387
	31577	31538	99	$\nu_e + \nu_1(s)$
				31537

TABLE II—(continued)

Designation	v obs. cm <sup>-1</sup>	Interval between pairs	Suggested interpretation	v calc	
a <sub>1</sub>	31737 ) 31798 )	31767	61	$v_r + v_1(s) + \delta_1(s)$	31777
B	31879 ) 31969 )	31924	90	$v_r + v_4(a)$	31924
b <sub>1</sub>	32061 ) 32113 )	32087	52	$v_r + v_1(s) + \delta_1(a)$	32077
c <sub>4</sub>	32185 ) 32248 )	32216	63	$v_r + v_1(s) + \delta_1(a) + \delta_2(a)$	32227
A''	32331 ) 32436 )	32384	105	$v_r + 2v_1(s)$	32377
a <sub>3</sub>	32573 ) 32626 )	32600	53	$v_r + 2v_1(s) + \delta_3(s)$	32617
c <sub>5</sub>	32680 ) 32744 )	32712	64	$v_r + 2v_1(s) + \delta_3(s) + \delta_5(a)$	32769
C	32808 ) 32906 )	32857	98	$v_r + v_5(s)$	32857
d	~ 33005	—	$v_r + v_5(s) + \delta_5(a)$	33007	
A'''	33156 ) 33257 )	33206	101	$v_r + 3v_1(s)$	33217
	33290 )		—	?	—
	33346 )	33318	56	?	—
a <sub>5</sub>	33390 ) 33468 )	33429	78	$v_r + 3v_1(s) + \delta_5(s)$	33457
c <sub>4</sub>	33569 ) 33626 )	33597	57	$v_r + 3v_1(s) + \delta_3(s) + \delta_5(a)$	33607
b <sub>5</sub>	33694 ) 33752 )	33723	58	$v_r + 3v_1(s) + \delta_1(a)$	33757
	33832 )		—	?	—
	33936 )	33884	104	?	—
other pairs of bands to shorter wave-lengths					

At first sight the spectrum between A (30697 cm.<sup>-1</sup>) and A'' (32384 cm.<sup>-1</sup>) appears to be reproduced between A'' and 33900 cm<sup>-1</sup>, but closer examination of the various intervals suggests that this is really accidental. Taking the pair A as corresponding to the origin of the system, a satisfactory interpretation of the system can, however, be given.

On this basis it is natural first to correlate the intense band-pairs, each having a wider separation of ca. 100 cm.<sup>-1</sup>. We see at once a fairly good agreement between the A-A', A'-A'', A''-A''', intervals, each being ca. 840. The other pairs are interpreted as given in Table II. The scheme

suggests valency vibrations in the excited state of *ca.* 840, 1227, and 2160. The less intense and closer pairs are then regarded as small deformation vibrations superposed upon the former, and of values *ca.* 150, 240, and 540. The latter are assigned to  $\delta_2(a)$ ,  $\delta_3(s)$ , and  $\delta_1(a)$ .

This scheme of energy levels in the excited state cannot at all be regarded as proved, but it has several advantages

(1) The frequencies suggested by it are, assuming little change occurs on electronic excitation, close to what would be expected on the basis of the above calculations. Thus,

	Calculated	Observed
$v_1(s)$ . . .	750	840
$v_2(s)$ ..... .	2150	2160
$v_3(a)$ ..... .	2450	—
$v_4(a)$ . . . . .	1450	1227
$\delta_1(a)$ . . . . .		540
$\delta_2(a)$ . . . . .	< 750	150
$\delta_3(s)$ . . . . .		240

(2) The band-pairs associated with valency vibrations alone are uniformly split to a greater extent than band pairs associated with deformation vibrations. Although no explanation of the difference is immediately obvious, there does therefore appear to be a differentiation between the two types.

(3) The most prominent valency vibration excited  $v_1(s)$  is totally symmetrical, in agreement with the rules of Herzberg and Teller.\*

(4) The scheme of energy levels is symmetrical within itself, and with very few exceptions the observed and "calculated" band frequencies given in Table II agree well within experimental error.

On the other hand, there are several difficulties.

(a) The origin of the system chosen above may be wrong.

(b) It is difficult to interpret the bands to the long-wave side of A.

(c) The scheme does not show coupling of the deformations with the  $v_4(a)$  and  $v_3(s)$  valency vibrations to the same extent as with the  $v_1(s)$  vibration. This may, however, arise from a superposition of such bands with the main bands, e.g.,  $[v_1 + v_3(s) + \delta_1(a)]$  would lie very close to the strongly observed band  $[v_1 + 3v_1(s) + \delta_3(s)]$ .

(d) We should expect to find the smaller deformations excited in the ground state, and find transitions from such levels. It is, however, possible

\* Z. phys. Chem., B, vol. 21, p. 410 (1933).

that their feebleness causes them to be masked, for none of the bands can be regarded as strong.

It is hoped that measurements on the infra-red spectrum will give more definite evidence.

5.—*The Photochemistry*—As already explained, the absence of fluorescence and the diffuse nature of the bands in the region 3000 Å cannot be regarded as a conclusive proof of a primary process of predissociation. Illumination of carbon suboxide with the light of a mercury arc leads predominantly to a polymerization and little decomposition, but this will be described more fully in a later paper.

We are grateful to The Royal Society for a grant, to Dr. W. Jevons and Dr. D. A. Jackson for the loan of apparatus, and to Dr. H. Kuhn for helpful discussions.

#### SUMMARY

The ultra-violet absorption spectrum of carbon suboxide has been measured. It is composed of both banded and continuous regions. With a view to analysis of the band system, the frequencies of the normal valency vibrations of the molecule have been calculated, on the basis of the force constants of the linkages involved. A scheme of energy levels for the molecule is suggested which is supported by many considerations.

Attempts to excite fluorescence were unsuccessful. Preliminary considerations of the photochemistry of the substance are given.

The data on the spectrum are in disagreement with those given recently by Badger and Barton.

## The Formation of Ethers by the Interaction of Primary Alcohols and Olefines at High Pressure

By D. M. NEWITT and G. SFMERANO

(Communicated by W. A. Bone, F.R.S.—Received 23 May, 1936)

Although it is known that olefines will condense with phenols in the presence of catalysts to give aromatic ethers, and that tertiary olefines will react with aliphatic alcohols in a similar manner, no corresponding reaction between the simple olefines and aliphatic alcohols has hitherto been reported. In some recent work upon the slow combustion of olefines at high pressures, however, we have detected ethers in the products in circumstances suggesting that they arise from the direct interactions of the olefine with alcohol produced during the combustion; and on testing the matter further it has been found that in the presence of a suitable catalyst and at high pressures ethylene, propylene, and butylene will combine with aliphatic alcohols in the vapour phase, the reaction



being reversible and slightly exothermic with respect to ether formation. At temperatures between 200° and 300° C. and pressures of about 50 atm., all three components of the system are present in measurable quantities at equilibrium and the equilibrium constant can be determined by approach from either side.

In the present paper the results are given of experiments with ethylene, propylene, and butylene, and a number of the lower aliphatic alcohols, the equilibrium constants for the system alcohol-olefine-ether having been determined in each case.

An account is also given of the secondary reactions in which the alcohols and olefines take part.

### EXPERIMENTAL PROCEDURE

In outline the method employed was to allow the alcohol and olefine to react, usually in stoichiometric proportions, in the presence of a catalyst and for a time sufficiently long to allow of equilibrium conditions being substantially reached, and then to make a complete analysis of the products.

The apparatus used is shown diagrammatically in fig. 1. It consisted essentially of a cylindrical steel reaction vessel A, of 500 cc. capacity, containing the catalyst and maintained at constant temperature by means of an electric furnace which entirely surrounded it. The liquid reactants were forced by means of compressed nitrogen from the container B, through an inlet valve into A. The gaseous reactants were then added separately from their respective storage cylinders and the inlet valve closed. After an interval sufficiently long for equilibrium substantially to be reached the products were released through a reducing valve V and were cooled and condensed in one or more glass containers D. Any gaseous products or adventitious nitrogen were collected in a gas holder,

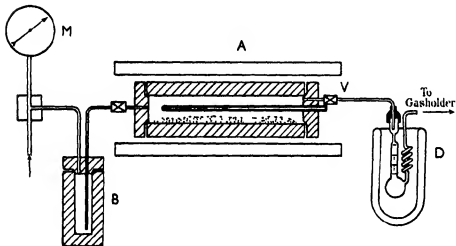


FIG. 1.

measured and analysed. The partial pressures of the reactants and the total pressure of the system were indicated by the gauge M, and the reaction temperature was measured by a platinum/platinum-rhodium thermocouple placed in a tube running axially through the reaction chamber.

#### THE CATALYST

The principal constituent of all the catalysts employed was an active form of alumina prepared by precipitation with carbon dioxide from a dilute solution of sodium aluminate. To this was added the phosphate of one of the metals of Group III in the proportion of 2 parts by weight of alumina to 1 part by weight of phosphate. The mixture was moistened with water, a little alundum cement was added, and the resultant paste

pressed into pellets and dried at 300° C. These catalysts proved very efficient in respect of the alcohol-olefine reaction and maintained their activity unimpaired over long periods. At the same time, however, they accelerated a number of secondary reactions of which the most important were the following resulting in the dehydration of the alcohol, namely,



Polymerization of the olefines occurred only to a slight extent

Whilst olefine formation by dehydration could be partially suppressed by the use of sufficiently high pressures, both the above reactions always proceeded to equilibrium, and considerable quantities of ether formed by dehydration were always found in the products.

The equilibrium constants of reaction (3) have been determined experimentally for ethyl alcohol between 215° and 250°, but not at higher temperatures. For propyl and butyl alcohols no data are available owing to the fact that dehydration normally proceeds almost entirely by reaction (2). By working at high pressures, however, the difficulties arising from excessive olefine formation may be largely obviated, and since a knowledge of the constants for all three alcohols is required for interpreting the results of the alcohol and olefine reactions this determination was undertaken as part of the present investigation.

#### ANALYSES OF ALCOHOL-ETHER-WATER MIXTURES

The products from reactions (1) and (3) contained ethers, alcohols, olefines, and water vapour in varying proportions. The method of analysis was first to remove the water by a suitable dehydrating agent and then to salt out the ethers from the residue by means of a saturated sodium chloride solution. The ethers and alcohols were then separated by fractional distillation and were identified by means of their boiling points, refractive indices, and densities. The procedure was briefly as follows: the contents of the reaction vessel were passed into a glass bulb into which was sealed a graduated neck and a condensing coil (D, fig. 1) cooled by means of solid carbon dioxide and ether. The dimensions of the bulb were such that it was almost completely filled by the condensate. The condensate was weighed and an approximately equal quantity of pure anhydrous potassium carbonate added. The tube was then stoppered and the contents allowed to stand for some 12 hours with constant shaking. Sufficient of a saturated potassium carbonate solution was then added to force the dehydrated alcohol-ether mixture up into the

graduated neck where, after standing for some time in a thermostat, its volume was measured. The potassium carbonate solution was then replaced by a saturated sodium chloride solution together with a small quantity of solid sodium chloride. After well shaking and allowing to stand for some hours in a thermostat, the volume of separated ethers was measured. The volume of alcohol was then obtained by difference. Corrections were necessary (*a*) for the slight solubility of alcohol and ether in the potassium carbonate solution, (*b*) for the solubility of ether in the sodium chloride solution, and (*c*) for the contraction in volume due to the admixture of alcohol and ether.

The separation of the ethers was effected by careful fractional distillation using a long column packed with Lessing rings. The various fractions were redistilled and the ethers identified by comparison of their vapour pressures, densities, and in some instances viscosities with authentic specimens prepared in the laboratory. Where the quantities of secondary ethers were too small to admit of complete separation they have been grouped together. The alcohols were also separated by fractional distillation, the purity of the fractions being confirmed by their refractive indices and vapour pressures; the normal secondary and *iso*-alcohols were identified by preparing their 3-5 dinitrobenzoate derivatives.

#### EXPERIMENTS WITH *n*-BUTYL ALCOHOLS

1—*Equilibrium in the System*  $2C_4H_9OH \rightleftharpoons (C_4H_9)_2O + H_2O$  *at*  $250^\circ C$   
 —Before studying the reaction between butyl alcohol and the olefines, a determination was made of the equilibrium constant of the dehydration reaction giving rise to dibutyl ether. For this purpose either the pure alcohol or an equimolecular dibutyl ether-water mixture was introduced into the previously heated reaction vessel, up to a total pressure of 12 atms., and the temperature was maintained constant at  $250^\circ$  until equilibrium was reached. The products were then rapidly withdrawn and analysed.

The analysis of the equilibrium mixtures approached by decomposition and by synthesis, respectively, are given in Table I.

TABLE I

	By decomposition	By synthesis
	gm.	gm.
Butyl alcohol . . . . .	0.355	0.300
Dibutyl ether . . . . .	2.279	1.928
Water . . . . .	0.270	0.224
from which $K_e$ equals . . . . .	11.3	11.5
Mean = 11.4		

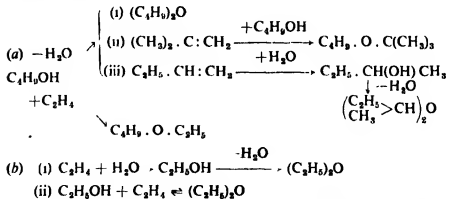
The equilibrium constant corresponds with a conversion of alcohol to ether of 87.5%.

During both experiments, some dehydration to butylene occurred, the quantity formed representing 9% of the alcohol decomposed. It was also noted that the *n*-butyl alcohol in the equilibrium mixture contained small quantities of *iso*-butyl alcohol probably formed by the rehydration of butylene.

**2—Reaction with Ethylene**—At 50 atm. pressure combination occurred between the alcohol and ethylene at a measurable rate at temperatures of 240° C. and upwards. Above about 265° C., however, considerable quantities of butylene were formed by the direct dehydration of the alcohol and the mixed ethers resulting from the olefine-alcohol reactions began to undergo thermal decomposition. The optimum temperature for their formation and survival under our experimental conditions was about 250° C. At this temperature and with a 1:5 alcohol-olefine mixture at 73 atm. total pressure reaction occurred rapidly and was three-quarters complete in about 1 hour. A further 4 hours' heating were required, however, before equilibrium was finally attained. The composition of the anhydrous liquid products is given in Table II.

During the course of the experiment, butylene and *iso*-butylene were formed, the composition of the residual gases being: ethylene = 94.1 and butylenes = 5.9 gm. mols. %.

All these products result from the operation of reactions (1), (2), and (3) as follows:



The predominant reactions were those resulting in the direct dehydration of the alcohol to the corresponding ether or isomeric olefines. Thus taking into account the butylene formed it was found that 49.9 gm. mols. % of the alcohol used went to form dibutyl ether, 40.8 to butylene, and

9.3 to ethyl-butyl ether. At the same time some hydration of the ethylene to ethyl alcohol with subsequent dehydration of the alcohol to diethyl ether also took place. The formation of secondary butyl alcohol and secondary dibutyl ether resulted from the hydration of the butylene.

In spite of the number of compounds present in the equilibrium mixture it is possible to obtain from the analytical results an approximate value for the equilibrium constant of the system butyl alcohol-ethylene-ethyl butyl ether. For example, there were present in the equilibrium mixture 1.74 gm. of ethyl butyl ether, 1.31 gm. of butyl alcohol and 17.19 gm.

TABLE II

	gm mol. %
Dibutyl ether	65.0
Ethyl-butyl ether	24.1
Ethyl alcohol	6.1
Secondary dibutyl ether	}
Normal secondary dibutyl ether	2.4
Normal tertiary dibutyl ether	}
Secondary butyl alcohol	1.6
Ethyl ether	0.8
	<hr/>
	100.0

of ethylene, from which  $K_e = C_{\text{ethene}} / C_{\text{alcohol}} \times C_{\text{ethylene}} = 1.6$ . This value of the constant indicates that starting with an equimolecular alcohol-olefine mixture at 250° C a 46.3% conversion of alcohol to ethyl butyl ether is theoretically possible.

3—*Reaction with Propylene*—Propylene reacted readily with butyl alcohol and with water liberated by the direct dehydration of the alcohol to give mainly *iso*-propyl derivatives. No *n*-propyl ethers and only traces of *n*-propyl alcohol were found in the products.

An equimolecular *n*-butyl alcohol-propylene mixture at 20 atms. and 251° reacted slowly, equilibrium being reached after the lapse of some 7 hours. The composition of the anhydrous liquid products are given in Table III.

The gaseous products consisted, as before, of butylenes and unreacted propylene.

The results show that dehydration of the alcohol occurred to a considerable extent and that much of the propylene was hydrated giving *iso*-propyl alcohol and *iso*-propyl ether. Of the alcohol used up only 10.4% was accounted for as *iso*-propyl butyl ether.

By analysis the equilibrium mixture was found to contain 4.39 gm. of butyl alcohol, 4.67 gm. of *iso*-propyl butyl ether, and 4.37 gm. of pro-

pylene, giving a value of 6.5 for the equilibrium constant of the alcohol-olefine-ether system at 251°.

### EXPERIMENTS WITH *n*-PROPYL ALCOHOL

1—*Equilibrium in the System*  $2 \text{C}_3\text{H}_7\text{OH} \rightleftharpoons (\text{C}_3\text{H}_7)_2\text{O} + \text{H}_2\text{O}$ —Two determinations of the equilibrium constant for the dehydration reaction

TABLE III

	gm. mol. %
Diethyl ether . . . . .	64.9
<i>Iso</i> -propyl ethyl ether . . . . .	21.6
Di- <i>iso</i> -propyl ether . . . . .	1.9
Secondary diethyl ether . . . . .	1.6
Normal tertiary diethyl ether . . . . .	0.8
Normal secondary diethyl ether . . . . .	1.6
<i>Iso</i> -propyl secondary ethyl ether . . . . .	1.4
<i>Iso</i> -propyl alcohol . . . . .	5.4
Propyl and <i>iso</i> -butyl alcohols . . . . .	0.8
	<hr/> 100.0

to ether were made at 250° C., and a pressure of 10 atm., the composition of the equilibrium mixture as approached by decomposition and by synthesis being given in Table IV.

TABLE IV

	By decomposition	By synthesis
	gm.	gm.
Propyl alcohol . . . . .	0.395	0.452
Propyl ether . . . . .	1.940	2.230
Water . . . . .	0.392	0.444
from which $K_e$ equals . . . . .	9.3	9.5
Mean = 9.4		

During these experiments very little decomposition to propylene took place, the gaseous products representing only 2.5% of the alcohol decomposed. The value of the equilibrium constant corresponds with a maximum conversion of alcohol to ether of 86%.

2—*Reaction with Ethylene*—At 253° C. an equimolecular propyl alcohol-ethylene mixture at 50 atm. reacted slowly, giving principally the dehydration product of the alcohol together with ethyl propyl ether. With a similar mixture at 295° the reaction was considerably accelerated and a greater proportion of the alcohol underwent dehydration to propy-

lene. The distribution of the alcohol consumed in the two experiments was as follows:—

	At 253° C.	At 295° C.
By dehydration to propyl ether . . . .	68·4	18·8
" propylene ..... .	7·3	77·0
By addition of the olefine to give ethyl propyl ether ..... . . . .	24·3	4·2

The effect of increase of temperature is perhaps best shown by a comparison of the anhydrous liquid products in the two cases, Table V.

TABLE V—PRODUCTS AS GM. MOLES % FROM REACTIONS

	At 253° C. gm. mol. %	At 295° C. gm. mol. %
Dipropyl ether	51·0	50·5
Ethyl propyl ether	36·3	23·0
Ethyl iso-propyl ether	1·9	8·2
Ethyl ether	1·3	13·8
Propyl iso-propyl ether	0·5	4·5
Ethyl alcohol .	9·0	Nil
	<hr/> 100·0	<hr/> 100·0

It will be seen that with increased temperature there was a greater tendency for iso-propyl derivatives to be formed, although the total amount of mixed ethers decreased by 7%. Also, whereas at 253° C. hydration of the ethylene resulted mainly in the formation of ethyl alcohol, at the higher temperature it gave ethyl ether only.

From the analysis of the equilibrium mixture at the two temperatures the equilibrium constants for the system propyl alcohol-ethylene-ethyl propyl ether are  $K_e$  (253°) = 1·54 and  $K_e$  (295°) = 1·23, corresponding with theoretical conversions of alcohol to mixed ethers of 46·5 and 41·5% respectively. The change of  $K_e$  with temperature indicates that the reaction is slightly exothermic with respect to ether formation.

#### EXPERIMENTS WITH ETHYL ALCOHOL

1—*Equilibrium in the System  $2C_2H_5OH \rightleftharpoons (C_2H_5)_2O + H_2O$  at 266° C.*—Several attempts have been made to measure the equilibrium constants for the above system at temperatures between 215° and 275° with results summarized in Table VI.

Of these results the value of 275° C., determined by Pease and Young, is almost certainly too low. The remaining figures, whilst showing better

agreement, are not entirely satisfactory. Thus, if 5700 calories are taken as the most probable value of the heat of hydration of ethyl alcohol and  $K(215^\circ) = 11.1$  is used as a basis of calculation, then the values of  $228^\circ$  and  $250^\circ$  would be 9.5 and 7.48 respectively.

TABLE VI

Temperature ° C.	K	Authors
215	11.1	Jatkar and Watson
220	10.0	"
228	7.0	"
250	8.0	Clark, Graham, and Winter.
275	0.66	Pease and Young.

We have determined the constant at  $266^\circ$  and 10 atm. approaching equilibrium by decomposition and synthesis. The compositions of the two equilibrium mixtures are given in Table VII.

TABLE VII

	By decomposition gm.	By synthesis gm
Ethyl alcohol . . . . .	0.745	0.655
Ethyl ether . . . . .	2.118	2.610
Water . . . . .	1.290	0.799
from which $K_e$ equals . . . . .	7.8	7.7

In neither experiment was more than a trace of ethylene found in the products. The mean value of the constant corresponds with a maximum conversion of alcohol to ether of 84.7%.

*Reaction with Ethylene*—We have been able to confirm this value from the results of an experiment in which an equimolecular alcohol-ethylene mixture at 50 atm. was allowed to react at  $267^\circ$  until equilibrium was substantially reached. The composition of the resulting mixture was: ethyl ether = 0.0273 gm. mol., ethyl alcohol = 0.0093 gm. mol., ethylene = 0.1450 gm. mol., and water = 0.0253 gm. mol. From these figures the equilibrium constant ( $K_e = C_{\text{ether}} \times C_{\text{water}} / C_{\text{alcohol}}$ ) is 8.0, a value agreeing reasonably well with the previous determinations.

The difference between the amounts of ether and water in the equilibrium mixture, namely 0.002 gm. mol., gives a measure of the ether formed by the direct interaction of ethylene and alcohol and corresponds with a maximum conversion of alcohol to ether by this reaction of 46%.

2—*Reaction with Propylene*—The rate of reaction between ethyl alcohol and propylene was too slow to be readily measurable at 250°. At 270.5° C., however, it proceeded more rapidly and starting with a 1:3.3 alcohol-propylene mixture at 44 atm. equilibrium was reached in about 10 hr. The composition of the anhydrous liquid products is given in Table VIII.

TABLE VIII

	Product as gm. mol. %
Ethyl ether . . . . .	92.1
Ethyl <i>iso</i> -propyl ether . . . . .	2.8
Ethyl propyl ether . . . . .	0.8
<i>Iso</i> -propyl ether . . . . .	0.2
<i>Iso</i> -propyl alcohol . . . . .	4.1

Taking into account the ethylene formed by dehydration the products correspond with the following distribution of alcohol:

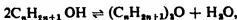
To diethyl ether . . . . .	97.5 gm. mol. %
To ethylene . . . . .	0.5 ..
To propyl and <i>iso</i> -propyl ether . . . . .	1.9 ..

It is evident from the above results that dehydration of ethyl alcohol took place much more readily than with either propyl or butyl alcohol. As in previous experiments, hydration of the propylene occurred simultaneously and resulted in the formation of *iso*-propyl derivatives. No *n*-propyl alcohol could be detected in the products and only relatively small quantities of ethyl propyl ether were formed.

The equilibrium mixture contained 0.60 gm. of ethyl *iso*-propyl ether, 0.17 gm. of ethyl propyl ether, 5.0 gm. of propylene and 3.31 gm. of ethyl alcohol, giving a value of 1.0 for the equilibrium constant at 270.5° C.

#### SUMMARY

The equilibrium constant for the system



has been determined for ethyl, propyl and butyl alcohols with the following results :

Alcohol	$K_e = \frac{C_{\text{ether}} \times C_{\text{water}}}{C_{\text{alcohol}}^2}$
Ethyl alcohol . . . . .	7.75 (266°)
Propyl alcohol . . . . .	9.40 (250°)
Butyl alcohol . . . . .	11.40 (250°)

At pressures of 10 atms. and upwards, and in the presence of suitable catalysts, ethylene and propylene combine with ethyl, propyl, and butyl alcohols to give the corresponding mixed ethers. The reaction is always accompanied by some direct dehydration of the alcohol and by partial hydration of the olefine to produce, in the former case, the corresponding ether and in the latter the alcohol.

The equilibrium constants for the system



have been determined in a number of instances with the following results:

Alcohol	Ethylene		Propylene	
	$K_s$	% conversion of alcohol to mixed ethers	$K_s$	% conversion of alcohol to mixed ethers
Ethyl alcohol . . .	1.54 (267°)	46.5	1.0 (270.5°)	38.0
Propyl alcohol . . .	1.54 (253°)	46.5	—	—
" . . .	1.23 (295°)	41.5	—	—
Butyl alcohol . . .	1.60 (250°)	45.0	6.5 (250°)	68.5

## A Critical Experimental Investigation of the "Force" Method of Determining the Dielectric Capacity of Conducting Liquids at Low Frequencies: Univalent Electrolytes in Aqueous Solution

By W. J. SHUTT, D.Sc., Lecturer in Electro-chemistry, and H. ROGAN, Ph.D., the Muspratt Laboratory, The University, Liverpool

(Communicated by W. C. M. Lewis, F.R.S.—Received 26 May, 1936)

The theories of Debye, Onsager, and Falkenhagen, stressing the connexion between the dielectric constant and the other properties of solutions of electrolytes, have focussed a considerable amount of attention on the problem of the accurate determination of the dielectric properties of conducting solutions. The results, however, of work published by various investigators during the past few years show wide discrepancies and, in fact, it can hardly be said that even the sign of the effect of electrolytes upon the dielectric constant of water has yet been established with any degree of certainty. That the results have been so unsatisfactory is not altogether surprising in view of the inherent difficulties of the problem; the system itself is a complicated one, consisting of simple water dipoles, the polymers dihydrol and trihydrol, and the solute molecules or ions dispersed throughout the liquid; furthermore, the experimental technique is frequently complicated by the requirement that the dielectric constants shall be determined at frequencies low enough to permit of computation of the maximum possible polarization of the system, including the rotational polarization of all polar molecules which may be present.

Methods involving the direct determination of the capacity of a condenser containing the liquid, whether by capacity-bridge or by resonance, are rendered difficult or inaccurate through the poor capacity sensitivity of such systems in presence of an appreciable ohmic conductivity between the condenser plates. This difficulty is minimized by the use of very high frequencies, and a considerable amount of work has been carried out under these conditions by Wien, Röver, Falkenhagen, and others in connexion with the theory of strong electrolytes. The need has arisen, however, for the values of the dielectric constants of solutions of large polar molecules such as long-chained amino acids, polypeptides, and soluble proteins. Such substances have considerably enhanced periods of relaxation, and proportionately low frequencies of alternating current

must be employed to avoid loss of the orientation polarization of the system. In the case of pure egg-albumin solution, dispersion of hertzian waves occurs at all frequencies above about  $10^5$  sec.<sup>-1</sup>.\* In view of this difficulty it seemed desirable that a thorough investigation should be made into the question as to whether precision results might be obtained from some general method which uses comparatively low frequencies of alternating current. The "force" method theoretically developed by Fürth,† in 1924, seemed the most promising. Various modifications of this method have been used by many workers, unfortunately, however, with by no means concordant results, so far as conducting solutions are concerned. It consists broadly in the determination of the force exerted upon an ellipsoid, mounted to rotate about one of its minor axes, in a liquid dielectric across which an alternating field is applied in a direction at right angles to the axis of rotation of the ellipsoid. For such a system Fürth has shown that the torque on the ellipsoid may be expressed by  $\epsilon E^2 \sin 2\theta A$ , where  $\epsilon$  represents the dielectric constant of the liquid,  $E$  the potential gradient,  $\theta$  the angle between the major axis of the ellipsoid and the direction of the field, and  $A$  a constant involving the dimensions of the ellipsoid. This form of Fürth's equation applies only so long as the resistance of the liquid dielectric is high relative to that of the ellipsoid itself.

It has been suggested by Cohn‡ that the Fürth method is unsuited to the absolute determination of dielectric constant, although quite satisfactory as a comparison method, furthermore, under these conditions, the ellipsoidal form of suspended body is quite unnecessary, any convenient shape being equally reliable. Nevertheless, it was felt that a wide divergence from the form of the ellipsoid would bring in several factors of uncertain significance, and the original form of apparatus has, as far as possible, been maintained in this work. Preliminary experiments, however, soon indicated that the passage of any part of the moving system through the liquid-air interface was a weak point in the Fürth design. The torsional force of the electric field on the ellipsoid is so minute that any irregularities in surface tension at the point of penetration of the liquid surface are sufficient to vitiate the results, and laborious precautions are necessary to maintain perfection of surface. To avoid this difficulty, the apparatus was finally constructed so as to allow of complete immersion of the moving system, including the whole of the quartz fibre suspension. This mode of construction extended the range

\* Errera, 'J. Chim. phys.', vol. 29, p. 577 (1932).

† 'Z. Phys.', vol. 22, p. 98 (1924); vol. 44, p. 256 (1927).

‡ 'Phys. Z.', vol. 32, p. 687 (1931).

of the method to a wide variety of liquids, and it was possible to examine even solutions of proteins—substances which orientate at the surface of the liquid to form a semi-solid layer.\*

### EXPERIMENTAL

*Apparatus.*—The form of cell finally adopted is shown diagrammatically in fig. 1a. It consisted essentially of an open-ended quartz cylinder AB,

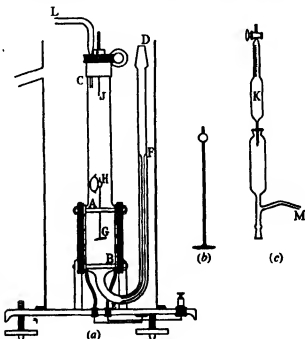


FIG. 1.

6 cm. in diameter, and 2·5 cm. in length; to this was attached the vertical tube AC and the bent tube BD used for filling and evacuating the cell. A length of capillary tubing, EF, was inserted into BD to break the force of the incoming liquid and avoid undue disturbance of the suspended system GH. The latter consisted of a platinum ellipsoid G (*ca.* 9 mm. long and *ca.* 0·8 mm. thick) drilled through one of its minor axes and spot-welded to a fine platinum-iridium wire, which passed through the hole in the ellipsoid and formed a means of attachment for the stainless steel mirror H and the lower end of the quartz fibre, shown at H. For some

\* Ramsden, 'Z. phys. Chem.', vol. 47, p. 336 (1904).

time the mirror was directly cemented to the platinum-iridium wire, but this type of suspended system was found to be extremely fragile in use, and the rigidity of the weld at the ellipsoid was a matter of some doubt; in consequence, the system was modified to the form shown in fig. 1*b*. The wire was cut short, to within a few millimetres of its lower end and slipped into a fine glass capillary tube, which could be fused rigidly to the body of the ellipsoid itself. The upper end of the capillary was sealed and slightly etched to facilitate attachment of the mirror and fibre. The latter was anchored both to its platinum support and to the suspended system by means of shellac. The upper end of the fibre was attached to a stout platinum wire soldered to a brass rod which, in turn, was held in a torsion head operated in the usual manner by worm and wheel. The mirror, which was 4 mm. in diameter, was viewed through a plane quartz window fused to the side of the tube AC at an angle of 45° with respect to the axis of the cylinder AB and at about 3° to the vertical. This deflexion from the vertical avoided direct reflexion of the light beam employed to measure the rotation of H. The optical system was completed by the usual telescope and illuminated scale placed at a distance of about a metre and a half from the cell. An alternating field was applied to the dielectric by means of copper-backed platinum disks clamped to the ground ends of the quartz cylinder AB. These disks were backed by circular sheets of rubber and held in position by stout blocks of ebonite bolted together in the manner shown in the sketch.

The whole apparatus was enclosed in a cylindrical copper vessel fitted with a window which registered with the window in the quartz tube AC, and a brisk stream of water was circulated through this jacket from a thermostat. Considerable difficulty was experienced in maintaining electrical insulation between the water jacket and the contents of the cell. Best results were obtained by first coating the outer rims of the quartz cylinder and the edges of the platinum and rubber disks with a thin layer of soft red wax, a hot iron being used to ensure good contact between the wax and the solid surfaces, and then the whole space between the ebonite blocks was repeatedly painted with a mixture of two parts of soft red wax to one of golaz cement until a thickness of several millimetres of the insulator had been built up. The alternating current leads were liberally coated with the same mixture. In spite of most elaborate precautions, the life of this insulation was not, in general, more than about ten days.

Two  $\frac{1}{2}$  K.V.A. machines, designed and supplied by Loughborough College, provided a source of alternating current, the one at frequencies ranging from 20 to 200 cycles and the other at 1000 to 2000 cycles per second. Both were excited from a storage battery of large capacity and

the drive was furnished by constant speed motors. Although the power required to actuate the suspension was infinitesimal, in order to maintain a constant potential at the cell terminals, a comparatively heavy current was generated and the bulk of it was shunted through large, adjustable carbon-plate rheostats from which the working voltage for the cell was tapped. A thermo-galvanometer of the Duddell type served to measure this voltage and the circuit was closed on the cell by means of a double pole mercury switch. The series resistances of the galvanometer were non-inductively wound and placed in sealed glass tubes immersed in a thermostat maintained at 20° C.

#### EXPERIMENTAL METHOD

Throughout the research, water was used as standard, and, since both the ellipsoid and the platinum disks were heavily platinized to guard against electrolytic polarization, considerable care had to be taken to remove all traces of electrolyte which might have been occluded in the electrodes from a previous measurement. The cell was repeatedly washed with distilled water and the process of diffusion of the electrolyte was hastened by application of a slowly alternating potential of 230 volts to the plates. For this purpose a motor-driven commutator provided the alternations from the D.C. lighting circuit at a periodicity of about ten seconds.

An hour or so before any readings were taken, the dynamo, thermostat pump, etc., were set in motion in order that the rheostats, thermogalvanometer, and cell itself might attain constant conditions. The cell was then filled with the aid of the apparatus shown in fig. 1c. The pipette was filled with a volume of water slightly greater than the pre-determined capacity of the cell by a sharp evacuation on the water pump. This process had the advantage of removing a large fraction of the dissolved air and so preventing the formation of bubbles of gas on the ellipsoid. The water was then transmitted to the cell via the vessel K which fitted on the quartz ground-joint D. Final adjustment of the level of liquid in the cell was made by means of the capillary tube L, which passed through the brass torsion cap and could be connected to a vacuum line at will. The cell was emptied by closing the top of K and putting the tube M into communication with the same vacuum line.

After filling, the cell and its contents were left undisturbed for ten or fifteen minutes, after which time the position of the suspension was usually steady and the zero position of the mirror, as read through the telescope, could be relied upon to remain constant to within a millimetre or so of

the scale divisions throughout an extended series of measurements. The zero was adjusted to such a value that the swing of the mirror (a matter of 100 or 120 millimetres of scale divisions) was equally disposed about the centre of the scale. It will be obvious that with such a small deflexion of the mirror, the error produced by reading divisions on a flat scale as angular deflexions is negligible. In fact, calculation showed that for the most exacting cases studied in this work (e.g., 0·03 N. KCl) the error was less than one-tenth of 1%.

There are two methods by which the torsion of a quartz fibre may be used to determine the torque on a suspended system; the displacing force, in this case an alternating potential, can be applied continuously and the final equilibrium position taken up by the suspension can be determined (the "static method"), or, on the other hand, the field may be applied only for so long as is required for the ellipsoid to complete its first throw, the maximum reading on the scale being taken as a measure of the torque on the system (the "ballistic method"). The latter method possesses the advantage of requiring that only a minimum of current be passed through the liquid, but it is obviously unsuited to the comparison of the dielectric constants of two liquids which differ in viscosity. Since the object of this work was to extend the measurements to solutions of as high a conductivity as possible and since a very small amount of joule heating of the solution was sufficient to set up convection currents which completely vitiated the results, the ballistic method was used throughout. Justification for this procedure was derived from the fact that for low concentrations of electrolyte (e.g., to N/200 KCl) both methods yielded the same result. Furthermore, for even the most strongly conducting solutions employed, a single equilibrium throw could usually be obtained, and its value invariably corresponded within experimental error (about 0·2%) to the result given by the ballistic method.

When the apparatus had attained constant conditions, some five or six measurements of the throw of the ellipsoid were made with water in the cell, the corresponding reading of the thermo-galvanometer being noted for each. The cell was then left for about a quarter of an hour and a second series of readings were taken. If the two series agreed among themselves, the cell was refilled with water and the process repeated. In general, the "water throw" was not considered reliable until at least three fillings of the cell had yielded results steady to within about 0·2%. It may be stated, however, that the agreement between consecutive fillings of the cell was usually better than this and the variation from day to day was not more than about 0·2%. Satisfactory results having been obtained for water, the cell was filled with the solution to be examined and several

series of readings were taken. The length of each series depended on the conductivity of the solution and in extreme cases not more than one or two successive measurements could be made before convection currents were created in the liquid. The mutual agreement between results was, however, in general as good as that for water. This high order of reproducibility in the behaviour of a quartz fibre was at first somewhat surprising and can only be attributed to the constant environment (water or a dilute solution in water) maintained about the thread. The voltage applied to the plates lay between 12 and 20 volts, but its precise value depended upon the thickness of the quartz fibre in use. The fibres were shot in the usual manner and tested for suitability by a count of the vibration frequency when the suspension hung freely from the fibre in air. The series resistances of the thermo-galvanometer were then adjusted until a "throw" of the ellipsoid (in water) of some 10 or 12 cm. corresponded with a reading of 90 or 95 on the 100 arbitrary divisions of the galvanometer scale. The voltage did not usually vary by more than 0.1% during any one series of measurements, but correction had to be made even for this small variation, since the throw of the ellipsoid is proportional to the square of the potential. The question of precise voltage measurement became of serious moment when dealing with conducting solutions. Although the resistance of the carbon rheostats was of the order of only about one ohm, the act of closing the circuit across the cell caused an appreciable drop in voltage. This difficulty was countered by pre-determining the open-circuit potential which would give the standard voltage represented by 90 or 95 on the arbitrary galvanometer scale when a "throw" was being measured. With the most strongly conducting solutions employed, this involved setting the galvanometer to a value about 4 or 5% greater than the standard value. Final correction was made by reading the voltage at the plates immediately after a series of throws had been measured. This comparatively prolonged passage of electricity of course intensified the convection currents within the cell, and the apparatus had, in consequence, to be allowed a proportionately longer time to regain equilibrium before a further series of throws could be measured.

#### POLARIZATION

Electrolytic polarization has been a continuous menace to accuracy in the determination of dielectric constants by the Fürth method. Its action is to oppose the applied field by back-electromotive forces generated at the electrode surfaces (both plates and ellipsoid), and so to detract from the applied voltage, which should, theoretically, be engaged solely in

maintaining a potential gradient across the liquid. Thus the net effect of electrolytic polarization is a "throw" abnormally low in respect to the voltage registered at the cell terminals, and a correspondingly low value for the dielectric constant. Some time was devoted to a study of this effect, and it is now felt that the experimental method may be considered to be free of any objection on the score of polarization. In this connexion measurements were carried out with a cell fitted with bright platinum plates and ellipsoid—conditions under which polarization might be expected to occur at all but the highest of alternating current fre-

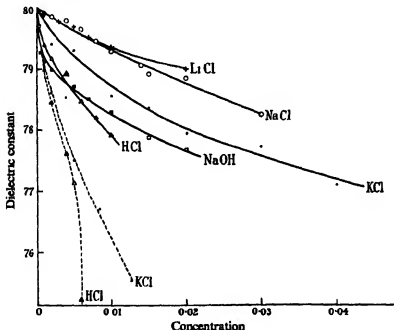


FIG. 2.

quencies—and the "throw" was found to increase with increasing frequency. This effect is readily explained by assuming that, with the small current densities employed, the full over-voltages of hydrogen and oxygen (chlorine for chloride solutions) were not fully developed in the short period of one-half cycle of the alternating current. With further reduction of this period, *i.e.*, with increasing frequency, still less was the degree of polarization built upon the plates and a greater fraction of the applied voltage was spread across the liquid dielectric, to manifest itself in the enhanced "throw" of the suspended system. With the bright electrodes it is likely that electrolytic polarization was still occurring at the highest

frequency available, 2000 cycles/second, since the values of the dielectric constants obtained under these conditions were invariably lower than those obtained with platinized plates and ellipsoid. For instance, the broken-line curves in fig. 2 indicate values for the dielectric constants of potassium chloride and hydrochloric acid solutions as determined in a cell fitted with bright electrodes. It will be seen that the effect of polarization, evidenced by the widening discrepancy between the dotted and full curves, increases with the conductivity of the electrolyte, as is only to be expected from the increase in current density under such circumstances.

After these tests, the same plates and ellipsoid were platinized in the usual manner and the measurements were repeated. Under these conditions, no variation whatsoever was observed in the "throw" on changing the frequency of the applied voltage and the apparatus was considered to be free of polarization.

An early difficulty experienced with the Fürth method lay in a slight change in the value of the observed dielectric constant with a change in the intensity of the field, and this effect, too, has been attributed to polarization. It may be stated at once that, in these experiments, no such discrepancy arose. With well platinized plates and ellipsoid, the torque developed was, within the accuracy of the meters available, strictly proportional to the square of the applied r.m.s. voltage, as demanded by the Fürth equation.

#### PRELIMINARY TESTS

Aqueous solutions of amino acids, urea, etc., have comparatively low conductivities and the determination of their dielectric constants presents no serious difficulty. Accurate data are available and such solutes possess an added advantage, for the purpose of experimental test, in the fact that they affect the dielectric constant of water to a marked extent. Series of measurements have been made on these solutions and the full results will be presented elsewhere. The cases of pure glycine and urea solutions may, however, be cited in brief. A linear relationship between concentration and dielectric constant was observed in both cases. The value of  $d\epsilon/dc$  for glycine\* obtained with this apparatus was identical with that given by Hedeström† (22·4), who used a high frequency capacity bridge method, and was within 0·5% of the more recent figure of Wyman and McMeekin,‡ who employed the resonance method, but were working

\* The measurements on glycine were made by Dr. H. Evans of this Laboratory, to whom our thanks are due.

† 'Z. phys. Chem.', vol. 135, p. 40 (1928).

‡ 'J. Amer. Chem. Soc.', vol. 55, p. 908 (1933).

at a somewhat different temperature (25° C.). As regards urea, the value of 2.90 for  $d\varepsilon/dc$  agrees exactly with the result found both by Devoto\* and by Wyman.†

Although these results were obtained under conditions considerably less onerous than those imposed by the more strongly conducting solutions for which the apparatus was primarily designed, their close agreement with figures obtained from methods involving much higher frequencies is considered to be ample evidence for the general reliability of this type of apparatus and technique.

### RESULTS FOR SIMPLE ELECTROLYTES

The mean results are given in Table I, of which the first column represents the concentration in grammolecules per litre and the others the dielectric constants of the various electrolytes all referred to the value 80.0 as the dielectric constant of pure water at 20° C.

TABLE I  
Temperature = 20° C.  $\pm 0.02$

Concentration of electrolyte	Dielectric constants				
	LiCl	NaCl	KCl	HCl	NaOH
0.0005	—	—	—	—	79.27
0.001	79.90	79.90	79.86	79.39	79.13
0.002	—	79.86	79.52	79.16	78.99
0.003	79.76	—	—	—	—
0.004	—	79.79	—	78.90	78.92
0.005	79.69	—	79.32	—	78.72
0.006	—	79.65	—	78.47	—
0.0075	79.50	—	—	—	78.50
0.008	—	79.46	—	78.20	—
0.010	79.35	79.28	78.55	77.93	78.29
0.014	—	79.05	—	—	—
0.015	—	78.91	78.36	—	77.87
0.020	78.98	78.85	77.93	—	77.67
0.030	77.96	78.25	77.74	—	—
0.040	—	77.21	77.09	—	—

A more general impression of the results may be gained from fig. 2 (full lines), where the same figures are indicated graphically. The curves show that, up to the maximum concentrations studied, the effect of the presence of univalent ions upon the dielectric constant of water is com-

\* 'Gazz. chim. ital.', vol. 63, pp. 50, 119 (1933).

† 'J. Amer. Chem. Soc.', vol. 55, p. 4116 (1933).

paratively slight, only about 4% in all. This small difference emphasizes the necessity for extreme accuracy and sensitivity of experimental technique; an error of 0·2% in the measured dielectric constant represents about 5% inaccuracy in the estimation of the greatest lowering of dielectric constant observed. The relation between concentration and dielectric constant is comparatively simple, although by no means linear, and there is no evidence of the minimum previously observed by several investigators. It is remarkable that results indicating a minimum dielectric constant at a low concentration have been obtained almost exclusively by workers employing "force" methods and yet, with the present modification of the Fürth method, we are quite unable to reproduce such minima. All the electrolytes mentioned in Table I have been examined in this way either by Schmidt,\* by Pechhold,† or by Millicka and Slama,‡ and in every case a minimum value of the dielectric constant was found for comparatively dilute solutions. The minima lay at concentrations ranging from  $3\cdot9 \times 10^{-3}$  (for NaOH) to  $7\cdot5 \times 10^{-3}$  (NaCl) gram molecules per litre and the values of these minimum dielectric constants were very low compared with the results given in this paper. The value for HCl was 71·9 (Pechhold) or 70 (Millicka and Slama), for NaOH 74, and for KCl 77·7. It may be noted, however, that there is a strong resemblance between the descending portions of the curves obtained by the earlier investigators of this method and the dotted lines of fig. 2, where polarization of the electrodes was undoubtedly present; so marked is this similarity that it is impossible to avoid the suspicion that the question of polarization has not hitherto received adequate attention. In view of this doubt Fürth's hypothesis§ of an extremely large sheath of water of hydration around each ion need not, at present, be considered.

Since the completion of the work described in this paper, some interesting figures for the dielectric constants of solutions of electrolytes have been published by Fischer and Schaffeld.|| They have employed the Fürth method as modified by Orthmann.¶ They opposed the effects of electrolytic polarization by the use of high frequencies and at 200,000 cycles they found that platinization of the ellipsoid was unnecessary, perfectly satisfactory results being obtained with a smooth gold surface. At lower frequencies (50,000 cycles and below) a variation of throw was

\* 'Phys. Rev.,' vol. 30, p. 925 (1927).

† 'Ann. Physik,' vol. 83, p. 427 (1929).

‡ 'Ann. Physik,' vol. 8, p. 663 (1931).

§ 'Phys. Z.,' vol. 32, p. 184 (1931).

|| 'Ann. Physik,' vol. 25, p. 450 (1936).

¶ 'Ann. Physik,' vol. 9, p. 537 (1931).

observed on changing the frequency of the applied field. This is contrary to our experience, and it can only be inferred that their mode of platinization was in some way faulty. This inference is supported by the fact that they found the throws of the ellipsoid in presence of water too unsteady to permit of the use of the pure solvent as a standard. Whilst it must be admitted that, of all the liquids so far examined, water is undoubtedly the most exacting in the matter of perfection of the ellipsoid surface, this fact was rather welcomed by us as affording a means of testing the apparatus, since experience seemed to indicate that it was advisable to trust only such results as could be compared directly with water itself.

Their results for uni-univalent electrolytes are very similar to those given in Table I. Their curves for  $d\epsilon/dc$  do not exhibit the minimum previously observed by Milicka and Slama and others, but they differ from the curves given in fig. 2 in that the slope increases with increasing concentration of electrolyte.

#### CONCLUSION

Since the measurements seem to indicate a marked difference in dielectric constant between solutions of the same strength of different uni-univalent electrolytes they cannot be said to represent a marked confirmation of the Debye-Falkenhagen theory. On the other hand, the results for alkali chlorides do conform, within experimental error, with a relation of the type  $\epsilon = \epsilon_0(1 + \alpha\sqrt{c} - \beta c)$  if it be assumed that the maximum of the  $d\epsilon/dc$  curve, to which this expression leads, is relatively small and occurs at some concentration less than  $0.0005 n$ . This equation represents the Debye-Falkenhagen relation between the dielectric constant of the solution,  $\epsilon$ , that of pure water,  $\epsilon_0$ , and the concentration,  $c$ , together with the correction  $\beta c$  applied by Sack\* to take account of the saturation effect of the ionic charges upon the water dipoles. At low or zero frequency,  $\alpha$  is assigned the value 0.047 for all uni-univalent salts, and the value 3 was proposed by Sack for the constant  $\beta$ . A comparison between the observed dielectric constants of sodium chloride solutions and values calculated from  $\epsilon = \epsilon_0(1 + 0.047\sqrt{c} - 1.1c)$  is made in fig. 3. It will be seen that the agreement is poor over the range of concentrations at which the Debye-Falkenhagen factor  $\alpha$  has the predominating influence and the value of 1.1 has to be adopted for  $\beta$ .

It is not, at present, possible to account satisfactorily for this discrepancy between the theory and the practical results; it should be

\* 'Phys. Z.,' vol. 28, p. 199 (1927).

remembered, however, that the frequencies employed in this work are very low and it is not impossible that, under these conditions, large molecular aggregates (e.g., "hydrates") are playing a part in the orientation polarization of the system in a manner not allowed for either in the derivation of the Debye-Falkenhagen equation or in the correction term  $\beta$  due to Sack.

### SUMMARY

The Fürth force method for the determination of dielectric constant has been modified and the new apparatus is described in detail. The

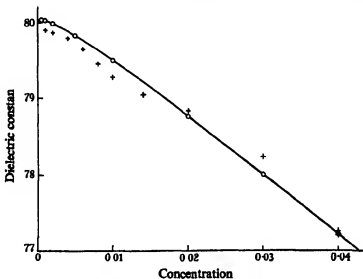


FIG. 3.—+ observed NaCl; O  $\epsilon = \epsilon_0 (1 + 0.047 \sqrt{c} - 1.1 c)$ .

method is now considered to be reliable to within an accuracy of  $\pm 0.2\%$  for solutions of electrolytes having conductivities less than 0.005 mho.

The occurrence of electrolytic polarization of the electrode surfaces is discussed. The effect of frequency of applied alternating field has been tested over a range of from 50 to 2000 cycles per second and, with a well platinized ellipsoid, such variation of frequency has been found to be without influence upon the observed dielectric constant of dilute electrolytes.

The apparatus has been tested with aqueous solutions which have well-defined dielectric constants.

Figures are given for the dielectric constants of solutions of LiCl, NaCl, and KCl up to a concentration of about 0.04  $n$ , of HCl up to 0.01  $n$ ,

and of NaOH to 0·02 n. All these electrolytes affect the dielectric constant of water to a comparatively small extent; a lowering of only about 4% is observed with the strongest solutions studied. The dielectric constant falls continuously with increasing concentration of electrolyte over the range of concentration used.

The discrepancies between the experimental results and the Debye-Falkenhagen theory are discussed briefly.

## Transmutation of the Lithium Isotope of Mass Seven by Deuterons

By A. E. KEMPTON,\* B. C. BROWNE, and R. MAASDORP†

(Communicated by Lord Rutherford, O.M., F.R.S.—Received 29 May, 1936)

### INTRODUCTION

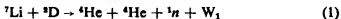
Recent investigations on the transmutations of the light elements have shown that the mass number 5 is the only one not occupied by a stable element. In a letter to 'Nature,' Dr. Oliphant‡ has pointed out that the mass defects of the light elements show a periodic variation, and has deduced from this that the missing element should have a mass of about 5·0125. It is to be expected that the place should be occupied either by an isotope of helium or of lithium of mass five, but more probably by the former. These investigations were initially undertaken to test whether the isotope of helium of mass five arose in certain transmutations. In considering the whole field of artificial transmutations, experience has shown that practically every type of reaction which is energetically possible does take place, but the relative frequency of each reaction is governed by factors which are not yet understood. Among the light elements the nuclei  $^2\text{H}$ ,  $^3\text{D}$ ,  $^3\text{T}$ ,  $^3\text{He}$ ,  $^4\text{He}$ , and  $^6\text{Li}$ ,  $^7\text{Li}$ ,  $^8\text{Be}$ , etc., all appear as products of nuclear transmutations, and it is reasonable to expect that the nucleus of mass five, if it exists, should also make itself evident. For example, we

\* Coutts Trotter Student.

† Beit Railway Trust Rhodesian Fellow.

‡ 'Nature,' vol. 137, p. 396 (1936).

might expect that the transmutation of  $^7\text{Li}$  when bombarded by deuterons should proceed in the alternative ways:



The bombardment of  $^7\text{Li}$  with deuterons is therefore a likely experiment in which to search for a  $^6\text{He}$  nucleus.

It has been shown that (1) results in a continuous distribution of  $\alpha$ -particles with energies ranging from the lowest observable ( $0.6 \text{ m. e-volts}$ ) to a maximum of  $8.1 \text{ m. e-volts}$ .\* The reality of (2) would be revealed by the presence of two homogeneous groups of particles superimposed on this continuous distribution. The work described in this paper has been done in order to ascertain whether or not the second of the above transmutations does occur.

We may notice in the first place that the reaction energy of (2) is greater or less than that of (1) (*i.e.*,  $W_2 \gtrless W_1$ ) according as the  $^6\text{He}$  nucleus is stable or unstable. (Stability here denotes that the binding energy of the  $^6\text{He}$  nucleus considered as formed from an  $\alpha$ -particle and a neutron is positive.) It follows that on the hypothesis of a stable  $^6\text{He}$  nucleus the  $\alpha$ -particle liberated in (2) will have a greater energy and therefore a greater range than the most energetic  $\alpha$ -particles liberated in (1). Conversely, the formation of an unstable  $^6\text{He}$  nucleus would be accompanied by the presence of an  $\alpha$ -particle group of energy less than the maximum of (1). Clearly such a group unless large would be much more difficult to detect in the latter case than in the former.

Using the mass 5.0125, the ranges of the  $^4\text{He}$  and  $^6\text{He}$  liberated in (2) are calculated to be 8.05 and 4.95 cm. respectively. We may state with certainty that no homogeneous group of  $\alpha$ -particles is emitted, when  $^7\text{Li}$  is bombarded with deuterons, with energy greater than the maximum of (1); or more exactly, no such group exists with a yield as great as 1% of (1). We therefore conclude that the probability of the formation of a stable  $^6\text{He}$  nucleus is less than 1% of the probability of the transmutation (1).

During some further experiments on the continuous distribution of  $\alpha$ -particles, indications of certain irregularities in the shape of the number-absorption curve were obtained. In the total number-absorption curve these irregularities take the form of a rapid and discontinuous change of

\* Oliphant, Kempton, and Rutherford, 'Proc. Roy. Soc.,' A, vol. 149, p. 406 (1935).

slope, while on the differential number-absorption curve they appear as "peaks". The presence of homogeneous groups of particles would be revealed in precisely this manner. However, experiments done from day to day showed little or no consistency in the values of the ranges at which these irregularities occurred, and it was clear that if precision was to be obtained the experimental method must be improved.

One of the chief difficulties inherent in counting experiments when using high voltage sources is the capricious fluctuations occurring in the activity of the source. The number of particles emitted per unit time per unit current fluctuates by factors often as high as 50% or more. These are to be ascribed to small variations in the accelerating voltage, the nature of the target, etc., and their complete removal would seem impossible. It is therefore desirable to employ a second counter, the sole function of which is to determine the activity of the source. In the next series of experiments we therefore employed two counters. The target\* of separated  $^7\text{Li}$  was scanned by two windows, the normals to which were perpendicular. The one counter was an ordinary ionization chamber and served only to measure the activity of the source during the course of an experiment. It remained fixed in position and counted particles over a definite energy range. To increase the chance of detecting small homogeneous groups superimposed on the continuous distribution the second counter was of the differential type. It had three parallel electrodes, the centre one being the collector and connected to the grid of the D.E.V., and the two outer ones having potentials of  $\pm 240$  volts respectively. Circular apertures in the two electrodes nearest the target allowed the particles to traverse both halves of the chamber, and these apertures were of such relative sizes that all particles passing through the first half of the chamber also passed through the second half. The apertures were covered with aluminium foils of about  $\frac{1}{2}$  mm. of air stopping-power. If a pure range is investigated with such a counter, the number-absorption curve obtained has the form of a sharp peak. The sharpness of the peak, and therefore the resolving power of the counter, depends upon the stopping-power of the gas between the electrodes, and it is therefore desirable to have the distance between the electrodes as small as possible. On the other hand, decrease of the inter-electrode distance leads to an increase both in the capacity of the counter and also in the microphonics. Both these difficulties can be overcome by filling the counter with hydrogen, which has a stopping-power relative to that of air of 0.25, and by making the inter-

\* We wish to thank Mr. E. L. Yates for supplying us with a target of separated  $^7\text{Li}$ , which was more than 99% pure.

electrode distance fairly large (in our case 1 cm.). The equivalent air thickness of the counter is then only 0·25 cm. It was impracticable to fix the differential chamber rigidly to the air-absorption tube, so that it was necessary to circulate hydrogen continuously through the counter. A thin rubber tube served as a flexible connexion which would not appreciably disturb the counter, but which sufficed to prevent the hydrogen escaping too quickly. In practice it was found that the hydrogen must be

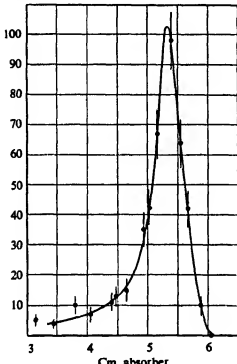


FIG. 1.

thoroughly dried before introduction into the counter. The performance as regards resolving power can be gauged from fig. 1, which shows the differential number-absorption curves for a pure range, viz., the homogeneous range of  $\alpha$ -particles formed in the transmutation



As regards "dirtiness" of source, this distribution corresponds with the  $\alpha$ -particle distribution to be investigated, and the width at half-height is only 5 mm., so that two ranges differing by about 5 mm. would be separated sufficiently for their detection.

When using two counters in this manner it is not necessary to employ two amplifiers. The voltages applied to the two counters were of such sign that one gave positive and the other negative impulses. Both were connected to the same D.E.V., linear amplifier, and oscillosograph. As long as the number of positive impulses applied to the grid of the D.E.V. greatly exceeds the number of negative impulses, no choking of the D.E.V. grid will occur. In our experiments, this condition was always satisfied. The number of positive and negative kicks can be counted separately, and the ratio of the two numbers gives a measure of the

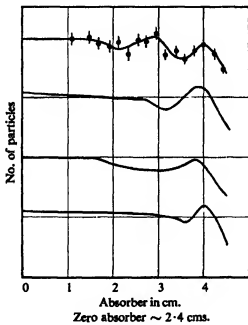


FIG. 2.

number of particles counted in the differential chamber which is independent of any fluctuations of the source.

The whole of the absorption curve for the continuous distribution of  $\alpha$ -particles from  $^7\text{Li}$  (*i.e.*, from  $\sim 2$  cm. up to the maximum range of 7.8 cm.) was investigated many times using this arrangement; but although the agreement between independent experiments was much better than before it was still insufficient to allow of unambiguous interpretation. A typical set of curves obtained in this way is shown in fig. 2.\* Despite the large number of particles counted, the discrepancies

\* In fig. 2 the zeroes have been shifted in order to avoid superposing the curves.

between different experiments do not lie within the ordinary statistical probable errors. The only irregularity common to all curves is the slight rise and maximum at a range of about 6.8 cm.

It is clear from the foregoing that unless millions of particles are to be counted and the statistical errors thus reduced to a minimum, no certainty can be attained by this approach. We were therefore led to a consideration of alternative methods of investigation. The advantages of a Wilson chamber for such a purpose are obvious. Each particle is treated individually, and one is completely independent of capricious fluctuations. There is, on the other hand, the tediousness of the method and the difficulty of measuring a large number of tracks with precision. In an experiment of this kind, one can avail oneself of the advantages of a Wilson chamber, without incurring its disadvantages, by constructing an ionization chamber

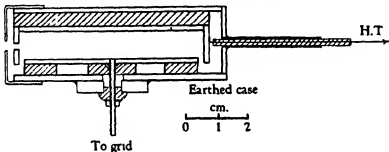


FIG. 3.

such that the actual length of track of each particle passing into it is determined. Such a chamber is represented in fig. 3. The chamber is connected to a linear amplifier and oscillograph, and gives "kicks" the sizes of which are determined by the amounts of ionization produced by the  $\alpha$ -particles.

An investigation of the distribution in size of these kicks plus a calibration using particles of known range will then determine the distribution in range (or energy) of the original particles. For a counter of this type it is necessary that the particles should be sufficiently collimated to ensure that they do not strike either of the counting electrodes. This is easily satisfied by placing slits of suitable dimensions between the source and the counter. The chamber and collimating system once clamped firmly in position, it is then only necessary to count sufficient particles and obtain their range distribution as indicated above.

The dependence of size of kick on range of particle in the chamber can be obtained by considering the Bragg curve for a single  $\alpha$ -particle. If a

length  $ab$  of the range is included in the chamber, then the ionization produced by the particle in the chamber is given by  $I = \int_a^b I_R dR$ , where  $I_R dR$  is the ionization produced between the ranges  $R$  and  $R + dR$ . Since both amplifier and oscillograph have linear responses, the size of kick  $S$  will be given by  $S \propto \int_a^b I_R dR$ . Evaluating this integral graphically, fig. 4 is obtained.

We see that  $S$  rapidly increases as the particles penetrate further into the chamber up to about 2 cm., after which the rate of increase is appreciably slower. When the particles pass right through the chamber the size of kick begins to decrease again, but not very rapidly. This curve is

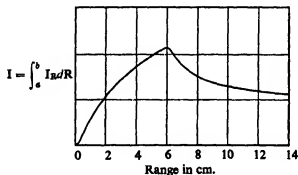


FIG. 4.

not suitable for the conversion of the number-size curve to a number-range curve; for in the first place the Bragg curve for an  $\alpha$ -particle is not known with sufficient precision, and secondly we cannot be certain of the length over which to integrate owing to possible end-effects of the counting electrodes. For this purpose then, it is necessary to use  $\alpha$ -particles of known range and find the size of kick when they penetrate a known depth into the chamber. In this way a calibration curve equivalent to that of fig. 4, but essentially more reliable, is obtained.

It is interesting in this connexion to consider fig. 5, which is the experimental size distribution of kicks from ThC'  $\alpha$ -particles which penetrated 4 cm. into the chamber.

The peak is seen to be very narrow and the width at half-height corresponds to only 8 mm. respectively, so that we may safely say that ranges at least 7 mm. apart would be resolved sufficiently for their separate detection. The linearity of response of the recording system was tested by inducing known charges on to the grid of the D.E.V.

This chamber in operation was found to be much more microphonic than the usual type of shallow chamber, probably because the chamber had to be fastened fairly rigidly to the collimating system. As the amount of ionization is about ten times as great as in the shallow chamber, the ratio of kick-size to background is certainly no smaller and possibly greater than in the shallow chamber experiments. This fact is of some importance in deciding the resolving power; for it is clear that the wider the background the greater will be the variation in the size of kick for a given impulse applied to the grid of the first valve. Thus for a homogeneous range of particles for which the size-distribution curve must have the

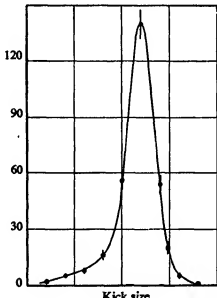


FIG. 5.

form of a very sharp peak, the sharpness of this peak will depend on the width of the background; and consequently the resolving power, *i.e.*, the ability to distinguish between two close ranges, will decrease as the background width increases.

In fig. 6 is shown the result of counting about 17,000 particles. The large peak appearing at a range of about 2.5 cm. is to be ascribed to the protons formed in the transmutation



These protons are known to have a range of about 14 cm., and consequently passed completely through our detecting chamber. The ioniza-

tion and therefore the size of kick due to such particles may be estimated from the curve of fig. 4, if we remember that the ionization produced by a proton is just one-quarter of that produced by an  $\alpha$ -particle of the same velocity and hence same range. The two values, measured and calculated, agree so well that the above assumption is justified. The fact that the proportion of these particles in the distribution was found to vary irregularly by large factors may be counted as additional evidence that they are not due to the transmutation of lithium. The presence of these protons in all transmutations effected by deuterium has already been

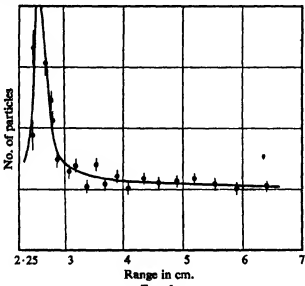


FIG. 6.

noted, and they are to be ascribed to the deposition of deuterium on the target and its subsequent bombardment by the beam of deuterons.

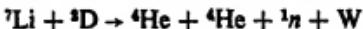
The curve of fig. 6 is the number-size curve transformed by the method described above to the number-range curve. It is clear from this curve that no irregularity such as would indicate the existence of a homogeneous group of particles can with any certainty be said to exist. As before, there are indications of such irregularities which agree in some measure with those previously obtained. We may instance the irregularity at a range of 3.5 cm. It would require a much longer investigation to determine whether such irregularities are in fact real. All we can say for certain is that no such irregularity exists having a height greater than 10% of the height of the horizontal portion of the curve, *i.e.*, if a homogeneous group be superimposed on the continuous distribution it contains less than 1% of the particles in the continuous distribution.

In conclusion we may point out that an irregularity in such curves does not necessarily imply the presence of a homogeneous group, and therefore the occurrence of transmutations other than (1). If they do occur they may well be occasioned by relatively more probable modes of (1).

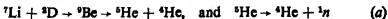
### MECHANISM OF THE TRANSMUTATION

The experiments just described and those of Bonner and Brubaker,\* though deficient and uncertain in detail, do at least present considerable information as to the energy distribution of the  $\alpha$ -particles and neutrons. The forms of the number-energy distribution curves are known with sufficient accuracy to warrant a more detailed consideration of the "mechanism" of the transmutation than was previously possible.

A complete theory of the nucleus would enable us to calculate both the  $\alpha$ -particle and the neutron energy distributions, but failing such a detailed solution of the problem it is only possible to make some simple assumption which will be sufficient to enable us to calculate the one from the other. The new conceptions of nuclear structure recently advanced by Bohr† indicate the general lines along which we should proceed. From Bohr's viewpoint, we may consider that the reaction



takes place with the temporary formation and subsequent break-up of a  $^6\text{Be}$  nucleus. This nucleus will be formed in an excited state of about 14.5 m. e-volts energy. To liberate this energy the  $^6\text{Be}$  nucleus must emit either a  $\gamma$ -ray quantum or a heavy particle. From the experimental data one sees that the emission of a  $\gamma$ -ray must be relatively improbable since no such  $\gamma$ -ray has ever been observed. We must therefore consider the alternative possibilities:



While the possibility of the first reaction cannot be excluded, we may well imagine that it is less possible than the second which, in the first stage, involves the liberation of a single elementary particle. We know from Bonner and Brubaker's investigation of the neutron distribution that there is a well-defined group of neutrons with energy about 13.5 m. e-volts which can be satisfactorily explained in terms of the formation of a

\* 'Phys. Rev.,' vol. 49, p. 19 (1936).

† 'Nature,' vol. 137, p. 344 (1936).

stable  $^6\text{Be}$  nucleus, and we shall therefore assume that the majority of these  $^7\text{Li}$  transmutations occur with the temporary formation of a  $^6\text{Be}$  nucleus in an excited state.

On this view the results of Bonner and Brubaker represent the energy distribution of the neutrons emitted in (b). If  $T$  be the kinetic energy of the neutron emitted in (b), and  $W$  be the total energy liberated in the two stages of (b), i.e.,  $W$  is defined by



then the excitation energy of the  $^6\text{Be}$  nucleus will be  $(W - 9/8T)$ . In addition to this, however, the  $^6\text{Be}$  nucleus will have a recoil energy  $T/8$ . If now we make the natural assumption that the angular distribution of the  $\alpha$ -particles ejected in (b) is isotropic with respect to the centre of gravity of the recoiling  $^6\text{Be}$  nucleus, it is easily shown that these  $\alpha$ -particles have a uniform continuous distribution in energy between

$$\frac{E_{\min}^{\max}}{E_{\min}} = \frac{1}{2} \left[ (W - T) \pm 2 \sqrt{\frac{T}{8}(W - \frac{9}{8}T)} \right].$$

Defining  $\lambda(T)dT$  as the number of neutrons with energies between  $T$  and  $T + dT$ , one finds that the number of  $\alpha$ -particles with energies between  $E$  and  $E + dE$  is given by

$$P(E)dE = dE \int_{x_1}^{x_2} \frac{\lambda(x)dx}{\sqrt{\frac{x}{8}(1 - \frac{9}{8}x)}},$$

where

$$x = \frac{T}{W}, \quad x_1 = \left[ \frac{2}{5} (\sqrt{\eta} \pm \sqrt{5 - 9\eta}) \right]^2,$$

and

$$= \eta \frac{E}{W}.$$

This integral can be evaluated graphically, using some assumed neutron energy distribution for  $\lambda(x)$ . In fig. 7 is shown the neutron energy distribution found by Bonner and Brubaker (curve B), except that the peak at 13 m. e-volts has not been included since it arises from the formation of  $^6\text{Be}$  in the ground state. In fig. 8 is shown our experimental energy distribution curve for the  $\alpha$ -particles (curve A) and also the distribution as calculated in the above manner from Bonner and Brubaker's results (fig. 8, curve B).

It will be seen that the agreement is fairly satisfactory, the chief difference being that the calculated  $\alpha$ -particle distribution shows a rather broader

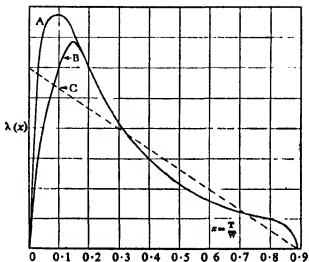


FIG. 7.

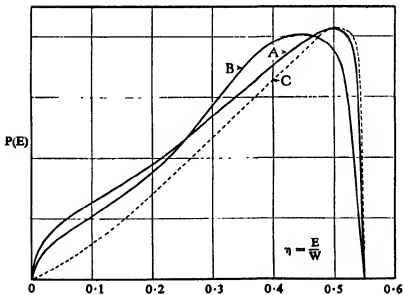


FIG. 8.

maximum at an energy some million volts lower than the observed value. The high energy end of the calculated  $\alpha$ -particle distribution depends on the accuracy of Bonner and Brubaker's results at low energies. In order to give an idea of the magnitude of this discrepancy, we have included curve A (fig. 7) which shows the shape of the neutron distribution curve which would be necessary to give the observed  $\alpha$ -particle distribution. The general shape of the calculated  $\alpha$ -particle distribution is not, however, very sensitive to small changes in the shape of the assumed neutron distribution, as can be seen from the dotted curve (fig. 8C) which shows the calculated  $\alpha$ -particle distribution assuming a linear neutron distribution as shown in fig. 7C. In view of the uncertainties inherent in the determination of the neutron energy distribution from the experimental proton distribution, the differences are perhaps not outside the experimental error. Unfortunately, it is not possible to correlate the two distributions (neutron and  $\alpha$ -particle) with certainty, for neither is known with sufficient precision; but the substantial qualitative agreement already obtained offers some justification for the assumption that the transmutation of  $^7\text{Li}$  by deuterons occurs in the two stages as suggested above.

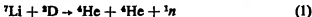
Expressed differently our assumption implies that the  $^9\text{Be}$  nucleus has a number of virtual levels or positive energy levels. Having granted the existence of such levels, it is then necessary to consider their nature, *i.e.*, their width, and the very important question as to whether they constitute a discrete set or a continuous manifold. On these points we have no definite evidence, unless the work of Dee and Gilbert\* on the disintegration of  $^{11}\text{B}$  by protons be taken as such. These authors interpret the continuous energy distribution of the  $\alpha$ -particles emitted in the boron transmutations as due to a virtual level of  $^9\text{Be}$  of about 3 m. e-volts positive energy, which possesses a width, *i.e.*, an energy spread, of about 1 m. e-volts. This level for  $^9\text{Be}$  would correspond to a neutron energy of about 10 m. e-volts in our reaction and a spread of  $\alpha$ -particles of from 0 to 4.5 m. e-volts. In the transmutation of  $^7\text{Li}$  we are considering excitations of the order of 0 to 14.5 m. e-volts. It might be expected that for the lower part of this energy range the levels would be discrete and for the upper part continuous. This being so the lower energy neutrons should have a continuous energy distribution, while those of higher energy should be resolvable into a number of discrete groups. The present results are not sufficiently precise to warrant any categorical statement either for or against this view.

\* 'Proc. Roy. Soc.,' A, vol. 154, p. 279 (1936).

We wish to express our thanks to Professor Lord Rutherford and to Dr. M. L. E. Oliphant for their help and unfailing interest in this work, and to Mr. G. R. Crowe for his technical assistance. One of us (B. C. B.) is indebted to the D.S.I.R. for financial assistance.

#### SUMMARY

The continuous distribution of  $\alpha$ -particles formed in the transmutation



has been investigated in detail. Counters not previously used in high voltage research are described. The possibility of the formation of a  $^5\text{He}$  nucleus is discussed, but the experimental evidence so far obtained on this point is negative.

It is shown that the observed neutron energy distribution (Bonner and Brubaker) and the  $\alpha$ -particle distribution are in qualitative agreement if we make the assumption that (1) occurs in two stages, an excited  $^8\text{Be}$  nucleus being temporarily formed.

---

Angular Distributions of the Protons and Neutrons  
Emitted in Some Transmutations of Deuterium

By A E KEMPTON \* B C BROWNE and R MAASDORF†

(Communicated by Lord Rutherford O M, FRS—Received 29 May,  
1936)

INTRODUCTION

The nature of the angular distribution of the particles emitted in artificial transmutations is a matter which has received little attention. Hitherto experimental investigation has been mainly concentrated on the determination of the energy release and nature of various transmutations. But it is now clear that we have sufficiently precise data concerning the nature of many transmutations to make profitable their further investigation, and in particular the investigation of the angular distribution of the transmutation products. Moreover, in much of the literature it is implicitly assumed that the transmutation products are uniformly distributed in space when referred to relative coordinates *i.e.*, coordinates in which the centre of gravity of the system is considered to be at rest, in particular all attempts to determine absolute yields depend upon the correctness of this assumption. The work so far published on this subject‡ appears to support the uniformity of angular distribution, but further investigation is clearly of some importance.

During the course of some cloud chamber experiments on the transmutation



Dee formed the tentative opinion that the angular distribution of the protons emitted was not uniform. The alternative transmutation



is very similar to (1), since the spins of the particles are probably identical and the energy balances of the same order of magnitude. We have therefore investigated the angular distribution for both these transmutations.

\* Coutts Trotter Student

† Bent Railway Trust Rhodesian Fellow

‡ Giarratana and Brennecke, 'Phys. Rev.', vol 49, p 35 (1936)

## NEUTRON INVESTIGATION

The investigation of the angular distribution of neutrons is simpler than the corresponding investigation for charged particles, in that it is not necessary to provide a window system through which the particles may pass and so be counted. The neutron source consists of a target containing deuterium bombarded with deuterons. The target is held in a brass tube through which the neutrons easily pass. By far the most sensitive detector of fast neutrons, and the most convenient, is an ionization chamber containing helium under pressure. Such a chamber containing about 12 atmospheres of helium was therefore used, and was so mounted that it could be swung about the neutron source at a constant distance from it. (The ionization chamber being about 2 cm. deep, its counting efficiency was about 1 in 2000.) The range of angles which it was possible to investigate was  $0^\circ$  to  $\sim 150^\circ$  with respect to the direction of the incident deuterons.

This arrangement of counter and source would suffice to determine the angular distribution of the neutrons emitted from a constant or known source. But the activity of a high voltage source does not remain constant or even proportional to the bombarding current for any great length of time. It is therefore convenient to employ a second counter, fixed relative to the source, which will serve to measure its activity. For this purpose we adapted one of our standard ionization chambers by placing a sheet of boron inside it and surrounding it with paraffin wax. The experimental arrangement of counters and source is indicated in fig. 1. The efficiency of neutron counters being small, it was necessary to forgo the magnetic separation of the deuteron beam in order to obtain as large a yield as possible. In the first experiments the target consisted of  $(ND_2)_2SO_4$  and gave a neutron source equivalent to about 100 mc. of Rn + Be. Such a target, however, is not very satisfactory owing to its rapid decomposition under bombardment. In the later experiments we were fortunate in being able to use  $Al(OD)_3$  as target, which lasted longer under bombardment and gave a more intense source (about 400 mc.). The two counters were connected to separate amplifiers, which fed an oscillosograph through a centre-tapped transformer. The impulses from the two amplifiers therefore produced deflexions of opposite sign and could be recorded simultaneously.

Before describing the results obtained, it will be convenient to discuss the possible perturbing factors in our experimental arrangement. The energy of the recoils in the helium counter varies from 0 to  $16/25$  of the neutron energy according to the angle between the recoil and the incident

neutron. The oscillograph "kicks" have therefore a continuous distribution in size, and since the background is of finite width the smaller kicks are indistinguishable from the background variations. One must therefore adopt some criterion as to what to count. For any one angle  $\theta$  this is of little importance and presents no difficulty, for it is permissible to count over any arbitrary constant size. The energy of the neutrons depends appreciably upon the angle  $\theta$ , however, owing to the momentum of the incident deuterons. The average size of kick for given  $\theta$  is therefore likewise dependent on  $\theta$ , and it is meaningless to count traces for different values of  $\theta$  over the same size. It may be assumed that the kick

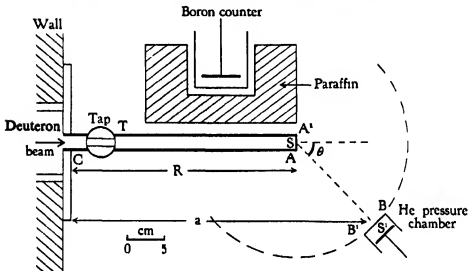


FIG. 1.

size is proportional to the energy of the recoil, and that the average kick size within the energy range considered is approximately proportional to the energy of the neutrons. This assumes that the angular distribution of helium recoils does not vary with the neutron velocity. This matter is considered in more detail in the next paragraph. The different traces were therefore counted over scale-sizes proportional to the neutron energies. It is easily shown that

$$\frac{T}{W} \sim 1 + \sqrt{\frac{E}{2W}} \cos \theta,$$

$T$ , being the neutron energy for angle  $\theta$ ,  $E$  the energy of the incident deuteron, and  $W$  the neutron energy for  $E = 0$ . From this expression

$T_s$  may be calculated and the relative scale sizes chosen. Assuming  $W = 2 \cdot 0$  m. e-volts and  $E = 100$  or  $200$  kv., the scale sizes used are given in Table I.

TABLE I

$\theta$	$T_s/W$		Size in mm.	
	200 kv.	100 kv.	200 kv.	100 kv.
0°	1.22	1.16	3.86	3.66
30°	1.19	1.14	3.76	3.60
60°	1.11	1.08	3.51	3.41
90°	1.00	1.00	3.16	3.16

Since the experiments were performed, Bonner and Brubaker\* have redetermined the neutron energy as  $W = 2 \cdot 4$  m. e-volts; but using this figure there is no sensible difference in the counting scales, as such differences amount only to a few hundredths of a millimetre and are within the experimental error of counting. It may be of interest to note the order of magnitude of the error which would be introduced if we had not used the calculated scale sizes, but had counted all traces over one constant size. For  $E = 200$  kv. the error introduced between  $\theta = 0^\circ$  and  $\theta = 90^\circ$  is about 20%.

We must now consider the possible variation with neutron velocity in the cross-section of helium ( $\sigma$ ) for elastic collisions with neutrons and the associated variation in angular distribution of the recoil helium nuclei; for it is clear that variations in these will greatly influence the number and distribution in size of the "kicks" observed. The neutron energy for  $E = 200$  kv. varies as the ratio  $1.22/0.84$  for the angular range  $\theta = 0^\circ$  to  $\theta = 135^\circ$ , so that the velocity of the neutrons changes by about 20%. One would not expect any large variation in  $\sigma$  or the angular distribution of recoils over such a small velocity range, either from theoretical considerations or from the few experiments relating to the collision of fast neutrons in helium. No experimental evidence whatever has been obtained relating to the variation in the angular distribution of the recoils in helium, but this matter is essentially connected with the variation of  $\sigma$  with neutron velocity, and we may therefore assume that if no large variation occurs in the one, none is to be expected in the other. We shall return later to the possible variation in  $\sigma$  in connexion with the experimental results.

To obtain sufficient counts in the helium chamber, the distances  $SS'$  (see fig. 1) could not be increased much above 15 cm. The source  $AA'$  is

\* 'Phys. Rev.', vol. 49, p. 19 (1936).

about 2 cm., and the counter BB' about 4 cm. in diameter. The average solid angle subtended by the counter over the surface of the source was calculated for the simplified case in which the source is considered as a circle of diameter AA' and the counter as a circle of diameter BB' the plane of which was normal to SS'. It can be shown that

$$\frac{\bar{\Omega}_{90^\circ}}{\bar{\Omega}_0} \sim 1 + \frac{1}{\pi} \left( \frac{1}{SS'} \right)^2,$$

where  $\bar{\Omega}_{90^\circ}$  and  $\bar{\Omega}_0$  are the average solid angles for  $\theta = 90^\circ$  and  $\theta = 0^\circ$ . For  $SS' = 15$  cm. as obtained in the experiment, the change in solid angle is therefore less than  $\frac{1}{2}\%$  and may be neglected. We see also that the

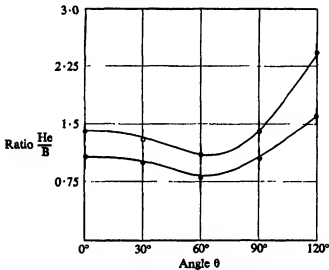


FIG. 2—○ 100 kV.; ● 200 kV.

angular definition in these experiments is approximately  $3/15$  radians, or about  $10^\circ$ .

It might be thought that neutrons scattered from the paraffin surrounding the boron counter would be counted in the helium chamber, and that owing to the lack of symmetry (for different values of  $\theta$ ) this would affect the apparent angular distribution. But for this to occur the scattering angle must be large, and the neutrons must make several collisions in the paraffin, and will therefore be reasonably slow. The helium counter is insensitive to slow neutrons since we counted over fairly large scale sizes. This important point was verified experimentally. For this purpose a series of short runs ( $\frac{1}{2}$  minute) was done with the helium

counter alone in a fixed position. The paraffin was alternately placed in position and removed. With several runs of this kind, fluctuations in the source are averaged out and any difference between the two sets must be ascribed to neutrons scattered from the paraffin into the helium counter. In several experiments no difference outside the statistical errors was ever found. We may therefore conclude that the scattering due to the paraffin is of no importance.

The first experiments, performed with the arrangement shown in fig. 1, showed a marked asymmetry about  $\theta = 90^\circ$  for bombarding voltages of both 100 and 200 kv. This asymmetry, as shown in fig. 2, takes the form of a marked increase in the number of neutrons observed at angles greater than  $60^\circ$  to the bombarding beam. When such curves are reduced to relative coordinates (which correction is never more than about 30%) the number of neutrons observed at an angle of  $(\pi/2 + \phi)$  is much greater than that observed at  $(\pi/2 - \phi)$ . But it is clear that in relative coordinates, *i.e.*, the centre of gravity of the system being at rest, the directions  $(\pi/2 + \phi)$  and  $(\pi/2 - \phi)$  must be equally probable unless the incident deuterons have a definite orientation. As such an orientation is very unlikely, it seemed probable that the observed rise for angles greater than  $60^\circ$  was spurious. Such a spurious effect might arise from either or both of two causes. This work was done with the high voltage set constructed by Oliphant,\* and in this the beam of deuterons is led through a large wall of heavy brick. The wall is between the high voltage set, discharge tube, etc., and the actual target and counters, its function being to protect the workers from the X-rays produced. The target A (see fig. 1) in these experiments was comparatively close to C, so that an appreciable number of neutrons might have been scattered backwards from the wall into the counter. Alternatively the tube AC itself, and in particular the tap T (on account of its constriction), might be acting as a neutron source owing to the deposition of deuterium from the beam. Both of these effects would be manifested as an anomalous increase in the number of neutrons observed at large angles.

A calculation of the order of magnitude of scattering by the wall was attempted on the assumption that the neutron collisions in the wall result in a uniform angular distribution, and that the cross-section for collision was of the order of  $8 \times 10^{-26}$  cm.<sup>2</sup>. For  $R = 30$  cm. and  $a = 20$  cm. (fig. 1), as in these experiments, the number of neutrons scattered from the wall into the counter was calculated to be about 6% of the number passing directly through the counter. In the experiments described below, R was

\* 'Proc. Roy. Soc.,' A, vol. 144, p. 692 (1934).

increased to about 60 cm., so that the corresponding ratio is about  $\frac{1}{2}\%$ . This source of error can therefore be considered as removed.

Most of the contamination effect of the deuterium in the target tube was found to be due to the tap T. In fact, the tap acted as a neutron source of about one-fifth the strength of our  $(ND_4)_2SO_4$  target, the rest of the tube emitting fewer but a still appreciable number of neutrons. After much trouble the effect of the neutrons coming from the tap and the target tube was obviated by using the arrangement shown in fig. 3. It is clear that the large blocks of paraffin PP serve effectively to slow down and

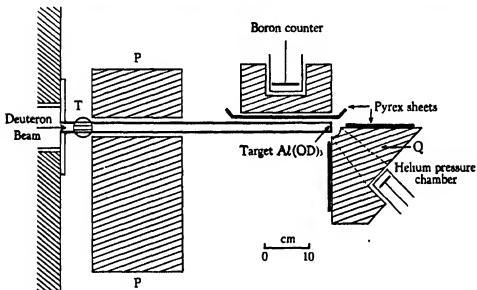


FIG. 3.

absorb the neutrons emitted at T. The majority of these neutrons which reach the helium counter will consequently be so slow as not to be counted. The paraffin block Q moved with the helium counter, and it was found that within experimental error this was effective in eliminating the neutrons from the target tube. Pyrex sheets shown in the figure prevented neutrons scattered in Q from affecting the boron counter.

Check experiments showed that the pyrex acted in the desired way. Another contributory factor to the removal of this difficulty of the counting of neutrons not emitted directly from the target was the use, as already stated, of  $Al(OD)_3$  as a target in place of  $(ND_4)_2SO_4$ . The relative effect of deuterium contamination was greatly reduced by the increased yield

of neutrons. A curve obtained with this arrangement is shown in fig. 4 and is symmetrical about  $90^\circ$ .

We have already remarked on the possibility of a variation with neutron velocity of the cross-section of helium nuclei ( $\sigma$ ) for neutron collisions and its consequent effect on the observed distribution. That such a variation over the neutron velocity range considered is inappreciable is at once seen from the symmetry of the curve of fig. 4 about  $\theta = 90^\circ$ . For the neutron velocities, for  $\pi/2 - \phi$  and  $\pi/2 + \phi$  are different, and any appreciable difference in  $\sigma$  would be revealed by a difference in the yield of recoils at these angles and therefore in asymmetry of the observed curve about  $\theta = 90^\circ$ . It can therefore be stated that the variation in  $\sigma$  with neutron velocity is within the experimental error, say, 10% at most.

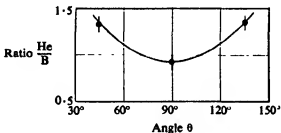


FIG. 4.

It was clear by this time that no really accurate data could be obtained without great difficulty and the expenditure of a disproportionate amount of time; so that it was decided only to determine the ratio of emission for  $\theta = 0^\circ$  and  $\theta = 90^\circ$ . For this purpose two experiments were decided upon.

A—With the above arrangement, neutrons from places other than the target, and in particular the target tube, have their maximum effect at  $0^\circ$ , for owing to the conical hole in Q the paraffin does not stop any of them at this angle. This arrangement should therefore give a *maximum* for the  $0^\circ$  to  $90^\circ$  ratio.

B—Running without the paraffin Q, the effect of the target tube should be greater for  $\theta = 90^\circ$  than for  $\theta = 0^\circ$ , owing to the solid angles involved. In this way, therefore, one should obtain a *minimum* for the  $0^\circ$  to  $90^\circ$  ratio.

Actually, although the results in A were slightly higher than in B, about 20%, the difference was not so large as we had expected from our first experiments. As explained above, this is to be attributed to the much greater efficiency of an  $\text{Al}(\text{OD})_3$  target as compared with  $(\text{ND}_4)_2\text{SO}_4$ .

The final curves for 200 kv. and 100 kv., each of which represents the

mean of several experiments, are shown in fig. 5. These curves in themselves are of no obvious significance but must be transformed into relative coordinates. Since the energy of the incident deuterons and the reaction energy are both known, this transformation is easily effected and results in the curves shown in fig. 6. In passing we may note that this correction is probably too large; for the average energy of the bombarding deuterons will be less than that of the accelerating voltage owing to penetration into

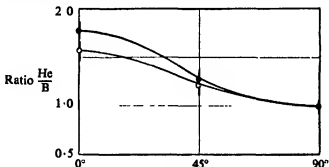


FIG. 5—● = 200 kV., ○ = 100 kV.

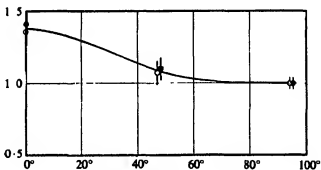


FIG. 6—● = 200 kV.; ○ = 100 kV.

the target and the fact that no magnetic analysis was used. It is difficult to estimate how important this over-correction is, but a consideration of the factors involved shows it not to be large.

The difference between the results for 100 kV. and 200 kV. is as seen in fig. 6, small and within the experimental error. This is somewhat surprising in view of the fact that the wave-length of the deuterons changes by a factor of  $\sqrt{2}$  for  $E = 100$  and  $200$  kV., and indicates that the non-uniformity of the angular distribution is at best only slightly velocity sensitive.

The actual shape of the curve between  $0^\circ$  and  $90^\circ$  is not well established

in these experiments. In the proton experiments, which are described later, more attention has been paid to this matter, and one may assume, in the absence of experimental data, that the distribution of both neutrons and protons are qualitatively the same. From the neutron experiments alone one can only say that the angular distribution in relative coordinates is not uniform, but that the neutron emission is about  $3/2$  times as great forwards as at right angles, and that the distribution is symmetrical about  $\theta = 90^\circ$ .

#### PROTON INVESTIGATION

The difficulties inherent in the investigation of the angular distribution of charged particles are much greater than for neutrons. For either one

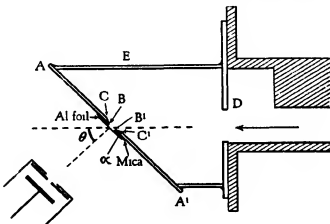


FIG. 7.

must have a complicated series of windows at all the angles at which one wishes to measure, or one must construct a counter which can be rotated under vacuum in the evacuated space containing the target. In the reaction now considered these difficulties can, however, be obviated by using the contaminating property of a deuteron beam. A target of any substance bombarded with deuterons adsorbs sufficient deuterium to constitute an effective deuterium target. If, in particular, a thin foil be bombarded with deuterons, the protons emitted in the transmutation



which have a range in air of about 15 cm., will pass through it and may be counted.

Our experimental arrangement is indicated in fig. 7. A brass tube

about 5 cm. in diameter is cut at angle of  $45^\circ$  with respect to its axis and closed by a flat elliptical brass plate AA'. At the centre of this and parallel to its minor axis is cut a slit BB' about 2 mm. wide and 1 cm. long. The back edges of the slit are milled away so that the angle  $\alpha$  is  $30^\circ$ . An aluminium foil, of 5 cm. of air equivalent stopping power, is waxed over the slit, being insulated from the plate by a thin mica sheet from which a slit of the above size is also cut. The current of deuterons hitting the aluminium foil can therefore be measured.

The counter is mounted so that it can be rotated, at a fixed distance, about the middle point of BB'. The width of the brass tube, the diaphragm D, and the bevelling of the slits, ensure that at any angle between  $\theta = 0^\circ$  and  $\theta = 90^\circ$  no protons can be counted other than those coming from the strip of aluminium covering BB'. For example, protons coming from BC and B'C' cannot reach the counter, nor is it likely that the deuteron beam will spread sufficiently to give an appreciable number of protons from the tube wall at E.

In these experiments only one counter was used. Apart from the experimental inconvenience of mounting another counter in the proton investigation, the second counter is not so essential as in the previous neutron experiments. In those, the counting rate was low, and the runs were often 2 or 3 minutes in length. But in the proton case, half a minute was usually sufficient to obtain a reasonable number of counts. By repeating these short runs many times for the same apparent conditions, fluctuations in the source were averaged out. To ensure that violent fluctuations did not occur, the current of deuterons to the aluminium was measured, and all runs discarded unless this current remained constant.

The chief inconvenience of this arrangement is that angles greater than  $90^\circ$  cannot be investigated.\* On the other hand, it is particularly satisfactory in that the geometry for  $\theta = 0^\circ$  and  $\theta = 90^\circ$  is almost identical, there being symmetry about  $\theta = 45^\circ$ .

The maximum stopping power of the aluminium foil used is obtained for  $\theta = 0^\circ$  and  $\theta = 90^\circ$  and is about 7 cm. of air. As the proton range for  $\theta = 90^\circ$  is about 15 cm. and increases with decreasing  $\theta$  up to nearly 20 cm. for  $\theta = 0^\circ$ , we have a minimum path of protons outside the aluminium of about 7 cm. In all the experiments the distance between the counter front and BB' was approximately  $3\frac{1}{2}$  cm. The counter front also had a bevelled slit 2 mm.  $\times$  1 cm. parallel to the slit-shaped proton

\* It was actually possible to make  $\theta$  as great as  $100^\circ$ , and this was done to ensure that there was no rapid dropping off in yield beyond  $90^\circ$ .

source, so that the angular definition was about  $3^\circ$ . The distance between source and counter was at least constant to 1 mm., so that the variation in the solid angle subtended by the counter at the source was at most  $(0.1/3.5)^2$ , i.e., about 6%. As each angle was investigated many times, the actual errors due to this cause must be much less than this upper limit.

Typical curves obtained are shown in figs. 8 and 9. It is seen that the general appearance is identical with that already obtained for the neutrons.

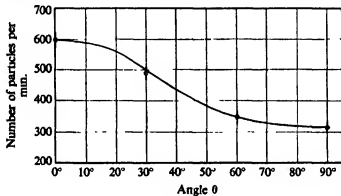


FIG. 8—100 kV.

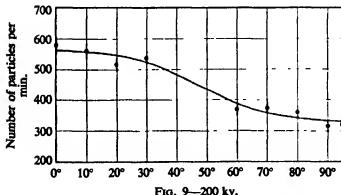


FIG. 9—200 kV.

and in particular the ratio of the intensities at  $0^\circ$  and  $90^\circ$  is approximately the same for both. In the proton experiments it was, however, possible to investigate the shape of the curve in more detail, and as shown in fig. 9 the curve between  $0^\circ$  and  $30^\circ$  and between  $60^\circ$  and  $90^\circ$  is approximately flat, most of the fall between  $0^\circ$  and  $90^\circ$  occurring between  $30^\circ$  and  $60^\circ$ .

In fig. 10 are shown the final weighted mean curves of a considerable number of separate experiments, and the root mean square errors are indicated. These curves transformed to relative coordinates are shown in

fig. 11. One sees that the non-uniformity of the angular distribution appears to be more marked for 100 kv. than for 200 kv., a somewhat surprising result. The difference between the two is, however, not very much greater than the root mean square errors, so we should not like to

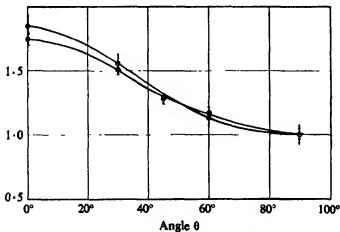


FIG. 10— $\circ$  100 kv.;  $\bullet$  200 kv.

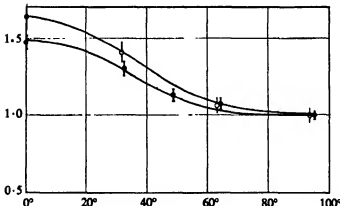


FIG. 11— $\circ$  100 kv.;  $\bullet$  200 kv.

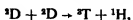
insist too much on its possible significance. Apart from this the proton distribution, as shown in fig. 11, and the neutron distribution, as shown in fig. 6, are remarkably similar, in particular the ratio of the intensity of emissions at  $0^\circ$  and  $90^\circ$  being approximately 3:2 in both cases.

We wish to express our thanks to Professor Lord Rutherford and to Dr. M. L. E. Oliphant for their help and unfailing interest in this work,

and to Mr. G. R. Crowe for his technical assistance. One of us (B. C. B.) is indebted to the D.S.I.R. for financial assistance.

### SUMMARY

The angular distribution of the protons and neutrons emitted in the transmutations



has been investigated. For the coordinates in which the centre of gravity of the system is at rest it is found that the angular distributions are symmetrical about an angle of  $90^\circ$  to the direction of the incident particles, but that the intensity of emission at  $0^\circ$  is about  $3/2$  times that at  $90^\circ$ . Both distributions are relatively insensitive to the energy of the incident deuterons between 100 and 200 kv.

---

## The Structure of Isatin—I

By E. G. COX, T. H. GOODWIN, and A. I. WAGSTAFF

(Communicated by W. N. Haworth, F.R.S.—Received 3 June, 1936)

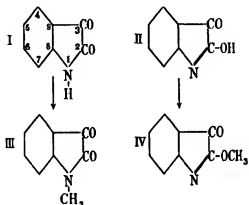
[PLATE 10]

### I—INTRODUCTION

The constitution of isatin has long presented a problem of considerable interest. This substance may react either as a lactam (I) or as a lactim (II), giving rise, for example, to two quite distinct methyl ethers, the nitrogen-ether (III) or the somewhat unstable oxygen-ether (IV). The failure of purely chemical methods to determine which of the structures (I) or (II) is to be assigned to isatin has led various workers to investigate the problem by means of optical absorption spectra. Hartley and Dobbie,\* owing to the difficulty of ensuring the stability of the oxygen-ether in solution, concluded that the spectrum of isatin resembled that of

\* J. Chem. Soc., vol. 55, p. 640 (1889).

the *N*-ether more closely than that of the *O*-ether, and inferred that isatin possessed the lactam structure (I). Later workers,\* however, taking precautions to prevent the decomposition of the *O*-ether, found that its absorption spectrum, while certainly different from those of the other two substances, is not sufficiently so to lead to any definite decision as to the structure of isatin itself.



The present investigation was therefore undertaken in the hope that X-ray methods would yield more conclusive results; since the C=O and C—OH bonds differ by nearly 20%, and the C=N and C—N bonds by at least 5%, a quantitative study of isatin should distinguish clearly between the formulae (I) and (II). Apart from the variation in bond lengths, however, differentiation between the molecules represented by (I) and (II) might be possible on the basis of their arrangement in the crystal lattice. Experience suggests that, subject to the exigencies of molecular shape, organic molecules containing groups capable of dipole association, formation of hydroxyl bonds, etc., tend to arrange themselves in the solid state so that such association or coordination does take place to a very large extent; thus, for example, in the present case a molecular arrangement involving juxtaposition of oxygen atoms would indicate hydroxyl bonds and therefore favour the lactim structure (II) while the close approach of a nitrogen atom to a nitrogen or oxygen in neighbouring molecules might suggest "amino" bonds between molecules of the lactam (I). The present paper contains an account of the determination of the molecular arrangement in crystalline isatin together with the conclusions to be drawn from it, and also X-ray data for several

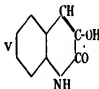
\* Morton and Rogers, 'J. Chem. Soc.', vol. 127, p. 2698 (1925); Ault, Hirst, and Morton, *ibid.*, p. 1653 (1935).

related substances whose structures might be expected to throw light on that of isatin; these are the two methyl ethers (III) and (IV), 3-hydroxy-quinolone (V), and the so-called "methyl isatoide" (see § V). The decomposition of the *O*-ether has also been studied by X-ray methods. The detailed structure of isatin as determined by Fourier analysis will be published in Part II.

## II—ISATIN

The results of earlier crystallographic measurements on isatin are recorded by Groth;\* it is described as crystallizing in elongated monoclinic prismatic combinations of  $m\{110\}$  and  $b\{010\}$  terminated by  $q\{011\}$  or  $r\{10\bar{2}\}$ , and exhibiting good cleavage parallel to the latter form. The axial ratios are

$$a:b:c = 0.4251:1:0.5025; \beta = 94^\circ 42'.$$



The plane of the optic axes is  $b\{010\}$ .

The material used in the present investigation was recrystallized from hot water. Goniometric examination confirmed the above data while the optical results were extended. The crystals exhibit very high negative birefringence the refractive indices for yellow light being as follows:

- $\alpha$   $1.46 \pm 0.005$  perpendicular to  $r\{10\bar{2}\}$ .
- $\beta$   $1.80 \pm 0.03$  perpendicular to  $b\{010\}$ .
- $\gamma$   $1.90 \pm 0.03$  parallel to [201].

A centred acute bisectrix figure is visible through  $r\{10\bar{2}\}$ , the optic axial angle in air being about  $100^\circ$ .

X-ray single crystal rotation photographs about the  $a$ ,  $b$ ,  $c$ ,  $[110]$  and  $[011]$  axes together with measurements of the spacings of the  $(020)$  and  $(100)$  planes led to the following values for the cell dimensions:

$a = 6.19$  Å.,  $b = 14.55$  Å.,  $c = 7.19$  Å.;  $\beta = 95^\circ 00'$ , whence  $a:b:c = 0.4254:1:0.4941$  (cf. values above). These measurements and all others recorded in this paper were made with copper  $K\alpha$  radiation.

By the flotation method the density was found to be  $1.51$  gm./cm.<sup>3</sup>, so that the number of molecules in the unit cell is  $3.97 \approx 4$ . The lattice is a simple one, and analysis of the  $b$ - and  $c$ -axis oscillation photographs shows that the only abnormal spacings are  $(0k0)$  absent for  $k$  odd, and  $(h0l)$  absent for  $l$  odd. Thus the space-group is  $P2_1/c$  ( $C_{2h}^5$ ) and the molecular symmetry is 1, i.e., none. An X-ray powder photograph of isatin is reproduced in fig. 2b.

\* 'Chem. Krystallogr.', vol. 5, p. 564.

The cell dimensions recorded above do not give any indication of the molecular arrangement in crystalline isatin. The high negative birefringence (0.44) shows, however, that the molecules (which must undoubtedly be nearly or quite flat) are all approximately parallel to one plane, namely  $r(10\bar{2})$ , which contains the two high refractive indices  $\beta$  and  $\gamma$ . The spacing of  $(10\bar{2})$  (3.25 Å.) is of the expected order for the perpendicular separation of flat molecules, while the good cleavage parallel to this face, and the very high intensity of its X-ray reflexion (Table I) both point to the same conclusion. Owing to the uncertainty in estimating extinction effects in the small crystals available, it is difficult to decide from the measured intensity of  $(10\bar{2})$  whether the molecules lie exactly in the plane or not, but the divergence is evidently very small, and in the following discussion it is assumed that all the atoms (with the possible exception of hydrogen) are situated in the  $\{10\bar{2}\}$  planes.

All possible distributions of the molecules in the  $(10\bar{2})$  planes have been considered, the criteria for a satisfactory structure being the maintenance of the appropriate intermolecular distances and good agreement between observed and calculated X-ray intensities. For this purpose lactam and lactim models based on the following bond length were used:—

	A.		A.
C—C in benzene ring	1.42*	C=N	1.31†
C <sub>6</sub> —C <sub>2</sub>	1.48*	C—O	1.46
C <sub>3</sub> —C <sub>2</sub>	1.54*	C=O	1.15‡
C—N	1.38†		

We have taken the minimum permissible intermolecular distances to be C...C = 3.5 Å., and C...O = 3.2 Å. The distances =O...>NH and >O...N< are less certain, but since both =O...NH<sub>2</sub> in urea§ and >N...N< in cyanuric triazide† are approximately 3.2 Å., it may be assumed that the same figure is valid for them provided no coordination takes place.

In spite of systematic trials, it was found impossible to obtain an arrangement either of lactam or lactim molecules which satisfied the above conditions. It appeared, however, that if neighbouring molecules were permitted to approach so that the O...N distance was reduced to about 2.8 Å., then a structure which was otherwise satisfactory might be found. O...N distances of this order would imply the existence of some form of bond, and although there has previously been no direct evidence of it,

\* Robertson, "Report of International Congress on Physics," vol. 2, p. 46 (1934).

† Knaggs, "Proc. Roy. Soc., A, vol. 150, p. 576 (1935).

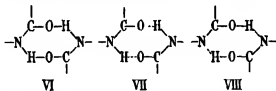
‡ Robertson, "Proc. Roy. Soc., A, vol. 150, p. 106 (1935).

§ Wyckoff, "Z. Krystallogr., vol. 81, p. 102 (1932).

it seems probable that the linking of oxygen to nitrogen through a hydrogen atom is of fairly frequent occurrence. In this case, the hydrogen would evidently play the same role as in the hydrogen and hydroxyl bonds\* between oxygen atoms, although the binding cannot, in general, be expected to be quite so marked on account of the smaller electrical anisotropy of the nitrogen atom. We may thus anticipate the existence of either hydrogen bonds N—H—O or "amino" bonds N—H..O in isatin in addition to the hybrid hydroxyl bonds N..H—O.

Very close packing of the molecules is further suggested by the high density of isatin (1.51 gm./cc.) as compared with the densities found for its *N*- and O-ethers, viz., 1.40 gm./cc. and 1.38 gm./cc. respectively. The corresponding molecular volumes are: isatin 161 A.<sup>3</sup>; *N*-ether 190 A.<sup>3</sup>; O-ether 193 A.<sup>3</sup>. The mean increment for the CH<sub>3</sub> group is therefore 30.5 A.<sup>3</sup>. This figure is considerably higher than the average (24 A.<sup>3</sup>) found from representative homologous series of solid organic compounds, and the inference is therefore that the packing of isatin molecules in the lattice is appreciably greater than in its ethers where no coordination can be expected.

Actually, owing to the relative positions of the nitrogen and oxygen atoms in the same molecule and to space group considerations, the only possibilities of coordination which need be considered, are the centrosymmetrical arrangements shown below (VI), (VII), and (VIII). Owing to lack of data regarding bonds involving nitrogen, it is not practicable at



the present stage to differentiate between these alternatives, but it is clear that in any case the intramolecular bond lengths will lie between those corresponding to the lactam and lactim structures. We have therefore adopted the following interatomic distances in making up a model from which to calculate X-ray intensities for comparison with the experimental observations:—

	A.	A. <sub>4</sub>	
C to C in benzene ring	1.42	C <sub>8</sub> to N	1.35
C <sub>8</sub> to C <sub>3</sub>	1.48	C <sub>8</sub> to O <sub>2</sub>	1.25
C <sub>8</sub> to C <sub>1</sub>	1.54	C <sub>8</sub> to O <sub>3</sub>	1.15
C <sub>8</sub> to N	1.38		

\* Bernal and Megaw, ' Proc. Roy. Soc.,' A, vol. 151, p. 413 (1935).

In order to distort the valency angles in the heterocyclic ring as little as possible, we have assumed the  $C_6C_3$  and  $C_4N$  bonds each to be deflected  $10^\circ$  towards the other from their normal position (radial to the benzene ring), while the CO bonds have been made to bisect the  $C_3$  and  $C_4$  angles.

Of the numerous possible arrangements of these molecules in the

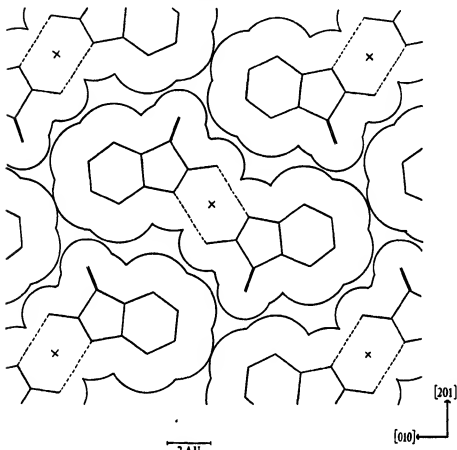


FIG. 1.

( $10\bar{2}$ ) plane, those involving intermolecular distances of less than  $3.5 \text{ \AA}$ . (between carbon atoms) were first eliminated. The remainder were systematically tested by means of the intensities of various reflexions, and in one case only was a satisfactory agreement between observed and calculated intensities obtained. The molecular arrangement so found is shown in fig. 1 as a projection on ( $10\bar{2}$ ). The molecules are associated in pairs about the centres of symmetry so that the O....N distance is

2.8 Å., and are oriented so that the line joining C<sub>7</sub> to the symmetry centre is parallel to the *b*-axis and 4.18 Å. in length. The agreement between experimental ( $F_{exp}$ ) and theoretical ( $F_{theo}$ ) structure factors is shown in Table I for various planes; the low experimental values for the two strongest planes (102) and (110) are probably largely due to extinction effects. The observed intensities ( $I$ ) are the absolute integrated intensities for a crystal of unit volume (corrected for absorption). They were estimated in the first instance by comparison with calibration spots of known intensities recorded on the photographs by means of a rotating stepped sector disk, taking the (040) reflexion as standard; the absolute intensity of (040) was then measured by comparison with the (400)

TABLE I

<i>hkl</i>	$I \times 10^4$	$F_{exp}$	$F_{theo.}$
020	128	20	32
040	211	37	33
060	11.6	11	12
080	85	37	25
100	6.4	4.8	3.2
200	0.25	1.4	0.3
300	64	29	23
400	0.5	3.2	1.2
302	1.0	4.2	6.5
312	26	21	15
322	37	26	40
332	2.6	7	12
342	28	24	19
110	455	43	68
220	82	29	30
330	0.8	3.4	8
102	1230	97	160

rocksalt reflexion, using a procedure previously described,\* modified appropriately for the small crystals available. The structure factors ( $F_{exp}$ ) have been obtained from the intensities by means of the usual formula for a mosaic crystal

$$I = \frac{N^4 e^4 \lambda^3}{2m^4 c^4} \cdot \frac{1 + \cos^2 2\theta}{\sin 2\theta} F^2,$$

while the theoretical structure factors  $F_{theo.}$  have been calculated from the structure shown in fig. 1, using atomic scattering factors for carbon based

\* Cox, Wardlaw, and Webster, 'J. Chem. Soc.', p. 780 (1936).

on the data of James and Brindley.\* For the present purpose of determining the molecular arrangement, it has been considered sufficiently accurate to ignore the differences in the scattering powers of carbon, nitrogen, and oxygen, particularly as the first of these elements preponderates in the molecule.

In view of the uncertainties to the precise values to be ascribed to the bond lengths, and of the approximation just mentioned, the agreement between the experimental and theoretical structure factors is satisfactory, and there can be no doubt that the molecular arrangement shown in fig. 1 is substantially correct. In particular the association of the molecules through N...O linkages appears to be definitely established, and it is therefore highly probable that in the crystalline state isatin is neither truly lactam nor truly lactim, but exists in some form intermediate between the two. Whether this intermediate form has a resonance structure involving hydrogen bonds, such as (VI), or has a structure exhibiting "amino" (VII) or hydroxyl bonds (VIII) cannot be decided at present. The elucidation of this point and an investigation of the possible persistence of molecular coordination in the dissolved state will be reported in Part II.

### III—*N*-METHYLISATIN

No previous crystallographic work on *N*-methylisatin had been recorded. It is polymorphous, two forms having been definitely recognized, while certain evidence points to the probable occurrence of a third form. Their absorption spectra in solution are indistinguishable, while their melting points and mixed melting points are the same. Consequently there can be no doubt that they are chemically identical. They have been designated  $\alpha$ ,  $\beta$ , and  $\gamma$ .

Both  $\alpha$  and  $\beta$  forms are orthorhombic. The  $\alpha$ -modification crystallizes from water in long red needles elongated parallel to the *c*-axis with the prism form  $k\{410\}$  fully developed,  $a\{100\}$  being frequently present. The  $\beta$ -variety is obtained from benzene-ether solution as thin yellow plates elongated parallel to the *c*-axis and tabular on  $a\{100\}$  and exhibiting the forms  $b\{010\}$  and  $q\{011\}$ . The  $\gamma$ -*N*-ether is also acicular, fan-like growths of rather thick needles showing straight extinction being common. In habit and colour in non-polarized light it is definitely different from the  $\alpha$ -form but it has not been examined sufficiently to show whether any more fundamental differences exist. It crystallizes with the  $\alpha$ -modification

\* Phil. Mag., vol. 12, p. 81 (1931); Cox and Goodwin, J. Chem. Soc. p. 773 (1936).

from which it can be separated by hand picking. All three types of crystal are pleochroic.

The optical and X-ray data for the  $\alpha$ - and  $\beta$ -modifications are summarized in Table II. Since the structures of both forms are evidently very complex and are not related in any simple way to those of isatin and the *O*-ether, no attempt has been made to determine the molecular arrangement, although it is clear from the optical properties (high birefringence with the minimum index parallel to the *c*-axis) that in both cases the molecules are arranged with their planes not greatly inclined to the (001) planes, the parallelism being closer in the  $\alpha$ -form. In neither modification is the parallelism so complete as in isatin, as is shown by the higher values of the minimum refractive indices (1.52 and 1.56, as compared with 1.46 for isatin) and by the absence of any outstandingly strong X-ray reflexion intensities. Since the methyl group is presumably not in the same plane as the remainder of the molecule, a less perfect alignment is to be expected.

The  $\alpha$ -modification provides an excellent example of the "enhancement principle," for the *a*-axis is nearly quartered and the *c*-axis nearly halved. This last observation confirms that the molecules are approximately parallel to the (002) planes.

It seems likely that the molecular arrangements in the two forms are not very different since  $[a]_a \approx [a]_\beta$  while  $[b]_a \approx [011]_\beta$ . Thus in the  $\beta$ -form the molecules are probably more nearly parallel to the {011} planes (whose spacing of 6.5 Å. corresponds with  $[c]$ ) than to {001}.

A powder photograph of  $\alpha$ -*N*-methylisatin is reproduced in fig. 2d.

#### IV—*O*-METHYLISATIN

This compound (IV) crystallizes from benzene in blood red monoclinic prismatic combinations of  $c\{001\}$  and  $s\{20\bar{1}\}$  equally developed, with  $a\{100\}$  very much smaller; they are somewhat elongated parallel to the *b*-axis and are terminated by the prism form  $q\{210\}$ . Crystals of a different habit sometimes occur, being tabular on  $c\{001\}$  and bounded by  $q\{210\}$ . The angle  $c\{001\}: s\{20\bar{1}\} = 53^\circ 01'$ ; owing to the poorness of the faces the other interfacial angles could only be measured approximately.

The optical and X-ray data are summarized in Table II.

The instability of the *O*-ether has been recognized for some time,\* but the exact nature of the decomposition products has been uncertain. It

\* E.g., Morton and Rogers, *loc. cit.*

X-ray data— System	$\alpha$ -N-ether	$\beta$ -N-ether	Orthorhombic	$O$ -ether	Methylisatoide	3-Hydroxyquinalone
$a$ . . . . .	. . . . .	31 51 Å	33 45 Å	15 49 Å	9 42 Å	8 70 Å.
$b$ . . . . .	. . . . .	13·62 Å	10 60 Å	6 14 Å	18 36 Å.	6 77 Å
$c$ . . . . .	. . . . .	7 09 Å	8 39 Å	8 32 Å	7 87 Å.	7 29 Å.
$a$ . . . . .	. . . . .	—	—	—	—	93° 25'
$\beta$ . . . . .	. . . . .	—	—	101°	100½°	123° 02'
$\gamma$ . . . . .	. . . . .	—	—	—	—	97° 55'
Mols./unit cell	16	16	4	4	2	Pi
Space group	?	?	P2 <sub>1</sub> /m or P2 <sub>1</sub> α	P2 <sub>1</sub> /m	1 50 g./cc.	1 50 g./cc.
Density (X-rays)	1·41 g./cc.	1·43 g./cc.	1·38 g./cc.	1·51 g./cc.	1·49	1·50
Density (flotation)	1·40	1·40	1·37	1·49	—	—
Optical data—						
$\alpha$ . . . . .	1·52	1·56	1·51	1·57	—	—
$\beta$ . . . . .	1·74	1·71	perp to $a$ (001) perp to $b$ (010)	perp to $a$ (100) perp to $b$ (010)	perp to $b$ (010) perp to $c$ (001)	perp. to (012) perp. to (001) birefringence high
$\gamma$ . . . . .	—	1·78	1·74	1·81	1·83	—

\* Refractive indices for sodium light and accurate to 0.01 unless otherwise stated.

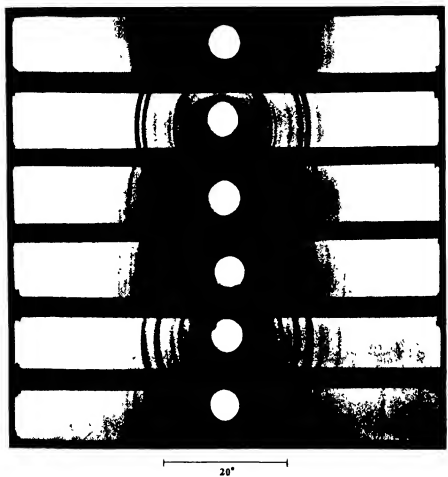
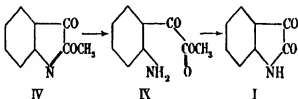


FIG. 2.—(a) 3-methoxyquinolone, (b) isatin, (c) methylisatoide, (d) *N*-methylisatin, (e) *O*-methylisatin, (f) 3-hydroxyquinolone



is now found that the changes which occur in solution are entirely different from those taking place in moist air. Thus, when an alcoholic solution which had been allowed to stand for two days was evaporated to dryness, crystals of isatin were obtained. These were identified by microscopic and X-ray examination as well as by their melting point and mixed melting point. The absorption spectrum of a two-days-old solution of *O*-methylisatin is not, however, that of isatin.\* It therefore seems probable that the first product of decomposition of the *O*-ether (IV) is *o*-aminobenzoylformic ester (IX) (or acid), which then, on evaporation, eliminates methyl alcohol (or water) to form isatin (I).



In air of normal humidity, on the other hand, the decomposition proceeds much more slowly and may take several months to reach completion. The product is a yellow powder which sublimes on to the covering vessel. This is the "methylisatoide" described by von Baeyer† and Hantzsch‡ (*vide § V*). The course of this decomposition has been followed by X-ray methods; powder photographs of the initial *O*-ether and of the final product (methylisatoide) are reproduced in figs. 2 (e) and (c).

#### V—"METHYLISATOIDE"

Von Baeyer,§ Hantzsch,§ and other workers have attempted with only partial success to determine the constitution of this substance, which is apparently formed by the combination of isatin and its *O*-methyl ether during the decomposition of the latter in moist air. The X-ray results confirm that the molecular weight corresponds with the formula C<sub>12</sub>H<sub>10</sub>O<sub>4</sub>N<sub>2</sub>; moreover, the substance does not appear to be a compound of isatin with its *N*-methyl derivative since recrystallization together of equimolecular proportions of these two substances yields only a mixture of them.

\* Ault, Hirst, and Morton, *loc. cit.*

† 'Ber. deuts. chem. Ges.,' vol. 15, p. 2094 (1882).

‡ *Ibid.*, vol. 54, p. 1221 (1921); vol. 55, p. 3180 (1922); etc.

§ *Loc. cit.*

Methylisatoide crystallizes from alcohol in monoclinic prismatic combinations of  $m\{011\}$  fully developed, with  $c\{001\}$  and  $b\{010\}$  frequently occurring as very narrow faces. The prisms are terminated by  $a\{100\}$ .

The X-ray and optical data are summarized in Table II; the assumption of eight molecules in the unit cell (apart from its improbability on general grounds) would lead to a molecular weight of  $151 \pm 2$ , which is incompatible with the formula of any isatin derivative.

#### VI—3-HYDROXYQUINOLONE

When isatin is treated with a slight excess of diazomethane in dry acetone, a colourless or light brown compound is produced. This substance has been identified as 3-hydroxyquinolone by Ault, Hirst, and Morton.\* It is triclinic and usually crystallizes with the pinacoidal forms  $a\{100\}$ ,  $b\{010\}$ , and  $c\{001\}$ .

The X-ray and optical data are summarized in Table II. The  $c$ -axis rotation photograph shows weak odd layer lines; this indicates interleaving of molecules along the  $c$ -axis and consequently there are two molecules in the unit cell. The molecular weight is therefore  $160.3 \pm 1$  since the density was found to be  $1.497$  g./cc.;  $C_6H_7O_2N = 161.1$ .

Powder photographs of 3-hydroxyquinolone and of 3-methoxy-quinolone are shown in figs. 2*f* and 2*a*. The former is remarkably like that of isatin (fig. 2*b*), suggesting a similarity of molecular arrangement. It is reasonable to suppose that here also association of molecules through imino and carbonyl groups occurs. Since the birefringence is high, the molecules are presumably coplanar with their planes normal to the minimum refractive index, *i.e.*, in the  $\{0\bar{1}2\}$  planes. The spacing of these planes ( $3.2$  Å.) corresponds closely with that of the  $\{0\bar{1}2\}$  planes of isatin. Moreover, the length of the  $[021]$  axis ( $15.0$  Å.) and the spacing of the  $(100)$  plane ( $7.14$  Å.), both of which lie in the  $(0\bar{1}2)$  plane, correspond respectively with the  $[010]$  and  $[201]$  axes of isatin ( $14.55$  Å. and  $2 \times 6.89$  Å.). Since, in solution at least,\* 3-hydroxyquinolone appears definitely to have a lactam structure, a detailed comparison of its solid structure with that of isatin should be of special value and will be reported in Part II.

We are indebted to H.M. Department of Scientific and Industrial Research for a Senior Research Award to one of us (T. H. G.), and to

\* Ault, Hirst, and Morton, *loc. cit.*

Professor W. N. Haworth, F.R.S., and Dr. E. L. Hirst, F.R.S., for their continued interest and valuable discussions. We have also to thank Dr. R. A. Morton and Dr. R. G. Ault for supplying various specimens.

#### VII—SUMMARY

The failure of chemical and spectroscopic methods to decide between the lactam and lactim structures for isatin has suggested an attempt on the problem by X-ray methods. The present paper contains an account of the determination of the molecular arrangement in crystalline isatin, from which it is concluded that the structure is intermediate between the two. The molecules are found to be disposed in parallel layers in such a way that the nitrogen atom and adjacent oxygen atom in one molecule approach very closely ( $2\cdot8$  Å.) to the oxygen and nitrogen atoms respectively in the next molecule. It is inferred from this that some type of coordination (hydrogen, hydroxyl, or "amino" bonds) occurs.

Several related substances have also been examined, but with the exception of 3-hydroxyquinolone their structures do not appear to bear any marked similarity to that of isatin, and they have therefore not been studied in great detail.

---

## Spectroscopic Identification and Manometric Measurement of Artificially Produced Helium\*

By F. A. PANETH, E. GLÜCKAUF, and H. LOLEIT

(Communicated by J. C. Phillip, F.R.S.—Received 3 June, 1936)

The evidence for artificially produced elements has so far been based entirely on radioactive methods (fluorescent screen, electrometric device, or Wilson chamber); either the rays accompanying the process of transmutation have been observed, or, in the case of artificial radio-elements, the rays emitted by the products of transmutation have been used for their detection and the study of their behaviour. The amount of new matter is usually so small that there is no possibility of discovering it by any non-radioactive method; attempts to detect hydrogen spectroscopically have failed,† but with helium where the limit of identification is so low (see I) there was more hope of success.

There are at present several processes of artificial transmutation of which helium is known to be a product. In high-voltage apparatus it is difficult completely to exclude the possibility of contamination by helium from the air, or from glass walls;‡ but bombardment by radioactive sources can be carried out under conditions much better suited to our purpose. Chadwick and Goldhaber§ and Fermi and co-workers|| have

\* 'Helium Researches XIII.' As previous numbers of the 'Helium Researches' are frequently quoted, we give the references here: I, II, and III, Paneth and Peters, 'Z. phys. Chem.', vol. 134, p. 353 (1928); *ibid.*, B, vol. I, pp. 170, 253 (1928); IV, Paneth, Gehlen, and Peters, 'Z. anorg. Chem.', vol. 175, p. 383 (1928); V, Paneth, Gehlen, and Günther, 'Z. Elektrochem.', vol. 34, p. 645 (1928); VI, Paneth, Petersen, and Chloupek, 'Ber. deuts. chem. Ges.', vol. 62, p. 801 (1929); VII, VIII, and IX, Paneth and Urry, 'Mikrochem,' Emich-Festschrift, p. 233 (1930); 'Z. phys. Chem.', A, vol. 152, pp. 110, 127 (1931); X, Paneth and Koeck, 'Z. phys. Chem.', Bodenstein-Festband, p. 145 (1931); XI, Günther and Paneth, 'Z. phys. Chem.', A, vol. 173, p. 401 (1935); XII, Holmes and Paneth, 'Proc. Roy. Soc.,' A, vol. 154, p. 385 (1936); referred to later as I, etc.

† Paneth and Günther, 'Nature,' vol. 131, p. 652 (1933). See also XI.

‡ See Paneth and Thomson, 'Nature,' vol. 136, p. 334 (1935).

§ Chadwick and Goldhaber, 'Nature,' vol. 135, p. 65 (1935); 'Proc. Camb. Phil. Soc.,' vol. 31, p. 612 (1935); Taylor and Goldhaber, 'Nature,' vol. 135, p. 341 (1936); see also Taylor, 'Proc. Phys. Soc.,' vol. 47, p. 873 (1935); Taylor and Dabholkar, *ibid.*, vol. 48, p. 285 (1936); Kurichatow, Kurichatow, and Latyshev, 'C.R. Acad. Sci. Paris,' vol. 200, p. 1199 (1935).

|| Amaldi, D'Agostino, Fermi, Pontecorvo, Rasetti, and Segré, 'Proc. Roy. Soc.,' A, vol. 149, p. 522 (1935).

found that under the impact of slow neutrons lithium and boron produce helium, the latter according to the reaction:



We decided to try boron because this element can be obtained in the form of volatile liquid esters from which it is easy to drive out the helium; the presence of hydrogen atoms in the esters is an additional advantage, since it is essential to slow down the neutrons before they collide with the boron atoms. The methyl ester of boric acid which we used,  $\text{B}(\text{OCH}_3)_3$ , contains nine hydrogen atoms for every boron atom; these hydrogen atoms, as well as the oxygen and carbon atoms, have, compared with boron, a negligible absorbing power for slow neutrons.\* 1 cc. of ester,  $d_{40} = 0.915$ , contains 0.095 gm. boron and 0.080 gm. hydrogen.

#### APPARATUS AND EXPERIMENTAL PROCEDURE

To avoid contamination by helium from glass, the ester was in contact exclusively with metal during the whole irradiation, which had to be continued for months. It was contained in a spherical copper flask (A in fig. 2) with a gun-metal stopcock. The radius of the flask in its final form was 10 cm.; the neutron sources could be placed at the centre of the flask by means of a cylindrical pocket of 1.2 cm. radius. The flask was inserted in a cylindrical water tank of 40 cm. diameter. As neutron sources we used mainly glass tubes filled with finely powdered beryllium and radon, supplied to us from time to time from three different sources: St. Bartholomew's and the Middlesex Hospitals in London, and the Institute for Radium Research in Vienna.

Before the experiment starts the boron ester has to be freed from atmospheric air and the Ne and He contained therein. This is achieved by opening the stopcock *a* of the copper flask and the glass stopcocks *b*, *c*, *d*, and *i* to the high-vacuum pump and keeping the ester boiling for about 15 minutes; the distillate is collected in the traps *B* and *B'* which are cooled by liquid air. The same operation is then performed as described below for the collection of helium from the ester; in this blank test the quantity of neon + helium observed in the capillary on top of the bulb *L* and measured by the manometric device *N* must not exceed  $10^{-9}$  cc. We found that with methyl borate this point can be reached fairly quickly, and, further, that a second test, carried out weeks or months later, gives

\* Fermi and co-workers, *loc. cit.*; Bjerje and Westcott, 'Proc. Roy. Soc.,' A, vol. 150, p. 709 (1935).

the same result: no release of any detectable amount of helium from the walls of the copper vessel takes place. The interval between the two tests was in one experiment 9 weeks.

The actual experiment, the bombardment of the ester with neutrons, was carried out four times. In the first three experiments we used a somewhat smaller copper flask (radius 7.5 cm.) with a larger pocket (1.5 cm.). The rest of the apparatus was in all cases identical, but the neutron sources were of very different strength. In addition to the radon-beryllium tubes mentioned above, we employed also a radium-beryllium, and a radiothorium-beryllium, source which happened to be at our disposal. The efficiency of the various preparations, as neutron sources, was determined by comparing the intensity, measured by a Geiger-Müller counter, of the artificial radioactivity they produced in silver and in rhodium. We found no appreciable variation in the neutron efficiency of the numerous radon tubes, although the fineness of the powder and the free space left was slightly different. Our radium-beryllium mixture had only 0.75 of the neutron efficiency of a radon-beryllium tube of equal  $\gamma$ -ray intensity; our radiothorium-beryllium mixture, on the other hand, being prepared from a radiothorium source of high emanating power, was 1.8 times as efficient a neutron source as a  $\gamma$ -equivalent radon-beryllium tube. As neither radium nor radiothorium decays appreciably during the time of one experiment, the intensity of their radiation, taking for radiothorium the mean value, can be considered as constant. As to the radon, since its period of average life is 5.52 days, the total radiation emitted from 1 millicurie (mc.) radon, during its complete decay, is equivalent to a constant radiation of 5.52 mc. days or  $4.77 \times 10^6$  mc. seconds.

The quantities of radon which were allowed to decay in our four experiments, and the strengths of the constant sources, together with the duration of their application, are given in Table I.

After the irradiation by neutrons, the analysis of the methyl borate for helium was carried out, the procedure being the same in all four experiments. It was based on previous work on the detection and measurement of small quantities of helium (see especially I and VIII), but could be somewhat simplified since little hydrogen had to be removed. It was unnecessary, therefore, to use the calcium furnace or the palladium capillary, the palladium furnace being sufficient. As the new model of this furnace, which has been in use in our laboratory for some time, has so far not been described in detail it is shown in a special diagram, fig. 1. For delicate helium analyses, where the complete removal of hydrogen is essential, it can be strongly recommended. The innermost part A, made of soda

glass and sealed to the rest of the analysing apparatus, contains at the bottom about 0.2 gm. of palladium sponge. It is inserted in a jacket B so that it can be heated while the latter is cooled by water. B, made of Jena glass, carries inside a cylinder supporting a flat "Nichrome" wire by means of which the heating of the palladium to a dull red heat can be effected with an energy of 50 watt; B is evacuated through a side tube c. As can be seen from the drawing, part A contains an inner glass tube a, reaching almost to the bottom, and a second inlet b; this makes it possible to let the hydrogen-oxygen mixture pass over the hot palladium as many

TABLE I

	Experiment			
	1	2	3	4
Radon-beryllium sources—				
Mc. decayed . . . . .	57	446	1975	1858
Equivalent to $10^6$ mc. sec. . . . .	0.27	2.13	9.42	8.86
Radium-beryllium source—				
$\gamma$ -equivalent to mc. radon . . . . .	—	—	—	50.9
Neutron-equivalent to mc. radon . . . . .	—	—	—	38
Time of irradiation in days . . . . .	—	—	—	26.7
Effect equivalent to $10^6$ mc. sec. radon . . . . .	—	—	—	0.88
Radio-thorium beryllium source—				
$\gamma$ -equivalent to mc. radon . . . . .	18	—	21	—
Neutron-equivalent to mc. radon . . . . .	32.4	—	38	—
Time of irradiation in days . . . . .	14.5	—	47.6	—
Effect equivalent to $10^6$ mc. sec. radon . . . . .	0.41	—	1.56	—
Total activity applied—				
In mc. radon decayed . . . . .	140	446	2300	2040
In $10^6$ mc. sec. radon . . . . .	0.68	2.13	10.98	9.74

times as seems desirable (see description below), thus ensuring complete combustion.

In order to drive out the helium formed in the methyl borate, the latter is kept boiling just as was done initially for the removal of air (see p. 413); but this time the outlet of the traps B and B' (fig. 2) is closed to the pump and opened through stopcocks k, l, and n to the three tubes E, F, J (each containing 12 gm. charcoal), to the palladium furnace G, and to the bulb L (volume 600 cc.). As B and B' are cooled by liquid air the gas filling the space just described consists, apart from the traces of helium, almost exclusively of hydrogen and methane which have been evolved as a conse-

quence of the irradiation of the boron ester by  $\gamma$ -rays and neutrons.\* For the elimination of hydrogen and, at the same time, the transport of all the helium contained between *c* and *l* into the analysing apparatus, a surplus of oxygen is admitted through stopcock *h*. This oxygen has

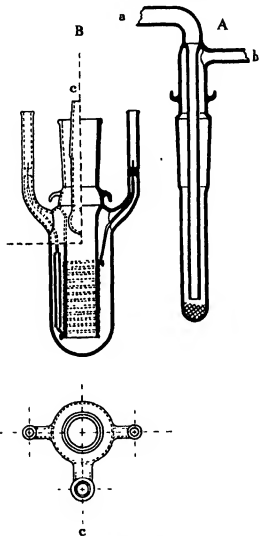


FIG. 1 (half natural size).

\* Very little is known so far about the chemical influence of neutron bombardment; according to Hopwood and Phillips ('Nature,' vol. 136, p. 1026 (1935)), the chemical effects of the neutrons of a radon-beryllium source are of the same order of magnitude as those due to its  $\gamma$ -rays.

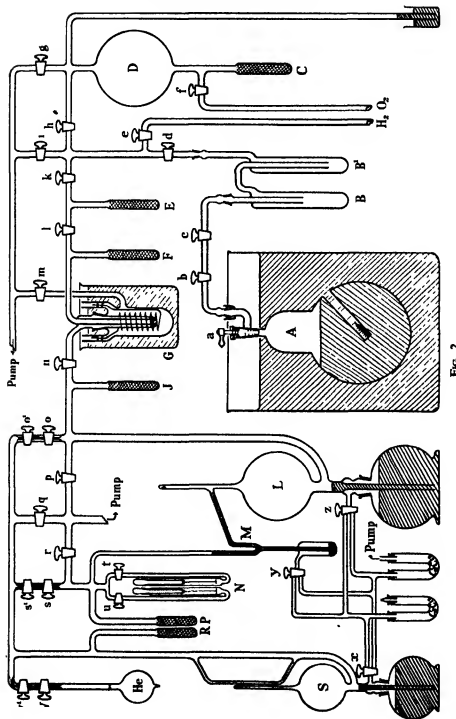


FIG. 2.

been electrolytically prepared,\* freed from hydrogen and a possible contamination of helium and neon by condensation in charcoal C, and afterwards stored in bulb D. It is first admitted into B' and B, and then, by opening *k* for short intervals, adsorbed in E which is cooled by liquid oxygen, so acting as a carrier for the helium (see II, p. 173). After repeating this process six times all the helium should be present in the apparatus behind *k*. To ensure that no helium is retained by the comparatively large quantity of ester condensed in B, we made it simmer by surrounding B with hot water, B' remaining in liquid air; during this operation tap *d* is closed and oxygen of about 10 cm. Hg pressure present.

From now onwards *k* remains closed. To separate the helium contained in E from the bulk of the oxygen the temperature of E is slightly raised by removing the liquid oxygen bath for about 1 minute, while *l* is closed; by repeatedly opening *l* for short intervals all this helium is carried beyond *l*. In the last and most important experiment 4 we made sure that no helium was left in A, B, B', and E by repeating the whole process onwards from boiling the methyl borate; no measurable amount of helium was recovered.

The oxygen released into the analysing apparatus should have a pressure of not more than about 12 cm. and is now used for the combustion of the hydrogen. The palladium in furnace G is heated and the mixture of gases, the major part of which is contained in the large volume L, passed over the palladium by cooling charcoal F in liquid air and thereby adsorbing the oxygen. Subsequent heating of F by means of hot water causes the oxygen to expand again and so to return through the palladium furnace to bulb L. Eight repetitions of this operation of alternate cooling and heating are always sufficient to burn all the hydrogen present to water. This water and the surplus of oxygen is removed by cooling first charcoal F and finally J for about 30 minutes each.

At the end of this cooling all gases with the exception of helium should have been removed. In order to test this, mercury is now raised into L, and the gas compressed into the capillary on the top of it and spectroscopically examined. If there has been any leakage of air into the vessel A during the weeks of irradiation, or into the glass parts of the apparatus during the separation of the helium, this contamination reveals itself immediately by the presence of neon lines in the helium spectrum. This is a very valuable check (see I and II) and it is, therefore, essential to use as cooling agent liquid oxygen and not liquid nitrogen or liquid air, for charcoal cooled to the temperature of liquid nitrogen retains a very considerable part of the neon. As has been shown previously, less than

\* See I, fig. 3, p. 365.

0.01% of neon in helium is spectroscopically easily visible, and a comparison of the relative strength of the lines permits of a fairly accurate estimate of the percentage of neon in the helium (see XI). While in the first three of our experiments the neon present amounted to about 20% of the helium, in the last experiment we succeeded in keeping the boron ester air-free to such an extent that, according to spectroscopic examination, the neon was certainly less than 10% of the helium.

The measurement of a minimum of  $10^{-8}$  cc. of helium can be carried out by means of a Pirani gauge (see VIII). For this purpose the mercury in bulb L is lowered below the tube leading to M; then with the help of stopcock y the mercury in M is withdrawn till the gas gains access to one side of the Pirani gauge N. For the calibration of the latter known quantities of helium from bulb He (volume measured in the capillary s-s<sup>1</sup>, pressure in the McLeod gauge S) are distributed through exactly the same volumes, P, N, M and upper part of L. (The cooled charcoals R and P are applied in order to remove all other gases, especially tap grease, and to make sure that only helium and neon are measured in the Pirani gauge.)

A certain quantity of the helium has, of course, not been included in the bulb L when the mercury was raised, but has remained in the palladium furnace G, the charcoals, and the connecting glass tubes up to stopcock l, according to the respective volumes and temperatures. The necessary correction for this part of the helium is found by introducing into the whole apparatus from L to l a known quantity of helium (measured by means of the capillary o-o<sup>1</sup> and the McLeod gauge S) and treating this in exactly the same way. The helium measured in the Pirani gauge has to be multiplied by the factor so determined; in our case this was 1.33.

A few other details in fig. 2 are self-explanatory, or their purpose can be found from our previous publications.

#### RESULTS\*

In experiment 1 the quantity of helium was sufficient only for a qualitative identification but not for a measurement in the Pirani gauge. From the lines visible in the spectroscope 5875.63, 5015.68, 4921.93, and, faintly, 4471.48 Å., we could roughly estimate† the amount of helium as of the order of  $10^{-8}$  cc. The experiment is interesting as showing that

\* The results of the second and third experiment have already been briefly communicated 'Nature,' vol. 136, p. 950, (1935).

† See table on p. 371 in I; or 'Mikrochem.,' vol. 7, p. 425 (1929).

a quantity of not more than 140 mc. radon, mixed with beryllium, is sufficient for a production of detectable amounts of helium from boron; but here we are near to the limit of sensitivity of our micro-method.

In the second experiment, carried out with 446 mc. radon, the helium quantity produced was still too small for an exact measurement, although in this experiment the helium line 4471·48, hardly visible in the first experiment, was very distinct; this is in good agreement with the increase in the strength of the radon source. In experiments 3 and 4 two more lines, 6678·15 and 4713·15, could be easily seen, and here the Pirani gauge could be applied. We found in experiment 3, making allowance for the 20% neon present (see formula in XI),  $1\cdot4 \pm 0\cdot2 \times 10^{-7}$  cc. helium, and in experiment 4, where the quantity of neon was negligible,  $2\cdot4 \pm 0\cdot2 \times 10^{-7}$  cc. helium (N.T.P.).

Although the activity in experiment 3 exceeded that applied in experiment 4 by almost 13%, the helium found was only about 0·6 as much. The reason for the greater yield in the last experiment is no doubt the increased volume of the copper vessel A filled with boron ester, and it is very likely that a further increase of the volume would result in a still higher value. It is hardly possible to calculate exactly the proportion of neutrons which is still not caught even in the bigger vessel. A fraction of the neutrons produced in the beryllium source is certainly not slowed down by the hydrogen of the boron ester, but only by the water of the tank outside; some of them, however, get back by diffusion from here into the vessel A and are finally caught by boron atoms. One has also to consider that during the experiments the vessel A was not completely filled with the liquid ester; not only the dome on top but also a part of the spherical vessel was empty because, as described above, some of the ester had to be distilled into B in order to get it air-free; as, however, the surface of the boron ester was still 4 cm. above the centre of the sphere in experiment 4 (and 2 cm. in experiment 3), the influence of the incomplete filling on the final result can only be small and by a slightly changed arrangement in a repetition of the experiment this source of error could easily be avoided. It will be more troublesome to make the vessel A large enough to ensure capture of practically all the neutrons produced in the radon-beryllium source, but if the experiment is deemed sufficiently important, it could no doubt be done. An increase of the radius of A from 7·5 cm. to 10 cm., together with a reduction of the radius of the pocket and a rising of the level of the ester, enabled us to catch 1·9 times as many neutrons in experiment 4 as in experiment 3; from this fact, as well as from theoretical considerations based on work on the diffusion of neutrons in water, it seems that another substantial increase might be expected if

all neutrons could be used up by reaction (1) inside a still larger copper vessel.

Although, therefore, the helium found is only a minimum value it is quite interesting to make use of this figure for a calculation of the minimum number of neutrons generated in the beryllium source. In experiment 4,  $9.74 \times 10^8$  mc. sec. radon produced  $2.4 \times 10^{-7}$  cc., or  $6.5 \times 10^{22}$  atoms of helium; according to equation (1) the same number of neutrons has been used up, from which it follows that 1 mc. sec. of a radon beryllium source emits at least  $6.7 \times 10^8$  neutrons. This figure is considerably higher than the value  $1 \times 10^8$  deduced from early experiments.\* More recent observations in a Wilson chamber made  $10^4$  neutrons per mc. sec. seem a likely value.† Our figure is obtained by a quite different and very direct way; being a minimum value, it is consistent with this result. It may be pointed out that in experiment 4, on which our figure is based, only 10% of the activity was provided by a radium beryllium source, so that any uncertainty in determining the neutron equivalent of such a source to radon beryllium is of very little influence.

From a minimum neutron efficiency of  $6.7 \times 10^8$  neutrons per mc. sec. it follows that one  $\alpha$ -particle from a ( $Rd + RaA + RaC'$ ) source by its impact on beryllium produces at least  $6 \times 10^{-6}$  neutrons, i.e., more than one neutron per 17,000  $\alpha$ -particles; but as the three  $\alpha$ -particles have very different energies, not much physical significance can be attached to such an average value.

As to the origin of the helium, the objection could be made that possibly the  $\gamma$ -rays and not the neutrons were the efficient agent. Chadwick and Goldhaber,‡ however, were able to detect nuclear disintegration as a product of  $\gamma$ -radiation only in deuterium and in beryllium and not in any of the elements contained in the vessel A (boron, carbon, oxygen, copper). And in a control experiment in which 193 mc. radon, without beryllium, decayed in the centre of vessel A, we did not find any helium in the boron ester.

In the present experiments an artificially produced element has been spectroscopically identified and quantitatively measured for the first time. The reaction by which the helium is formed has already been known from physical experiments; but it is not without interest that the

\* Ellis and Henderson, 'Nature,' vol. 133, p. 530 (1934); see also Fermi, Amaldi, D'Agostino, Rasetti, and Segré, 'Proc. Roy. Soc.,' A, vol. 146, p. 483 (1934).

† Jaekel, 'Z. phys. Chem.,' vol. 91, p. 493 (1934). The result can hardly claim to give more than the order of magnitude as three quantities entering the calculation are given only with one significant figure.

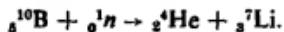
‡ Chadwick and Goldhaber, 'Proc. Roy. Soc.,' A, vol. 151, p. 479 (1935).

methods of chemistry are sensitive enough to detect the products of artificial transmutation and to permit an entirely independent quantitative study.\* It may be that there are atomic processes going on with so little energy that radio-physical or radio-chemical methods cannot be applied at all, yet where a chemical procedure, similar to the one described, may be able to discover the newly formed elements. Experiments on these lines are in progress.

The senior author wishes to express his thanks to the Imperial College for laboratory facilities; to Imperial Chemical Industries, Ltd., for their assistance; to Professor F. L. Hopwood, director of the Radium Department, St. Bartholomew's Hospital, London, Professor S. Russ, director of the Radium Department, Middlesex Hospital, London, and Professor Stefan Meyer, director of the Institute for Radium Research in Vienna, for kindly supplying the radon-beryllium tubes.

#### SUMMARY

By a micro-method it was possible to collect, in a pure state, the helium produced by neutron bombardment from boron according to the following reaction:



The neutrons from a radioactive source equivalent to the decay of only 140 mc. radon gave sufficient helium for a spectroscopic identification. With stronger radioactive sources, of the order of 2 curie radon, enough helium was obtained for its quantitative determination; the neutrons from 2.04 curie radon, mixed with beryllium, produced during its decay  $2.4 \times 10^{-7}$  cc. helium. From this figure it can be deduced that 1 mc. sec. of a radon beryllium source emits at least  $6.7 \times 10^3$  neutrons.

\* See also 'Nature,' vol. 137, p. 560 (1936).

---

## Hydrogen Overvoltage and the Reversible Hydrogen Electrode

By J. A. V. BUTLER, D.Sc., University of Edinburgh

(Communicated by J. Kendall, F.R.S.—Received 3 June, 1936)

There are two fairly sharply contrasted methods by which hydrogen is liberated in electrolysis. At high overvoltage electrodes Tafel\* found that the current and electrode potential were related by  $i = ke^{-\alpha V/RT}$ , a relation more recently confirmed by Bowden.† These electrodes are not reversible and there is no evidence that the process  $H_2 \rightarrow 2H^+ + 2e^-$  can occur to any appreciable extent at potentials accessible to observation. Even at ordinary bright platinum, which has a fairly low overvoltage, Armstrong and Butler‡ found that the ionization of hydrogen occurred to only a slight extent in the region between the reversible hydrogen potential and the potential at which oxygen begins to be formed. On the other hand, reversible hydrogen potentials have long been known at platinized platinum and similar electrodes, and it has been found that bright platinum and similar metals can be "activated" in various ways,§ whereby it is brought into a condition in which the reversible hydrogen potential can be realized. In this state the hydrogen overvoltage is low and at small displacements from the reversible value the potential varies linearly with the current, i.e.,  $V = V_0 - ki$ . This relation can be accounted for|| on the assumption that there are two processes at the reversible electrode which are influenced exponentially by the potential, but in opposite directions.

The theories of overvoltage which have been put forward have been concerned mainly with the behaviour of high overvoltage electrodes. In Gurney's theory|| the potential determining process was the transfer of electrons from the metal to the hydrogen ions in the solution. As

\* 'Z. phys. Chem.', vol. 50, p. 641 (1905).

† 'Proc. Roy. Soc.,' A, vol. 125, p. 446 (1929); vol. 126, p. 107 (1929).

‡ 'Proc. Roy. Soc.,' A, vol. 137, p. 604 (1932).

§ Butler and Armstrong, 'J. Chem. Soc.,' p. 743 (1934); Volmer and Wick, 'Z. phys. Chem.,' A, vol. 172, p. 429 (1935).

|| Erdy Grúsz and Volmer, 'Z. phys. Chem.,' A, vol. 150, p. 203 (1930); Butler, 'Trans. Faraday Soc.,' vol. 28, p. 379 (1932); Hammett, *ibid.*, vol. 29, p. 770 (1933); Hoekstra, 'Z. phys. Chem.,' A, vol. 166, p. 77 (1933).

|| 'Proc. Roy. Soc.,' A, vol. 134, p. 137 (1931).

Gurney pointed out,\* this process is essentially irreversible, for the reverse transfer of electrons from either free hydrogen atoms or molecules cannot occur to an appreciable extent in the same potential region. Horiuti and Polanyi† have suggested an alternative mechanism in which the primary process is the transference of hydrogen ions to adsorption positions at the surface of the metal, in the course of which neutralization occurs. This process may under some circumstances be reversible, but on the assumptions made has a high activation energy of 20–30 k.cals.

The object of this paper is to suggest a scheme which contains features of both these theories and includes as possible cases reversible and irreversible electrodes. It is shown that when the adsorption energy of hydrogen atoms on the metal is appreciable, these can be deposited at a lower potential than is required for the liberation of free hydrogen. But hydrogen cannot be continuously liberated in this way unless the rate of desorption as hydrogen molecules is greater than the current.

#### FORMATION OF FREE ATOMIC HYDROGEN

According to Gurney, the condition for the neutralization of hydrogen ions near the electrode is approximately stated as  $\phi + \epsilon V < N$ , where  $\phi$  is the thermionic work function of the metal,  $V$  the potential difference between the metal and the ions, and  $N$  the neutralization potential of hydrogen ions. The latter is  $N = \mathcal{I} - L - R$ , where  $\mathcal{I}$  is the ionization potential of gaseous atomic hydrogen,  $L$  the hydration energy of protons, and  $R$  the repulsive potential between hydrogen atoms and the water molecule.  $L$  and  $R$  are to be evaluated for the state of the hydrogen ion in which neutralization occurs. Writing this condition as

$$\phi + \epsilon V + R < \mathcal{I} - L,$$

it can be represented graphically as in fig. 1. The curve AA represents  $\mathcal{I} - L$  plotted as a function of the distance of the proton from the centre of the water molecule, and the curve BB is that of the corresponding values of  $\phi + \epsilon V + R$ . The condition is satisfied for points lying to the left of the point of intersection X of the two curves, and if  $E'$  is the energy of the point of intersection,  $E' - E_0$  is the activation energy required for the process. This representation is, however, only approximate, because it is based on the assumption that the electron levels of the metal are completely filled for values  $> \phi$  and completely unoccupied

\* 'Trans. Faraday Soc.', vol. 28, p. 447 (1932).

† 'Acta Physicochim., U.R.S.S.', vol. 2, p. 505 (1935).

for values  $< \phi$ . Gurney took into account the fact that there is a range of energies in which the levels are partly filled and partly unfilled. There will then be occupied levels of the metal with values  $< \phi$  and therefore an appreciable probability of the neutralization of ions to the right of X. In fact, since the number of ions in levels above X diminishes rapidly, the greater part of the current is employed in the neutralization of ions with energies below X. Nevertheless, it can be shown that the activation

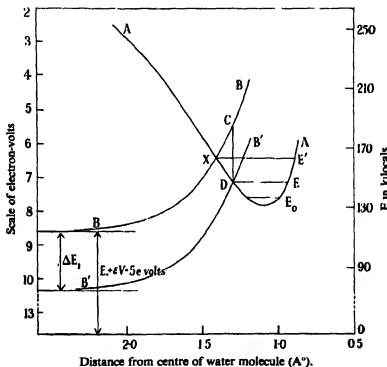


FIG. 1.—Discharge of proton in  $\text{H}_3\text{O}^+$ . AA, curve of  $\mathcal{J} - L$ ; BB, curve of  $E_1 + \epsilon V + R$ .

energy  $\Delta$ , as measured by  $(d \log i / dT)_v = \Delta / RT^2$ , is approximately equal to  $E' - E_0$ .

Let BB be the curve of  $\phi + \epsilon V + R$  for  $\phi = E_1$ , where  $E_1$  is the energy of the electronic level in the metal, which is half occupied by electrons, and let  $B'B'$  be the corresponding curve for the electronic level  $E_1 - \Delta E_1$ . The probability of finding an electron in the level  $E_1 - \Delta E_1$  is given by  $e^{-\Delta E_1 / kT}$ . The curve  $B'B'$  intersects AA at D, and an electron in the level  $E_1 - \Delta E_1$  is therefore able to neutralize an ion in the ionic level E which

passes through D. The probability of an ion having this energy is  $e^{(E_0 - E/kT)}$ . The rate of neutralization is thus an expression of the form

$$i = \int_{E_0}^{E'} e^{(E_0 - E)/kT} \cdot e^{-\Delta E/kT} \cdot \text{const. } dE.$$

But we see from the diagram that

$$\Delta E_1 = CD = \gamma(E' - E),$$

where to the first approximation  $\gamma$  is a constant.

Hence

$$i = \int_{E_0}^{E'} e^{(E_0 - E)/kT} \cdot e^{-\gamma(E' - E)} \cdot \text{const. } dE,$$

so that

$$\log i = \text{const.} + (E_0 - E)/kT \quad (1)$$

and

$$d(\log i)/dT = (E' - E_0)/kT^2. \quad (2)$$

The Tafel-Bowden relation also follows easily from this construction, if  $\gamma$  be taken as 2, for

$$-d(\log i)/dV = (dE'/dV)/kT = \epsilon/\gamma kT. \quad (3)$$

The curves of fig. 1 were constructed from the following data. The total hydration energy of the proton is about 270 k.cals.,\* but this includes the energy of hydration of the ion  $H_3O^+$ , which may reasonably be taken as about 90 k.cals., leaving  $L_0 = 180$  k.cals. for the interaction of  $H_3O$  and  $H^+$ . The curve of  $L$  is constructed by means of the Morse equation  $L = L_0(e^{-2a(r-r_0)} - 2e^{-a(r-r_0)})$ , where the value of  $a$  corresponding to the fundamental frequency  $\omega_r = 3660 \text{ cm.}^{-1}$  is  $a = 1.735 \times 10^8 \text{ cm.}^{-1}$ . The distance of the protons from the centre of the water molecule is 0.97 Å., but a somewhat greater value may be expected in  $H_3O^+$ , so we take  $r_0 = 1.1 \text{ Å.}^{\dagger}$   $\mathcal{F}$  is 13.5 e-volts or 313 k.cals.

A suitable value of the repulsive potential  $R(H_3O - H)$  is more difficult to estimate. Bleick and Mayer‡ have calculated the repulsive potential between two neon atoms, and have obtained values which are in reasonable agreement with the expression  $\log_{10} R(r) = 8.43 - 2.077 \times 10^8 r$ , while Slater's values§ for the repulsive potential of two helium atoms are represented by  $\log_{10} R(r) = 7.05 - 1.99 \times 10^8 r$ . Judging

\* Bernal and Fowler, 'J. Chem. Phys.', vol. 1, p. 515 (1933).

† Bernal and Fowler, loc. cit.

‡ *Ibid.*, vol. 2, p. 252 (1934).

§ 'Phys. Rev.', vol. 32, p. 349 (1928).

by the values of the repulsive potential of H — He, calculated by Gentile,\* the repulsive curve of H — Ne will be somewhat flatter than that of Ne — Ne. Its position can be estimated from the rule† that for a given value of R ( $r$ ) the values of  $r$  are approximately additive for the two atoms concerned. On these grounds the expression  $\log_{10} R(r) = 6.96 - 1.6r$  was chosen as a reasonable estimate of the H — Ne curve and the H — H<sub>2</sub>O may be expected to be similar. The position of this curve with reference to the calculated repulsions of the other cases is shown in fig. 2.

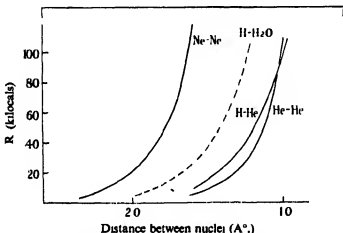


FIG. 2—Repulsive potentials of Ne — Ne, He — He, and H — He. —, curve assumed for H — H<sub>2</sub>O.

Using these curves and taking the zero point energy of the proton in H<sub>3</sub>O<sup>+</sup> as 5 k.cals., the following values of  $\Delta = E' - E_0$  are obtained:

$E_1 + \epsilon V$ .....	3	4	5	6	$\epsilon$ -volts
$\Delta$ .....	8	16	27	38	kilocalcs.

Now Bowden‡ found that at the potential  $V = -1.0$  volts against saturated calomel, the value of  $\Delta$  obtained from the  $d \log l/dT$  curve of a mercury electrode was 0.43  $\epsilon$ -volts or 9.9 k.cals. This corresponds to the value  $E_1 + \epsilon V = 3.2$  volts, or taking the absolute value of  $V$  as  $-0.47$  volts, to  $E_1 = 3.7$   $\epsilon$ -volts. The photoelectric threshold of mercury corresponds to a thermionic work function of 4.5  $\epsilon$ -volts, which is in reasonable agreement with this figure. It may therefore be concluded

\* 'Z. Physik,' vol. 63, p. 795 (1930).

† Cf. Born and Mayer, 'Z. Physik,' vol. 75, p. 1 (1932).

‡ 'Proc. Roy. Soc.,' A, vol. 126, p. 107 (1930).

that Gurney's mechanism gives a reasonable quantitative agreement with the observations at a high overvoltage metal.

#### FORMATION OF ADSORBED HYDROGEN ATOMS

We shall now consider the case in which the hydrogen atoms may be adsorbed on the metal surface. The energy of a hydrogen atom in the

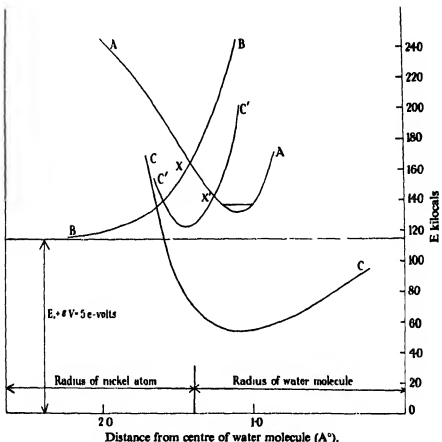


FIG. 3—Formation of adsorbed hydrogen. AA, curve of  $\mathcal{F} - L$ ; BB, curve of  $E_1 + \epsilon V + R$ ; CC, curve of A; C'C', curve of  $E_1 + \epsilon V + R - A$ .

region between the metal surface and the adjacent water molecules must be obtained by combining its energy of adsorption on the surface of the metal A with the repulsive energy R between it and the water molecule. In fig. 3 CC is the curve of A, plotted against the distance of the hydrogen from the surface of the metal, displaced upwards a distance  $E_1 + \epsilon V$ . The curve C'C', obtained by adding the values of R represented by BB,

thus represents  $E_1 + \epsilon V - A + R$ . The curve AA, as in fig. 1, is that of  $\mathcal{S} - L$ . The condition of neutralization is now  $\phi + \epsilon V - A + R < \mathcal{S} - L$ , and as before the energy of activation of the process is equal to the difference between the energy at the point of intersection X' of the two curves and the energy of the proton in its ground level.

The activation energy for this process is thus smaller than that required for the formation of "free" atomic hydrogen by the amount represented by the vertical distance between X' and X, or alternatively the potential difference may be increased (positively) by the same amount to keep the activation energy (and the rate of discharge) the same. It is easily shown that, assuming the potential curves to be straight lines in the neighbourhood of the intersection, the difference of potential is

$$\epsilon \cdot \Delta V = A / (1 - dR/dL - dA/dL),$$

where A is the adsorption energy near the point of intersection.  $dA/dL$  is small compared with  $dR/dL$  and in a rough estimate may be neglected. In Gurney's theory the experimental facts required that  $dR/dL = -1$ , whence  $\epsilon \cdot \Delta V = A/2$ . With metals which are capable of adsorbing hydrogen in the atomic condition the energy of adsorption is of the same order as D/2, where D is the dissociation energy of the hydrogen molecule, i.e.,  $A = ca. 2$  e-volts and  $\Delta V$  is of the order of 1 volt. It is clear that adsorbed hydrogen may be formed at a considerably less negative voltage than is required for the production of free hydrogen by Gurney's mechanism.

#### CONDITIONS OF REVERSIBILITY

The process considered in the last section can also take place in the opposite direction, and the reversible hydrogen potential is that at which the transfers occur at the same rate in both directions. Ignoring the influence of the amount of adsorbed hydrogen present, this will happen when the potential difference is such that *the energy of activation is the same from either side*. At a practical reversible electrode it should be possible to pass appreciable currents through the electrode without appreciably displacing the equilibrium potential difference. For this purpose the rates of transfer in either direction must be comparatively large compared with the current used, and the activation energy correspondingly small.

In order to see under what circumstances this condition is satisfied, the activation energies have been estimated for nickel, for which the data required are available. In constructing the curve of A (Ni - H)

the heat of evaporation of hydrogen atoms from the surface was taken as 60 k.cals. and the equilibrium distance of the hydrogen atoms from the nickel nuclei as 1.56 Å., and the curve is determined by Morse's equation, taking  $a = 1.39 \times 10^8$  cm.<sup>1</sup>.\*

In combining the curves of A and R it is also necessary to know the distance between the centres of the metal atoms and the adjacent water molecules. The radius of the nickel atom may be taken as 1.25 Å., and that of the water molecule as 1.38 Å., giving the shortest distance of approach of the two as 2.63 Å. The distance of the protons from the centre of the H<sub>3</sub>O<sup>+</sup> ion has been taken as 1.1 Å. If it be supposed that the electron surface of the metal coincides with the radius given above, the thickness of the electrolytic double layer, *i.e.*, the distance between the nearest protons of H<sub>3</sub>O<sup>+</sup> and the surface of the metal, is about 0.3 Å. This is considerably smaller than Bowden and Rideal's original estimate of the double layer thickness from the capacity of mercury electrodes (*viz.*, 1.5 Å.). But Frumkin and Proskurnin,† taking stringent precautions to prevent the contamination of the electrodes by paraffins, obtained a value of the capacity three times as great, which corresponds to a double layer thickness of 0.5 Å., which is reasonably concordant with these dimensions.

TABLE I—ACTIVATION ENERGIES OF REVERSIBLE TRANSFER FROM IONIC STATE TO ADSORPTION POSITIONS

Distance between Ni and H <sub>3</sub> O <sup>+</sup> Å.	$E' - E_0$ (k.cals.)			
	1.0	1.1	1.2	1.3
2.46	7	0	—	—
2.56	13	5	—	—
2.66	18	10	3	—
2.76	23	15	7	0
2.86	27	19	11	4

Table I shows the values of the activation energy required for the reversible transfer, determined graphically, as in fig. 3, by adjusting the potential difference until the minima of the curves for the ionic and adsorbed states are at the same level. The values given are for various Ni—H<sub>3</sub>O distances, and assuming the equilibrium distances of the proton from the centre of the water molecule in H<sub>3</sub>O<sup>+</sup> to be 1.0, 1.1, 1.3 Å. respectively.

\* Sherman, Sun, and Eyring, 'J. Chem. Phys.', vol. 3, p. 49 (1935).

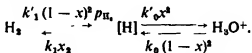
† 'Proc. Roy. Soc.,' A, vol. 120, p. 59 (1928).

‡ 'Trans. Faraday Soc.,' vol. 31, p. 110 (1935).

It can be seen that the mechanism described leads in favourable cases to small values of the activation energy of the reversible transfer. The most probable configuration, viz., total distance 2.63 Å., and proton distance 1.1 Å., has an activation energy of about 8 k.cals. According to the measurements of Bowden cited above, the transfer rate from the ionic side is  $10^{-6}$  amps./cm.<sup>2</sup> when the activation energy is 10 k.cals. This is independent of the nature of the metal and it follows from (1) that with  $E' - E_0 = 8$  k.cals. the rate of transfer is about  $2.5 \times 10^{-4}$  amps. At such an electrode the passage of currents of the order of  $10^{-5}$  amps./cm.<sup>2</sup> would not greatly disturb the equilibrium potential.

### THE DESORPTION OF HYDROGEN

At the reversible hydrogen electrode it is also necessary that the adsorbed hydrogen shall be in reversible equilibrium with the atmosphere of gaseous hydrogen. We shall consider the equilibrium of the adsorbed hydrogen with the hydrogen atmosphere on the one hand and the ions of the solution on the other:



Let  $x$  be the fraction of the adsorption positions at the surface which is occupied by hydrogen. The rate of desorption of hydrogen may be written as  $k_1 x^2$  and the rate of adsorption (which is proportional to the probability of finding two adjacent adsorption places vacant) is  $k'_1 (1-x)^2 p_{\text{H}_2}$ . The equilibrium is thus defined by  $k_1 x^2 = k'_1 (1-x)^2 p_{\text{H}_2}$ .\* When hydrogen is being liberated at the electrode, this equilibrium is disturbed and the rate of formation of hydrogen ( $i$ ) is

$$i = k_1 x^2 - k'_1 (1-x)^2 p_{\text{H}_2}. \quad (4)$$

It is evident from this that (1) if  $k_1$  is large compared with  $i$  the displacement of the adsorption equilibrium caused by the current is small; (2) the rate at which hydrogen is produced in this way cannot exceed the value  $k_1$ .

Consider now the equilibrium between the adsorbed hydrogen and the ions of the solution. Let the rate of transfer of protons at the equilibrium potential difference  $V_0$  to a completely unoccupied surface ( $x = 0$ ) be

\* There are other possible equations for the adsorptive equilibrium of hydrogen (cf. Roberts, 'Proc. Camb. Phil. Soc.', vol. 32, p. 152 (1936)), but the argument of this section is not thereby affected.

$k_0$ , and the rate of transfer in the opposite direction from a completely occupied surface ( $x = 1$ ) be  $k'_0$ . The condition of equilibrium at the potential  $V_0$  is  $k_0(1 - x) = k'_0x$ . When the potential is displaced by the amount  $\Delta V$  from  $V_0$ , these rates become  $k_0(1 - x)e^{-\epsilon \Delta V/\gamma kT}$  and  $k'_0x e^{\epsilon \Delta V/\gamma kT}$ , and the current is

$$i = k_0(1 - x)e^{-\epsilon \Delta V/\gamma kT} - k'_0x e^{\epsilon \Delta V/\gamma kT}, \quad (5)$$

and  $x$  is determined by (4). The following conclusions can be drawn.

(1) When  $i$  is small compared with  $k_1$ , the adsorption equilibrium is not appreciably disturbed by the current, and writing  $i_0 = k_0(1 - x)$  for the rate of the reversible transfer at  $V_0$ , we have approximately for small values of  $\Delta V$ ,

$$i/i_0 = -2\epsilon \cdot \Delta V/\gamma kT, \quad (6)$$

i.e., for small displacements of the potential difference, the latter varies linearly with the current. This has been found to be the case for reversible electrodes.

(2) As  $i$  approaches  $k_1$ ,  $(1 - x)$  approaches zero, and therefore  $-\Delta V$  will increase more rapidly than in case (1).

(3) When  $i > k_1$ , this mechanism is no longer capable of accounting for the whole of the current, and the potential of the electrode must rise until some other discharge process becomes possible, e.g., by Gurney's mechanism.

The behaviour of an electrode is thus determined by the magnitude of  $k_1$ . If this is large, hydrogen may be liberated at a correspondingly large rate by the reversible mechanism and at a low overvoltage. If it is small, the liberation of hydrogen at an appreciable rate by this process cannot take place and the higher overvoltage of the alternative mechanism is exhibited. This is presumably the case with the high overvoltage metals.

The value of  $k_1$  is determined by the activation energy of the desorption process. Sherman and Eyring\* calculated the activation energy for the adsorption of  $H_2$  on carbon as a function of the spacing of the carbon atoms and found that it was a minimum for a certain spacing (3.5 Å.), which is considerably greater than the normal C-C distance. Although these calculations are not very reliable quantitatively, the conclusion that there is an optimum spacing for each metal is reasonable, and the difficulty of realizing the reversible hydrogen potential at most bright metallic surfaces may be attributed to unsuitable spacings. The ease with which the potential is established at platinum black and similar materials may

\* J. Amer. Chem. Soc., vol. 54, p. 2661 (1932).

perhaps be due to the greater probability of finding a suitable spacing on the surface.

In conclusion, it may be noted that although the formation of adsorbed oxygen can easily be demonstrated at anodes,\* the formation of adsorbed hydrogen below the normal overvoltage has not been observed. Experiments on the establishment of the hydrogen overvoltage have, however, usually been made in an atmosphere of hydrogen, and after a preliminary cathodic polarization to remove traces of oxygen. Under these conditions the adsorbed hydrogen would be present at the start and no indication of its formation would be found.

#### SUMMARY

In the discharge of hydrogen ions at metallic cathodes adsorbed hydrogen may be formed at a lower potential than "free" hydrogen, liberated according to Gurney's mechanism.

There is a potential difference at which the rates of transfer of hydrogen ions to adsorption positions and the reverse are equal, and it is shown that in favourable cases the activation energy of the reversible transfer is sufficiently low to give rise to a practically reversible electrode.

Hydrogen can, however, only be continuously evolved by this process with currents which are less than the rate of desorption of  $H_2$  from a saturated surface, and with greater currents an alternative mechanism must come into action. It is suggested that at high overvoltage electrodes the rate of desorption is small, and hydrogen is formed by Gurney's or some similar mechanism.

\* Armstrong, Himsworth, and Butler, ' Proc. Roy. Soc.,' A, vol. 143, p. 89 (1933); Butler and Drever, ' Trans. Faraday Soc.,' vol. 32, p. 427 (1936).

---

## Integral Electromagnetic Theorems in General Relativity

By J. L. SYNGE

*(Communicated by E. T. Whittaker, F.R.S.—Received 5 June, 1936)*

### 1—INTRODUCTION

In classical physics Gauss's theorem, connecting normal flux of intensity with enclosed mass or charge, has one single form for gravitation and for electrostatics: it is, in fact, a direct consequence of the inverse square law. In the general theory of relativity gravitation and electricity play very different parts, and one might expect a divergence between an extension of Gauss's gravitational theorem to general relativity and an extension of his electrostatic theorem. Whittaker,<sup>†</sup> and Ruse,<sup>‡</sup> have developed the gravitational extension, and Whittaker has indicated the electrical extension. It is the purpose of the present paper to complete the electrical extension. It is found that for an electromagnetic field in general relativity there exists a theorem which is expressed naturally in precisely the same form as the classical theorem of Gauss, but which admits a more general interpretation. Other integral theorems are also obtained by systematic application of the three Green-Stokes theorems available in four-dimensional space-time.

The fact that the fundamental form of space-time is not positive-definite does not affect certain results, such as (2.1) below. But when we seek physical interpretations, this fact must be taken into consideration, as the presence of the indicators in (3.13), (3.15), (3.28) shows. It is through careful attention to this detail that the results obtained differ from those given by Pauli.<sup>§</sup> The utility of the classical formulae of Green and Stokes depends to a great extent on the fact that they are expressed in forms involving essentially positive elements of area and volume: it would seem that the value of their extensions to space-time depends similarly on the use of essentially positive elements of area, volume, and 4-volume, with explicit attention to the indefinite character of the fundamental form.

<sup>†</sup> 'Proc. Roy. Soc.,' A, vol. 149, p. 384 (1935).

<sup>‡</sup> 'Proc. Edin. Math. Soc.,' vol. 4, p. 144 (1935).

<sup>§</sup> "Relativitätstheorie," "Encyk. d. math. Wiss.," vol. 5, part 19, p. 606 (1920).

## 2—GREEN-STOKES THEOREMS IN SPACE-TIME

If in a space of  $N$  dimensions  $V_N$  (not necessarily metrical) there exists an  $(M+1)$ -dimensional region  $V_{M+1}$  bounded by a closed  $V_M$ , and if  $v_{i_1 \dots i_M}$  is any continuous differentiable field of quantities with  $M$  suffixes, then†

$$\int_{(N)} v_{i_1 \dots i_M} d\omega^{i_1 \dots i_N} = \int_{(M+1)} \partial_{i_{M+1}} v_{i_1 \dots i_M} d\omega^{i_1 \dots i_{M+1}}; \quad (2.1)$$

the suffixes have the range 1, 2, ...,  $N$ , with summation on account of repetition,  $x^i$  are coordinates in  $V_N$ , and

$$\left. \begin{aligned} \partial_i &= \partial/\partial x^i, \\ d\omega^{i_1 \dots i_N} &= \delta_{i_1 \dots i_M}^{i_1 \dots i_N} d_{(1)} x^{i_1} \dots d_{(M)} x^{i_M}, \\ d\omega^{i_1 \dots i_{M+1}} &= \delta_{i_1 \dots i_{M+1}}^{i_1 \dots i_{M+1}} d_{(1)} x^{i_1} \dots d_{(M+1)} x^{i_{M+1}}, \end{aligned} \right\} \quad (2.2)$$

these  $\delta$ 's being the generalized Kronecker deltas.‡ The integral on the left of (2.1) is taken over  $V_M$  and that on the right over the enclosed portion of  $V_{M+1}$ . It is assumed that  $V_{M+1}$  is an orientable space and  $V_M$  a two-sided surface in it. The  $M$ -cells in  $V_M$  have a unique, but arbitrary, orientation: when that is assigned, the  $(M+1)$ -cells in  $V_{M+1}$  have a unique orientation, namely, that obtained by adding to an  $M$ -cell of  $V_M$  as a final edge  $d_{(M+1)} x^{i_{M+1}}$  an element of the outward normal to  $V_M$  in  $V_{M+1}$ .

In the applications of this theorem to space-time we are to take  $N = 4$ . There are then three cases to be considered, namely,  $M = 1$ ,  $M = 2$ ,  $M = 3$ . These give the following statements:

$$\left. \begin{aligned} \int_{(1)} v_t d_{(1)} x^t &= \int_{(2)} \partial_t v_t d\omega^t, \\ d\omega^t &= \delta_{tt}^{ij} d_{(1)} x^k d_{(2)} x^l; \end{aligned} \right\} \quad (2.3)$$

$$\left. \begin{aligned} \int_{(2)} v_{tl} d\omega^{tl} &= \int_{(3)} \partial_k v_{tl} d\omega^{tk}, \\ d\omega^{tl} &= \delta_{tl}^{ij} d_{(1)} x^k d_{(2)} x^l, \\ d\omega^{tk} &= \delta_{tk}^{ij} d_{(1)} x^l d_{(2)} x^m d_{(3)} x^n; \end{aligned} \right\} \quad (2.4)$$

$$\left. \begin{aligned} \int_{(3)} v_{tik} d\omega^{tik} &= \int_{(4)} \partial_l v_{tik} d\omega^{lik}, \\ d\omega^{tik} &= \delta_{lik}^{ij} d_{(1)} x^l d_{(2)} x^m d_{(3)} x^n, \\ d\omega^{lik} &= \delta_{lmn}^{ijk} d_{(1)} x^m d_{(2)} x^n d_{(3)} x^p d_{(4)} x^q. \end{aligned} \right\} \quad (2.5)$$

† This result will be found in slightly different notation in Schouten, "Der Ricci-Kalkül," p. 97 (1924). It is perhaps most easily established by a variational method.

‡ Cf. Veblen, "Invariants of Quadratic Differential Forms," Cambridge (1927), p. 3.

We shall now convert these into alternative forms. We shall assume that in (2.4)  $v_{\mu\nu}$  is skew-symmetric and that in (2.5)  $v_{\mu\nu k}$  is skew-symmetric in each pair of suffixes. In the statements made above no metrical properties of the space concerned are involved, but we shall now assume that  $V_4$  is Riemannian with fundamental form

$$\Phi = g_{\mu} dx^{\mu} dx^{\nu}. \quad (2.6)$$

The signature of this form will be taken to be  $+++ -$ . The indicator  $\epsilon$  of a vector  $t^{\mu}$  is chosen equal to  $\pm 1$  to make  $\epsilon g_{\mu\nu} t^{\mu} t^{\nu} > 0$ .

We shall write

$$\eta_{\mu\nu k} = \epsilon_{\mu\nu k} \sqrt{-g}, \quad (2.7)$$

$\epsilon_{\mu\nu k}$  being the usual permutation symbol, and  $g$  the determinant of  $g_{\mu\nu}$ : this is a covariant tensor, but only with respect to transformations having a positive Jacobian. Raising the subscripts in the usual way, we find the contravariant form

$$\eta^{\mu\nu k} = -\epsilon_{\mu\nu k} / \sqrt{-g}. \quad (2.8)$$

Let  $t_{(1)}^{\mu}, t_{(2)}^{\mu}, t_{(3)}^{\mu}, t_{(4)}^{\mu}$  be a field of tetrads of mutually orthogonal unit vectors with indicators  $\epsilon_1, \epsilon_2, \epsilon_3, \epsilon_4$ . (Since these carry one suffix and the permutation symbols four, there can be no confusion due to this notation.) From the signature of  $\Phi$  we have

$$\epsilon_1 \epsilon_2 \epsilon_3 \epsilon_4 = -1. \quad (2.9)$$

Since the  $\eta$ 's are tensors only with respect to transformations with positive Jacobian, we shall restrict our attention to such transformations. The orientation of the parametric lines of  $x^1, x^2, x^3, x^4$  is then invariant, and we shall choose the tetrad of  $t$ -vectors with this same orientation. It will then be possible by allowed transformations to reduce the fundamental form at an assigned point to

$$\Phi = \epsilon_1 (dx^1)^2 + \epsilon_2 (dx^2)^2 + \epsilon_3 (dx^3)^2 + \epsilon_4 (dx^4)^2, \quad (2.10)$$

and at the same time to bring it about that all the contravariant components  $t_{(j)}^{\mu}$  vanish there except

$$t_{(1)}^1 = 1, \quad t_{(2)}^2 = 1, \quad t_{(3)}^3 = 1, \quad t_{(4)}^4 = 1, \quad (2.11)$$

and all the covariant components  $t_{(\mu)}^{\nu}$  vanish except

$$t_{(1)1} = \epsilon_1, \quad t_{(2)2} = \epsilon_2, \quad t_{(3)3} = \epsilon_3, \quad t_{(4)4} = \epsilon_4. \quad (2.12)$$

We shall have also  $\sqrt{-g} = 1$ .

The following equations are tensor equations, and since (as is easily verified) they are true for the special system of coordinates just described, they are true in general for all allowed coordinate systems:

$$\left. \begin{aligned} \delta_{kl}^{ij} t_{(1)}^k t_{(2)}^l &= -\eta^{ijkl} t_{(3)k} t_{(4)l} \epsilon_3 \epsilon_4, \\ \delta_{lmn}^{ijk} t_{(1)}^l t_{(2)}^m t_{(3)}^n &= -\eta^{ijkl} t_{(4)k} \epsilon_4, \\ \delta_{mnpq}^{jkl} t_{(1)}^l t_{(2)}^m t_{(3)}^p t_{(4)}^q &= -\eta^{ijkl}. \end{aligned} \right\} \quad (2.13)$$

We shall define conjugates to skew-symmetric tensors as follows:

$$\left. \begin{aligned} v^{*ij} &= \frac{1}{2} \eta^{ijkl} v_{kl}, \\ v^{*i} &= \frac{1}{3} \eta^{ijkl} v_{jkl}. \end{aligned} \right\} \quad (2.14)$$

These give the covariant forms

$$\left. \begin{aligned} v_{ij}^* &= \frac{1}{2} \eta_{ijkl} v^{kl}, \\ v_i^* &= \frac{1}{3} \eta_{ijkl} v^{kl}. \end{aligned} \right\} \quad (2.15)$$

Since

$$\left. \begin{aligned} \eta_{ijkl} \eta^{imjn} &= -2 \delta_{kl}^{mn}, \\ \eta_{ijkl} \eta^{imnp} &= -\delta_{jl}^{mnp}, \end{aligned} \right\} \quad (2.16)$$

we obtain from (2.14) and (2.15)

$$\left. \begin{aligned} v_{ij} &= -\frac{1}{2} \eta_{ijkl} v^{*kl}, \\ v_{jkl} &= -\eta_{ijkl} v^{*i}, \end{aligned} \right\} \quad (2.17)$$

and

$$\left. \begin{aligned} v^{ij} &= -\frac{1}{2} \eta^{ijkl} v_k^*, \\ v^{kl} &= -\eta^{ijkl} v_i^*. \end{aligned} \right\} \quad (2.18)$$

We know (*cf.* Schouten, *loc. cit.*) that it is permissible in (2.3), (2.4), (2.5) to replace the symbol  $\partial$  of partial differentiation by the symbol D, indicating covariant differentiation. We also note that the covariant derivative of  $\eta_{ijkl}$  or  $\eta^{ijkl}$  is zero.

We shall now proceed to convert (2.3). Assigning a positive sense on the curve  $V_1$ , we shall choose our  $t$ -tetrad such that on  $V_1$ ,  $t_{(1)}^i$  and  $t_{(2)}^i$  lie in  $V_2$ , and on  $V_1$ ,  $t_{(1)}^i$  points along  $V_1$  in the positive sense. We choose  $t_{(2)}^i$  so that on  $V_1$  it points along the outward normal to  $V_1$  in  $V_2$ . We complete the tetrad with  $t_{(3)}^i$ ,  $t_{(4)}^i$  so as to obtain the same orientation as that of the parametric lines of the coordinates. Then in (2.3) we may write

$$\left. \begin{aligned} \text{on } V_1: d_{(1)} x^i &= t_{(1)}^i ds, \\ \text{on } V_2: d_{(1)} x^i d_{(2)} x^j &= t_{(1)}^i t_{(2)}^j dS, \end{aligned} \right\} \quad (2.19)$$

where  $ds$  is the element of arc on  $V_1$  and  $dS$  the element of area on  $V_3$ , both positive quantities. Then (2.3) may be written

$$\int_{(1)} v_i t'_{(1)} ds = \int_{(2)} (\mathbf{D}_i v_k - \mathbf{D}_k v_i) t'_{(1)} t'_{(2)} dS. \quad (2.20)$$

But, by use of (2.13) it may also be written

$$\boxed{\int_{(1)} v_i t'_{(1)} ds = - \int_{(2)} \mathbf{D}_j v_i \cdot \eta^{ijkl} t_{(3)k} t_{(4)l} \epsilon_3 \epsilon_4 dS,} \quad (2.21)$$

or, again, if we first substitute  $v^*_i$  for  $v_i$ , and then use (2.18),

$$\boxed{\int_{(1)} v^*_i t'_{(1)} ds = \int_{(2)} \mathbf{D}_j v^{*kl} \cdot t_{(3)k} t_{(4)l} \epsilon_3 \epsilon_4 dS.} \quad (2.22)$$

Here we have three alternative forms for (2.3). It would appear that (2.21) is most closely analogous to the classical Stokes's theorem: we shall find it most useful in the electromagnetic interpretation.

We shall now convert (2.4). We shall choose  $t'_{(1)}$ ,  $t'_{(2)}$ ,  $t'_{(3)}$  so that on  $V_3$  they lie in  $V_3$ , and on  $V_3$   $t'_{(3)}$  points along the outward normal to  $V_3$  in  $V_3$ :  $t'_{(4)}$  is then normal to  $V_3$ , with a sense chosen to give to the tetrad the orientation of the parametric lines of the coordinates. Then in (2.4) we may write, using (2.13),

$$\left. \begin{aligned} d\omega^{ij} &= \delta_{kl}^{ij} t'_{(1)} t'_{(2)} dS = - \eta^{ijkl} t_{(3)k} t_{(4)l} \epsilon_3 \epsilon_4 dS, \\ d\omega^{ik} &= \delta_{lm}^{ik} t'_{(1)} t'_{(2)} t'_{(3)} d\sigma = - \eta^{ijkl} t_{(4)l} \epsilon_4 d\sigma, \end{aligned} \right\} \quad (2.23)$$

where  $dS$  is an element of area of  $V_3$  and  $d\sigma$  an element of volume of  $V_3$ , both positive quantities. Then (2.4) may be written

$$\int_{(2)} v_{ij} \eta^{ijkl} t_{(3)k} t_{(4)l} \epsilon_3 \epsilon_4 dS = \int_{(3)} \mathbf{D}_k v_{ij} \cdot \eta^{ijkl} t_{(4)l} \epsilon_4 d\sigma. \quad (2.24)$$

If we now write  $v^*_{ij}$  instead of  $v_{ij}$  on both sides, and then make use of (2.18), we obtain

$$\boxed{\int_{(2)} v^*_{ij} t_{(3)k} t_{(4)l} \epsilon_3 \epsilon_4 dS = - \int_{(3)} \mathbf{D}_j v^{*kl} \cdot t_{(4)l} \epsilon_4 d\sigma.} \quad (2.25)$$

The convenience of this form lies in the fact that it involves the minimum of trouble with respect to orientation. We have simply to remember that  $t'_{(3)}$  is the unit outward normal to  $V_3$  in  $V_3$ . As for  $t'_{(4)}$ , it is either unit normal vector to  $V_3$ , since a reversal of its sign leaves (2.25) unaltered.

We now proceed to the conversion of (2.5). It will be seen that this leads to Green's theorem, which I have examined in detail elsewhere by a different method.<sup>†</sup> We choose  $t'_{(4)}$  normal to  $V_3$  on  $V_3$ , pointing outward; then on  $V_3$   $t'_{(1)}, t'_{(2)}, t'_{(3)}$  lie in  $V_3$ ; we choose the orientation which gives to the tetrad the orientation of the parametric lines of the coordinates. Then using (2.13), we may write in (2.5)

$$\left. \begin{aligned} d\omega^{ijk} &= \delta_{lmn}^{ijk} t'_{(1)} t'_{(2)} t'_{(3)} d\sigma = - \eta^{ijkl} t_{(4)i} e_4 d\sigma, \\ d\omega^{ijkl} &= \delta_{mnpq}^{ijkl} t'_{(1)} t'_{(2)} t'_{(3)} t'_{(4)} d\tau = - \eta^{ijkl} d\tau, \end{aligned} \right\} \quad (2.26)$$

where  $d\sigma$  is an element of volume of  $V_3$  and  $d\tau$  an element of 4-volume of  $V_4$ , both *positive* quantities. Then (2.5) may be written

$$\int_{(3)} v_{ijk} \eta^{ijkl} t_{(4)i} e_4 d\sigma = \int_{(4)} D_i v_{ijk} \cdot \eta^{ijkl} d\tau. \quad (2.27)$$

If we now use (2.14), and then drop the star (since  $v^{*i}$  may be any vector), we have

$$\boxed{\int_{(3)} v^i t_{(4)i} e_4 d\sigma = \int_{(4)} D_i v^i \cdot d\tau.} \quad (2.28)$$

All we have to remember concerning orientation here is that  $t'_{(4)}$  points along the *outward* normal to  $V_3$ .

### 3—APPLICATIONS TO ELECTROMAGNETISM

In the general theory of relativity the electromagnetic field is characterized by the skew-symmetric tensor  $F_{ij}$  and the current 4-vector  $J^i$ . The conjugate tensor being defined by

$$F^{*ij} = \frac{1}{2} \eta^{ijkl} F_{kl}, \quad (3.1)$$

Maxwell's equations read

$$D_j F^{ij} = J^i, \quad (3.2)$$

$$D_i F^{*ij} = 0, \quad (3.3)$$

$D_i$  being the symbol of covariant differentiation. (3.3) imply the existence of the potential 4-vector  $\phi_i$  such that

$$F_{ij} = \partial_i \phi_j - \partial_j \phi_i - D_i \phi_j - D_j \phi_i. \quad (3.4)$$

The 4-force on a charge  $e$  moving on a world-line with unit tangent vector (or 4-velocity)  $\lambda^i$  is

$$X^i = e F^{ij} \lambda_j. \quad (3.5)$$

<sup>†</sup> Trans. Roy. Soc. Can., Sect. III, vol. 28, p. 168 (1934).

The equations of motion of a particle of proper energy  $W$  carrying a charge  $e$  are then

$$\frac{\delta}{\delta s} (W \lambda^t) = X^t, \quad (3.6)$$

$\delta/\delta s$  indicating the absolute derivative.†

These formulae naturally suggest that we should define *the electric intensity associated with the unit vector  $\lambda^t$*  to be

$$E^t(\lambda) = F^{tu} \lambda_u, \quad (3.7)$$

and similarly *the magnetic intensity associated with the unit vector  $\lambda^t$*  to be

$$H^t(\lambda) = F^{*u} \lambda_u. \quad (3.8)$$

Obviously the vectors  $E^t(\lambda)$ ,  $H^t(\lambda)$  are perpendicular to  $\lambda^t$ . They are respectively the 4-forces exerted on unit electric charge and unit magnetic pole proceeding with 4-velocity  $\lambda^t$ .

Consider now a space-like  $V_3$ , and let  $\lambda^t$ ,  $\mu^t$  be orthogonal unit vectors normal to it,  $\lambda^t$  being time-like and  $\mu^t$  space-like. Then, as judged by an observer moving along  $\lambda^t$ , the element of  $V_3$  is instantaneously at rest and  $\mu^t$  is its instantaneous unit normal. The *component of electric intensity normal to  $V_3$*  is then

$$E(\mu, \lambda) = \mu_t E^t(\lambda) = F^{tu} \mu_t \lambda_u = -F^{tu} \lambda_t \mu_u = -E(\lambda, \mu), \quad (3.9)$$

and the *component of magnetic intensity normal to  $V_3$*  is

$$H(\mu, \lambda) = \mu_t H^t(\lambda) = F^{*tu} \mu_t \lambda_u = -F^{*tu} \lambda_t \mu_u = -H(\lambda, \mu). \quad (3.10)$$

Since the world-line of a particle must be time-like, this physical interpretation applies only to the case where  $V_3$  is space-like. We may, however, extend our definition to cover the case of a  $V_3$  which cuts the null-cone by defining *the components of electric intensity and magnetic intensities normal to  $V_3$  (to which  $\lambda^t$ ,  $\mu^t$  are ordered mutually orthogonal normal unit vectors) to be respectively*

$$\left. \begin{aligned} E(\lambda, \mu) &= -\epsilon(\lambda) \epsilon(\mu) F^{tu} \lambda_t \mu_u, \\ H(\lambda, \mu) &= -\epsilon(\lambda) \epsilon(\mu) F^{*tu} \lambda_t \mu_u. \end{aligned} \right\} \quad (3.11)$$

These formulae agree formally with (3.9), (3.10), since in the case there considered  $\epsilon(\lambda) = -1$ ,  $\epsilon(\mu) = 1$ .

† By referring to proper energy (the more fundamental concept) instead of to proper mass, we avoid the appearance of a factor  $c^4$  which is out of place in discussions in the general theory of relativity.

Let us now apply (2.21), putting  $v_i = \phi_i$ . Then

$$D_i \phi_i \cdot \eta^{ikl} = -\frac{1}{2} F_{ij} \eta^{ijk} = -F^{ikl}, \quad (3.12)$$

and (2.21) may be written

$$\int_{(1)} \phi_i dx^i = \int_{(2)} F^{ikl} t_{(3)i} t_{(4)j} \epsilon_3 \epsilon_4 dS = \int_{(2)} H(4, 3) dS. \quad (3.13)$$

We have in words the following result:

**Theorem I:** *The line integral of the potential 4-vector taken round any closed circuit in space-time bounding a  $V_3$  is equal to the flux of magnetic intensity across  $V_3$ .*

With regard to signs, we are to remember that, in order, the positive tangent to the circuit, the outward normal to it in its two-space, and the vectors  $t_{(3)}$ ,  $t_{(4)}$  are to form a tetrad having the orientation of the parametric lines of the coordinates; the flux is to be calculated in accordance with (3.11) and (3.13).

Let us now apply (2.25), putting first  $v^i = F^{ikl}$ . The equation then reads

$$\int_{(2)} F^{ikl} t_{(3)i} t_{(4)j} \epsilon_3 \epsilon_4 dS = 0, \quad (3.14)$$

and we have the following result:

**Theorem II:** *The flux of magnetic intensity across any closed  $V_3$  in space-time is zero.*

Let us now put  $v^i = F^{ikl}$  in (2.25). We get

$$\int_{(2)} F^{ikl} t_{(3)i} t_{(4)j} \epsilon_3 \epsilon_4 dS = - \int_{(3)} J^l t_{(4)j} \epsilon_4 d\sigma. \quad (3.15)$$

Let  $\rho_0$  be the proper density of charge, so that

$$J^l = \rho_0 \lambda^l, \quad (3.16)$$

$\lambda^l$  being the unit vector of 4-velocity of the charge. There being assigned a positive sense on the normal to  $V_3$ , viz., that given by  $t_{(4)}$ , we naturally define the flux of electricity across  $V_3$  as follows:

Flux of electricity across  $V_3$  = [total charge associated with world-lines crossing  $V_3$  in the positive sense] — [total charge associated with world-lines crossing  $V_3$  in the negative sense]. (3.17)

We note that if  $V_3$  is space-like, and  $t_{(4)}$  points into the future, then the flux of electricity across  $V_3$  is simply the total charge associated with all the world-lines cutting  $V_3$ .

Consider a thin tube of world-lines of normal 3-section  $d\sigma_0$ . The total charge associated with it is  $\rho_0 d\sigma_0$ . It cuts  $V_3$  in  $d\sigma$  where†

$$d\sigma_0 = d\sigma |\lambda^4 t_{(4)4}|. \quad (3.18)$$

But the world-line  $\lambda^4$  cuts  $V_3$  in the positive or negative sense according as

$$\lambda^4 t_{(4)4} \epsilon_4 > \text{ or } < 0. \quad (3.19)$$

Hence the contribution to the flux across  $V_3$  from the tube is

$$\rho_0 \lambda^4 t_{(4)4} \epsilon_4 d\sigma = J^4 t_{(4)4} \epsilon_4 d\sigma. \quad (3.20)$$

Thus (3.15) may be written

$$\int_{(3)} E(3, 4) dS = F, \quad (3.21)$$

where  $F$  is the flux of electricity across  $V_3$ . Hence we have this result:

**Theorem III:** *The flux of electric intensity across a closed  $V_3$  is equal to the flux of electricity across any  $V_3$  bounded by  $V_3$ .*

Taking a space-like  $V_3$ , we have precisely Gauss's theorem: *The flux of electric intensity across a closed  $V_3$  bounding  $V_3$  is equal to the total electric charge associated with the world-lines cutting  $V_3$  (i.e., the total charge in  $V_3$ ).*

To make the result more definite, let us suppose that the parametric lines of the time coordinate  $x^4$  are normal to  $V_3$ , for which  $x^4 = \text{const}$ . Let us use Greek suffixes for the range 1, 2, 3. Then, since  $g_{\alpha 4} = 0$  on  $V_3$ ,

$$t_{(4)}^0 = 0, \quad t_{(4)\alpha} = 0, \quad t_{(\alpha)}^4 = 0, \quad t_{(\alpha)4} = 0, \quad \epsilon_3 = 1, \quad \epsilon_4 = -1. \quad (3.22)$$

Let us further suppose that the charges are at rest, so that

$$J^\alpha = 0, \quad J^4 = \rho_0 t_{(4)}^4. \quad (3.23)$$

Then (3.15) becomes

$$\int_{(3)} F^{*\alpha} t_{(3)\alpha} t_{(4)4} dS = \int_{(3)} \rho_0 d\sigma. \quad (3.24)$$

Now by (3.7) we have for the electric intensity associated with the charges in question, or, by (3.5), the 3-vector of force per unit charge acting on the charges,

$$E^* = F^{*\alpha} t_{(4)\alpha} : \quad (3.25)$$

remembering that  $t_{(3)}$  is the unit outward normal to  $V_3$  in  $V_3$ , we have for the normal (outward) component of intensity

$$N = E^* t_{(3)\alpha} = F^{*\alpha} t_{(3)\alpha} t_{(4)4}, \quad (3.26)$$

† Synge, loc. cit.

and (3.24) takes the familiar Gaussian form

$$\int_{(2)} \mathbf{N} \cdot d\mathbf{S} = \int_{(3)} \rho_0 \, d\sigma. \quad (3.27)$$

The applications of (2.28) are rather obvious. If we put  $v^t = J^t$ , we get

$$\int_{(3)} J^t t_{(4)t} \epsilon_4 \, d\sigma = 0, \quad (3.28)$$

which simply confirms the conservation of charge by stating that the flux of electricity across any closed  $V_3$  in space-time is zero. If we put  $v^t = \phi^t$ , and make use of  $D_t \phi^t = 0$ , the relation to which the potential 4-vector is conventionally subjected, we get

$$\int_{(3)} \phi^t t_{(4)t} \epsilon_4 \, d\sigma = 0, \quad (3.29)$$

which may be expressed by stating that *the flux of potential 4-vector across any closed  $V_3$  in space-time is zero.*

### SUMMARY

The general Green-Stokes theorem, connecting M-fold and  $(M + 1)$ -fold integrals in an N-space, is applied to space-time, yielding forms involving essentially positive elements of area, volume, and 4-volume. The indefinite character of the fundamental form in space-time is given explicit consideration, certain indicators ( $\pm 1$ ) appearing in the formulae on that account. The results are applied to the electromagnetic field in general relativity. Electric and magnetic intensities are defined, and it is shown that (I) the line integral of the potential 4-vector taken round a closed circuit is equal to the flux of magnetic intensity across any  $V_3$  bounded by the circuit, (II) the flux of magnetic intensity across a closed  $V_3$  is zero, (III) the flux of electric intensity across a closed  $V_3$  is equal to the flux of electricity across any  $V_3$  bounded by  $V_3$ . This last result yields, in particular, the classical electrostatic theorem of Gauss extended to general relativity.

## The Elastic Constants and Specific Heats of the Alkali Metals

By K. FUCHS, H. H. WILLS PHYSICAL LABORATORY, UNIVERSITY OF BRISTOL

(Communicated by N. F. MOTT, F.R.S.—Received 5 June, 1936)

In a recent paper\* the author has given a theoretical calculation of the elastic constants of copper and of the alkali metals. The purpose of this note is: firstly, to correct some mistakes in the calculation for the alkali metals (that for copper is correct); secondly, to compare these results with a recent experimental determination of the elastic constants for sodium;† and thirdly, to attempt an explanation of the observed fact that the specific heats of the alkalis show abnormally large deviations from the Debye form.

The corrections are as follows: the formulae in Table II, p. 630, for the body centred cubic structure should read

$$A^T = \frac{1}{8} \rho \frac{dw}{d\rho}$$

$$2B^T = \frac{5}{8} \rho^3 \frac{d^3 w}{d\rho^3} + \frac{1}{8} \rho \frac{dw}{d\rho}.$$

In formulae (17A) and (18) a factor 2 should be inserted on the left-hand side, since  $w$  is defined as the potential energy per ion, whereas Born and Mayer's values relate to the energy per pair of ions.

In formula (23), p. 633, the term  $37008 D^6$  in the coefficient of  $a_8$  should read  $19056 D^6$ .

With these corrections the values of the elastic constants (in c.g.s. units  $\times 10^{11}$ ) and the Debye temperatures for the alkalis are shown in Table I.

TABLE I

	$2C =$	$A =$	$2B =$			
	$1/\kappa$	$c_{11} - c_{12}$	$c_{44}$	$c_{11}$	$c_{12}$	$\Theta$
Li .....	1.30	0.341	1.329	1.53	1.19	354
Na .....	0.87 <sub>s</sub>	0.141	0.580	0.97 <sub>s</sub>	0.83 <sub>s</sub>	143
Exp. ....	0.85 <sub>s</sub>	0.16 <sub>s</sub>	0.55 <sub>s</sub>	0.96 <sub>s</sub>	0.79 <sub>s</sub>	—
K .....	0.40 <sub>s</sub>	0.061 <sub>s</sub>	0.260	0.44 <sub>s</sub>	0.38 <sub>s</sub>	77

\* Proc. Roy. Soc., A, vol. 153, p. 622 (1936).

† The possibility of an error in the calculation was suggested by Professor E. Grünisen, since the theoretical values disagreed with the experimental results of Herr Bender. I wish to thank him also for the privilege of quoting these results.

In the original paper, extrapolated experimental values of the compressibility were used, since the theoretical values obtained from the numerical integration of the wave equation were rather uncertain. Fröhlich\* has now developed an analytical method of determining the wave functions for the alkalis, which makes possible a more accurate calculation of the compressibility, at least if the effective number of electrons is unity. This is the case for Na and K but not for Li.<sup>†</sup>

According to Fröhlich, the energy  $W_0$  of the lowest electronic state can be shown to be ( $W_0$  in Rydberg units,  $r$  in atomic units)

$$W_0 = -\frac{2}{r} + \frac{r_0^2 - r^2}{r^3} - \frac{4\pi}{3} r^3 = \Omega,$$

where  $\Omega$  is the atomic volume and  $r_0$  the radius at the minimum of  $W_0$ . The total energy per atom of the crystal is then

$$W = W_0 + W_F + W_I = -\frac{2}{r} + \frac{r_0^2 - r^2}{r^3} + \frac{2 \cdot 210}{r^3} + W_I.$$

Here  $W_F$  is the Fermi energy and  $W_I$  the energy between the ions.<sup>‡</sup> At the actual atomic radius, we have

$$\frac{dW}{dr} = \frac{3}{r^2} - \frac{3r_0^2}{r^4} - 2 \frac{2 \cdot 210}{r^3} + \frac{dW_I}{dr} = 0.$$

This formula allows us to calculate  $r_0$  from the atomic radius. For the compressibility, we thus obtain

$$\frac{1}{\kappa} = \frac{1}{9\Omega} r^2 \frac{d^2W}{dr^2} = \frac{1}{4\pi r^3} \left[ \frac{2}{r} - \frac{1 \cdot 473}{r^2} + \frac{1}{r} \frac{dW_I}{dr} + \frac{1}{r^2} r^2 \frac{d^2W_I}{dr^2} \right].$$

The values given in the table for Na and K are calculated from this formula.

Recently the elastic constants of Na have been measured by Benders<sup>§</sup> at a temperature of  $-183^\circ$  C.; his results are also given in the table.

#### THE SPECIFIC HEAT OF THE ALKALIS

Debye's theory of the specific heat of solids agrees very well with experiment for monatomic substances which crystallize in a cubic structure.

\* I wish to thank Dr. Fröhlich for allowing me to see the manuscript. ('Proc. Roy. Soc.,' A, vol. 155, p. 640 (1936).)

<sup>†</sup> Cf. Seitz, 'Phys. Rev.,' vol. 47, p. 400 (1935).

<sup>‡</sup> For expressions for  $W_I$ , cf. the original paper.

<sup>§</sup> 'Naturwiss.' (to be published).

There are, however, a few exceptions to this rule. For the alkalis, in particular, the variation of the specific heat with temperature shows considerable deviations from Debye's formula. The success of Debye's theory for other similar substances has led to the suggestion being made that this anomaly is not due to the lattice oscillations, but to another effect; Simon,\* in particular, has suggested that Schottky's theory of the excitation of some higher quantum level would give a satisfactory explanation.

This interpretation of the anomaly of the specific heat, however, assumes that Debye's theory can be regarded as satisfactory. Blackman† has recently dealt with this question, and he has shown that large variations with temperature can be expected in the  $\Theta$ -value in Debye's theory. Pankow‡ has measured directly the amplitude of the thermal oscillations of lithium and has found that the total specific heat may be accounted for by the lattice oscillations.

In Debye's theory the dependence of the velocity of the elastic waves on the direction in the crystal and also the dispersion, or change of velocity with wave-length, are both neglected.

The elastic constants of the alkalis, as shown by the author's theoretical calculations as well as the experimental determination for sodium by Bender, are highly anisotropic, so that the wave velocity depends on the direction much more than for the other metals with cubic structure. We shall show that, if the dispersion is neglected, this anisotropy gives the sort of divergence from a Debye form observed for the alkalis.

Let  $\lambda$  be the wave-length,  $v$  the frequency, and  $c$  the velocity of a lattice oscillation. The exact formula for the number of frequencies with given polarization in the interval  $d(1/\lambda)$  and with wave vectors within the solid angle  $d\omega$  has been given by Born and Karmann§

$$Na^3 \frac{1}{\lambda^3} d\left(\frac{1}{\lambda}\right) d\omega \quad \lambda v = c \quad a = \sqrt[3]{\Omega}, \quad (1)$$

where  $N$  is the number of atoms and  $\Omega$  the atomic volume. We neglect the dispersion and assume that the velocity  $c$  in any given direction does not depend on the wave-length  $\lambda$ . In this case formula (1) reduces to

$$N \frac{a^3}{c^3} v^2 d\omega. \quad (2)$$

\* Simon and Swain, 'Z. phys. Chem.,' B, vol. 28, p. 189 (1935); Simon and Seidler, 'Z. phys. Chem.,' A, vol. 123, p. 383 (1926).

† 'Proc. Roy. Soc.,' A, vol. 148, p. 365; vol. 149, p. 117 (1935).

‡ 'Helv. phys. Acta,' vol. 9, p. 87 (1936).

§ 'Phys. Z.,' vol. 14, p. 15 (1913).

If we neglect the dependence of the velocity on the direction, this formula leads to Debye's expression for the specific heat.

In order to obtain a finite number of frequencies, we have to assume a maximum frequency  $v_m$ , as in Debye's theory; we shall, however, assume that  $v_m$  depends on the direction. The number of normal modes with given polarization and wave vectors in the solid angle  $d\omega$  is  $N d\omega/4\pi$ ; equating this to the integral of (2) from 0 to  $v_m$  we have

$$d\omega \int_0^{v_m} v^2 N \frac{a^3}{c^3} dv = \frac{v_m^3}{3} N \frac{a^3}{c^3} d\omega = N \frac{d\omega}{4\pi},$$

which leads to

$$v_m = c/a (3/4\pi)^{1/3} \quad \lambda_m = c/v_m = a (4\pi/3)^{1/3}. \quad (3)$$

Our assumption is thus equivalent to assuming that the frequency spectrum in any direction extends to one and the same minimum *wave-length*  $\lambda_m$ , which is of the order of magnitude of the distance between the atoms.

Finally, from equations (2) and (3), we obtain for the number of frequencies per frequency interval  $dv$

$$N(v) dv = \sum_{i=1}^3 v^2 N a^3 dv \int \frac{d\omega}{c_i^3}. \quad (4)$$

Here the integration is over all values of  $c$  for which

$$c \geq \lambda_m v,$$

and the summation is over the three directions of polarization.

The velocities  $c$  can be calculated from the elastic constants according to the well-known formula of Born and Karmann.\* Fig. 1 shows the dependence of the velocities  $c$ , calculated in this way, on the direction in the crystal. Thus the frequency spectrum can be obtained from equation (4). The result is shown in fig. 2. Except at very low frequencies, it has no similarity to a Debye continuum. The three maxima are due to the three directions of polarization of the elastic waves.

From the frequency spectrum, the thermal energy and the specific heat can easily be obtained†

$$U = \int \frac{hv}{e^{h\nu/kT} - 1} N(v) dv \quad C_v = k \int \left( \frac{hv}{kT} \right)^2 \frac{e^{h\nu/kT}}{(e^{h\nu/kT} - 1)^2} N(v) dv. \quad (5)$$

The result for  $C_v$  is shown in fig. 3, as a  $\Theta$ -curve plotted against tempera-

\* Loc. cit.

† Cf., for example, Schrödinger, 'Handb. d. Physik,' vol. 10, p. 301 (1926).

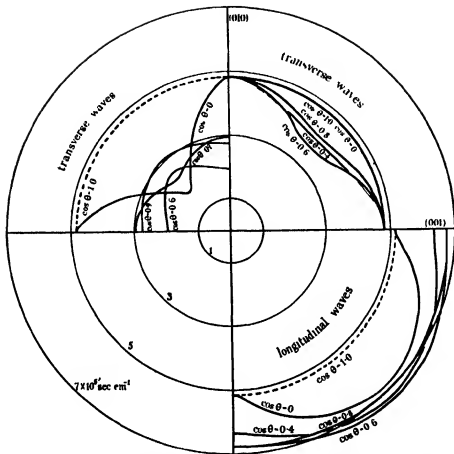


FIG. 1—Dependence of the velocity of elastic waves on the direction in the crystal. The (100) axis of the crystal is supposed to be perpendicular to the plane of the figure. The velocity of waves moving in a direction making an angle  $\theta$  with the (100) axis is given by the radius vector from the centre to the appropriate curve. Each curve, therefore, if continued in the other four quadrants, gives the velocities of waves in directions lying on a cone with the angle of aperture  $2\theta$  and the axis in the (100) direction. The curves for  $\cos \theta = 1$  are dotted, since they refer to one direction only. The curves in the three quadrants refer to longitudinal waves and transverse waves with two different directions of polarization.

ture. This representation shows a deviation from Debye's theory of the type observed. The experimental results of Simon and Swain\* are also shown.

It may be emphasized again that the rise of the  $\Theta$ -value in our present calculation is solely due to the anisotropy of the crystal. Similar curves

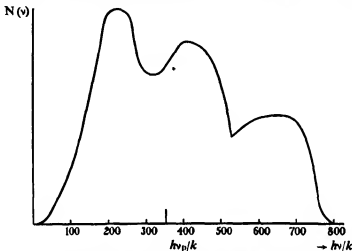


FIG. 2—The frequency spectrum of lithium.  $v_0$  is the limiting frequency calculated from the elastic constants on the assumptions of Debye's theory.

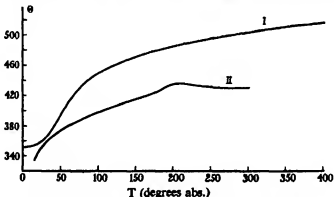


FIG. 3—The specific heat of lithium, plotted as a  $\Theta$ -curve against temperature. I, calculated; II, observed.

may be expected for sodium and potassium. Since, however, the effect of the dispersion seems to be large, it is hardly worth while to evaluate formula (4) for further elements. It may be sufficient to demonstrate the anisotropy of these metals, as compared with that of lithium, on the

\* Loc. cit.

one hand, and copper and aluminium on the other. For isotropic substances the following relation holds between the elastic constants

$$c_{44} = (c_{11} - c_{12})/2.$$

The two quantities on the right- and left-hand side and the ratio between them are

	Li	Na	K	Cu	Al*
$c_{44}$	1.329	0.580	0.260	8.9	2.8 <sub>4</sub>
$(c_{11} - c_{12})/2$	0.170	0.070	0.031	2.5	2.3 <sub>0</sub>
$\frac{2c_{44}}{c_{11} - c_{12}}$	7.8	8.3	8.4	3.6	1.23

$$\times 10^{11} \text{ erg./cm.}^3$$

The calculated divergence of the  $\Theta$ -value from a constant value is greater than that observed. We may conclude that the dispersion has the opposite effect to the anisotropy. This is perhaps to be expected, since there is no reason why the anisotropy should be so great for short wave-lengths as we have calculated for long waves.

The success of Debye's theory for Cu and Al is thus rather to be found in the fact that the effect of the anisotropy and the dispersion largely cancel each other, whereas for the anomalous elements the anisotropy is so large that this does not occur.

I wish to thank Professor N. F. Mott, who suggested to me the present calculation, for the interest he has taken in it.

#### SUMMARY

Some mistakes in a recent calculation of the author of the elastic constants of the alkalis are corrected. The results for sodium are compared with recent experimental results. An attempt is made to explain the observed fact that the specific heats of the alkalis show abnormally large deviations from a Debye function.

\* Goens, 'Ann. Phys.', vol. 17, p. 233 (1933).

## The Electrical Properties of High Permeability Wires Carrying Alternating Current

By E. P. HARRISON, G. L. TURNER, H. ROWE, and H. GOLLOP

(Communicated by Sir Frank Smith, Sec.R.S.—Received 10 June, 1936)

### I—INTRODUCTION

It is well known that certain alloys of nickel and iron of the "perm-alloy" and "mumetal" group have abnormally high values of magnetic permeability in small fields, and the properties of these alloys have been the subject of a considerable amount of research during the past ten or twelve years. It seems to have escaped attention that their high magnetizability at low field-strengths causes wires of these alloys to have many interesting properties when used as conductors of alternating current.

Owing to the "skin effect", the A.C. resistance of a wire bears to its D.C. resistance a definite ratio which is a function of the frequency of the current, and of the diameter, the electrical conductivity, and for ferromagnetics the permeability of the wire. With fine wires (diameter 0.5 mm. or less) of non-magnetic material such as copper, this ratio does not materially exceed unity until the frequency approaches  $10^5$  cycles per second. But with wires of ferro-magnetic alloys, whose permeability may be in the neighbourhood of 50,000, the ratio  $R_{AC}/R_{DC}$  is appreciably greater than unity even at the lowest audio-frequencies. Furthermore, a ferro-magnetic wire possesses an internal self-inductance, which, with alternating current, is also a function of the frequency, diameter, conductivity, and permeability. Now permeability is a function of magnetization, and since a wire carrying A.C. is magnetized by the current as well as by the external field in which it may be situated, it may be expected that its A.C. resistance and inductance will show some sort of dependence on both current and external field.

In this paper an account is given of an investigation of these phenomena, of which perhaps the most striking is the very large change of A.C. resistance which occurs when an external magnetic field of the order of that of the earth is applied to a wire in the direction of its axis. A letter

describing briefly this change of effective resistance was published in June, 1935.\* The resistance change is many times greater than the corresponding magneto-resistance change with direct current, which, as is well known, is itself remarkably large in these alloys.

## II—EXPERIMENTAL DETAILS

It is necessary to remark at the outset that the material used in these experiments is one or other of the high permeability alloys of nickel and iron of range near to 78% nickel prepared in the form of wire, usually of 26 standard wire gauge, and annealed in some special way. Since the particular alloy used and the heat treatment given to it have an important effect on the character and magnitude of the observed phenomena, § VII is devoted to these details. For the moment it is enough to state that in the experiments described below all the material has been subject to some quite definite annealing process, which at present may conveniently be left unspecified.

*Apparatus*—A valve oscillator was used as source of alternating current in all the measurements. This instrument provides a reasonably pure wave form if the frequency is not too low and if the iron core in the oscillator inductance is removed; to the degree of accuracy aimed at in these experiments its small harmonic content did not seriously affect the results. Since, however, the impedance varies with the frequency of the A.C. supply, it is evident on general grounds that in making quantitative measurements of the highest degree of accuracy, which shall also be strictly repetitive, it will be essential to use a really pure sine wave oscillator.

A very convenient bridge for the determination of the resistance and inductance of various specimens of wire is a modified Kelvin double bridge whose circuit is shown in fig. 1.  $P$ ,  $Q$ , and  $R_1$  are non-inductive resistances,  $R_1$  being variable,  $R$ ,  $L$  are the resistance and inductance of the nickel iron wire,  $MA$  is a thermomilliammeter of resistance  $r$ , and  $C$  is a variable capacity.

The indicator is a Campbell vibration galvanometer VG.

The conditions for balance are:—

$$R = QR_1/P$$

$$L = CQ \left[ R_1 + \frac{rP}{P + Q + r} \right],$$

and it was generally found convenient to make  $P = 100$  ohms,  $Q = 1$  ohm.

\* Harrison, Turney, and Rowe, 'Nature,' vol. 135, p. 961, 8 June (1935).

To find the current  $i$  in the specimen in terms of the current  $i_1$  observed in the ammeter, we have

$$i = i_1 \left[ 1 + \frac{r}{P+Q} \right].$$

By introducing a battery instead of the oscillator and an ordinary galvanometer at VG, d.c. resistances can also be measured.

The accuracy with which the instrumental measurements can be made is such that at a frequency of 500 cycles/second, the effective resistance is determined to one-tenth of 1% and the inductance to one-fifth of 1%.

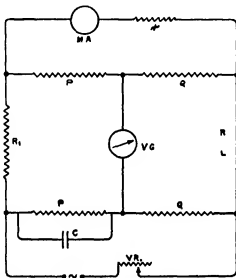


FIG. 1—Kelvin double bridge adapted to A.C. measurements.

No particular precautions were taken in measuring the absolute value of the frequency, but variations did not exceed  $\frac{1}{2}$ -cycle/second.

In order to apply a uniform longitudinal field to a wire, two alternative methods were used, a pair of Helmholtz coils, or a solenoid long compared with the wire.

*Method of Mounting the Wires*—The effect of strain on the properties with which we are concerned has been found to be extremely important. The relations between strain and impedance have not been investigated, but it became evident that it was vital to eliminate both strain and temperature variations in order to ensure that all impedance measurements should be repetitive within the limits of accuracy determined by the character of the A.C. supply, and the nature of the bridge. Constancy

of temperature was easy to attain, but much experimental work was necessary before a satisfactory way was achieved of mounting isolated wires so as to avoid strain. As a result of these experiments two necessary conditions emerged:—

(i) The wire must, if horizontal, be supported along its length; in other words it should lie along a plane surface, or be embedded in some form of vaseline or petroleum jelly.

(ii) One end of the wire only may be fixed by solder or otherwise to a copper or brass terminal on the base plate; the other end must be as nearly free from constraint as may be, consistent with the necessity of conducting current into the wire. The most practicable method for purely experimental purposes was to keep *both* ends free by soldering short lengths of thin copper wire to the ends of the specimen, allowing these copper end pieces to dip into mercury cups. For other purposes, where it may be necessary to transport the specimen, one end may be fixed by solder and the free end attached to its fixed contact piece by a fine copper spiral.

### III—RESULTS

Except where otherwise specified, the results given below were obtained with a mumetal wire, 0·445 mm. in diameter and 15·25 cm. long, having the following percentage composition : Fe,  $16\cdot6 \pm 0\cdot2$ ; Cu,  $5\cdot0 \pm 0\cdot1$ ; Mn,  $0\cdot5 \pm 0\cdot1$ ; Cr, 1·4 to 1·8; Si, 0·2 to 0·25; Ni, 77·3% by subtraction.

After being straightened by electric heating under tension it was annealed by heating in hydrogen for two hours at  $900^\circ$  to  $920^\circ$  C. and cooling slowly with the furnace.

*Zero Longitudinal Magnetic Field*—The wire, lying horizontally at right angles to the magnetic meridian, was demagnetized, and measurements were made of its effective resistance and reactance at various frequencies and with various currents. Some results are shown graphically in fig. 2. The outstanding feature of the curves at each frequency is the maximum through which the effective resistance passes as the current is varied; for convenience the current value at which the maximum occurs will throughout this paper be termed the "optimum current" for the wire in question in the prevailing conditions. Effective resistance and optimum current both show a regular increase with increasing frequency, and these characteristics have been found in all the wires investigated, though the actual values vary widely according to the composition of the wire and the heat treatment it has received.

The reactance also has a maximum value for each frequency, in the case shown in fig. 2 at a value of current less than the optimum. But this is by no means an invariable characteristic, and the reactance curves are

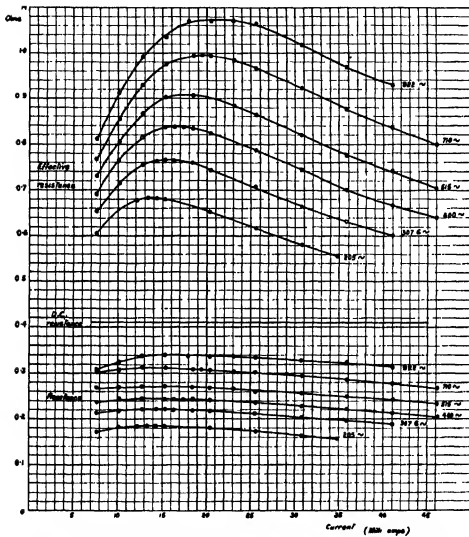


FIG. 2—Variation of effective resistance and reactance with current at different frequencies. Wire 15·25 cm. long, 0·445 mm. diameter.

found to differ considerably in character as the composition of the alloy is varied. For some alloys the maximum reactance occurs at a current above the optimum; in others a minimum occurs near the optimum

current, followed by a maximum at a much higher value. Since, however, the reactance component is in general only about one-third of the effective resistance, these irregularities have no very pronounced effect on the impedance.

When the current is taken through a cycle of increasing and decreasing values there is a small but measurable hysteresis of both resistance and reactance with respect to current. A typical result, obtained with a wire different from that to which the curves of fig. 2 refer, is shown in fig. 3, curve 1, and illustrates the nature of the resistance hysteresis.

*The Effect of External Magnetic Fields*—When an external magnetic field is applied at right angles to the length of the wire we have been unable to detect any change in either component of the impedance. But we have found that marked changes are caused by the application of a steady longitudinal field. In fig. 4 are shown the values of the two components in various fields up to 1 gauss and at various frequencies, the current in the wire being the optimum, as determined from fig. 2, at each frequency. Fuller results for the same wire, using a wide range of currents at each frequency, are set out in Table I. Inspection shows that the greatest change of effective resistance with field occurs with a current at or near the optimum for each frequency, and that the optimum current, as previously defined, does not alter when a field is applied.

There is a small hysteresis effect, which is illustrated in fig. 3, curve 2, when the wire is taken round a magnetic half-cycle of increasing and decreasing field. The curve shown was obtained with the same wire as that of fig. 3, curve 1.

The existence of hysteresis with respect to current makes necessary two experimental precautions which are worthy of note. First, in making a series of measurements with different currents as in Table I, it is essential in order to obtain consistent results either to carry out a complete circular demagnetization of the wire initially and work with increasing current values on the lower branch of fig. 3, curve 1, or else to start with a saturating value of current and work with decreasing values on the upper branch.

Secondly, during measurements with varying field at any particular current value, when the field is increased by a step the effective resistance of the wire decreases. To restore balance the variable arm of the bridge must also be decreased, and since the ratio is 100/1 this leads to an appreciable increase of current above the chosen value. If we are working with increasing current values (the first method described above) the subsequent restoration of the current to its chosen value will not, owing

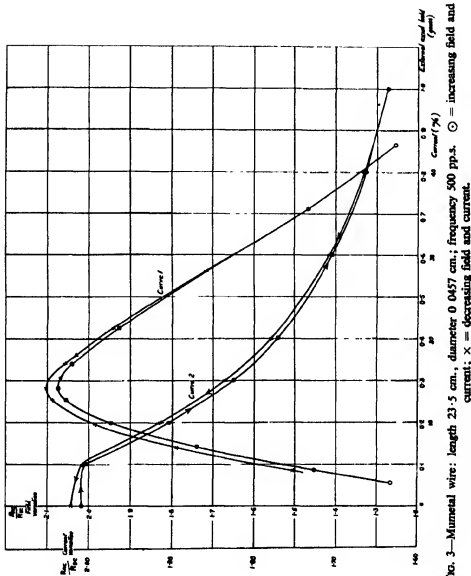


FIG. 3—Mumetal wire: length 23.5 cm., diameter 0.0457 cm.; frequency 500 p.p.s. ○ = increasing field and current; × = decreasing field and current.

to hysteresis, restore the wire to its original state of circular magnetization, and it is therefore necessary before re-balancing the bridge to reduce the current slightly. If we are working with decreasing current values the

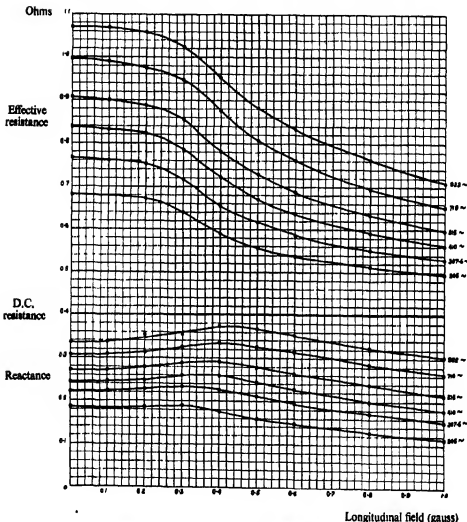


FIG. 4—Variation of effective resistance and reactance with longitudinal field at different frequencies and optimum current. Wire 15.25 cm. long; 0.445 mm. diameter.

need for this precaution does not arise, and this was the method actually employed in obtaining the curves of fig. 4.

*Wires of Different Dimensions*—With wires of different lengths, but

TABLE I.—The variation of A.C. resistance and reactance with current and applied longitudinal field at constant frequency

Wire from heat 94—0.02225 cm. radius, 15.25 cm. length, 0.410 ohm  
D.C. resistance; frequency 515~

Field in gauss	Current in m/A.	A.C. resistance ohms	Reactance in ohms	Field in gauss	Current in m/A.	A.C. resistance ohms	Reactance in ohms
0	170.7	0.478	0.131	0	150.7	0.489	0.141
0.2		0.475	0.131	0.2		0.485	0.141
0.4		0.469	0.129	0.4		0.477	0.139
0.6		0.462	0.126	0.6		0.468	0.135
0.8		0.454	0.121	0.8		0.459	0.130
1.0		0.449	0.116	1.0		0.452	0.124
0	135.6	0.500	0.150	0	119.0	0.514	0.162
0.2		0.495	0.148	0.2		0.509	0.161
0.4		0.486	0.146	0.4		0.496	0.159
0.6		0.476	0.144	0.6		0.484	0.155
0.8		0.466	0.138	0.8		0.472	0.147
1.0		0.458	0.132	1.0		0.462	0.139
0	101.2	0.533	0.172	0	91.0	0.551	0.182
0.2		0.526	0.173	0.2		0.543	0.184
0.4		0.511	0.172	0.4		0.524	0.182
0.6		0.495	0.168	0.6		0.505	0.178
0.8		0.481	0.161	0.8		0.490	0.170
1.0		0.471	0.151	1.0		0.476	0.159
0	80.9	0.573	0.192	0	70.8	0.598	0.205
0.2		0.562	0.195	0.2		0.586	0.209
0.4		0.542	0.194	0.4		0.558	0.210
0.6		0.519	0.190	0.6		0.530	0.204
0.8		0.499	0.180	0.8		0.507	0.190
1.0		0.484	0.166	1.0		0.491	0.175
0	60.7	0.635	0.217	0	50.6	0.681	0.230
0.2		0.621	0.222	0.2		0.666	0.237
0.4		0.584	0.225	0.4		0.621	0.244
0.6		0.549	0.218	0.6		0.573	0.234
0.8		0.521	0.200	0.8		0.540	0.214
1.0		0.502	0.186	1.0		0.520	0.196
0	45.5	0.708	0.237	0	41.0	0.743	0.245
0.2		0.696	0.246	0.2		0.726	0.255
0.4		0.639	0.254	0.4		0.664	0.264
0.6		0.589	0.242	0.6		0.616	0.251

TABLE I—(continued)

Field in gauss	Current in m/A.	A.C. resistance in ohms	Reactance in ohms	Field in gauss	Current in m/A.	A.C. resistance in ohms	Reactance in ohms
0.8	45.5	0.549	0.217	0.8	41.0	0.565	0.226
1.0		0.527	0.200	1.0		0.540	0.204
0	35.9	0.778	0.253	0	30.8	0.822	0.260
0.2		0.764	0.262	0.2		0.808	0.272
0.4		0.690	0.274	0.4		0.722	0.283
0.6		0.623	0.258	0.6		0.644	0.265
0.8		0.579	0.232	0.8		0.598	0.238
1.0		0.552	0.210	1.0		0.566	0.214
0	25.6	0.866	0.264	0	20.5	0.902	0.270
0.2		0.856	0.276	0.2		0.892	0.275
0.4		0.757	0.292	0.4		0.781	0.292
0.6		0.669	0.268	0.6		0.687	0.266
0.8		0.615	0.239	0.8		0.633	0.239
1.0		0.581	0.214	1.0		0.596	0.215
0	18.5	0.904	0.271	0	15.4	0.894	0.271
0.2		0.895	0.276	0.2		0.883	0.275
0.4		0.786	0.289	0.4		0.778	0.287
0.6		0.688	0.263	0.6		0.683	0.260
0.8		0.635	0.238	0.8		0.630	0.234
1.0		0.597	0.214	1.0		0.593	0.211

otherwise identical, it has been found, as is natural, that the optimum currents and the ratios,

$$\frac{\text{A.C. effective resistance}}{\text{D.C. resistance}},$$

in zero field do not vary but that the effect of applying longitudinal fields increases with the length, owing to the reduction in self-demagnetization. This is shown in the graphs of fig. 5 which were obtained by cutting down a 26 S.W.G. wire originally 41 cm. long.

In wires of different diameter, on the other hand, there are differences not only in the longitudinal self-demagnetization but also in the distribution of current over the cross-section, so that their A.C. properties are fundamentally different. In investigating the variations in these properties with diameter an experimental difficulty arises.

It will be shown in § VII that heat treatment has a very important effect on the characteristics of a wire of any particular composition. In a batch of wires having the same length, diameter, and composition all

subjected to the same heat treatment, there is always found to be a gradation of quality, so that no two wires of the same batch are strictly alike magnetically. It is not, therefore, an easy matter to devise a satisfactory way of making comparable measurements on wires drawn

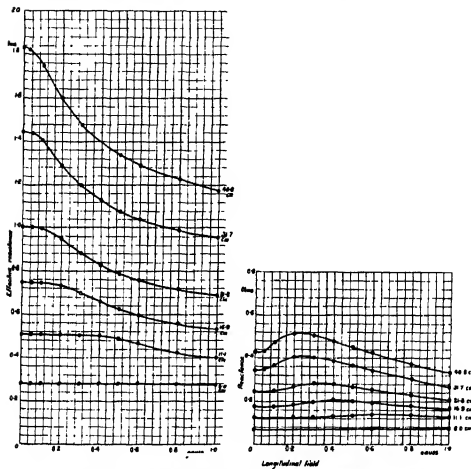


FIG. 5—Variation of resistance and reactance with longitudinal field. Wires of diameter 0.445 cm., and different lengths. Frequency 515~. "Optimum current" 25 m/a.

to different diameters and subsequently annealed, even though annealed in the same "heat", the less so since the effect of cold working on a wire previous to its annealing has a marked and uncontrollable influence upon its magnetic properties.

The best way hitherto discovered for producing comparable wires of different diameter is to choose specimens of the same length and diameter

from one heat-treated batch which differ as little as may be in their magnetic properties, and to etch them with an acid mixture for different lengths of time. By this means we obtained a series of wires having as nearly as possible the same physical characteristics and differing only in diameter. Their diameters lay between 0.445 mm. and 0.1 mm. and they were all 15.25 cm. long, the  $\frac{\text{length}}{\text{diameter}}$  ratios thus ranging between 343 and 1525.

The impedance measurements on these wires at optimum current with a frequency of 515 cycles per second, and in zero longitudinal field, are set out in Table II. It will be seen that the optimum current decreases with decreasing diameter. It is also found that the resistance-maximum at optimum current is sharper the smaller the diameter of the wire.

TABLE II—Wires of different diameter, length 15.25 cm.; frequency 515 c./sec.; zero longitudinal field.  $R_0$  = D.C. resistance (ohms);  $R$  = A.C. effective resistance (ohms);  $\omega L$  = reactance (ohms); at optimum current  $I$  m./A.

Diameter mm.	I m./A.	R	$\omega L$	$R/R_0$	$\omega L/R_0$
0.445	25.5	0.713	0.159	1.870	0.416
0.437	22.5	0.777	0.195	2.000	0.501
0.427	21.0	0.864	0.240	2.067	0.574
0.376	12.5	1.218	0.412	2.248	0.761
0.346	9.0	1.433	0.498	2.316	0.805
0.315	8.5	1.615	0.506	2.150	0.674
0.264	5.5	2.231	0.624	2.039	0.570
0.183	4.2	3.558	0.830	1.510	0.352
0.102	3.5	7.278	0.623	1.115	0.095

Very large percentage changes in effective resistance are observed when a longitudinal field is applied to wires of small diameter. An example, for a wire of diameter 0.183 mm., is shown in fig. 6. It will be noticed that the resistance changes by about 20%, or 0.6 ohm, when the field is reduced from 0.18 gauss to zero, so that a change of this magnitude is produced by simply rotating a horizontal wire through 90° in the earth's magnetic field.

*The Temperature Coefficient*—The temperature coefficient of effective resistance was measured for the wire from which the curves of figs. 2 and 4 were obtained, using the optimum current at 515 cycles per second, and with longitudinal fields between zero and 1 gauss. The relation

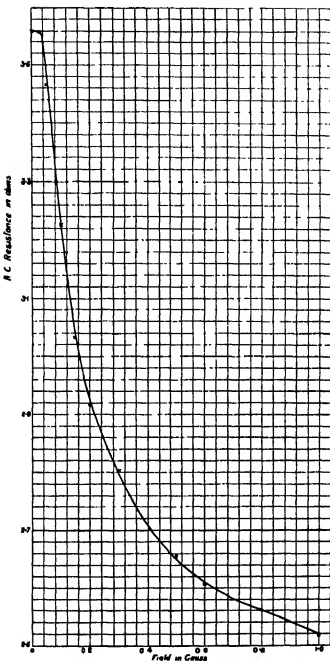


FIG. 6—Variation of A.C. resistance with applied longitudinal field. Frequency 515~, optimum current. Length 15.25 cm.; diameter 0.0183 cm.

between resistance and temperature is linear for each field value, but the coefficient decreases as the field increases, some measured values being

0.00306 in zero field.

0.00303 in 0.2 gauss.

0.00211 in 1.0 gauss.

The D.C. temperature coefficient for the same wire was 0.0026.

#### IV—THEORETICAL CONSIDERATIONS

Consider a straight cylindrical wire of circular section with radius  $a$ , electrical conductivity  $\sigma$  and constant permeability  $\mu_0$ .

Let  $R_0$  be its D.C. resistance.

$R$  be the effective resistance and  $L$  the inductance at frequency  $\omega/2\pi$ . It is well known\* that  $R$  and  $L$  are given by the equation

$$\frac{R + j\omega L}{R_0} = \sqrt{2} \xi \frac{J_0(\xi \sqrt{8})}{J_1(\xi \sqrt{8})}, \quad (1)$$

where

$$\xi = a \sqrt{\frac{-\pi \mu_0 \omega \sigma}{2}}, \quad (2)$$

from which  $R/R_0$  and  $\omega L/R_0$  can be obtained in terms of the *ber* and *bei* functions of Kelvin.

With ferro-magnetic material the permeability is not a constant and the fundamental equation of conduction in the wire cannot in general be solved.

It is well known,† however, that if the magnetic field  $H$  due to the current at any point in the wire is assumed to be a simple sine-wave without harmonics, and the induction  $B$  at the same point to be another sine-wave lagging an angle  $\psi$  behind  $H$ , an elliptical relation between  $B$  and  $H$  is obtained which is a fair approximation to an actual ferro-magnetic hysteresis loop.

The relation may be written

$$B = \mu e^{-j\psi} H, \quad (3)$$

where  $\mu$  is the permeability and is a constant defined by

$$B_0 = \mu H_0, \quad (4)$$

\* Zenneck, 'Ann. Physik,' vol. 2, p. 1135 (1903).

† Russell, "Alternating Currents," vol. 2, chap. x; Gall and Sims, 'J. Instn. elect. Engrs.', vol. 74, p. 453 (May, 1934).

$B_0$  and  $H_0$  being the maximum values of induction and field respectively in the ellipse.

For the simple permeability  $\mu_0$  in (2) we must therefore in ferromagnetic material substitute the complex expression

$$\begin{aligned}\mu_0 &= \mu e^{-j\psi} \\ &= \mu_1 (1 - jb),\end{aligned}\quad (5)$$

where

$$\mu_1 = \mu \cos \psi,\quad (6)$$

and

$$b = \tan \psi.\quad (7)$$

It may easily be shown that if  $W$  be the hysteresis loss in the wire in ergs/cycle/cc.

$$W = \frac{\sin \psi}{4\mu} B_0^2 = KB_0^2,$$

where

$$K = \frac{\sin \psi}{4\mu}.\quad (8)$$

Thus the angle  $\psi$  is given in terms of  $\mu$  and the quantity  $K$ , which as a rough approximation may be taken as the Steinmetz coefficient of the material.

It must be remembered, however, that in a wire the value of  $H_0$  varies from zero at the axis to a maximum at the circumference, and that with actual material  $\mu$  as defined by (4) is not a constant, but varies with  $H_0$  and is therefore a function of the distance from the axis.

But the solution (1) of the equation of conduction can only be obtained on the hypothesis of constant permeability, so that it is necessary to assume a constant value of  $\mu$ , or in other words to take  $\mu$  as a mean value averaged over the whole cross-section of the wire. The same probably applies also to the value of  $\psi$ .

With this understanding we can substitute for  $\mu_0$  in (2) the complex expression (5), so that

$$\xi^2 = -(b + j)k^2,$$

where

$$k = a \sqrt{\frac{\pi \mu_1 \omega \sigma}{2}}.\quad (9)$$

This substitution makes it less easy than in the classical case to obtain from (1) the values of  $R/R_0$  and  $\omega L/R_0$ , but the computation for a considerable range of values of  $k$  and  $b$  has been carried out by Wwedensky,\*

\* Wwedensky and Schillerow, 'Z. Physik,' vol. 34, p. 309 (1925); see also Mittelstrass, 'Arch. Elektrotech.,' vol. 18, p. 595 (1927); Ermolaev, *Ibid.*, vol. 23, p. 101 (1929); Antik, *Ibid.*, vol. 25, p. 125 (1931).

who has given his results in a convenient form as a mesh diagram in which values of  $R/R_0$  and  $\omega L/R_0$  are plotted as abscissae and ordinates respectively for various values of  $k$  and  $b$ , and curves of constant  $k$  and constant  $b$  drawn to form the mesh. In the present work  $R/R_0$  and  $\omega L/R_0$  have been measured, so that the corresponding values of  $k$  and  $b$  can at once be read off from the diagram.  $\mu$  follows from (6), (7), and (9) for

$$\begin{aligned}\mu &= \frac{\mu_1}{\cos \psi} \\ &= \frac{2k^2}{\pi a^2 \omega \sigma \cos \psi} \\ &= \frac{2R_0}{\omega L \cos \psi} \cdot k^2,\end{aligned}\quad (10)$$

where  $l$  = length of wire.

$K$  then follows at once from (8).

It may be noted that the conception that hysteresis losses in alternating fields are the cause of a lag between  $B$  and  $H$ , which makes the permeability a complex function, is essentially that of Arkadiew.\*

The treatment outlined above avoids the introduction of the fictitious "magnetic conductivity" postulated by that worker, and as has been seen leads to a solution in terms of recognized properties of ferro-magnetic material.

## V—APPLICATION TO EXPERIMENTAL RESULTS

i—*Axial Field Zero*—In Table III,  $a$  and  $b$ , are shown the values of  $\mu$  and  $K$  computed from the measured values of  $R/R_0$  and  $\omega L/R_0$  for a particular wire at various currents and frequencies, with zero axial field. The wire was of mumetal, 23.5 cm. long and 0.457 mm. in diameter.

The values of  $\mu$  at constant frequency, when plotted against current, are found to lie on smooth curves which resemble in form the ordinary  $\mu$ - $H$  curve of ferro-magnetic material. The variations in  $K$  with current are, on the other hand, somewhat irregular, and very much smaller than those of  $\mu$ , the values being, in fact, appreciably constant over a wide range of current. By taking the maximum value of  $\mu$  and its corresponding value of  $K$  at each frequency we obtain Table IV.

The variation with frequency suggests that in order to compare directly the values of  $\mu$  and  $K$  obtained from impedance measurements with those which can be derived from magnetic measurements, it is necessary that

\* 'Phys. Z.,' vol. 14, p. 928 (1913).

TABLE III  
 $a$ -VALUES OF  $\mu \times 10^{-4}$

Current m/A.	Frequency, cycles/sec.					
	55	100	150	210	350	500
3.0	2.09	1.98	1.55	1.58	1.52	1.26
5.0	3.02	2.80	2.48	2.21	2.00	1.60
7.5	4.18	3.85	3.29	2.93	2.49	1.96
10.0	4.85	4.20	3.82	3.38	2.84	2.25
15.0	4.24	3.80	3.55	3.41	3.01	2.50
20.0	3.30	3.14	3.10	3.01	2.80	2.44
30.0	2.35	2.20	2.30	2.26	2.22	2.06
35.0	2.07	1.94	2.03	2.07	1.98	1.91

$b$ -VALUES OF $K \times 10^4$					
3.0	5.0	7.5	10.0	15.0	20.0
4.7	5.4	4.7	4.4	4.5	3.9
6.4	6.1	5.4	5.0	5.0	5.2
6.4	7.0	6.2	6.0	5.9	6.0
7.3	7.9	7.3	7.0	7.7	7.0
8.2	9.4	8.9	8.6	8.1	8.1
9.9	9.4	8.9	8.6	8.1	8.1

the frequency should be extremely small. If we extrapolate the results in Table IV to zero frequency we get the following values of  $\mu$  and  $K$ :

$$\mu = 5.8 \times 10^4$$

$$K = 1.7 \times 10^4.$$

TABLE IV—MAXIMUM VALUES OF  $\mu$  AND CORRESPONDING VALUES OF  $K$  AT DIFFERENT FREQUENCIES

Frequency	$\mu \times 10^{-4}$	$K \times 10^4$
55	4.86	3.4
100	4.41	4.4
150	3.85	5.0
210	3.53	5.9
350	3.03	6.7
500	2.51	8.1

The B-H curve for the wire and hysteresis loops with various values of maximum induction  $B_s$  were found by enclosing the wire in a solenoid and using the standard ballistic method of magnetic measurement. The

self-demagnetization effect was eliminated, approximately at any rate, by applying the correction appropriate to cylindrical wires.

The maximum permeability found in this way was  $8.5 \times 10^4$  and the values of K calculated from the formula  $W = KB_0^2$ <sup>3</sup> are shown in Table V.

TABLE V

B <sub>0</sub>	W (ergs/cc.)	K × 10 <sup>4</sup>
3000	14.4	1.6
4600	30.0	1.42
4900	34.5	1.44

If it is borne in mind that  $\mu$  as derived from impedance measurements is by definition an average value of permeability over a range of fields from zero upwards, and therefore essentially less than the actual maximum permeability in the wire, it appears that the two results are in reasonable concordance. A more exact comparison is a matter of great difficulty, since we have no knowledge as to how to arrive at the mean value of permeability which it is necessary to assume in order to solve the equation of conduction in the wire. It is possible, however, to give a general qualitative interpretation of the results shown in Table III, *a*.

The variation of  $\mu$  with current, at constant frequency, clearly derives from the normal variation of permeability with field. For the value of  $\mu$  for any current must be some sort of average value of permeability calculated over a range of field between zero and the field at the surface of the wire, which is proportional to the current. Thus, whatever method of calculation of the average be employed, the  $\mu$ -current curve must have the same general form as the curve connecting permeability and field, namely a rather sharp rise to a maximum followed by a slower decrease.

As the frequency increases, the total current in the wire remaining constant, the distribution of the current over the cross-section changes so that it is concentrated more and more in the outer layers, with the result that the field at points within the wire becomes smaller, although that at the surface is unchanged since it depends only on the total current. If in fig. 7, curve 1 represents the distribution of permeability from the axis to the circumference of the wire (of radius *a*) at some given low frequency, the corresponding distribution for the same current at a higher frequency will be given by a curve of the form of curve 2. The average permeability over the cross-section, or  $\mu$ , will evidently be smaller when calculated from curve 2 than from curve 1, particularly for small or moderate current values. When the current is so large that the field at the surface approaches saturation, and the permeability there is small, it can be easily seen that

the average values of permeability at different frequencies will tend to equality. It is also easy to see that the maximum values of  $\mu$  (the average permeability) will decrease and will occur at higher values of current as the frequency increases. Reference to Table III, *a*, shows that these are the salient features of the experimental results, which can thus be broadly and qualitatively interpreted in terms of the ordinary magnetic properties of the wire.

In attempting a quantitative explanation it must be remembered first of all that we have assumed that at any point in the wire the hysteresis loop due to a single cycle of current is an ellipse.

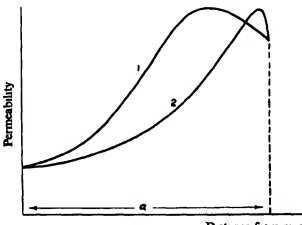


FIG. 7.

Let fig. 8 represent one such ellipse, at a point distant  $r$  from the axis, with a maximum value of field  $H_0$  and of induction  $B_0$ . The permeability at this point is defined as  $\mu_r = \frac{B_0}{H_0} = \frac{PX}{OX}$  in fig. 8. If we proceed from the axis to the surface of the wire we get a family of ellipses in which  $H_0$  varies from zero at the axis to  $\frac{2\sqrt{2}I}{a}$  at the surface, where  $a$  is the radius and  $I$  the R.M.S. value of current. To obtain  $\mu_r$  in terms of the measured permeability of the wire it is assumed that the locus of P is the B-H curve of the wire, so that the value of  $\mu_r$  for any value of  $H_0$  is equal to the measured permeability for a field-strength  $H = H_0$ .

Now except when the frequency is infinitesimally small the variation of  $H_0$  from axis to surface is not linear, so that it is next necessary to determine the distribution of field over the cross-section. It may easily be shown from the classical equation of conduction in a wire that the

amplitude of field ( $H_0$ ) at a point distant  $r$  from the axis is given by  $H_r$ , where

$$H_r = \frac{(ber'^2 x + bei'^2 x)i}{(ber'^2 z + bei'^2 z)i} \cdot H_0 \quad (11)$$

in which

$$z = 2 \sqrt{\frac{\mu \omega}{R_0}}$$

$$x = \frac{r}{a} \cdot z$$

$$H_0 = \frac{2\sqrt{2}I}{a}$$

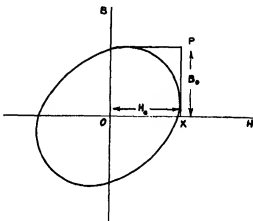


FIG. 8.

Since, however, we have substituted for  $\mu$  in the classical equation the complex quantity  $\mu_1(1 - jb)$  (vide p. 465), the parameter  $z$  becomes complex, and it is not easy to obtain numerical values of  $H_r$  from (11). To a first approximation, therefore, the distribution of field is calculated on the assumption that hysteresis may be ignored, so that  $b = 0$ , the values of  $z$  being obtained by using those of  $\mu$  given in Table III, *a*. The values of  $\mu_r$  over the cross-section then follow, according to assumption, from the B-H curve obtained ballistically, and may be plotted to give curves of the type shown in fig. 7.

It is finally necessary to average  $\mu_r$  over the cross-section in order to establish the value of  $\mu$  for the whole wire, which should, if the assumptions made are reasonable, be in agreement with that deduced from the impedance measurements and given in Table III, *a*. It is very doubtful

how this average should be calculated, but for simplicity it has been taken as the arithmetic mean of  $\mu_r$  over the cross-section, i.e., we write

$$\mu = \frac{1}{a} \int_0^a \mu_r dr.$$

On this basis it has been attempted to construct Table III, *a*, from the B-H curve of the wire, but the results are not particularly encouraging. The calculated maximum values of  $\mu$  at each frequency are always greater than those shown in the table, and the discrepancy increases with the frequency. Thus, if the distribution of field over the cross-section is linear, which is so for very low frequencies, the calculated value of  $\mu$  is  $6 \times 10^4$ , that obtained by extrapolation from Table III, *a*, is  $5.8 \times 10^4$ , which is in good agreement. But at 500 cycles per second the experimental value of  $\mu_{\max}$  is  $2.5 \times 10^4$  while that calculated is about  $5 \times 10^4$ . The theory, therefore, is inadequate to account quantitatively for the decrease in  $\mu_{\max}$  with frequency shown by the impedance measurements. This may indicate that the concentration of current in the surface of the wire is greater than has been calculated approximately on the classical theory. A further discrepancy is that at any frequency the maximum value of  $\mu$  shown in Table III, *a*, occurs at a value of current considerably greater than that which the theory would indicate. From this it would appear that the amplitude of field at the surface of the wire must actually be less than  $\frac{2\sqrt{2}I}{a}$ . But there remains the possibility that the hysteresis loop traversed at a point in the wire during a cycle of current cannot be related, as has been assumed, to the loop measured ballistically with longitudinal magnetization, and in this case the whole basis of comparison must break down.\*

If we turn to Table III, *b*, and consider the variations in  $K$ , the hysteresis constant deduced from impedance measurements, this view appears to find some support, for these variations are very difficult to account for by means of the ballistic hysteresis loops of the material, since we have found that  $K$  determined ballistically is appreciably constant over a wide range of flux density. In Table III, *b*, the variations of  $K$  with current at constant frequency are perhaps small and irregular enough to be attributed to fortuitous divergences from a constant value which, as has been seen, agrees well enough with the ballistic value when the frequency is sufficiently low. But the marked increase in  $K$  which occurs with increasing frequency

\* There actually appears to be some evidence of magnetic anisotropy in ferromagnetic wires, *vide* Ermolaev, 'Arch. Elektrotech.', vol. 23, p. 101 (1929).

seems to indicate either that the hysteresis loop in these conditions is quite different from that obtained ballistically, or that the postulated lag between field and induction in the wire is due not only to hysteresis but to some other property, such as magnetic viscosity, which increases with frequency.

ii—*The Effect of Applying an Axial Field*—The values of  $\mu$  and  $K$  have been computed as above for the same wire with the same range of frequency and current, and with applied axial fields up to 0.6 gauss. As an example of the effect of axial field the values at a frequency of 55 cycles per second are shown in Table VI, *a* and *b*. The results at higher frequencies are similar in character.

TABLE VI

*a*—VALUES OF  $\mu \times 10^{-4}$ . FREQUENCY 55 C./SEC.

Current m/A.	Axial field in gauss				
	0	0.1	0.2	0.4	0.6
3.0	2.09	1.78	1.32	1.14	1.10
5.0	3.02	2.90	2.10	1.56	1.30
7.5	4.18	3.87	2.69	1.93	1.51
10.0	4.85	4.16	2.93	1.95	1.58
15.0	4.24	3.60	2.72	1.85	1.50
20.0	3.30	2.95	2.33	1.71	1.32
30.0	2.35	2.12	1.86	1.49	1.08
35.0	2.07	1.92	1.68	1.38	1.01

*b*—VALUES OF  $K \times 10^4$ . FREQUENCY 55 C./SEC.

3.0	4.7	5.0	5.6	7.0	6.3
5.0	5.0	4.7	5.1	7.2	8.1
7.5	4.2	4.3	4.8	6.3	7.9
10.0	3.4	3.8	4.5	6.4	7.3
15.0	3.4	3.7	4.0	5.5	6.5
20.0	3.9	3.8	4.1	4.4	6.5
30.0	4.0	4.0	4.2	4.7	6.3
35.0	4.3	3.9	4.2	4.5	5.7

Now when a wire is subjected simultaneously to an alternating circular and a direct longitudinal magnetic field, its resultant magnetization is of an alternating screw type, the mathematical investigation of which is not within the scope of this paper. No quantitative explanation of the experimental results shown in Table VI will therefore be attempted. The results can, however, at any rate as far as  $\mu$  is concerned, be broadly explained by means of the theory of ferro-magnetism. A ferro-magnetic body is conceived to consist of a very large number of domains, which, in the absence of an external field, are spontaneously magnetized in

directions distributed at random over the aggregate, so that the resultant magnetization of the body is zero. If the body is a wire and a circular field is applied to it by the passage of current, direct or alternating, the directions of magnetization of the domains tend to conform to the direction of the field and the body becomes circularly magnetized, the circular permeability at any point in the wire assuming the value appropriate to the field at that point. If a direct longitudinal field of increasing magnitude is superposed on an alternating circular field, the directions of magnetization of the domains tend to lie along the axis of the wire, and the constraint thus imposed renders them less able to conform to the alternations of the circular field, and the circular permeability is decreased, slightly for small axial fields, and then at a rate which increases rapidly with the field for a time but finally dies away as the magnetization of the domains approaches perfect alignment with the field and the wire becomes saturated. The values of  $\mu$  given in Table VI,  $a$ , show just this type of variation as the axial field is increased.

A somewhat analogous phenomenon is the well-known fact that when a direct current is passed through a wire so as to give it a steady circular magnetization the longitudinal permeability is decreased. On the other hand, when the circular field is alternating the longitudinal permeability for small fields is known to be increased, probably in the same way as it is increased by the agitation due to mechanical vibration. Thus in the case considered here the decrease in circular permeability caused by the axial field is accompanied by an increase in longitudinal permeability.

It will be remembered that when an external field is applied at right angles to the axis of the wire there is no measurable change of impedance, and consequently of mean circular permeability. During any half-cycle of current the applied transverse field and the circular field due to the current are in the same direction in one half of the cross-section of the wire and in opposite directions in the other half. It is to be expected, then, that the effect of a transverse field over the whole cross-section will be zero.

#### VI—DISCUSSION OF RESULTS

The experimental results which have been described in § III show that the A.C. resistance and reactance of a highly permeable wire undergo changes of considerable magnitude when its circular or longitudinal magnetizations are altered by variations in current or external field. It is evident that this variation of impedance with external field affords a novel method of measuring or detecting small changes in a magnetic

field of the order of that of the earth, or even of measuring absolute values of field. It is not the purpose of this paper to discuss or describe in any detail such possible applications of the effect which has been discovered, but certain considerations which arise from the experimental results may briefly be touched upon.

We have seen that the reactance of a wire is small compared with its resistance, so that in general the power factor considerably exceeds 0.9. Therefore, although a change in external field produces a change of impedance in the wire, this may be considered for practical purposes to be due to a change of ohmic resistance, the reactive change being negligible. It is desirable at this stage to introduce some quantity which will define the sensitivity of a wire to changes in external field. If in an axial field  $H$  the A.C. resistance is  $R$ , and if a small change of field  $\delta H$  gives rise to a change of resistance  $\delta R$ , then  $\delta R = \frac{dR}{dH} \cdot \delta H$ , where  $\frac{dR}{dH}$  is the slope of the

$R$ - $H$  curve at the point  $H$ . We define the sensitivity of the wire in a field  $H$  as the percentage change of resistance caused by 0.1 gauss change of field, i.e.,

$$S = \frac{100}{R} \cdot \frac{dR}{dH} \times 0.1 = \frac{10}{R} \frac{dR}{dH}.$$

It will be realized that this is not necessarily in all cases the most suitable definition of sensitivity, but it has been found a convenient term to use in discussing the characteristics of a particular specimen of material.

It is clear at once from the data which have been given that the sensitivity of a wire of given diameter varies between very wide limits according to its length, the external magnetic field, and the amplitude and frequency of the current.

Reference to Table I shows that, *ceteris paribus*, the sensitivity is greatest with the optimum current flowing in the wire. This, it will be recalled, is the current at which the resistance has its maximum value and is therefore least affected by accidental current variations, so that stability as well as sensitivity is a maximum. On the other hand, the sensitivity of any network in which the wire may be placed is proportional to the current, so that in some cases it may be practically advantageous to sacrifice some intrinsic sensitivity and stability in order to obtain greater network sensitivity. Theoretically, however, it is desirable to work at optimum current, and this will be taken as the basis of further discussion.

The  $R$ - $H$  curves at different frequencies (using the optimum current) for a particular wire sample are shown in fig. 4. Although the maximum slope of the curve increases with frequency, the sensitivity as defined above

in a field of 0·4 gauss (that of the earth's vertical component) is greatest at a frequency of about 500 cycles per second, and this would therefore appear to be in general the best working frequency.

As regards the dimensions of the wire, the curves of fig. 6 show that for a given diameter the sensitivity increases with the length, since with wires of small dimension ratio the effect of self-demagnetization is to reduce the sensitivity in small fields. If the length is less than 20 cm. there is practically no change of resistance in a wire of 0·445 mm. diameter for fields between zero and 0·2 gauss. Adequate length is thus essential. If length is restricted, for any reason, greater sensitivity in small fields may be obtained by using wires of smaller diameter. This, however, introduces considerations other than that of the dimension ratio, since the "skin effect", which determines the A.C. resistance, is a function of the diameter, and, as we have seen (Table II), wires of different diameters show fundamental differences in behaviour when used as conductors of A.C. Thus the optimum current decreases with the diameter, and the resistance-maximum which occurs at this current becomes sharper the finer the wire, so that a decrease in diameter entails a loss not only of network sensitivity but of stability to accidental current variations.

It is clear that in applying the field-sensitivity of the A.C. resistance of nickel-iron alloy wires to the measurement of magnetic fields or changes of field there exists a wide choice of working conditions, and that the optimum conditions can only be determined by reference to the particular circumstances of the measurement required. Enough has been said to indicate the application to such determination of the experimental results which form the subject matter of this paper.

In the next section some account is given of experiments which have been carried out with the object of producing wires of as high sensitivity as possible by means of suitable heat treatment.

## VII—HEAT TREATMENT

It is evident from the theory which has been developed earlier that the change of impedance with axial field is an extremely complex phenomenon, and uncertainty must exist as to the precise magnetic qualities which it is necessary to develop in a wire by heat treatment in order that it should have the greatest possible value of  $\frac{1}{R} \cdot \frac{dR}{dH}$ . But high permeability in small fields, say less than 0·5 gauss, is clearly essential, and the methods of heat treatment employed have been those found most effective in producing

this property. The actual value of the permeability developed in a given wire depends in detail not only on the heat treatment, which must be found by experiment for each particular "wire draw" made from an ingot, but also on the strain history and annealing history during the wire drawing and its antecedent physical processes.

It is not proposed here to discuss in detail the effects either of composition or of strain history; but it is necessary to emphasize the great importance of preventing oxidation. In the present experiments, owing to the small diameter of the specimens, the question of oxidation becomes particularly important, and its prevention imperative. Various ways of avoiding oxidation have been tried, and the results combine to show that heat treatment should be carried out in an atmosphere of hydrogen, either under high pressure or at atmospheric pressure. In order to develop the highest permeability, it was found to be definitely advantageous to take precautions against oxidation, not only during the main heat treatment but during the wire drawing process itself, by performing the intermediate annealings in hydrogen during drawing. As regards the final heat treatments, the heating of the drawn wires for a considerable length of time in hydrogen does more, of course, than merely prevent oxidation: it completes the reduction of any oxide still remaining included in the wire after the drawing.

Although many wires showing unusually high values of mean permeability over ranges of field from 0·4 to 0·5 gauss have been obtained after heating in hydrogen under pressures of 60 lb. per sq. in. (above atmospheric pressure), the present experiments give no direct evidence either for or against the theory proposed by Cioffi\* that hydrogen, mechanically retained in the cooled metal, is itself a contributory cause of exceptionally high initial permeability.

The method of experiment eventually developed for finding the best heat treatment for samples taken from a batch of wires drawn from one particular ingot consists in varying separately the maximum temperature to which the sample is heated and the length of time it is held at that temperature. Additional variation is caused by a second or even a third heat treatment to the top temperature. The rate of cooling was sometimes controlled and sometimes that of the furnace itself—but in all cases kept the same when the other variables were altered.

For the binary alloys—78·5% Ni. 21·5% Fe (the original permalloy) the heat treatment recommended by Arnold and Elman† has been found

\* Cioffi, 'Nature,' vol. 126, p. 200 (9 August, 1930).

† Arnold and Elman, 'J. Franklin Instn.,' vol. 195, p. 621 (1923).

to be the best. The treatment most likely to be successful with alloys containing copper and chromium, "Mumetal" for instance, is to heat to 1200° C. for several hours and cool slowly with the furnace. It has often been found that a second heating exactly repeating the first materially improved the permeability value of a wire.

The general conclusions reached, as to heat treatment of fine wires of the more complex alloys in which copper and chromium are present, are (i) that special precautions against oxidation must be taken during the wire drawing process as well as during the main heating and that the latter must be done in hydrogen, not only to prevent fresh oxidation but to reduce the oxide already in the wire; (ii) that, in general, high permeability is favoured by the highest annealing temperatures and slow cooling. The effect of short or long exposure to the top temperature remains in doubt.

It has become plain from a large series of measurements of  $\mu$  in fields of 0.2 gauss made on wires prepared in the way described that a specified heat-treatment applied to individual wires of batch can never be guaranteed to produce the highest value of  $\mu$ . The results as regards success are analogous to those observed in metal crystal growing: the element of chance plays an important part.

When we proceed to examine the "sensitivity", as defined on p. 474, of wires in which the appropriate heat treatment has produced high values of permeability, we find a further uncertainty. Although there is a fairly strong correlation between the permeability and the sensitivity of a wire over a given range of fields, we have found that their inter-dependence is far from complete, as is shown by the following experiments.

From several batches of wires, each of 26 S.W.G. and 23 cm. long, of the same composition and subjected to various heat treatments, fifteen wires were selected by a rough ballistic test to fall into a graded series as regards their permeability in a field of 0.2 gauss. The sensitivity  $S = \frac{10}{R} \cdot \frac{dR}{dH}$  of each wire was then measured between 0.2 and 0.3 gauss (where the R-H curve is steepest for wires of this dimension ratio), and the B-H curve of each wire determined ballistically over the range 0-0.5 gauss. From the latter the values of  $\mu$  in any field were deduced, being defined as the ratio  $B/H$ , where  $H$  is the external field, and denoting, therefore, the effective permeability in a wire of given dimension ratio. The values of  $S$  and those of  $\mu$  in fields between 0.2 and 0.3 gauss were found to be fairly well correlated, but the relation between the two quantities is far from perfect.

An investigation was therefore made of the frequency distribution of the coefficient  $S$  among a large number of wires, all similarly annealed

in batches of 50 at a time, and selected so that their  $\mu$  values fell within a specified narrow range.

The result of two such experiments with separate batches of 340 and 166 wires was to show that the distribution of the values of the coefficient amongst them was governed by the laws of probability. The standard deviation was roughly 10% of the mean value of S.

This is not a very surprising result, since by fixing the permeability of a wire for a single value of field we merely fix one point on its B-H curve. Theory shows that the impedance of the wire depends upon the form of the complete hysteresis loop over a given range of field, so that the frequency distribution of S indicates little more than the possible variations of a hysteresis loop which passes through a single given point. The magnitude of the standard deviation is, however, noteworthy.

To sum up the conclusions as regards heat treatment, we may say that while it is a necessary condition of the production of wires of high S value that they should be so annealed as to be endowed with high permeability in the same field, this condition is not sufficient, and ensures only a certain probability of high S.

In conclusion, the authors wish to express their indebtedness to Mr. S. Butterworth for help and suggestions in the theoretical treatment, and to the Admiralty for permission to publish this paper.

### VIII—SUMMARY AND CONCLUSION

The variations of the effective resistance and inductance of nickel-iron wires of high permeability have been investigated when the wires are supplied with alternating current of varying frequency and amplitude. It has also been discovered that large changes in effective resistance occur when external longitudinal fields are applied to the wire. In order to explain the experimental results, the classical theory of alternating-current conduction has been extended to take account of the hysteresis property of ferro-magnetics, but to render the equations soluble, it is necessary to assume a constant value of permeability over the cross-section of the wire, whereas actually the permeability varies from the axis to the circumference. While the experimental results are generally in accordance with theory, it has not been found possible to obtain numerical correlation between the magnetic properties of a wire deduced from the impedance measurements and those measured by direct magnetic methods. Still less is it possible to predict the A.C. resistance or inductance of a wire from its measured magnetic properties.

In a suitably heat-treated wire the change of A.C. resistance caused by the application of small longitudinal fields, of the order of that of the earth, is so large as to suggest the use of the effect in the measurement or detection of small changes of magnetic field. The heat-treatment required to produce the maximum effect depends upon the composition and strain history of the wire, and must be found by experiment. While no detailed general rules can be laid down, annealing in an atmosphere of hydrogen is always an essential. Even when the best treatment for any particular sample has been determined, there is no certainty that it will be effective in producing a high resistance-field sensitivity in any individual wire, for the sensitivity coefficients of a large number of similar wires, similarly annealed, are found to be distributed over a wide range of values, approximately according to the probability law.

---



In a suitably heat-treated wire the change of A.C. resistance caused by the application of small longitudinal fields, of the order of that of the earth, is so large as to suggest the use of the effect in the measurement or detection of small changes of magnetic field. The heat-treatment required to produce the maximum effect depends upon the composition and strain history of the wire, and must be found by experiment. While no detailed general rules can be laid down, annealing in an atmosphere of hydrogen is always an essential. Even when the best treatment for any particular sample has been determined, there is no certainty that it will be effective in producing a high resistance-field sensitivity in any individual wire, for the sensitivity coefficients of a large number of similar wires, similarly annealed, are found to be distributed over a wide range of values, approximately according to the probability law.

---

## Photochemical Reactions in the Fluorite Region

### I—Photochemical Decomposition of Ethylene

By R. D. McDONALD and R. G. W. NORRISH, F.R.S.

(Received 3 July, 1936)

Studies of the photochemical decomposition of carbonyl compounds have shown the importance of investigations on homologous compounds as evidence for the mechanisms of the primary photochemical processes in the individual substances. It seemed of interest, therefore, to undertake a similar study of a number of hydrocarbons. With these somewhat more stable compounds, it is important to be able to extend the investigations beyond the wave-length limits arbitrarily imposed by the use of quartz apparatus to include the shorter wave-lengths transmitted by fluorite. For this purpose a special apparatus has been developed.

In the interpretation of results a knowledge of the absorption spectrum of the hydrocarbon concerned is of great assistance, and it seemed advisable, therefore, in the first instance to concentrate on the simpler hydrocarbons, the spectra of which had been measured. In the case of ethylene, which is the subject of the investigation reported here, such measurements have been made by Price\* and by Hilgendorff.†

That ethylene is polymerized by the action of ultra-violet light has been known for some time.‡ More recently, interest in the reactions of atomic hydrogen has led to careful investigations of its action on ethylene and of the hydrogen-ethylene reaction sensitized by mercury vapour.§ In these experiments the ethylene pressures were of the order of hundreds of millimetres. The results showed that the reaction was not simply a hydrogenation of the ethylene to ethane, although that was the predominant process, especially when there was a large excess of free hydrogen.

Thus, Kelmenc and Patat found that in the first stages of the illumination appreciable quantities of acetylene were formed. When the atomic

\* 'Phys. Rev.,' vol. 47, p. 444 (1935).

† 'Z. Physik,' vol. 95, p. 781 (1935).

‡ Berthelet and Gauduchon, 'C.R. Acad. Sci. Paris,' vol. 150, p. 1169 (1910); Landau, *Itid.*, vol. 155, p. 403 (1910).

§ Taylor and Bates, 'J. Amer. chem. Soc.,' vol. 49, p. 2438 (1927); Olson and Meyers, *ibid.*, vol. 48, p. 389 (1926); vol. 49, p. 3131 (1927); Taylor and Hill, *ibid.*, vol. 51, p. 2922 (1929); 'Z. phys. Chem.,' B, vol. 2, p. 449 (1929); Bonhoeffer and Harteck, 'Z. phys. Chem.,' A, vol. 139, p. 64 (1928); Kelmenc and Patat, 'Z. phys. Chem.,' B, vol. 3, p. 289 (1929).

hydrogen was prepared by Wood's method rather than by the resonance method a similar result was obtained, and it was concluded that the hydrogen atoms could dehydrogenate as well as hydrogenate the ethylene. It was also observed that the polymerization of ethylene by light in the absence of hydrogen, if not entirely dependent on, was at least greatly catalysed by the presence of mercury vapour. Concurrent with this polymerization there was a decomposition of the ethylene into hydrogen and acetylene, a reaction which, as far as they were able to ascertain, was independent of mercury.

Taylor and Hill's results were somewhat similar, though they ascribe the formation of acetylene to collisions of excited mercury atoms with ethylene molecules. The detailed mechanism which they suggest can account for the formation of the higher hydrocarbons which have been detected.

In all these investigations a mercury arc was used as the light source. Mooney and Ludlam\* found that ethylene did not appreciably absorb light of wave-lengths longer than  $213 \mu\mu$  and pointed out that it was not to be expected, therefore, that the longer wave-lengths previously used would lead directly to reaction. By using a condensed aluminium spark which gave strong emission at  $186 \mu\mu$ , they were able to show that acetylene was formed from ethylene even in the absence of mercury.

More recently, Taylor and Emeléus† found that ethylene alone was polymerized by light from a mercury arc under conditions where a mercury sensitized reaction was impossible, and concluded that this must be a direct polymerization following the absorption by the ethylene of light of wave-length near the lower limit of transmission of the quartz.

The use of the shorter wave-lengths transmitted by fluorite in the present work has enabled us to study the reaction produced by direct absorption. Since absorption at such wave-lengths is very strong, low pressures were used. This should reduce complications due to secondary reactions.

#### EXPERIMENTAL METHOD

The apparatus which was developed for this series of investigations is shown in fig. 1. The light source was the water-jacketed pyrex hydrogen lamp, B, which operated at 2000 volts and, usually, 1 ampere. At the one end the lamp extended for some distance beyond the electrode and was closed at C by a glass plate with a hole cut in its centre. A fluorite

\* 'Trans. Faraday Soc.', vol. 25, p. 442 (1929).

† 'J. Amer. chem. Soc.', vol. 53, pp. 562, 3370 (1931).

plate was sealed over this hole with pineine. The extension on the lamp was of uniform tubing, so that a fluorite lens in its supporting carriage could be moved along it in order to focus the light at any desired point in the reaction system, but the lens was not used in the present investigation and is omitted from the figure. At D was a ground joint which could be water cooled if desired, and the quartz reaction chamber, E, fitted over this. Plane windows parallel to and at right angles to the path of the light made it possible to photograph the original beam and the fluorescence, if any. Pressures were measured on the McLeod gauge, F,

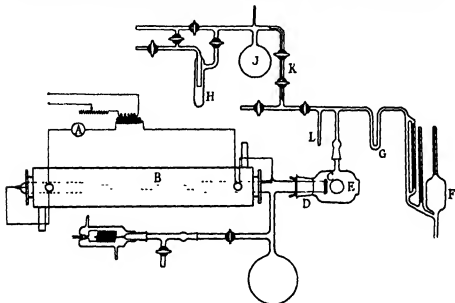


FIG. 1.

which was in effect a double one so that a wide range of pressures might be covered. The tubing at G could be cooled in carbon dioxide-ether in order to trap mercury vapour.

Ethylene from a steel cylinder was condensed in H and fractionated, the middle third being stored in the bulb, J, which was connected to a mercury manometer. The small amounts required for each experiment were taken out in the capillary, K, and thence admitted to the system. Condensable gases could be removed at any time by cooling the side tube, L, in the appropriate refrigerant.

#### EXPERIMENTAL RESULTS

*Production of Hydrogen*—Preliminary experiments showed that with this arrangement the rapid decrease in pressure characteristic of the

mercury sensitized reaction did not occur. Even after several hours' illumination, the pressure usually remained at its initial value, and when a decrease was recorded it only amounted to a very few per cent. However, when runs were made in which the side tube of the reaction system was cooled in liquid nitrogen at intervals, usually of one hour, and the pressure measured after equilibrium was established, it was found that a non-condensable gas was formed. The results of six of these runs are shown in fig. 2 in which the pressure of permanent gas is plotted against the time. That this gas was hydrogen was shown by experiments in which the side tube was cooled in liquid hydrogen. The additional drop in pressure which this caused was almost exactly equal to the vapour

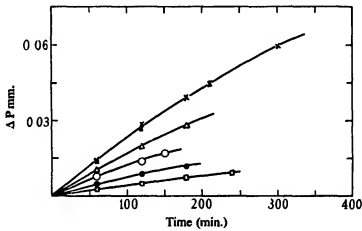


FIG. 2.

pressure of the ethylene at liquid nitrogen temperature as given by the blank at the beginning of the runs.

In the runs at the two lowest pressures, the total pressure in the system was no longer constant but increased somewhat. In the run at 0.0275 mm. this increase was equal, within the experimental error, to the pressure of the hydrogen formed.

*Effect of Pressure*—Direct evidence for the formation of a polymer was obtained when experiments were made at higher pressures. Successive experiments under apparently identical conditions showed decreasing rates, presumably due to a decrease in light transmission because of a film of polymer on the fluorite window. In accordance with this, when the apparatus was taken apart and the front surface of the window wiped with ether, subsequent runs showed an increase in rate of several hundred per cent. This is illustrated in the difference between the rates in runs

19 and 20 in Table I. The fact that the rate in run 20 is greater than that in run 11 is of no significance since the window had not been cleaned after the preliminary runs. For this reason it was almost impossible to obtain an accurate measurement of the effect of the initial pressure on the rate, but the results which are given in Table I, where the order in which the experiments were carried out can be seen, and which are plotted in

TABLE I—EFFECT OF PRESSURE ON RATE

Run No.	$P_{C_2H_4}$	Rate	Run No.	$P_{C_2H_4}$	Rate
14	0.0275	0.0025	—	—	—
15	0.065	0.0040	22	0.070	0.0105
12	0.135	0.0075	20	0.475	0.0355
13	0.290	0.0105	21	0.82	0.0405
18	0.465	0.0115	—	—	—
11	0.515	0.0140	24	0.82	0.0225
19	0.99	0.0105	25	2.18	0.0260
16	2.36	0.0140	26	4.97	0.0240
17	15.8	0.0120	—	—	—

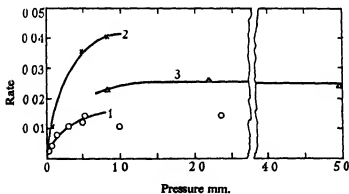


FIG. 3.

fig. 3, show clearly enough the general nature of the relation. Rates are given in mm. of hydrogen formed in the first hour. The results really form three distinct series and are treated as such.

Before run 18, the McLeod gauge was shut off from the reaction system and the U-tube between it and the system cooled in liquid air over night in order to remove any mercury vapour. During the run the trap was cooled in carbon dioxide-ether so that no mercury vapour could enter from the gauge. Since, however, the rate conforms closely to the results represented in curve 1, the reaction must be independent of mercury.

Between runs 18 and 19 the window was cleaned with ether as described

above. Subsequent experiments, 19, 20, and 21, show a much greater velocity (curve 2). In run 20 a layer of copper oxide was placed in the reaction chamber in an attempt to detect atomic hydrogen. Since the rate of formation of hydrogen was satisfactorily in accord with that of the next two experiments the result is a negative one, but not necessarily conclusive. Another attempt to detect hydrogen atoms was made in run 23 in which oxygen was added, but the result was again negative, hydrogen being produced at much the same rate as would have been expected had no oxygen been present.

Taken together, the three series of results indicate a rate of production of hydrogen proportional to the ethylene pressure when that is low, becoming less dependent on it as it increases and finally reaching a constant value. This is what would be expected if absorption were incomplete at the low pressures, becoming complete at the higher pressures.

*Condensable Products*—Since hydrogen is a product of the reaction, the formation of acetylene might also be expected. However, it is known that acetylene can be rapidly polymerized by ultra-violet light,\* so that it was possible that it might be removed almost as quickly as it was formed. Therefore, a few measurements were made using acetylene—taken from a cylinder and carefully purified—under conditions similar to those used with ethylene. It was found that, though a measurable decrease in pressure did occur, this was so slow as to make it very doubtful whether acetylene, at the low pressures at which it would occur in the work with ethylene, would be appreciably polymerized. Pressure measurements with the side tube cooled in liquid air indicated that a very small but definite amount of non-condensable gas was formed from the acetylene.

The amounts of gas concerned in reactions at these low pressures are so very small that it is quite impractical to determine the products by any modification of direct gas analysis. However, some information may be obtained by determining the temperatures at which they pass into the gas phase. This method has been applied to ethylene. Unfortunately, no vapour pressure measurements have been made on the hydrocarbons in the pressure range which is involved here, and it was therefore necessary to obtain approximations by the extrapolation of vapour pressure equations considerably below the limits for which they were developed.

As liquid nitrogen condenses everything except the hydrogen and a small amount of ethylene (*ca.* 0.002 mm.), it seemed possible that a

\* Lind and Livingston, 'J. Amer. chem. Soc.', vol. 54, p. 94 (1932); vol. 56, p. 1550 (1934).

refrigerant at a slightly higher temperature might permit the evaporation of the ethylene while keeping the hydrocarbon products, if any, from the gas phase. Liquid oxygen, however, is not suitable unless the ethylene pressure is of the order of 0.03 mm., which is too low for convenient working. By using petrol ether cooled by liquid nitrogen to about  $-170^{\circ}$  and bringing it to the same temperature, as measured by a thermocouple, before each reading, the results given in Table II were obtained. Here  $P_c$  represents the pressure of condensable gas.

TABLE II—CONDENSABLE PRODUCTS

No.	$P_{C_2H_4}$	$P_{H_2}$	$P_c$	No.	$P_{C_2H_4}$	$P_{H_2}$	$P_c$
34	0.195	0.017	0.041			0.012	0.027
35	0.20	0.021	0.044			0.022	0.060
		0.011	0.020	37	0.35	0.040	0.110
36	0.20	0.020	0.047			0.055	0.145
		0.027	0.064	40	0.07	0.008	0.014
39	0.30	0.025	0.066	41	0.32	0.019	0.049

This was obtained as the difference between the pressure with the side tube cooled in the petrol ether-nitrogen bath and the total pressure, due allowance being made for the effect of cooling alone. All pressures are given in millimetres. In runs 36 and 37 readings were taken at intervals during the course of the runs, in the remaining cases final readings only were taken. In the majority of the runs, where the total pressure remained constant, the ethylene which had reacted is necessarily given by the sum of the hydrogen and the condensable gas formed. It is apparent from the table that the latter was generally from two to three times the former.

In runs 37, 39, and 40 the cooling mixture was allowed to warm slowly and the changes in pressure measured. In this way a further separation was obtained. After increasing regularly up to  $-160^{\circ}$ , the pressure remained constant until  $-140^{\circ}$  was reached. The remainder of the condensable product then evaporated over the next  $10^{\circ}$  interval. The amounts of the two fractions were:—

Run	$-170^{\circ}$ to $-160^{\circ}$	$-140^{\circ}$ to $-130^{\circ}$
37	0.089	(0.056)
39	0.050	0.016
40	0.041	0.008

In run 37 a breakage after reaching  $-150^{\circ}$  stopped the experiment, the second fraction is therefore obtained by difference. In run 40 the quantity of this second fraction is only about twice the experimental

error, so the ratio of the two fractions is not of great significance. However, the first is always very definitely the greater of the two.

Because of the uncertainties in the vapour pressures, as mentioned above, it is impossible to deduce the composition of each of these fractions. However, from the vapour pressure equations it would appear that, at the pressures concerned, all hydrocarbons with three or less carbon atoms would evaporate on warming up to  $-160^{\circ}$ . The first fraction may therefore be rather complex, though on other grounds it seems likely that acetylene would be its chief constituent. The butanes would, however, have vapour pressures of the required magnitude at  $-140^{\circ}$  to  $-130^{\circ}$  and may possibly form the second fraction.

### DISCUSSION

Hilgendorff (*loc. cit.*) states that the absorption spectrum of ethylene consists of a number of diffuse main bands and a series of sharp secondary bands. In discussing the former, he writes: "Probably the ethylene molecule breaks down here into the two halves  $\text{CH}_2$ . This breakdown is certainly to be expected since a dissociation at 1750 A. corresponds to a heat of dissociation of 158.6 Cal./mol. This value also corresponds very well to the chemical data for the breaking of the C=C double bond (162 Cal./mol). This observation agrees with Price's short communication\* that the spectrum of ethylene in the Schumann region is very highly diffuse and that at 1750 A. continuous absorption sets in." In his paper referred to here, Price also speaks of the ethylene breaking down into  $\text{CH}_2$  radicals and, while no mention of that is made in the more detailed paper referred to in the introduction, there is nothing there to rule out this possibility.

It is natural, therefore, to attempt an explanation of the present results on the basis of such a decomposition. Certainly the primary formation of  $\text{CH}_2$  radicals can conveniently explain a polymerization, for these might reasonably be expected to give, on reaction with ethylene, at least some long chain hydrocarbons.

The formation of hydrogen is not so easy to explain, for its rate is greatest in the early stages of the reaction and it cannot, therefore, be due to the photodecomposition of any intermediate substance. If the primary process be the formation of  $\text{CH}_2$  radicals we must conclude, then, that hydrogen is formed by the reaction



\* 'Phys. Rev.', vol. 45, p. 843 (1934).

This is certainly possible on energy grounds, but it would seem much more probable for the  $\text{CH}_3$  radicals, once separated, to collide and react with ethylene molecules rather than with other  $\text{CH}_3$  radicals.

As alternative primary processes, the following, the second of which had been suggested previously by Mooney and Ludlam (*loc. cit.*), may be considered:



All of these are energetically possible, while (3) has the advantage that the energy which it requires, 145,000 cals. (using heats of formation from the International Critical Tables), corresponds to the absorption of light of wave-length 196  $\mu\mu$ , which is near the threshold of strong absorption in ethylene. The fact that no hydrogen atoms were detected with either copper oxide or oxygen is explained if the hydrogenation of ethylene takes place readily enough to remove the hydrogen atoms before they can react with either of these substances.

Moreover, the present experimental results can be explained if reactions (3) and (4) occur simultaneously and to about the same extent. The hydrogen atoms from (3) may react with other ethylene molecules to give  $\text{C}_2\text{H}_5$  radicals, which may be further hydrogenated to ethane or may combine to give butane. The overall reaction resulting from the decomposition of one ethylene molecule according to this scheme could then be represented as made up of the processes:



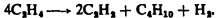
and



With another ethylene molecule reacting according to (4), the total result would lie between



and



These equations would require a condensable product three times as great as the hydrogen and consisting of two fractions, the more volatile one considerably greater than the other. The total pressure change would be small and, when allowance was made for the formation of a higher polymer, would be still further reduced. All these points are in satisfactory agreement with the experimental results.

It may be that processes (3) and (4) are really the same, that is, that on the absorption of the light the molecule loses two of its hydrogen atoms. Whether these separate as such, or as molecular hydrogen, may depend on a probability factor, which in turn is determined by factors such as the wave-length of the light absorbed.

However, with illumination by light of a wide range of wave-lengths the assumption of two or more primary processes is not unreasonable. For the present, therefore, we are inclined to accept this sequence of reactions as a tentative explanation of the results reported here.

It is hoped in subsequent work to control the wave-lengths transmitted, by the use of appropriate filters, and so to determine to what extent the different products are formed independently.

The authors wish to express their thanks to the Royal Society of Canada for a maintenance grant to the one of them (R. D. McD.) and to the Royal Society for an apparatus grant.

#### SUMMARY

Light from a hydrogen lamp is passed directly through a fluorite window into ethylene at pressures mostly below one millimetre. The total pressure never varies by more than a few per cent., although a polymer is deposited on the window, and hydrogen as well as a condensable gas is formed. The latter can be separated into two fractions, one of which evaporates at  $-170^{\circ}$  to  $-160^{\circ}$ , the other at  $-140^{\circ}$  to  $-130^{\circ}$  at the low pressures involved. The variation of the rate of hydrogen formation with the ethylene pressure is such as to indicate that the light is not completely absorbed at the lowest pressures used. Possible mechanisms for the reaction are discussed.

---

# Self-Consistent Field, with Exchange, for Cu<sup>+</sup>

By D. R. HARTREE, F.R.S., and W. HARTREE

*(Received 8 July, 1936)*

## 1—INTRODUCTION

Solutions of Fock's equations\* for the self-consistent field of a many-electron atom, including exchange effects, have already been carried out for several atoms by Fock and Petrashen† and the present authors.‡ The heaviest atom for which results of such calculations have previously been published is Cl<sup>-</sup>; Cu<sup>+</sup> was selected as the next atom for which to attempt the solution of Fock's equations, for the following reasons. As already pointed out in Paper IV, the results of the solution of Fock's equations are most interesting for atoms for which exchange effects are large; the self-consistent field without exchange, which is an almost necessary preliminary to the solution of Fock's equation, had already been worked out for Cu<sup>+</sup>,§ and from this work it was known that the (3d)<sup>10</sup> group of Cu<sup>+</sup> is very sensitive to the atomic field, so that it is likely to be considerably affected by the inclusion of exchange terms in the equations. Further, in view of the interest of Cu from the point of view of metal theory,|| it is desirable to have as good wave functions for Cu<sup>+</sup> as possible, particularly for the outer groups, which are those likely to be most affected by the inclusion of exchange terms in the equation from which they are determined.

The number of radial wave functions involved in the normal configuration of Cu<sup>+</sup> is perhaps almost the largest for which a complete solution of Fock's equations is practicable, for the following reason.

In the self-consistent field without exchange, the addition of one extra (*nl*) group to any configuration simply increases by one the number of functions  $2(2l+1)Z_0(nl, nl|r)$ , giving (when divided by  $r^3$ ) the contributions to the field from the different groups, which have to be estimated and adjusted by trial till the final functions, calculated from the solutions of the equations, agree with the estimates. And although this

\* 'Z. Physik,' vol. 61, p. 126 (1930).

† 'Phys. Z. Sowjet.' vol. 6, p. 368 (1934); vol. 8, p. 547 (1935).

‡ 'Proc. Roy. Soc.,' A, vol. 150, p. 9 (1935); vol. 154, p. 588 (1936); vol. 156, p. 45 (1936). These will be referred to as II, III, and IV.

§ D. R. Hartree, 'Proc. Roy. Soc.,' A, vol. 141, p. 282 (1933). This will be referred to as I.

|| See, for example, Fuchs, 'Proc. Roy. Soc.,' A, vol. 151, p. 585 (1935).

increase of one in the number of functions to be adjusted, together with the addition to the number of equations to be solved, and possible decreases of length of the steps of the numerical integration, increases the amount of work to be done to obtain a solution of the equations of the self-consistent field, it does not increase it to an overwhelming extent; and it has been found practicable to carry out calculations of the self-consistent field, without exchange, for atoms as heavy as Hg, with 14 groups.

But when exchange terms are included in the equations, there are introduced a number of other Z functions all of which have to be estimated and adjusted similarly, both functions involving two different groups,  $Z_k(nl, n'l'|r)$ , which may be called "non-diagonal" functions, and functions  $Z_k(nl, nl|r)$  involving a single group, but with  $k \neq 0$ , which, with the corresponding functions with  $k = 0$ , may be called "diagonal" functions. The addition of a (3d)<sup>10</sup> group to an argon-like configuration increases the number of  $Z_k$  functions by no less than 10, so that for the normal configuration of Cu<sup>+</sup>, with exchange, there are altogether 28 such functions, or already twice as many as for Hg without exchange. The further addition of the (4s)<sup>8</sup> and (4p)<sup>6</sup> groups to form the normal configuration of Kr would further increase the number of  $Z_k$  functions by 22, and the complete solution of Fock's equations would probably be so lengthy as to be impracticable.

Besides being somewhat heavy on account of the large number of Z functions involved, the work of solving Fock's equations for Cu<sup>+</sup> was made particularly tricky by the extreme sensitiveness of the (3d)<sup>10</sup> group, already mentioned. This sensitiveness is not due to a very small value of the energy parameter  $\epsilon$  (as it is for the (3p)<sup>6</sup> group of Cl<sup>-</sup>), so much as to the large range over which the attractive force on a d-electron due to the atomic field is not much larger than the centrifugal force, so that a small change in the atomic field gives a large proportional change in the net force on the electron. Consequently the effect of the exchange terms in lessening the sensitiveness of the outermost group, already noted in the case of the (3p)<sup>6</sup> group of Cl<sup>-</sup>, is not so pronounced in the case of the (3d)<sup>10</sup> group of Cu<sup>+</sup>.

However, the calculations have been carried to a successful conclusion, and the results are given in the present paper.

## 2—FOCK'S EQUATIONS FOR Cu<sup>+</sup>, AND METHOD OF SOLUTION

General formulae and tables for enabling Fock's equations to be written down directly for any configuration consisting of complete groups

only have already been given in a previous paper.\* Typical equations for the normal configuration of  $\text{Cu}^+$ , namely those for the (3s), (3p), and (3d) radial wave functions, are given here for reference, viz.:

$$\left[ \frac{d^2}{dr^2} + \frac{1}{r} \{ T + 2 - 2(1 - Y_0(3s, 3s)) \} - \epsilon_{3s, 3s} \right] P_N(3s)$$

$$+ \sum_{n=1}^{\infty} \left[ \frac{2}{r} Y_0(ns, 3s) - \epsilon_{ns, 3s} \right] P_N(ns)$$

$$+ \frac{2}{r} \left[ \sum_{n=2}^{\infty} Y_1(3s, np) P_N(np) + Y_2(3s, 3d) P_N(3d) \right] = 0 \quad (1)$$

$$\left[ \frac{d^2}{dr^2} + \frac{1}{r} \{ T + 2 - 2(1 - Y_0(3p, 3p)) + \frac{1}{3} Y_2(3p, 3p) \} - \epsilon_{3p, 3p} - \frac{2}{r^2} \right] P_N(3p)$$

$$+ \frac{2}{3r} \sum_{n=1}^{\infty} Y_1(ns, 3p) P_N(ns)$$

$$+ \left[ \frac{1}{r} \{ 2Y_0(2p, 3p) + \frac{1}{6} Y_2(2p, 3p) \} - \epsilon_{2p, 3p} \right] P_N(2p)$$

$$+ \frac{1}{r} [\frac{1}{3} Y_1(3p, 3d) + \frac{1}{3} Y_2(3p, 3d)] P_N(3d) = 0 \quad (2)$$

$$\left[ \frac{d^2}{dr^2} + \frac{1}{r} \{ T + 2 - 2(1 - Y_0(3d, 3d)) + \frac{1}{4} (Y_2(3d, 3d) + Y_4(3d, 3d)) \right.$$

$$\left. - \epsilon_{3d, 3d} - \frac{6}{r^2} \right] P_N(3d) + \frac{2}{5r} \sum_{n=1}^{\infty} Y_2(ns, 3d) P_N(ns)$$

$$+ \frac{1}{r} \sum_{n=2}^{\infty} \left\{ \frac{1}{3} Y_1(np, 3d) + \frac{1}{30} Y_2(np, 3d) \right\} P_N(np) = 0, \quad (3)$$

where  $T$  is the total  $2Z_\alpha$  for the whole atom, namely

$$T = 2N - \sum_{nl} 4(2l+1) Y_0(nl, nl)$$

$$= \sum_{nl} 4(2l+1) [1 - Y_0(nl, nl)] + 2C, \quad (4)$$

where  $C$  is the total charge of the atomic system under consideration ( $C = 1$  for  $\text{Cu}^+$ ), and the notation is that of the writers' previous papers.<sup>†</sup>

The general method adopted for the solution of these equations was the same as that used for  $\text{Cl}^-$  and already explained in IV. Briefly, the relevant functions  $r^k Z_k(nl, n'l|r)$  are first estimated, and corresponding

\* IV, formulae (12)-(14) and Table I.

<sup>†</sup> See particularly III and IV. As explained in IV, in the numerical work it is more convenient to work with  $(1 - Y_0(nl, nl))$  than with  $Y_0(nl, nl)$ , and formulae (1)-(4) have been written in the form in which they are actually used in the numerical work.

functions  $r^k Y_k(nl, n'l'|r)$  calculated from them by integration of the equation

$$\frac{d}{dr} [r^k Y_k(nl, n'l'|r)] = \frac{2k+1}{r} [r^k Y_k(nl, n'l'|r) - r^k Z_k(nl, n'l'|r)]. \quad (5)$$

The equations for the radial wave functions, of which (1)-(3) are specimens, are then solved with these  $Y_k$  functions, the conditions of orthogonality and normalization being satisfied by suitable choice of initial values of each  $P_N(nl)/r^{l+1}$  and of the non-diagonal parameters  $\epsilon_{nl, n'l'}$ . These non-diagonal parameters are then reduced to zero by suitable linear transformations of the corresponding radial wave functions  $P_N(nl)$ ; "final"  $Z_k$  functions are then calculated from the transformed radial wave functions and are compared with the estimated functions. These estimates are then adjusted until the final calculated  $Z_k$  functions agree with the estimated functions. As already mentioned, for Cu<sup>+</sup> there are altogether 28 such  $Z_k$  functions to be estimated, calculated, and adjusted.

For (3d), inward integration of the equation for  $\eta = -\frac{d}{dr}(\log P)$

was used for large  $r$ , over the range for which exchange terms are negligible. For the other wave functions, outward integration of the equation for  $P$  was used over the whole range.

On account of the sensitiveness of the (3d)<sup>10</sup> group, a special order of procedure had to be adopted for this atom. For each trial set of  $Z_k$  functions not involving (3d), two calculations of the (3d) radial wave function were made; first a set of estimates of the  $Z_k$  functions involving (3d) were made, and equation (3) solved for  $P_N(3d)$ ; then the estimates of 10[1 -  $Z_0(3d, 3d)$ ],  $Z_1(3d, 3d)$ , and  $Z_4(3d, 3d)$  were revised, and equation (3) solved again; the solution and corresponding  $Y_k$  functions were then used in the exchange terms in the equations such as (1) and (2) for the other wave functions. Early in the work, it appeared that for the second of these calculations, a good approximation to 10[1 -  $Z_0(3d, 3d)$ ] was given by taking one-third of the way between the estimated and final values for the first of the calculations; this empirical rule was remarkably successful in reducing the maximum discrepancy between estimated and calculated values of this function,\* and was a great help in hastening the convergence to a self-consistent set of  $Z_k$  and  $P_N$  func-

\* It has also been found very effective in the case of the (5d)<sup>10</sup> group of Au, for which calculations of the self-consistent field, without exchange, are in progress. It may apply somewhat generally to the highly sensitive (nd)<sup>10</sup> groups of atoms following the transition metals.

tions. The estimates of the functions  $Z_k(3d, 3d)$ , ( $k = 2, 4$ ) were usually derived from those of  $Z_0(3d, 3d)$  by use of the general relation

$$r^k Z_k(nl, n'l'|r) = \int_{r_1=0}^r r_1^k dZ_0(nl, n'l'|r_1), \quad (6)$$

and not made independently.\*

The initial estimates of the functions  $Z_k(nl, n'l'|r)$  not involving  $(3d)$  were obtained by taking the corresponding functions calculated from the results of the self-consistent field without exchange, and modifying them by estimates of the effects of exchange terms, based on the corresponding effects for  $\text{Cl}^-$  already calculated. In particular the estimates of the  $Z_0(nl, n'l')$  functions were adjusted so as to tend to 0 as  $r \rightarrow \infty$ , as recommended in IV as a result of experience of the work on  $\text{Cl}^-$ .

For the  $Z_k$  functions involving  $(3d)$ , there were no results of previous calculations to serve as a basis for the effects of exchange terms. For the non-diagonal functions, the results of the self-consistent field without exchange were taken without modification; for  $10[1 - Z_0(3d, 3d|r)]$  a guess was made of the effect of exchange terms, by taking the change of  $Z_0$  to be the same function of  $Z_0$  as for the  $(3p)$  group of  $\text{Cl}^-$ ; estimates of  $Z_2(3d, 3d|r)$  and  $Z_4(3d, 3d|r)$  were calculated from the estimated  $10[1 - Z_0(3d, 3d|r)]$  by (6). This guess, though not good, was fortunately better than nothing; even so, the result of this first estimate was that the maximum difference between the estimated and final values of  $10[1 - Z_0(3d, 3d|r)]$  was as much as 1.5, and the estimated and final values of  $\lim_{r \rightarrow \infty} r^4 Z_4(3d, 3d|r)$ , which is particularly sensitive to the behaviour of the wave function at large  $r$ , differed by a factor of about  $3\frac{1}{2}$ . For the second estimate, these differences were about half as great, in the opposite direction; for the third, the maximum difference between estimated and final values of  $10[1 - Z_0(3d, 3d|r)]$  was reduced to 0.17, thanks to the method of revising the estimates of this quantity already mentioned, and the estimated and final values of

$$\lim_{r \rightarrow \infty} r^4 Z_4(3d, 3d|r)$$

differed by only 20%. At this stage the first solutions of the equations for  $(3s)$  and  $(3p)$  were carried out.

Altogether eight stages of approximation have been made, four of these being concerned with  $(3d)$  only. In the final approximation, the

\* Since  $Z_0$  is specified at equal intervals of  $r_1$ , not vice versa, this formula is not suitable for the accurate evaluation of  $Z_4$ , but it is convenient for estimating either  $Z_4$  itself or the variation of  $Z_4$  corresponding to a variation of  $Z_0$ .

maximum difference between estimated and final values of

$$10 [1 - Z_0(3d, 3d|r)]$$

is 0·01, which is as good as the agreement obtained in the calculations of the self-consistent field without exchange; for the other functions  $2(2l+1)[1 - Z_0(nl, nl|r)]$  the corresponding maximum difference is 0·005.

There is one general comment to be made on the work as a whole. It might seem at first sight that the work of solving Fock's equations is a very suitable field for the application of mechanical means of integrating differential equations, such as are provided by the differential analyzer of Bush,\* which has already been used on calculations of the self-consistent field without exchange.† But the experience of the present work and that on Cl<sup>-</sup> suggests that the scope of the differential analyzer here is not so great as appears at first sight.

The calculations involved in the evaluation of the self-consistent field of an atom, either with or without exchange, fall into two groups; firstly the numerical integration of the equations such as (1)-(3) for the radial wave functions, with given values of the functions and parameters occurring in them, and secondly the evaluation of the  $Z_k$ ,  $Y_k$  functions and of the exchange terms (if any), and subsidiary calculations such as interpolations to satisfy the conditions of orthogonality and normalization, and transformations to eliminate the non-diagonal parameters. In the calculation of a self-consistent field without exchange, the second group is comparatively small and light, as there are only the diagonal  $Z_0$ ,  $Y_0$  functions to consider, no exchange terms and no orthogonality conditions or transformations. But in the solution of Fock's equation these calculations in the second group take up much the greater part of the time, and are the most tedious part of the whole work and the most difficult to check; the first group of calculations, consisting of the actual numerical integration of the equations for the radial wave functions, is a comparatively small part of the whole work, and is the most pleasant and interesting part of it to carry out.

This first group of calculations is the only part of the work for which the differential analyzer would probably be used in practice, unless a machine were built of sufficient capacity to handle Fock's equations on the lines of

\* 'J. Franklin Inst.', vol. 212, p. 447 (1931); D. R. Hartree, 'Nature', vol. 135, p. 940 (1935).

† D. R. Hartree, 'Phys. Rev.', vol. 46, p. 738 (1934); Porter, 'Proc. Manc. Lit. Phil. Soc.', vol. 79, p. 75 (1935); Manning and Millman, 'Phys. Rev.', vol. 49, p. 848 (1936).

Torrance's treatment\* of the equations of the self-consistent field without exchange; the laborious calculations of the second group would still have to be done by hand computation, and the saving of time and labour by the use of the differential analyzer would probably not be very marked.

### 3—RESULTS AND DISCUSSION

The final results are given in Tables I and II. Table I gives the normalized radial wave functions  $P_N(nl|r)$ , the values of  $P_N(nl|r)/r^{l+1}$  for small  $r$ , and the values of the diagonal energy parameters  $\epsilon_{n,l,n}$ ; the non-diagonal parameters have been reduced to zero by orthogonal transformation of the radial wave functions. Table II gives the functions  $2(2l+1)[1 - Z_0(nl, nl|r)]$ , which are the contributions to  $Z$  from

TABLE I—Cu<sup>+</sup>. SOLUTION OF FOCK'S EQUATIONS. NORMALIZED RADIAL WAVE FUNCTIONS  $P_N(nl|r)$

TABLE OF  $P_N(nl|r)/r^{l+1}$

$r$	(1s)	(2s)	(2p)	(3s)	(3p)	(3d)
0.000	307.0	94.5	708	35.2	260½	244½
0.005	265.7	81.5	659	30.4	242	233
0.010	229.9	70.0	613	26.1	225½	222
0.015	199.0	59.7	571	22.2	209½	211½
0.020	172.3	50.6	532	18.8	195	202

TABLE OF  $P_N(nl|r)$

0.000	0.000	0.000	0.000	0.000	0.000	0.000
0.005	1.328	0.407	0.016	0.152	0.006	0.000
0.010	2.299	0.700	0.061	0.261	0.022	0.000
0.015	2.985	0.896	0.128	0.334	0.047	0.001
0.020	3.445	1.011	0.213	0.376	0.078	0.002
0.025	3.729	1.061	0.310	0.393	0.113	0.003
0.030	3.876	1.057	0.416	0.389	0.152	0.005
0.035	3.918	1.009	0.528	0.368	0.193	0.008
0.040	3.881	0.926	0.644	0.334	0.234	0.011
0.05	3.645	0.686	0.877	0.238	0.317	0.019
0.06	3.290	0.384	1.103	0.119	0.395	0.030
0.07	2.890	0.054	1.312	-0.010	0.465	0.044
0.08	2.488	-0.280	1.500	-0.139	0.524	0.061
0.09	2.110	-0.602	1.663	-0.260	0.572	0.080
0.10	1.769	-0.900	1.801	-0.370	0.607	0.101

\* 'Phys. Rev.', vol. 46, p. 388 (1934). See II, § 6, for the extension of Torrance's method to Fock's equation.

TABLE I—(continued)

<i>r</i>	(1s)	(2s)	(2p)	(3s)	(3p)	(3d)
0.12	1.211	-1.403	2.002	-0.544	0.642	0.149
0.14	0.809	-1.770	2.111	-0.651	0.632	0.203
0.16	0.530	-2.007	2.142	-0.692	0.583	0.261
0.18	0.344	2.132	2.113	-0.677	0.503	0.321
0.20	0.221	-2.168	2.040	-0.614	0.400	0.382
0.22	0.141	-2.134	1.934	-0.515	0.281	0.442
0.24	0.089	-2.050	1.808	-0.390	0.152	0.501
0.26	0.056	-1.932	1.670	-0.247	0.018	0.557
0.28	0.036	-1.795	1.528	-0.094	-0.116	0.610
0.30	0.023	-1.646	1.386	+0.062	-0.249	0.660
0.35	0.007	-1.270	1.055	0.438	-0.554	0.770
0.40	0.002	-0.940	0.778	0.757	-0.804	0.855
0.45	0.001	-0.674	0.561	1.001	-0.993	0.917
0.50	—	-0.474	0.398	1.170	1.123	0.958
0.55	—	-0.328	0.279	1.268	-1.200	0.981
0.60	—	0.225	0.195	1.311	-1.235	0.991
0.7	—	-0.104	0.093	1.275	-1.212	0.978
0.8	—	-0.048	0.045	1.147	-1.115	0.937
0.9	—	-0.022	0.022	0.983	-0.986	0.882
1.0	—	-0.011	0.011	0.817	-0.848	0.821
1.1	—	-0.004	0.005	0.663	-0.717	0.759
1.2	—	-0.002	0.002	0.531	-0.598	0.698
1.3	—	-0.001	0.001	0.420	-0.494	0.639
1.4	—	—	—	0.329	-0.405	0.585
1.6	—	—	—	0.198	-0.269	0.488
1.8	—	—	—	0.117	-0.176	0.406
2.0	—	—	—	0.069	-0.114	0.337
2.2	—	—	—	0.040	-0.073	0.279
2.4	—	—	—	0.023	-0.047	0.231
2.6	—	—	—	0.014	-0.030	0.191
2.8	—	—	—	0.008	-0.019	0.158
3.0	—	—	—	0.004	-0.012	0.136
3.2	—	—	—	0.002	-0.007	0.107
3.4	—	—	—	0.001	-0.004	0.088
3.6	—	—	—	—	-0.002	0.072
3.8	—	—	—	—	-0.001	0.059
4.0	—	—	—	—	—	0.049
4.5	—	—	—	—	—	0.029
5.0	—	—	—	—	—	0.018
5.5	—	—	—	—	—	0.010
6.0	—	—	—	—	—	0.006
7	—	—	—	—	—	0.002
8	—	—	—	—	—	0.001
$a_{nl, ml}$	658.4	82.30	71.83	10.651	7.279	1.613

the different ( $nl$ ) groups, in the sense used in the papers in which the results of calculation of the self-consistent field without exchange have been published;\* Table II also gives the function  $T$  defined by (5), which is the total  $2Z_p$  of the field of the nucleus and the Schrodinger charge distribution of the whole atom;† this is one of the quantities required in calculating the wave functions of a further electron (either the series electron of a free neutral atom, or a "free" electron of a metal) in the

TABLE II— $\text{Cu}^+$ . SOLUTION OF FOCK'S EQUATIONS. CONTRIBUTIONS TO  $Z_p$  AND TOTAL  $2Z_p$

<i>r</i>	Contributions to $Z_p$ ; $2(2l+1)[1 - Z_0(nl, nl r)]$						Total $2Z_p$
0 000	2 000	2 000	6 000	2 000	6 000	10 00	58 00
0 005	1.994	1 999	6 000	2 000	6 000	10 00	56.66
0.010	1.959	1 996	6 000	1 999	6 000	10 00	55.35
0.015	1.888	1 990	6 000	1.999	6 000	10 00	54.10
0.020	1.784	1 981	5.999	1.997	6 000	10 00	52.92
0.025	1.654	1 970	5.997	1 996	6 000	10 00	51.80
0.030	1.508	1 959	5.993	1.994	5 999	10 00	50.75
0.035	1.356	1 948	5.986	1.993	5 998	10 00	49.75
0.040	1 203	1 938	5.976	1.992	5 997	10 00	48.80
0.05	0.918	1.925	5.941	1.990	5.992	10.00	47.02
0.06	0.676	1 919	5.882	1 989	5.984	10 00	45.38
0.07	0.484	1.918	5.794	1 989	5.973	10 00	43.84
0.08	0.340	1 917	5.675	1 989	5.959	10 00	42.38
0.09	0.234	1.913	5.524	1.988	5.941	10 00	40.99
0.10	0.159	1.902	5.344	1.986	5.920	10 00	39.66
0.12	0.071	1 847	4.906	1.978	5.873	9.99	37.18
0.14	0.030	1.744	4.395	1.963	5.823	9.99	34.94
0.16	0.013	1.600	3.850	1.945	5.779	9.98	32.91
0.18	0.005	1.427	3.304	1.926	5.743	9.96	31.07
0.20	0.002	1.241	2.785	1.909	5.718	9.93	29.42
0.22	0.001	1.055	2.310	1.896	5.704	9.90	27.91
0.24	—	0.879	1.890	1.888	5.698	9.86	26.54
0.26	—	0.720	1.527	1.884	5.697	9.80	25.26
0.28	—	0.581	1.220	1.882	5.697	9.73	24.07
0.30	—	0.462	0.965	1.882	5.693	9.65	22.95

\* See I. In comparing Table II of the present paper with Table IV of Paper I, note that in the latter, three entries have been omitted at the end of the  $(1s)^8$  column. These entries are the same as the corresponding entries in the present Table II.

†  $Z_p(r)$  is defined as  $r \times (\text{potential at radius } r)$ .

TABLE II—(continued)

<i>r</i>	(1s) <sup>8</sup>	(2s) <sup>8</sup>	(2p) <sup>6</sup>	(3s) <sup>8</sup>	(3p) <sup>6</sup>	(3d) <sup>10</sup>	Total 2Z <sub>p</sub>
0.35	—	0.249	0.518	1.874	5.641	9.39	20.38
0.40	—	0.127	0.267	1.837	5.500	9.06	18.08
0.45	—	0.062	0.133	1.758	5.254	8.67	16.00
0.50	—	0.029	0.065	1.639	4.915	8.23	14.13
0.55	—	0.013	0.031	1.489	4.507	7.76	12.47
0.60	—	0.006	0.015	1.322	4.061	7.27	11.01
0.7	—	0.001	0.003	0.982	3.150	6.29	8.65
0.8	—	—	0.001	0.686	2.331	5.37	6.91
0.9	—	—	—	0.457	1.666	4.54	5.64
1.0	—	—	—	0.295	1.161	3.82	4.72
1.1	—	—	—	0.186	0.794	3.19	4.05
1.2	—	—	—	0.114	0.535	2.66	3.56
1.3	—	—	—	0.069	0.356	2.21	3.19
1.4	—	—	—	0.041	0.235	1.84	2.91
1.6	—	—	—	0.014	0.100	1.27	2.55
1.8	—	—	—	0.005	0.042	0.87	2.34
2.0	—	—	—	0.001	0.017	0.59	2.21
2.2	—	—	—	—	0.007	0.41	2.13
2.4	—	—	—	—	0.003	0.28	2.08
2.6	—	—	—	—	0.001	0.19	2.05
2.8	—	—	—	—	—	0.13	2.03
3.0	—	—	—	—	—	0.09	2.02
3.2	—	—	—	—	—	0.06	2.01
3.4	—	—	—	—	—	0.04	2.00
3.6	—	—	—	—	—	0.02	—
3.8	—	—	—	—	—	0.01	—
4.0	—	—	—	—	—	0.01	—

field of the ion. The third decimal is given in all the contributions to Z except that from the (3d)<sup>10</sup> group, as it is probably dependable to  $\pm 1$  for all groups out to (3s)<sup>8</sup>, and is of some value for (3p)<sup>6</sup>, and it may be of interest in comparing the results with those of the self-consistent field without exchange.

As in Cl<sup>-</sup>, the main features of the effect of the exchange terms are a very considerable contraction of the outermost (*nl*) group (here (3d)<sup>10</sup>) and a comparatively small alteration of the other groups of the outer shell, on account of the partial compensation of the attractive effect of the exchange terms in the equation, and the repulsive effect of the contraction of the outermost group and consequent increased screening of the nucleus by it. The maximum changes in  $2(2l + 1)[1 - Z_0(3l, 3l|r)]$ , and those

in  $[1 - Z_0(3l, 3l|r)]$  which give the changes per electron of each ( $3l$ ) group, and the latter figures for  $\text{Cl}^-$ , are as follows:

	Max. change in $I \quad 2(2l+1)[1-Z_0(3l, 3l r)]$	Max. change in $[1-Z_0(3l, 3l r)]$	Max. change in $[1-Z_0(3l, 3l r)]$
	$\text{Cu}^+$	$\text{Cu}^+$	$\text{Cl}^-$
0 (s)	0.03 <sub>s</sub>	0.01 <sub>s</sub>	0.01 <sub>s</sub>
1 (p)	0.10 <sub>s</sub>	0.01 <sub>s</sub>	0.10 <sub>s</sub>
2 (d)	0.77	0.07 <sub>s</sub>	

The changes per electron for  $\text{Cu}^+$  are about the same for the (3s) and (3p) group, whereas for  $\text{Cl}^-$  the change per electron for the (3p) group is about six times that for the (3s) group; and for  $\text{Cu}^+$  the change per electron for the (3d) group is about  $4\frac{1}{2}$  times that for the (3p) group. It is interesting to note that the change per electron for the (3s) group is almost the same for  $\text{Cl}^-$  and  $\text{Cu}^+$ ; this would hardly be expected *a priori* in view of the considerably looser binding in the former atom, and emphasizes the extent to which the direct attractive effect of the exchange terms on the (3s) wave function of  $\text{Cl}^-$  is counteracted by the indirect effect through the large contraction of the (3p) wave function.

The results for  $\text{Cu}^+$  also confirm the effect of the exchange terms on the (2s)<sup>2</sup> group of  $\text{Cl}^-$ , which was unexpectedly large. The maximum changes in the contributions to  $Z$  from the groups with  $n = 2$  are:—

	Max. change in $I \quad 2(2l+1)[1-Z_0(2l, 2l r)]$	Max. change in $2(2l+1)[1-Z_0(2l, 2l r)]$
	$\text{Cu}^+$	$\text{Cl}^-$
0 (s)	0.031	0.06 <sub>s</sub>
1 (p)	0.035	0.10 <sub>s</sub>

Since the size screening constant for the M shell is about 4, it might be expected that from  $\text{Cl}^-$  to  $\text{Cu}^+$  the effect of the exchange terms on the groups of the M shell would be reduced roughly in the ratio of the values of  $(N - 4)$  for Cl and Cu, that is by a factor of about 2, and this is seen to be the case.

Table III gives the total radial charge densities

$$U(r) = \sum_n 2(2l+1) P_n^2(nl|r)$$

for  $\text{Cu}^+$ , calculated from the results of the self-consistent field with and without exchange, and the difference between them. Table IV gives the values of  $\bar{r}^4$  for the different groups calculated from the results of the

TABLE III—Cu<sup>+</sup> CHARGE DISTRIBUTION. TOTAL RADIAL DENSITY IN ATOMIC UNITS, U(r) =  $\sum_{nl} 2(2l+1) P_n^l (nl|r)$ . CALCULATED BY SELF-CONSISTENT FIELD (a) WITHOUT EXCHANGE, (b) WITH EXCHANGE, AND THE DIFFERENCE (b) - (a)

r	U(r) (a)	U(r) (b)	$\delta U(r)$ (b) - (a)	r	U(r) (a)	U(r) (b)	$\delta U(r)$ (b) - (a)
0.000	0.00	0.00	—	0.7	20.45	21.70	1.25
0.005	3.9 <sub>1</sub>	3.9 <sub>1</sub>	0.0 <sub>0</sub>	0.8	18.02	18.89	0.87
0.010	11.7 <sub>1</sub>	11.7 <sub>1</sub>	0.0 <sub>0</sub>	0.9	15.02	15.54	0.52
0.015	19.7 <sub>4</sub>	19.7 <sub>4</sub>	0.0 <sub>0</sub>	1.0	12.17	12.39	0.22
0.020	26.3 <sub>6</sub>	26.3 <sub>6</sub>	0.0 <sub>0</sub>	1.1	9.72	9.72	0.00
0.025	31.0 <sub>4</sub>	31.0 <sub>4</sub>	0.0 <sub>1</sub>	1.2	7.75	7.57	-0.18
0.030	33.7 <sub>7</sub>	33.7 <sub>6</sub>	-0.0 <sub>1</sub>	1.3	6.21	5.91	-0.30
0.035	34.9 <sub>0</sub>	34.9 <sub>1</sub>	0.0 <sub>1</sub>	1.4	5.01 <sub>3</sub>	4.62 <sub>3</sub>	-0.39
0.040	34.8 <sub>8</sub>	34.8 <sub>7</sub>	0.0 <sub>0</sub>				
				1.6	3.37	2.89	-0.48
0.05	32.7 <sub>9</sub>	32.8 <sub>1</sub>	0.0 <sub>0</sub>	1.8	2.35 <sub>8</sub>	1.86	-0.49 <sub>4</sub>
0.06	30.0 <sub>8</sub>	30.2 <sub>1</sub>	0.1 <sub>1</sub>	2.0	1.69	1.21 <sub>1</sub>	-0.47 <sub>1</sub>
0.07	28.1 <sub>3</sub>	28.3 <sub>5</sub>	0.2 <sub>4</sub>	2.2	1.24	0.81 <sub>1</sub>	-0.42 <sub>1</sub>
0.08	27.4 <sub>4</sub>	27.7 <sub>4</sub>	0.3 <sub>1</sub>	2.4	0.91	0.55	-0.36
0.09	27.9 <sub>0</sub>	28.3 <sub>6</sub>	0.3 <sub>4</sub>	2.6	0.67 <sub>4</sub>	0.37	0.30 <sub>1</sub>
0.10	29.4 <sub>4</sub>	29.9 <sub>3</sub>	0.4 <sub>9</sub>	2.8	0.50 <sub>5</sub>	0.25 <sub>1</sub>	-0.25
				3.0	0.37 <sub>6</sub>	0.17	-0.20 <sub>1</sub>
0.12	33.61	34.20	0.59	3.2	0.28	0.11 <sub>1</sub>	-0.16 <sub>1</sub>
0.14	37.35	37.96	0.61	3.4	0.20 <sub>6</sub>	0.08	-0.12 <sub>1</sub>
0.16	39.32	39.83	0.51	3.6	0.15	0.05 <sub>6</sub>	-0.09 <sub>1</sub>
0.18	39.23	39.59	0.36	3.8	0.11	0.03 <sub>1</sub>	-0.07 <sub>1</sub>
0.20	37.36	37.62	0.26	4.0	0.08 <sub>1</sub>	0.02 <sub>1</sub>	-0.05 <sub>1</sub>
0.22	34.35	34.53	0.18				
0.24	30.81	30.97	0.16	4.5	0.03 <sub>7</sub>	0.00 <sub>6</sub>	-0.02 <sub>1</sub>
0.26	27.24	27.43	0.19	5.0	0.01 <sub>6</sub>	0.00 <sub>5</sub>	-0.01 <sub>1</sub>
0.28	23.98	24.26	0.28	5.5	0.00 <sub>7</sub>	0.00 <sub>1</sub>	-0.00 <sub>6</sub>
0.30	21.26	21.67	0.41	6.0	0.00 <sub>8</sub>	—	-0.00 <sub>1</sub>
				6.5	0.00 <sub>1</sub>	—	-0.00 <sub>1</sub>
0.35	17.19	18.04	0.85				
0.40	16.48	17.72	1.24				
0.45	17.61	19.13	1.52				
0.50	19.22	20.89	1.67				
0.55	20.53	22.17	1.64				
0.60	21.16	22.74	1.58				

present paper, and the diamagnetic susceptibility calculated from the results of the self-consistent field with and without exchange, in the same way as similar results were obtained for Cl<sup>-</sup> in IV. The "observed" susceptibility as given by Stoner\* is also shown in Table IV; the agreement with the value calculated from the results of the present paper appears very satisfactory.

TABLE IV—DIAMAGNETIC SUSCEPTIBILITY OF Cu<sup>+</sup>

	Group	$\bar{r}^2$	$2(2l+1)\bar{r}^2$	
Self-consistent field, with exchange	(1s) <sup>2</sup>	0.0037	0.01	
	(2s) <sup>2</sup>	0.0665	0.13	
	(2p) <sup>6</sup>	0.0528	0.32	
	(3s) <sup>2</sup>	0.604	1.21	
	(3p) <sup>6</sup>	0.679	4.07	
	(3d) <sup>10</sup>	1.285	12.85	
S.c.f., without exchange	$\Sigma 2(2l+1)\bar{r}^2$	18.58	$-\chi \cdot 10^{-4} = 14.67$	
	$-\int_0^\infty r^2 \delta U(r) dr$	4.89		
	$\Sigma 2(2l+1)\bar{r}^2$	23.47	$-\chi \cdot 10^{-4} = 18.54$	
	Observed		$-\chi \cdot 10^{-4} = 14$	

## 4—SUMMARY

The numerical solution of Fock's equation for the self-consistent field, including exchange effects, for the Cu<sup>+</sup> ion has been carried to a successful conclusion. The work is made rather troublesome by the very sensitive character of the (3d)<sup>10</sup> group, but otherwise presents no particular features except its length.

The results are given and the effects of the exchange terms discussed and compared with the corresponding effects for Cl<sup>-</sup>; in both cases the most striking feature is a considerable contraction of the outermost (*n*l) group, accompanied by a comparatively small contraction of the other groups of the outer shell.

The diamagnetic susceptibility is calculated and found to be in good agreement with experiment.

\* "Magnetism and Matter" (Methuen, 1934), ch. 9, Table 4.2, p. 272. This value is based on measured values of the susceptibilities of cuprous salts. For a discussion of the analysis of the susceptibility of a salt into those of its ions, see Stoner, *op. cit.*, ch. 9, § 4.

## The Kinetics of the Combustion of Methane

By R. G. W. NORRISH, F.R.S., and S. G. FOORD, Laboratory of Physical Chemistry, Cambridge

(Received 9 July, 1936)

### INTRODUCTION

The kinetics of oxidation of methane at pressures comparable with atmospheric pressure presents many features of great interest and of considerable importance to the elucidation of the nature of combustion processes in general. The facts which have accumulated to date, though fairly precise and definite, require in some cases amplification and further study in view of the realization that combustion has the character of a chain reaction.

It has been found\* that the temperature of ignition of methane, which lies in the region 700–800°C., is dependent on the composition and total pressure of the mixture. For equimolecular mixtures of  $\text{CH}_4$  and  $\text{O}_2$ , no lower limit phenomena of the kind associated with hydrogen or carbon monoxide ignition have been observed. Below the ignition limit there is a readily measurable reaction velocity, and it was shown by Fort and Hinshelwood† that the pressure-time curve is comprised of three distinct parts: (a) an induction period of several seconds' or minutes' duration, during which almost no reaction can be detected; (b) a period of acceleration to a steady velocity, followed by (c) a gradual decline of the velocity to zero as the reactants are used up. Fort and Hinshelwood showed that the velocity during the reaction period was much more dependent on the pressure of methane than that of oxygen. They further established the fact that the reaction is almost completely inhibited by packing the vessel with pieces of quartz tubing. Bone and Allum‡ showed that the most reactive mixture consists of methane and oxygen in the ratio 2:1, the induction period being shortest and the reaction velocity greatest for this proportion. It was further found that the reaction is subject to sensitization, small quantities of nitrogen peroxide, iodine, or formaldehyde practically removing the induction period and increasing the reaction rate. An analysis of the products of the reaction showed that it followed the general course:



\* Neumann and Serbinov, 'Phys. Z. Sowjet.', vol. 4, p. 433 (1933).

† 'Proc. Roy. Soc.,' A, vol. 129, p. 284 (1930).

‡ 'Proc. Roy. Soc.,' A, vol. 134, p. 578 (1932).

During the process of the reaction, small quantities of intermediates were isolated, chief among which in the matter of quantity was formaldehyde. It is significant that this substance has been shown to be readily formed by the oxidation of methane, yields up to 20% being obtained by Bone and Wheeler\* using a flow method.

It has been pointed out by one of us† that neither the hydroxylation nor the peroxidation theory is adequate fully to account for the kinetic phenomena of this reaction, and that in particular they have not been able to give an adequate explanation of such effects as the induction period, the promotion by inert gases, the inhibition by increase of surface, and the phenomena of sensitization and inhibition by small amounts of added substances. These are all characteristics of a chain reaction, and in order to take account of such kinetic phenomena as well as the stoichiometric relationships covered by the hydroxylation theory a mechanism has been proposed based upon the propagation of chains by oxygen atoms and methylene radicals with the primary production of formaldehyde. Semenoff‡ simultaneously has developed the theory of "degenerate branching" of reaction chains, and has shown that much of the kinetics of combustion of hydrocarbons, previously obscure, may be readily interpreted. In the present paper, with an improved technique for the measurement of pressure changes, we have made a detailed study of the slow reaction, and have found that a synthesis of the atom chain hypothesis and the theory of degenerate branching gives a remarkably complete interpretation of the very varied kinetic relationships, including the catalytic effect of inert gas which we have discovered to be a marked feature of the reaction. We have also studied the effect of catalysts on the ignition temperature, and from the steady increase of reaction velocity up to very high values as the temperature is raised towards the ignition limit, we conclude that the ignition of methane is undoubtedly a thermal phenomenon which sets in when the reaction velocity exceeds a limiting value and the reaction process becomes approximately adiabatic.

#### EXPERIMENTAL METHOD

*Apparatus*—The apparatus used was of the type described by us in a recent paper.§ It consisted of an electrically heated reaction vessel into which a gas mixture could be admitted from a separate mixing vessel.

\* Trans. Chem. Soc., p. 1074 (1903).

† Norrish, Proc. Roy. Soc., A, vol. 150, p. 36 (1935).

‡ "Chemical Kinetics and Chain Reactions," Oxford (1935).

§ Foord and Norrish, Proc. Roy. Soc., A, vol. 152, p. 196 (1935).

Subsequent explosion of the mixture could be observed visually through a small window in the entry tube, and the course of slow reactions could be followed by the pressure change in the system as observed on a special type of Bourdon gauge connected with the reaction vessel. Measurements of pressure change were made with an accuracy within 0·02 mm. of mercury or less. Where it was required to follow the slow reaction for a considerable proportion of the total change, steps had to be taken to avoid condensation, in the entry tube, of water formed during the reaction. This was accomplished by using a coiled entry tube of 3 mm. bore heated by a circulatory steam system to 100° C. for about 50 cm. of its length. By this means no interference with the pressure of the system could occur by water condensation until a partial pressure of 12 to 15 mm. of water vapour was attained at the cool end of the entry tube by diffusion. Cylindrical reaction vessels of soda-glass, pyrex, or quartz were used. The length of the vessels was standardized at 20 cm. (*i.e.*, less than the length of furnace over which the temperature was constant within 1° C. at a mean temperature of 500° C.), but the diameter was varied as required. The apparatus could be evacuated to  $10^{-6}$ – $10^{-8}$  mm. by "Hyvac" and mercury diffusion pumps.

*Preparation of Gases*—Oxygen was prepared by the electrolysis of 10% sodium hydroxide solution saturated with barium hydroxide, and purified from ozone and hydrogen by passage over heated platinized asbestos. Methane was made by reduction of methyl iodide, by methyl alcohol, and a zinc-copper couple, mainly as described by Vanino,\* and purified by two fractional distillations of the liquid methane. Particular care was taken during the preparation to avoid contamination of the product by iodine. Both methane and oxygen were stored over water in aspirators, and on analysis always proved to be between 99% and 100% pure, the residue being mainly due to the gradual diffusion of air from the aspirator water as the gas was used. Before use the gases were dried with phosphorus pentoxide. Nitrogen used as inert gas was taken direct from cylinders and used without further purification, apart from drying. Hydrochloric acid gas was obtained by dehydration of its concentrated solution by strong sulphuric acid, and stored in a large bulb. It was given a final drying before use by passage over calcium chloride. Known amounts of iodine were introduced into gaseous mixtures by storing oxygen at a constant pressure in a series of tubes containing iodine and held in a bath of cold water, and admitting the appropriate amount of the saturated gas to the mixing vessel. The amount of iodine was calcu-

\* "Präparative Chemie," vol. 2.

lable from the vapour pressure at the temperature of the water bath. Chlorine was obtained from a cylinder and purified by repeated fractional distillation.

#### EXPERIMENTAL RESULTS

*Slow Reaction Velocity*—At 480° C., using a soda-glass reaction vessel of 28.5 mm. diameter, the general form of pressure-time curve obtained was similar to that recorded by previous workers;\* it commenced with an induction period of the order of several minutes, during which no appreciable change of pressure occurred, followed by a pressure change which gradually increased to a maximum rate after a further period of a few minutes. The rate of reaction, after remaining constant for a short time, gradually fell as the reactants were consumed. The pressure change at the point of maximum rate was small compared with the total change for complete reaction, so that the maximum rate could justifiably be taken as that corresponding to the original concentrations of reactants within a small limit of error. On account of the sensitivity of the pressure measuring device, this rate could be measured fairly accurately over a small length of the curve, even for small pressure changes of a few millimetres.

Using the above method of rate determinations, three series of measurements have been made to investigate the individual effects of the three variables, viz., concentration of methane, concentration of oxygen, and the total pressure, on the velocity of the slow reaction at 480° C. Obviously any effect of total pressure on the rate has to be allowed for in examining the effect of each of the other two variables, and is therefore considered first. Fig. 1 shows the effect of varying the total pressure by adding nitrogen to a mixture of methane and oxygen of fixed composition (*i.e.*, 250 mm. methane; 100 mm. oxygen). There is a nearly linear increase in velocity with total pressure. For this reason, in investigating the effect of varying the concentrations of methane and oxygen, allowance has been made for the simultaneous change in total pressure, assuming a linear law. An approximate proportionality between reaction velocity and total pressure has also been found to hold at higher temperatures, up to 600° C. in a pyrex reaction vessel.

Fig. 2 shows the effect on the reaction rate (at 480° C.) of varying the concentration of methane, at a constant concentration of oxygen. A plot of  $[CH_4]^n P$  against the rate, where  $P$  is the total pressure, gives a

\* Fort and Hinshelwood, 'Proc. Roy. Soc.,' A, vol. 129, p. 284 (1930); Bone and Allum, *ibid.*, vol. 134, p. 578 (1932).

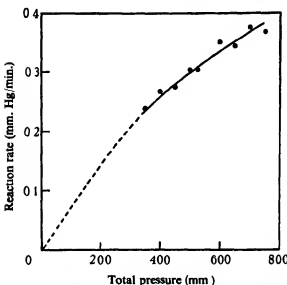
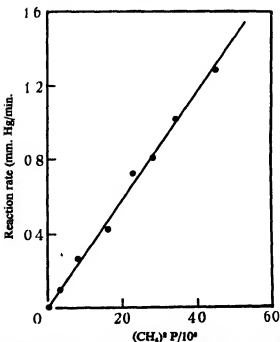


FIG. 1—Variation of slow reaction velocity with total pressure.

FIG. 2—Variation of slow reaction velocity with  $\text{CH}_4$  concentration

close approximation to a straight line. Similarly, at constant concentration of methane, and varying concentration of oxygen, a plot of  $[O_2]P$  against the rate gives an approximately straight line with the exception of one point for a low concentration of oxygen (fig. 3). Combining the results of the above measurements, the reaction rate is given by an expression of the form :

$$\frac{d}{dt} [CH_4] = k [CH_4]^3 [O_2] P. \quad (1)$$

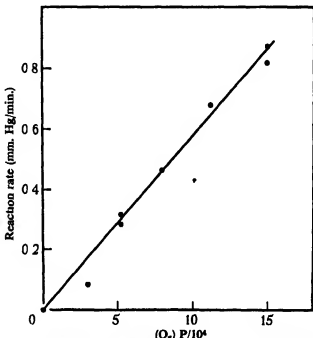


FIG. 3—Variation of slow reaction velocity with  $O_2$  concentration.

It should be mentioned that in measuring the above velocities, the absolute values of the reaction velocity were susceptible to fortuitous changes in the surface conditions in the reaction vessel, and concordant and reproducible results (*i.e.*, within 5%) could only be obtained by carrying out a complete series of measurements without allowing the reaction vessel to cool, and pumping out the vessel for at least half an hour between successive experiments. In particular, the experience of other workers that the reaction rate is considerably lowered by allowing the reaction vessel to remain full of air, was confirmed. The law obtained above is in approximate agreement with the reaction order of 3.5 obtained by Frear\*

\* 'J. Amer. Chem. Soc.', vol. 56, p. 305 (1934).

for a mixture of constant proportions of methane and oxygen, although a rather lower order was indicated by the results of Fort and Hinshelwood.\* It also includes the result that for a given total pressure the most reactive mixture is  $2\text{CH}_4 + \text{O}_2$ , as shown by Bone and Allum.†

To extend the proof of the expression for the reaction rate obtained above to lower concentrations of reactants, it was necessary to raise the temperature to obtain conveniently measurable rates of reaction. Pressure-time curves were therefore plotted for equimolecular mixtures of methane and oxygen at various pressures in a quartz reaction vessel of 23 mm. diameter, at a temperature of  $620^\circ\text{ C}$ . Similar curves to those at  $480^\circ\text{ C}$ . were obtained, with the exception that the rate of change of pressure did not reach a maximum value until 20–30% of the total change had occurred, and then rapidly fell away again. Approximate maximum rates are given in Table I.

TABLE I—SLOW REACTION AT  $620^\circ\text{ C}$ .  $[\text{CH}_4]:[\text{O}_2] = 1$ .

Total pressure (mm.) . . . .	200	150	100	50
Maximum rate (mm./sec.) . . . .	0·64	0·345	0·105	0·015

The rate is here approximately proportional to  $P^3$  but, in view of the considerable amount of reactants consumed at the point of measurement, a higher order reaction was probably occurring. More satisfactory results are given for a lower temperature ( $530^\circ\text{ C}$ .) in connexion with experiments described below on the effect of surface, which bear an approximate fourth order relation.

*Surface Effect on the Slow Reaction*—Quantitative data on the effect of surface on the velocity of slow reaction are not available, although several workers have reported a reduction of the velocity and increase in the induction period by increase of the surface factor. In particular, Fort and Hinshelwood obtained a very marked suppression of the reaction by packing the reaction vessel with tubing, while Frear noted that the surface had an inhibiting effect at pressures greater than 300 mm. and a promoting effect at pressures lower than 300 mm.; however, the flow method adopted by the latter is open to criticism when dealing with a reaction accompanied by an induction period.

Measurements have therefore been made of the slow reaction velocity at  $530^\circ\text{ C}$ . in a series of pyrex vessels of equal length but varying in diameter from 5 mm. to 37·5 mm., using an equimolecular mixture of

\* 'Proc. Roy. Soc.,' A, vol. 129, p. 284 (1930).

† 'Proc. Roy. Soc.,' A, vol. 134, p. 578 (1932).

methane and oxygen at total pressures between 150 mm. and 300 mm. The smaller vessels were composed of a number of units of the standard length and the stated diameter connected together in parallel, to avoid the use of a large correction factor for the volume of the pressure gauge in computing the reaction velocity. The value obtained for the velocity in any set of circumstances was dependent to a considerable extent upon the previous treatment of the surface, but by standardizing the procedure, both in cleaning the vessels and in making the measurements comparable, results could be obtained, and the reaction rate reproduced within about 10% in duplicate series of runs at different pressures. The rate of change of pressure was in each case corrected for the volume of the pressure gauge and connecting tubing. The results obtained are given in Table II.

TABLE II—SLOW REACTION AT 530° C. IN PYREX VESSELS  
 $[\text{CH}_4]/[\text{O}_2] = 1$

Vessel diameter (mm.)	Number of sections	Reaction velocity at total pressure P (mm. Hg/min.)			Reaction order <i>n</i>
		P = 150	P = 200	P = 300	
5.0	19	—	0.61	6.11	5.7
7.5	9	0.76	2.66	14.3	4.2
11.1	4	0.98	2.72	18.3	4.2
16.7	2	1.31	4.25	18.1	3.9
28.1	1	1.66	4.09	22.1	3.8
37.5	1	1.72	5.83	27.5	3.7

The reaction velocity figures are each mean values of between two and four determinations, which when taken as a whole show a standard deviation from their means of approximately 10%, indicating the degree of agreement obtainable. This figure for the error includes measurements taken from time to time on the same vessel or on different vessels of the same diameter, and may therefore be taken to include variations in the catalytic activity of the surface from vessel to vessel. The calculated order of reaction *n* is given, and is seen to be approximately four except for the smallest vessel, and is in agreement with equation (1), which for equimolecular mixtures of methane and oxygen requires a value of *n* = 4.

An examination of the data of Table II shows that, in spite of a wide variation with pressure, there is a general tendency for the velocity to decrease as the diameter of the reaction vessel is reduced. With the smallest vessel used the effect is very much greater than for the larger

vessels, and the apparent order of reaction has increased considerably. This suggests that a surface effect of a different order becomes effective for high surface to volume ratios, particularly in view of the complete inhibition of the reaction obtained by Fort and Hinshelwood\* on packing their vessels with silica tubes. In order to find whether similar inhibition by packing occurred with our conditions of experiment, we carried out several determinations with packed vessels of a surface to volume ratio equal to that of a cylindrical vessel of 2 mm. diameter, which fully confirmed the almost complete inhibition observed by the earlier workers. There thus appears to be a critical diameter (2 to 5 mm.) below which the reaction is strongly inhibited, and above which a less marked but quite definite inhibition by surface occurs. It is interesting that similar results were obtained by Spence† in the oxidation of acetylene, when he found a limiting diameter (4 to 6 mm.) of vessel below which strong inhibition occurred, but above which reaction proceeded with a steady velocity nearly independent of diameter. This remarkable effect will be referred to later in the discussion, where it is represented as a consequence of the theory of degenerate branching of reaction chains.

The general effect of surface is shown graphically in fig. 4, in which the results at different pressures have been combined by dividing the reaction velocity by the fourth power of the pressure and plotting the mean value for each vessel diameter, a procedure which reduces the probable error in the value adopted for any particular vessel.

*Transition from Slow Reaction to Ignition*—We have shown‡ for the hydrogen oxygen reaction catalysed by nitrogen peroxide that by a steady change in one of the variables of the system (e.g., concentration of nitrogen peroxide or oxygen) a transition can be effected from a region of slow reaction to one of ignition, and that the length of the induction period varies continuously in passing from one region to the other.

Similar measurements have been carried out with an equimolecular mixture of methane and oxygen, the transition from slow reaction to explosion being brought about by increasing the total pressure of the mixture. At 720° C. with a 23 mm. quartz reaction vessel, a pressure limit of ignition was reached at a total pressure of 270–280 mm. Below this pressure, the increasing reading on the pressure gauge indicated a rapidly accelerating reaction which reached a well-defined maximum rate in the course of a few seconds, and fell soon afterwards to zero, after which a

\* Proc. Roy. Soc., A, vol. 134, p. 578 (1932).

† J. Chem. Soc., p. 686 (1932).

‡ Foord and Norrish, Proc. Roy. Soc., A, vol. 152, p. 196 (1935).

slow steady fall of pressure occurred, presumably due to combustion of carbon monoxide formed in the main reaction. Above the critical pressure, the same type of growth of reaction was observable, but terminated in a sharp momentarily large increase in pressure as a visible general ignition occurred in the reaction vessel. The point of particular importance arising from these experiments is that a plot of induction period against total pressure is a continuous curve (fig. 5), provided that the induction period of the slow reaction is measured to the time of

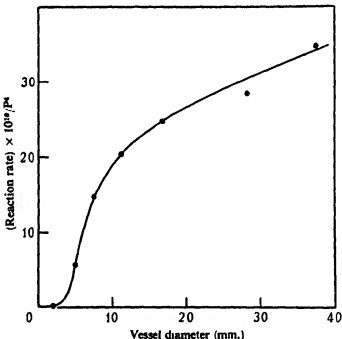


FIG. 4—Variation of slow reaction velocity with vessel diameter.

*maximum rate*, and not to the onset of the observable pressure change. This leads to the conclusion that whatever be the mechanism of the growth of the reaction during the induction period, ignition is a thermal process following the attainment of a critical reaction velocity.

*Effect of Reaction Products*—To determine whether the products of the reaction had any retarding influence on the slow reaction, the rate of reaction at 530° C. was measured with and without addition of carbon monoxide, carbon dioxide, and water vapour. Using 200 mm. of the methane oxygen mixture, addition of up to 150 mm. of either carbon dioxide or water vapour had no other effect on the velocity of the reaction

than the normal increase approximately proportional to the total pressure obtained by addition of an inert gas. Carbon monoxide in small quantities (up to 30 mm.) had no appreciable effect on the reaction rate as mentioned by the rate of rise of pressure. With larger amounts, combustion of the carbon monoxide with its attendant fall in pressure rendered it impossible to measure the methane combustion rate by observation of the pressure change.

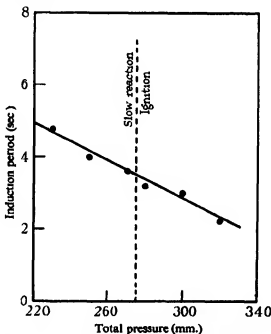


FIG. 5.—Continuity of induction period for ignition and slow reaction of  $\text{CH}_4$  and  $\text{O}_2$  at  $720^\circ \text{C}$ . Concentration:  $[\text{CH}_4] = [\text{O}_2] = P/2$ . ● Time of maximum rate of slow reaction; ○ time of ignition.

*Relation Between Ignition Temperature and Total Pressure*—Early in the present work an attempt was made to extend the work of Neumann and Serbinov,\* in which the existence of three pressure limits of ignition over a limited temperature range was described. The results obtained, using a mixture of methane and oxygen in equimolecular proportions, will not be elaborated as they merely confirm further work of the above authors† which appeared soon afterwards, describing the

\* "Nature," vol. 128, p. 1040 (1931); "J. phys. Chem., Russia," vol. 3, p. 75 (1932).

† *Ibid.*, vol. 4, p. 433 (1933).

disappearance of these limits with the proportions used by us, a result which has recently been repeated with methane-air mixtures.\* A matter of immediate importance, however, is the difficulty experienced in this work of repeating an ignition temperature determination after a period of several days. Differences of the order of 10° to 20° C. were observed in this way, presumably owing to a gradual change in the catalytic activity of the surface. Measurements with two sizes of reaction vessel gave the qualitative result that the one of largest diameter gave slightly lower ignition temperatures.

*Effect of Sensitizers and Inhibitors*—The effect of the addition of hydrochloric acid gas on the ignition temperature of an equimolecular mixture

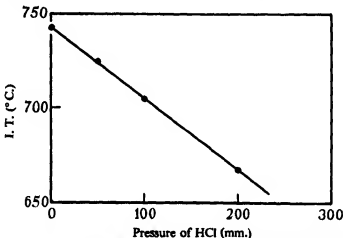


FIG. 6—Effect of HCl on ignition temperature. Concentrations:  $[CH_4] = [O_2] = 100$  mm. at 500° C.

of methane and oxygen is shown in fig. 6. It is seen to have a mild sensitizing action. The importance of this fact in studying the mechanism of the reaction will appear in view of the observation of Medvedev† that small amounts of hydrochloric acid considerably raise the yield of formaldehyde in the catalytic oxidation of methane.

Chlorine in much smaller quantities has at first an anticatalytic effect (fig. 7), but addition of more than 10 mm. of chlorine reverses the effect, possibly due to hydrochloric acid formed by the interaction of methane and chlorine.

Iodine has been shown by Bone and Allum to increase the velocity of

\* Naylor and Wheeler, 'J. Chem. Soc.', p. 1427 (1935).

† 'Trans. Karpov. Inst. Chem.', No. 3, p. 54 (1924); No. 4, p. 117 (1925).

the slow reaction at 447° C., and to remove the induction period. In the present work, addition of considerably smaller amounts of iodine (0.1%) had no effect on the main reaction velocity, but reduced the induction period from three minutes to one minute at 460° C. At higher temperatures, on the other hand, iodine was found to act as a powerful anti-

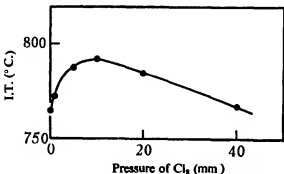


FIG. 7—Effect of  $\text{Cl}_2$  on ignition temperature. Concentrations:  $[\text{CH}_4] = [\text{O}_2] \approx 100 \text{ mm. at } 500^\circ \text{ C.}$

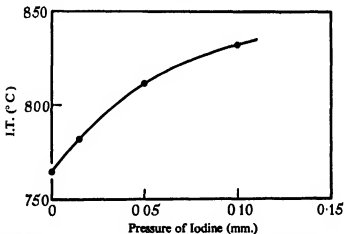


FIG. 8—Effect of iodine on ignition temperature. Concentrations:  $[\text{CH}_4] = [\text{O}_2] = 100 \text{ mm. at } 500^\circ \text{ C.}$

catalyst, as shown by the curve of fig. 8, the ignition temperature of the methane oxygen mixture being raised 100° C. by 0.1 mm. of iodine.

The effect of small amounts of formaldehyde on the slow reaction at 550° C. was investigated. A pyrex reaction vessel 27 mm. in diameter and an equimolecular methane oxygen mixture at a total pressure of 200 mm. were used. The final steady reaction velocity attained was in no

way affected by the addition of up to 5 mm. of formaldehyde, but the induction period was progressively reduced and practically disappeared with the addition of 2 mm. of the aldehyde (fig. 9).

### DISCUSSION

The results described may be summarized as follows:

(1) In the neighbourhood of 480° C., the reaction between methane and oxygen exhibits a marked induction period during which no appreciable change of pressure occurs.

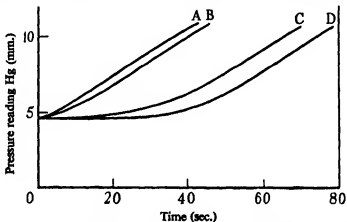


FIG. 9—Effect of HCHO on slow reaction.  $[CH_4] = [O_2] = 100$  mm.

Curve .....	A	B	C	D
HCHO pressure on mm. Hg .....	5	2	0.5	0

able change of pressure occurs. This is followed by a pressure increase in the system which reaches a steady maximum rate given by:

$$\text{Rate} = k [CH_4]^n [O_2] P,$$

where  $P$  is the total pressure.

(2) The magnitude of  $k$  in the above expression is strongly dependent upon the catalytic activity of the surface of the vessel, while for small diameters, a marked dependence upon the linear dimensions of the reaction vessel is superimposed.

(3) The reaction is almost completely inhibited by packing the reaction vessel with small diameter quartz tubing, as was shown by Fort and Hinshelwood.

(4) Ignition occurs by a thermal process when the velocity of the slow reaction reaches a sufficiently high value for the system to become self-heating.

(5) Carbon monoxide, carbon dioxide, and water vapour have no appreciable influence on the velocity of the slow reaction other than that normally obtained with an inert gas.

(6) Hydrochloric acid has a sensitizing action in reducing the ignition temperature.

(7) Chlorine at low pressures inhibits the reaction, but at high pressures catalyses it.

(8) Iodine has a marked anticatalytic effect in the neighbourhood of the ignition temperature. At lower temperatures it has a slight effect on the slow reaction velocity, but brings about a large reduction of the induction period.

(9) Addition of small amounts of formaldehyde removes the induction period of the slow reaction, as was also found by Bone and Allum,\* but does not alter the maximum velocity of reaction.

To these data may be added some important results obtained by other workers.

(10) Nitrogen peroxide has a strong sensitizing action, 1 or 2% reducing the ignition temperature by more than 100° C.†

(11) Hydrochloric acid catalyses the production of formaldehyde in the catalytic oxidation of methane.‡

*Slow Reaction*—The marked induction periods, followed by the gradual increase in the reaction velocity, the catalytic effect of small quantities of nitrogen peroxide and other substances, and the inhibiting effect of traces of iodine and chlorine at high temperatures, all indicate that a chain mechanism is involved, and the remarkable increase in velocity produced by the addition of inert gas shows that the active chain carriers are destroyed at the surface. Fort and Hinshelwood pointed out that the form of the pressure-time curves is such as to suggest that the main reaction is developing from some intermediate whose concentration is tending towards an equilibrium value at which the rates of production and removal are equal, and Semenoff further showed how the development of the maximum velocity from zero in the space of minutes could be interpreted in terms of a branching chain mechanism of the type termed degenerate. According to these ideas, we must conclude that in the present instance methane is oxidized by a straight chain with the production of a comparatively stable intermediate, which by its subse-

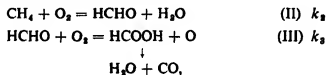
\* 'Proc. Roy. Soc.,' A, vol. 134, p. 578 (1932).

† Norrish and Wallace, 'Proc. Roy. Soc.,' A, vol. 145, p. 307 (1934).

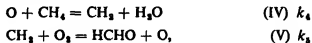
‡ Medvedev, 'Trans. Karpov. Inst. Chem.,' No. 3, p. 54 (1924); No. 4, p. 117 (1925).

quent oxidation is capable from time to time of starting fresh methane chains. There is thus established a process of delayed branching which, if the effective branching factor  $\phi$  is positive, will cause a growth of the reaction rate. The reaction will first start very slowly from certain adventitious centres, but after a period of induction, during which the intermediate is growing in concentration, the reaction will proceed more and more rapidly until in the absence of other factors the rate would tend to infinity by an exponential law. The rate will, however, reach a maximum value if an equilibrium concentration of intermediate is reached at which its rate of oxidation is equal to its rate of production, and this can only occur if the value of  $\phi$  is reduced to zero during the progress of the reaction.

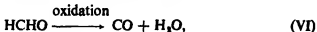
The atom chain hypothesis requires but slight modification to take into account these requirements. Although immaterial, it is probable that the first oxygen atoms are produced from traces of formaldehyde formed at the surface, by reactions such as:



but any other adventitious production of a few oxygen atoms in the gas phase will serve as well. Once they are formed, formaldehyde may be assumed steadily to increase in concentration by the operation of a straight chain of the type:



while from the formaldehyde fresh chains may occasionally start by the reaction (III) above. Alternatively the formaldehyde may be removed by oxidation without forming a chain, and this will be represented by



since the principal products of the reaction are carbon monoxide and water.

The growth of the formaldehyde concentration is given by the relation:

$$\frac{d}{dt} [\text{F}] = \theta + \phi [\text{F}], \quad (2)$$

where  $\theta$  is the rate of production by the primary process,  $[F]$  the concentration of formaldehyde, and  $\phi [F]$  the rate of production by the branching mechanism. Now, at the beginning of the induction period, the velocity is immeasurably small, and the primary process must therefore be negligible in magnitude compared with the process generating centres from formaldehyde in the later stages of the reaction. Under these circumstances, the term  $\theta$  may be neglected, and the concentration of formaldehyde will therefore grow according to the relation:

$$[F] = Ae^{\alpha t}. \quad (3)$$

This will increase indefinitely unless the value of  $\phi$  is reduced to zero, which will then give a point of maximum velocity. According to the relation given by Semenoff,  $\phi$  in the present instance will be given by the equation:

$$\phi [F] = k_3(v - 1)[O_2][F] - R, \quad (4)$$

where  $v$  is the chain length of reactions (IV) and (V), and  $R$  is the rate of removal of formaldehyde by reaction (VI).  $\phi$  may be reduced to zero by reduction of  $v$  or an increase in  $R$ , and a choice between these two possibilities necessitates some assumption as to the mechanism of oxidation of the formaldehyde. This oxidation is known to occur by a chain mechanism, and in view of the fact that the chief products of reaction are carbon monoxide and water, and not carbon dioxide, we shall assume that at these high temperatures oxidation occurs by a process in which the primary step is the reaction of a formaldehyde molecule with an oxygen atom, the latter being regenerated in a subsequent link of the formaldehyde oxidation chain, together with carbon monoxide. The initial reaction will be represented by:



and is part of the complete process represented by reaction (VI). Under these circumstances,  $\phi$  will fall to zero as  $R$  increases by the growth of the concentration of oxygen atoms in the system.

We have now a complete scheme explaining the existence of the induction period and the slow growth of the reaction to a maximum value, and it remains to deduce an expression for the velocity of the slow reaction.

**Formaldehyde Equilibrium**—At the point of maximum velocity, the rates of production and removal of formaldehyde are equal. If  $k_1[F][O]$

be the rate of the straight chain oxidation of formaldehyde, of which reaction (VII) is the initial step, then

$$\frac{d}{dt} [F] = \text{zero} = k_4 [\text{CH}_4] [\text{O}] - k_7 [\text{F}] [\text{O}], \quad (5)$$

neglecting the comparatively small effect of reaction (III). Whence,

$$[\text{F}] = \frac{k_4}{k_7} [\text{CH}_4]. \quad (6)$$

*Oxygen Atom Equilibrium*—The equilibrium of oxygen atoms is controlled by their rate of production and the rate of their removal, which in the latter case is considered to occur in two ways:

1—At the surface



2—At high pressures in the body of the gas, in accord with the fact that methyl alcohol is formed in increasing quantities at high pressures,



Then putting  $\frac{d}{dt} [\text{O}] = \text{zero}$ , for equilibrium,

$$k_8 [\text{F}] [\text{O}_2] = \frac{k_9 S}{Pd} [\text{O}] + k_9 [\text{CH}_4] [\text{O}] P, \quad (7)$$

S being the surface activity per unit area, P the total pressure,  $1/P$  proportional to the diffusion coefficient of centres through the gas, and  $d$  the diameter of the vessel. Thus,

$$[\text{O}] = \frac{k_8 [\text{F}] [\text{O}_2] Pd}{k_9 S + k_9 [\text{CH}_4] P^2 d}. \quad (8)$$

The rate of reaction is given by :

$$\frac{d}{dt} [\text{CH}_4] = k_4 [\text{CH}_4] [\text{O}] \quad (9)$$

$$= \frac{k_9 k_8 [\text{CH}_4] [\text{F}] [\text{O}_2] Pd}{k_9 S + k_9 [\text{CH}_4] P^2 d}. \quad (10)$$

Thus the maximum velocity is attained when the concentration of aldehyde reaches its maximum value, as is readily seen to occur from the experimental curves for ethane and ethylene obtained by Bone and his co-workers.\*

\* Bone, Haffner, and Rance, ' Proc. Roy. Soc.,' A, vol. 143, p. 16 (1933); Bone and Hill, ' Proc. Roy. Soc.,' A, vol. 129, p. 434 (1930).

Eliminating [F] from equations (10) and (6),

$$\frac{d}{dt} [\text{CH}_4] = \frac{k_3 k_4^*}{k_7} \frac{[\text{CH}_4]^2 [\text{O}_2] P d}{k_8 S + k_9 [\text{CH}_4] P^2 d}. \quad (11)$$

The pressure change in the system occurs as a result of the oxidation of the formaldehyde, the production of aldehyde in the chain occurring without change of volume. However, the rate of oxidation of aldehyde at the point of maximum velocity is equal to the rate of its production from methane, so that the latter may be taken as accurately represented by the rate of change of pressure. Neglecting the gas phase deactivation term from equation (11), as only being of importance at high pressures, we obtain

$$\frac{d}{dt} [\text{CH}_4] = \frac{k_3 k_4^* [\text{CH}_4]^2 [\text{O}_2] P d}{k_7 k_8 S}. \quad (12)$$

in agreement with the experimental results obtained on pp. 508, 510.

This expression shows how the maximum velocity can vary with the catalytic activity of the surface (S), and indicates that the velocity should be a linear function of the diameter of the vessel, and though on account of the difficulty of standardizing S it is hard to prove the latter, the results of Table II show such a variation in a qualitative way.

One of the most remarkable effects observed in this and in similar reactions, however, is the *completeness* of the inhibition in packed vessels. This inhibition is so great that it cannot be produced by the operation of the *d* factor in equation (12). It must be remembered also that this equation refers to the maximum velocity, while the effect of packing is rather to prolong the induction period to infinity. In our opinion, the effect of packing is to reduce the value of  $\phi$  in equation (3) to zero or some negative value at an early stage, by reducing the value of  $v$ , the chain length (equation (4)). For a straight chain,  $v$  is proportional to  $d^4$ ; thus it follows that for vessels of a diameter less than a limiting value  $\phi$  becomes negative and the reaction can never develop. This corresponds to an infinite induction period, and it is evident that practically complete inhibition will result if the effective diameter of the packed vessel is very small. It seems possible that an explanation of this kind will account also for the results of Spence\* in the oxidation of acetylene in which a similar critical diameter below which oxidation is inhibited is evident.

*Ignition*—The evidence presented on p. 513 shows that the process of ignition of methane is of a thermal kind. As the pressure of the reactants

\* 'J. Chem. Soc.,' p. 686 (1932).

is increased, the velocity of the slow reaction is progressively increased up to large values, until finally ignition occurs. In agreement with this, the induction periods measured to the point of maximum velocity or ignition fall on a smooth curve, showing that the process of development of the reaction is the same for slow reaction as for ignition.

As a general condition for ignition, we may therefore write:

$$\frac{d}{dt} [\text{CH}_4] = K, \quad (13)$$

where  $K$  represents a limiting velocity beyond which the reaction process ceases to be isothermal, and becomes self-heating.

Referring to the coefficients in equation (11),  $k_3$ , corresponding to reaction (III) is the only one which will show marked temperature dependence. All the others, which refer to processes involving atoms of oxygen or free radicals, will probably be but slightly affected by change of temperature. The condition for ignition may therefore be written

$$K' = \frac{[\text{CH}_4]^n [\text{O}_2] P d e^{-\frac{E}{RT}}}{k'_S + [\text{CH}_4] P^a d}. \quad (14)$$

At atmospheric pressure, when the second term of the denominator is negligible, we therefore have:

$$\frac{E}{RT} + B = \log \frac{[\text{CH}_4]^n [\text{O}_2] P d}{S}. \quad (15)$$

Thus the ignition temperature is markedly dependent on  $S$  the specific catalytic activity of the surface, as has been found, and is also seen to be the higher the smaller the diameter of the vessel, in agreement with observation. The expression is in accord with the experimental equation of Sagulin,\*

$$\log p = \frac{A}{T} + B, \quad (16)$$

where  $p$  is the total pressure of a mixture of methane and oxygen of constant composition.

At high pressures, when the first term in the denominator of equation (14) is small compared with the second, the ignition temperatures will be given by the equation:

$$\frac{E}{T} + B = \log \frac{[\text{CH}_4] [\text{O}_2]}{P}.$$

\* "Z. phys. Chem.," B, vol. 1, p. 275 (1928).

This gives a falling ignition temperature with rise of pressure, the rate of change with pressure falling off towards high pressures, properties which have been realized experimentally.\*

*Effect of Formaldehyde*—It has been shown above (fig. 9) that while successive additions of formaldehyde progressively reduce the induction period of the slow reaction there is no effect on the ultimate velocity. This is to be expected on the view that the induction period is concerned with the development of the concentration of formaldehyde to the equilibrium value which governs the velocity of reaction. Thus addition of formaldehyde eliminates the early stages of the induction period, but has no influence on the subsequent equilibrium concentration of formaldehyde, which is dependent only on the temperature and concentration of methane (*see equation (6)*). If, therefore, formaldehyde be added at this equilibrium concentration the induction period will be suppressed altogether.

*Inhibitors and Catalysts*—It has been shown that any factor which changes  $v$  or  $k_s$ , and thus affects the value of  $\phi$  (*equation (4)*) will have a considerable influence on the development of the reaction. It is possible that an effect of this character is responsible for the mild catalytic effect of hydrochloric acid (fig. 6), while the dual effect of iodine may be similarly interpreted. At high temperatures in the region of ignition iodine acts as an anticatalyst, a small quantity producing a considerable rise in the ignition temperature (fig. 8). At lower temperatures, however, in the region of slow reaction, it catalyses the reaction during the induction period while having no appreciable effect on the final maximum velocity. The exact mechanism of these opposing effects is somewhat uncertain, but may readily be explained in terms of *equation (4)* if it be assumed that iodine exerts a catalytic or an inhibitory influence on each of the processes represented by the two terms of this equation. Addition of iodine will then either catalyse or inhibit the reaction as a whole according as the value of  $\phi$  is increased or decreased by the combined changes in the two terms, and both these possibilities may be realized within different ranges of temperature.

It may be said that the kinetic results previously established, together with the new results presented in this paper, are in accord with the chain mechanism previously suggested, modified to take account of the theory of degenerate branching.

*Note on Recent Work*—Since the completion of the manuscript for this paper, two papers dealing with the combustion of methane have appeared

\* Townend and Chamberlain, 'Proc. Roy. Soc.,' A, vol. 154, p. 95 (1936).

which may briefly be discussed in the light of the present theory. Bone and Gardner\* have investigated the combustion of methane, and also the combustion of its possible oxidation products according to the hydroxylation theory. Decreasing the diameter of the reaction vessel over a twofold range retarded the slow reaction, in qualitative agreement with our work. The concentration of formaldehyde present was measured at various stages during the reaction. It was found to increase during the induction period and reach a steady value at the point of maximum velocity, which is an essential feature of the mechanism adopted in the present paper. The fact that very little formaldehyde was detectable during the first half of the induction period is just what is to be expected on the theory of degenerate branching, since the growth in concentration of the formaldehyde is of an exponential character, and the rate vanishingly small in the earlier stages. If, on the other hand, methyl alcohol is formed in any measurable quantity during these earlier stages, as is considered possible by Bone and Gardner, there would be a reduction of pressure which is not observed in practice. It is also of great significance that the addition of small amounts of formaldehyde progressively reduces and finally removes the induction period, whereas the addition of considerably larger amounts of methyl alcohol, as Bone and Gardner have shown, while reducing it does *not* remove it, in confirmation of the view that the essential preliminary to the development of the reaction is the initial formation of formaldehyde. If methyl alcohol be added, the formation of formaldehyde is obviously facilitated and the induction period reduced, but since time is required for the oxidation of the alcohol, the induction period can never be completely eliminated.

In a second paper, Newitt and Gardner† have shown that methyl alcohol in quantities comparable with the formaldehyde may be isolated during the combustion of methane at pressures of the order of one atmosphere if the gas mixture be drawn through the pores of a hot porcelain tube at the centre of the reaction vessel. The difference in experimental technique required to obtain this result indicates that the catalytic production of methyl alcohol at a surface may occur, quite possibly as a preliminary to the formation of formaldehyde; but this evidence can have no bearing on the origin of formaldehyde in the homogeneous chain reaction. In the experiments of Newitt and Gardner the length of the chains in the pores will be cut down to negligible dimensions, while the primary surface reaction will be enormously increased. Thus while methyl alcohol may precede the formation of formaldehyde at the surface

\* Proc. Roy. Soc., A. vol. 154, p. 297 (1936).

† Proc. Roy. Soc., A, vol. 154, p. 329 (1936).

this will in no way affect the explanation given above, for there is no evidence that it plays any part in the main chain propagation which constitutes the homogeneous oxidation process.

The authors desire to express their thanks to the Royal Society and to Imperial Chemical Industries, Ltd., for grants which have made this work possible.

#### SUMMARY

The kinetics of the combustion of methane have been investigated with particular reference to the slow reaction. The velocity of the reaction has been found to be proportional to the square of the concentration of methane and the first power of the concentration of oxygen, and approximately proportional to the total pressure. The effect of surface has been examined and the almost complete inhibition of the reaction in packed vessels confirmed. Ignition has been shown to be a thermal process consequent upon the attainment of a critical reaction velocity. The inhibiting and catalytic properties of various added substances have been determined by their effect on both the slow reaction and the ignition temperature. A kinetic mechanism for the combustion of methane has been proposed, based on the atom chain theory originally suggested by one of us and modified to include the phenomenon of degenerate branching, and has been found substantially to represent the experimental data. An explanation of the complete inhibition of certain reactions by packing or reduction of vessel diameter is advanced.

---

## The Forces on a Circular Cylinder Submerged in a Uniform Stream

By T. H. HAVELOCK, F.R.S.

(Received 18 August, 1936)

1—Although many investigations have been made on the wave resistance of submerged bodies, no case has been solved completely in the sense of taking fully into account the condition of zero normal velocity at the surface of the body. The simplest case is that of the two-dimensional motion produced by a long circular cylinder, with its axis horizontal and perpendicular to the stream, submerged at a certain depth below the upper free surface. This problem was propounded many years ago by Kelvin, and it was solved later, as regards a first approximation, by Lamb; in that solution the cylinder was replaced by a doublet, and the effect of the disturbance at the surface of the cylinder was neglected. Applying the method of images, I examined a second approximation,<sup>†</sup> and also by the same method obtained a first approximation for the vertical force on the cylinder.<sup>‡</sup>

Although the problem is not in itself of practical importance, it seems of sufficient interest to obtain a more complete analytical solution, and this is given in the present paper. The solution contains an infinite series, whose coefficients are given by an infinite set of linear equations; expansions are given for the coefficients in terms of a certain parameter, and corresponding expressions obtained for both the wave resistance and the vertical force. Numerical calculations have been made from these for various velocities and for different ratios of the radius of the cylinder to the depth of its axis. These confirm the general impression that the first approximation is a good one over a considerable range. The effect of the complete expressions appears in an increase in the wave resistance at lower velocities and a slight decrease at high velocities; this may be described as due largely to a shifting of the maximum of resistance towards the lower velocities, an effect which might have been anticipated.

The similar three-dimensional problems of the submerged sphere, or spheroid, are of more practical interest, as the first approximations which I have given for these cases have had certain applications in ship resis-

<sup>†</sup> 'Proc. Roy. Soc.,' A, vol. 115, p. 268 (1926).

<sup>‡</sup> 'Proc. Roy. Soc.,' A, vol. 122, p. 387 (1928).

tance; the corresponding extension of the solutions would require more complicated analysis than for the two-dimensional case, but it seems probable that the general deductions on the range of applicability of the approximate formulae would be of a similar character.

2—Consider the two-dimensional fluid motion due to a fixed circular cylinder, of radius  $a$ , placed in a uniform stream of great depth, the axis of the cylinder being at a depth  $f$  below the undisturbed surface of the stream. Take the origin at the centre of the circular section, with  $Ox$  horizontal and  $Oy$  vertically upwards, and suppose the stream to be of velocity  $c$  in the negative direction of  $Ox$ . We write the velocity potential of the motion as

$$\phi = cx + \phi_0. \quad (1)$$

To obtain a solution which gives regular waves to the rear of the cylinder, we adopt the hypothesis of a frictional force proportional to the deviation of the fluid velocity from the uniform flow  $c$ , thus introducing a coefficient  $\mu'$  which is made zero after the various analytical calculations have been effected. The pressure is then given by†

$$\frac{p}{\rho} = \text{const} - gy + \mu' \phi_0 - \frac{1}{2} q^2. \quad (2)$$

If  $\eta$  is the surface elevation and we make the usual approximation for small surface disturbances, we have

$$-c \frac{\partial \eta}{\partial x} = -\frac{\partial \phi}{\partial y}; \quad y = f. \quad (3)$$

Hence, from (2), the condition to be satisfied at the free surface is

$$\frac{\partial^2 \phi_0}{\partial x^2} + \kappa_0 \frac{\partial \phi_0}{\partial y} - \mu \frac{\partial \phi_0}{\partial x} = 0; \quad y = f, \quad (4)$$

where  $\kappa_0 = g/c^2$ , and  $\mu = \mu'/c$ .

We may regard  $\phi_0$  as made up of two parts, one part having singularities within the circle  $r = a$ , and the other having singularities in the region of the plane for which  $y > f$ . The first part is the potential of a system of sources and sinks, of total strength zero, within the circle, and can clearly be expressed by the real part of a series

$$\sum_1^{\infty} A_n z^{-n}, \quad (5)$$

† Lamb, "Hydrodynamics," 6th ed., p. 399.

where  $z = x + iy$ , and the coefficients are complex. Now we have

$$z^{-n} = \frac{(-i)^n}{(n-1)!} \int_0^\infty \kappa^{n-1} e^{i\kappa z} d\kappa, \quad y > 0. \quad (6)$$

Hence, in order to satisfy (4), we write  $\phi_0$  in the form

$$\phi_0 = \int_0^\infty F(\kappa) e^{i\kappa x - i\kappa y} d\kappa + \int_0^\infty G(\kappa) e^{i\kappa x + i\kappa(y-2f)} d\kappa, \quad (7)$$

where the real part is to be taken, and

$$F(\kappa) = \sum_1^\infty (-i)^n A_n \kappa^{n-1} / (n-1)!. \quad (8)$$

Putting (7) in (4), we obtain

$$G(\kappa) = -\frac{\kappa + \kappa_0 + i\mu}{\kappa - \kappa_0 + i\mu} F(\kappa). \quad (9)$$

With this value in (7) the surface condition is satisfied. Further, we may change the sign of  $i$  throughout the second term of (7), and we obtain

$$\phi_0 = \int_0^\infty F(\kappa) e^{i\kappa x - i\kappa y} - \int_0^\infty \frac{\kappa + \kappa_0 - i\mu}{\kappa - \kappa_0 - i\mu} F^*(\kappa) e^{-i\kappa x + i\kappa(y-2f)} d\kappa, \quad (10)$$

where the real part is to be taken, and the asterisk denotes the conjugate complex quantity. It may be noted that this method of satisfying the condition at the free surface is quite general, and independent of the form of the submerged body.

It is convenient for the present problem to alter the notation slightly from (8), and we write

$$\left. \begin{aligned} F(\kappa) &= -ica^3 f(\kappa) \\ f(\kappa) &= b_0 + b_1(\kappa a) + \frac{b_2}{2!} (\kappa a)^2 + \frac{b_3}{3!} (\kappa a)^3 + \dots \end{aligned} \right\}. \quad (11)$$

Further, the expression (10) is a function of the complex variable  $z$ ; hence we have for the complex potential function  $w$ , or  $\phi + i\psi$ ,

$$w = cz - ica^3 \int_0^\infty f(\kappa) e^{i\kappa z} d\kappa - ica^3 \int_0^\infty \frac{\kappa + \kappa_0 - i\mu}{\kappa - \kappa_0 - i\mu} f^*(\kappa) e^{i\kappa z - 2\pi f} d\kappa, \quad (12)$$

this being in a form valid in the liquid in the region  $y > 0$ , it also being noted that ultimately  $\mu$  is to be made zero.

3.—We have now to determine the function  $f(\kappa)$  so as to satisfy the condition  $\partial\phi/\partial r = 0$  for  $r = a$ . For this we turn the second term in

(12) back to the form (5); it gives, with the form (11) for  $f(\kappa)$ , the series

$$\sum_{n=1}^{\infty} ca^n (ia)^{n-1} b_{n-1} z^{-n}. \quad (13)$$

Further, the last term in (12) represents the potential of image sources and sinks in the region of the plane for which  $y > f$ , and hence it can be expanded in the neighbourhood of the circle  $|z| = a$  in a series of ascending powers of  $z$ . Thus we obtain  $w$  in the form

$$w = \text{const} + cz + \sum_{n=1}^{\infty} ca^n (ia)^{n-1} b_{n-1} z^{-n} + \sum_{n=1}^{\infty} B_n z^n,$$

$$B_n = ca^n \frac{(-i)^{n+1}}{n!} \int_0^\infty \frac{\kappa + \kappa_0 - i\mu}{\kappa - \kappa_0 + i\mu} \kappa^n e^{-2\pi\kappa f} f^*(\kappa) d\kappa. \quad (14)$$

With the potential in the form

$$w = \text{const} + \sum_{n=1}^{\infty} (C_n z^n + D_n z^{-n}), \quad (15)$$

the condition of zero normal velocity on the circle  $|z| = a$  is satisfied, provided

$$D_n = a^{2n} C^*_n. \quad (16)$$

Hence, from (14) we obtain the equations

$$b_0 = 1 - a^2 \int_0^\infty \frac{\kappa + \kappa_0 + i\mu}{\kappa - \kappa_0 + i\mu} \kappa f(\kappa) e^{-2\pi\kappa f} d\kappa,$$

$$b_{n-1} = - \frac{a^{n+1}}{n!} \int_0^\infty \frac{\kappa + \kappa_0 + i\mu}{\kappa - \kappa_0 + i\mu} \kappa^n f(\kappa) e^{-2\pi\kappa f} d\kappa. \quad (17)$$

These relations, with (11), may be expressed in the form of an integral equation satisfied by the function  $f(\kappa a)$ ; it is easily found to be

$$v^{\frac{1}{2}} f(v) = v^{\frac{1}{2}} - \int_0^\infty \frac{u + \gamma + i\mu}{u - \gamma + i\mu} e^{-2\pi u/v} u^{\frac{1}{2}} f(u) I_1(2\sqrt{uv}) du, \quad (18)$$

where  $\gamma = \kappa_0 a$ ,  $I_1$  is the modified Bessel function, and the limit of the integral is to be taken as the positive quantity,  $\mu$  approaches zero.

For purposes of calculation, we use (17) as a set of linear equations for the coefficients  $b_0, b_1, \dots$ . We write

$$q_n = \lim_{\mu \rightarrow 0} \int_0^\infty \frac{u + 1 + i\mu}{u - 1 + i\mu} e^{-2\pi u/v} u^n du. \quad (19)$$

Substituting the power series (11) for  $f(\kappa)$  on the right of (17), we obtain the infinite set of equations

$$\left. \begin{aligned} b_0(1 + q_1\gamma^2) + q_2\gamma^3 b_1 + \frac{q_3\gamma^4}{2!} b_2 + \frac{q_4\gamma^5}{3!} b_3 + \dots &= 1 \\ \frac{q_2\gamma^4}{2!} b_0 + \left(1 + \frac{q_3\gamma^4}{2!}\right) b_1 + \frac{q_4\gamma^5}{2!2!} b_2 + \frac{q_5\gamma^6}{2!3!} b_3 + \dots &= 0 \\ \frac{q_3\gamma^4}{3!} b_0 + \frac{q_4\gamma^5}{3!} b_1 + \left(1 + \frac{q_5\gamma^6}{2!3!}\right) b_2 + \frac{q_6\gamma^7}{3!3!} b_3 + \dots &= 0 \\ \dots &= 0 \end{aligned} \right\}. \quad (20)$$

From the integral expression for  $q_n$  given in (19), and also the fact that  $a/f < 1$ , it can readily be shown that the infinite determinant formed by the coefficients of  $b_0, b_1, \dots$ , on the left of (20) is convergent.

Evaluating the expression (19) and putting

$$q_n = r_n - is, \quad (21)$$

we find

$$\begin{aligned} r_n &= \frac{n!}{\alpha^{n+1}} + 2 \left\{ \frac{(n-1)!}{\alpha^n} + \frac{(n-2)!}{\alpha^{n-1}} + \dots + \frac{1}{\alpha} - e^{-s} \text{li}(e^s) \right\}, \\ s &= 2\pi e^{-s}, \end{aligned} \quad (22)$$

where  $\alpha = 2\kappa_0 f$ , and  $\text{li}$  denotes the logarithmic integral.

For any given values of  $a, f$ , and  $c$ , we have in (20) a set of equations for the  $b$ 's with complex numerical coefficients.

Although expansions in terms of other parameters may be more suitable for special ranges, it is convenient to assume that the coefficients  $b$  can be expanded in power series of the quantity  $\gamma$ , that is  $\kappa_0 a$ . These expansions will be of the form

$$\left. \begin{aligned} b_0 &= 1 + b_{02}\gamma^2 + b_{04}\gamma^4 + b_{06}\gamma^6 + \dots \\ b_1 &= b_{13}\gamma^3 + b_{15}\gamma^5 + b_{17}\gamma^7 + \dots \\ b_2 &= b_{24}\gamma^4 + b_{26}\gamma^6 + b_{28}\gamma^8 + \dots \\ \dots &= \dots \end{aligned} \right\}. \quad (23)$$

Substituting in (21) and collecting the various powers of  $\gamma$ , the new coefficients may be found to any required stage. For the calculations which follow, it was found sufficient to obtain the results:

$$b_{02} = -q_1$$

$$b_{04} = q_1^2$$

$$b_{06} = \frac{1}{2}q_1^3 - q_1^2$$

$$b_{08} = q_1^4 - q_1 q_1^2 + \frac{1}{12}q_1^3$$

$$\begin{aligned}
 b_{00} &= -q_1^6 + \frac{1}{2}q_1^3q_2^3 - \frac{1}{12}q_1q_2^3 - \frac{1}{2}q_2^3q_3 - \frac{1}{12}q_1q_2q_3 + \frac{1}{12}q_4 \\
 b_{10} &= -\frac{1}{2}q_2 \\
 b_{15} &= \frac{1}{2}q_1q_2 \\
 b_{17} &= \frac{1}{2}q_2q_3 - \frac{1}{2}q_1^3q_2 \\
 b_{19} &= -\frac{1}{2}q_2^3 + \frac{1}{2}q_1^3q_2 - \frac{1}{2}q_1q_2q_3 + \frac{1}{12}q_2q_4 \\
 b_{111} &= -\frac{1}{6}q_2q_3^3 + \frac{1}{2}q_1^3q_2q_3 - \frac{1}{2}q_1^4q_2 + \frac{1}{2}q_1q_2^3 - \frac{1}{12}q_1q_2q_4 + \frac{1}{12}q_2q_4q_5 \\
 b_{24} &= -\frac{1}{6}q_3 \\
 b_{26} &= \frac{1}{2}q_1q_3 \\
 b_{28} &= -\frac{1}{2}q_1^3q_3 + \frac{1}{12}q_2q_4 \\
 b_{35} &= -\frac{1}{12}q_4 \\
 b_{37} &= \frac{1}{2}q_1q_4 \\
 b_{46} &= -\frac{1}{12}q_5.
 \end{aligned} \tag{24}$$

4—Consider now the forces acting on the cylinder per unit length. The pressure is given by

$$P/\rho = \text{const} - gy - \frac{1}{2}q^2. \tag{25}$$

The term in  $gy$  gives the usual buoyancy, equal to the weight of displaced liquid, as part of the vertical force on the cylinder. Apart from this term, let  $X$ ,  $Y$  be the resultant horizontal and vertical forces on the cylinder in the positive directions of  $Ox$ ,  $Oy$ . Then, by the Blasius formula, we have

$$X - iY = \frac{1}{2}\rho i \oint \left( \frac{dw}{dz} \right)^2 dz, \tag{26}$$

taken round the circle  $|z| = a$ .

We note that  $-X$  will be the force known as the wave resistance, while  $Y$  is the addition to the upward force of buoyancy arising from the fluid motion. The value of the integral in (26) is  $2\pi i$  times the residue of the integrand; with  $w$  given in the form (15), and, using (16), this gives

$$X - iY = 2\pi\rho \sum_1^\infty \frac{n(n+1)}{a^{2n+1}} D_n D_{n+1}^*. \tag{27}$$

Using (14), we have the result

$$\begin{aligned}
 X - iY &= -2\pi\rho c^3 a \{ 1 \cdot 2b_0 b_1^* + 2 \cdot 3b_1 b_2^* + \dots \\
 &\quad + n(n+1)b_{n-1} b_n^* + \dots \}.
 \end{aligned} \tag{28}$$

This may be expanded in powers of  $\gamma$ , that is of  $\kappa_0 a$ , by substituting from (23) and (24), the results given there being sufficient to include the term

in  $\gamma^{11}$ . Using the notation of (21), and separating out the real and imaginary parts, we obtain, after some reduction,

$$\begin{aligned} -X = & 4\pi^2 \rho c^3 a (\kappa_0 a)^8 e^{-2xJ} [1 - 2r_1(\kappa_0 a)^3 - (r_2 - 3r_1^2 + s^2)(\kappa_0 a)^6 \\ & - (4r_1^3 - r_2^2 - 2r_1 r_2 + \frac{1}{2}r_2 - 4r_1^2 + s^2)(\kappa_0 a)^8 \\ & + \{5r_1^4 - 3r_1 r_2^2 - 3r_1^2 r_2 + \frac{1}{2}r_2^3 + \frac{1}{2}r_2^2 + \frac{1}{2}r_1 r_2 + \frac{1}{2}r_2 r_1 - \frac{1}{2}r_4 \\ & - (10r_1^2 - 3r_1 - 3r_2 + \frac{1}{2}s^2 + s^4)(\kappa_0 a)^8 + \dots], \end{aligned} \quad (29)$$

$$\begin{aligned} Y = & 4\pi\rho c^3 a (\kappa_0 a)^8 [-\frac{1}{2}r_1 + r_1 r_2 (\kappa_0 a)^2 + \frac{1}{4}(r_2 r_3 - 3r_1^2 r_2 + r_2 s^2)(\kappa_0 a)^4 \\ & + (2r_1^2 r_2 - \frac{1}{2}r_2^3 - r_1 r_2 r_3 + \frac{1}{2}r_2 r_3 r_4 + \frac{1}{2}r_2 s^2 - 2r_1 r_2 s^2)(\kappa_0 a)^6 \\ & + \{\frac{3}{2}r_1 r_2^2 - \frac{3}{2}r_1^2 r_2 - \frac{1}{2}r_2^3 r_3 + \frac{3}{2}r_1^2 r_2 r_3 - \frac{1}{2}r_2^2 r_4 - \frac{1}{2}r_1 r_2 r_4 + \frac{1}{2}r_2 r_3 r_4 \\ & + (5r_1^3 r_2 - \frac{1}{2}r_1 r_2 - \frac{1}{2}r_2 r_3 - \frac{1}{2}r_2^2 r_3 + \frac{1}{2}r_3 - \frac{1}{2}r_4 + \frac{1}{2}s^2 \\ & - r_2 s^4)(\kappa_0 a)^8 + \dots], \end{aligned} \quad (30)$$

with  $r_n, s$  given by (22).

The first term in (29) is the expression for the wave resistance of a circular cylinder which was obtained by Lamb. The first term in (30) is, after putting in the value of  $r_2$  from (22), the first approximation for the vertical force which I obtained by the method of images in the paper already quoted.

5—It is of interest to obtain the wave resistance, which should be equal to  $-X$ , from considerations of energy applied to the regular waves behind the cylinder. The current function  $\psi$  is given by the imaginary part of the expression (12). Putting  $y = f + \eta$ , we obtain at once the complete expression for the surface elevation as

$$\eta = ia^2 \int_0^\infty f(\kappa) e^{i\kappa x - iJ} d\kappa + ia^2 \int_0^\infty \frac{\kappa + \kappa_0 - i\mu}{\kappa - \kappa_0 - i\mu} f^*(\kappa) e^{-i\kappa x - iJ} d\kappa, \quad (31)$$

where the imaginary part is to be taken,  $f(\kappa)$  is given by (11), and  $\mu$  is to be made zero ultimately. This expression separates into two parts, a local disturbance  $\eta_1$  which decreases with increasing distance from the cylinder, and a system of regular waves  $\eta_2$  to the rear, that is, for negative values of  $x$ . The latter part is found, by methods familiar in these problems, to be given by

$$\eta_2 = -4\pi\kappa_0 a^2 f^*(\kappa_0) e^{-i\kappa_0 x - i\kappa_0 J}, \quad (32)$$

the imaginary part to be taken.

If  $h$  is the amplitude of the regular waves at a great distance behind the cylinder, the wave resistance  $R$  is given by

$$R = \frac{1}{2}g\rho h^2. \quad (33)$$

Hence from (32) we have

$$R = 4\pi^2 \kappa_0^2 a^2 f(\kappa_0) f''(\kappa_0) e^{-2\alpha f}. \quad (34)$$

With

$$f(\kappa_0) = b_0 + b_1 (\kappa_0 a) + \frac{b_2}{2!} (\kappa_0 a)^2 + \dots,$$

and with the equations (20), it could presumably be shown that (34) is the same as the real part, with sign changed, of the expression (28). However, it has been used here simply to verify the previous expansion; substituting from (23) and (24) we obtain from (34) the same result as is given in (29).

6—We may now examine the expressions (29) and (30) numerically. It is easily seen that if the ratio  $a/f$  is small, the first term in each case gives a close approximation at all velocities. Further, the ratio of the second term to the first in (29) and in (30) is  $-2r_1 \kappa_0^2 a^2$ , that is

$$-\frac{1}{2} \frac{a^2}{f^2} \{1 + 2\alpha - 2\alpha^2 e^{-\alpha} ll(e^\alpha)\}, \quad (35)$$

with  $\alpha = 2\kappa_0 f = 2gf/c^2$ .

The quantity in brackets in (35) approaches the value  $-1$  as  $c$  becomes zero and the value  $+1$  as  $c$  becomes infinite. It has a maximum negative value of  $-2.57$  at  $\alpha = 4.5$  approximately, and a maximum positive value of  $1.9$  at about  $\alpha = 0.6$ . Hence the effect of the second approximation in (29) is to increase the wave resistance at low velocities and to give a rather smaller value at high speeds.

Taking  $a/f = \frac{1}{2}$ , as a moderate value of this ratio, and calculating the resistance from (29), it is found that the value does not differ by more than about 9% of the value of the first approximation at any velocity. As an example of the numerical values in this case, for  $\alpha = 6$ , that is for  $c = 0.58 \sqrt{(gf)}$ , the following are the values of the successive terms in the expansion in square brackets in (29):

$$1 + 0.0746 + 0.0134 + 0.0015 + 0.0001.$$

Another case which has been worked out in some detail is  $a/f = \frac{1}{2}$ , this being definitely outside the range of the first approximation for the most part. Numerical values were calculated for both  $X$  and  $Y$  for  $\alpha = 8, 6, 5, 4, 3, 2.5, 2$ , and  $1$ . On account of slower convergence of the series at the higher values of  $\alpha$ , an estimate was made of the next term beyond those shown in (29) and (30). The results are shown in fig. 1.

The curves  $R$  and  $Y$  are the wave resistance and vertical force calculated from (29) and (30);  $R_1, Y_1$  are the curves given by the first approximations,

that is by the first term in (29) or (30). The unit of force in each case is  $\pi g \rho a^3$ , that is the weight of liquid displaced by the cylinder per unit length. It should be noted also that, in addition to the vertical force  $Y$ , there is the usual hydrostatic buoyancy. The curves for the wave resistance show clearly the increased values at lower velocities and also the displacement of the position of maximum resistance, the latter occurring at a lower speed than the value  $\sqrt{gf}$  given by the first approximation.

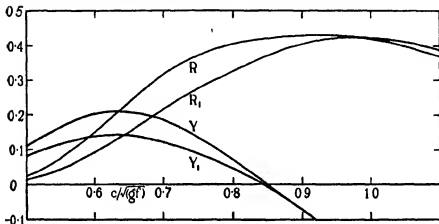


FIG. 1.

### SUMMARY

A solution is given for the two-dimensional wave motion due to a circular cylinder in a uniform stream, taking fully into account the condition at the surface of the cylinder. Expressions for the horizontal and vertical forces on the cylinder are obtained in the form of infinite series in ascending powers of a certain parameter. Numerical calculations are made from these and compared with the known first approximations. The main effect of the additional terms upon the wave resistance is to increase the calculated value at low velocities and to decrease it slightly at high velocities.

## The Oscillations of the Atmosphere

By HAROLD JEFFREYS, F.R.S.

With a Note by Professor G. I. TAYLOR, F.R.S.

(Received 31 August, 1936)

In a paper with the above title\* Professor G. I. Taylor offers some criticisms of a paper of mine on the winds produced in the atmosphere by differences of temperature and humidity. As they seem to depend in part on a misunderstanding, and as other meteorologists have expressed analogous difficulties to me in conversation, I think some further explanation is desirable.

My problem† was to find the periodic winds associated with a given periodic variation of temperature or of virtual temperature, the latter being a modification of the actual temperature to allow for the effect of humidity on the density. In these conditions we have as unknowns the three components of velocity and the density; given the density and the virtual temperature, the pressure is known. Thus we have four unknowns, which satisfy the three equations of motion and the equation of continuity, and the problem is therefore determinate. It is necessary to notice that the virtual temperature is taken as known from observation as a function of position and time.

If the temperature were taken as unknown and to be found from the rate of supply of heat to the atmosphere, a further equation would be needed to express the changes of temperature due to receipt of heat, transfer by radiation, turbulence, conduction, and adiabatic changes of pressure. My problem was framed to avoid this necessity, because the temperature is better known than the magnitudes of the various terms that would be needed in such an equation. But this device, while convenient for dealing with winds, makes the method inapplicable to free oscillations of the type treated by Taylor. If in my equations the variation of temperature is put equal to zero, we shall obtain a soluble problem, and there will be a calculable set of free periods analogous to those of a uniform ocean covering the earth. But these will be the periods of oscillations such that the temperature does not change at any point during the motion; if, for instance, new air rises to a place, heat must be lost to or brought in from the outside in just such amount as

\* 'Proc. Roy. Soc.,' A, vol. 156, pp. 318-326 (1936).

† 'Quart. J. R. Met. Soc.,' vol. 52, pp. 85-88 (1926).

will neutralize the change of the local temperature due to the convective terms and the adiabatic expansion. Such a condition has no obvious application, and in any case is not satisfied in Taylor's problem, for he adopts (equation (13) of his paper) the adiabatic equation of state, thus assuming no exchange of heat with the surroundings. Thus it need not have been expected that the equivalent depth in my solution would have any application to Taylor's problem. My equations would be true in Taylor's problem, but the change of virtual temperature at any point would be, not zero, but a function of the vertical displacement of the air there, and the presence of this term would alter the free periods. When the displacement is isothermal, but the initial state is not, there will still be a term of this kind.

Taylor objects (p. 325) that I have neglected  $w\partial/\partial z$  when operating on quantities that do not vanish in equilibrium. This is not so; it is neglected in the equations of motion, where it gives only a second order error, but in the equation of continuity the corresponding term  $\frac{\partial}{\partial z}(\rho w)$  is written exactly (equation (6) of my paper). On integration with regard to  $z$ , however, it makes no contribution to (8) since  $\rho w$  vanishes for  $z = 0$  and  $z = \infty$ .

I should mention that the device used to obtain the term on the right of my (15) is wrong, and has been corrected by C. A. Coulson.\* The correction appears to improve the agreement with observation, but an accurate test would require more knowledge of the annual variation of upper-air temperature than I possess.

*Note by Professor G. I. Taylor.*

Dr. Jeffreys's note clears up a difficulty several people have felt in regard to his paper, and I readily admit that my criticism was based on a misunderstanding, and was quite unjustified.

Dr. Jeffreys's assumption that the temperature at a fixed point in space remains unchanged during an oscillation has enabled him to derive an equivalent height in the form of an integral through the height of the atmosphere, but this equivalent height has little connexion with the free oscillations of the atmosphere.

That it is not possible to use such integrals, giving equivalent heights in calculating the free oscillations of the atmosphere, has not always been understood. Chapman, Pramanik, and Topping,<sup>†</sup> for instance, quote

\* 'Quart. J. R. Met. Soc.', vol. 57, p. 161 (1931).

† 'Beitr. Geophys.', vol. 33 (1931).

Jeffreys's integral as being applicable when the changes are isothermal and another integral as applying in the case of adiabatic changes. As Dr. Jeffreys points out in his note, his integral does not apply to isothermal changes but to cases where the air immediately assumes the temperature of the point in space to which it moves. The other formula (equation (6)) quoted by Chapman, Pramanik, and Topping as applying when the changes are adiabatic must rest on some mathematical fallacy, for in my paper to which Dr. Jeffreys refers I have shown that though equivalent depths exist which are significant in relation to the free oscillations of the atmosphere, they are not expressible as definite integrals through the height of the atmosphere.

---

## Correlation Measurements in a Turbulent Flow Through a Pipe

By G. I. TAYLOR, F.R.S.

(Received 31 August, 1936)

Measurements of the correlation between the velocity at pairs of points in a turbulent stream flowing between two planes 24·6 cc. apart (*i.e.*, a two-dimensional pipe) have been made by Reichardt.

Reichardt's first measurements were made by estimating the ratio of the diameters of the elliptical area blackened on a photographic plate by a spot of light, which moved so that the velocity variations at the two hot wires caused the spot to move in two perpendicular directions over the plate. This method has the disadvantage that unless the blackened area is truly elliptical some difficulty must arise in calculating the correlation coefficient. The method is also inaccurate when there is very little correlation between the velocity variations at the two wires.

Another method for measuring correlations, also mentioned by Dr. Reichardt, consists in passing the amplified disturbances from the two hot wires through the two coils of an electro-dynamometer.\* This method measures  $\overline{u_1 u_2}$ ,  $u_1$  and  $u_2$  being the components of turbulent velocity parallel to the mean wind direction at the two points, and  $\overline{u_1 u_2}$  the

\* Similar measurements were also made independently by Mr. L. F. G. Simmons. See Taylor, "Statistical Theory of Turbulence," "Proc. Roy. Soc., A," vol. 151, fig. 1, p. 445 (1935).

mean value of their product. To obtain  $R$ , the correlation coefficient, it is necessary to measure  $\overline{u_1^2}$  and  $\overline{u_2^2}$  as well as  $\overline{u_1 u_2}$  for

$$R = \frac{\overline{u_1 u_2}}{(\overline{u_1^2})^{1/2} \cdot (\overline{u_2^2})^{1/2}}. \quad (1)$$

Reichardt's measurements did not measure correlations below  $R = 0.5$ .

On the other hand, it can be proved that if the correlation between the component of velocity at a fixed point and that at a point which can take up any position on the same cross-section is considered, there must be some positions of the variable point where  $R$  is negative.

In an incompressible fluid the mean flow across each section of a pipe is constant at all sections down the pipe, so that any temporary departure from the mean velocity over any section must occur simultaneously at all sections. To produce variations of this type it would be necessary to apply a pressure difference between the ends of the pipe which varies with time. In flow under a steady pressure difference, therefore, there can be no time variations in the mean flow across a section. Now suppose that the correlation  $R$  has been measured between the component,  $u_1$ , at a fixed point  $P$ , and  $u_2$  at a variable point  $Q$  on the same cross-section. Since the mean flow across the section is constant with regard to time

$$\int (U + u_1) dy dz = \text{const} = \int U dy dz, \quad (2)$$

where  $U$  is the time mean of the velocity at the point  $Q$  whose coordinates are  $(y, z)$  and the integration extends over the whole cross-section of the pipe. At any instant, therefore,

$$\int u_2 dy dz = 0, \quad (3)$$

and therefore

$$u_1 \int u_2 dy dz = 0. \quad (4)$$

Since  $u_1$  is a constant so far as integration over the cross-section at any instant is concerned, (4) may be written

$$\int u_1 u_2 dy dz = 0, \quad (5)$$

and since (5) is true at every instant, the integral of (5) over an interval of time  $T$  is zero, thus

$$\frac{1}{T} \int_0^T \left[ \int u_1 u_2 dy dz \right] dt = 0. \quad (6)$$

Changing the order of integration and remembering that when  $T$  is large,

$$\frac{1}{T} \int u_1 u_2 dt$$

is the mean value of  $u_1 u_2$  (6) becomes

$$\int \overline{u_1 u_2} dy dz = 0, \quad (7)$$

writing  $u'_1$  for  $\sqrt{\overline{u_1^2}}$  and  $u'_2$  for  $\sqrt{\overline{u_2^2}}$ , and bearing in mind the definition of  $R$  contained in (1) it will be seen that (7) may be written

$$u'_1 \int R u'_2 dy dz = 0,$$

or

$$\int R u'_2 dy dz = 0. \quad (8)$$

Since  $u'_1$  and  $u'_2$  are necessarily positive quantities, it is clear that negative as well as positive values of  $R$  must occur in the section.

*Application to a Circular Pipe*—The simplest case to which (8) can be applied is that of a circular pipe. If the fixed hot wire is placed in the centre, and the values of  $R$  are measured at various distances  $r$  of the variable hot wire from the axis of the pipe, then (8) becomes

$$\int_0^a u' r dr = 0, \quad (9)$$

where  $u'$  is the value  $\sqrt{\overline{u^2}}$  at radius  $r$ , and  $a$  is the radius of the pipe.

It seemed worth while to verify this result by making measurements of  $R$  and  $u'$ , for various values of  $r$ . Measurements of this kind have been made recently by Mr. L. F. G. Simmons, of the National Physical Laboratory, in a wind tunnel. Accordingly, at my request he made similar measurements in a circular pipe.

*New Method for Measuring  $R$* —Before discussing the experimental results a new method for measuring  $R$  must be described. It has been mentioned that the method so far adopted consists in using two compensated amplifiers, one for each hot wire, and then passing the amplified disturbances through an electrodynamometer. Three consecutive measurements must be made in order to get  $\overline{u_1^2}$ ,  $\overline{u_2^2}$  and  $\overline{u_1 u_2}$ . If  $R$  is very nearly equal to 1.0 (*i.e.*, when the two wires are close together) the small differences between  $R$  and 1.0 are very sensitive to small changes in the

measuring apparatus, which may occur while the three sets of measurements are being made. Since the wires used are only 0.0002 cm. diameter and 1 mm. long, particles of dust accidentally adhering to them may cause considerable changes in their calibration. An error of 1% in R will be produced by an error of 1% in any one of the three dynamometer measurements, and if these measurements are taken when, say,  $R = 0.98$  the error in  $1 - R$  will be 50%.

For cases where  $R$  is nearly 1.0 a new method is desired which gives  $1 - R$  directly. Such a method will now be described.

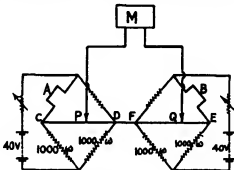


FIG. 1

The arrangement of the circuits is shown in fig. 1. The steady current through each hot wire (A and B, fig. 1) is balanced out in the ordinary way by means of bridges and galvanometers (not shown in fig. 1). The two bridges are connected together at the points D, F. Thus the mean potentials at C, D, F, E are identical.

A speed variation  $u_1$  at hot wire A produces a potential  $E_1$ , between C and D which is proportional to  $u_1$  and similarly a variation  $u_2$  at B produces a potential  $E_2$  in FE proportional to  $u_2$ . Thus

$$R = \frac{\overline{E_1 E_2}}{(E_1^2)^{\frac{1}{2}} (E_2^2)^{\frac{1}{2}}} \quad (10)$$

The points C and D (fig. 1) and also E and F are connected by means of potentiometer wires (or other equivalent resistances) which can be divided at the points P and Q. The potential difference between P and Q is fed into the input side of a compensated amplifier, the output of which is connected to an alternating current voltmeter (M, fig. 1) or other apparatus for measuring the mean square value of a variable potential.

It will be seen that if the indications of the hot wires A and B are exactly proportional to one another, as they are when  $R = 1.0$ , positions of P and Q can always be found such that the potentials of P and Q

remain equal to one another, even though the potential differences between C and D and E and F are fluctuating. By adjusting either P or Q while the other is fixed, it is therefore possible to get zero deflection in M when  $R = 1 \cdot 0$ .

On the other hand, if the indications of the hot wires are not exactly proportional to one another, i.e., R is not exactly equal to 1·0, no possible positions of P and Q will be found such that no current passes through M. If, however, R is only slightly smaller than 1·0 there will be a sharp minimum value of the deflection in M which will indicate how far the indications A and B are from being perfectly correlated.

*Theory of the Method*—If  $\alpha$  represents  $PD/DC$ ,  $\beta = FQ/EF$  (i.e.,  $\alpha$  and  $\beta$  are the ratios into which the potentiometer wires are divided) the potential difference applied to the input of the amplifier is

$$\alpha E_1 - \beta E_2,$$

and its mean square value is

$$\alpha^2 \overline{E_1^2} + \beta^2 \overline{E_2^2} - 2\alpha\beta \overline{E_1 E_2}. \quad (11)$$

Suppose now that with P fixed, Q is adjusted till the minimum deflection is attained in M. This deflection then measures the minimum value of (11). The minimum value of (11) as  $\beta$  varies is evidently, when

$$\beta = \alpha \overline{E_1 E_2} / \overline{E_2^2}, \quad (12)$$

and substituting from (12) in (11) the minimum value of (11) is

$$\alpha^2 \left( \overline{E_1^2} + \frac{(\overline{E_1 E_2})^2}{\overline{E_2^2}} - 2 \frac{(\overline{E_1 E_2})^2}{\overline{E_2^2}} \right),$$

which may be written

$$\alpha^2 \overline{E_1^2} (1 - R^2) \quad (13)$$

in virtue of (10).

Thus if  $I_1$  is the minimum deflection of M as Q is varied,

$$I_1 = K \alpha^2 \overline{E_1^2} (1 - R^2), \quad (14)$$

when K is the factor of amplification.

Now move Q (fig. 1) up to the point F and again take the reading,  $I_2$ , of M. This is equivalent to taking  $\beta = 0$  in (11) so that

$$I_2 = K \alpha^2 \overline{E_1^2}. \quad (15)$$

From (14) and (15)

$$1 - R^2 = I_1/I_2. \quad (16)$$

It will be noticed that the quantities which come into (16) are only the two deflections of M, so that only two consecutive readings must be taken

instead of the three which are necessary in the electrodynamometer method. It may be objected that the determination of a position of  $Q$  for which the deflexion is a minimum is a difficult matter, because the deflexion will probably fluctuate slightly. This is true, but it must be remembered that it is  $I_1$ , the minimum deflexion as  $\beta$  varies, that is wanted, and that the deflexion near its minimum value is insensitive to variations in  $\beta$ .

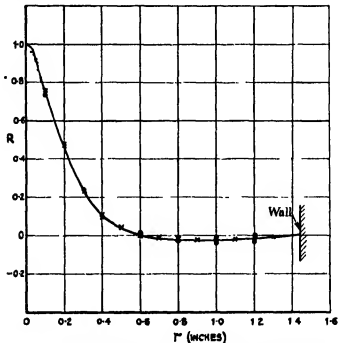


FIG. 2—Correlation between velocity at centre and velocity at radius  $r$ . • New method for measuring  $1 - R^2$ ; ○ and × electrodynamometer.

#### CORRELATION MEASUREMENTS IN A PIPE

Mr. L. F. G. Simmons, of the National Physical Laboratory, has made correlation measurements in a pipe  $2\frac{1}{4}$  inches diameter. He fixed one hot wire in the centre of the pipe and moved the other one along a radius.  $r$  is the distance apart of the wires. For values of  $r$  less than  $1/10$ th inch Mr. Simmons used the method described above, while for greater values of  $R$  he used an electrodynamometer.

The results of these measurements are shown in fig. 2 and an enlarged diagram showing the individual measurements for  $r < 0.08$  inches is

given in fig. 3. The parabola predicted by theory\* is shown marked in fig. 3, and it will be seen that it fits the observations fairly well.

*Comparison with Present Theory*—Returning to fig. 2, it will be seen that  $R$  is positive when  $r < 0.6$  inches but that when  $r > 0.6$  inches  $R$  is negative. Thus the observations are in accordance with the prediction given above.

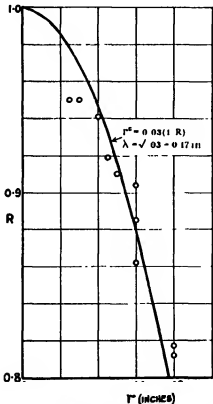


FIG. 3—Correlation measurements near the axis.

To test the formula (8) it was necessary to measure  $u'$ . The necessary measurements were made by means of the electrodynamometer during the determination of  $R$ . Fig. 4 shows the measured values of  $u'$ .

Taking the values of  $u'$  from the curve, fig. 4 and  $R$  from fig. 2, the values of  $u'Rr$  were found. These are shown in the curve fig. 5. It will be seen that  $u'Rr$  is positive from  $r = 0$  to  $r = 0.6$  inches while it is negative for  $r = 0.6$  inches to the wall of the pipe.

\* "Statistical Theory of Turbulence," Parts I and III.

Taking the areas of the positive and negative points of the curve in fig. 5, I find that the contribution to

$$\int_0^R u' r R \, dr$$

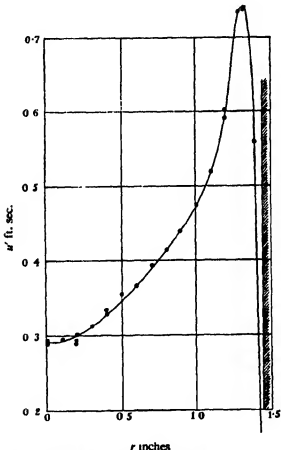


FIG. 4—Measured values of  $u'$  when velocity at centre is 9.5 ft. per sec.

from  $r = 0$  to  $r = 0.6$  inches is

$$+ 0.0098$$

while the contribution of the negative point from 0.6 inches to the wall is

$$- 0.0097.$$

The negative part of

$$\int_0^R r R u' \, dr$$

is therefore nearly equal to the positive part, thus verifying the theoretical prediction that

$$\int_0^r r R u' dr = 0.$$

In conclusion, I wish to express my thanks to Mr. L. F. G. Simmons for supplying me with the results of his measurements.

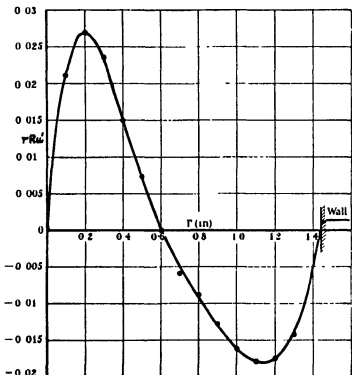


FIG. 5.

### SUMMARY

A new method for measuring  $R$ , the correlation coefficient between two fluctuating currents, is described. An advantage of the method is that the ratio of the two necessary measurements is  $1 - R^2$ , so that small deviations from perfect correlation can be measured accurately.

In all correlation measurements in turbulent flow the complexity of the apparatus is so great that independent verification of the results is desirable. It is proved theoretically that if  $R$  is the correlation between the

turbulent component of velocity at the centre of a circular pipe of radius  $a$  and that at radius  $r$ ,

$$\int_0^a r R u' dr = 0$$

where  $u' = \sqrt{u^2}$  and  $u$  is the component parallel to the axis at radius  $r$ . This integral forms a useful check on the accuracy of the methods used in measuring turbulence. It is verified in measurements made at the National Physical Laboratory by Mr. L. F. G. Simmons.

---

## Fluid Friction Between Rotating Cylinders

### I—Torque Measurements

By G. I. TAYLOR, F.R.S.

(Received 31 August, 1936)

The stability of fluid contained between concentric rotating cylinders has been investigated and it has been shown that, when only the inner cylinder rotates, the flow becomes unstable when a certain Reynolds number of the flow is exceeded. When the outer cylinder only is rotated, the flow is stable so far as disturbances of the type produced in the former case are concerned, but provided the Reynolds number of the flow exceeds a certain value, turbulence sets in. The object of the present experiments was partly to measure the torque reaction between two cylinders in the two cases in order to find the effect of centrifugal force on the turbulence, and partly to find the critical Reynolds numbers for the transition from stream-line to turbulent flow.

The apparatus is shown diagrammatically in fig. 1.\*

#### DESCRIPTION OF APPARATUS

The outer cylinder was made of brass turned inside and out. It measured 8·11 cm. inside diameter by 84·4 cm. long. The centre portion was a brass casting which contained two circular brass trapdoors made so that, when in place, they fitted flush with the inside surface

\* This sketch merely indicates the general nature of the measurements. More detail is given in fig. 1, Part II.

without a break. The cylinder was balanced so that it could rotate without vibration and was then fitted centrally on a turn-table which ran between two ball-bearing collars and rested on a ball-bearing thrust

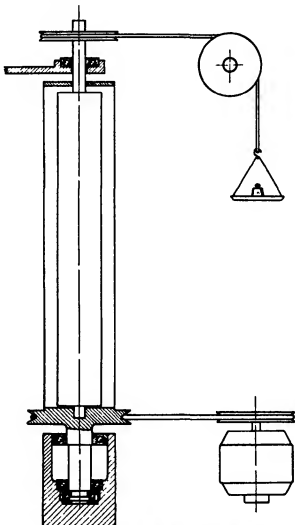


FIG. 1—Sketch illustrating method employed.

block. This table could either be rotated by means of a tight belt or held against friction when the inner cylinder was revolving by a thread which ran over an accurately made ball-bearing pulley and was attached to a scale pan.

The inner cylinder was supported on a single steel ball rotating on a

flat, hard, bronze end-plate, being kept in position by a plain bearing which was lubricated by grease forced in from below.

The inner cylinder was made of a pile of cylindrical blocks of ebonite threaded on a turned steel rod. The blocks were kept in place by circular end nuts so shaped that they cleared the bottom and top of the inner cylinder by about 1 mm. As the experiments proceeded, the inner cylinder was turned down so that an increasing series of thicknesses were obtained for the annular space between the cylinders.

The top of the inner cylinder was slightly conical in shape and the cover of the outer cylinder was similarly shaped on its under side. A hole was bored horizontally through the cap to the highest point of the cone, and this hole was sealed with a needle valve as soon as the overflow began, while the apparatus was being filled with fluid. To fill the apparatus, a long funnel was screwed to a cock at the bottom of the outer cylinder. It was filled with the fluid while the cock was closed and all bubbles allowed to rise to the surface. The cock was then opened and the level of the fluid in the funnel was kept up till overflow started at the top. The needle valve was then closed and the cock turned off. The inner cylinder was set rotating to free the bubbles at intervals during the filling process.

The upper bearing between the two cylinders was a greased ball race, set between two narrow disks which only just cleared the spindle.

The upper bearing between the fixed upper support and the inner cylinder was a ball-bearing carried on a brass plate. In setting up the apparatus the inner cylinder was trued up. The brass plate and ball bearing were slipped over the top. The upper fixed support was then brought into position so that a hole in it was concentric with the top of the inner cylinder. The plate containing the ball-bearing was then fixed to the upper fixed support by means of three bolts which held it firm against three adjustable pins. In this way the whole apparatus was set up true so that the friction between the cylinders when empty was very small.

A driving belt or torque thread could be fitted to the inner cylinder in the same way as to the outer one.

To make a measurement, the inner or outer cylinder was driven by a tight belt and its speed measured by timing a revolution counter attached to it. The torque required to hold the other cylinder in position was measured by putting weights in the scale pans (*a*) till the cylinder was just able to move in the same direction as the belt driven cylinder, and (*b*) till it just moved in the opposite direction. The difference between the two was due to the friction against fixed supports, so that the friction torque between the two cylinders was taken as the mean of (*a*) and (*b*).

The torque between the cylinders is due partly to friction between the bearings and partly to fluid friction. The torque was measured both when the apparatus was full and when it was empty. The difference is due to fluid friction, nearly all of which was due to the tangential stress on the cylindrical walls, though a small fraction must have been due to fluid friction between the top of the inner cylinder and the top of the outer cylinder and between the bottom of the inner cylinder and the bottom of the outer cylinder.

*Fluids Used*—The following fluids were used: water, pentane, aviation spirit, and various mixtures of glycerine and water. Their viscosities depended on the temperature, and they were determined by means of calibrated capillary tubes for a range of temperatures.

The relevant properties at 15° C are given in Table I.

TABLE I

Liquid	Density	Viscosity	v
Water .....	1.00	0.0114	0.0114
Pentane .....	0.634	0.0024	0.00379
Glycerine and water .....	1.120	0.0524	0.0468
" .....	1.171	0.153	0.131
" .....	1.083	0.0263	0.0243
" .....	1.046	0.0174	0.0167
Aviation spirit (18° C) .....	0.729	0.00457	0.00625

With pentane great precautions were necessary to ensure that the apparatus was full and that there were no bubbles.

## DATA

The radius of the torque pulley on the outer cylinder was 9.78 cm. The radius of the torque pulley on the inner cylinder was 5.01 cm. As an example of the action of the apparatus the results of a set of observations made with water are given below.

Outer cylinder diameter 8.11 cm.

Inner cylinder diameter 7.78 cm.

W = weight of scale pan = 22.5 gm.

The tension in the thread round the torque arm is

$$\begin{aligned} W + \text{load in pan} &= P_1 \text{ when the pan is just falling} \\ &= P_2 \text{ when the pan is just rising.} \end{aligned}$$

The weight which counterbalances the torque due to fluid friction is taken to be

$$P = \frac{1}{2}(P_1 + P_2)_{\text{full}} - \frac{1}{2}(P_1 + P_2)_{\text{empty}}.$$

$G$  = torque expressed as  $Pg \times (\text{radius of torque pulley in cm.})$ .

$N$  = number of revolutions per second.

### OBSERVATIONS

*Outer cylinder rotating, water*

$$\left\{ \begin{array}{l} N = 16, \text{ apparatus empty } P_1 = W + 20 \\ \quad \quad \quad P_2 = W + 10 \\ N = 15.6, \text{ apparatus full } P_1 = W + 170 \\ \quad \quad \quad P_2 = W + 160 \end{array} \right\} P = 150 \text{ gm.}$$

$$G = 7.38 \times 10^6$$

$$G/\rho N^2 = 3.03 \times 10^3, \quad N/v = 1.45 \times 10^3.$$

$$\left\{ \begin{array}{l} N = 22.4, \text{ full } P_1 = W + 350 \\ T = 17.5^\circ \text{ C. } P_2 = W + 360 \end{array} \right\} P = 330 \text{ gm.}$$

$$G = 16.23 \times 10^6$$

$$G/\rho N^2 = 3.2 \times 10^3, \quad N/v = 2.17 \times 10^3.$$

$$\left\{ \begin{array}{l} N = 11.48, \text{ empty } P_1 = W + 10 \\ \quad \quad \quad P_2 = W + 0 \\ N = 11.28, \text{ full } P_1 = W + 90 \\ \quad \quad \quad P_2 = W + 80 \end{array} \right\} P = 80 \text{ gm.}$$

$$G = 3.94 \times 10^6$$

$$G/\rho N^2 = 3.10 \times 10^3, \quad N/v = 1.04 \times 10^3.$$

$$N = 15.0 \quad P = 145, \quad G = 7.12 \times 10^6, \quad G/\rho N^2 = 3.17 \times 10^3$$

$$N/v = 1.37 \times 10^3$$

$$N = 10.78 \quad P = 75, \quad G = 3.69 \times 10^6, \quad G/\rho N^2 = 3.17 \times 10^3$$

$$N/v = 1.00 \times 10^3$$

$$N = 17.65 \quad P = 190, \quad G = 9.33 \times 10^6, \quad G/\rho N^2 = 3.00 \times 10^3$$

$$N/v = 1.62 \times 10^3$$

$$N = 20.55 \quad P = 280, \quad G = 13.7 \times 10^6, \quad G/\rho N^2 = 3.25 \times 10^3$$

$$N/v = 1.96 \times 10^3$$

$$N = 22.8 \quad P = 355, \quad G = 17.5 \times 10^6, \quad G/\rho N^2 = 3.36 \times 10^3$$

$$N/v = 2.23 \times 10^3$$

*Inner cylinder rotating, water*

$$\left\{ \begin{array}{l} N = 20, \text{empty} \quad P_1 = O + 30 \\ \qquad \qquad \qquad P_2 = O + 0 \\ N = 21.1, \text{full} \quad P_1 = W + 260 \\ \qquad \qquad \qquad P_2 = W + 230 \end{array} \right\} P = 245 + W - 15 = 253 \text{ gm.}$$

$$G = 253 \times 981 \times 9.78 = 24.3 \times 10^5$$

$$G/\rho N^2 = 5.45 = 10^4, \quad N/v = 1.92 \times 10^3.$$

$$N = 17.58 \quad P = 185, \quad G = 17.8 \times 10^5, \quad G/\rho N^2 = 5.75 \times 10^4 \\ N/v = 1.58 \times 10^3$$

$$N = 24.4 \quad P = 323, \quad G = 31.0 \times 10^5, \quad G/\rho N^2 = 5.21 \times 10^4 \\ N/v = 7.22 \times 10^3$$

$$N = 29.7 \quad P = 478, \quad G = 45.9 \times 10^5, \quad G/\rho N^2 = 5.21 \times 10^4 \\ N/v = 2.7 \times 10^3$$

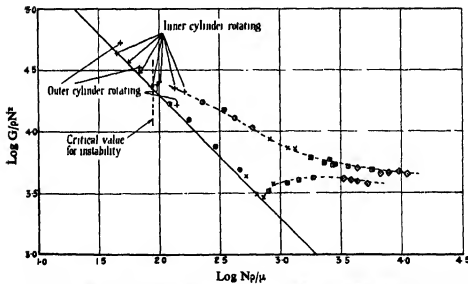


FIG. 2— $R_1 = 4.05$ ,  $R_2 = 3.94$ . Upper curve, inner cylinder rotating. Lower curve, outer cylinder rotating. Full line, calculated critical line for inner cylinder rotating.  $+ v = 0.131$ ;  $\circ v = 0.047$ ;  $\times v = 0.024$ ;  $\square v = 0.011$ ;  $\diamond v = 0.0038$ .

#### COMPLETE RESULTS

In representing the results, it must be remembered that the theory of Dynamical Similarity demands that for any given pair of diameters

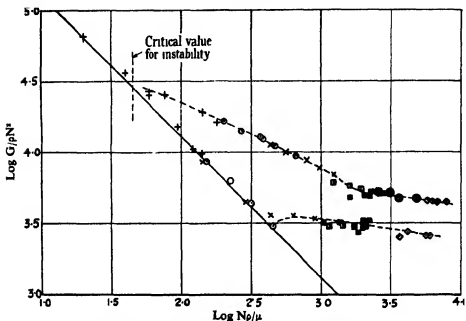


FIG. 3— $R_1 = 4.05$ ,  $R_2 = 3.89$ .  $+ \nu = 0.131$ ;  $\circ \nu = 0.047$ ;  $\times \nu = 0.024$ ;  
 $\square \nu = 0.011$ ;  $\diamond \nu = 0.0062$ ;  $\diamond \nu = 0.0038$ .

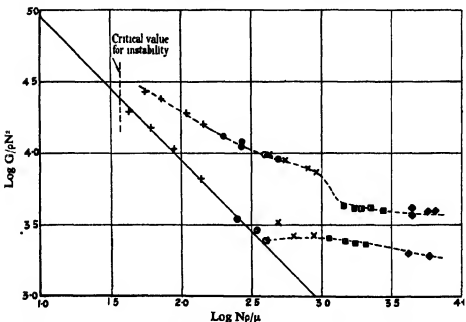


FIG. 4— $R_1 = 4.05$ ,  $R_2 = 3.83$ .  $+ \nu = 0.131$ ;  $\circ \nu = 0.047$ ;  $\times \nu = 0.024$ ;  
 $\square \nu = 0.011$ ;  $\diamond \nu = 0.0038$ .

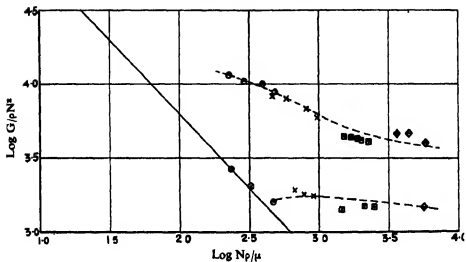


FIG. 5— $R_1 = 4.05$ ;  $R_2 = 3.74$ .  $\circ$   $v = 0.047$ ;  $\times$   $v = 0.024$ ;  $\square$   $v = 0.011$ ;  $\diamond$   $v = 0.0038$ .

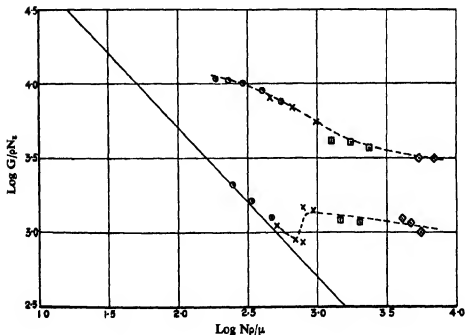


FIG. 6— $R_1 = 4.05$ ,  $R_2 = 3.68$ .  $\circ$   $v = 0.047$ ;  $\times$   $v = 0.024$ ;  $\square$   $v = 0.011$ ;  $\diamond$   $v = 0.0038$ .

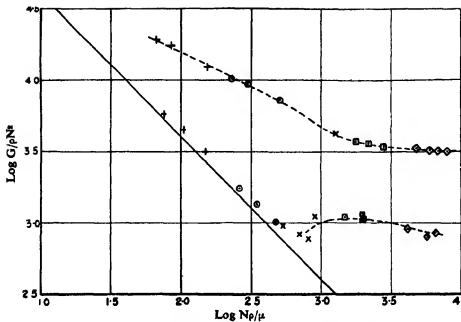


FIG. 7— $R_1 = 4.05$ ,  $R_2 = 3.59$ . +  $v = 0.131$ ; ○  $v = 0.047$ ; ×  $v = 0.024$ ; □  $v = 0.011$ ; ◇  $v = 0.0038$ .

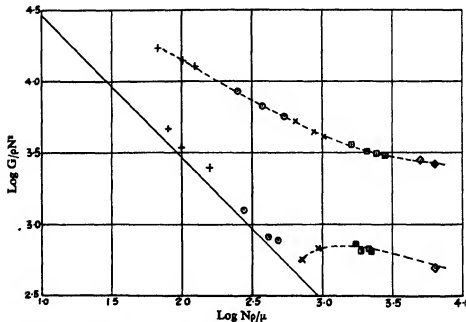


FIG. 8— $R_1 = 4.05$ ,  $R_2 = 3.45$ . +  $v = 0.131$ ; ○  $v = 0.047$ ; ×  $v = 0.024$ ; □  $v = 0.011$ ; ◇  $v = 0.0038$ .

$G/\rho N^2$  must be a function of  $N/v$ . In each case, therefore, these two quantities were calculated. In figs. 2-9 all the results are represented on diagrams giving  $\log_{10}(G/\rho N^2)$  and  $\log_{10}(N/v)$ . A separate curve is given for each diameter of the inner cylinder, namely 7.89, 7.78, 7.66, 7.48, 7.36, 7.18, 6.91, 6.40 cm. The outer one is the same for all, namely, 8.11 cm. The points for both types of measurement, inner

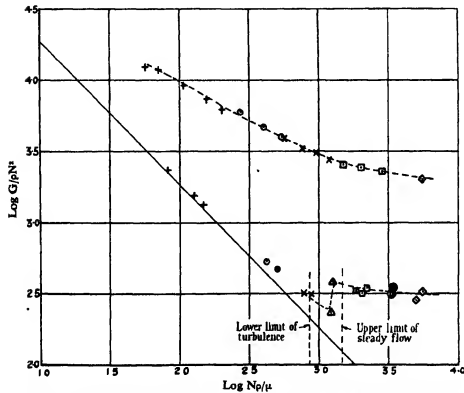


FIG. 9.— $R = 4.05$ ,  $R_i = 3.20$ . +  $v = 0.131$ ; ○  $v = 0.047$ ; ×  $v = 0.024$ ; □  $v = 0.011$ ; ◇  $v = 0.0062$ ; ◇  $v = 0.0038$ ; △ glycerine and water,  $\rho = 1.046$ ,  $v = 0.017$ .

cylinder rotating and outer cylinder rotating, are given on the same figure. The points corresponding with the former case are always above those corresponding with the latter except for the lowest values of  $N/v$ . When there is any possibility of confusion the points are distinguished on the diagram.

In order to see the effect of rotation on the turbulence, the theoretical value of  $G$  for steady motion was calculated in each case. Since in that case  $G$  is proportional to  $N$ ,  $G/\rho N^2$  is proportional to  $1/N$ , so that with

the logarithmic coordinates of figs. 2-9 this theoretical curve is always a straight line at  $-45^\circ$  to the horizontal axis. The calculated value for  $G$  is

$$G = \frac{2\pi^2 D_1^2 D_2^2 l \mu N}{(D_1 + D_2)(D_1 - D_2)}, \quad (1)$$

where  $D_1$  is the diameter of the outer cylinder, namely 8.11 cm.,  $D_2$  is the diameter of the inner cylinder,  $l$  is the length, namely 84.2 cm.

(1) may be written in the form

$$\log(G/\rho N^2) - \log(N/v) = \log(2\pi^2/D_1^2) + \log D_2 - \log(D_1 + D_2) - \log(2t) = C, \quad (2)$$

where  $t = \frac{1}{2}(D_1 - D_2)$  is the thickness of the annular space between the two cylinders and  $C$  represents the right-hand side of (2).

Table II gives the values of  $C$  for the values of  $D_2$  used in the course of the work

TABLE II

$D_2$ , cm. .	7.89	7.78	7.66	7.48	7.36	7.18	6.91	6.40
$C^*$ .....	6.286	6.10	5.956	5.794	5.708	5.598	5.462	5.256
$t$ (cm.) .....	0.110	0.165	0.225	0.315	0.375	0.465	0.600	0.855
$\log(t/R_1)$ ..	2.433	2.609	2.744	2.890	2.966	3.059	3.170	3.324
$t/R_1$ .....	0.0271	0.0407	0.0555	0.0776	0.0924	0.1146	0.1480	0.210
Number in fig. 10	1	2	3	4	5	6	7	8

\* See equation (2).

Inner cylinder used for velocity distribution measurement (see Part II),  $t/R_1 = 0.226$ .

#### CRITERION OF TURBULENCE

1—Outer Cylinder Rotating—In all the results given in figs. 2-9 it will be seen that for low values of  $N/v$  the observed values of  $G/\rho N^2$  are close to those calculated on the assumption that the flow is steady. At a value of  $N/v$  which depends on the ratio of the radii of the cylinders, the observed values of  $G/\rho N^2$  begin to leave the straight line which represents the conditions in stream line motion. The value of  $N/v$  at which this takes place is taken to be the critical value at which turbulence sets in. In the neighbourhood of this point the flow can be either steady or turbulent. In general there is a lower critical point below which the flow is in all cases steady, and an upper critical point above which the flow is always turbulent. At intermediate points the flow is usually stable if the rotation of the outer cylinder is steadily increased through the lower

critical point, but a slight disturbance, such as that produced by a slight rotation of the inner cylinder in the opposite direction to that of the outer one, will make the flow permanently turbulent.

As an example of the limits found in this way, experiments with the inner cylinder 6·40 cm. diameter may be cited. The fluid used was a mixture of glycerine and water of density 1·046. The relevant observations are given below:

*Apparatus Empty*

$$N = 21 \begin{cases} P = 10 \\ P = 8 \end{cases} \text{ mean } 9 \text{ gm.}$$

*Apparatus Full*

Speed increased gradually  $\begin{cases} P_1 = W + 10 \\ P_2 = W + 5 \end{cases} P = 22\frac{1}{2} + 7\frac{1}{2} - 9 = 21 \text{ gm.}$   
 $N = 20\cdot8$

Speed increased gradually  $\begin{cases} P_1 = W + 10 \\ P_2 = W + 7 \end{cases} P = 22 \text{ gm.}$   
 $N = 21\cdot0$

After turning inner cylinder backwards to start turbulence,  $N = 21\cdot0$   $\begin{cases} P_1 = W + 25 \\ P_2 = W + 20 \end{cases} P \approx 36 \text{ gm.}$

The points corresponding with these observations are marked with points  $\Delta$  in fig. 9. The value of  $\log Ut/v$  corresponding with  $N = 21\cdot0$  rev. per sec. is marked at D in fig. 11. It will be seen that it is in the middle of the range between the points A and B.

The critical range in which turbulent and steady flow were both possible could not always be determined from the torque measurements. A pair of glass windows was therefore fitted to replace the brass windows in the outer cylinder. The inner surface of the glass was ground to the same radius as the inside of the outer cylinder and was fitted flush, so that there was no obstruction to the flow. The steel axle of the inner cylinder had a hole down the centre so that a thin film of coloured fluid could be spread over the inner cylinder.\* The upper and lower criteria found in this way with the smallest inner cylinder (6·40 cm. diameter) are shown in fig. 9, and are marked in fig. 11 by the points A and B.

\* This method is described in "Stability of a Viscous Liquid Contained Between Two Rotating Cylinders," *Phil. Trans.*, A, vol. 223, p. 289 (1923).

**2—Inner Cylinder Rotating**—The stability of the flow when the inner cylinder is rotating was discussed by the present writer\* some years ago, and it was shown that when the speed of rotation is gradually increased instability sets in as soon as the calculated criterion of instability is reached.

This criterion is

$$P = 0.0571 \left(1 - 0.652 \frac{t}{R_s}\right) + 0.00056 \left(1 - 0.652 \frac{t}{R_s}\right)^{-1}, \quad (3)$$

where

$$P = \frac{\pi^4 v^4 (R_1 + R_s)}{2\Omega^2 t^4 R_s^3}, \quad (4)$$

and  $t$  is the thickness of annulus.

When  $t/R_s$  is small,  $P = 0.0571$  and  $R_1 + R_s$  may be taken as  $2R$ , so that (4) may be written approximately

$$0.0571 = \pi^4 \left(\frac{v^4}{U^4 t^4}\right) \frac{R_1}{t} \quad (5)$$

or

$$\log t/R_1 + 2 \log Ut/v = 4 \log \pi - \log 0.0571 = 3.232, \quad (6)$$

where

$$U = \Omega R_1 = 2\pi N R_1 \quad (7)$$

is the velocity of the outer cylinder relative to the inner one and  $N$  is the number of revolutions per second. Another expression equivalent to (6) is

$$[\log(N/v)]_{crit} = 0.818 - \frac{1}{2} \log R_1 - \frac{3}{2} \log t, \quad (8)$$

and when  $R_1 = 4.055$  this becomes

$$[\log N/v]_{crit} = 0.514 - \frac{3}{2} \log t. \quad (9)$$

In most cases the lowest speeds of rotation were above the critical speed, but in the cases  $D_1 = 7.89$  and  $R_1 = 7.78$  cm. the critical value of  $N/v$  falls within the range of observations. Values for  $[\log(N/v)]_{crit}$  given by (9) are:

TABLE III

$D_1$	$t$	$[\log N/v]_{crit}$
7.89	0.11	1.95
7.78	0.165	1.68

\* Loc. cit., p. 318, equation (7.11). In the present paper  $R_1$  is the outer cylinder and  $R_s$  the inner, whereas in the paper here referred to  $R_1$  was the inner cylinder and  $R_s$  the outer cylinder.

These values are marked by broken lines in figs. 2 and 3. It will be seen that they correspond with the points where the observed points leave the calculated curves for steady motion.

#### EFFECT OF ROTATION ON TURBULENT STRESSES

The effect of rotation on the Reynolds stress which causes the torque between the cylinders can be seen by comparing the values of  $G/\rho N^2$  at the same value of  $N/v$  (*a*) when the inner cylinder is revolving, and (*b*) when the outer cylinder revolves. Up to the critical value in case (*a*) the torque in the two cases is identical for a given speed of rotation (see fig. 2). Above that the torque becomes greater in (*a*) than in (*b*). Above the critical speed in case (*b*) the ratio of the torques in (*a*) and (*b*) may decrease, though that in (*a*) still remains greater than that in (*b*). The ratio  $G$  (case *a*)/ $G$  (case *b*) may be taken to represent the effect of rotation on the Reynolds stress in turbulent motion.

To compare the effects of rotations for various thicknesses of the annulus, the results have been plotted in fig. 10 so as to show  $\log \tau/\rho U^2$  as a function of  $\log Ut/v$  for each value of  $t/R_1$ . Here  $\tau$  is the tangential stress on the outer cylinder, and  $U = 2\pi NR_1$  as before. In fig. 10 the curves are traced directly from figs. 2-9, and in each case the origin shifted by the amount necessary to make the curves represent  $\tau/\rho U^2$  and  $Ut/v$  instead of  $G/\rho N^2$  and  $N/v$ . The correspondence between the data given in Table II and the numbers of the curves in fig. 10 is given at the foot of Table II.

The full lines represent observations taken with the inner cylinder rotating. The dotted lines with the outer cylinder rotating. It will be seen that the full lines are close together, whereas the dotted lines show a rapidly decreasing friction as  $t/R_1$  increases. It seems, therefore, that rotation does not very greatly affect the Reynolds stresses when the inner cylinder rotates, but has a large effect when the outer cylinder rotates.

The former of these effects might have been expected because it has been shown that when  $t/R_1 = 0.49$  and the inner cylinder rotates, the distribution of velocity is such that over 83% of the thickness of the annulus  $Ur$  is constant.\* In that region, therefore, the effect of rotation is likely to be small. The effect of decreasing  $t/R_1$  might be expected to reduce the proportion of the whole volume of the annulus in which  $Ur = \text{constant}$  without affecting very greatly the transition layers close to the surfaces of the cylinders.

\* "Distribution of Velocity and Temperature Between Concentric Cylinders," Proc. Roy. Soc., A, vol. 151, p. 494 (1935).

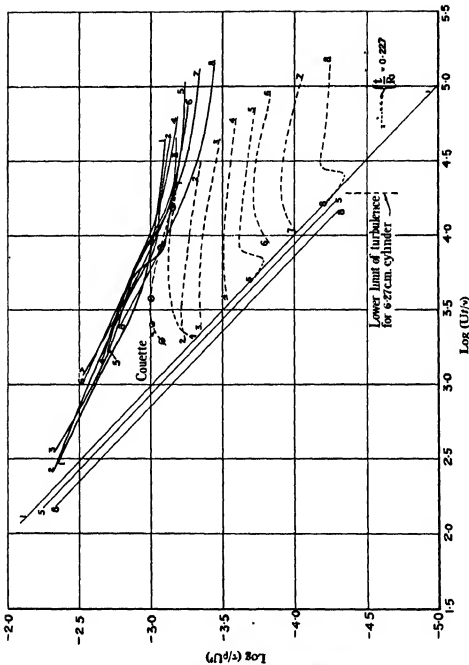


FIG. 10—Results compared in non-dimensional form.

The distribution of velocity when the outer cylinder rotates will form the subject of the second part of this paper. It seems that the distribution is then of a type which might be expected to be greatly influenced by rotation.

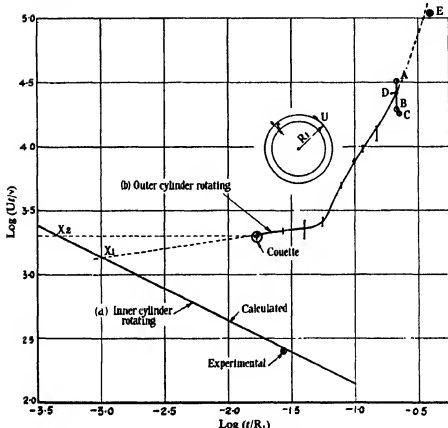


FIG. 11—Critical speeds.

#### EFFECT OF ROTATION ON CRITICAL SPEEDS

The observed upper and lower critical speeds for the case when the outer cylinder is revolving are shown in fig. 11. The ordinates represent the critical values of  $\log(tU/v)$  or  $\log(t\Omega R_1/v)$ . The upper and lower critical values are shown joined by a line to represent the range of states at which the change from steady to turbulent flow can take place. The abscissae are  $\log(t/R_1)$ .

The calculated critical speeds (see equation (9)) when the inner cylinder

is revolving are also shown, and an experimental point in one case, namely when  $R_2 = 8.11$ ,  $R_1 = 7.89$ ,  $t = 0.11$ .

#### COMPARISON WITH COUETTE'S OBSERVATIONS ON THE CRITICAL SPEED

The smallest ratio  $t/R_1$  used in the experiments here described was 0.0271. The experiments were not carried to a lower value because it was thought that if  $t$  were less than 1 mm. difficulty would be experienced in securing accuracy and uniformity in the thickness of the annulus and at the same time preserving sufficient freedom from non-fluid friction between the cylinders. The apparatus of Couette\* had a larger radius and less length than mine. This is permissible when small values of  $t/R_1$  are being used, and Couette's value of  $t/R_1$  was only 0.01685. His experiments were designed primarily to measure viscosity, but he measured the critical speed of the outer cylinder when turbulence set in. He found it to be  $N' = 55.69$  rev. per minute at a temperature of  $16.3^\circ C.$

Taking  $\mu = 0.01108$  at this temperature,  $t = 0.2465$  cm.  $R_2 = 14.639$  cm.,  $[\log(Ut)/v]_{crit} = 3.28$ , and  $\log(t/R_1) = -1.77$ .

The point corresponding with Couette's experiments is shown in fig. 11. It will be seen that it fits in well with the present results.

#### EXTRAPOLATION TO CASE OF TWO PARALLEL PLATES

The limiting critical value  $tU/v$  when  $t/R_1$  is very small, must be that corresponding with the case of two parallel planes distant  $t$  apart and moving tangentially with relative velocity  $U$ . In fact, the critical values for the two cases shown in fig. 11 must ultimately coincide for large negative values of  $\log t/R_1$ . If we consider the course of the upper curve (*b*), fig. 11, it will be seen that it descends rapidly till about  $\log t/R_1 = -1.3$ . At that point it flattens out, gradually descending. This flat part of the curve (from Couette's  $\log t/R_1 = -1.77$  to  $\log t/R_1 = -1.3$ ) indicates that the critical value of  $\log Ut/v$  for parallel plates must be less than 3.28, i.e.,  $[Ut/v]_{crit} < 2000$ . On the other hand, it hardly seems likely that the effect of a very minute curvature in the flow will be felt, so that it is unlikely that the critical value of  $Ut/v$  will fall very far below 2000.

Now consider the lower curve (*a*), fig. 11. It seems that steady motion will break down into cellular vortices† as soon as  $Ut/v$  exceeds the values on the line (*a*). If, however, this line is produced till it cuts the pro-

\* 'Ann. chim. (Phys.)', vol. 21, p. 433 (1890).

† *Loc. cit.*, p. 327.

longation of (b) it seems certain that the line will no longer represent the critical condition for values of  $U_t/v$  which are lower still. In fact, turbulence due to another cause, the cause which causes turbulence in case (b), must now set in before  $tU/v$  has risen to the value necessary for the cellular vortices. Since the curve (b) is descending slowly towards the rising line (a) their point of intersection\* must fall in the limited range between the points  $X_1$  and  $X_2$  where the line (a) cuts (1) the prolongation of (b) produced as a straight line with the same slope that it had in the lowest part of the observed range of  $t/R_1$ ; (2) a horizontal line through the lowest observed point on (b), namely  $\log(U_t/v) = 3.28$ . In this way  $X_1$  corresponds with  $t/R_1 = 0.001$ , and  $X_2$  corresponds with  $t/R_1 = 0.00045$ .

It appears, therefore, that in order that curvature may have no effect on the critical Reynolds number of the flow between concentric rotating cylinders,  $t/R_1$  must be less than 1/1000.

The corresponding limits to the critical value of  $U_t/v$  for flat parallel plates are, for  $X_1$ ,  $tU/v = 1260$ ; for  $X_2$ ,  $tU/v = 2000$ .

#### COMPARISON WITH COUETTE'S TORQUE MEASUREMENTS

In Couette's apparatus the outer cylinder rotated and the inner cylinder was held in position by a load  $P$ . Couette measured the number of revolutions  $N'$  per minute so that  $N' = 60N$ . Some of his observations, for values of  $N'$  above the critical value, are given in columns 1 and 2 of Table IV.

TABLE IV

$N'$	$P/N'$	$\log(\tau/\rho U^3)$	$\log(U_t/v)$
56.08	0.3067	4.916	3.297
71.56	0.4704	4.996	3.398
107.9	0.6883	4.993	3.581
249.7	1.327	4.903	3.929
453.3	2.111	4.846	4.192

Using the dimensions of Couette's apparatus, I find that

$$\left. \begin{aligned} \log(\tau/\rho U^3) &= \log(P/N') - \log N' + 1.1777 \\ \log(U_t/v) &= \log N' - \log v + 1.5773 \end{aligned} \right\}. \quad (10)$$

The values of  $\tau/\rho U^3$  and  $U_t/v$  calculated from (10) are given in columns 3 and 4 of Table IV and are marked in fig. 10. It will be seen that they compare very well with the present results for larger values of  $t/R_1$ .

\* Loc. cit., p. 327.

**STRESS CALCULATED FROM VELOCITY MEASUREMENTS**

In Part II of this paper the distribution of velocity is given when the outer cylinder rotates and the inner cylinder has a diameter of 6.27 cm., the outer one being 8.11 cm., so that  $t/R_1 = 0.227$ . The tangential stress at the outer surface was calculated from the velocity measurements and the results shown in fig. 10. It will be seen that the stress is very low, being rather lower than the lowest stress observed directly with the slightly larger inner cylinder 6.40 cm. diameter. This might have been expected because the direct measurements are necessarily too high owing to the fact that the fluid friction on the ends of the inner cylinder was not allowed for. On the other hand, the friction deduced from velocity distribution measurements taken near the middle of the cylinders is likely to give too low a result. It seems, therefore, that the true values  $\tau/\rho U^2$  for the values of  $t/R_1$  less than 0.227 are not likely to be very much in error.

**SUMMARY**

The torque between concentric rotating cylinders was measured in two cases, (a) inner cylinder rotating, outer cylinder fixed, (b) inner cylinder fixed, outer cylinder rotating.

It was found, as was to be expected, that the critical speed at which turbulence begins is very much lower in case (a) than in case (b). The difference between the critical speeds in the two cases becomes rapidly greater as  $t/R_1$  increases,  $t$  being the difference between the radii, and  $R_1$  the radius of the outer cylinder. When  $t/R_1 = 0.38$  the ratio of the critical speeds in the two cases exceeds 1000, when  $t/R_1 = 0.1$  it is about 50, when  $t/R_1 = 0.017$  it is 6. It appears that  $t/R_1$  must be less than 0.001 before the effect of rotation on the critical speed disappears.

When the flow is turbulent the effect of rotation on the torque is small in case (a) but large in case (b).

---

## Fluid Friction Between Rotating Cylinders

### II—Distribution of Velocity Between Concentric Cylinders when Outer One is Rotating and Inner One is at Rest

By G. I. TAYLOR, F.R.S.

(Received 31 August, 1936)

Measurements of the distribution of velocity between two cylinders when the outer one is at rest have been made\* by means of small Pitot tubes. The Pitot was traversed in from the outer wall towards the inner cylinder and the difference in pressure  $P$  between the Pitot tube and a hole in the outer cylinder was measured. The connexion between the velocity  $U$  and  $P$  is

$$\frac{2}{\rho} \int_0^r r^2 dP = U^2 r, \quad (1)$$

where  $U$  is the velocity at radius  $r$ .

A similar method can be used to determine the velocity between rotating cylinders when the inner cylinder is fixed and the outer one rotates. The small Pitot tube must now be fixed projecting from the inner cylinder. The formula (1) still applies for determining  $U$ . It may be conveniently expressed in the form

$$\frac{2}{\rho} \int_0^P \frac{dP}{N^2} = \frac{U^2 r^2}{N^2}, \quad (2)$$

where  $N$  is the number of revolutions of the outer cylinder per second.

Though the theory of these measurements is simple, the design of apparatus for carrying it into effect and making measurements at high speed of rotation is difficult. The difficulty arises entirely because it is necessary, after each change in the position of the Pitot tube, to fill the apparatus in such a way that one can be certain that all the internal passages in the inner cylinder are full of water. (The fluid used was water.) The internal passages are essential because the pressure from the Pitot tube, and also the pressure from holes on the surface of the inner cylinder, must be conveyed out through the small axle on which the fixed inner cylinder is mounted.

\* Taylor, 'Proc. Roy. Soc.,' A, vol. 151, pp. 494, 512 (1935); Wattendorf, 'Proc. Roy. Soc.,' A, vol. 148, p. 565 (1935).

The outer cylinder previously used for torque measurements\* was available. This had a pair of holes situated on opposite sides of the cylinder and at half its height. These holes, 5 cm. diameter, were fitted with removable brass plugs or doors cut to the same radius as the inside surface of the cylinder. When these plugs were fitted there was no break in the smooth finish of the outer cylinder. The inner cylinder was designed so that the fitting carrying the small Pitot tube could be loosened and the Pitot moved, by uncovering the brass doors, leaving the cylinders in position. The position of the Pitot was measured by means of a micrometer fixed to another plug fitting the same hole as one of the brass plugs.

The inner cylinder was designed for me by Mr. W. S. Farren. The central part is shown in the sketch, fig. 6, and Mr. Farren's description of the mode of operation is given in the Appendix. The general arrangement of the cylinders is shown in fig. 1.

#### METHOD OF MEASURING PRESSURE

The Pitot tube used in most of the measurements had an external diameter of 0.85 mm. A larger Pitot, 1.2 mm. diameter, and a smaller one 0.48 mm., were also tried but it was found that no measurable difference could be detected in the results obtained in the three cases. This is in marked contrast to what is found when the inner cylinder rotates. The difference between the two cases is due, no doubt, to the fact that the water retarded by the Pitot tube is driven inwards by the radial pressure gradient. When the Pitot tube projects from a fixed outer wall the fluid which strikes the mouth of the Pitot tube has therefore come from a region where it has already been retarded by passing (possibly many times) over the stem of the Pitot tube. In the present case, where the Pitot tube projects from the inner cylinder the fluid retarded by the mouth of the Pitot is also driven inwards by the radial pressure gradient so that it strikes the stem of the Pitot between the mouth and the surface of the inner cylinder. Unretarded fluid is therefore continually striking the mouth of the Pitot.

To measure the difference between the pressure at the holes in the surface of the inner cylinder and that in the Pitot tube, one cannot use a manometer directly, because the fluid would flow so slowly through the small bore of the Pitot tube that a very long time would be necessary for

\* Described in Part I.

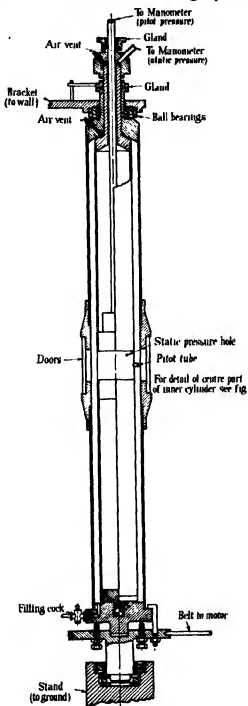


FIG. 1.

each measurement. A null reading capillary manometer\* designed to get over this difficulty was inserted between the manometer and the Pitot. The general arrangement of the measuring apparatus is shown in fig. 2. In that diagram A is the capillary manometer. The pressure from the Pitot tube is taken through a glass tube to the vessel B, which is partially filled with mercury. The lower surface of the mercury is situated in a converging capillary tube in which it is observed through a microscope M. The capillary tube projects into a vessel filled with dilute sulphuric acid. This vessel is part of a U-tube, the bottom of which is filled with mercury. The manometer C which contains mercury—or if small pressures are

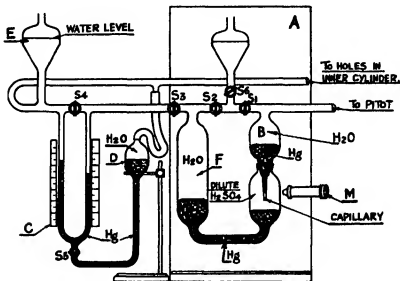


FIG. 2—Manometer.

being measured,  $CHCl_3$ —is connected at its lower end with a vessel containing mercury by means of rubber tubes. The vessel is also connected with the water pipe as shown in fig. 2. A number of glass stop-cocks  $S_1$ ,  $S_2$ , ...,  $S_5$  can cut off some parts of the apparatus from other parts. The pressure in the apparatus is controlled by the level of the water in the open funnel E.

To operate the apparatus,  $S_4$  is opened and  $S_3$  and  $S_5$  are closed. The readings of the manometer C are taken. This gives the reading for zero pressure difference. Next, keeping  $S_3$  and  $S_5$  closed,  $S_1$  and  $S_2$  open, the microscope is adjusted till the level of the mercury meniscus in the

\* Described in "A Manometer for Use with Small Pitot Tubes," "Proc. Camb. Phil. Soc.", vol. 24, p. 74 (1927).

capillary is on the crosswire. Next, close  $S_1$  or  $S_3$ , open  $S_4$  and  $S_5$ . If the apparatus is working the meniscus will stay on the crosswire of M, but if there is a bubble anywhere in the circuit the meniscus will move. With  $S_5$  closed, the level of D is then raised so that there is a good head of mercury.

Having made these preliminary adjustments,  $S_4$  is closed ( $S_3$  open,  $S_2$  closed). The cylinders are then rotated with increasing speed. Directly the pressure in the Pitot rises, the meniscus in the capillary begins to descend, the volume of water flowing through the pipe connecting the Pitot with B being very small. Keeping his eye on the meniscus, the observer then opens  $S_3$  very slightly and allows mercury to flow into C. Since the volume of water between the mercury in D and the mercury in F is nearly constant, the mercury level in C practically only rises on one side of the U-tube. Thus the pressures in B and F are brought to equality, the meniscus being brought to its zero position. The difference in level H of the mercury on the two sides of the manometer C is then read. The difference in pressure P between the Pitot and the holes in the inner cylinder is then  $P = Hg(\rho_m - 1)$ , where  $\rho_m$  is the density of mercury (or  $\text{CHCl}_3$  if that is being used).

#### MEASUREMENTS WITH INNER CYLINDER 5·02 CM. IN DIAMETER

Measurements were first made with an inner cylinder 5·02 cm. in diameter. If H is the measured distance between the mercury levels on the two sides of the U-tube C (fig. 2)  $H/N^2$  was found to be constant at any given radius as N varied. The values of  $H/N^2$ , measured at  $N = 33$  revs. per sec., are given in Table I, column 2. In column 3 are given the values of  $r^4 dH/N^2$ , where  $r$  is taken as the mean radius during the interval in which  $dH$  is measured (e.g., between  $r = 2\cdot6$  and  $r = 2\cdot7$  cm.,  $dH/N^2 = (1\cdot8 - 0\cdot8) \times 10^{-3}$ , and  $r^4 dH/N^2 = (2\cdot65)^4 \times 10 \times 10^{-3} = 7\cdot02 \times 10^{-3}$ ). The values of  $\int_{r_1}^{r_2} r^4 dH/N^2$  are found by adding the figures in column 3. These are given in column 4.

To find  $U^2 r^3 / N^2$  it is necessary to multiply the figures in column 3 by  $2g(\rho_m - 1) = 2 \times 981 \times 12\cdot6 = 24\cdot7 \times 10^3$ . Taking the square root of the figures derived in this way the values of  $Ur/N$  given in column 5 are obtained and hence dividing by  $r$  the values of  $U/N$  given in column 6.

These results are plotted in fig. 3. It will be seen that the distribution of velocity near the outer wall is nearly a uniform shearing motion, as it is

TABLE I— $R_1 = 4.05$ ,  $R_2 = 2.51$ ,  $N = 33$ 

$r$	1	2	3	4	5	6*	7†
		$\frac{H}{N^2} \times 10^3$	$\frac{r^2 dH}{N^2} \times 10^4$	$\int \frac{r^2 dH}{N^2} \times 10^4$	$\frac{Ur}{N}$	$\frac{U}{N}$	$\frac{U}{N}$ calculated streamline flow
2.51	0	0	0	0	0	0	0
2.6	0.8	5.22	5.22	11.3	4.3	1.8	
2.7	1.8	7.02	12.24	17.3	6.4	3.7	
2.8	2.8	7.56	19.80	22.1	7.9	5.6	
2.9	4.0	9.75	29.55	27.0	9.3	7.4	
3.0	5.3	11.30	40.85	31.7	10.5	9.2	
3.1	7.0	15.81	56.66	37.3	12.0	10.9	
3.2	8.8	17.86	74.52	42.8	13.4	12.6	
3.3	10.8	21.15	95.67	48.7	14.8	14.2	
3.4	12.9	23.60	119.27	54.2	15.9	15.8	
3.5	15.3	28.55	147.82	60.4	17.2	17.3	
3.6	18.4	39.1	186.9	68.0	18.9	18.9	
3.7	21.7	43.9	230.8	75.5	20.4	20.4	
3.8	25.1	47.8	278.6	83.0	21.8	21.9	
3.9	29.1	59.3	337.9	91.2	23.4	23.3	
3.953	31.2	32.4	370.3	95.6	24.2	24.1	
4.045	—	—	—	—	—	—	25.5

\* Crosses, fig. 3.

† Dots, fig. 3.

if the motion is non-turbulent. For this reason the theoretical values for non-turbulent flow were calculated from the formula

$$U/N = 10.22r - 64.4/r,$$

which vanishes when  $r = 2.51$  and is equal to  $2\pi(4.05)$  when  $r = 4.05$ . These are given in column 7, Table I, and shown in fig. 3. It will be seen that except near the inner cylinder the distribution of velocity is very close to that which would be expected if the flow were non-turbulent.

It will be noticed that the velocity of the outer cylinder, and therefore the velocity of the fluid very close to it, is known. It is

$$U = 2\pi N (4.05) = 25.5N,$$

so that the value of  $U/N$  at the outer cylinder is 25.5. This value is marked in all the subsequent diagrams and is given in column 7, Table I.

The fact that the observed velocity near the inner cylinder is greater than that calculated, is due to the action of the ends which cause outward flow there and a corresponding inward flow in the middle. This explanation was verified by fitting annular ends to the fixed inner cylinder. Radial

pressure then causes an inward flow at the ends and therefore a corresponding outward flow in the middle. This outward flow gives rise to a reduction in velocity near the middle of the inner cylinder. The measured

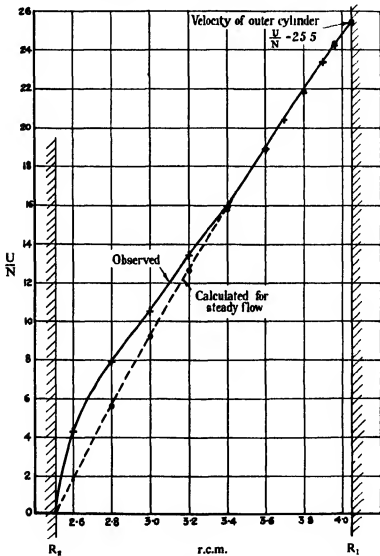


FIG. 3—Distribution of velocity when  $R_1 = 4.05$  cm.,  $R_2 = 2.51$  cm.  $N = 33$  revs. per sec.

velocity near the inner cylinder in this case was less than that calculated.

The conclusion derived from these experiments is that, at  $N = 33$  revs. per sec., the motion is still non-turbulent when  $R_2 = 2.51$ ,

$R_1 = 4.05$  cm. This was confirmed by watching coloured water emitted from the surface of the inner cylinder. This coloured fluid showed, incidentally, the flow over the surface of the inner cylinder from the centre to the ends.

The Reynolds number  $U t / v$  was, in the case when  $N = 33$  revs. per sec.,

$$\left. \begin{aligned} Ut/v &= 1.1 + 10^5 \\ t/R_1 &= 0.38 \end{aligned} \right\}. \quad (3)$$

and

This result is represented in fig. 11, Part I, by the point E. The fact that the motion is not turbulent under the conditions represented by E is indicated in fig. 11, Part I, by producing the critical line dividing stable from unstable states so that it passes above the point E.

#### MEASUREMENTS WITH CYLINDER 6.27 CM. DIAMETER

The diameter of the inner cylinder was increased by adding a concentric sleeve which brought its diameter up to 6.27 cm., thus leaving an annulus 0.92 cm. thick. Readings were taken at approximately 23.0, 26.7, 30.0, 33.0 revs. per sec.

Two typical sets of readings at  $N = 26.7$  revs. per sec. are shown in fig. 4, where the ordinates represent  $H/N^2 \times 10^3$ , and the abscissae are radii in cm. After drawing a smooth curve through the observed points, values of  $H/N^2$  were read off at each millimetre difference in radius and a table similar to Table I was constructed.

The values of  $U/N$  calculated in this way for  $N = 23.0, 26.7, 30.0, 33.0$  are shown in fig. 5 and the values of  $U/N$  for streamline flow are also shown. It will be noticed that in each case the  $U/N$  curve is nearly a straight line near the outer cylinder and that these straight lines pass very nearly through the value  $U/N = 25.5$  at  $r = 4.05$ , which is the value for the surface of the outer cylinder. This fact verifies the accuracy of the method of measuring velocities by integrating the Pitot pressures in the manner described,\* and also indicates that turbulence is not very effective in the outer layers.

Close to the fixed inner cylinder the measurements indicate too high a velocity. This appears to be due to a flow parallel to the length of the inner cylinder in a layer very close to the surface. This effect has already been discussed in connexion with the 5.10 cm. cylinder.

\* This method was used when the inner cylinder rotated and gave consistent results, *loc. cit.*, p. 565 (Part II).

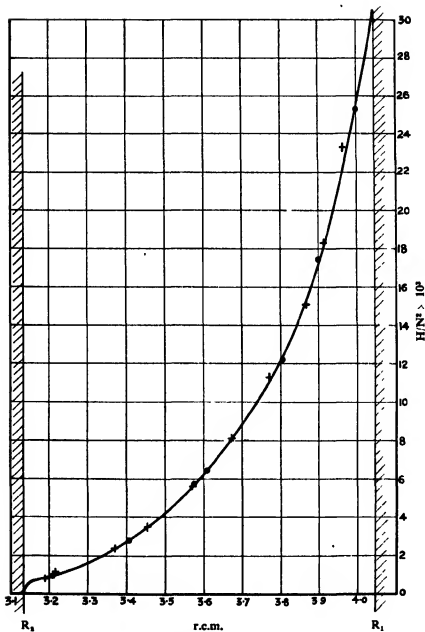


FIG. 4— $H/N^2 \times 10^3$ , when  $R_1 = 4.05$ ,  $R_2 = 3.13$ ,  $N = 26.7$ .

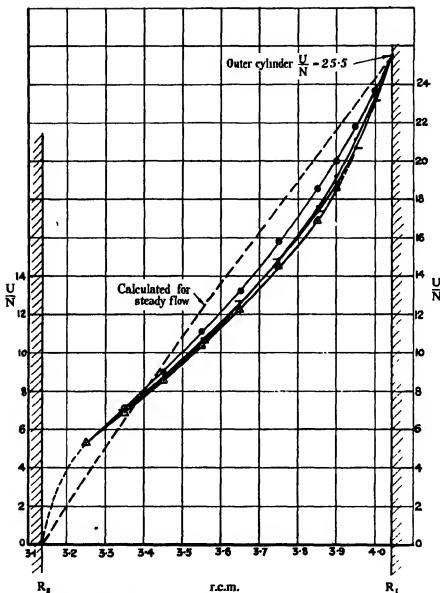


FIG. 5—Distribution of velocity,  $R_1 = 4.05$ ,  $R_2 = 3.13$ .  $\Delta$   $N = 33.0$ ;  $\bullet$   $N = 30.0$ ;  $*$   $N = 26.7$ ;  $\odot$   $N = 23.0$ .

## CALCULATION OF TORQUE

The torque between the two cylinders can be calculated from the velocity distribution, if it is assumed that the flow is non-turbulent very close to the wall. The nearly straight portion of the velocity curve near the outer cylinder wall gives  $dU/dr$ , and  $\tau$ , the shear stress, can therefore be calculated from the formula  $\tau = \mu \left( \frac{dU}{dr} - \frac{U}{R_1} \right)$ . The torque  $G$ , is  $2\pi R_1 \tau l$ , when  $l$  is the length of the cylinder.

TABLE II

1 N revs. per sec.	2 $\frac{1}{N} \frac{dU}{dr}$	3 $\frac{1}{N} \left( \frac{dU}{dr} \frac{U}{R_1} \right)$	4 $\frac{\tau}{\rho U^2}$	5 $\frac{tU}{v}$
23.3	39.5	33.2	$2.4 \times 10^{-4}$	$5.4 \times 10^4$
26.7	47.5	41.2	$2.6 \times 10^{-4}$	$6.2 \times 10^4$
30.0	50.1	43.8	$2.5 \times 10^{-4}$	$7.0 \times 10^4$
33.3	55.9	49.6	$2.5 \times 10^{-4}$	$7.7 \times 10^4$
8.3      Lower limit for turbulence	.....	.....	.....	$1.8 \times 10^4$

The values of  $\frac{1}{N} \left( \frac{dU}{dr} \right)_{r=R_1}$  given in column 2, Table II, were calculated from measurements of the curves shown in fig. 5.

The value of  $U/R_1 N$  is  $2\pi$  or  $6.3$ . Column 3 is found by subtracting  $6.3$  from column 2. The result may be expressed in a non-dimensional form by calculating  $\tau/\rho U^2$ , where  $U = 2\pi R_1 N$ . Thus

$$\frac{\tau}{\rho U^2} = \frac{\mu}{4\pi^2 R_1^2 N^2} \left( \frac{1}{N} \right) \left( \frac{dU}{dr} - \frac{U}{R_1} \right). \quad (4)$$

The values of  $\tau/\rho U^2$  are given in column 4, Table II. They are found by multiplying the figures in column 3 by  $\frac{\mu}{4\pi^2 R_1^2 N^2}$ .

The most suitable non-dimensional independent variable is  $tU/v$  when  $t$  is the thickness of the annulus, i.e., 0.92 cm. Taking  $v = 0.011$ ,  $U = 2\pi R_1 N$ ,  $tU/v = 2.32 \times 10^3 \times N$ . The values of  $tU/v$  are given in column 5, Table II. These results are shown in fig. 10 of Part I, where they may be compared with those obtained by direct torque measurement.

## CRITICAL POINT FOR TURBULENCE WITH 6.27 CM. CYLINDER

Passing some dye through the hole in the surface of the inner tube, it was found that the lower limit of velocity at which turbulence would persist was when  $N = 8.05$  revs. per sec. This corresponds with  $U_t/v = 1.8 \times 10^4$ . It is shown in fig. 11, Part I, at the point C.

Since finishing the work described above, I have seen a paper by F. Wendt\* in which measurements of the flow between rotating cylinders are described. These measurements were more complete than mine in the sense that they included cases where both cylinders rotated, but the design of the apparatus was such that only qualitative results could be expected. The height of the cylinders was only twice their diameter, and when in action the height of the fluid was lessened owing to the slope of the free surface till it was only 1.36 times the diameter of the outer cylinder. In the experiments described above, it was found that the effect of the bottom introduces serious errors in certain cases when the height is as little as 10 times the diameter. For this reason it is not possible to compare the two sets of results from a quantitative point of view. Qualitatively, the results agree in showing that when only the outer cylinder rotates there is a large gradient of velocity in the space between the cylinders, but when only the inner cylinder rotates the large gradients of velocity are confined to thin layers close to the walls.

In conclusion, I wish to express my thanks to Lord Rutherford for his permission to carry out these measurements in the Cavendish Laboratory.

## APPENDIX

By W. S. FARREN

The Pitot tube 1, fig. 6, is held by a spring chuck 2 in a transverse hole in the solid centre part of the inner cylinder 3. The chuck is tightened by a threaded plug 4 and the transverse hole is sealed by another plug 5 whose outer surface is turned so as to form part of the surface of the cylinder 3. Communication with the pitot tube is by a central hole 6, whose upper end is made conical. Into this fits the conical lower end of a long tube 7, which passes up, through the centre of the upper bearing, to the manometer. The conical joint between 6 and 7 acts as a union which can be disconnected by rotating the tube 7 from the outside. The lower end of the tube is threaded and screws into a nut 8, which is prevented from rotating by keys 9, though free to move axially. On a flange

\* "Turbulente Strömung Zwischen Zwei Rotierenden Konaxialen Zylindern," 'Ingen.-Arch.,' p. 577 (1933).

on this nut is a fibre washer 10, and, when the tube 7 is screwed downwards, the axial movement of the nut upwards brings the washer 10 into contact with an internal flange on the central block, and thus forces the conical end of the tube into the coned end of the central hole 6. At

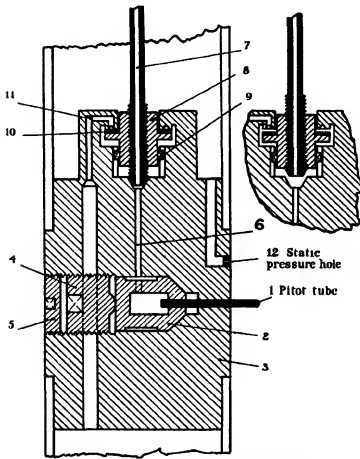


FIG. 6—Section of centre part of inner cylinder.

the same time the washer 10 seals the ends of a number of holes 11 which communicate with the space below the central block.

The two sketches show the parts in the two essential positions; on the left with the holes 11 sealed and the communication between the Pitot tube and the manometer established by the closing of the conical joint; on the right, with the holes 11 and the conical joint open, so that, when the apparatus is filled from below, the rising water can find its way quickly

into the whole of the inner cylinder. If the cylinder were filled, with the apparatus in the condition shown on the left, the water could reach the upper part of the inner cylinder only through the very small static hole 12, and not only would filling take an inconveniently long time, but it would be very difficult to ensure that all air was removed. Moreover, the whole of the connecting passages from the Pitot tube to the manometer would have to be filled through the Pitot tube itself. With the apparatus in the condition shown on the right, the water has free access to all the passages.

#### SUMMARY

In case (a) the distribution of velocity between the cylinders has previously been measured. The far greater technical difficulty of measuring the distribution in case (b) has now been overcome by a new design for the inner cylinder due to Mr. W. S. Farren. It is found that the stabilizing effect of rotation makes it possible for large gradients of velocity to exist throughout the space between the cylinders. The distribution is therefore more like that which occurs in non-turbulent flow than that observed in case (a), where nearly the whole velocity changes occur quite close to the wall.

---

## Further Work on Two Types of Diamond

By Sir ROBERT ROBERTSON, F.R.S., J. J. FOX, D.Sc., and A. E. MARTIN,  
Ph.D.

(Received 2 September, 1936)

[PLATE 11]

### INTRODUCTION

In the paper "Two Types of Diamond"\*\* many physical properties of diamond are described, and on p. 516 are collected features of difference and of similarity between the two types. Briefly, the ordinary type (Type 1) is characterized by greater apparent homogeneity, Type 2 having a mosaic structure but greater isotropy in polarized light; in infra-red absorption Type 1 has a strong band at  $8\text{ }\mu$ , this being absent in Type 2; in the ultra-violet Type 1 absorbs up to a point much nearer the visible region than Type 2 which is transparent nearly as far out as quartz; Type 1 has little, Type 2 a marked photo-conductivity; while the X-ray pattern exhibits slight differences† interpreted as supporting the greater degree of mosaicism of Type 2.‡

The two types were similar in respect of the electron diffraction, the Raman spectrum, tribo-luminescence, dielectric constant, refractive index, specific gravity, and colour.

The most striking differences were in the absorption of long and short wave light, and in the photoelectric response with its remarkable features of selective frequencies for activation and quenching. A fundamental Raman frequency of vibration at  $7.5\text{ }\mu$  was shown to be identical in the two types. The differences appeared to be connected with mosaicism.

This work has been continued both on some of the features mentioned above and also in other directions. Thus the work now reported relates to the further exploration of finer structure of the infra-red absorption spectrum by the aid of a grating, and of the photoelectric effect taken down to a lower temperature ( $20^\circ\text{ K.}$ ) than before; while the emission spectrum and the specific heats of diamonds of the two types are subjects not before included.

\* 'Phil. Trans.,' A, vol. 232, pp. 463-535 (1934).

† *Ibid.*, p. 474.

‡ See also Renninger (of Professor Ewald's laboratory), 'Z. tech. Phys.', vol. 11, p. 440 (1935), on X-ray intensities of "ideal" and of "mosaic" diamonds.

## INFRA-RED SPECTRUM OF DIAMONDS EXPLORED BY GRATING

On the curve of absorption given in fig. 7 of the original paper there appears beside the broad outlines of the absorption curve some evidence of a fine structure. Certain regularities in the frequency of these small bands were discovered, and they were considered to be connected with a nutation of low frequency (p. 522). But for the purpose of the allocation of the bands to atomic motions, greater resolution was thought desirable in the region 4 to 4.8  $\mu$  (p. 486) than could be obtained with the prism spectrometer then used (p. 478).

Consequently, a concave grating of 1 metre focus of echelle type was mounted in conjunction with the prism instrument. No new details of the bands at 3  $\mu$ , and 4.1  $\mu$  were obtained, but the band at 4.8  $\mu$  was further resolved (fig. 1a) and the small band C $\alpha$ \* on the side of the 8  $\mu$  band was definitely split into two (fig. 1b). The positions of these new bands are shown in Table I.

TABLE I—POSITIONS OF INFRA-RED BANDS OF DIAMOND. VALUES OF WAVE-LENGTHS AND WAVE NUMBERS

Band	$\text{cm.}^{-1}$	$\mu$	Previous value
$4.8 \mu$ B $\alpha_1$	2217	4.511	B $\alpha$ 4.59 $\mu$
	2170	4.608	
B $\beta_1$	2028	4.931	B $\beta$ 4.98 $\mu$
	1976	5.061	
$7.3 \mu$ C $\alpha_1$	1376	7.266	C $\alpha$ 7.29 $\mu$
	1368	7.311	

PHOTOELECTRIC PROPERTIES OF DIAMOND AT TEMPERATURES TO  
20° K

*Introductory*

In the apparatus figured on p. 480 of the original paper the temperature,  $-160^\circ\text{C}.$ , was attained by the use of liquid air, and the photoelectric effect was measured at that temperature, with the results given on pp. 514 *et seq.* It was desired to see if at a lower temperature, namely, that of liquid hydrogen, a diamond which appeared to lose its sensitiveness to light at about  $-100^\circ\text{C}.$  would persist in this condition at the still lower temperatures reached.

\* For this notation see original paper, p. 482.

In the earlier experiments heat was conducted from the diamond by way of a metal sleeve cooled internally by liquid air and in contact with the diamond-container which occupied a position in the vacuous space. To avoid the possibility of lag in the withdrawal of heat and to attain lower temperatures, the silica Dewar vessel (fig. 2) was now used. It was devised by Professor Simon of Oxford and gave a more direct cooling while readings could be made down to  $-250^{\circ}$  C. by the use of liquid hydrogen.

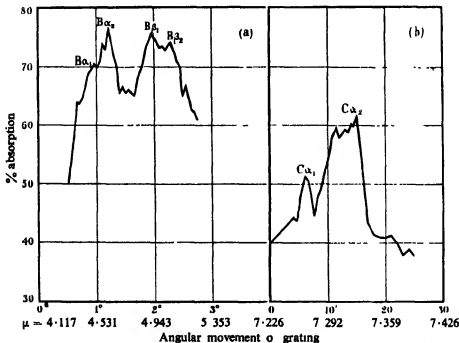


FIG. 1—Finer details of infra-red spectrum of diamond. Type I—D.26—thickness 0.8 mm.

#### *Experimental Arrangement*

In fig. 2 is shown the silica Dewar vessel with its tight-fitting metal cap and apertures for admitting liquid oxygen or air, and for leading off or pumping off the evolved gas. In this vessel the diamond, with its fittings as shown, is first of all cooled by being immersed in liquefied gas. Liquid oxygen was used for the initial reduction of temperature and then liquid hydrogen, for which we are indebted to Professor F. A. Lindemann, F.R.S., of Oxford. Only after the liquid hydrogen had evaporated so as to come below the diamond were readings of the photo-conductivity

taken, the diamond then being illuminated by either ultra-violet or red light, or both through the double silica windows of the vessel. This was internally silvered except for the windows and a narrow vertical slit for observation of the liquid level. Measurement of the currents was made in the manner described in the original paper, and most conveniently as the diamond gradually rose in temperature throughout about two hours.

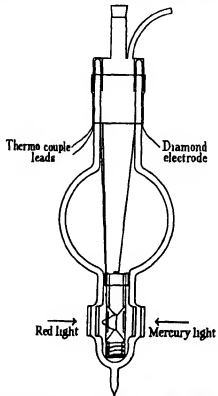


FIG. 2—Silica Dewar vessel for determining the photo-conductivity of diamond at the temperature of liquid hydrogen.

### Results

Readings of the total current generated in a diamond of Type 2 (D.22)\* by light from the mercury arc alone, and from this lamp with the addition of red light were made. The results are displayed in fig. 3a where the variation with temperature from  $-253^{\circ}\text{C}$ . to  $20^{\circ}\text{C}$ . is given for light from the mercury arc alone, and for the extra currents generated by the addition of red light. It will be seen that there is little change throughout

\* See p. 468 of original paper.

the interval between the temperature of liquid hydrogen and that of liquid air—the photo-conductivity induced by the full mercury arc keeping at a low value, while the effect of the added red light is constant throughout this range and appreciable. The rise in photo-conductivity from  $-100^{\circ}$  C. obtained formerly is confirmed. The effect of red light

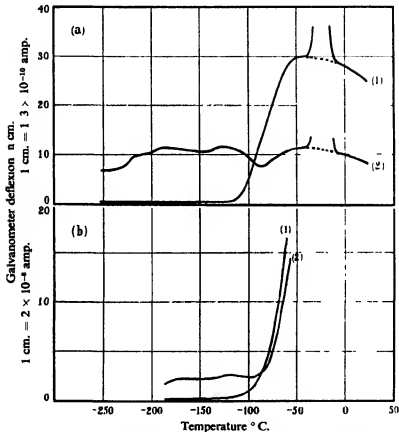


FIG. 3—Curves (1). Variation with temperature of currents generated by diamond D.22 on imposition of light from mercury lamp, without applied voltage (a), and with 30 volts applied (b). Curves (2): Variation with temperature of extra currents generated by addition of red light, without applied voltage (a), and with 30 volts applied (b).

does not show much variation from  $-253^{\circ}$  C. to  $20^{\circ}$  C. except for a diminution at the lowest temperatures and another at about  $-90^{\circ}$  C. Fig. 3b shows the results obtained for D.22 under an applied potential of about 30 volts. It will be seen that the voltage only begins to produce an effect above  $-95^{\circ}$  C.

Although the effects at a temperature lower by 90° C. than in the earlier experiments are the same, difference of behaviour was observed with this diamond in this series of experiments from that of the same diamond under the previous conditions when it was in a vacuum. Probably as a result of having been immersed in liquids containing some CO<sub>2</sub> and a trace of moisture, a large increase in conductivity took place at about -40° C., but on approaching 0° C. the conductivity returned to the same level as for the dry diamond, and the more easily if the apparatus was pumped out. Similar effects could be obtained with the diamond in air at room temperature by breathing lightly on it and illuminating with the mercury lamp. The normal current generated by the diamond was readily increased tenfold by this means and persisted so long as the moisture film remained. The effect appears to be due to the short-circuiting of insulating areas which are normally present on the diamond surface and impede the passage of the current. A large increase in current is also obtained by immersing the diamond between electrodes in distilled water contained in a silica tube, the light from a mercury lamp passing through the silica and water to the diamond.

#### INFRA-RED EMISSION SPECTRA OF DIAMONDS

##### *Introductory*

Friedel has examined the optical isotropy of diamonds at high temperatures up to 1885° C., and some account of this work will be found in our original paper (pp. 472 and 520). He finds that birefringence persists up to this temperature, but that the diamond then breaks into fragments on account of a rapid change in volume, and birefringence is no longer noticed in the fragments so long as they are not allowed to cool. He also found that at 1885° C. the transformation to graphite is very rapid. It was suggested by us (p. 520) that the differences between diamonds of Types 1 and 2 might be explained by the manner in which they passed through the point of transformation, those diamonds in which the strain had been relieved giving rise to the more isotropic Type 2.

It seemed possible that on heating a diamond of Type 1 to a temperature of 1885° C. the strain might be relieved and a diamond of Type 2 result, though to maintain the change on cooling to room temperature would probably require rather careful annealing. In order to follow any change in the diamond as it was heated, the emitted infra-red radiation was examined, an emission band at 8 μ clearly indicating the persistence of the character of Type 1 diamond.

*Apparatus and Procedure*

Through the courtesy of the General Electric Company, the design was obtained for a small molybdenum furnace capable of use for a considerable time at 1600° C. This furnace with associated apparatus is shown in fig. 4. The alundum tube A, 4 inches long and  $\frac{1}{4}$  inch diameter, is wound with Kanthal wire for moderate temperatures, or with molybdenum wire for the higher temperatures. The furnace casing was made from iron tube fitted with end plates through which passed the furnace tube, excessive gas leakage being prevented by asbestos packing B. Alumina was used for furnace packing C and provided good heat insulation. The diamond D was held in a disk of alundum E, faced with polished platinum

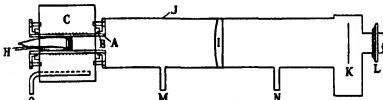
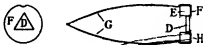


FIG. 4—Electric furnace and associated apparatus used for determining the emission spectrum of diamond

sheet F, to which were attached platinum wires G by which the diamond in its mount could be pushed to the centre of the furnace. The temperature of the diamond was determined by a Pt/PtRh thermocouple H.

The radiation from the diamond and its mount was condensed on to the slit of the infra-red spectrometer by means of the rocksalt lens I mounted in the brass tube J. One end of this tube joins on to the furnace and the other end is fitted to the enclosed electromagnetic shutter K which is attached to the slit L of the spectrometer. The correct alignment of the furnace was secured by placing a pea-lamp inside the furnace tube in the position normally occupied by the diamond, and making sure that the collimating mirror of the spectrometer was completely filled with light. As a check, the diamond holder without the diamond was placed in the furnace tube and the slit of the spectrometer illuminated. On looking down the furnace tube an image of the slit could be seen centrally in the aperture in the mount.

As carbon dioxide and water vapour have strong absorption bands in the region  $4\text{--}7 \mu$ , purified dry air was pumped into the spectrometer and into the brass tube through M and N when the temperature of the furnace was low. A small part of the diamond mount was cut away to allow easy passage of gas through the tube. At higher temperatures a reducing gas (4 parts nitrogen and 1 part hydrogen) was passed into the brass tube at M and into the furnace through O. Since the central part of the furnace tube was at the highest temperature and hence the most porous, the gas diffused through it and passed out of the furnace, thereby protecting the diamond as well as the molybdenum from oxidation.

The spectrometer and galvanometer system were arranged as described in the earlier paper (p. 478). During the examination of an emission spectrum, the temperature of the furnace was maintained constant; the procedure was to advance the wave-length drum by small regular steps, the galvanometer deflexion with the shutter alternately open and closed being obtained for each successive position in the spectrum. Emission spectra were obtained for the mount alone and with diamond, the emission being obtained by difference. This is permissible since only a small amount of the energy radiated from the walls of the open furnace tube reaches the spectrometer, and only a negligible proportion of this passes through the aperture of the mount in the absence of the diamond.

Emission curves were obtained for both types of diamond and for comparison from substances behaving nearly as black body radiators. The substances used were graphite roughened with No. 2 emery paper, oxidized iron and a surface coated with soot from burning camphor. Each of these could be slipped into the holder so as to occupy the position of the diamond. The emissivity of these three surfaces from 2 to  $15 \mu$  did not vary to any considerable extent, the graphite and camphor soot being particularly close. Graphite was finally selected as being generally the most satisfactory and was used for black body emission in all the measurements given in this paper, since it gave a curve nearly in accordance with a true black body.

### Results

The emission curves for a diamond of each type, together with graphite at temperatures of approximately  $200$  and  $400^\circ \text{C}$ . are given in fig. 5. The spectrometer slits were  $0.3 \text{ mm}$ . for the lower temperature and  $0.1 \text{ mm}$ . for the higher at which greater resolution was obtained.

It will be seen that even at the low temperature of about  $200^\circ \text{C}$ . each diamond is emitting radiation in accordance with its type, as indicated by the presence or absence of a band at  $8 \mu$ .

In fig. 6 have been drawn the absorption and also the emission curves of the two types of diamond, and in these will be observed a striking likeness even in details of fine structure. The diamonds used were D.10 (see previous paper), D.26 of about the same thickness, both having all the characteristics of Type 1, and D.2 a somewhat thicker diamond of Type 2.

We have thus an example of the validity of Kirchhoff's Law obtaining not at one restricted region but persisting throughout the whole band

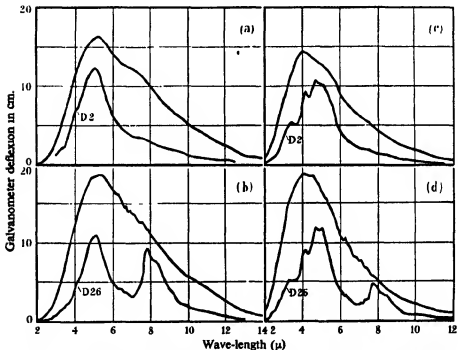
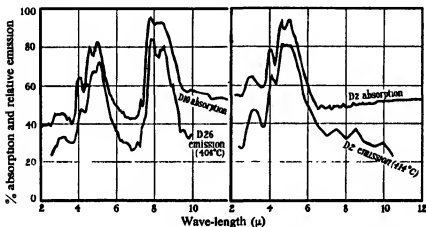


FIG. 5—Emission spectra of diamonds and graphite. (a) Graphite and diamond of Type 2 (D.2) at 198° C.; (b) graphite and diamond of Type 1 (D.26) at 198° C.; (c) graphite and diamond of Type 2 (D.2) at 414° C.; (d) Graphite and diamond of Type 1 (D.26) at 408° C.

range of the diamonds to such an extent that the curves of absorption and emission respectively can almost be superimposed even in their detail, except for some small reflexion losses.

The absence of the  $8 \mu$  band for the diamond of Type 2 in the emission spectrum is clearly shown. This band was observed for the diamond of Type 1 at temperatures up to 1025° C., but at higher temperatures (*ca.* 1400° C.) in an inert atmosphere the diamond was found to be superficially changing over to graphite, and the spectrum became indistinguishable from that of a black body. For this reason further experiments at

the higher temperatures were not attempted; but the diamond was repolished and then gave its normal emission spectrum. In an early experiment at 700° C. the diamond (Type 1) was in air and not in a reducing atmosphere, and after cooling it was noticed that one surface on which the air impinged had become slightly opalescent. On examination under the microscope, it was seen that the surface was covered with triangular etchings. Photographs of the etched surface are shown in fig. 7, Plate 11.



Thickness of diamonds: D2 = 2.09 mm., D10 = 1.08 mm.; D26 = 0.80 mm.

FIG. 6—Emission at ca. 400° C. of diamonds of both types relative to graphite, together with their absorption spectra at room temperature.

#### SPECIFIC HEAT OF DIAMOND

##### *Introductory*

The specific heat of diamond has been determined by many workers, but it was not known which of the two types was being investigated. The chief investigators are Nernst and Eucken who developed the method for low temperatures down to 30° K., Weber, who made measurements up to 1169° C., and Magnus. The variation of the specific heat of diamond with temperature has been discussed by Nernst, Lindemann, and Debye. For the present measurements the method of Nernst and Eucken, somewhat modified, was used for both types of diamond, the temperature range being from 90 to 320° K.

##### *Apparatus*

The diamond of either type under examination (weight about 0.5 gm.) was sealed up in a small container made from thin silver sheet. The

weight of silver was known and also the weight of solder used for sealing. Air was left in the container to assist in the rapid attainment of thermal equilibrium during the specific heat experiments in which the diamond in its case was isolated in a vacuum and supplied with a measured quantity of electrical energy. The case was rectangular in shape and wound with about 50 turns of enamelled copper wire, S.W.G. 47, as shown in fig. 8. The wire was knotted at the start and the finish of the winding to hold it in position, and could be kept completely insulated from the case. The same wire served for leads, a length of 15 mm. being used for each. Platinum wires were sealed through short tubes joined to a glass bulb and were attached to the thin copper leads so that the diamond in its case was suspended inside the glass vessel. Stout copper leads were soldered to the free ends of the platinum wires and finally connected to a Wheatstone bridge. The glass bulb was supported inside a Dewar vessel by means of a glass tube connected to a mercury diffusion pump, backed by a "Hyvac". The copper leads were bent downwards inside the Dewar vessel, as shown in fig. 8, in order to minimize the amount of heat conveyed along them to or from the platinum wires. The Dewar vessel contained solid carbon dioxide or liquid oxygen for the lower temperatures, and transformer oil for room temperature and above. A small electrical heater was provided for maintaining the oil at steady temperatures up to 50° C. The contents of the Dewar vessel completely covered the glass bulb and several inches of the leads. The glass vessel could be evacuated to such a degree that the heat conduction of the residual gas was quite negligible. A carbon dioxide trap was used to prevent mercury vapour from diffusing into the vessel.

The temperature of the case and its contents was obtained from a measurement of the resistance of the copper wire wound on the case, and the rate at which electrical energy was being supplied could also be determined from a knowledge of the current passing through the wire together with its resistance. The details of the circuit are shown in fig. 9. Current from a 2-volt accumulator was passed through the resistance P, milliammeter M, and the Wheatstone bridge. The resistance R was

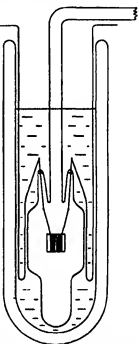


FIG. 8—Apparatus for measurement of specific heat of diamond.

about 13 ohms at room temperature and could be determined to 0·01 ohm directly from the bridge. The Moll galvanometer G was rapid in response and sufficiently sensitive to enable resistance differences to be measured to 0·0001 ohm from the out of balance current. It can be shown that when the bridge is balanced as in fig. 9 the out of balance current produced by increasing or decreasing the resistance 100 R by 1 ohm is very nearly

$$\frac{E}{[10(10R + G(10 + R))] [10 \cdot 1 P + (R + 10) 10]}.$$

The scale deflexion caused by the variation of 1 ohm in the 100 R resistance having been determined for one value of R, the out of balance

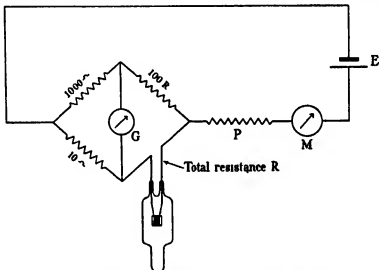


FIG. 9—Circuit used for measurement of specific heat of diamond.

current can then be used for measuring R to 0·0001 ohm for any other value. The purpose of this is to measure the rate of increase of temperature of the case and diamond by means of the rapidly changing resistance values.

Before starting an experiment, the glass vessel and its contents are allowed to attain the temperature of the surrounding substance with some air left inside the bulb to promote rapid thermal equilibrium. The glass vessel is finally evacuated and the heating current switched on. Resistance measurements are made at  $\frac{1}{2}$ -minute intervals at first and then less rapidly as the rate of temperature rise decreases. The resistance box is manipulated so as to keep the galvanometer spot close to its zero, and both resistance and galvanometer deflexion are recorded for the exact subse-

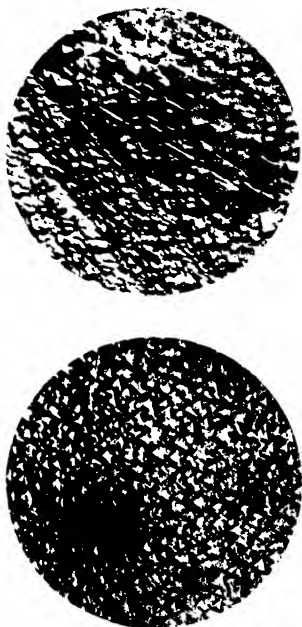


FIG. 7.—Portion of surface of diamond (Type I—D 26) etched by oxidation in air at 700 °C. : 2000.



quent determination of  $R$  as already outlined. The current supplied to the bridge is noted at frequent intervals, and if its value is denoted by  $C$ , then the energy supplied to the case and its contents is

$$\frac{C^2}{(1.01)^2} \times (R - I) \text{ watts},$$

where  $I$  is the resistance of all the leads right up to the case.

The variation of resistance of the copper wire with temperature is obtained from the resistance value at the start of each experiment (obtained by extrapolation) and the known bath temperature. It is necessary to correct for the portion of the copper leads outside the Dewar vessel which remain approximately at room temperature, and also for the platinum wires. The resistance of the platinum wires having been measured at room temperature, the value at any other temperature can be calculated from the known variation of resistance with temperature, the correction in any case being small.

During a specific heat determination the case is heated and also the thin copper leads to some extent. Since the ends of the leads in contact with the case are at the temperature of the case, and the ends attached to the comparatively massive platinum leads have not risen in temperature, we will assume that the average rise in temperature of the thin copper leads is half that of the case. If  $p$  is the resistance of the winding on the case,  $r$  the resistance of the thin copper leads, and  $r'$  the resistance of the thick copper leads outside the glass vessel but immersed in the contents of the Dewar vessel, all these resistances being for the same temperature, then the part of the total copper resistance  $p + r + r'$  which will have the temperature of the case when this is being heated by a current will be  $p + (r/2)$ , and the resistance change per  $1^\circ\text{C}$ . obtained from the measurements at different bath temperatures must be multiplied by  $\frac{p + (r/2)}{p + r + r'}$  to obtain the value to be used in determining the temperature rise of the case when heated electrically.

If at a given instant the electrical energy supplied per unit time to the case and contents is equivalent to  $H$  calories, the rate of temperature rise is  $d\theta/dt$ , and the total temperature rise  $\theta$ , then  $H = \Sigma ws \frac{d\theta}{dt} + f(\theta)$ ,

where  $\Sigma ws$  is the sum of the component heat capacities of the case and its contents, and  $f(\theta)$  represents the loss of heat from the system due to radiation and conduction through the leads. When  $\theta$  is small  $f(\theta)$  can be replaced by  $k\theta$ ,  $k$  being constant, and at the completion of the experiment when  $\theta$  becomes constant at the value  $\theta_0$ , we have

$$H_0 = k\theta_0,$$

so that

$$H = \Sigma ws \frac{d\theta}{dt} + H, \frac{\theta}{\theta_0},$$

It was found to be impracticable to determine  $\theta_0$  directly owing to the length of time required; actually it was calculated from the measurements made at the end of each experiment, the variation of  $\theta$  with time then being given by a single exponential expression. From the above equation  $\Sigma ws$  can then be obtained. The heat capacity of the silver was calculated from the known value of the specific heat; the heat capacity of the copper heating wire was similarly obtained, the exact weight of wire on the case being found at the completion of each set of experiments by cutting the wires close to the case and finding the total weight. The experiments with the empty case gave the heat capacity of the solder by difference, and the weight of solder being known, the specific heat was obtained and used for the experiments employing the diamonds. In these latter experiments the heat capacity of each diamond was finally obtained by difference and the results are set out in Table II. It was found that the specific heats of the two types of diamond do not differ from each other to any significant extent, nor do they differ appreciably from the figures given by other observers, as is shown in Table II.

We desire to acknowledge again our indebtedness to the Diamond Corporation Ltd. for lending us some of the stones, to Professor W. T. Gordon for the use of some from his own collection, and to Mr. F. S. Benge for his valuable assistance in the construction of the apparatus.

#### SUMMARY

Further work on the physical properties has been done on diamonds of the two types previously described.\*

*Absorption Spectrum*—This was explored by means of the addition of a grating to the spectrometer, and some further resolution of the band at  $4.8 \mu$  and of the small band on the side of that at  $8 \mu$  (in the case of Type 1 diamond) was obtained.

*Photoelectric Properties at Lower Temperatures*—By using liquid hydrogen the current produced in a diamond of Type 2 by the imposition of light of short wave-length and also of red light was determined at a temperature about  $100^\circ C.$  lower than had been done previously. At the temperature of  $-253^\circ C.$ , no abrupt change in the effects observed at  $-160^\circ C.$  was found.

\* 'Phil. Trans.' A, vol. 232, p. 463-535 (1934).

TABLE II—VALUES OF THE SPECIFIC HEAT OF DIAMOND

Temp. ° K.	Sp. ht. of diamond by others	Observer	Sp. ht. of	Sp. ht. of
			diamond of Type 1 (present authors)	diamond of Type 2 (present authors)
30	0.000	Nernst	—	—
42	0.000	"	—	—
88	0.0025	"	—	—
92	0.0025	"	0.0045	0.0033
201	—	—	0.048	—
203	—	—	—	0.052
205	0.052	Nernst	—	—
209	0.055	"	—	—
220	0.060	"	—	—
222	0.063	Weber	—	—
232	0.072	Koref	—	—
243	0.079	Dewar	—	—
262	0.095	Weber	—	—
284	0.113	"	—	—
295	—	—	0.121	0.118
306	0.132	"	—	—
325	—	—	0.148	—
327	—	—	—	0.142
331	0.153	"	—	—
358	0.177	"	—	—
413	0.222	"	—	—
1169	0.454	"	—	—

*Infra-red Emission Spectra of Diamonds*—As in the previous work on absorption, a clear differentiation of the two types of diamond in either possessing or not possessing a band at  $8 \mu$  was obtained also in emission. It was found possible to get the characteristic spectra of the respective types of diamond in the infra-red when they were heated at a temperature as low as  $200^{\circ}$  C. The agreement between the bands of emission and absorption is so close that even details of the structure of the bands are reproduced, thus affording a striking example of Kirchhoff's Law over a range of wave-length and in a spectral region not usually examined for this purpose. When air had access to the diamond at a temperature of  $700^{\circ}$  C. a finely etched surface with inverted pyramidal pits was obtained.

*Specific Heat of Diamonds*—This was done by the method of Nernst and Eucken, and it was found that the diamonds of both types had the same specific heat throughout the critical range of low temperature and also at higher temperatures.

## The Movement of Desert Sand

By R. A. BAGNOLD

(Communicated by G. I. Taylor, F.R.S.—Received 23 March, 1936)

[Plates 12, 13, 14]

### 1—INTRODUCTION

It is well known that on a dry sand beach and, on a much larger scale, on sand-strewn desert country the wind, if above a certain strength, will cause the surface sand grains to rise and to travel down-wind as a low-flying cloud. The mechanism, however, by which (a) the grains composing this cloud are raised, (b) the rate of mass movement of the sand depends upon the wind velocity, or (c) the wind velocity close to the surface is affected by the presence of the sand cloud, does not appear to have been previously investigated experimentally. This mutual interaction of wind and sand grains is of interest both in connexion with the problem of the tendency of sand to heap itself up into dunes even in totally flat uniform plains, and also for the light it may throw on certain aspects of the allied problem of the transport of sediment by liquid currents.

Sand found in the desert is usually composed of rounded quartz grains whose sizes range from small pebbles 2 to 3 mm. in diameter down to small particles 0·01 mm. in diameter, which must be regarded as dust. Mechanical analysis of eolian sand for grain size† show, when curves of percentage weight are plotted against grain size, that the peaks of such curves never occur on the small side of 0·15 mm. diameter. Sand having this smallest peak size is found at the crests of dunes. Here the grains approach uniformity of size, so that the diagrams are sharp-peaked. On the other hand, sand deposits clear of the actual dunes give broad, low diagrams with the peak at a larger diameter. In every case the diagrams show only a few per cent by weight at a size of 0·03 mm. In fact, it is a peculiarity of all sand accumulations that they are practically free from dust.

If dust is defined as particles which are so small that their low terminal velocity of fall allows of their being raised and maintained aloft for long periods by the upward vertical components of the internal movement of

† Wentworth, 'Univ. Ia. Stud. Phys.', vol. 14, No. 3 (1932).

the wind, then it becomes possible to define the dividing line between dust and sand in terms of the air and its motion. The larger particles, *i.e.*, sand, are those which, while still capable of being set in initial motion by the direct forward velocity of the wind, are yet incapable of being seriously affected by the less violent velocities of the wind's internal movement. The dividing line between sand and dust cannot be expressed in terms of grain size only, since material which behaves as sand in normal regions may be truly regarded as dust in regions where the wind speeds are unusually great.

I have already described† experiments which show that:—

(a) The motion in air of the average sand grain of a sample sifted for uniformity of grain size can be predicted with fair accuracy by (i) the replacement of the real grains by an ideal smooth sphere of a certain "equivalent diameter", and (ii) the use of a quantity which is defined in terms of the equivalent diameter and the relative velocity; this quantity is the ratio of the force of the air to that of gravity acting on the grain. I have called it the "susceptibility"  $S$  of the grain to the air in which it is moving.

(b) It is possible to attribute the uniform cloud of low-flying sand grains observed over an open desert surface, during sand-driving, to a continued bouncing motion of the grains whereby they move as projectiles, being shot upwards into the air after bouncing off a pebble or other solid object.

Assuming that the phenomena of sand-driving result from this bounding motion and are therefore surface effects, they should be, contrary to current ideas, largely independent of the natural eddies in the wind. Consequently, it should be possible to reproduce the effects in a wind tunnel of suitable design.

## 2—THE WIND TUNNEL USED

A tunnel 30 cm. square in section and 30 feet long was constructed during the spring of 1935. The discharge end opens into a wooden chamber A (fig. 1, Plates 12, 13), 5 feet cube, in the roof of which is a suction fan. The sand having passed through the tunnel settles in this chamber, where it falls into a hopper at the bottom, and is collected out of the door B for re-use. The tunnel itself is made of ply-wood, with glass sides and, for convenience, a removable roof. It is composed of sections 3 feet long, jointed together and supported at the joints by spring balances.

† Bagnold, 'Geogr. J.', vol. 85, p. 342 (1935).

By the changes in the readings of these, the rates of sand deposition and erosion, and therefore, by summation, the net flow of sand past any section can be measured at any place in the tunnel. Since this demanded flexibility at the joints, somewhat careful designing was necessary to ensure that air-tightness and internal smoothness were retained. Fig. 2 shows the design of the joints in detail.

Wind velocities were measured with a small total head tube made of hypodermic steel tube whose internal diameter of 0·8 mm. was about

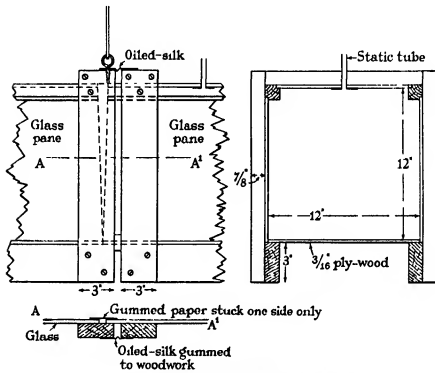


FIG. 2—Details of the joints between tunnel sections.

three times the diameter of the sand grains. The tube, in addition to being adjustable as to height, could also be moved from section to section of the tunnel. The static pressure was obtained from a series of orifices flush with the tunnel wall, any one of which could be connected with the manometer C by means of plugs, on the lines of a telephone exchange. The manometer pressures ranged from 0·05 to 12 mm. of water. Owing to the limited time available during a run, before the sand in the tunnel began to disappear and uncover the wood floor, it was essential that the manometer should be such that readings could be taken speedily. A

zero-reading instrument of the type described by Ower<sup>†</sup> was used, viz., an adjustable U-tube with an inclined tube on one limb which can be raised and lowered with a micrometer screw.

At the mouth of the tunnel was a sand reservoir D, also carried on a spring balance. This reservoir fed into a mechanical distributor E driven by an electric motor, and thence a stream of sand could be fed into the mouth of the tunnel at any required rate.

For the observation of ripples, a 1000-watt lamp was made to shine down the tunnel from some distance beyond the mouth.

Before each run the tunnel floor was covered with a layer of sand 1.5 cm. thick, smoothed out by means of a long-handled raker provided with thin legs 1.5 cm. long at each side, the feet of which rested on the tunnel floor so that an even thickness of sand was ensured.

The sand used was screened to exclude all grains other than those between 0.3 and 0.18 mm. diameter. This particular grade was chosen because, as already stated, it forms a very large proportion of the more mobile parts of desert dune fields.

### 3—DESCRIPTION OF THE SAND MOVEMENT

Beginning with a wind speed well below the threshold value at which the wind first starts to move the grains, the effects will be described as the wind is increased up to the highest speeds used.

At low wind speeds there was no sand movement whatever. When the sand distributor was switched on, so that a small but steady supply was started at the mouth, the incoming grains disturbed other surface grains, causing a small movement to take place along the tunnel. This movement, however, died away after a short distance.

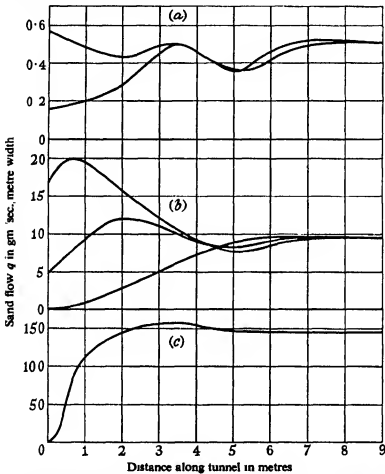
At a rather greater speed, but still considerably less than that required to start grain movement without an initial disturbance, a sudden change took place. The movement along the tunnel, instead of dying away, continued apparently indefinitely down wind, approaching as the distance increased a certain steady rate of flow.

Fig. 3a shows the sand flow in terms of the distance along the tunnel from the mouth.<sup>‡</sup> If the initial sand supply (as indicated by the ordinate

<sup>†</sup> "The Measurement of Air Flow" (1933).

<sup>‡</sup> The rate of sand flow through a given section of the tunnel was found as follows : Starting from the intake end, there are spring balances supporting (1) the sand reservoir, (2) the bell-mouth, (3) the first tunnel joint, (4), (5), etc., the succeeding joints. At the end of a run lasting  $t$  seconds the balance readings changed by amounts  $W_1, W_2, W_3, \dots$ , etc. For simplicity it was assumed that each of the changes referred

at  $x = 0$ ) was smaller than the ultimate rate, the flow built up, while if greater, the flow decreased till the same ultimate rate was reached. By standing at the down-wind end of the tunnel and operating the distributor switch from there, it was possible to measure the speed at which the disturbance travelled along the tunnel.



a, Mean air speed 430 cm./sec. (below threshold)  $V_{th} = 19.5$ ; b, mean air speed 490 cm./sec.,  $V_{th} = 36$ ; c, mean air speed 930 cm./sec.,  $V_{th} = 92$

FIG. 3—Variation of the flow of sand with the distance along the tunnel.

The first sign of the arrival of the disturbance could be seen in two ways. First, if the sand floor had previously been pressed very smooth to deposition or erosion in the half-section of the tunnel immediately on either side of the joint concerned. With this approximation the average rate of sand movement past any mid-section XY during the run was  $(W_1 + W_2 + W_3 + \dots W_n)/t$ .

with a sheet of metal or glass, small craters a millimetre or so in diameter could be seen to appear suddenly as if erupting spontaneously out of the sand. The craters rapidly increased in numbers until the whole surface assumed the typical finely-irregular appearance of wind-blown sand.

The sand movement could also be observed with the aid of an intense narrow beam of light† directed vertically downwards through a lengthwise slot in the roof. The after-image retained in the eye caused the grain paths to stand out against a black background like a skein of silver threads. The effect was of considerable beauty. The first grains to appear after the sand supply had been switched on were those whose paths rose to a maximum height—some 5 cm. These were rapidly followed by grains of lower and shorter paths until the flow became steady. On switching off the supply, the lapse of time before the motion ceased at the point of observation was rather longer than before. The rate of propagation of the disturbance down the tunnel was slow—about a third that of the air speed at the height at which the highest paths were seen.

By this method of intense vertical illumination large portions of the paths of the sand grains can be seen with the naked eye, and if the beam is sufficiently strong, can also be photographed. If either the camera or the light source is open for about 1/500 second the threads appear as lines of limited length, thus enabling the speed of the grains to be measured. A spinning grain appears as a dotted line, as the reflecting positions of the facets recur. Rotation does not seem to be the rule, though occasionally a grain was seen to rotate about once in ten diameters of path.

There can be little doubt, after watching the motion, that the grains behave as though scarcely affected by any air movement except its direct forward advance.

In particular, every path is concave downwards. The rise is almost vertical and the fall is of a nearly constant inclination from 10° to 16° to the horizontal. In fig. 4 (Plate 14) the actual paths as photographed are compared with typical theoretical paths calculated in the manner described in § 5 and the Appendix. The following points of special interest should be noted in them: The fainter downward tracks are those of fast-moving grains. More than one instance can be seen in (a) of an actual impact. The descending grain disappears into a little crater below the surface outline, and from the crater a slow speed grain rises almost vertically. In another case a descending grain has clearly ricocheted off the surface and continued forward at a flat angle and without losing much speed. One

† The source of light used was a mercury arc in a capillary tube of pyrex glass.

instance can be seen, in (b), of a rapidly spinning grain, and several tracks where a slow rotation has caused a track of uneven brightness. In (c), which was taken during a more violent sand movement, the connexion between the ripple phase and the density of the impacts is well shown.

As the flow proceeded, the little craters were seen to coalesce laterally into ridges, which slowly combined and separated out into the final ripple-mark.

The phenomena at low air speeds, when the wind was incapable of initiating sand movement, have been described in some detail. But they have all the characteristics of sand movement at higher air speeds, and their occurrence suggests strongly that the sand flow is maintained, once it is started, by the impact and splashing up of the sand grains themselves on the loose sand surface rather than by the direct action of the wind in picking the grains off the surface. The manner of the onset of the sand movement at the threshold speed, when there is no initial sand supply, illustrates this point.

When the wind was further increased, there came a moment when slight but unavoidable fluctuations, due to draughts outside the tunnel mouth, caused intermittent but strongly marked movements on the sand floor. The first occurrence of these took place, rather surprisingly, near the down-wind end of the tunnel. The disturbance ran rapidly down the rest of the tunnel and in a short time ceased as suddenly as it began, cessation beginning at the upstream end of the disturbed patch.

A further slight increase in the air speed caused such movements to occur more and more frequently until a steady sand flow was maintained. The point in the tunnel at which motion began, at first near the extreme down-wind end, moved further and further up the tunnel until it reached half a metre or less from the bell-mouth. Sand placed at the mouth itself was never disturbed even at the highest speeds used, despite the fact that the drag and the normal velocity gradient must be a maximum here.

The threshold wind at which movement began had no very clearly defined value. It was noticeable that if, after the sand movement had continued for a little time, the wind was reduced to below the threshold speed and again increased, sand movement occurred at a higher wind speed than if the surface was freshly raked over. This is understandable since on the old surface it is to be expected that all the grains have already been dislodged from the more unstable or more exposed positions. Two threshold speeds must be accepted: an upper, or "static" threshold, corresponding to an old stable surface, and a lower or "dynamic threshold", of which more later, corresponding to a disturbed surface. When

the motion has once been initiated at the higher threshold wind speed, we may picture the bombarding grains as disturbing the surface so that motion will persist, as long as the sand flow lasts, even though the wind is reduced to the lower threshold speed. If, however, grains cease to arrive from up-wind to disturb the surface, the latter will become stable at the up-wind end and a condition of greater stability will work along the surface, bringing a cessation of movement with it.

Again, since the sand surface is never disturbed even by the highest wind within a certain distance of the sand's up-wind extremity, the distance varying inversely with the wind speed, it seems that the threshold condition depends in some way on the length of the exposed surface. A point worth noting is the persistence of this undisturbed length of sand surface immediately down-wind, not only of the tunnel mouth, but of the boundary of an area of pebbles with which the up-wind half of the tunnel floor has been covered.

The rate of sand flow, at a wind speed just above the threshold, increased slowly with the distance along the tunnel until the ultimate steady rate was reached. If the sand supply was switched on at the tunnel mouth, sand movement began at the point at which the incoming grains struck the surface, and an excavation of the surface was formed there. The rate of increase of the sand flow was much greater than before, as can be seen in fig. 3b. It will be noticed that owing to the excavation of sand at the point of entry, the flow rises to a maximum which is higher than the ultimate rate, and falls to a minimum before the ultimate rate is reached. An increase in the incoming supply caused a more violent excavation and a correspondingly higher maximum, but the steady rate remained the same. Thus, for any given wind speed there is a certain ultimate steady rate of sand flow.

The ripple length, or the distance between one ripple crest and the next, increased with rising wind speed from 2·4 cm. at the lowest speed used—that at which the sand motion was only just stable even when stimulated by an incoming supply—to about 3 cm. at the threshold speed, and to a maximum of nearly 12 cm. When the wind exceeded a certain speed the ripples flattened out and disappeared, leaving a smooth, flat surface.

The appearance, at very low wind speeds, of bombardment craters has been described. Apart from the formation of these craters, little or no forward movement of the surface grains *along the surface* was seen. As the wind speed increased, however, the formation of the craters was accompanied by a forward jerking movement, at first only a few millimetres at a time, but gradually increasing with rising wind speed till at

high speeds the whole surface appeared to be creeping slowly forward.

Efforts were made to determine the mass-distribution of the sand flow with the height above the surface by weighing the sand collected in each of a set of tubes held at a range of heights. This was not entirely successful owing to the continual variation of the height of the surface itself as the ripples advanced, and also owing to the difficulty that however the collectors were placed the flow was interfered with. Neither of these troubles was serious at great heights but both became apparently insuperable within a few millimetres of the surface—just where the bulk of the sand was flowing. Other methods have been tried but with still less success.

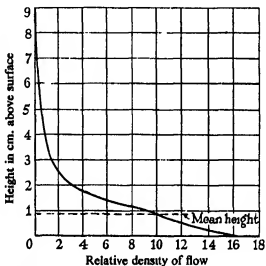


FIG. 5—Approximate curve showing distribution of sand grains according to height above the surface.

However, the fact emerged that the mean height of the sand cloud, that is, the height at which as much sand was collected above as below, varied from about 0.5 cm. at the lowest wind speeds to about 1.5 cm. at the highest speed used, which corresponded to about 34 miles per hour if measured at a height of one metre.

Visually the cloud is very deceptive; for the top, as seen quite clearly in a bright light when looking down the tunnel, is some ten times higher than the mean height. Fig. 5 shows a typical curve connecting the quantity of sand collected in a given time with the height of collection. It will be seen that a small change in the zero height of the surface will make a serious error in the mean height.

## 4—WIND VELOCITY AND SURFACE DRAG

The wind velocity varies, of course, for any given pressure drop, from zero at the tunnel surface to a maximum at some height near the centre of the tunnel depending on the relative drag of the top and bottom surfaces. A search was made for some standard method, whereby the wind velocity distribution at which a given sand flow, ripple length, or pressure drop took place could be specified independently of the tunnel dimensions.

As a preliminary to velocity measurements with flowing sand, the characteristics of the air flow were found for the case when the identical sand surface was fixed so that no sand movement could take place. To do this the sand surface was first allowed to conform to the wind conditions corresponding to a particular fan rate by driving the sand until the ripples were well developed. The whole surface was then fixed without disturbing any of the grains by spraying with water vapour from an "atomizer". The fan was again turned on and the wind velocity explored with the pitot tube from a minimum height of 0·2 cm. This process was repeated for the whole range of wind speeds used. In order to minimize any errors in estimating the true height above such an irregular surface as that of sand, and also to guard against the measurement near the surface being affected by the particular ripple phase at which measurement took place, the readings were repeated at four different places one metre from each other along the tunnel.

The mean of the four readings for each height was plotted against the log height, and the results gave straight lines conforming well with Prandtl's equation

$$v = \sqrt{\frac{\tau}{\rho}} \left( 5.75 \log \frac{z}{k} + 8.5 \right), \quad (1)$$

where  $v$  is the mean horizontal air velocity at any height  $z$ ,  $\tau$  is the surface drag in dynes per cm.<sup>2</sup>,  $\rho$  is the density of the air, and  $k$  a length representing the dimension of the surface irregularity. Since when  $v$  is zero,  $z$  must be equal to  $k/30$  in order to satisfy equation (1), and since the surface irregularity should, when the surface is fixed, be the same for all wind speeds, all the plots should converge to one focus on the log  $z$  axis and this intercept should give a height  $z$  equal to 1/30 of the size of the irregularity. The actual lines do so converge, to within a small margin of error, and the mean intercept gives a value for  $k$  equal to 0·06 cm., which is about half-way between the grain size and that of the little impact craters in the surface.

The quantity  $\sqrt{\frac{\tau}{\rho}}$  has the dimensions of a velocity, and specifies the distribution of the velocity with height for any surface for which  $k$  is constant. In accordance with the accepted notation,  $\sqrt{\frac{\tau}{\rho}}$  is denoted by  $V_*$ . By differentiating equation (1) with regard to  $\log z$  it will be seen that  $\frac{dv}{d(\log z)} = 5.75 V_*$ , so that the value of  $V_*$  can be read off at sight from any experimental plot of the normal velocity distribution; and hence the drag  $\tau = \rho V_*^2$  can also be readily found from the plot. ( $\rho$  is regarded as constant and equal to  $1.2 \times 10^{-3}$ .)

The dotted lines in fig. 6 show a set of curves plotted on a logarithm scale connecting wind velocity with height for different fan speeds when the surface was fixed. It will be noted that the velocity, even at as low a height as 0.2 cm. above the surface, increases considerably as the general wind speed is raised.

On repeating the measurements when the surface had dried off and the sand was again mobile, it was found that the steepest rays, corresponding to the lowest speeds below the threshold value, were much the same as before. But the unexpected fact emerged that for wind speeds above the threshold the Pitot tube placed near the surface at a height of 0.2 cm. never gave a pressure corresponding to an air speed greater than 210 cm./sec. In fact, the velocity at this height dropped suddenly from 260 cm./sec. when the sand movement started to 200 cm./sec. when the movement became continuous, and subsequently decreased still further to 175 cm./sec. when the wind speed was greatly raised. The rays crossed each other at a height between 0.2 and 0.4 cm., and intersected at an approximately fixed point for all winds above the threshold.

The point ( $v = 250$ ,  $z = 0.3$ ) thus became a new focus for the velocity rays in place of the usual intercept ( $v = 0$ ,  $z = k/30$ ). The continuous lines in fig. 6 show the arrangement of the velocity distribution when this sand flows over its own loose surface.

Before proceeding further, it was necessary to consider whether the Pitot tube was showing the total head of a fluid consisting of a mixture of air molecules and sand whose density could be taken as the total mass of matter in unit volume, or whether it was the total head due to the air alone. A sand grain of the size dealt with is so little affected by the fluid that if travelling at, say, 400 cm./sec. and suddenly entering still air, its velocity will not be reduced to half-value till it has travelled 20 cm. Since the Pitot tube used was only 3 cm. long, there seemed no possibility that the column of air in it could have absorbed any appreciable part of

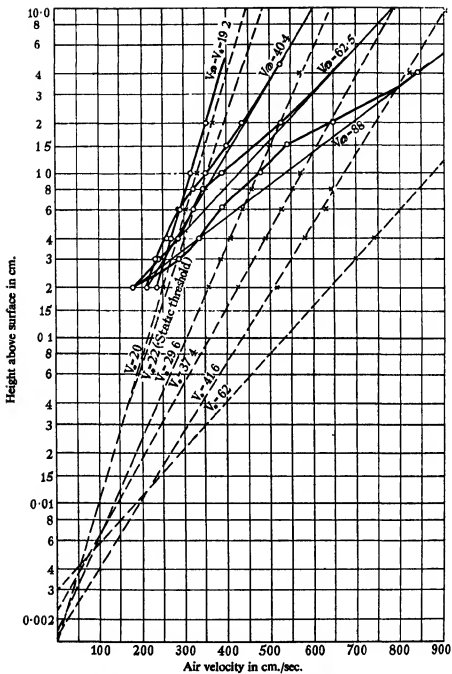


FIG. 6—Normal wind velocity distributions. Dotted lines refer to flow without sand movement; heavy continuous lines to flow during sand movement.

the momentum of the grains that entered the tube. Nor, owing to its comparatively low susceptibility, *i.e.*, the stopping or deflecting power of the air on the grain, could the passage of the latter outside the tube have any appreciable influence on the air inside.

In order to make certain, however, that the pressures measured could really be attributed to the air alone the experiments were repeated with very coarse sand of 10 mm diameter—as large as the whole outside diameter of the Pitot. Exactly the same arrangement of velocity distributions was found, though naturally the fixed focus occurred at a higher wind speed.

Prandtl's equation  $v = \sqrt{\frac{\tau}{\rho}} \left( 5.75 \log \frac{z}{k} + 8.5 \right)$  for the velocity distribution of the fluid flow near a boundary is derived from his general equation  $\tau = \rho l^2 \left( \frac{\partial v}{\partial z} \right)^2$  by taking  $l$  the Mischungsweg as proportional to the distance from the boundary and equal to 0.4 times that distance. If this condition should approximate to the truth in the region above the layer of air affected by the sand cloud, it should be possible to replace the actual crooked velocity curves found by experiment by straight lines which would give the velocity distribution and shear stress in the air above the disturbed layer.

Transferring the origin to the experimental fixed focus Prandtl's equation (1) reduces to

$$v - 5.75 V_{w_0} \log \frac{z}{k} + V_t \quad (2)$$

where  $V_t$  is a constant velocity (approximately 250 cm/sec in the case of sand here dealt with),  $k$  is now the height of the focus above the surface, and  $V_{w_0}$  is equal to  $\sqrt{\frac{\tau}{\rho}}$  ( $\tau$  being the total drag or the shear stress per unit area of surface in the air above the sand flow).

In fig. 6, a straight line will be noticed marked  $V_{w_0} = V_t = 19.2$ . This line represents the wind distribution at the lower or "dynamic" threshold. It also passes through the focus ( $v = 250, z = k$ ), so that it appears that the velocity at which the feeblest sustained movement of sand will start, if stimulated by a shower of grains upon the surface, remains the same, at the height  $k$ , at all higher velocities also, when sand is moving freely. This identification of the constant velocity of equation (2) with the dynamic threshold wind velocity is also true for uniform sands of other grain sizes, even up to 10 mm in diameter.

The constant height  $k'$  at which  $V_t$  is measured appears from my

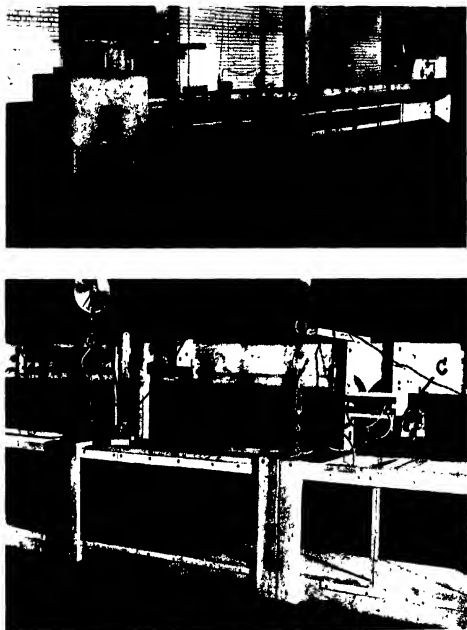


FIG. 1.—Special wind tunnel.

(Facing p. 806)

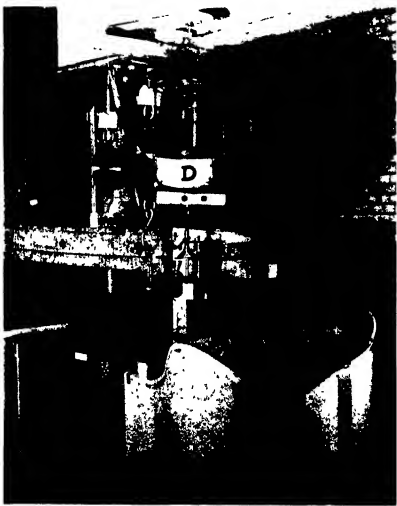


FIG. 1—Special wind tunnel used.



(a)



20<sub>1</sub>

(b)



(c)



(d)

FIG. 4.



experiments to remain the same for larger grain sizes. Existing theory,<sup>†</sup> based on the fluid force acting on a grain resting on the surface, indicates that the threshold velocity for different grains should vary as the square root of the diameter, the velocity being taken as that at the top of the grain, so that  $v^* = A' \frac{\sigma - \rho}{\rho} gd$ . Experimental support, however, has been forthcoming only from observations on the general velocity of the fluid at far greater heights. I find experimentally that the square root relation does not hold when the velocity is measured at a fixed height, but that it is very closely true when the velocity in each case is taken at a height  $z$  equal to  $k$  of equation (1), that is, at a height equal to the diameter  $d$  of the grain; the velocity at such a small height being read off the continuation of the straight line velocity plot (e.g., the dotted line of fig. 6) which gives the velocity distribution at the dynamic threshold.

Equation (1) can be written  $v = 5.75 V_* \log \frac{30z}{k}$  and when  $z = k$ ,  $v$  is proportional to  $V_*$  for all values of  $k$ , i.e., for all dimensions of the surface irregularity. Hence

$$V_* = A'' \frac{\sigma - \rho}{\rho} gd,$$

so that

$$V_t = A \log \frac{30k'}{d} \times \sqrt{\frac{\sigma - \rho}{\rho} gd}, \quad (3)$$

where  $k' = 0.3$ ,  $\sigma = 2.65$  (quartz),  $d$  is the mean diameter of the grain, and  $A$  is found to have the value 0.43.

It now remains to discover whether the drag as obtained from the estimated ultimate direction of the velocity rays (the continuous lines of fig. 6) agrees in any way with the actual drag which the moving sand bottom now contributes to the pressure drop along the tunnel.

The pressure drop along the tunnel is caused by the total of the resisting forces contributed by each unit of area of the walls, roof, and bottom. The walls and roof remaining the same whatever kind of surface is placed upon the floor, it is possible to estimate the drag caused by them by subtracting from the total pressure drop the contribution thereto due to the floor surface, when this is known. The result should be the same whatever fixed floor surface is used. Thus, once a curve is obtained for the drag due to the walls and roof of the tunnel in terms of the mean tunnel air speed, it is possible to arrive at the drag due to the flowing

<sup>†</sup> Owens, 'Geogr. J.', vol. 31, p. 418 (1908); Jeffreys, 'Proc. Camb. phil. Soc.', vol. 25, pt. 3, p. 272 (1929); Davis, 'Engineering', vol. 140, pp. 2, 124 (1935).

sand on the floor at any given mean air speed, by subtracting the drag of the walls and roof from the total drag as obtained from the pressure drop.

This was done for the whole range of wind speeds dealt with, using as a check in obtaining the drag of the walls and roof three different kinds of fixed floor surface, (i) sand fixed by spraying, (ii) coarse grit scattered evenly over the wood floor, and (iii) the bare wood floor. The drag due to the bottom was in each case deduced from the velocity distribution. As the figures for (ii) and (iii) lay closely along the same curve as those for condition (i), it was concluded that the curve gave reliably the drag due to the walls and roof.

If equation (2) represents the actual state of affairs, the drag due to the sand flow along the bottom ought to be obtainable from the slope of the straight line rays, drawn from the focus to meet the actual experimental curves well above the top of the sand cloud. This drag should be the same as that found above from the pressure drop measured during the same experiments in which the velocity curves were taken. A comparison of these two sets of results is given below:—

Mean tunnel speed, cm./sec	...	508	620	703	880
$\tau$ from pressure drop	.....	2.1	3.7	4.7	10.6
$\tau = \rho V_w^2$	.....	1.9	3.1	4.7	9.4

On the assumption that equation (2) is a fair approximation to the truth, it is of interest to compare the surface drag at a standard height of one metre with and without sand flow over a surface of the same sand. For the flowing sand condition we have

$$v - 250 = 5.75 \sqrt{\frac{\tau}{\rho}} \log 333,$$

so that

$$\tau = 5.75 \times 10^{-6} (v - 250)^2,$$

and for the fixed surface

$$v = \sqrt{\frac{\tau}{\rho}} \left( 5.75 \log \frac{100}{0.075} + 8.5 \right),$$

so that

$$\tau = 1.7 \times 10^{-6} v^2.$$

V in cm./sec.	...	530	583	1000	2000
V in m.p.h.	...	11.9	13.1	22.5	45
$\tau$ for sand flow	.....	0.44	0.63	3.20	17.4
$\tau$ without flow	.....	0.44	0.58	1.7	6.8

These figures give a good idea of the extent to which a loose sand surface can affect the wind which blows over it.

It will be seen from equation (2) that the velocity distribution above the sand cloud (for sand of a given grain size) is uniquely determined by the value of  $V_{\infty} = \sqrt{\frac{\tau}{\rho}}$ . In what follows all the sand effects described will be specified in terms of  $V_{\infty}$ , for the flowing sand condition and the wind over any fixed surface will be specified in terms of  $V$ .

Reference to fig. 6 will show that the velocity distribution departs from the straight line relation of equation (2) in the neighbourhood of 1 cm. height, and that the curves make a pronounced kink, the thickest part of which rises in height as  $V_{\infty}$  increases in value. It seemed likely that this kink indicated the height at which the grains receive most of their forward momentum from the air. If the grains describe ballistic paths from impact to impact, the height of the centre of the kink might indicate some sort of mean height to which the grains rise. This is strongly supported by the similarity between this height and that found for the mean height of the mass-flow by the collecting tube method.

When originally trying to devise some manageable way of dealing with such heterogeneous things as sand grains, I used the idea of replacing the real grains by an ideal grain which would behave in the same manner, under the given conditions, as the average grain of a sample. Since we are here dealing with a similarly heterogeneous collection of grain paths, of all heights and velocities, we might, by pursuing the same idea, obtain an ideal grain path which would have the same effect upon the air as the real sand cloud, and would therefore characterize the sand flow for a particular wind velocity. In order to follow this up, it is necessary to examine the nature of the ideal paths traced out by ideal grains when they are projected into air streams of different velocities at various initial speeds.

##### 5—GRAIN PATHS AND RIPPLE LENGTH

I have supposed the ideal grain to start vertically upwards with initial velocity  $w_1$  and the air velocity distribution to be that of the experimental curves of fig. 6. Having chosen one particular velocity distribution,  $V_{\infty}$ , I traced by the approximate method given in the Appendix the path which an ideal smooth sphere of the same equivalent diameter as the experimental sand grains (0.018 cm.) would follow if given some arbitrarily chosen initial velocity  $w_1$ . Several such paths corresponding to different values of  $w_1$  were traced for the same wind, and then similar sets of paths were traced, for the same set of values of  $w_1$  but for new wind speeds.

The paths are purely mathematical curves, based on nothing but the accepted drag on a smooth sphere as defined in terms of the Reynolds number. Since the work of path tracing does not lend itself to analytical treatment and can only be done by a laborious approximate method, it is impracticable to obtain any path at will. I have therefore linked together the sets of paths already traced by approximate relations from which the principal elements can be obtained for any intermediate paths.

The most important of these elements are:

$V_{eq}$  which defines the distribution of wind velocity.

$d$  the equivalent grain diameter, which has remained unchanged throughout the present work.

$w_1$  the initial velocity of rise.

$u_s$  the final horizontal velocity of the grain at impact.

$l$  the range, or total distance travelled down-wind between take-off and impact.

$z$  the maximum height of rise.

The following approximate connexions were found between these quantities:

(a) The height  $z$  can be expressed by the empirical expression

$$z = \frac{w_1^2}{2g} \left\{ 1 - 0.021 \left( \frac{w_1^2 V v}{d^3 g^2} \right)^{\frac{1}{2}} \right\}, \quad (4)$$

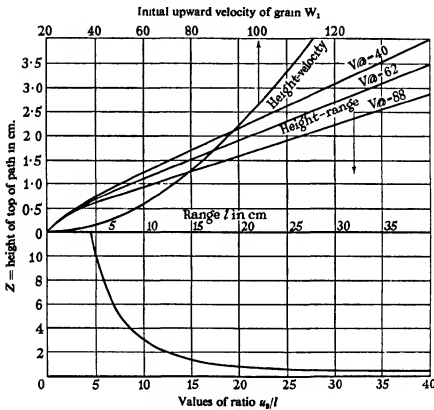
where  $V$  is here the wind velocity at the height  $z$ . The negative dimensionless term was found by trial and error to give values for  $z$  in agreement with those found from the traced paths over a wide range of values of both  $w_1$  and grain diameter  $d$ . The effect of changes of  $V$  on the value of  $z$  is very small, and in most cases it suffices to retain some mean value of  $V$  for a wide range of  $w_1$ .

(b) The ratio  $l/u_s$  was found to be equal to the time of rise of the grain if no drag were acting. So that

$$w_1 = gl/u_s \quad \text{or} \quad \frac{u_s}{l} \times w_1 = g \quad (\text{to within 5% error}). \quad (5)$$

(c) Owing to the complicated nature of the velocity distribution, I have only been able to complete the relation of the grain path elements graphically. Fig. 7 gives the connexion between the wind velocity distribution as defined for a grain of 0.018 equivalent diameter, the range  $l$  and the height  $z$ . Curves showing the values of  $w_1$  and  $u_s/l$  both in terms of  $z$  are also added for convenience.

On the ballistic hypothesis, the drag opposed by the sand movement to the air stream is due to the extraction of momentum from the latter in accelerating the grain during its passage along its path. For any given path, therefore, the maximum effect upon the air will take place at the height at which the grain receives the bulk of its forward momentum. From an examination of the figures obtained in calculating the above



Path elements for a grain of equivalent diameter = 0.018 cm.

FIG. 7.

grain paths, it appears that the grain receives 50% of its momentum between the ground and  $0.8z$ , and the remainder between  $0.8z$  and  $z$ . On the other hand, the 50% level as regards the quantity of sand that would be collected by orifices placed at every height is the level at which 50% of the total range  $l$  is gained above and 50% below. This height is  $0.75z$ .

After examination of the evidence, it was decided that if the whole sand flow could be replaced by a single imaginary path which every grain

pursued, this characteristic path should have a maximum height equal to 1·3 times the level to which the evidence points as being that of maximum interaction between air and sand; that is, the height of the maximum width of the kink in the velocity curves.

Two assumptions were now made. (1) The initial velocity of rise  $w_1$  of the characteristic grain bears some constant ratio to the velocity distribution  $V_w$  of the air. This seems reasonable since the characteristic grain is supposed to be ejected from the surface by the impact of a grain whose final velocity of impact is the mean of that of all the grains describing all possible paths in the sand cloud. Since these grains are exposed to the air stream at all heights, their mean velocity of impact is likely to be controlled by  $V_w$ , which defines the whole distribution of air speed. Thus it was assumed that:

$$W_1 = BV_w, \quad (6)$$

where  $B$  may be regarded as an "impact coefficient". (Note—The block letters  $W_1$ ,  $U_2$ ,  $L$ , and  $Z$  refer in what follows to the elements of the characteristic path whereas the corresponding small letters refer to any path.)

(2) The height of rise  $Z$  is to be measured from the origin of equation (2), that is, from a height  $k'$  above the surface, so that

$$Z = (Z_0 - k') - (1·3H - k') \quad (k' = 0·3 \text{ cm.}). \quad (7)$$

Substituting in equation (3) we have

$$Z = \frac{B^2 V_w^2}{2g} \left\{ 1 - CB^2 V_w^2 V^2 \right\},$$

where

$$C = 0·021 \left( \frac{v}{d^2 g^2} \right)^{\frac{1}{4}}.$$

Putting  $B = 0·8$ , the right-hand side was evaluated for each experimental value of  $V_w$ , and values found for  $Z_0$  and  $H$  in each case.  $H$  as thus found agreed fairly closely with the heights of the centres of the kinks in the velocity curves of fig. 6.

Using the curves of fig. 7, the range  $L$  was taken out for each value of  $Z_0$ . Below are tabulated the values of  $H$ ,  $Z_0$ , and  $L$  corresponding to the different wind speeds  $V_w$  used in the experiments. The figures are based on (a) equations (6) and (7), (b) the calculated theoretical grain path relations, and (c) an arbitrary value of  $B$  chosen so as to make  $H$  agree

with the height of the centre of the kink in the experimental velocity curves.

$V_{w_0}$ .....	19.2	25	40.4	50.5	62.5	88
$Z_0$ .....	0.4	0.47	0.73	0.94	1.23	2.0
H .....	0.31	0.36	0.56	0.72	0.95	1.54
L .....	2.5	3.0	5.4	8.0	11.6	27.0
Ripple .....	2.4	3.0	5.3	9.15	11.3	(no ripples)

The ripple length, which is also shown above, was found experimentally by counting the number of ripples along a considerable length of tunnel in the same actual experiments in which the curves of fig. 6 were taken and from which the other figures are derived. The remarkable correspondence between the range of the characteristic path and the experimental ripple length may, of course, be a pure coincidence. But it is likely, I think, that there is a physical basis of fact behind it. For even though there is no evidence that the majority of the grains pursue the characteristic path, yet if this path is real enough for its height to appear in the observed effect of the sand flow upon the air, it is just as likely that its range should also appear in the effect of the sand bombardment upon the surface.

With regard to the height  $k'$ , which appeared as the height at which the limiting air velocity  $V_t$  occurred, and is introduced into equation (7); its physical significance may be the height of the top of the ripple above the mean height of the surface. Experimentally, owing to the length of time taken in making the velocity readings which created  $k'$ , the ripples were always well formed while the readings were made. The ripple height is of very much the same order as  $k'$  and the ripples flatten out at high wind speeds much as  $k'$  is seen to fall in value at high wind speeds in fig. 6.

#### 6—THE DRAG CAUSED BY THE SAND FLOW OVER A LOOSE SAND SURFACE

If a stationary sand grain rises from the surface with a forward velocity  $u_1$  and strikes it again, after travelling a distance  $l$ , with horizontal velocity  $u_2$ , all of which is lost on impact, the momentum extracted from the sand-influenced layer of air will be  $m(u_2 - u_1)$ , where  $m$  is the mass of one grain. The loss will be distributed over the distance  $l$  along the surface.

If, of a total heterogeneous sand flow in which a mass  $q$  passes a fixed line per second, a mass  $\delta q$  has a certain range  $l$ , this elementary mass of

sand must take off somewhere in the length  $l$  every second, and as, for a steady flow, a like mass must also land on the same length, the rate of loss of momentum by the air due to the elementary flow  $\delta q$  must be  $\delta q(u_s - u_1)$ , so that the drag caused by  $\delta q$  will be  $\delta F = \delta q \frac{(u_s - u_1)}{l}$  and the whole drag due to the whole flow will be

$$F = \Sigma \delta q \frac{(u_s - u_1)}{l}.$$

If we replace the total heterogeneous flow by an ideal one in which all the grains pursue one path, we shall have

$$F = q \frac{(U_s - U_1)}{L}, \quad (8)$$

for the drag due to the flow. This will act on the air, not on the surface, but at a height comparable with that to which the grains rise, the drag diminishing both above and below the level of maximum effect.

If the above ideal grain path can be identified with the characteristic path referred to in the last section,  $F$  should be equal to  $\tau$ . By neglecting  $U_1$ , as being very small compared with  $U_s$ , we have

$$F = q \frac{U_s}{L}, \quad (8A)$$

and since  $U_s/L$  is a grain path relation obtainable from fig. 7 for any given value of  $V_{\text{g}}$ , by making  $W_1$  equal to  $0.8V_{\text{g}}$  (equation (6) *et seq.*) it is possible to compare  $F$  with  $\tau$ . The following table gives the experimental values found for the sand flow  $q$  in terms of  $V_{\text{g}}$  together with two sets of values for  $\tau$ ; the first,  $\tau = q \frac{U_s}{L}$ , being deduced from the quantity of sand flowing over the surface, and the second,  $\tau = \rho V_{\text{g}}^2$ , being deduced from the air velocity distribution as modified by the sand flow. The value of  $q$  is expressed in grams per second passing a transverse line 1 cm. long. It was measured directly by dividing the algebraic sum of the changes in the readings of the spring balances supporting the tunnel by the time of the run.

$V_{\text{g}}$ .....	19.2	25	40.4	50.5	62	88
$q$ .....	0.0042	0.029	0.118	0.25	0.44	1.22
$U_s/L = \frac{g}{0.8 V_{\text{g}}}$	64	49	31	24	20	14
(by (5) and (6))						
$\tau = q U_s/L$ ....	0.27	1.4	3.6	6.0	8.7	17
$\tau = \rho V_{\text{g}}^2$ .....	0.44	0.75	2.0	3.1	4.7	9.4

It will be seen that the drag as calculated from the assumed type of motion of the grains is of the same order as that estimated from measurements of air velocity. It is, however, too high by an almost constant factor 1.9 (except for the extreme case of the feeble wind  $V_w = 19.2$ ). A discrepancy in this direction is rather to be expected since it was assumed that all the grains rise vertically into the air so that  $U_1$  is zero. If  $U_1$  is not negligible the value of the expression for the drag  $\tau = q(U_2 - U_1)/L$  will be reduced.

Allowing for this discrepancy, the measured sand flow  $q$  can be expressed in terms of wind motion. Thus

$$\begin{aligned} q &= 1.9 \tau L/U_2 = 1.9 \rho V_e^2 L/U_2 \\ &= 1.9 \rho V_e^2 B V_d/g \text{ by (5) and (6)} \\ &= 1.9 \frac{\rho}{g} B V_e^3 \end{aligned} \quad (10)$$

or  $q = 1.8 \times 10^{-8} V_e^3$  approximately for sand of 0.025 cm. diameter.

Since by equation (2)  $V_d$  is proportional to  $v_s - V_t$ , it appears that the flow  $q$  for a uniform sand is proportional to  $(v_s - V_t)^3$ , where  $v_s$  is the wind velocity measured at any height  $z$  and  $V_t$  is given by equation (3).

#### 7—EXTENSION TO OTHER SURFACES—CONCLUSION

It must be emphasized that the foregoing results can only be expected to hold good for sand of uniform grain size. But the theory should provide a basis upon which investigation can be extended to the more practical case of sands composed of grains of mixed sizes, driven over a surface of similar mixed sand or of pebbles. By way of conclusion, an outline may be given of preliminary results obtained for the extreme case of a mixture composed of the same uniform fine sand used in the preceding experiments and a coarse grit 3 mm. in diameter.

The grit pebbles were scattered as evenly as possible over the surface of fine sand, the density of distribution being fairly thin—about one pebble per sq. cm. The grit was much too coarse to be moved at all either by the wind or by the bombardment of the finer grains.

After an initial period during which surplus fine sand was removed from between the pebbles, a condition of stability was reached when no further sand grains were moved by even the strongest wind, i.e., the scattered surface pebbles completely protected the sand from disturbance either by the wind itself or by the granular bombardment.

A stream of sand was now, as before, allowed to enter the tunnel

mouth. This sand passed down the tunnel without causing any changes in the surface. The behaviour of the sand cloud as observed and photographed was now very different from that of the corresponding sand cloud passing over a bare sand surface. In particular:—

(a) The grain paths were far higher and their distribution with height was nearly uniform instead of their being confined largely to the bottom 2 cm. Grains were seen to strike the roof and to rebound downwards. A hole was cut in the roof, and grains were seen to shoot out of it (against the in-draught of air through the hole) and to rise to a height of more than 80 cm. above the surface.

(b) The grains, instead of splashing into a soft yielding surface of fine sand, now continued on their way striking the pebbles and rebounding with very high velocities approaching that of the wind itself.

(c) The average grain, instead of moving in a path whose length was of the order of 10 cm., now moved in long hops, rising to a considerable height and having a range of several metres

From equations (5) and (8) we should expect that with this type of motion where  $w_1$  has a much larger value than before and where  $U_s/L$  is correspondingly smaller, the drag caused by the sand movement should be considerably less than before. This was confirmed by experiment. Comparing similar conditions of wind and sand flow, the drag as measured by the change of pressure drop between sand flow and no sand flow was less than a tenth of that for a surface of plain fine sand.

The intensity of sand flow along the tunnel is that of the incoming sand, since after the initial sweeping-up there is no surplus sand on the surface to be picked up *en route*. Hence the former limiting mechanism by which the surface movement so checked the air stream that no further surface grains could be set in motion to augment the flow, is here absent altogether. In other words, for a given wind strength the rate of sand movement over a plain surface of fine sand is limited, whereas that over a pebble surface is not. It follows that such a pebble-covered surface can, for a given pressure drop, pass a larger quantity of sand than can a bare surface of fine sand.

Consequently, when a wind, in moving over a normal pebbly desert surface, has picked up and is driving along a heavy charge of surplus grains which have been lying about between the pebbles, it must, when it reaches a surface of bare fine sand such as a dune, deposit any excess of charge over and above the limiting charge which the sand surface can pass for that particular wind speed. I think this is undoubtedly the explanation of the striking phenomenon observed in desert countries that

all the sand is swept up neatly into dunes leaving the surrounding desert floor almost devoid of sand.

Finally, I must express my thanks to the authorities of the City and Guilds (Engineering) College for their kindness in providing accommodation for the apparatus used; and to Dr. C. M. White for his valuable advice and assistance.

#### APPENDIX

*Calculation of Grain Paths*—The ideal grain is supposed to start vertically upwards from the surface with velocity  $w_1$ , and the air is supposed to have the same velocity distribution as that found experimentally and

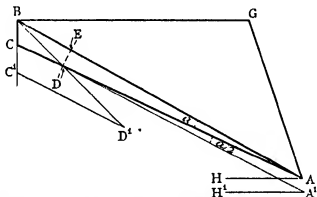


FIG. 8—Approximate construction used in calculating theoretical grain paths.

given in fig. 6. The air stream is divided into a convenient number of, say six, horizontal layers and the velocity in each is supposed constant. Within the bottom layer the path is found as follows (see diagram in fig. 8).

From the initial velocity vector AG (in this case of the bottom layer AG is vertical and equal to  $w_1$ ) is subtracted the velocity GB of the air in layer 1 so that the conditions are changed to those of the grain being fired backwards into still air with velocity AB and at an angle BAH.

The magnitude of the grain's velocity is allowed to fall by a small arbitrarily chosen amount BE, and during this period  $t$  the magnitude is assumed constant and equal to  $(AB + AD)/2 = V_m$ . By the end of the period the direction has changed to AD by an angle  $\alpha$ . The total change of velocity has been made up of a change  $BC = gt$  vertically downwards due to gravity, and a change  $CD = Ft$  due to the air resistance whose direction is always opposite to that of the relative velocity. It is assumed

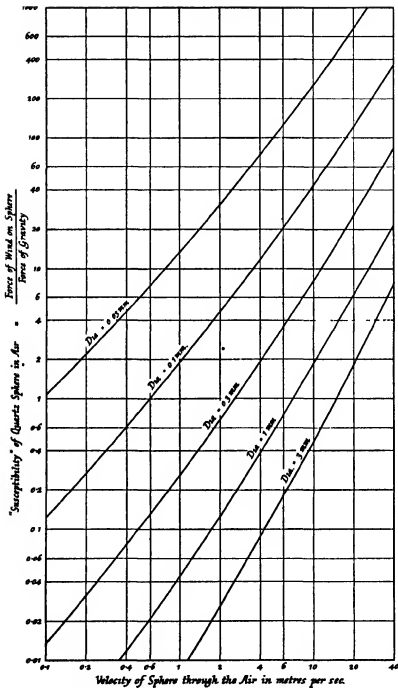


FIG. 9.—The "susceptibility" of a smooth sphere in air, calculated for the density 2.65 of quartz.

as an approximation that during the period this direction is parallel to the bisector of the angle BAD, making an angle  $\alpha/2$  with AB.

The value of  $t$  is unknown, but the ratio of  $F$  to  $g$  is the "susceptibility"  $S$  found for the velocity  $V_m$  from the diagram of fig. 9 reproduced from my previous paper (by permission of the R.G.S.). Lines CC' and C'D' are drawn so that  $C'D'/CC' = S$ , C'D' being made parallel to the estimated final angle BAH -  $\alpha/2$ ). (A small error in this estimation only makes a second order error in the result.)

The intercept D of the arc ED with the line BD' then gives the final velocity vector AD, and if DC is drawn parallel to C'D', the length  $CD = gSt$ , so that  $t = CD/gS$ , whence  $l$  the distance travelled (backwards through the air) during the period is  $V_m t$  and its direction with the horizontal is  $(BAH - \alpha/2) = DA'H$ .

The backward horizontal travel is therefore  $l \cos DA'H$ . But during the period the air itself has moved forward a distance  $U_1 t$ , so that the range element relative to the ground is  $U_1 t - l \cos DA'H$ . Similarly the height element is  $l \sin DA'H$ .

With a little experience, a good guess can be made at the velocity change BE which will bring the grain to a height approximately equal to that of the top of layer 1.

A new diagram is now constructed starting with AD as the initial velocity vector. From this is subtracted a horizontal velocity equal to the increase in air speed between layer 1 and layer 2.

Thus the whole path can be traced out, by dead-reckoning so to speak, from layer to layer. It is unfortunate that no analytical method seems to be possible owing to the complex nature both of the air velocity and the susceptibility. The latter is based on the accepted relation between the drag on a smooth sphere and the appropriate Reynolds number. The diameter of the sphere is taken as 0.75, the mean dimensions, as measured microscopically, of the average sand grain of the approximately uniform sand used.

#### SUMMARY

The motion of sand grains and their reaction on the air stream when wind blew over a thick layer of dry uniform sand on the floor of a wind tunnel was investigated experimentally. The paths of the individual grains were photographed. The wind velocity distribution and the pressure drop were measured during the sand movement and compared with results obtained over the same surface when movement was prevented. At the same time the total mass flow of sand past various sections of the tunnel was measured directly.

The grain motion was found to consist of a series of bounds; the grains rose steeply into the air stream and fell slowly, gathering forward velocity and striking the sand surface with sufficient impact to splash up more grains into the air stream. Irregularities in the grain paths due to internal air movements were undetected.

The wind velocity at a height comparable with the surface sand ripple amplitude—about 0·3 cm.—remained constant for all mean tunnel speeds above that at which sand movement started; this constant velocity is a function of the grain diameter.

The drag due to the sand movement is measurable. This drag was found to be a maximum at the height above the surface at which maximum acceleration of the grains took place. By the replacement of the actual movement of the grains in heterogeneous paths by an ideal movement in which all the grains follow one characteristic path calculated from the forces acting on a smooth sphere rising into the same air stream with a certain initial velocity of rise, values were obtained for the drag which such a movement would exert. These values were found to agree with the actual drag as deduced from the pressure drop along the tunnel and also from the normal velocity distribution curves.

The length of the characteristic path from impact to impact was found in all experiments to be the same as the measured wave-lengths of the ripples formed on the surface.

---

## A Note on the Quantum Yield of the Photosensitized Decomposition of Water and of Ammonia

By H. W. MELVILLE

(Communicated by E. K. Rideal, F.R.S.—Received 5 May, 1936)

When hydrogen atoms are produced by collisions between hydrogen molecules and excited mercury atoms in mixtures containing gases other than hydrogen, there is always a complication introduced by the fact that these gases may also react with the excited Hg atoms. This difficulty appeared when studying the kinetics of the exchange reactions of deuterium atoms with hydrides. In the latter reactions exchange may occur by the dissociation of the hydride and subsequent recombination of the fragments with atomic deuterium. With the object of finding the maximum possible rate of this type of exchange, measurements have been made of the quantum yields of the decomposition of  $H_2O$ ,  $D_2O$ , and  $NH_3$  at different temperatures. These measurements are of importance, for in the water exchange experiments it was not possible at higher temperatures to decide unequivocally that the exchange went by way of the chain reaction  $D + H_2O = HDO + H$ ,  $H + D_2 = HD + D$ .

The experimental arrangements were similar to those described for the exchange experiments with the exception that a Pirani gauge was employed to measure the pressure of gas after the water or ammonia had been frozen out by means of liquid air. Droplets of mercury were distilled on to the surface of the tube leading to the reaction vessel to ensure that mercury vapour was present throughout the run.

### WATER

First it was necessary to determine the nature of the products of the reaction. This was done by measuring the pressure of the gas with a Pirani and with a McLeod gauge. The gas proved to be hydrogen. Had there been any oxygen in addition, the sensitivity of the gauges was such that 2% of  $O_2$  could have been detected. The oxygen must therefore combine with the mercury, the simplest reaction being  $Hg + H_2O \rightarrow HgO + H_2$ . From the present point of view, it is the rate of the back reaction, namely the reduction of the mercuric oxide, which controls the rate of exchange. The water was therefore condensed out and the rate of disappearance of hydrogen measured, keeping the vessel illuminated.

Some runs are shown in fig. 1 where it will be seen that as soon as the hydrogen begins to accumulate, the rate of decomposition slows down. The rate of disappearance of hydrogen is, however, smaller than would correspond to the decrease in rate of decomposition. Using a pressure of water vapour of 8.5 mm., the quantum yields for the decomposition have been measured by observing the initial rate of dissociation. The results are shown in Table I. In the third column of the table the quantum yield for dissociation has been calculated for a mixture of 12 mm. H<sub>2</sub>O and 50 mm. D<sub>2</sub>, using the values of the quenching radii found by Evans,\*

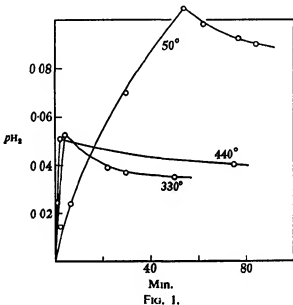


FIG. 1.

and in the last column are given the observed quantum yields for the exchange reaction under comparable condition of light intensity. It will be seen at once that the exchange  $\gamma$ 's are much larger than those observed in the present experiments and hence it must be concluded that the exchange does not take place appreciably by the dissociation and subsequent reformation of the water molecule.

#### AMMONIA

If exchange between deuterium and hydrides goes by way of a back reaction, the quantum yield cannot exceed unity. When  $\gamma$  is greater than unity, there is no doubt that the chain mechanism is the correct inter-

\* 'J. Chem. Phys.', vol. 2, p. 486 (1934).

TABLE I—QUANTUM INPUT  $2.0 \times 10^{16}$  PER SEC. VOLUME OF VESSEL 86.8 CC. PRESSURE OF  $\text{H}_2\text{O}$  8.5 MM.

Temperature °C.	$\gamma$ ( $\text{H}_2\text{O}$ decomp.)	$\gamma$ ( $\text{H}_2\text{O}-\text{D}_2$ mixture)	$\gamma$ (exchange)
45	0.018	$2.4 \times 10^{-4}$	0.1
220	0.028	$3.8 \times 10^{-4}$	—
330	0.032	$4.4 \times 10^{-4}$	0.7
430	0.037	$4.9 \times 10^{-4}$	—
580	0.036	$4.9 \times 10^{-4}$	2.4
	$\text{D}_2\text{O}$		
50	0.007		
210	0.023		

pretation; this happens with ammonia above 300° C. In previous work on the kinetics of the decomposition of ammonia\* an expression was deduced which predicted the temperature coefficient of the rate of dissociation. The experiments described below were made to test the validity of the formula. To complete the work on ammonia, it was also essential to determine the quantum yield of the sensitized decomposition

TABLE II—INPUT  $2.0 \times 10^{16}$  QUANTA SEC.<sup>-1</sup>. HG PRESS. 0.001 MM.

Press. mm.	Temp. °C.	Init. rate mm. min. <sup>-1</sup>	$\gamma$	$\gamma_{p=\infty}$	$\gamma^*$ (direct)	$p_{\text{NH}_3}$ for $\gamma_{\alpha}/2$ (press. re- duced to 0° C.)
73	50	0.0231	0.045	0.05	0.14	11.1
5.0	50	0.0097	0.020	—	—	—
75	260	0.0880	0.17	0.26	0.34	12.5
5.0	260	0.0165	0.032	—	—	—
75	432	0.234	0.45	0.65	0.56	7.9
5.0	432	0.054	0.11	—	—	—

\* Ogg, Leighton, and Bergstrom, 'J. Amer. Chem. Soc.', vol. 56, p. 320 (1934).

in order to see if it is identical with that of the direct reaction as is required by the theory (*loc. cit.*). The data at three temperatures are given in Table II.

First, it will be noted that the value of  $\gamma$  for  $p = \infty$  increases with temperature at about the same rate as that for the direct reaction, and that  $\gamma$  for sensitized reaction is practically identical with that for the

\* Melville, 'Proc. Roy. Soc.,' A, vol. 152, p. 325 (1935).

direct reaction. This provides further evidence that once the molecule is dissociated the secondary reactions which occur are the same in both cases. Secondly, it will be observed that the concentration of ammonia at which the rate of decomposition falls off to half its value at high pressures slightly decreases on increasing the temperature to 430°. Now it has already been shown that

$$\frac{1}{[\text{NH}_3]_{1/2}} = \frac{k_1\tau}{1 + k_1^1/k_4},$$

where  $[\text{NH}_3]_{1/2}$  is the concentration at which  $R = \frac{1}{2}R_\infty$ ,  $k_1$ ,  $k_1^1$ , and  $k_4$  are respectively the velocity coefficients for the deactivation of excited Hg atoms to the metastable state by ammonia, for raising the  ${}^3\text{P}_0$  Hg atom to the  ${}^3\text{P}_1$  state by collisions with ammonia and for the rate of dissociation of ammonia by  ${}^3\text{P}_0$  atoms,  $\tau$  is the mean life of the  ${}^3\text{P}_1$  atom. At 20° C.,  $k_1^1/k_4$  is 5·9, which corresponds to a difference in energy of activation of the two reactions of 1000 cals. Assuming that  $k_1$  is independent of temperature, which appears to be the case for quenching of mercury resonance radiation, then the value of  $k_1^1/k_4$  at 432° C. is 2·5, which therefore reduces the value of  $1/[\text{NH}_3]_{1/2}$  by a factor of 2·0 compared with that at 50°, whereas the observed decrease is  $11\cdot1/7\cdot9 = 1\cdot4$ .

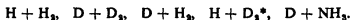


## The Mercury Photosensitized Exchange Reactions of Deuterium with Ammonia, Methane, and Water

By A. FARKAS and H. W. MELVILLE (Department of Colloid Science, The University, Cambridge)

(Communicated by E. K. Rideal, F.R.S.—Received 5 May, 1936)

Amongst the simplest reactions in chemical kinetics are those involving an interchange between a free atom and an atom in a polyatomic molecule. One example of this kind of reaction is the exchange of a deuterium atom with a hydride, namely  $D + HX \rightleftharpoons DX + H$ . The deuterium atoms required to start the reaction may be produced electrically, photochemically, or thermally. The following reactions have been investigated by the thermal method:



Exchange reactions involving  $CH_4$  and  $NH_3$  and deuterium atoms produced photochemically have been demonstrated by Taylor, Jungers,<sup>†</sup> Morikava and Benedict,<sup>‡</sup> but the results do not lead to quantitative conclusions regarding the mechanism. Geib and Steacie<sup>§</sup> have used H atoms from a Wood's tube to effect exchange with  $CH_4$ ,  $NH_3$ , and  $C_2H_2$ , but in the light of subsequent results this method is attended by the intrusion of complicating factors, to be discussed later, whose magnitude is difficult to assess accurately.

The subject of the present paper is the investigation over a wide range of operating conditions, of the mercury photosensitized exchange reactions of hydrogen and deuterium with the simplest hydrides, namely water, ammonia, and methane.

Anticipating the results, it may be stated that the experiments permit quantitative conclusions being drawn with regard to the energetics of these processes.

\* Farkas and Farkas, 'Proc. Roy. Soc.,' A, vol. 152, p. 124 (1936).

† Taylor and Jungers, 'J. Chem. Phys.,' vol. 2, p. 452 (1934).

‡ Taylor, Morikava, and Benedict, 'J. Amer. Chem. Soc.,' vol. 57, p. 383 (1935).

§ 'Z. phys. Chem.,' B, vol. 29, p. 215 (1935).

### EXPERIMENTAL

In an exchange reaction of the type  $H + DX$  the rate is proportional to the hydrogen atom concentration. The hydrogen atom concentration may be measured by observing the rate of conversion of para-hydrogen which takes place by the mechanism  $H + p\text{-H}_2 = o\text{-H}_2 + H$  since the kinetics of the Hg sensitized conversion have already been investigated by Farkas and Sachse.\* The procedure in carrying out all the experiments to be described below is to mix *p*-hydrogen with deuterides (*e.g.*,  $p\text{-H}_2 + ND_3$ ) or *o*-deuterium with hydrides (*e.g.*,  $o\text{-D}_2 + CH_4$ ), illuminate in presence of Hg vapour, and observe the rate of ortho-para conversion and the exchange in the same mixture.

Since it was expected that the velocity of the exchange reaction would be small, particular care was taken to obtain the highest possible intensity of resonance radiation. Hitherto, in performing photochemical reactions at high temperatures, it has been necessary to place the source of light outside the furnace, a procedure which leads to a serious reduction in the intensity. This difficulty was overcome in the present experiments by using a Hg-Ne high voltage discharge lamp,† the construction of which permitted its operation inside the furnace, the electrode chambers, naturally remaining outside. Fortunately, the intensity of the light is practically independent of the operating temperature even up to  $600^\circ C.$ , and, moreover, remained sensibly constant (within 20%) over a period of several weeks. A further advantage of this type of lamp is that at least 90% of the energy radiated is in the resonance line at  $2537 \text{ \AA}$ , and therefore no special filters need be used to prevent direct photochemical reaction. Another advantage in having the lamp and reaction vessel at the same temperature is that the shape of the emission line (or separate components) and of the absorption line is changed to the same extent by alteration of temperature. Although this may not be an important factor for the present experiments, none the less it will be of particular importance if the absorption of light is not complete. It may also be mentioned that the lamp is started simply by switching on, no tilting being necessary, and that a steady operating condition is attained within a few minutes of starting up. Though the input was only 60 watts the total output attained the large value of about  $10^{19}$  quanta per second.

The arrangement of the lamp and reaction vessel in the furnace is shown in fig. 1. The reaction vessel R of silica, length 12 cm., and dia-

\* "Z. phys. Chem." B, vol. 27, p. 111 (1934).

† Melville (*in the press*).

meter 2 cm., is enclosed within a shutter consisting of two cylinders  $S_1$  and  $S_2$  of aluminium foil each having a rectangular opening.  $S_1$  was maintained in a fixed position and  $S_2$  was supported on the bearing B and rotated by the handle H. Only one limb of the lamp was used, the other being covered with aluminum foil. To reduce the intensity of the light, a filter F was constructed of aluminium foil with one 1 mm. hole per square cm. This filter could be moved along the limb of the lamp by means of an attached wire W. Temperatures were measured with a chrome-alumel thermocouple and millivoltmeter.

The following gases and vapours were used,  $H_2$ ,  $p-H_2$ ,  $D_2$ ,  $\alpha-D_2$ ,  $H_2O$ ,  $D_2O$ ,  $NH_3$ ,  $ND_3$ , and  $CH_4$ . Special care was taken to eliminate small traces of oxygen from these gases. The hydrogen and deuterium were

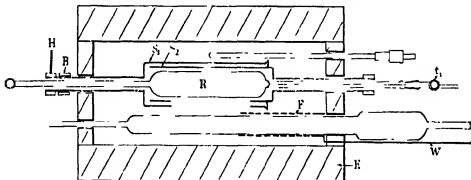


FIG. 1.

diffused through palladium and subsequently converted in the usual way. The deuterium was 80–90% D. The "D<sub>2</sub>O" contained 92% D. The ammonia was prepared from Mg<sub>3</sub>N<sub>2</sub> and H<sub>2</sub>O and D<sub>2</sub>O. By weighing, the ND<sub>3</sub> was found to contain 90% D. The first sample of methane prepared by the interaction of Al<sub>4</sub>C<sub>3</sub> and water exhibited an anomaly to be described later and therefore three other samples were prepared to ensure that the effect was not due to an impurity. These were made (1) from another sample of Al<sub>4</sub>C<sub>3</sub>, (2) by the reduction of methyl iodide with Zn-Cu couple, (3) from a cylinder of natural methane. All samples were purified by the usual methods and finally fractionated by means of liquid nitrogen.

Usually a 50:50 mixture of gases was used except with water where the vapour pressure was too small. Pressures were measured by a capillary mercury manometer and by a Bourdon gauge for smaller pressures. Total pressures were not allowed to fall below 100 mm. to ensure that the hydrogen atoms mainly combined in the gas phase. After a suitable

time of illumination, a sample was withdrawn, after waiting for a few minutes' diffusion to establish uniformity in the gaseous mixture in the capillary, by means of the tap  $t_1$  the key of which was partially filled with picein. The para-content and D-content were measured by the micro-thermal conductivity method,\* water and ammonia being frozen out with liquid air and the methane with liquid hydrogen.

Exposures were made with three intensities: (1) without filter, (2) filter partially in, and (3) filter completely in. The relative rates were 35:17:1.

#### EXPERIMENTAL RESULTS

Before describing the results obtained in the several exchange reactions, some general features common to all will be discussed.

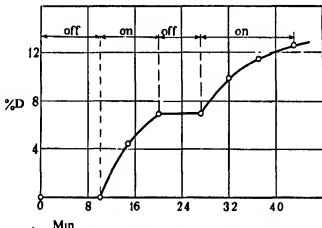


FIG. 2—485° C., 80 mm. H<sub>2</sub>, 12 mm. D<sub>2</sub>O.

To ascertain whether a heterogeneous exchange reaction occurs at higher temperatures, the gases were left in the reaction vessel for a considerable time (on the basis of previous experiments a homogeneous† reaction does not take place at the temperature employed). In fig. 2 the percentage D-content in 80 mm. hydrogen when mixed with 12 mm. D<sub>2</sub>O is shown as a function of the time of heating. It is evident that an increase in the D-content due to exchange reaction only occurs when the vessel is illuminated and stops immediately the light is switched off—a fact which clearly demonstrates that the progress of the exchange reaction

\* A. Farkas, 'Z. phys. Chem.,' B, vol. 22, p. 344 (1933); A. Farkas and L. Farkas, 'Proc. Roy. Soc.,' A, vol. 144, p. 467 (1934).

† A. Farkas, 'J. Chem. Soc.,' p. 36 (1936).

is not complicated by induction periods nor by photochemical after-effects. Similar results were also obtained for the exchange reactions of methane and ammonia.

As has already been mentioned, in all experiments the progress of the

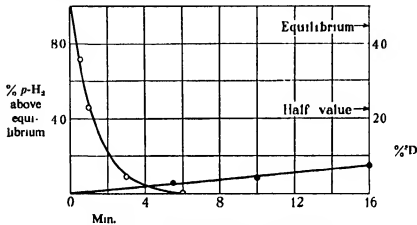


FIG. 3—50 mm. *p*-H<sub>3</sub>; 50 mm. ND<sub>3</sub>, 208° C.

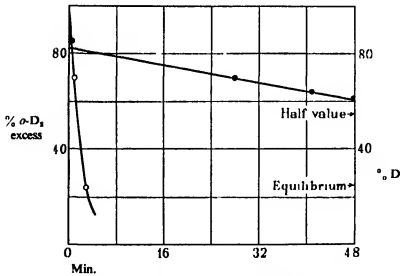


FIG. 4—610° C.; 51 mm. *o*-D<sub>3</sub>; 50 mm. CH<sub>4</sub>.

ortho-para conversion and of the exchange reaction were measured consecutively. Fig. 3 shows the progress of the conversion and exchange in a mixture of 50 mm. *p*-H<sub>3</sub> and 50 mm. ND<sub>3</sub>, and fig. 4 for 51 mm. *o*-D<sub>3</sub> and 50 mm. CH<sub>4</sub>. The left-hand ordinate refers to the conversion reactions (curve 1, open circles) and the right to the exchange reaction

(curve II, full circles). The progress of the exchange reaction was followed until equilibrium was reached, the latter composition of the gas being indicated on the right-hand ordinate. Although the progress of the conversion obeys the exponential law  $V = V_0 e^{-k[H]t}$  ( $V$  = excess of the ortho or para component relative to normal  $D_2$  or  $H_2$ ), the same law applies only approximately, but with sufficient accuracy, to the progress of the exchange reaction, namely

$$Z = Z_0 e^{-k[H]t},$$

where  $Z = u_\infty - u$ ,  $u$  being the D-percentage of the hydrogen measured experimentally and  $u_\infty$  the percentage D at equilibrium (cf. figs. 3, 4, and 5). The half-life times may therefore be used to characterize the velocity of both reactions.

*Effect of  $NH_3$ ,  $H_2O$ , and  $CH_4$  on Stationary H Atom Concentration—* Experiments were also made to determine whether the H atom concentration is affected by the addition of these hydrides. With  $NH_3$  and  $H_2O$ , no considerable effect could be detected at any temperature, but with  $CH_4$  above 150° C. the H atom concentration was reduced considerably. The results for  $NH_3$ ,  $H_2O$ , and  $CH_4$  are shown in Table I.

TABLE I—EFFECT OF  $NH_3$ ,  $H_2O$ ,  $CH_4$  ON THE STATIONARY H ATOM CONCENTRATION

Temperature °C.	$\rho-H_2$	$\tau_1$ (conversion)
40	98.0	2.7'
33	80.2 + 19.8 $CH_4$	3.0'
39	50.0	5.6'
30	41.8 + 37.2 $ND_2$	5.5'
238	95.2	2.1"
238	83.0 + 19.0 $NH_3$	3.0"
238	83.0 + 13.0 $D_2O$	2.8"
238	81.8 + 20.2 $CH_4$	17.0"

$\tau_1$  is half-life time.

The establishment of the equilibrium is shown in fig. 5 for a mixture of  $CH_4 + D_2$  and for a mixture of  $H_2O + D_2$  in fig. 11. The equilibrium reached in these experiments is in agreement with calculations.

For example, consider the exchange reaction of methane and deuterium. To a first approximation the ratio of the ratio (H/D) in the hydrogen to the ratio (H/D) in the methane at equilibrium is given by the equation

$$\frac{(H/D)_{\text{hydrogen}}}{(H/D)_{\text{methane}}} = K/2,$$

where  $K$  is the equilibrium constant of the reaction



It is assumed that the equilibria

$$\frac{[\text{CH}_3\text{D}]^2}{[\text{CH}_4][\text{CH}_3\text{D}_2]}, \quad \frac{[\text{CH}_3\text{D}_2]^2}{[\text{CH}_3\text{D}][\text{CHD}_3]}, \quad \text{and} \quad \frac{[\text{CHD}_3]^2}{[\text{CH}_3\text{D}_2][\text{CD}_4]}$$

have the classical values.

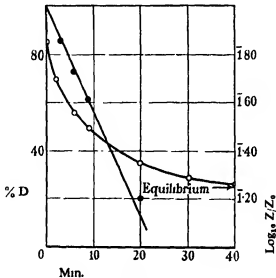
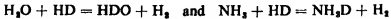


FIG. 5—610° C.; 49.2 mm. D<sub>2</sub>; 55.8 mm. CH<sub>4</sub>

$K$  is calculated from the formula

$$-\ln K = \frac{\Delta E}{RT} - \frac{1}{2} \ln \frac{M_{\text{CH}_3\text{D}} \cdot M_{\text{H}_2}}{M_{\text{CH}_4} \cdot M_{\text{HD}}} - \ln \frac{\bar{I}_{\text{CH}_3\text{D}} \cdot I_{\text{H}_2}}{\bar{I}_{\text{CH}_4} \cdot I_{\text{HD}}} - \ln 2,$$

where  $\Delta E$  is the heat content change in the reaction and the other symbols have their usual significance. For methane  $\Delta E$  and  $\bar{I}_{\text{CH}_3\text{D}}$  may be computed from the measurements of the vibrational frequencies of CH<sub>3</sub>D.\* In a similar way the equilibrium constants for the reactions



may be calculated. The values so obtained at different temperatures are given in Table II.

\* Howard, 'J. Chem. Phys.', vol. 3, p. 207 (1935); Ginsburg and Barker, *ibid.*, vol. 3, p. 668 (1935).

The number of quanta entering the reaction vessel was measured by observing the rate of decomposition of oxalic acid sensitized by the  $\text{UO}_2^{++}$  ion\* and the rate of hydrolysis of monochlor-acetic acid.† The procedure was first to measure the rate of the *p*-H<sub>2</sub> conversion, then fill the reaction vessel with the appropriate solution, and after illumination withdraw the solution for analysis. The pressure of the mercury vapour in the reaction vessel was 0.001 mm. and consequently half the resonance light is absorbed in a layer of vapour 2 mm. thick. For practical purposes,

TABLE II

Temperature ° K . . .	300	400	600	800	1000
K = $\frac{[\text{H}_2][\text{HDO}]}{[\text{HD}][\text{H}_2\text{O}]}$	2.6	1.9	1.4	1.2	1.0
K = $\frac{[\text{H}_2][\text{NH}_3\text{D}]}{[\text{HD}][\text{NH}_3]}$	3.5	2.6	1.9	1.6	1.4
K = $\frac{[\text{H}_2][\text{CH}_3\text{D}]}{[\text{HD}][\text{CH}_3]}$	4.8	3.4	2.4	2.0	1.8

therefore, all the resonance light is absorbed in the reaction vessel. Similarly the concentration of the  $\text{UO}_2^{++}$  ion was such



that all the light was absorbed. On the other hand, the monochlor-acetic acid is not quite so opaque. The extinction coefficients of the 0.1 N solution used were calculated from Rudberg's figures, and correction was applied (25%) to the quantum input in order to arrive at the total number of quanta passing through the reaction vessel. The chloride was estimated by adding excess silver nitrate, filtering off the silver chloride, and back titrating the filtrate with potassium thiocyanate, and the oxalate by titration with 0.01 N  $\text{KMnO}_4$  as recommended by Forbes and Heidt.

With reaction vessel II the values so obtained for the number of quanta entering the bulb per sec. were

$5 \times 10^{18}$  estimated by means of chloracetic acid‡

and

$10 \times 10^{18}$  estimated by means of uranyl oxalate,

the half-life of para-hydrogen being 1.5 minutes at 43° C.

For the present purpose, the agreement between these two measurements may be regarded as satisfactory though the discrepancy is far

\* Forbe and Heidt, 'J. Amer. Chem. Soc.', vol. 56, p. 2313 (1934).

† Rudberg, 'Z. Phys.', vol. 24, p. 247 (1924).

‡ In subsequent calculations, the chloracetic value will be taken.

outside the limits of experimental error. Somewhat less satisfactory is the relation between the rate of para-hydrogen conversion and the light intensity as compared with Farkas and Sachse's results, where  $2 \times 10^{17}$  quanta per sec. gave a half-life of 20 sec. or 40 sec. with  $5 \times 10^{16}$  quanta compared with 90 sec. in the above experiments.

At higher temperatures, where the half-life of para-hydrogen decreases to a fraction of a second, accurate measurement is not possible. The procedure adopted was therefore to cut down the light intensity by interposing the filter. The decrease in intensity was measured directly by performing two para-hydrogen conversion runs at a lower temperature with and without the filter. In this way the half-life could be increased by a factor of 17, as shown in Table III.

TABLE III

Mixture, mm	Temperature ° C.	$\tau_f$ Filter out	$\tau_f$ Filter in	Factor
50·5p-H <sub>2</sub> 12·5D <sub>2</sub> O	40	258'	3600'	14
55·4p-H <sub>2</sub> 9·5D <sub>2</sub> O	160	40"	670"	16·7
52·2p-H <sub>2</sub> 50·4NH <sub>3</sub>	311	5·6"	102"	18

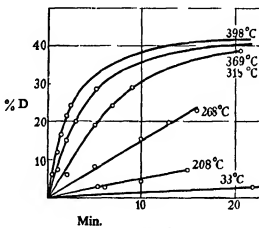


FIG. 6.

It appears that with the exchange reaction the filter factor may be slightly smaller, e.g., 50:50 mixture of ammonia and deuterium at 578° the half-life without the filter was 0·79' and 9·5' with filter, giving a factor of 12.

*Exchange with Ammonia*—The kinetics of the separate exchange reaction will now be discussed in detail. Fig. 6 shows a typical series of experiments with a 50:50 mixture of H<sub>2</sub> and ND<sub>2</sub>, at a total pressure of

100 mm. at constant light intensity. From these curves the half-life for exchange has been computed by taking the equilibrium value calculated above and taking into account the fact that the composition was not always exactly 50: 50 (variation  $\pm 10\%$ ) and that the D-content of the "ND<sub>3</sub>" was 90%. The values obtained are shown in Table IV.

TABLE IV—EXCHANGE WITH ND<sub>3</sub> (R.V.I.). EFFECT OF TEMPERATURE.  
QUANTUM INPUT  $2 \times 10^{16}$  PER SEC.

Temperature ° C.	$\tau_i$ (exchange)	$\tau_i$ (conversion)	$\frac{\tau_i}{\tau_t}$ (exchange) $\frac{\tau_i}{\tau_t}$ (conversion)
30	12000	330	36
208	3200	53	60
268	900	22	40
318	390	13	30
369	200	10	20
398	120	—	—

Table V shows the influence of composition of the mixture on the rate of exchange. The pressure was maintained constant in order to keep the stationary concentration of atomic hydrogen at a constant value

TABLE V—EFFECT OF COMPOSITION. TEMPERATURE 290° C.

ND <sub>3</sub> press.	H <sub>2</sub> press.	Total press.	$\tau_i$ (sec.)
52	49	101	720
30	73	103	840
15	89	104	1080

In a separate series of experiments runs were made with H<sub>2</sub> and ND<sub>3</sub>, on the one hand, and D<sub>2</sub> and NH<sub>3</sub> on the other. The results are shown in fig. 7 in which the mixtures were 50 mm. ND<sub>3</sub>, 52 mm. H<sub>2</sub>, and 48 mm. NH<sub>3</sub>, and 52.6 D<sub>2</sub> (92.5%) at 259° C., and 50.4 mm. ND<sub>3</sub>, 60.2 mm. H<sub>2</sub>, and 51 mm. NH<sub>3</sub> + 50 mm. D<sub>2</sub> at 397° C., the change in D and H content respectively being plotted against time. As is usual, the reaction with ND<sub>3</sub> proceeds more slowly.

The ammonia experiments were repeated in the second reaction vessel, when the measurements could be extended to higher temperatures without the intrusion of a heterogeneous reaction which vitiated the results in the first reaction vessel. Similar results were obtained. The extended data are given in Table VI. Again the mixtures were 50: 50, the total pressure being 100 mm. The D-content of the hydrogen was 61%. The *p*-H<sub>2</sub> conversion was determined in a neighbouring run. The filter was

employed at the highest temperature, as both exchange and conversion were too quick to measure accurately at this temperature.

TABLE VI—QUANTUM INPUT  $2 \times 10^{16}$  PER SEC.

Temperature ° C.	$\tau_i$ (exchange)	$\tau_i$ ( $p$ -conversion)	$\frac{\tau_i}{\tau_j}$ (exchange) (conversion)
50	16800	318	53
178	2760	20	138
311	540	6	90
582	50	1.3	38
578	530*	21*	25

\* Filter in position.

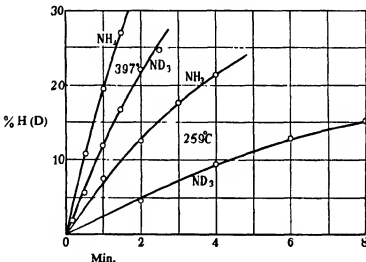


FIG. 7

#### DISCUSSION OF THE AMMONIA REACTION

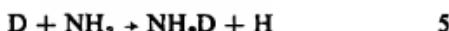
The hydrogen atoms are produced in the first place by the dissociation of hydrogen molecules colliding with excited mercury atoms, and disappear at the high pressure used in these experiments, mostly in three body collisions in the gas phase. Therefore a stationary concentration of atomic hydrogen is set up. The para-hydrogen is then converted by collisions between atomic hydrogen, and  $p$ -H<sub>2</sub>. The dissociation and subsequent recombination of atoms also leads to a conversion, but the quantum yield of the conversion in all experiments was invariably not less than twenty, and hence the conversion must almost exclusively be

due to the reaction  $H + p\text{-H}_2 \rightarrow o\text{-H}_2 + H$ , the activation energy being 6000–7000 cal.

Similarly the exchange reaction can occur in two different ways. The first mechanism is



the second mechanism is



The first reaction mechanism is characterized by the fact that its quantum yield cannot exceed unity even if all the excited mercury atoms were deactivated by ammonia. On the other hand, the second reaction may have a quantum yield ( $\gamma$ ) greater than unity as it is essentially a chain reaction. Furthermore, if the observed quantum yield for exchange is greater than unity then the second mechanism is only one whereby exchange can take place. Table VII shows that  $\gamma > 1$  above 300° C.

TABLE VII—INPUT IN QUANTA PER SEC.  $2 \cdot 0 \times 10^{18}$

Temperature ° C.	No. of para-hydrogen molecules converted per quantum absorbed	No. of hydrogen atoms exchanged with ammonia per quantum absorbed
30	16	0.30
178	152	1.32
311	480	5.4
580	1840	39

(The above results calculated from data in Table VI)

Below 300° C., the low quantum yield cannot be attributed wholly to the occurrence of the back reaction (e.g., 4) as the fraction of excited Hg atoms deactivated by ammonia is much smaller than  $\gamma$ ; for instance, at 50° C. this fraction for a 1 : 1 mixture is given by the usual formula

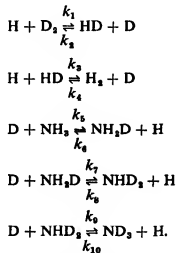
$$\frac{\sigma^2_{\text{HgNH}_3} - \mu^2_{\text{HgNH}_3}}{\sigma^2_{\text{HgNH}_3} + \mu^2_{\text{HgNH}_3}},$$

\* Melville, 'Trans. Faraday Soc.', vol. 28, p. 888 (1932).

where  $\sigma$  is the effective collision diameter and  $\mu$  is the reduced mass of the colliding particles.

The following values\* for  $\sigma$  were taken  $\sigma^2_{\text{H}_2\text{NH}_3} = 2.94 \times 10^{-16}$  cm.<sup>2</sup>,  $\sigma^2_{\text{H}_2\text{ND}_3} = 1.09 \times 10^{-16}$  cm.<sup>2</sup>,  $\sigma^2_{\text{H}_2\text{H}} = 6.01 \times 10^{-16}$  cm.<sup>2</sup>, and  $\sigma^2_{\text{H}_2\text{D}_2} = 8.41 \times 10^{-16}$  cm.<sup>2</sup>. The mean value of the fraction is about 1/14. Recent experiments† have shown that this fraction may be very much smaller since the ammonia molecules only deactivate the  $3P_1$  mercury atoms to the  $3P_0$  state. A part of the exchange observed at low temperatures is probably due to a small amount of direct photochemical dissociation of ammonia by light of  $\lambda < 2300$  Å.

To discuss the kinetics of the reaction, it is necessary to derive a relation connecting the observed half-life for exchange with the velocity constants of the various reactions which take place. The main reactions involved are



Assuming classical distribution of hydrogen and deuterium among the molecular species involved, and assigning the characteristic velocity constant  $k_1$  for the exchange reactions involving hydrogen molecules, then

$$k_1 = k_2 = k_3 = k_4,$$

and a characteristic velocity constant  $k_{11}$  for the exchange reactions involving the ammonia molecules, then

$$k_{11} = k_5 = 3k_6 = \frac{1}{2}k_7 = \frac{1}{2}k_8 = 3k_9.$$

\* Zemansky, 'Phys. Rev.', vol. 36, p. 919 (1930); Evans, 'J. Chem. Phys.', vol. 2, p. 486 (1934).

† Melville, 'Proc. Roy. Soc.,' A, vol. 152, p. 325 (1935).

The rate of exchange is given by the equation

$$-\frac{dz}{dt} = \frac{k_{II} ([NH_3] + \frac{2}{3} [D_2]) [D_0]}{[D_2] + k_{II}/k_I \cdot [NH_3]} \cdot Z,$$

where  $Z$  is the excess concentration relative to the equilibrium-value and is given by the equation

$$Z = u - [D_2]/(\frac{2}{3} [NH_3] + [D_2]),$$

$u$  being the percentage D content of the hydrogen as measured experimentally.  $[D_0]$  is the stationary concentration of atomic deuterium and is given by the equation

$$[D_0] = \{I/k_{III} ([D_2] + [NH_3])\}^{\frac{1}{2}},$$

where  $I$  is the intensity and  $k_{III}$  is the trimolecular velocity constant, assuming (a) that  $D_2$  and  $NH_3$  have the same trimolecular velocity constants, and (b) that all the H/D atoms disappear in this way. The above equation, of course, refers to  $NH_3$  and  $D_2$ , but it is obvious a similar equation holds for  $ND_2$  and  $H_2$ .

The half-life  $\tau_i$  (exch.) is therefore given by the equation

$$\frac{\ln 2}{\tau_i} = \frac{k_{II} ([NH_3] + \frac{2}{3} [D_0]) [D_0]}{[D_2] + k_{II}/k_I [NH_3]}. \quad (1)$$

The half-life  $\tau_i$  (con.) for the para-hydrogen conversion is given by an equation of a similar type

$$\frac{\ln 2}{\tau_i \text{ (con.)}} = k_I [D_0].$$

It must be emphasized that the approximation introduced here is that the velocity constants of the reactions  $H + H_2$  and  $D + D_2$  are equal to  $k_I$ . Hence

$$\frac{\tau_i \text{ (ex.)}}{\tau_i \text{ (con.)}} = \frac{k_I [D_2] + k_{II} [NH_3]}{k_{II} [NH_3] + \frac{2}{3} [D_2]}.$$

In the case where  $[NH_3] = [D_2]$  then

$$\frac{\tau_i \text{ (ex.)}}{\tau_i \text{ (con.)}} = \frac{k_I + k_{II}}{1.66 k_{II}}.$$

Using the values of  $\tau_i \text{ (ex.)}/\tau_i \text{ (con.)}$  given in Table VI the following results given in Table VIII were obtained.

This equation only holds at high temperatures where the equilibrium constant of the reaction  $HD + NH_3 = NH_2D + H_2$  has the classical

value of 3/2. At lower temperatures the value is greater than 3/2. This leads to a much more complicated equation in which the value of  $k_1/k_{II}$  does not appear explicitly. To avoid this difficulty, Z has been set equal to  $u - u_\infty$  where  $u_\infty$  is the equilibrium concentration calculated from the data given on p. 632.

The next question to decide is why the velocity constant  $k_{II}$  is so much smaller than  $k_I$ . In the first place it may be due to an energy of activation. The dependence of the absolute rate of the exchange reaction on temperature Table IV gives in the range 280 to 450° C., an energy of activation of 9.5 kcal. compared with 7 kcal. for the para-hydrogen conversion.

TABLE VIII

Temperature ° C. . . . .	187	311	369	580	(720)*
$k_I/k_{II}$ . . . . .	230	150	—	42	ca. 30

\* From thermal measurements.

Another check on the energy of activation for the exchange reaction is given by the dependence of the ratio  $k_I/k_{II}$  on temperature. From the results in Table VIII the additional energy of activation is computed to be 4 kcal., or a total energy of activation of 11 kcal. for the exchange reaction. Furthermore, assuming that the smaller rate of the exchange reaction is due wholly to an increased energy of activation, the additional energy of activation calculated from the absolute ratio  $k_I/k_{II}$  is 5 kcal. or 12 kcal. total energy of activation. The mean of these determinations is  $11 \pm 1$  kcal. which value is in agreement with the energy of activation obtained from the study of the thermal interchange of deuterium and ammonia.\*

The steric factor for the reaction must also be taken into consideration. This may be calculated by comparing the ratios  $k_I/k_{II}$  experimentally determined with those calculated on the basis of an additional energy of activation of 4 kcal. The latter computation would give 28 at 300° C. and 10 at 580° C. compared with the experimental values of 100 and 30 respectively. It will be seen that the order of magnitude of these values is as close as could be expected having regard to the simplifications made in the derivation of the kinetic formula. The discrepancy between the calculated and observed ratios may be increased, however, if more than two "square" terms of the ammonia molecule contribute to the activation. For example, taking 6 square terms for  $\text{NH}_3$  increases the rate of activation by a factor of 25 at 600° C., which would then be compensated by a correspondingly much smaller steric factor. It is not yet possible to separate the square terms and steric factors.

\* Farkas, 'J. Chem. Soc.', p. 26 (1936).

The dependence of the rate of the exchange on the composition as shown in Table V is in agreement with the formula, as may be seen from fig. 8 where the reciprocal of the half-life time is plotted against the  $[ND_3]/[H_2]$  ratio. It will be recognized that the experimental points lie on a straight line and that the ratio of the intercept to the slope of this line is 0.5, in satisfactory accordance with the calculated value of 0.66.

The last point to discuss is the different rates for the exchange reactions involving, on the one hand, a mixture of  $ND_3$  and  $H_2$  and, on the other, a mixture of  $NH_3$  and  $D_2$ , the relative rates being at  $259^\circ C.$ , 1:3.2, and 1:2 at  $397^\circ C.$ . The temperature dependence of this ratio corresponds to a difference in the activation energies 2.4 kcal. A similar figure

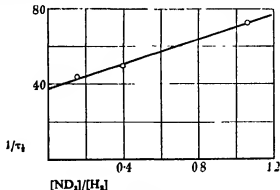


FIG. 8— $290^\circ C.$

(1.6 kcal.) is obtained from the ratio itself after allowing for a mass factor of  $\sqrt{2}$  which reduces the number of collisions by this factor in the reaction

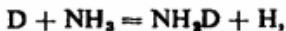


compared with that in the reaction



This difference in the activation energies is due to the different zero point energies of the molecules  $NH_3$  and  $ND_3$ , which is 2.4 kcal.

Since the energy of activation  $11 \pm 1$  kcal. measured experimentally in the exchange reaction is an average of those for the individual exchange reactions 1—10, p. 637, the energy of activation of the reaction



will be 1 kcal. smaller than this average value, *i.e.*, 10 kcal., and that of



1 kcal. larger, *i.e.*, 12 kcal.

From these data it also follows that the separation in the energy levels of the activated complexes  $\text{ND}_3\text{H}$  and  $\text{NH}_3\text{D}$  involved in the above, mentioned exchange reactions cannot be more than 1.5 kcal.

### EXCHANGE REACTIONS WITH METHANE

The exchange experiments with methane were done in the same way as those with ammonia, the only difference being that liquid hydrogen was used to freeze out the methane from the original mixture.

Fig. 9 shows the progress of the exchange reaction in the reaction vessel I in the temperature range 278–506°C., the mixture being approximately 50 mm.  $\text{CH}_4$  + 50 mm.  $\text{D}_2$  (82% D.) In this series the rate of

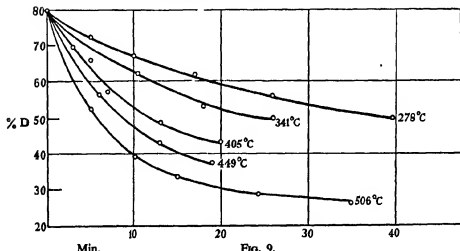


FIG. 9.

the para-hydrogen conversion was determined in parallel runs and corresponding half-lives are given for a mixture of para-hydrogen and methane and para-hydrogen alone.

TABLE IX—QUANTUM INPUT  $2.0 \times 10^{16}$  PER SEC.

Temperature °C.	Half-life times in seconds	
	Without $\text{CH}_4$	With $\text{CH}_4$
119	31	30
170	10	20
201	6	—
280	1.8	15
340	1.0	5

From Table IX it appears that above 150° C. the rate of the para-hydrogen conversion varies much less with temperature than would be expected, and that above this temperature the conversion goes more slowly in the presence of methane, e.g., the rates are equal for a mixture of methane and para-hydrogen at 340° C., and for pure para-hydrogen at 201° C. To investigate this anomaly further, experiments were made in which the CH<sub>4</sub> was not removed (there was no liquid H<sub>2</sub> available at the time); this circumstance decreased the accuracy of the measurements which were, however, accurate enough to demonstrate that the effect is real. Table X contains the results obtained, which refer to mixtures of 20 mm. CH<sub>4</sub> + 80 mm. p-H<sub>2</sub> or 100 p-H<sub>2</sub>, as the case may be. It will be recognized that the inhibiting effect is really characteristic of methane.

TABLE X

Temperature ° C.	Half-life of para-conversion		Source of CH <sub>4</sub>
	In absence of CH <sub>4</sub>	In presence of CH <sub>4</sub>	
37	180	162	ex Al <sub>4</sub> C <sub>9</sub> I
116	—	30	ex Al <sub>4</sub> C <sub>9</sub> I
235	2.4	17	ex Al <sub>4</sub> C <sub>9</sub> I
235	—	18	ex Al <sub>4</sub> C <sub>9</sub> II
235	—	22	ex CH <sub>4</sub> I
238	2.0	17	ex cylinder

In the reaction vessel II the exchange experiments were repeated using mixtures of ortho-deuterium and methane, thus eliminating the necessity of performing two experiments. In this series the CH<sub>4</sub> was again removed by liquid hydrogen. The results are summarized in Table XI.

TABLE XI—TOTAL PRESSURE 100 MM. 50CH<sub>4</sub> + 50D<sub>2</sub>

Temperature ° C.	Half-life of conversion (sec.)	Half-life of exchange (sec.)	Ratio	Remarks
40	900	—	—	Filter removed completely
134	270	—	—	—
189	270	9000	—	Quantum input
340	90	3900	43	— 5.0 × 10 <sup>16</sup> sec. <sup>-1</sup>
453	144	2220	15	—
610	48	372	8	—

To orientate these experiments with respect to the para-hydrogen conversion to which all the exchange reactions are referred, the ratio of

the rates of conversion of para-hydrogen have been compared with ortho-deuterium. At 40° C., the ratio is 5·5: 1 and at 184° C., 4·0: 1.

In order to show that the exchange reaction with methane is of the true exchange type  $D + CH_4 \rightarrow CH_3D + H$ , the quantum yields have been calculated in Table XII, and demonstrate unequivocally that above 400° C. the value of  $\gamma$  is greater than unity. The absolute values are somewhat smaller than with ammonia on account of the decrease in the hydrogen atom concentration at high temperatures.

TABLE XII

Temperature ° C.	$\gamma$ (conversion)	$\gamma$ (exchange)
189	3·3	0·10
340	7·6	0·18
453	4·1	0·27
610	9·8	1·2

The derivation of the expression for the exchange kinetics of methane is carried out in exactly the same way as for ammonia, except that there are now five different methanes and therefore four equations describing the exchange. Equation (1) (p. 638) under the same (*i.e.*, classical) assumptions now becomes

$$\frac{\ln 2}{\tau_t} = \frac{k_{II}([CH_4] + \frac{1}{2}[D_2]) [D]_0}{[D_2] + k_{II}/k_I \cdot [CH_4]},$$

and hence combining with the expression for the half-life of the ortho-conversion

$$\frac{\tau_t(\text{ex.})}{\tau_t(\text{con.})} = \frac{k_I + k_{II}}{1 \cdot 5k_{II}}.$$

The ratio of the values of  $k_I$  to  $k_{II}$  are given at different temperatures below.

TABLE XIII

Temperature ° C. ....	189	340	453	610
$k_I/k_{II}$ ....	51	63	23	12·2
$k_I/k_{II}^*$ ....	190	156	93	45

\* Calculated for  $\Delta E$  of 6000 cal. and same steric factor.

As may be seen from fig. 10, the plot of the  $\log. \tau_t(\text{ex.})$  against  $1/T$  gives an apparent energy of activation of only 7000 cal. This calculation is invalid on account of the decrease in D atom concentration with increasing temperature. To obtain the true energy of activation it is therefore

necessary to plot  $k_I/k_{II}$  against  $1/T$ , which gives directly the *additional* energy of activation for the exchange reaction compared with the ortho-deuterium conversion. This amounts to 6000 cal. The energy of activation may also be obtained from the absolute rate of  $k_I/k_{II}$ , and this amounts to 5000 cal. Table III also shows what the values of  $k_I/k_{II}$  should be, assuming that the whole difference is due to 6000 cal. additional energy of activation. The observed values are somewhat smaller, thus suggesting that, compared with the  $\text{H} + \text{H}_2$  reaction, the steric factor is

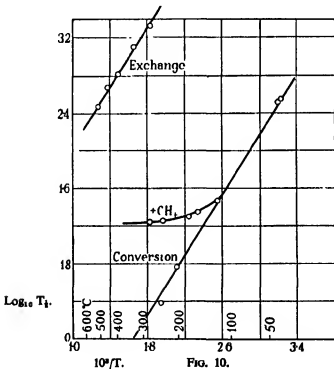


FIG. 10.

a little larger. This, of course, might also be due to the participation of more than two square terms. At all events, the agreement is within the error introduced by the uncertainties in the numerical calculation.

The energy of activation then is computed to be  $13 \pm 1$  kcal. This again is a mean value of the exchange reaction of the five methanes, and therefore the energy of activation for the reaction  $\text{D} + \text{CH}_4 = \text{CH}_3 + \text{H}$  will be the somewhat smaller and  $\text{H} + \text{CD}_4 = \text{CD}_3\text{H} + \text{D}$  somewhat larger than 13 kcal.

The next problem to be settled is the cause of the disappearance of the hydrogen atoms in the presence of methane. One explanation suggests

itself immediately. It is that the effect is due to the presence of some impurities. This, however, is invalid since the inhibiting effect was found with four different samples of methane.

A possible process which may account for the removal of the hydrogen atoms is the reaction



From the investigations of Polanyi and V. Hartel\* and Paneth,† it is known that such a reaction actually occurs, though the energy of activation is of the order of 15 kcal. (Geib and Harteck).‡§ This reaction will only reduce the hydrogen atom concentration effectively if it proceeds fast enough to compete with the three-body recombination of the hydrogen atoms. Furthermore, the equilibrium in the above reaction must lie on the right-hand side. The first postulate requires an energy of activation of somewhat less than 15 kcal., the latter an exothermic heat effect in the reaction



Although both requirements are not easily compatible with the data concerning this reaction at present available, the possibility of its occurring has been tested in the following way. If the concentration of the hydrogen atoms is reduced by a bimolecular process, then the atom concentration in the presence of methane should be directly proportional to the intensity, whereas in the absence of methane the H-atom-concentration varies as the square root of the light intensity, the atoms being removed in three-body collision. For example, with a mixture of 20 mm.  $\text{CH}_4$  and 83 mm.  $p\text{-H}_2$ , the filter increased the half-life at 389° C., from 20 sec. to 220 sec., corresponding to a factor of 11 compared with one of 15 obtained in absence of methane. This indicates that the above reaction is not responsible for the reduction of the hydrogen atom concentration.

Two other possibilities are (*a*) a large increase in the quenching radius of methane with temperatures or (*b*) an increase in the efficiency of three-body collisions including methane as the third body. Both (*a*) and (*b*), however, are improbable as there are no examples of such behaviour in processes of this kind, *i.e.*, the quenching radii independent of temperature for  $\text{H}_2$ ,  $\text{CO}$ ,  $\text{N}_2$ . With methane the quenching radius at 500° C. would need to be about 50 times that of hydrogen whereas at room temperature it is only 1/250 of that of hydrogen.

\* Hartel and Polanyi, 'Z. phys. Chem.,' B, vol. 11, p. 97 (1930).

† Paneth, Hofeditz, and Wunsch, 'J. Chem. Soc.,' p. 372 (1935).

‡ Harteck and Geib, 'Z. phys. Chem.,' A, vol. 170, p. 1 (1934).

§ Bonhoeffer and Harteck, 'Z. phys. Chem.,' A, vol. 139, p. 64 (1928).

Further experiments are, however, necessary to elucidate the nature of the collisions responsible for the disappearance of the hydrogen atoms.

#### EXCHANGE REACTIONS WITH WATER

The exchange experiments with water were carried out in the same way as those with ammonia, the only difference being that the water pressure was limited to 11–12 mm. Hg (vapour pressure at room temperature). The progress of some typical runs (in reaction vessel II) are shown in fig. 11 in the temperature region 318–585°C, the reaction mixture 50 mm.  $p\text{-H}_2 + 12 \text{ mm. D}_2\text{O}$  (90% D).

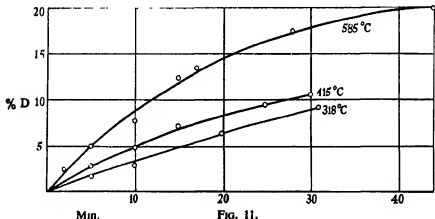


FIG. 11.

The conversion of para-hydrogen was measured simultaneously with the exchange reaction, but in these experiments it was found that the latter proceeded about one thousand times more slowly than the conversion (Table XIV).

TABLE XIV

Temperature °C.	$\tau_1$ (exchange) (sec.)	$\tau_1$ (conversion) (sec.)
318	1560	1·1
415	1200	0·8
585	750	—

Since the half-life times for the para-hydrogen-conversion were so short, it was not possible to measure them very accurately and therefore the rate of the para-hydrogen was re-determined after cutting down the light intensity using the filter. The results of two runs are given in Table XV.

TABLE XV—QUANTUM INPUT  $2.0 \times 10^{14}$  PER SEC.

Temperature ° C.	$\tau_t$ for exchange sec.	$\tau_t$ for conversion		$\frac{\tau_t}{\tau_t} (\text{ex.})$ $\frac{\tau_t}{\tau_t} (\text{conv.})$
		With filter sec.	Without filter calculated sec.	
368	3600	58	3.9	900
586	840	12	0.7	1200

In reaction vessel I in this temperature range similar results were obtained. Table XVI gives some results at lower temperatures in terms of the relative rates of the exchange the conversion rate being taken as unity in order to make the data independent of light intensity and geometrical arrangement of lamp and reaction vessels.

TABLE XVI

Temperature ° C.	$\tau_t$ conversion	$\tau_t$ exchange	$\frac{\tau_t}{\tau_t} (\text{exchange})$ $\frac{\tau_t}{\tau_t} (\text{conversion})$
50	75	15000	200
187	4	2100	530
317	1.8	1600	880

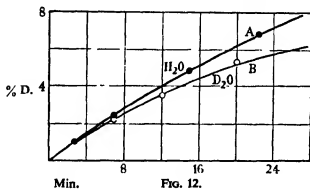


FIG. 12.

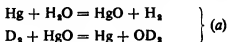
In two runs (in bulb I) again the rates of the exchange reactions between  $\text{H}_2\text{O} + \text{D}_2$ , on the one hand, and between  $\text{D}_2\text{O} + \text{H}_2$ , on the other, have been compared. The results are given in fig. 12 in a manner similar to that used in fig. 11. Curve A refers to a mixture 15.2 mm.  $\text{H}_2\text{O} + 85.8$  mm.  $\text{D}_2$  (89.5% D), and curve B to a mixture of 14.8 mm.  $\text{D}_2\text{O}$  (90% D) + 101.6 mm.  $p\text{H}_2$ . It appears that both reactions proceed with similar speeds in contrast to the results obtained with  $\text{NH}_3$  and  $\text{ND}_3$ .

The most striking feature about the exchange with water is its extreme slowness. Even the quantum efficiency at 585° C. is of the order of unity (Table XVII). For this reason alone it is not possible to say unambiguously that the exchange reaction goes by a mechanism similar to that of methane and ammonia. It might be suggested that the water is decomposed by the excited mercury atoms and that some kind of back

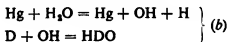
TABLE XVII

Temperature ° C.	$\gamma$ (exchange)	$\gamma$ (conversion)
50	0·1	29
167	0·8	370
368	0·7	630
585	2·8	2880

reaction takes place which leads to an exchange, for example,\*



or



In order to account for the quantum yield of unity at higher temperatures, it would then be necessary to assume that the majority of the excited mercury atoms are deactivated by water molecules leading to the decomposition of the latter according to mechanism (a) or (b). At room temperature the fraction of excited mercury atoms deactivated by water is about 1/20,000. The temperature coefficient of this fraction is not yet known, but will be the subject of a further investigation† to determine whether it increases sufficiently rapidly with temperature to account for the quantum yield at 500°.

The temperature coefficient of the rate of exchange gives an apparent energy of activation of only 7000 cal., i.e., the ratio of velocity conversion/exchange is practically independent of temperature. This is a surprising fact compared with the CH<sub>4</sub> and NH<sub>3</sub> reactions where the ratio, though much smaller, varies quite rapidly with temperature, showing that it is due mainly to an additional energy of activation to that of the para-hydrogen-conversion. Had the factor of 1000 at 500° C. been due to additional energy of activation of about 9000 cal., the ratio should have

\* Senftleben, 'Z. Phys.', vol. 32, p. 922 (1925); vol. 33, p. 871 (1925).

† Melville (*In the press*).

decreased from 300° to 500° by a factor of about 7·5 which would have been easily detected. To explain these results it would then be necessary to assume that the steric factor is about 1/1000 of that for the reaction  $H + H_2 = H_3 + H$  or that the decomposition reactions mentioned above are partly responsible for exchange. At present these possibilities cannot be distinguished.

At lower temperatures the ratio conversion/exchange decreases. Here the exchange may be due to decomposition of water or it may be due to exchange occurring between water adsorbed in the walls and atomic hydrogen in the gas phase.

Whereas the rate of the exchange reaction involving methane and ammonia is completely characterized by the corresponding energies of activation (13 and 11 kcal. respectively), the exchange reaction involving water proceeded very much more slowly than would be expected from the apparent energy of activation which is 7 kcal.

For purposes of comparison, therefore, Table VIII showing the rates of the exchange relative to that of the para-ortho-hydrogen conversion (which is taken as unity) has been compiled.

TABLE XVIII

	500° K.	800° K.	1000° K.
CH <sub>4</sub> . . . . .	1:45	1:10	1:5*
NH <sub>3</sub> . . . . .	1:90	1:40	1:30
OH <sub>2</sub>	1:900	1:1000	<1:100†

\* This is the ratio rate of exchange/rate of para-conversion in absence of CH<sub>4</sub>. The effect of the presence of CH<sub>4</sub> on the thermal *o-p*-H<sub>2</sub> conversion requires further investigation.

† The low ratio here may be due to a catalytic reaction.

The last column refers to exchange experiments initiated thermally, and it will be recognized that there is satisfactory agreement between the results obtained by the two methods. It may be mentioned that as far as the energy of activation of the exchange with ammonia is concerned the agreement is complete since the thermal measurements also give 11 ± 1 kcal.

It is now necessary to compare these results with those of other investigations. Taylor, Morikava, and Benedict\* have demonstrated that at 30° C. exchange reaction occurs when a mixture of methane deuterium and mercury vapour is illuminated with the mercury resonance line.

\* J. Amer. Chem. Soc., vol. 57, p. 383 (1935).

Without giving numerical results, they estimate the energy of activation for the atomic exchange reaction to be 5 kcal.

On the basis of the present experiments, this appears to be much too low. On the other hand, as far as the mechanism of the ammonia exchange at room temperature is concerned, Taylor and Jungers's\* results are in qualitative agreement with the present investigation. At this temperature the atomic reaction is too slow to contribute to the exchange which occurs by direct photochemical dissociation and subsequent recombination of the radicals with deuterium atoms.

Geib and Steacie† have investigated the exchange reaction occurring in the interaction of atomic hydrogen (produced in a Wood's tube) with methane, water, and ammonia. Although the energies of activations deduced by these authors are not much different from those given in this paper, there is a serious discrepancy in the absolute reaction rates.

Table XIX contains the collision efficiencies at 100° C. for the different exchange reactions according to Geib and Steacie compared with the collision efficiency of the para-hydrogen-conversion measured by Geib and Harteck,‡ using the same technique.

TABLE XIX

	Collision efficiency
D + H <sub>2</sub> O	$3.9 \times 10^{-7}$
D + NH <sub>3</sub>	$12 \times 10^{-7}$
H + H <sub>2</sub>	$7 \times 10^{-4}$

It will be seen that according to these figures the additional energy of activation for the exchange reaction compared with that of the para-hydrogen conversion could not be more than 2 kcal. since the collision efficiencies do not differ by more than a factor of 20, whereas in the present investigation at much higher temperatures factors of the order of 100 were found (*cf.* Table XVIII).

Consequently, taking these energies of activation and those of the present investigation, the rates found by Geib and Steacie are too fast. It may be suggested that these authors have underestimated the contribution of the reaction occurring at the walls. This is also supported by the observation that the quickest reaction is found with ammonia and water which are known to be strongly adsorbed, and practically no reaction with weakly adsorbed methane. On the other hand, the present results indicate that methane is the more reactive molecule and water the least when homogeneous atomic exchange is concerned.

\* 'J. Chem. Phys.', vol. 2, p. 452 (1934).

† 'Z. phys. Chem.', B, vol. 29, p. 215 (1935).

‡ 'Z. phys. Chem. Bodensteinfestband', p. 849 (1931).

The authors wish to thank Professor E. K. Rideal, F.R.S., for his interest in and his encouragement throughout the investigation. One of them (H. W. M.) thanks the Royal Commissioners of the Exhibition of 1851 for a Senior Studentship. The other thanks Imperial Chemical Industries, Ltd., for a grant.

### SUMMARY

The mercury photosensitized exchange reactions of hydrogen and deuterium with methane, ammonia, and water have been investigated.

The following parameters have been varied:—

- (1) The time of reaction up to the establishment of the equilibrium.
- (2) The temperature in the range 30–600° C.
- (3) The partial pressure of the components at a total pressure of 100 mm.
- (4) The components, e.g.,  $D_2 + NH_3$  and  $H_2 + ND_3$ .
- (5) The intensity of the illumination.

In each case the rate of the exchange reaction was compared with the absolute intensity of the light and the rate of the ortho-para-conversion of hydrogen or deuterium in order to measure the stationary H or D atom concentration.

With methane and ammonia it was possible to show from the kinetics that the exchange above 300° C. proceeded by the mechanism



followed by



and so on.

The energy of activation for methane exchange (*i.e.*, reaction (a)) is  $13 \pm 1$  kcal. and that for ammonia is  $11 \pm 1$  kcal. The steric factors involved are the same order of magnitude in the reaction  $H + H_3 = H_2 + H$ . The apparent energy of activation for exchange with water is 7 kcal.

This energy of activation does not account for the slowness of the rate of exchange (*i.e.*, 1/1000 that of para-conversion at 500° C.). This might be due either to a small steric factor or to the decomposition of water by excited mercury and subsequent reformation.

It is pointed out that especially at lower temperatures the mechanism of the exchanges becomes complicated by reactions, discussed in the paper, which may account for the results described by other experimenters.

---

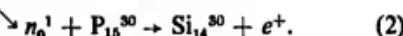
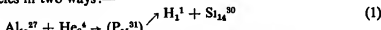
## The Formation of Radio-Phosphorus ( $P^{30}$ )

By J. R. S. WARING, Trinity College, Cambridge, and W. Y. CHANG, Jesus College, Cambridge

(Communicated by C. D. Ellis, F.R.S.—Received 15 June, 1936)

### 1—INTRODUCTION

It has been known for some time that aluminium could be disintegrated by  $\alpha$ -particles in two ways:—



The first reaction has been exhaustively studied by many workers. In particular the "resonance" levels, *i.e.*, levels of easy entry of the  $\alpha$ -particles, are well known. It was therefore of interest to discover whether "resonance" phenomena occurred in the second reaction, and if so to locate the levels, measure their relative intensities, and compare with the corresponding data for proton emission.

During the course of the present work a paper covering some of the same ground has been published by Fahlenbrach.\* This will be referred to later.

In principle, the method of measurement is quite simple. A target of aluminium is exposed to  $\alpha$ -particles of a given energy and the yield of neutrons is calculated from the observed positron activity, as measured by suitable counting apparatus. In practice, difficulties are encountered in obtaining at the same time both good resolving power and sufficient intensity, and a compromise has to be made.

Two types of experiment are described here—obtained with thick and thin targets respectively—which may be called (1) integral, and (2) differential measurements.

### 2—INTEGRAL MEASUREMENTS

The following was the experimental arrangement used: a cylindrical target of thick aluminium foil was activated by a radon source contained in a thin-walled glass tube placed along the axis of the cylinder. The activated foil was then coiled into a cylinder of half the diameter of the original one and placed over a long tube counter.

\* Z. Phys., vol. 94, p. 607 (March, 1935).

The maximum energy of the  $\alpha$ -particles hitting the aluminium could be varied by establishing a known pressure of  $CO_2$  in the activation apparatus. The maximum range of the emergent  $\alpha$ -particles was measured to an accuracy of 2 to 3 mm. by using a scintillation screen.

The homogeneity of the  $\alpha$ -particles hitting the target may be seen from Table I, which refers to the two extreme cases. Two factors are not taken into account here, namely (1) straggling of the  $\alpha$ -ranges, and (2) variation of the thickness of the glass wall of the radon tube. The figures are only an indication of the "geometry".

TABLE I

*Case I*—Using 7 cm.  $\alpha$ -particles from Ra C, and after passing through 3 cm. absorber (maximum energy  $5.35 \times 10^4$  e-volts).

80%	have an energy between	..... . .	5.05 and 5.35 M. e-volts
68%	" "	..... . .	5.15 and 5.35 "
55%	" "	..... . .	5.25 and 5.35 "

*Case II*—Using 5 cm. absorber (maximum energy  $3.2 \times 10^4$  e-volts).

64%	have an energy between	..... . .	2.9 and 3.2 M. e-volts
55%	" "	..... . .	3.0 and 3.2 "
43%	" "	..... . .	3.1 and 3.2 "

The general evidence indicates that resonance levels have a total width of the order of 0.3 M. e-volts, and it will therefore be seen that this arrangement should be effective at least in locating their positions.

The experimental results obtained in this way are shown in figs. 1 and 2. The curve in fig. 1 was obtained for the lower energy range of  $\alpha$ -particles (3 M. e-volts up to 5.6 M. e-volts), while that in fig. 2 was determined for the higher energy range (5.3 M. e-volts up to 7 M. e-volts) by using another radon tube. For the purpose of reference, the integral yield is expressed in absolute yield (number of positrons per  $\alpha$ -particle) as well as in actual yield per mg. for infinite exposure. In both cases the differential yield is shown by the dotted curves and is given as calculated in terms of cross-section for disintegration.

The two integral curves agree quite well with one another, as shown by the yield at the intermediate ranges of the  $\alpha$ -particles. The differential curve in fig. 1 indicates resonance levels at 4.0, (4.5), 5.0, and 5.55 M. e-volts, and that in fig. 2 indicates levels at 5.25, (6.0), and 6.7 M. e-volts. The two levels 5.25 M. e-volts and 6.7 M. e-volts are in good agreement with the levels 5.2 M. e-volts and 6.61 M. e-volts, as found by Fahlenbrach; the corresponding cross-sections and widths are approximately the same. Since the differential curves are obtained from the integral

curves merely by a graphical method, no great accuracy for the form or especially the peak values can be claimed.

Table II shows the comparison between the resonance levels found in the present work and those found for proton emission by Chadwick and Constable,\* and Duncanson and Miller.†

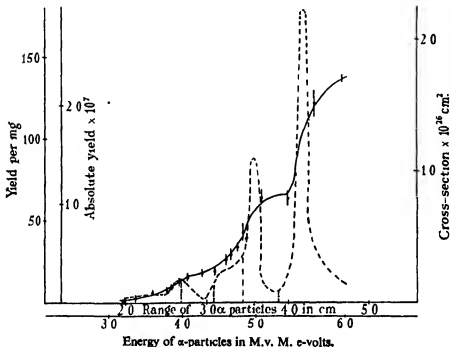


FIG. 1—Yield curve for low energy range. Full vertical lines = statistical error; dotted vertical lines denote levels found by Chadwick and Constable for protons.

TABLE II

Resonance levels in M. e-volts

Neutron emission .....	4.0	(4.51)	5.0	5.55		
					5.25	(6.0)
Proton emission .... ...	4.0	4.49	4.86	5.25	5.75	6.61

The figures in the brackets indicate broad or less definite levels.

The agreement between the positions of the resonance levels found for neutron and proton emission is as good as could be expected, as there is a certain indefiniteness in the range of the  $\alpha$ -particles due to (1) variable

\* Proc. Roy. Soc., A, vol. 135, p. 48 (1932).

† Proc. Roy. Soc., A, vol. 146, p. 413 (1934).

thickness of glass walls of the radon tubes, and (2) to straggling when much stopping power is introduced. The width of the levels appears to be from 150,000 to 300,000 e-volts at half intensity, agreeing well with the proton results. The level at 6.0 M. c-volts, however, appears to be anomalous

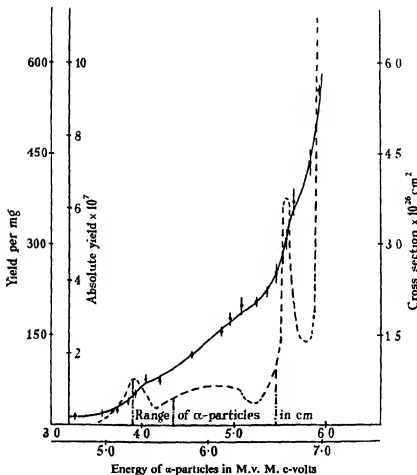


FIG. 2.—Yield curve for higher energy range. Full vertical lines — statistical error; dotted vertical lines denote levels found by Duncanson and Miller for protons.

where the width is more than 600,000 e-volts. This point will be discussed later.

Penetration of the top of the potential barrier begins at 6.9 M. e-volts with a corresponding rapid increase in the yield. This compares well

with Haxel's\* value of 6.7 M. e-volts found from observation of the protons.

Some values for the general variation of the yield of  $P^{20}$  with energy of  $\alpha$ -particles have been given by Ellis and Henderson.† It is difficult to make an exact comparison, but it is clear that the present measurements do not show such a rapid fall at low energies as was found by these authors. The starting point for neutron emission appears to be 3.2 M. e-volts or less; this figure is about 1.2 M. e-volts below that given in Ellis and Henderson's curve. We feel confident that the yields shown here are reasonable, since the experiments to be described later, using a thin target, would otherwise have been impracticable.

By far the most interesting result to be deduced from these measurements is the variation in the "branching ratio" (probability of neutron emission/probability of proton emission) with  $\alpha$ -ray energy. This is shown in Table III. The figures are very approximate.

TABLE III

$\alpha$ -particle energy in M. e-volts	Proton mean cross-section $P \times 10^{48} \text{ cm}^2$	Neutron mean cross-section $n \times 10^{48} \text{ cm}^2$	Branching ratio $n/P$
4.0	3	0.08	40
4.49	3	0.21	15
4.86	3	0.35	9
5.25	3	0.42	7
5.75	9	0.54	16
6.61	9	1.68	5

The mean cross-sections of the proton emission are taken from the data given by Chadwick and Constable.‡ It will be seen that as the range of the  $\alpha$ -particles is increased the branching ratio decreases. The measurements are not definite enough to settle whether there is really an irregular variation or not, but we can be reasonably certain that for increasing energy the ratio decreases approaching unity at an  $\alpha$ -range of say 7 cm. This suggests that for higher energies of the  $\alpha$ -particle the proton and neutron behave somewhat in the same way in regard to their escape through the potential barrier.

\* 'Z. Phys.,' vol. 90, p. 376 (1934).

† 'Proc. Roy. Soc.,' A, vol. 146, p. 206 (1934).

‡ Chadwick and Constable, 'Proc. Roy. Soc.,' A, vol. 135, p. 48 (1932). For the higher two energies, cf. also Duncanson and Miller, 'Proc. Roy. Soc.,' A, vol. 146, p. 408 (1934).

## 3—DIFFERENTIAL MEASUREMENTS

The difficulty of interpreting the results obtained from the "integral curves" and the errors which may be introduced in the process of differentiation, made it of great importance to obtain direct "differential" curves by the use of thin targets. The yield in such cases is considerably smaller and it was only found to be practicable with  $\alpha$ -particles of over 5·4 M. e-volts (*i.e.*, 4 cm. range). This region has, however, an additional advantage in that the two known resonance levels for protons are more than 0·9 M. e-volts apart and therefore relatively poor geometry should be able to resolve them.

Two sets of measurements were obtained using aluminium foils of 2·5 mm. and 1·25 mm. stopping power respectively. In the first set the experimental method was as follows: a brass disk carrying the aluminium foil was placed in front of a disk source of radium active deposit of 50 mg. strength or more. The source and the target were separated by a mica window of 1 cm. stopping power, and a known pressure of  $CO_2$  was established to alter the incident  $\alpha$ -ray range. The activated aluminium foil was then placed in front of the window of a large ball counter. In the second set a cylindrical method of activation was used. A disk source was enclosed in an evacuated brass cylinder, having a grid and mica window of 1 cm. stopping power on its circumference. The plane of the disk was perpendicular to the axis of the cylinder and slightly below the plane which included the bottom of the window. A larger and concentric brass cylinder carrying the aluminium foil surrounded the "virtual" source described above. The space between the two cylinders could be filled with a variable pressure of  $CO_2$ . Counting was carried out in the usual manner with a large cylindrical wire counter.

The homogeneity of the  $\alpha$ -particles hitting the targets in the two cases is shown in Table IV.

It will be seen that in both cases the geometry is reasonable; particularly the second set at higher pressure of  $CO_2$ , and, moreover, the targets used here were only half as thick as those in the first set. In addition, methods using active source have an advantage over those using radon tubes as there are in this case no errors due to unequal thickness of glass absorber.

The two curves in fig. 3 are the experimental results obtained respectively with the first and second methods after allowing for the difference in thickness of the foils. Taking into account the fact that the two experimental conditions are entirely different, the agreement is very satisfactory. Both curves show unambiguously a resonance level at about

6.5 M. e-volts, which as regards positions agrees well with the previous integral measurements and with Fahlenbrach's experiment as well as with the work of Duncanson and Miller on protons. At first sight it would seem that the form of the direct differential curve is quite different from that obtained by differentiation of the integral curve. However, as was pointed out in the discussion of the integral measurements, no great accuracy can be claimed in that case for the peak values of the cross-

TABLE IV

## A—Disk Method

(i) At zero pressure of CO <sub>2</sub> —				
100% of the $\alpha$ -particles have energy between . . . . .	6.65	and	6.92	M. e-volts
75% " "	6.82	and	6.92	"
50% " "	6.85	and	6.92	"
(ii) At 3/4 atmospheric pressure of CO <sub>2</sub> —				
100% of the $\alpha$ -particles have energy between . . . . .	4.7	and	5.4	M. e-volts
75% " "	5.05	and	5.4	"
50% " "	5.15	and	5.4	"

## B—Cylindrical Method

(i) At zero pressure of CO <sub>2</sub> —				
100% of the $\alpha$ -particles have energy between . . . . .	6.87	and	7.01	M. e-volts
75% " "	6.93	and	7.01	"
40% " "	7.00	and	7.01	"
(ii) At atmospheric pressure of CO <sub>2</sub> —				
100% of the $\alpha$ -particles have energy between . . . . .	4.74	and	5.2	M. e-volts
75% " "	4.92	and	5.2	"
40% " "	5.00	and	5.2	"

section at resonance. We therefore consider that the difference in the cross-section obtained with thin targets and those found by Fahlenbrach and us with thick targets is due to errors inherent in the process of graphical differentiation of the integral curves. In fact, if the direct differential curve obtained with a thin target is integrated, a curve is obtained which does not differ essentially from that shown in fig. 2. We therefore finally place more reliance on the figure of  $2.3 \times 10^{-26}$  cm.<sup>2</sup> for the cross-section at resonance than on the figure  $3.5 \times 10^{-26}$  cm.<sup>2</sup> obtained from the integral curves of either Fahlenbrach or ourselves. Similar considerations apply to the question of the width of the level, which from the direct differential curve would seem to be greater than 1 M. e-volt at half intensity, a value much greater than that obtained from the integral measurements.

Now turning our attention from the actual resonance level to the region just below, we notice a very striking feature, namely the large yield; in

other words the resonance levels in this region are not so pronounced as would have been expected. When one remembers the proton case, where the two levels 5.75 M. e-volts (4.35 cm. range) and 6.61 M. e-volts (5.45 cm. range) are far apart and have equal intensity, and the geometry

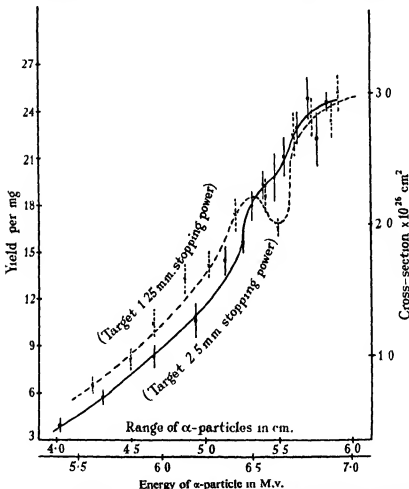


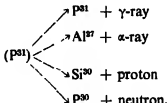
FIG. 3—Yield curves for thin targets of 1.25 mm — — —, and 2.5 cm. — — — stopping power. Vertical lines = statistical error; dotted curve is obtained from the cylindrical method and reduced to the same conditions as in the disc method.

in the differential measurements, one would expect some wide region with no yield. However, the curves in fig. 3 show a steady change of the yield with the energy of  $\alpha$ -particles. If there is a region of no yield, it must be less than 0.3 M. e-volts and must occur in the interval between two points determined of the curve. It may be mentioned again that the integral

measurements described above and in Fahlenbrach's work also show a very broad level or just a continuous yield in this region. This differs entirely from the proton case where Duncanson and Miller found a very small or practically zero proton yield in this region. Attempts are made to explain this phenomenon in the following section.

#### 4—DISCUSSION

The experimental results described above are in general consistent and can be brought into line with Bohr's theory\* of the formation of intermediate products. For example, in the case under consideration, a nuclear aggregate of mass 31 would be formed, which might break down in any of the following four ways:



Now it is reasonable to assume that the level system of the excited intermediate product is the same in all cases, *i.e.*, independent of the particular particle which is subsequently ejected. The probability of the different competing transformations of the intermediate product will vary with the degree of excitation, *i.e.*, with the energy of the incident particle. This will account for the branching ratio  $P/n$  varying with the energy, which has been noted experimentally. It seems possible that at different parts of the level system certain processes may be favoured at the expense of the others. A special case of this might be the complete absence of, say, a neutron "transition" where a proton "transition" is allowed (*cf.* selection rules in optics). Thus a zero or small yield of a disintegration product can be explained either as due to a small probability of a "transition", giving rise to this type of particle, or to a small yield of the intermediate product. The measurements described here, as well as the work of Fahlenbrach, show that the 5.75 M. e-volts proton level is either very broad or absent for neutrons. It seems possible that this level is preserved nearly exclusively for proton "transition". Also to explain the continuous yield of neutrons in the range 5.4 M. e-volts to 6.6 M. e-volts, it is necessary to assume a continuous yield of the intermediate product.

\* 'Nature,' vol. 137, p. 344 (29 February, 1936).

For some reason, therefore, only some levels give protons, whereas most give neutrons.

It appears to us, therefore, that we can obtain a better description of the phenomenon if we assume that  $\alpha$ -particles of any energy, above possibly a certain minimum energy, have a finite chance of entering the nucleus with formation of the intermediate product. The yield of the intermediate product when plotted against the energy of the  $\alpha$ -particle would be a continuous curve with only slight maxima if any. The maxima in the yield of protons or neutrons are in our opinion due to pronounced changes in the probability of the "transition" giving rise to these particular particles; hence "resonance" is to be associated more with the emitted particle than with the bombarding particle.

We wish to thank Lord Rutherford for his interest in this work, and Dr. C. D. Ellis for his constant encouragement and advice during the course of the experiment. We are also indebted to Mr. A. Szalay for his assistance in part of the work. One of us (J. R. S. W.) desires to thank the Department of Scientific and Industrial Research for a grant.

#### SUMMARY

The formation of radio-phosphorus ( $P^{30}$ ) from aluminium by the bombardment of  $\alpha$ -particles has been studied for different energies of the bombarding  $\alpha$ -particles. Both thin targets, *i.e.*, 1.25 mm. to 2.5 mm. stopping power, and thick targets were used. The resonance levels observed are discussed and compared with those found for proton emission. An explanation for the excitation curve is given in terms of Bohr's theory of the formation of intermediate products, and the results for proton emission are also discussed from the point of view of that theory.

---

## Auger Effect for the L Level of Xenon and Krypton

By J. C. BOWER, M.Sc., University of Melbourne

(Communicated by T. H. Laby, F.R.S.—Received 15 June, 1936)

[PLATE 15]

While a number of investigations have been carried out to determine the efficiency of emission of K series fluorescent radiation from various elements,\* only two determinations have been made of the L yield, that is the efficiency of emission of L series radiation.

Some years ago Auger,<sup>†</sup> using an expansion chamber, investigated the L yield for the two inert gases krypton and xenon, and recently Lay,<sup>‡</sup> using a photographic method, has determined this quantity for certain elements between atomic number 40 and 92. The results of the two investigations are not consistent, the values found by Auger for the L yields of krypton and xenon being much greater (100% and more) than the values for these gases given by interpolating and extrapolating the data published by Lay for neighbouring elements.

As pointed out in a previous paper,<sup>§</sup> the expansion chamber has the advantage that values of the efficiency of excitation can be calculated by a direct count, the only problem being the identification of tracks. In the present problem this presents little difficulty as the tracks are of two types, with and without a spur at their origins. Ionization and photographic methods yield values, the accuracy of which ultimately depends on the accuracy of existing absorption data, and in general where these exist the agreement between different workers leaves much to be desired. The difficulties of these methods will be discussed later.

In the present work measurements of the L yield for xenon and krypton have been repeated since these gases give spur tracks (due to internal conversion) which are sufficiently long to be readily recognized. Further, experience in the past has shown that they behave well in an expansion chamber.

\* Compton and Allison, "X-Rays in Theory and Experiment," p. 477 (1935).

† 'Ann Physique,' vol. 6, p. 183 (1926).

‡ 'Z. Phys.,' vol. 91, p. 533 (1934).

§ 'Proc. Roy. Soc.,' A, vol. 148, p. 40 (1935).

### EXPERIMENTAL

The expansion chamber used was similar in design to that described in a previous paper.\* The chief modification consisted in the inclusion of three iron piston rings which, when lubricated with colloidal graphite in oil, effectively prevented the passage of gas past the piston during an expansion. In addition the valve mechanism was improved so that the air beneath the piston could be swept out in a minimum of time, approximately 0·01 sec., as determined by a trace on a moving photographic film. The other arrangements were essentially the same.

Exciting beams of approximately homogeneous X-rays were produced by appropriately filtering the radiation from a standard Coolidge tube. To avoid the excitation of the K series radiation of the gases the potential across the X-ray tube, measured with an Abraham Villard electrostatic voltmeter, was kept below the K excitation potential. (35 k.v. for xenon and 14·7 k.v. for krypton.) Details of the tube potentials and the filters used are included in Table I, which also gives the energies of the primary and secondary photoelectrons emitted. (The terms primary and secondary photoelectrons are here used to denote respectively the photoelectrons ejected from the L shell by the incident X-radiation and the photoelectrons of energy  $h(v_i - 2v_M)$  emitted by atoms ionized in the L shell as the result of the internal conversion process.)

It was considered unnecessary to use a balanced filter to obtain an approximately homogeneous beam as the previous work on argon\* had shown the fluorescent yield to be independent of X-ray wave-length to within 5%. In each case the filters were so chosen so as to absorb any X-radiation of wave-length sufficiently short to excite the K level of the gas atoms. A sufficient thickness of absorber was used to eliminate X-radiation of wave-length too long to be capable of exciting the L levels of the respective gas atoms. In any case, tracks produced by the absorption of such radiation in the M level are so short as to be readily distinguishable (energies less than 5 k.v. in the case of xenon and 2 k.v. in the case of krypton).

In order to make the tracks sufficiently long, a 3% mixture of the inert gas with hydrogen was used in each case.

### OBSERVATIONS

Typical tracks produced in the xenon-hydrogen and krypton-hydrogen mixtures are shown on Plate 15. Figs. 1 and 2 are a stereoscopic pair of

\* Proc. Roy. Soc., A, vol. 148, p. 40 (1935).

photographs taken with the xenon-hydrogen mixture in the cloud chamber. The track, whose origin is marked by the intersection of AA and XX, is a typical Auger pair showing the long primary photoelectron track associated with the characteristic heavier short secondary photo-electron track. Other Auger pairs can be seen. Figs. 3 and 4 are

TABLE I

Gas	Target potential (k.v.)	Filter	Effective X-ray wave-length A.	Effective X-ray energy (e-k.v.)	Energy primary photo-electron (k.v.)	Energy secondary photo-electron (k.v.)
Xe	18	K Br (0.5 mm.)	0.8	15	9.5	3.5
Kr	11	Zn (0.003 mm.)	1.3	9.6	7.5	1.3

another stereoscopic pair showing one case of paired tracks and one ordinary track taken in the krypton-hydrogen mixture.

The tracks were examined under a threefold magnification. Each track was identified on both plates before classifying it, and in no case were the best tracks chosen at random. Either all the tracks on both plates, or at least several consecutive tracks had to be recognized before a count was made.

The results are collected in Table II.

TABLE II

Gas	Wave-length exciting radiation	No. of pairs of plates	Total no. of tracks	Paired tracks A	Ordinary tracks O	O/A + O	Probable error %	O/A + O (Auger)
Xe	0.8	105	706	449	257	0.364	3	0.359
Kr	1.3	90	633	483	150	0.237	4.5	0.251

The probable error in the ratio O/(A + O) given in the 8th column has been calculated on the assumption that if  $\pi$  is the proportion of ordinary tracks observed in a total count of  $n$  tracks then the probable error in  $\pi$

$$0.6475 \sqrt{\frac{\pi(1-\pi)}{n}}.$$

For the sake of comparison, values of O/(A + O) calculated from

\* Loc. cit.

Auger's data are given in the last column. The writer's values and Auger's for  $O/(A + O)$  agree to within the probable errors of both experiments.

The efficiency of excitation of fluorescent L radiation is given in terms of  $J_L$ , the L jump (the ratio of the ionization in the L shell to the ionization in the M + N--- shells) and the ratio  $O/(A + O)$  of the number of ordinary tracks to the total number of tracks by

$$\mu_L = \frac{J_L}{J_L - 1} \cdot \frac{O}{A + O} - \frac{1}{J_L - 1}. *$$

Few determinations of the L jump of elements have been made, and such values as have been obtained are not in general consistent. For elements of atomic number less than 60 the most satisfactory values of  $J_L$  are the value 5.3 given by Jönsson† for silver (atomic number 47) and the value 5.8 for the same element obtained from Kellström's‡ work of the  $L_{II}$ ,  $L_{III}$ , and  $L_{IV}$  jumps. Allen§ has given values of  $J_L$  for tin 7.2 and for silver 7.7, but as he did not use homogeneous radiation, his values cannot be given the same weight. Auger,|| from a statistical analysis of the track lengths of the photoelectrons produced in a xenon-hydrogen mixture, has deduced the value of the relative ionization in the L and M shells of xenon as 5.2. This corresponds to  $J_L = 6.2$ . The number of tracks counted was 226 and consequently the probable error in  $J_L$  is of the order of 10%.

On the basis of the two values 5.3 and 5.8 for silver, it seems that  $J_L$  for xenon should lie between 5 and 5.5, and for krypton between 5.5 and 6 allowing for the slow increase of  $J_L$  with decrease of atomic number indicated by the available experimental evidence.¶ Actually by taking  $J_L$  as the ratio of  $v_{T_A}/v_{M_I}$ , the values 4.8 and 5.8 are obtained. In view of these considerations values of  $J_L = 5$  for Xe and  $J_L = 5.7$  for Kr are assumed here as likely values, but the L yields are also calculated for the writer's observations for the higher values  $J_L = 6$  for Xe and  $J_L = 6.5$  for Kr. The values of the L yield for krypton and xenon obtained by the writer are tabulated in Table III.

The values of  $\mu_L$  obtained by Auger for xenon and krypton are respectively 0.25 and 0.13. It is thus apparent that the values of  $\mu_L$  obtained

\* *Loc. cit.*

† 'Diss.', Upsala, 1928.

‡ 'Z. Phys.', vol. 44, p. 269 (1926).

§ 'Phys. Rev.', vol. 28, p. 907 (1926).

|| 'Ann. Physique', vol. 6, p. 183 (1926).

¶ 'Wien Harms Handbuch der Experimental Physik.', vol. 24, i, p. 259 (1930).

by the writer when the lower values of  $J_L$  are taken are much less than the values given by Auger. The agreement is better when the higher values of  $J_L$  are assumed, particularly in the case of xenon. Actually Auger gives for the relative ionization in the L and M shells of xenon the value 5·2 which, corresponding as it does to a value of about 6·2 for  $J_L$ , is approximately in agreement with the higher values of  $J_L$  assumed here. The large differences apparent when the lower values of  $J_L$  are taken are due to these values of  $J_L$ , for inspection of Table II shows that the writer's and Auger's values of  $O/(A + O)$  are consistent within the limits of error.

TABLE III

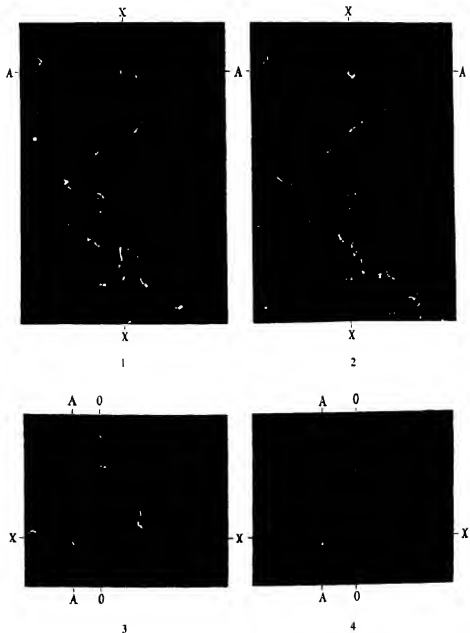
Gas	$O/(A + O)$	$J_L$	$\mu_L$
Xe .....	0·364	5	0·20 <sub>s</sub>
		6	0·23 <sub>s</sub>
Kr .....	0·237	5·7	0·07 <sub>s</sub>
		6·5	0·10 <sub>s</sub>

Interpolating and extrapolating the values of  $\mu_L$  given by Lay, for elements of atomic number between 60 and 40 gives values of 0·14<sub>s</sub> and 0·03<sub>s</sub> for the L yields of xenon and krypton. Both the experiments of Auger and this investigation show that these values are too low. To obtain values consistent with Lay's figures it would be necessary to assume a very low value for  $J_L$ . Actually examination of the experimental evidence suggests that it is unlikely that the values of  $J_L$  could be much smaller than the lower values assumed here.

The writer believes that the expansion chamber method possesses definite advantages over the photographic and ionization methods. These methods are technically difficult and require a knowledge of absorption data. In the photographic method calculations have to be made of the fraction of excited radiation escaping the radiator. A knowledge of the absorption coefficients, both of the exciting and excited radiation in the fluorescent material, is necessary, and in general these data are not available or at least can make no claim to a high degree of accuracy. The same can be said of the absorption data regarding the materials of the photographic film, a knowledge of which is essential in estimating the intensities of the exciting and excited radiation.

It is considered that the efficiency of emission of fluorescent radiation is about 20% in the case of xenon and about 8% in the case of krypton.

In conclusion, the writer wishes to express his indebtedness to Professor T. H. Laby, F.R.S., and Dr. L. H. Martin for advice and criticism, and Mr. Waters for technical assistance during the experiment.



FIGS. 1 and 2—Stereoscopic pair in 1% xenon-hydrogen mixture.

FIGS. 3 and 4—Stereoscopic pair in 3% krypton-hydrogen mixture.



## SUMMARY

An investigation of the efficiency of emission of L series fluorescent radiation from xenon and krypton using an expansion chamber is described. A statistical analysis of some 700 tracks in the case of xenon and 600 in the case of krypton gave values for the efficiency of 20% and 8% respectively. The results are compared with those obtained by previous workers.

---

## A Theory of Electro-Kinetic Effects in Solution; Reactions Between Ions and Polar Molecules

By E. A. MOELWYN-HUGHES

(Communicated by E. K. Rideal, F.R.S.—Received 16 June, 1936)

The experimental values of the velocity coefficient  $k$  for bimolecular reactions may be summarized in an equation of the form

$$k = Z \cdot P \cdot e^{-E_A/kT}, \quad (1)$$

where  $P$  and  $E_A$  are empirical constants, specific for each reacting system, and  $Z$  is the kinetic theory value for the frequency of binary collisions, namely,

$$Z = \frac{N_0}{1000} r_1 r_2^2 n_1 n_2 \left\{ 8\pi k T \left( \frac{1}{m_1} + \frac{1}{m_2} \right) \right\}. \quad (2)$$

The physical significance of the term  $P$  may be realized by considering the hypothetical case where the Arrhenius energy of activation  $E_A$  is identical with the true energy of activation  $E'$ . Since the theoretical expression for the maximum velocity of the bimolecular process is

$$k = Z \cdot e^{-E'/kT}, \quad (3)$$

it is seen that  $P$  measures the absolute probability that a binary collision of sufficient energy leads to chemical reaction. In general, however,  $E_A$  and  $E'$  are not identical, and the interpretation of the term  $P$  is not so simple.

As far as chemical reactions between two charged particles are concerned, it has, however, been possible to give a simple interpretation of

P values ranging from  $10^{-8}$  to  $10^{-8}$  by factorizing the true energy of activation ( $E'$ ) into a component E, which is assumed to be independent of temperature and of the medium, and  $E_A$ , the electrostatic contribution, which is a function of both variables.\* It is the object of this paper to see whether a similar treatment will prove helpful in gaining a clearer understanding of the mechanism of reactions with ions and polar molecules. Most of these reactions have normal velocities, that is, the factor P has the order of magnitude unity.† Selected data for one hundred of these reactions, which have attracted considerable attention within recent years, have recently been reviewed.‡ The new data in all cases agree with this generalization.§ The following treatment makes possible a finer analysis of the factor P, and allows us to correlate  $E_A$  and  $E'$  quantitatively. For reactions between ions and dipoles, it is known beforehand that the difference between  $E_A$  and  $E'$  is small, for the approximation  $E_A \approx E'$  underlies all the values of P quoted in the literature. Arguments have been advanced for rejecting the approximation completely in the case of the hydrolysis of glucosides,|| and the union of amines and halides.¶ On the other hand, for the reactions under discussion here, the approximation is valid. The conclusion was drawn on general chemical evidence, on the temperature invariance of  $E_A$ , and on the parallelism shown to exist between  $T_{l-1}$  and  $E_A$  for different reactions.\*\*

#### THEORY OF REACTION BETWEEN IONS AND Dipoles

We shall now follow the method outlined in the theory of reaction between two ions,†† by factorizing the total energy of activation,  $E'$  into

\* Moelwyn-Hughes, 'Proc. Roy. Soc.,' A, vol. 155, p. 308 (1936).

† Moelwyn-Hughes, 'Chem. Rev.,' vol. 10, p. 241 (1932).

‡ Moelwyn-Hughes, 'Acta Physicochim.,' U.R.S.S., vol. 4, p. 173 (1936).

§ Moelwyn-Hughes, 'Dissertation,' Oxford, chap. 3, p. 59 (1932).

|| Moelwyn-Hughes, 'Trans. Faraday Soc.,' vol. 25, p. 81 (1929).

¶ Moelwyn-Hughes, 'Chem. Rev.,' vol. 10, p. 241 (1932).

\*\* I am indebted to one of the referees for drawing my attention to an inconsistency which appeared in my previous paper ('Proc. Roy. Soc.,' A, vol. 155, p. 308 (1936)), but which I have averted in the present work. We have defined the empirical constant,  $E_A$ , by equation (1) which gives us  $d \ln k/dT = (E_A + \frac{1}{2}RT)/RT^2$ , and we have referred to  $E_A$  as the Arrhenius energy of activation. The empirical constant A used by Arrhenius is defined by the relation  $d \ln k/dT = A/RT^2$ , hence  $E_A = A - \frac{1}{2}RT$ . Throughout this paper we have consistently adhered to this convention. In our preceding paper, however, the terms  $E_A$  and A were used indiscriminately. Consequently, the term  $\frac{1}{2}RT$  should be deleted from equation (14), and the term  $e^{\frac{1}{2}}$  from equations (15) and (15A) of our previous paper. Numerically the correction is small.

†† Moelwyn-Hughes, 'Proc. Roy. Soc.,' A, vol. 155, p. 308 (1936).

$E$ , which is assumed to be constant, and  $E_r$ , which represents the mutual potential energy of the ion and the dipole, and is a function of the medium and of the temperature. Substituting into (3), we may express the rate of reaction as

$$k = Z \cdot e^{-E/RT} \cdot e^{-E_r/RT}. \quad (4)$$

By a method analogous to that employed by Debye and Hückel,\* we arrive at the following approximate expression for the average potential

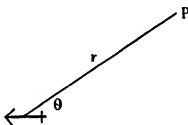


FIG. 1.

at a distance  $r$  and at an inclination  $\theta$  (fig. 1) from a dipole of moment  $\mu_A$  in a medium of fixed dielectric constant  $D$ :

$$\phi_A = \frac{\mu_A \cos \theta}{Dr^3} \cdot e^{-\epsilon r}. \quad (5)$$

Hence the mean electrostatic energy of interaction of the dipole with a charge  $z_B \epsilon$  is

$$E_r = \frac{z_B \epsilon \mu_A \cos \theta}{Dr^3} \cdot e^{-\epsilon r}. \quad (6)$$

Substituting into equation (4), the velocity coefficient becomes

$$k = Z \cdot e^{-E/RT} \cdot e^{-\frac{z_B \epsilon \mu_A \cos \theta}{Dr^3 k T} e^{-\epsilon r}}. \quad (7)$$

It then follows that

$$E_A = E - \frac{N_0 z_B \epsilon \mu_A \cos \theta}{Dr^3} (LT - 1) (1 - \frac{1}{2} \epsilon r) e^{-\epsilon r}, \quad (8)$$

and

$$P = \exp \left\{ - \frac{L z_B \epsilon \mu_A \cos \theta}{Dr^3 k} (1 - \frac{1}{2} \epsilon r) e^{-\epsilon r} - \frac{\kappa z_B \epsilon \mu_A \cos \theta}{2 Dr k T} e^{-\epsilon r} \right\}. \quad (9)$$

Derived expressions relating to infinite dilutions are:

$$\left( \frac{dE_A}{dT} \right)_{k=0} = - \frac{LN_0 z_B \epsilon \mu_A \cos \theta}{Dr^3} \quad (10)$$

\* *Phys. Z.*, vol. 24, p. 185 (1923).

and

$$P_{x=0} = e^{-\frac{z_B \epsilon^2 \mu_A \cos \theta}{DkT}}. \quad (11)$$

Abegg's constant, L, has the significance attached to it in our previous paper. The limiting law for the effect of ionic concentration at constant temperature becomes

$$\ln k_T = a_T + b_T \sqrt{j}, \quad (12)$$

where  $j$ , the ionic strength, may be identified with the concentration of electrolyte in the examples discussed here; and

$$b_T = \frac{z_B \epsilon^2 \mu_A \cos \theta}{r (DkT)^{3/2}} \cdot \left( \frac{8\pi N_A}{1000} \right)^{\frac{1}{2}}. \quad (13)$$

Spong\* has proposed the following expression for the average potential:

$$\phi_A = \frac{\mu_A \cos \theta}{Dr^2} (1 + \kappa r) e^{-\kappa r}, \quad (14)$$

which differs from equation (5). It can be shown, however, that the adoption of Spong's equation yields equations (10) and (11), but gives an exponential salt effect† instead of the square-root law. The limiting conditions become:

$$\ln k_T = a_T + g_T j \quad (15)$$

and

$$g_T = \frac{8\pi N_A z_B \epsilon^2 \mu_A \cos \theta}{1000 (DkT)^{\frac{3}{2}}}. \quad (16)$$

#### NUMERICAL APPLICATIONS TO REACTIONS IN HYDROXYLIC SOLVENTS

Let us consider a hypothetical reaction between a polar molecule, of moment 1.5 Debye units, and a univalent ion ( $z_B = \pm 1$ ) in ethyl alcohol ( $L = 6.02 \times 10^{-3}$ ) at 50° C. ( $D = 21.4$ ). Taking  $r$  to be 3 Å., and allowing for all possible angles of approach ( $\theta = 0$  to  $2\pi$ )  $P$  should, according to equation (11), lie within the limits 0.20 and 5.51. These limits include most of the  $P$  values out of the 100 cases cited above.‡

Under the same conditions,  $\left(\frac{dE_A}{dT}\right)_{x=0}$  should, according to equation (10), lie within the limits of +2.65 and -2.65 calories per gram-molecule per degree. These values are too low to be detected by ordinary methods of analysis, and are consistent with the constancy of  $E_A$  calcu-

\* J. Chem. Soc., p. 1283 (1934).

† Moelwyn-Hughes, "Acta Physico-chim." U.R.S.S., vol. 4, p. 173 (1936).

‡ See also "The Kinetics of Reactions in Solution," p. 79, Oxford (1933).

lated from the original results of Hecht, Conrad, and Brückner,\* and from the careful repetition of Gibson, Fawcett, and Perrin.†

In order to determine the direction of approach of the ion to the dipole, we shall use the very accurate measurements of Hecht, Conrad, and Brückner‡ on the velocity of the reaction between the ethylate ion and methyl iodide. Again taking  $r = 3$  A., the collision frequency by equation (2) becomes  $7.09 \times 10^{10}$  litres per gram-molecule per second. At infinite dilutions, the experimental results may be expressed as  $k = 4.84 \times 10^{11} \times e^{-19.400/RT}$  or  $k = 1.72 \times 10^{10} \times \sqrt{T} \times e^{-19.800/RT}$ , whence  $P_{k=0} = 4.15$ . Inserting this value in equation (11), we find  $r^2 \sec. 0 = 1.55 \times 10^{-16}$  cm<sup>2</sup>, indicating a virtually head-on collision. Even without a knowledge of  $r$ , it can be shown that a negative ion approaches the positive end of the dipole, in agreement with the supposition of Ogg and Polanyi ||

Equation (11) expresses in a satisfactory manner the relatively greater values of  $P$  which have been found for reactions between halides and anions of valency higher than one.¶ There is, therefore, no necessity to postulate a complicated activation process involving internal degrees of freedom for these reactions.

According to equation (12),  $\ln k$  at any given temperature should vary as the square-root of the ionic concentration. The influence of the concentration on the velocity of reactions between ions and dipoles has been inadequately studied. Nevertheless, an examination of the literature shows that there are marked tendencies to conformity with this law as a limiting condition. Fig. 2 shows Hardwick's data\*\* on the effect of ionic concentration for the reaction between ethyl iodide and m-4-xylyl oxide in ethyl alcoholic solution at 45.4° C. A comparison of the limiting slope with the theoretical expression (13) leads to the value 4.13 A. for  $r \sec. 0$ . Values for other reactions in the same solvent are given in Table I. The dipole moments have been taken from a list compiled by Sidgwick†† and the dielectric constant from the table in our previous paper.‡‡

\* 'Z. phys. Chem.', vol. 4, p. 273 (1889).

† 'Proc. Roy. Soc.,' A, vol. 150, p. 223 (1935).

‡ 'Z. phys. Chem.', vol. 5, p. 289 (1890).

§ Moelwyn-Hughes, "The Kinetics of Reactions in Solution," Oxford (1933), pp. 84 and 100.

|| 'Trans. Faraday Soc.,' vol. 31, p. 511 (1935).

¶ Moelwyn-Hughes, 'J. Chem. Soc.,' p. 1576 (1933).

\*\* 'J. Chem. Soc.,' p. 141 (1935).

†† 'Trans. Faraday Soc.,' vol. 30, p. 801 (1934).

‡‡ 'Proc. Roy. Soc.,' A, vol. 155, p. 308 (1936).

The last two results are of particular interest. Steger's results show that there is no appreciable salt effect, in spite of the powerful dipole possessed by ortho-dinitrobenzene. The data are consistent with the idea that the ion may approach in a force-free plane, as would occur if it traversed the prolongation of the line joining the 3:6 carbon atoms in the plane of the benzene ring. In view of the large value of  $P$  which holds for the corresponding reaction of the para compound, it is unfortunate that the dilution effect has not yet been studied. The data of Burke and

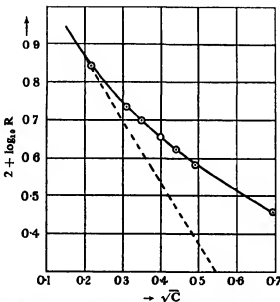


FIG. 2.—The influence of concentration on the velocity of reaction between anion and a dipole.

Donnan, in spite of some uncertainty in the exact value of the slope,\* indicate quite clearly that the attacking ion approaches the polar molecule against a repulsive field.

As mentioned above, the form of the dilution law given by equation (16) is not in such good harmony with experiment as that given by equation (12). There are instances, however, particularly in aqueous solution when  $z_B = +1$ , where  $\ln k$  varies linearly with the ionic strength. They have been noted by Grube and Schmid† who proposed the empirical relation

$$k = k_0 e^{ax}, \quad (17)$$

\* The value given here is obtained by linear extrapolation, omitting one point. If this is included, the evaluation of the tangent becomes precarious, leading to a value of  $r \sec \theta$  of about 0.6 Å.

† 'Z. phys. Chem.', vol. 119, p. 19 (1926).

TABLE I—ILLUSTRATING THE EVALUATION OF THE CRITICAL NUCLEAR SEPARATION AND THE ANGLE OF APPROACH,  
FROM DATA ON THE DILUTION EFFECT

Ref.	Reacting dipole	Moment (Dobies)	Reacting Ion	Valency	$\theta^{\circ}$ C.	Slope $\log_{10} \theta$	$r \sec \theta$
1	Ethyl iodide	1.65	m-4-xylyl oxide	-1	45.4	-0.84	4.13
2	Ethyl bromide	1.81	Hydroxide	-1	59.8	-0.87	3.66
3	Methyl iodide	1.51	Ethoxide	-1	24	-0.83	4.97
4	1:2 Dinitrobenzene	6.00	Ethoxide	-1	45	0	0
5	Butyl iodide	1.76	Silver	+1	24.5	+1.76	2.78

1—Hardwick, 'J. Chem. Soc.,' p 141 (1935).

2—Grant and Hinselwood, 'J. Chem. Soc.,' p. 258 (1933).

3—Hecht, Conrad, and Brückner, 'Z. phys. Chem.,' vol. 3, p. 450 (1889).

4—Sieger, 'Z. phys. Chem.,' vol. 49, p. 329 (1904).

5—Burke and Donnan, 'J. Chem. Soc.,' vol. 85, p. 555 (1904).

in which G is a constant specific for the reaction. The use of Spong's equation thus allows us to interpret the exponential salt effect in a manner somewhat more direct than that used by Brönsted.\* The latter derivation, however, has the advantage of resting on Debye and MacAulay's estimate of the variation in D,† a factor which is omitted in the present work. Until more experimental material is available, it would be futile to attempt to discriminate. In the meantime, we may apply equations (15) and (16) to the hydrogen-catalysed decomposition of acetal in water, for which an exponential salt effect has been found.‡ We then find  $\mu_A \cos \theta = 7.35$  debyes. The exact value of  $\mu_A$  for acetal is not yet known.

#### THE SUPERPOSITION OF AN ION-DIPOLE FIELD ON TO AN INTERIONIC ONE

The Debye-Hückel limiting law, as applied by Brönsted and by Bjerrum to the kinetics of interionic reactions, is obeyed by a certain number of reactions of varying ionic type in aqueous solution. There are, however, discrepancies, with which we must now deal.

It is significant that one of the reactant ions in most of the instances studied is capable of undergoing chemical reaction, and, in fact, often does react with the solvent. The necessity then arises for allowing with strictly quantitative accuracy for the simultaneous side reaction. In certain cases, the correction can apparently be carried out satisfactorily. In others, it eludes measurement,§ while for some reactions it has not even been attempted. What has been considered an "interesting and important contradiction of Brönsted's theory" was discovered by La Mer and Kammer,|| who found for the reaction between the thiosulphate and  $\beta$ -bromopropionate ions a pronounced salt effect in the opposite direction to that demanded by theory. The anomaly has been accepted as real by the authors themselves and by commentators, who attribute it to "orientation" effects. Experiments on a similar reaction, however, carried out by Moelwyn-Hughes,¶ showed that the concurrent chemical reaction occurring between the organic molecule and the solvent contributed a considerable proportion of the net observed rate. Further

\* 'Chem. Rev.', vol. 26, p. 22 (1925).

† 'Phys. Z.', vol. 26, p. 22 (1925).

‡ Brönsted and Wynne-Jones, 'Trans. Faraday Soc.', vol. 25, p. 59 (1929).

§ Soper and Williams, 'Proc. Roy. Soc.,' A, vol. 140, p. 59 (1933).

|| 'J. Amer. Chem. Soc.', vol. 53, p. 2883 (1931).

¶ 'J. Chem. Soc.', p. 1576 (1933).

work on the same lines by Nielsen\* has made it appear almost certain that the major part of the alleged anomaly will disappear when a quantitative correction for the side reaction is made.

A second, and more important cause for deviations from the limiting law of Debye and Hückel is due to the fact that most of the so-called ionic reactions are, in fact, chemical reactions with ions, on the one hand, and dipoles contained in charged molecules on the other hand. The distinction between true and apparent ionic reactions, although an important one,† has received no attention. Consider, for example, the reaction



The major contribution to the electrostatic energy of the reactant system is admittedly that due to the interaction of the inorganic ion and the organic ion. Otherwise it would be difficult to understand the sign and the order of magnitude of the kinetic salt effect. Nevertheless, the chemical reaction involved proceeds in virtue of the electrostatic attraction of the dipole  $\vec{C} - \vec{Br}$  for the ion  $\text{I}^-$ , and will take place in the absence of the charge on the organic molecule. The possibility, therefore, exists that the genuine deviations from the Debye-Hückel limiting law may be due to the omission to take into account the electrostatic interaction energy exerted between the ion and the dipole with which it undergoes chemical change. As far as it is possible to judge from the existing data, a genuine deviation of some 20% may exist. This magnitude is of interest, as it coincides with the ratio  $\mu/\epsilon r$ , which roughly measures the departure to be expected if the energy of interaction of ion and dipole is to be added to the interionic energy.

Let us, therefore, estimate the average potential at a point P (fig. 3), which is situated at a distance  $r_1$  from the centre of the dipole  $\mu_A$ , and at a distance  $r_2$  from a charge  $z_A e$  in the same molecule assuming that the two terms may be treated as independent. The average value of the total electrostatic energy is clearly

$$E_e = \frac{z_B e \mu_A \cos \theta}{Dr_1^2} e^{-\alpha r_1} + \frac{z_B z_A e^2}{Dr_2^2} e^{-\alpha r_2}. \quad (18)$$

The conditions for minimum energy are too difficult for us to obtain analytically, but the problem can be solved numerically in any given case. Let us take, for illustrative purposes,  $\alpha = 1.20 \text{ Å.}$ ,  $\beta = 1.35 \text{ Å.}$

\* J. Amer. Chem. Soc., vol. 58, p. 206 (1936).

† Moelwyn-Hughes, "The Kinetics of Reactions in Solution," p. 172.

$z_B = -2$ ,  $z_A = -1$ ,  $\mu_A = 1.81$  debyes,  $\kappa = 8.21 \times 10^6$  cm.<sup>-1</sup>. These figures correspond to the interaction of a divalent anion, in aqueous solution of ionic strength  $\sqrt{j} = 0.25$  at 25° C., with a β-brom-substituted carboxylic anion. The magnitudes  $\alpha$  and  $\beta$ , and the justification for treating the problem as two-dimensional, result from the construction of the solid model. The path of minimum electrostatic potential energy is shown in fig. 4, where the field due to the dipole is also illustrated. In the absence of this field the ion B would transcribe a circle of radius  $1/\kappa$  about the origin. At closer approaches, however, its course is deter-

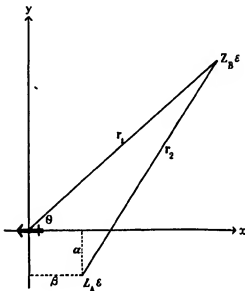


FIG. 3.

mined by the electrostatic attraction of the dipole. On physical grounds, therefore, a consistent extension of the simple treatment of interionic reactions should include a term to take account of this effect. The same remark applies to the treatment of solubility, heats of dilution, thermodynamic activity coefficients, and other non-kinetic properties derivable from the electrostatic contribution to the free energy of the solution.\*

\* A totally different attitude is adopted by many other workers, e.g., La Mer ('Annual Survey of American Chemistry,' p. 13 (1930)) who claims that his "purely mathematical extension (of the Debye-Hückel theory) gives a qualitatively correct interpretation for non-aqueous solutions, and a quantitatively correct one for symmetrical sulphates in water . . . without requiring new assumptions of a physical character".

## REACTIONS BETWEEN IONS AND MULTipoles

A quantitative kinetic treatment of the reaction between an ion and a neutral molecule possessing more than one dipole becomes complicated. A relatively simple comparative treatment becomes possible, however, if only one of the dipoles undergoes cleavage, the other remaining intact and exerting a modifying influence on the velocity of reaction. Such systems are well exemplified by the acid-catalysed prototropy of a series of para-substituted acetophenones. Denoting by  $(E_A)_s$  and  $(E_A)_u$ , the respective values of the Arrhenius energy of activation for the reaction of

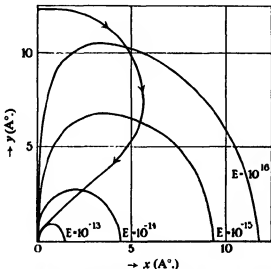


FIG. 4.—The approach of an ion to a charged dipole.

the substituted and unsubstituted ketone, Nathan and Watson\* found the following expression to hold:—

$$(E_A)_s - (E_A)_u = -C(\mu_s - 0.032 \mu_e^2), \quad (19)$$

in which  $\mu_s$  stands for the permanent dipole of  $C_6H_5X$ , and C is an empirical constant, shown to be to some extent a function of the concentration of catalyst. It is interesting to note that the effect of substitution on  $\Delta E_A$  should, according to this relation, be a maximum when  $\mu_s = 15.6$  Debye units, that is, when the para-substituent ionizes. The emergence of ionization from loose co-valent bonds has been discussed from various angles by Kendall† and by Moelwyn-Hughes and Sherman.‡

\* J. Chem. Soc., p. 890 (1933).

† J. Amer. Chem. Soc., vol. 39, p. 2303 (1917).

‡ J. Chem. Soc., p. 101 (1936).

The interpretation of what is now known as the Nathan and Watson rule was given by Waters,\* who had, in fact, anticipated it to some extent.† The theory of Waters, while being qualitatively satisfactory, is confined to the energetics of reaction. It is capable of being extended and made more general by incorporation into the scheme adopted here.

In the whole series of chemical changes studied by Nathan and Watson, the reacting dipole remains the same. Its contribution to the total electrostatic energy may therefore be included in the term E of equation (8). For different members of the same family of reactions, the latter equation gives us

$$(E_A)_s - (E_A)_u = - \frac{N_0 z_B \epsilon \mu_s \cos \theta}{Dr^2} (LT - 1) (1 - \frac{1}{2} \kappa r) e^{-\alpha r}. \quad (20)$$

The experimental data are not sufficiently complete to allow us to give this relation a fair test. That it is satisfactory as regards order of magnitude may be readily shown by ignoring the effect (which is known to be small) of induced polarity. We then find, from the experimental value of C, that  $r^2 \sec \theta = 1.7 \times 10^{-16}$  cm.<sup>2</sup>. This figure is consistent with the approach of the ion at an angle considerably inclined to the direction of the para-substituent dipole.

#### REACTIONS BETWEEN TWO DIPOLES

The application of the theory developed here to the chemical reaction between two polar molecules in a solvent with which neither interacts is fairly straightforward, the chief difficulty being the necessity of taking the average inclination of both dipoles into account. If it were justifiable to treat their approach as linear, we should have

$$E_s = \frac{2 \mu_A \mu_B}{Dr^3}; \quad E_A = E + (LT - 1) \frac{2 N_0 \mu_A \mu_B}{Dr^3};$$

and

$$P = \exp \left\{ \frac{2 \mu_A \mu_B L}{Dr^3 k} \right\}.$$

No experimental system has yet been examined which conforms to the postulate of this simple treatment. Reactions between halides and amines appear to proceed by an indirect route, the first step being chemical union of one of them with the solvent, and the second step involving reaction with the other reactant and the complex. The mechanism is thus more complicated, but there is qualitative agreement with the present theory.‡

\* *Ibid.*, p. 1551 (1933).

† *Idem.*, 'Phil. Mag.', vol. 8, p. 436 (1929).

‡ Moelwyn-Hughes and Sherman, 'J. Chem. Soc.', p. 101 (1936).

## OTHER REACTIONS BETWEEN IONS AND MOLECULES

Considered as a reaction between an ion and a multipole, the hydrogen-ion catalysed inversion of sucrose becomes too complex for treatment. As indicated in the opening section of this paper and elsewhere,\* the factor P for reactions of this type has an order of magnitude too great to be explained on the simple considerations advanced here. Among the missing factors which seem worthy of elaboration is the postulated temperature variation of  $r,\dagger$  which would aid in attaching some clear picture to the "entropy of activation".‡ Recent experiments on this reaction have revealed a genuine fall of  $E_A$  with rise in temperature, so that the entropy term may soon be evaluated.§ The ideas discussed in the present work, however, while being admittedly incomplete, appear to take us one stage further in the solution of some of the outstanding difficulties in this field.||

It is my privilege to thank Professor E. K. Rideal, F.R.S., for suggesting the present problem and for his consistent help in attacking it. The present treatment is, in fact, merely a consecutive account of ideas which occurred to us jointly during many discussions on the theme.

## SUMMARY

According to a theory of the kinetics of chemical reactions between ions and polar molecules advanced by us in 1932, the term P in the expression  $k = PZe^{-E_A/RT}$  has the order of magnitude unity. In the present paper we have refined the earlier work by introducing an approximate expression for the average electrostatic energy of interaction between the ion and the reacting dipole. We are thus able to understand how far, and under what conditions, P can deviate from unity. Theoretical predictions of the influence of electrolytes on  $k$ , of the temperature on  $E_A$ , and of the charge on the ion and the sign of the dipole on P are consistent with known facts. The treatment incorporates the rule of Nathan and Watson (1933), and suggests the desirability of allowing for the ion-dipole interaction in the theory of so-called interionic phenomena in solution. The limitations of the theory are admitted and outlined

\* Cf. Moelwyn-Hughes, 'Trans. Faraday Soc.', vol. 32, p. 75 (1936).

† Miller, 'Proc. Roy. Soc.,' A, vol. 151, p. 181 (1935).

‡ Cf. Soper, 'J. Chem. Soc.,' p. 1393 (1935).

§ Moelwyn-Hughes, 'Z. phys. Chem.,' B, vol. 26, p. 272 (1934).

|| Cf. Moelwyn-Hughes, 'Ann. Rep. Chem. Soc.,' vol. 32, p. 89 (1936).

## The Relativistic Interaction of Two Electrons in the Self-Consistent Field Method

By BERTHA SWIRLES, Ph.D., University of Manchester

(Communicated by D. R. Hartree, F.R.S.—Received 25 June, 1936)

### I—THE INTERACTION OF TWO ELECTRONS, TAKING INTO ACCOUNT THE SPIN INTERACTION AND RETARDATION

The extension of the self-consistent field method for the relativistic case has been discussed in a previous paper.<sup>†</sup> There no attempt was made to consider the interaction energy of two electrons to a greater degree of accuracy than that given by the Coulomb energy. In the present paper the interaction of the spins and the effect of retardation is introduced. The method is then applied to the evaluation of the separations of the components of the  $2^3P$  term of helium.

The relativistic expression for the interaction of two electrons has been discussed by several authors.<sup>‡</sup> The expressions they obtain may be shown to agree as far as terms of the first order in  $e^4$  and the square of the fine structure constant. We shall follow the discussion of Bethe and Fermi since this seems to be most suited for application to the self-consistent field method. We require the matrix elements of the interaction energy  $\mathcal{J}$  of two electrons 1 and 2, corresponding to given transitions of the two electrons. We denote the states of electron 1 by  $N_1, N'_1, N''_1, \dots$ , and those of electron 2 by  $N_2, N'_2, N''_2, \dots$ , where each  $N$  stands for the set of four quantum numbers specifying a state of the electron. Then the matrix element  $(N_1, N_2 | \mathcal{J} | N'_1, N'_2)$  corresponding to a transition  $N_1 \rightarrow N'_1$  for electron 1 and  $N_2 \rightarrow N'_2$  for electron 2 is found as follows. We form the charge and current density corresponding to a transition  $N_1 \rightarrow N'_1$  of electron 1. In Hartree atomic units these are

$$(N_1 | \rho | N'_1) = \psi^*(N'_1 | 1) \psi(N_1 | 1) e^{i(E'_1 - E_1)t}, \quad (1)$$

<sup>†</sup> Swirles, 'Proc. Roy. Soc.,' A, vol. 152, p. 625 (1935). Referred to as I.

<sup>‡</sup> Breit, 'Phys. Rev.,' vol. 34, p. 553 (1929); vol. 39, p. 616 (1932); Möller, 'Z. Physik,' vol. 70, p. 786 (1931). Bethe and Fermi, 'Z. Physik,' vol. 77, p. 296 (1932). For a summary, see Bethe, 'Handbuch der Physik,' vol. 24. The problem of the second order interaction energy, which gives a term of the first order in the square of the fine-structure constant, but which has been shown by Breit to lead to wrong results, is not discussed here.

and

$$\langle N_1 | j | N \rangle = \psi^*(N'_1 | 1) \alpha(1) \psi(N_1 | 1) e^{i(E'_1 - E_1)t}. \quad (2)$$

$E_1$  is the energy and  $\psi(N_1 | 1)$  the wave function in the state  $N_1$  and  $E'_1$  and  $\psi(N'_1 | 1)$  the corresponding quantities in the state  $N'_1$ .  $\alpha$  is the Dirac vector matrix with components  $\alpha_1, \alpha_2, \alpha_3, \dagger$ . The scalar potential  $(N_1 | \phi | N'_1)$  and vector potential  $(N_1 | A | N'_1)$ , due to this distribution of charge and current at the position  $r_2$  occupied by electron 2 are, putting  $|r_2 - r_1|$  the distance between the electrons equal to  $r$ ,

$$\langle N_1 | \phi | N'_1 \rangle = -e^{i(E'_1 - E_1)t} \int \frac{\psi^*(N'_1 | 1) \psi(N_1 | 1) e^{-i(E'_1 - E_1)r/c}}{r} d\tau_1 \quad (3)$$

$$\langle N_1 | A | N'_1 \rangle = e^{i(E'_1 - E_1)t} \int \frac{\psi^*(N'_1 | 1) \alpha(1) \psi(N_1 | 1) e^{-i(E'_1 - E_1)r/c}}{r} d\tau_1, \quad (4),$$

where the integration is taken over all the  $r_1$  space.‡

The Hamiltonian for the second electron in this field is

$$-[(N_1 | \phi | N'_1) + \alpha(2) \cdot (N_1 | A | N'_1)], \quad (5)$$

and the matrix element corresponding to the transition  $N_2 \rightarrow N'_2$  for the second electron is

$$e^{i(E'_2 - E_2 + h' - E_1)t}$$

$$\times \int \int \frac{\psi^*(N'_1 | 1) \psi^*(N'_2 | 2) (1 - \alpha(1) \cdot \alpha(2)) \psi(N_1 | 1) \psi(N_2 | 2) e^{-i(E'_1 - E_1)r_1/c}}{r_1} d\tau_1 d\tau_2. \quad (6)$$

We interpret this as  $\langle N_1, N_2 | J | N'_1, N'_2 \rangle$ . This expression (6) is unsymmetrical; the discussion as given here was originally applied by Bethe and Fermi to two *free* electrons. In that case the result can be brought into a symmetrical form. The problem of the interaction of two *bound* electrons has been discussed by Hulme,§ who has shown that if we use retarded potentials for two electrons, one in the ground state and one in an excited state, the particle in the excited state must be supposed to jump down first, i.e., it is the particle 1 in the treatment given above; the same result is obtained using advanced potentials supposing the particle in the ground state to jump up first.

In calculating the energy of an atom with many electrons, we construct the wave function as a determinant of one electron wave functions as in I.

† Cf. I, p. 627.

‡ In atomic units,  $c = 137$ .

§ Hulme, 'Proc. Roy. Soc.,' A, vol. 154, p. 487 (1936).

Then the only types of matrix element of the interaction energy which occur are  $\langle N_1, N_2 | \mathcal{J} | N_1, N_2 \rangle$ , the direct integral, and  $\langle N_1, N_2 | \mathcal{J} | N_2, N_1 \rangle$ , the exchange integral. The direct integral, given by

$$\langle N_1, N_2 | \mathcal{J} | N_1, N_2 \rangle$$

$$= \iint \frac{\psi^*(N_1|1) \psi^*(N_2|2) [1 - \alpha(1)\alpha(2)] \psi(N_1|1) \psi(N_1|2)}{r} d\tau_1 d\tau_2, \quad (7)$$

involves the spins but not retardation; this is what we should expect in this method of approximation. The exchange integral, on the other hand, involves both spin interaction and retardation. It is given by

$$\langle N_1, N_2 | \mathcal{J} | N_2, N_1 \rangle$$

$$= \iint \frac{\psi^*(N_2|1) \psi^*(N_1|2) [1 - \alpha(1)\alpha(2)] \psi(N_1|1) \psi(N_2|2) e^{i(h_1 - h_2)r/r}}{r}. \quad (8)$$

Here the suffix 1 refers to the state of higher energy.

The expression (6) for the general matrix element of the interaction energy may be expanded in powers of  $1/c$ , and it has been shown by Bethe and Fermi, that as far as terms in  $1/c^2$ , this leads to Breit's expression for the interaction energy. It has further been shown by Breit† that in this expression the Coulomb term may be considered as exact and not merely correct to the order  $1/c^2$ .

We shall find it more convenient to use a different method of expansion. Terms of the type (7) can be immediately evaluated by expanding  $1/r$  in a series of products of powers of  $r_1$  and  $r_2$  with surface harmonics as in equation (I, 34), and they give altogether for an atom with many electrons

$$\sum_{n, l, j, u; n', l', j', u'} [J(n, l, j, u; n', l', j', u') + J_{\text{spin}}(n, l, j, u; n', l', j', u')], \quad (9)$$

where  $J$  is the direct integral for the Coulomb interaction and  $J_{\text{spin}}$  that for the spin interaction. These can both be expressed as the sum of integrals over  $r_1$  and  $r_2$ . For  $J$  the coefficients of these integrals are the  $a$ 's evaluated in I.

The integral (8) can be expanded similarly,‡ for putting  $E_1 - E_2 = \kappa c$ , we have

$$\frac{e^{i\kappa r}}{r} = \sum_{k=0}^{\infty} \sum_{m=-k}^k (2k+1) \frac{(k-|m|)!}{(k+|m|)!} \frac{\zeta_{k(\sigma_1)} \eta_{k(\sigma_2)}}{r} P_k^{|m|}(\mu_1) P_k^{|m|}(\mu_2) e^{im(\phi_1 - \phi_2)} \quad (10)$$

† Breit, 'Phys. Rev.', vol. 39, p. 616 (1932).

‡ Lamb, 'Hydrodynamics,' 6th Ed., p. 503. Cf. Massey and Burhop, 'Proc. Roy. Soc.,' vol. 153, p. 661 (1936).

where  $r_a$  is the smaller and  $r_b$  the greater of  $r_1$  and  $r_2$ ,

$$\eta_k(x) = (\frac{1}{2}\pi x)^k J_{k+1}(x)$$

$$= \frac{x^{k+1}}{1 \cdot 3 \dots (2k+1)} \left[ 1 - \frac{x^2}{2(2k+3)} + \frac{x^4}{2 \cdot 4 \cdot (2k+3)(2k+5)} - \dots \right],$$

and

$$\zeta_k(x) = (\frac{1}{2}\pi x)^k [iJ_{k+1}(x) + (-1)^k J_{-k-1}(x)]$$

$$= \frac{ix^{k+1}}{1 \cdot 3 \dots (2k+1)} \left[ 1 - \frac{x^2}{2(2k+3)} + \frac{x^4}{2 \cdot 4 \cdot (2k+3)(2k+5)} - \dots \right] \\ + 1 \cdot 3 (2k-1) x^{-1} \left[ 1 - \frac{x^2}{2(1-2k)} + \frac{x^4}{2 \cdot 4 (1-2k)(3-2k)} - \dots \right].$$

(10) reduces to equation (I, 34) for  $\kappa = 0$ . As far as the dependence on the surface harmonics goes, the two expressions are the same, and (10) can be expressed as a sum of integrals over  $r_1$  and  $r_2$ . For the Coulomb term the coefficients of these integrals are the  $b$ 's evaluated in I.

The table of coefficients for the spin interactions, corresponding to the  $a$ 's and  $b$ 's for the Coulomb interaction, has not yet been constructed for all  $s$ -,  $p$ -,  $d$ -electrons. They have been calculated for the particular cases required in investigating the helium triplets. The construction of the complete table is quite straightforward but would be laborious.

## 2—THE SPIN SEPARATIONS OF THE $2^3P$ TERM OF HELIUM

The approximate wave functions for a helium atom with one ( $1s$ ) and one ( $2p$ ) electron may be written

$$\Psi = \frac{1}{\sqrt{2}} \begin{vmatrix} \psi(1s|1), \psi(2p|1) \\ \psi(1s|2), \psi(2p|2) \end{vmatrix},$$

where the  $\psi$ 's are Dirac  $\psi$ 's each with four components. When the interactions are neglected there are twelve ways of forming  $\Psi$ , since there are two possible wave functions for the ( $1s$ ) and six for the ( $2p$ ) state, and these all give the same value for the energy, neglecting terms of the order  $1/c^4$ . The correct zero order approximations to the wave functions for the  $1^1P$  and  $3^3P$  states are four independent linear combinations of these. In the non-relativistic case Slater† has shown how it is possible to find the triplet-singlet separation without first finding the correct linear combinations of the zero order wave functions. This method can be carried over

† Slater, 'Phys. Rev.', vol. 34, p. 1293 (1929), in particular, p. 1315.

to the relativistic case and extended to the determination of the triplet separations. We now show how this may be done.

We first construct a table of the wave functions  $\Psi$ , classifying them according to  $m + m'$ ; the two one-electron wave functions are specified by  $(j, u)$ ,  $(j, u')$  and  $m = u + \frac{1}{2}$ ,  $m' = u' + \frac{1}{2}$ . In the table we separate the  $2p$  and  $2\bar{p}$  wave functions.<sup>†</sup> When we come to evaluate the total energy to the order  $1/c^4$ , the difference between these must be taken into account.

TABLE I

$m + m'$	1s	2p	$2\bar{p}$
(1) -2	$\frac{1}{2}, -1$	$\frac{1}{2}, -2$	
(2) -1	$\frac{1}{2}, 0$	$\frac{1}{2}, -2$	
(3) -1	$\frac{1}{2}, -1$	$\frac{1}{2}, -1$	
(4) -1	$\frac{1}{2}, -1$		$\frac{1}{2}, -1$
(5) 0	$\frac{1}{2}, 0$	$\frac{1}{2}, -1$	
(6) 0	$\frac{1}{2}, 0$		$\frac{1}{2}, -1$
(7) 0	$\frac{1}{2}, -1$	$\frac{1}{2}, 0$	
(8) 0	$\frac{1}{2}, -1$		$\frac{1}{2}, 0$
(9) 1	$\frac{1}{2}, 0$	$\frac{1}{2}, 0$	
(10) 1	$\frac{1}{2}, 0$		$\frac{1}{2}, 0$
(11) 1	$\frac{1}{2}, -1$	$\frac{1}{2}, 1$	
(12) 2	$\frac{1}{2}, 0$	$\frac{1}{2}, 1$	

We now form a linear combination<sup>†</sup>  $c_u \Psi_j$  of these twelve wave functions and write down the variational equations obtained from varying the  $c_u$ 's separately, so as to make the total energy, including the interaction energy discussed in §1, a minimum, *i.e.*, if  $H$  is the total Hamiltonian for the whole atom,

$$\delta \iint c_u \Psi^* H c_u \Psi_j d\tau_1 d\tau_2 = 0, \quad (11)$$

subject to

$$\delta \iint c_u \Psi^* c_u \Psi_j d\tau_1 d\tau_2 = 0. \quad (12)$$

We obtain a determinantal equation for the total energy  $E$ , with twelve rows and columns, and elements  $-EU_{ij} + H_{ij}$  ( $i, j = 1, \dots, 12$ ) where  $U$  is the unit matrix and  $H_{ij}$  is the matrix component of the Hamiltonian between the state with wave function  $\Psi_i$  and that with wave function  $\Psi_j$ . (There are, in fact, non-vanishing matrix components of the interaction

<sup>†</sup> As in I,  $\beta$  denotes  $l = 1, j = \frac{1}{2}$ .

<sup>‡</sup> We use the convention that a respected suffix implies summation over that suffix.

energy between the states 1–12 and states belonging to other configurations of completely different energy. To take these into account would involve the consideration of "configuration interaction", which is beyond the scope of the present paper. As in Slater's non-relativistic treatment, they will be ignored for the present.) We shall now use the fact that the determinantal equation splits up into the form :

1	2	3	4	5	6	7	8	9	10	11	12
$-E + H_{11}$	1										
2		$-E + H_{22}$	$H_{23}$	$H_{24}$							
3			$H_{32}$	$-E + H_{33}$	$H_{34}$		$H_{43}$				
4				$H_{42}$	$H_{43}$	$-E + H_{44}$					
5											
6											
7											
8											
9											
10											
11											
12											

$\rightarrow 0 \quad (13)$

i.e., two one-rowed, two three-rowed, and one four-rowed determinant, corresponding to the classification in Table 1. The matrix components  $H_{\mu\nu}$  between states of different  $(m + m')$  vanish. Before proving this important result in the next section, we show how it enables us to find the

energies of the four states  ${}^1P_1$ ,  ${}^3P_0$ ,  ${}^3P_1$ ,  ${}^3P_2$ . The possible values of  $(m + m')$  for these states are :—

${}^1P_1$	-1	0	1
${}^3P_0$		0	
${}^3P_1$	-1	0	1
${}^3P_2$	-2	-1	0 1 2

We see that the equation (3) splits up into five separate equations. The roots of these are correlated to the states as follows :—

Determinant	Roots
I, V	${}^3P_2$
II, IV	${}^3P_2$ , ${}^3P_1$ , ${}^1P_1$
III	${}^3P_2$ , ${}^3P_1$ , ${}^3P_0$ , ${}^1P_1$

I gives immediately  ${}^3P_2$ . We then solve the determinantal equation II, obtaining in addition  ${}^3P_1$  and  ${}^1P_1$ . The sum of the diagonal terms in III then gives  ${}^3P_0$ . It should be noted here that the difference of the diagonal sums of II and IV gives  ${}^3P_0$  without requiring the determination of  ${}^1P_1$ . We should not therefore expect the degree of accuracy, with which given approximate wave functions give the spin separations of the triplet term  ${}^3P$ , to depend on the accuracy with which they give the triplet-singlet separation.

We now assume that we have suitable one electron wave functions for the  $1s$ ,  $2p$ , and  $2\bar{p}$  states. Let  $E_1$  be the total energy of the two electron system correct to order  $1/c^2$ , but neglecting the interaction energy, and calculated with a  $\Psi$  constructed from a  $1s$  and a  $2p$  wave function. The energy calculated with a  $\Psi$  constructed from a  $1s$  and a  $2\bar{p}$  wave function will differ from this by an amount of order  $1/c^4$ . We use the abbreviations  $F_0(sp)$  for  $F_0(1, 0; 2, 1)$  and  $G_1(sp)$  for  $G_1(1, 0; 2, 1)$  (see I).  $F_0(sp)$  ( $= F_0(1, 0; 2, -2)$ ) and  $G_1(sp)$  ( $= G_1(1, 0; 2, -2)$ ) differ from  $F_0(sp)$  and  $G_1(sp)$  by quantities of the order  $1/c^2$ . Each element of the determinant differs from some linear function of  $E$ ,  $E_1$ ,  $F_0(sp)$ ,  $G_1(sp)$ , by terms of the order  $1/c^4$ . These will be discussed in detail in § 4. For the present we write  $S_{ij}$  for the remainder of the terms of order  $1/c^4$  in each matrix component  $H_{ij}$ . Then the one-rowed determinant equation takes the form

$$-E + E_1 + F_0(sp) - \frac{1}{2}G_1(sp) + S_{11} = 0, \quad (14)$$

and the three-rowed equation given by determinant II is

$$\begin{vmatrix} -E + E_1 + F_0(sp) + S_{23}, & -\frac{1}{3^{\frac{1}{2}}} G_1(sp) + S_{23}, & \frac{2^{\frac{1}{2}}}{3^{\frac{1}{2}}} G_1(sp) + S_{34} \\ -\frac{1}{3^{\frac{1}{2}}} G_1(sp) + S_{23}, & -E + E_1 + F_0(sp) - \frac{2^{\frac{1}{2}}}{9} G_1(sp) + S_{23}, & -\frac{2^{\frac{1}{2}}}{9} G_1(sp) + S_{34} \\ \frac{2^{\frac{1}{2}}}{3^{\frac{1}{2}}} G_1(sp) + S_{24}, & -\frac{2^{\frac{1}{2}}}{9} G_1(sp) + S_{34}, & -E + E_1 + F_0(sp) - \frac{4}{9} G_1(sp) + S_{44} \end{vmatrix} = 0. \quad (15)$$

The diagonal terms  $H_{ii}$  in the determinant III are :—

$$\begin{aligned} H_{55} &= H_{77} = E_1 + F_0(sp) - \frac{4}{9} G_1(sp) + S_{55} \\ H_{66} &= H_{88} = E_1 + F_0(sp) - \frac{2}{9} G_1(sp) + S_{66}. \end{aligned}$$

The coefficients of  $F_0(sp)$  and  $G_1(sp)$  in the diagonal terms can be obtained from the tables in I. For the non-diagonal terms they are quite easily calculated. The  $S_{ij}$  are calculated in detail in § 4. We verify that the following relations are satisfied by the terms of order  $1/c^4$ ,

$$\left. \begin{aligned} S_{22} + 3^{\frac{1}{2}} S_{23} &= S_{11} \\ S_{33} + \frac{1}{3^{\frac{1}{2}}} S_{23} &= S_{11} \\ 3^{\frac{1}{2}} S_{24} + S_{24} &= 0 \end{aligned} \right\}. \quad (16)$$

Adding the first column of determinant II to  $3^{\frac{1}{2}}$  times the second, and further abbreviating  $F_0(sp)$ ,  $G_1(sp)$ , and  $F_0$ ,  $G_1$ , equation (5) becomes

$$(-E + E_1 + F_0 - \frac{4}{9} G_1 + S_{11})$$

$$\times \begin{vmatrix} -E + E_1 + F_0 + S_{23} & 1 & \frac{2^{\frac{1}{2}}}{3^{\frac{1}{2}}} G_1 + S_{24} \\ -\frac{1}{3^{\frac{1}{2}}} G_1 + S_{23} & 3^{\frac{1}{2}} & -\frac{2^{\frac{1}{2}}}{9} G_1 + S_{34} \\ \frac{2^{\frac{1}{2}}}{3^{\frac{1}{2}}} G_1 + S_{24} & 0 & -E + E_1 + F_0 - \frac{4}{9} G_1 + S_{44} \end{vmatrix} = 0. \quad (17)$$

This gives one root the same as that of the one-rowed determinant as it should. This root gives the energy of the  ${}^3P_2$  term. Solving the equation (17) we find the root corresponding to  ${}^3P_1$ . This is immediately distinguished from the root corresponding to  ${}^1P_1$ , since, apart from terms of order  $1/c^4$ , it is the same as the root already found, giving  ${}^3P_2$ . The triplet-

singlet separation is  $\frac{1}{2}G_1$ .<sup>†</sup> Finally, the  ${}^3P_0$  term is given by the difference of the sums of the diagonal terms of the matrix of  $H$  in the determinants II and III. In this way we obtain

$$\left. \begin{aligned} {}^3P_1 &= E_1 + F_0 - \frac{1}{2}G_1 + S_{11} \\ {}^3P_1 &= E_1 + F_0 - \frac{1}{2}G_1 - \frac{1}{6}S_{11} + \frac{1}{6}S_{33} + \frac{1}{3}S_{44} + \frac{2}{3}S_{34} \\ {}^3P_0 &= E_1 + F_0 - \frac{1}{2}G_1 + 2(S_{55} + S_{66}) - (S_{11} + S_{33} + S_{44}) \end{aligned} \right\}. \quad (18)$$

We have therefore the triplet separations by subtraction :—

$$\left. \begin{aligned} {}^3P_1 - {}^3P_2 &= -\frac{1}{6}S_{11} + \frac{1}{6}S_{33} + \frac{1}{3}S_{44} + \frac{2}{3}S_{34} \\ {}^3P_0 - {}^3P_2 &= 2(S_{55} + S_{66}) - (S_{11} + S_{33} + S_{44} + S_{66}) \end{aligned} \right\}. \quad (19)$$

The calculation of these quantities is given in § 4. Before proceeding to this we prove the important result mentioned above.

### 3.-PROOF THAT THE MATRIX COMPONENTS OF THE HAMILTONIAN BETWEEN STATES OF THE SAME ZERO ORDER ENERGY VANISH EXCEPT WHEN $m + m'$ IS UNCHANGED<sup>‡</sup>

Let  $\mu(1), \mu(2)$  be the orbital angular momenta of the two electrons,  $\alpha(1), \alpha(2)$  their spin matrices, and  $\mathbf{M}(1), \mathbf{M}(2)$  their total angular momenta. We show first that  $\mathbf{M}(1) + \mathbf{M}(2)$  is a constant of the motion as it should be, *i.e.*, that it commutes with the total Hamiltonian. We shall prove this for the Hamiltonian containing the interaction energy correct to the order  $1/c^2$ . For this purpose we use Breit's expression, which, as we have pointed out in § 1, can be obtained by expansion of (6) in powers of  $1/c^2$ . The interaction energy is then

$$\mathcal{F} = \frac{1}{r} - \frac{1}{2r} \left[ \alpha(1) \cdot \alpha(2) + \frac{\alpha(1) \cdot \mathbf{r} \alpha(2) \cdot \mathbf{r}}{r^2} \right]. \quad (20)$$

Now  $\mathbf{M}(1) + \mathbf{M}(2)$  commutes with the Hamiltonian for the two electrons moving separately in the field of the nucleus.<sup>§</sup> We have, therefore, only to show that  $\mathbf{M}(1) + \mathbf{M}(2)$  commutes with the expression (20).

If  $\mathbf{p}(1), \mathbf{p}(2)$  are the momenta of the two electrons, then

$$\mu(1) = \mathbf{r}(1) \wedge \mathbf{p}(1), \quad \mu(2) = \mathbf{r}(2) \wedge \mathbf{p}(2). \quad (21)$$

<sup>†</sup> Cf. Slater, *loc. cit.*, p. 1315.

<sup>‡</sup> Cf. Slater, *loc. cit.*, "Notes," p. 1319.

<sup>§</sup> Dirac, "Quantum Mechanics," 1st. ed., p. 250.

Now,

$$\mathbf{r}(1) \wedge \mathbf{p}(1) + \mathbf{r}(2) \wedge \mathbf{p}(2) = -i(\mathbf{r}(1) \wedge \nabla_{(1)} + \mathbf{r}(2) \wedge \nabla_{(2)}), \quad (22)$$

and therefore,

$$\begin{aligned} [\mu(1) + \mu(2)] \mathcal{F} - \mathcal{F} [\mu(1) + \mu(2)] &= -i(\mathbf{r}(1) \wedge \nabla_{(1)} + \mathbf{r}(2) \wedge \nabla_{(2)}) \mathcal{F} \\ &= -\frac{i}{2r^3} \left[ (\alpha(1) \wedge \mathbf{r}) (\alpha(2) \cdot \mathbf{r}) + (\alpha(2) \wedge \mathbf{r}) (\alpha(1) \cdot \mathbf{r}) \right]. \end{aligned} \quad (23)$$

We next consider

$$[\sigma(1) + \sigma(2)] \mathcal{F} - \mathcal{F} [\sigma(1) + \sigma(2)].$$

We first prove that if  $\mathbf{X}$  is any vector which commutes with  $\alpha(1)$ ,

$$\sigma(1) \alpha(1) \cdot \mathbf{X} - \alpha(1) \cdot \mathbf{X} \sigma(1) = -2i \alpha(1) \wedge \mathbf{X}. \quad (24)$$

For, using a suffix notation for the components of the vectors,

$$\sigma_s(1) = -\frac{1}{2} i \epsilon_{stu} \alpha_t(1) \alpha_u(1), \quad (25)$$

and

$$\alpha_t(1) \alpha_u(1) + \alpha_u(1) \alpha_t(1) = 2\delta_{ut} 1, \quad (26)$$

where  $\epsilon_{stu}$  is the alternating tensor,  $\delta_{ut} = 0$  ( $u \neq t$ ),  $\delta_{tt} = 1$  ( $u = t$ ) and  $1$  is the unit matrix with four rows and columns. We use the summation convention for repeated suffixes.

Then the  $s$ -component of the left-hand side of (24) is

$$\begin{aligned} \sigma_s(1) \alpha_v(1) \mathbf{X}_v - \alpha_v(1) \mathbf{X}_v \sigma_s(1) \\ &= -\frac{1}{2} i \epsilon_{stu} \alpha_t(1) \alpha_u(1) \mathbf{X}_v + \frac{1}{2} i \alpha_v(1) \mathbf{X}_v \epsilon_{stu} \alpha_t(1) \alpha_u(1) \\ &= -\frac{1}{2} i \epsilon_{stu} \{ \alpha_t(1) [2\delta_{uv} 1 - \alpha_v(1) \alpha_u(1)] - [2\delta_{tv} 1 - \alpha_t(1) \alpha_v(1)] \alpha_u(1) \} \mathbf{X}_v \\ &= -i (\epsilon_{stu} \alpha_t(1) - \epsilon_{stu} \alpha_u(1)) \mathbf{X}_v \\ &= -2i (\alpha(1) \wedge \mathbf{X})_s, \end{aligned} \quad (27)$$

and the result (24) follows at once.

It follows therefore that

$$\sigma(1) \mathcal{F} - \mathcal{F} \sigma(1) = \frac{i}{r} \left[ \alpha(1) \wedge \alpha(2) + \frac{(\alpha(2) \cdot \mathbf{r}) (\alpha(1) \wedge \mathbf{r})}{r^2} \right], \quad (28)$$

and similarly

$$\sigma(2) \mathcal{F} - \mathcal{F} \sigma(2) = \frac{i}{r} \left[ \alpha(2) \wedge \alpha(1) + \frac{(\alpha(1) \cdot \mathbf{r}) (\alpha(2) \wedge \mathbf{r})}{r^2} \right]. \quad (29)$$

Therefore,

$$[\sigma(1) + \alpha(2)] \mathcal{J} - \mathcal{J} [\sigma(1) + \alpha(2)] = \frac{i}{\hbar} [(\alpha(1) \wedge \mathbf{r}) (\alpha(2) \cdot \mathbf{r}) + (\alpha(2) \wedge \mathbf{r}) (\alpha(1) \cdot \mathbf{r})]. \quad (30)$$

Now,

$$\mathbf{M}(1) = \mu(1) + \frac{1}{2}\sigma(1) \quad \text{and} \quad \mathbf{M}(2) = \mu(2) + \frac{1}{2}\sigma(2).$$

It follows from (23) and (30) that  $\mathbf{M}(1) + \mathbf{M}(2)$  commutes with the interaction energy  $\mathcal{J}$  and hence with the total Hamiltonian as far as terms in  $1/c^4$ .

We next show that the  $z$ -component  $M_z(1) + M_z(2)$  of the total angular momentum has a diagonal matrix referred to our approximate wave functions formed as anti-symmetrical products of one electron wave functions; these are of the form of central field wave functions and may be taken to be of the form given by Darwin.<sup>†</sup> For a single electron wave function it may be seen that the matrix component of

$$M_z(1) (= -i \frac{\partial}{\partial \phi_1} + \frac{1}{2}\sigma_z(1))$$

vanishes on account of the properties of the spherical harmonics, except between states of the same  $(l, j, u)$ ; between states of the same  $(l, j, u)$  but different  $n$ , the matrix component of  $M_z(1)$  is simply  $m$  ( $= u + \frac{1}{2}$ ) times that of unity and therefore vanishes on account of the orthogonalizing condition. Since  $M_z(2)$  does not affect the wave function of electron 1, and *vice versa*, it follows that  $M_z(1) + M_z(2)$  is a diagonal matrix referred to the products of one electron central field relativistic wave functions.

The commutation relation of  $M_z$  ( $= M_z(1) + M_z(2)$ ) and  $H$ , the total Hamiltonian, can be written in matrix form, using  $N, N', N'', \dots$  to stand for the complete set of quantum numbers of both electrons,

$$\sum_N [(N | M_z | N') (N' | H | N'') - (N | H | N') (N' | M_z | N'')] = 0. \quad (31)$$

Since  $M_z$  is a diagonal matrix, *i.e.*,

$$(N | M_z | N') = 0, \quad \text{unless } N = N',$$

(12) becomes

$$[(N | M_z | N) - (N'' | M_z | N'')] (N | H | N'') = 0. \quad (32)$$

Therefore, either

$$(N | H | N'') = 0, \text{ or } (N | M_z | N) = (N'' | M_z | N''),$$

<sup>†</sup> 'Proc. Roy. Soc.,' vol. 118, p. 654 (1928). Cf. also I, p. 630.

which is the result required, namely, that the matrix components of the total energy vanish except between states for which  $M_s$ , the  $z$ -component of the total angular momentum has the same value, i.e., for which  $m + m'$  is the same

#### 4—THE $2^3P$ TERM OF HELIUM. NUMERICAL CALCULATION

We now evaluate the triplet separations given by (19). In this calculation we shall use relativistic hydrogen-like wave functions, for the  $s$ -state in the field of a nuclear charge 2 and for the  $p$ - and  $\bar{p}$ -states in the field of a unit nuclear charge. There is an obvious objection to the use of these wave functions, since to the order of accuracy to which we are working they may lead to relatively large errors. The calculation is intended as a preliminary investigation and shows the lines on which any calculation using relativistic wave functions which are products of one electron central field wave functions will have to go. We denote the normalized radial wave functions† for the  $1s$ -state by  $P_0$ ,  $Q_0$ , those for  $2p$  by  $P_1$ ,  $Q_1$ , and for  $2\bar{p}$  by  $P_{-2}$ ,  $Q_{-2}$ . Table II gives the wave functions to the order to which they will be required. We require the separations (9) correct to the first order in  $1/c^4$ .

TABLE II

$$\begin{aligned} 1s \quad P_0 &= 4\sqrt{2}re^{-2r} & Q_0 &= \frac{4\sqrt{2}}{c}re^{-2r} \\ 2p \quad P_1 &= \frac{1}{2\sqrt{6}} \left( 1 + 0.3457 \cdot \frac{1}{c^4} \right) r^2 e^{-ir} - \frac{1}{8\sqrt{6}c^4} r^2 e^{-ir} \log r & Q_1 &= \frac{1}{8\sqrt{6}c} r^2 e^{-ir} \\ 2^- \quad P_{-2} &= \frac{1}{2\sqrt{6}} \left( 1 + 1.0968 \cdot \frac{1}{c^4} \right) r^2 e^{-ir} \\ &\quad + \frac{1}{2\sqrt{6}c^4} r^2 e^{-ir} \left( \frac{3}{4r} - \frac{1}{4} - \frac{r}{16} - \frac{1}{4} \log r \right), & Q_{-2} &= \frac{1}{8\sqrt{6}c} e^{-ir} (r^2 - 6r) \end{aligned}$$

The contributions to the terms in (9) are divided into two classes ; first, those arising from the differences in the total energies of the separate electrons and the Coulomb interaction when calculated with  $2p$  and  $2\bar{p}$  wave functions ; second, those arising from the spin interactions.

We consider the first class. As we have pointed out in § 2,  $E_1$ ,  $F_0$ ,  $G_1$  are quantities calculated with  $2p$  wave functions. The wave functions (4) and (6) are constructed with  $2\bar{p}$  wave functions. Therefore in  $S_{44}$ ,  $S_{34}$ , and  $S_{43}$ , there will be terms arising from the differences between  $E_1(s\bar{p})$ ,  $F_0(s\bar{p})$ ,  $G_1(s\bar{p})$ , and  $E_1$ ,  $F_0$ , and  $G_1$  respectively.

† Cf. I (29), (30).

### I—Difference Between $E_1(sp)$ and $E_1(s\bar{p})$

We are using  $2p$  and  $2\bar{p}$  wave functions for an electron in the field of unit charge.

The energy of a  $2p$  electron is

$$E(2p) = c^4 \left[ 1 + \frac{1}{4c^2 - 1} \right]^{-\frac{1}{2}}, \quad (33)$$

while that of a  $2\bar{p}$  electron is

$$E(2\bar{p}) = c^4 \left[ 1 + \frac{1}{(c + \sqrt{c^2 - 1})^2} \right]^{-\frac{1}{2}}, \quad (34)$$

and to the order  $1/c^4$

$$E(2\bar{p}) - E(2p) = -0.0312 \cdot \frac{1}{c^4}. \quad (35)$$

We have further to take into account the fact that the potential energy of the two electrons in the field of the nucleus is  $-\frac{2}{r_1} - \frac{2}{r_2}$ , whereas the total energy for a  $1s$  and a  $2p$ , or  $2\bar{p}$  electron, calculated with our wave functions, includes only a potential energy  $-\frac{2}{r_1} - \frac{1}{r_2}$ . We have therefore to add to (3) the difference,

$$-\int_0^\infty \frac{(P_{-1}^2 + Q_{-1}^2) - (P_1^2 + Q_1^2)}{r} dr = -0.1250 \cdot \frac{1}{c^4}. \quad (36)$$

Adding this to (3) we have for the difference in the separate energies of the electrons using  $2p$  and  $2\bar{p}$  wave functions,  $-0.1562 \cdot 1/c^4$ . This will appear in  $S_{44}$  and  $S_{66}$ . The contributions to the separations are given in the first line of Table IV.

### II—Difference Between $F_0(s\bar{p})$ and $F_0(sp)$

Referring to equation (I, 38), we find that,

$$\begin{aligned} F_0(s\bar{p}) - F_0(sp) &= \frac{1}{c^4} \int_0^\infty \int_0^\infty \frac{e^{-4r_1 - r_2} r_1^3}{r(b)} (3r_2^3 + r_2^3 + 1.3374 r_2^4 - \frac{1}{2} r_2^5 \\ &\quad - \frac{3}{2} r_2^4 \log r_2) dr_1 dr_2 \\ &= 0.1161 \cdot \frac{1}{c^4}. \end{aligned} \quad (37)$$

This will appear in  $S_{44}$  and  $S_{66}$ . The result is shown in the second line of Table IV.

III—Difference Between  $G_1(s\bar{p})$  and  $G_1(sp)$ 

Referring to equation (I, 44), we find that

$$\begin{aligned} G_1(s\bar{p}) - G_1(sp) &= \frac{1}{c^3} \int_0^\infty \int_0^\infty \frac{e^{-i(r_1+r_2)} r(a) r_1^3}{r(b)^3} (-2r_2^2 + 1.3374 r_2^3 \\ &\quad - \frac{1}{6} r_2^4 - \frac{1}{3} r_2^3 \log r_2) dr_1 dr_2 \\ &= -0.0072 \cdot \frac{1}{c^3}. \end{aligned} \quad (38)$$

This will appear in  $S_{44}$  and  $S_{66}$ . Further, in  $H_{34}$  the exchange integral is calculated with one  $2p$  and one  $2\bar{p}$  wave function. Denoting this by  $G_1(sps\bar{p})$ , we find that

$$\begin{aligned} G_1(sps\bar{p}) - G_1(sp) &= \frac{1}{2} [G(s\bar{p}) - G(sp)] \\ &= -0.0036 \cdot \frac{1}{c^3}. \end{aligned} \quad (39)$$

This will appear in  $S_{34}$ . The results are shown in the third line of Table IV.

It should be pointed out that the retardation, i.e., the term in  $\kappa^2$  in the expansion of  $e^{i\kappa r}/r$  in (10), does not affect the *separations*, although it affects the absolute position of the terms.

We next come to the contributions arising from the matrix elements of  $-\alpha(1) \cdot \alpha(2)/r$ . We shall refer to this as the spin interaction.

## IV—The Direct Spin Interaction

We use the following abbreviation for the integrals which occur,

$$\begin{aligned} T_k(\alpha\beta; \gamma\delta) &= \int Q_\alpha(r_1) P_\beta(r_1) Q_\gamma(r_2) P_\delta(r_2) \frac{r(a)^k}{r(b)^{k+1}} dr_1 dr_2 \\ &= T_k(\gamma\delta; \alpha\beta) \neq T_k(\beta\alpha; \delta\gamma). \end{aligned} \quad (40)$$

The first letter in the bracket denotes the  $Q$  (the small wave function) and the second letter the  $P$  (the large wave function) of the electron 1; similarly the third and fourth letters denote the  $Q$  and  $P$  respectively of the electron 2. Since the  $Q$ 's are each of order  $1/c$ , we need only the zero order terms in the  $P$ 's, and these are the same for  $p$  and  $\bar{p}$  wave functions. The *second* letter of a pair may therefore be either  $p$  or  $\bar{p}$ , to our order of approximation; for the *first* letter of a pair, however, we must distinguish between  $p$  and  $\bar{p}$  since the  $Q$ 's are different. In the direct spin interaction the integrals which occur are :—

$$T_1(ss; pp) = 0.0147 \cdot \frac{1}{c^3}.$$

$$T_1(ss; \bar{p}\bar{p}) = T_1(ss; p\bar{p}) = -0.0237 \cdot \frac{1}{c^3}.$$

The terms in the matrix elements in the three-rowed determinant can be read from Table III. The others required are :—

$$S_{11} = \frac{1}{2} T_1(ss; pp)$$

$$S_{33} = \frac{1}{2} T_1(ss; pp)$$

$$S_{44} = \frac{1}{2} T_1(ss; \bar{p}\bar{p})$$

TABLE III

	2	3	4
	$\frac{1}{2} T_1(ss; pp)$	$-\frac{32}{31 \cdot 15} T_1(ss; pp)$	$(\frac{1}{2})! \left[ T_1(ss; pp) + T_1(ss; \bar{p}\bar{p}) \right]$
2		$\frac{4}{31} T_0(sp; sp)$	$(\frac{1}{2})! \left[ T_0(sp; sp) + 3T_0(sp; \bar{p}s) \right]$
	$\frac{1}{2} \left[ \begin{array}{l} T_1(sp; sp) \\ + 2T_1(sp; ps) \\ + T_1(ps; ps) \end{array} \right]$	$-\frac{1}{31 \cdot 75} \left[ \begin{array}{l} 11T_1(sp; sp) \\ + 42T_1(sp; ps) \\ - 9T_1(ps; ps) \end{array} \right]$	$-\frac{1}{2} (\frac{1}{2})! \left[ \begin{array}{l} T_1(sp; s\bar{p}) \\ - 3T_1(s\bar{p}; ps) \end{array} \right]$
3		$\frac{1}{2} T_1(ss; pp)$	$-\frac{21}{9} \left[ \begin{array}{l} T_1(ss; pp) \\ + T_1(ss; \bar{p}\bar{p}) \end{array} \right]$
		$\frac{1}{2} T_0(sp; sp)$	$-\frac{21}{9} \left[ \begin{array}{l} T_0(sp; sp) \\ + 3T_0(sp; \bar{p}s) \end{array} \right]$
	$\frac{1}{2} \left[ \begin{array}{l} 4T_1(sp; sp) \\ + 3T_1(sp; ps) \\ + 9T_1(ps; ps) \end{array} \right]$		$\frac{21}{45} \left[ \begin{array}{l} T_1(sp; s\bar{p}) \\ - 3T_1(s\bar{p}; ps) \end{array} \right]$
4			$\frac{1}{2} T_1(ss; \bar{p}\bar{p})$
			$\frac{1}{2} \left[ \begin{array}{l} T_0(sp; s\bar{p}) \\ + 6T_0(sp; \bar{p}s) \\ + 9T_0(\bar{p}s; \bar{p}s) \end{array} \right]$
			$\frac{1}{2} T_1(s\bar{p}; s\bar{p})$

The contributions to the separations are shown in the fourth line of Table IV.

## V—The Exchange Spin Interaction

The radial integrals which occur are :—

$$T_0(sp; sp) = T_0(s\bar{p}; s\bar{p}) = T_0(sp; s\bar{p}) = 0.0180 \cdot \frac{1}{c^2}$$

$$T_0(\bar{p}s; \bar{p}s) = 0.0268 \cdot \frac{1}{c^2}$$

$$T_0(sp; \bar{p}s) = T_0(s\bar{p}; \bar{p}s) = -0.0211 \cdot \frac{1}{c^2}$$

$$T_2(sp; sp) = T_2(s\bar{p}; s\bar{p}) = T_2(sp; s\bar{p}) = 0.0082 \cdot \frac{1}{c^2}$$

$$T_2(ps; ps) = 0.0005 \cdot \frac{1}{c^2}$$

$$T_2(sp; ps) = T_2(s\bar{p}; ps) = 0.0020 \cdot \frac{1}{c^2}.$$

The terms in the matrix elements in the three-rowed determinant can be read from Table III. The others required are :—

$$S_{11} = \frac{1}{2} T_0(sp; sp) + [\frac{1}{2} T_2(sp; sp) - \frac{1}{2} T_2(sp; ps) + \frac{1}{2} T_2(ps; ps)]$$

$$S_{33} = \frac{1}{2} T_0(sp; sp) + [\frac{1}{2} T_2(sp; sp) + \frac{1}{2} T_2(sp; ps) + \frac{1}{2} T_2(ps; ps)]$$

$$S_{44} = [\frac{1}{2} T_0(s\bar{p}; s\bar{p}) + \frac{1}{2} T_0(s\bar{p}; \bar{p}s) + 2 T_0(\bar{p}s; \bar{p}s)] + \frac{1}{2} T_2(s\bar{p}; s\bar{p}).$$

The contributions to the separations are shown in the fifth line of Table IV.

TABLE IV—THE ENERGY SEPARATIONS ARE GIVEN IN TERMS OF  $1/c^2$  IN ATOMIC UNITS

	${}^3P_1 - {}^3P_2$	${}^3P_0 - {}^3P_2$
$- \frac{1}{2} S_{11} + \frac{1}{2} S_{33} + \frac{1}{2} S_{44} + \frac{2}{3} S_{22}$	$2(S_{33} + S_{44}) - (S_{11} + S_{33} + S_{44} + S_{22})$	
I	0.1041	-0.1562
II	0.0774	0.1161
III	0.0016	0.0024
IV	0.0157	0.0788
V ( $k = 0$ )	0.0093	0.0202
( $k = 2$ )	0.0018	0.0036
Total	0.0017	0.0649

The separations in  $\text{cm}^{-1}$  are given below, with the observed values† for comparison :—

	${}^3P_1 - {}^3P_2$	${}^3P_0 - {}^3P_2$
Calculated	0.020	0.759
Observed	0.077	1.068

† Cf. Houston, ' Proc. Nat. Acad. Amer.,' vol. 13, p. 91 (1927); Hansen, ' Nature,' vol. 110, p. 237 (1927).

The agreement is as good as can be expected with the wave functions used.

Previous calculations by Gaunt<sup>†</sup> and Breit<sup>‡</sup> have involved the reduction of the Dirac equation to a second order equation. This has an advantage over the present method in that the physical meaning of the different contributions to the separations—from the "spin-spin" and "spin-orbit" interactions is readily seen. Since, however, in the relativistic theory of the electron, the "spin" cannot be separated from the orbital angular momentum, these terms are somewhat artificial. Moreover, Dirac's equation in its first order form is easier to handle than the second order equation derivable from it. Once the coefficients of the integrals over the radial wave functions have been determined, the present method depends simply on the insertion of the best obtainable wave functions in these integrals. The present paper is intended as a preliminary investigation of the practicability of the relativistic self-consistent field method. The results obtained are approximately the same as those obtained by Gaunt, using a similar approximation to Schrödinger wave functions; a great deal of the work involved in his paper in the formation of the correct zero order wave functions has been avoided. Breit has obtained much better agreement with experiment, using Schrödinger wave functions, including a dependence on  $r$ , the distance between the electrons, as well as on  $r_1$  and  $r_2$ . It is probable that in the present method the agreement can be materially improved by the use of more accurate wave functions obtained by a variational method; it is hoped to repeat the calculations with such wave functions.

In conclusion, the author wishes to thank Professor D. R. Hartree, F.R.S., for his continued interest in this work, and for helpful criticism.

#### SUMMARY

The relativistic self-consistent field method is extended to take account of the interaction of the spins of the electrons and retardation. The method is applied to the evaluation of the separations of the  $2^3P$  term of helium, using a modification of Slater's method of "diagonal sums". The agreement with experiment is as good as can be expected with the wave functions used.

<sup>†</sup> 'Phil. Trans.', A, vol. 228, p. 151 (1928).

<sup>‡</sup> 'Phys. Rev.', vol. 36, p. 483 (1930).

---

Address of the President,  
Sir William Bragg, O.M., at the  
Anniversary Meeting, 30 November, 1936

The year which has passed since our last Anniversary Meeting is sadly distinguished by the heavy losses which death has brought upon our Society.

First and most conspicuous is the death of our revered Patron His Majesty, KING GEORGE V. With all his peoples we mourn the close of a life devoted to the cause of peace and progress. As members of our Society we feel deeply the loss of a Patron who was a true friend to the purposes for which our Society exists.

By the death of RICHARD TETLEY GLAZEBROOK, at the age of eighty-two years, we lose one of the most active and efficient scientific workers and organizers of his generation. Glazebrook began his scientific career under Clerk Maxwell and the late Lord Rayleigh at the Cavendish Laboratory. His first investigations were on double refraction. In the early 'eighties he became interested in the absolute determination of the electrical units, which continued to occupy him up to the very end of his life.

He was for a time Senior Bursar of Trinity and then Principal of Liverpool University, but on the establishment of the National Physical Laboratory in 1899, Glazebrook was appointed the first director, and the present prosperity and national importance of that institution are more due to him than to any other single man. It remains as an abiding monument of his life's work. His retirement in 1919 by no means marked the close of his activities. As chairman of the Aeronautical Research Committee, and of the Executive Committee of the Laboratory, he was still able to do much to promote the work to which he had devoted his best years. He was elected to the Society as early as 1882, and received the Hughes Medal in 1909 and the Royal Medal in 1931. He was created K.C.B. in 1920, and received numerous other honours. The debt which the country owes to him in the development of aeronautics is very great.

PERCY CARLYLE GILCHRIST was associated with his cousin, the late Sidney Gilchrist Thomas, in experiments which ultimately led to the establishment of the Basic Bessemer Process. Bessemer had discovered

in 1855 that a stream of air when blown through molten pig iron contained in a converter removed its carbon and silicon by oxidation, the heat evolved being sufficient to retain the metal in a molten condition. The metal thus produced was brittle owing to its oxidized condition. Within a year Mushet made the important discovery that if manganese was added to the molten metal in the form of ferro-manganese it removed the absorbed oxygen and enabled sound malleable ingots to be cast. These discoveries led to the establishment of the "acid" Bessemer process in which the lining of the converter is a siliceous refractory material. But phosphoric irons were not amenable to this treatment since with an acid lining the phosphorus remains in the finished steel and renders it brittle.

In the early 'seventies Thomas conceived the idea of lining the converter with a basic material and making additions of lime with a view to eliminating the phosphorus in the converter. After preliminary experiments he enlisted the help of his cousin, P. C. Gilchrist, who was then a chemist at Cwm Avon in South Wales. Experiments were continued at these works and Thomas and Gilchrist took out two patents. They were greatly assisted in their work by Mr. Martin of the Blaenavon Steel Works, who came to their assistance, and on 6 March, 1878, another patent was taken out. After this, progress was rapid and at the autumn meeting of the Iron and Steel Institute, held that year in Paris, they presented a paper entitled "On the Elimination of Phosphorus in the Bessemer Converter". The paper was not read at this meeting and was adjourned until the following one in 1879 when it was read by Thomas and published in the Journal of the Institute. In this way the Basic Bessemer Process was established and has proved to be one of the main processes for producing cheap steel on a large scale.

STEWART RANKEN DOUGLAS was Deputy Director of the National Institute for Medical Research and Director of the Department of Experimental Pathology and Bacteriology. He will always be remembered for his work, in association with Sir Almroth Wright, on opsonins and vaccines. The discovery of opsonins was communicated to the Society in 1903, a second communication followed early in 1904, and further work on these subjects during the following decade laid the foundations of vaccine therapy as it is practised to-day. Douglas devised several valuable nutrient culture media for pathogenic bacteria, and one of these proved invaluable during the War, for it enabled large quantities of vaccines to be made for the Army at a time when the constituents of culture media as then compounded were becoming difficult to procure. After the War, Douglas organized the new pathological laboratories at

the National Institute for Medical Research and devoted himself to the initiation of new lines of research and the encouragement of his juniors. He was largely responsible for planning and directing the scheme of study of virus diseases at the Institute which proved so fruitful. Although the publications under his name in this branch of knowledge are few, he inspired and guided much of the work published by his juniors. He was elected to the Fellowship of the Society in 1922 and to the Fellowship of the Royal College of Physicians in 1933.

JAMES HARTLEY ASHWORTH was a distinguished zoologist and acquired a wide reputation as a teacher, more particularly in that branch of the subject which is usually referred to as medical zoology.

In the early part of his career he made an important contribution to our knowledge of the Alcyonaria and afterwards turned his attention to the anatomy and systematics of the lug-worms (*Arenicolidae*). His elaborate investigation of the histology of the nervous system of these worms and the distribution of the giant-cells they possess, yielded results of great interest and importance.

Soon after his appointment to a lectureship in the University of Edinburgh, he was invited to provide a course on medical zoology for post-graduate students. As it was the first course of this kind to be given in this country, it was difficult at first to obtain a sufficient supply of specimens to illustrate his lectures; but with characteristic energy and skill he soon remedied the deficiency. In a few years the course acquired a wide reputation and attracted a large number of young medical men.

In connexion with this class, original research was encouraged and stimulated, his own great monograph on the organism *Rhinosporidium* which causes a polypus in the nose, being a contribution to our knowledge of outstanding importance.

Professor Ashworth will also be long remembered for the energy he displayed in obtaining the necessary funds for the magnificent new Zoological Laboratory in Edinburgh which now bears his name, and also for the wide knowledge and skill that he showed in expressing his wishes to the architects of that great building.

Professor IVAN PETROVITCH PAVLOV, best known of Russian men of science and greatest of Russian physiologists, died on 27 February last at the age of 86. He had been a Foreign Member since 1907, was Copley Medallist in 1915, and Croonian Lecturer in 1928. He was Nobel Laureate in 1904.

Pavlov was the son of a village priest and the grandson of a priest, and throughout his life, in spite of fame and position, he kept the simplicity of his origin, and in his teaching some of the attributes of the

priest. He preserved his vigour to the end, and in August, 1935, presided over an International Congress of Physiologists which his prestige, and the affection of physiologists for him, had brought to Leningrad. His position in Russia was unique among scientific men and unique in public estimation. The attention paid to science in the Soviet Union is due, to a significant extent, to Pavlov's character and achievements.

Pavlov's earliest researches were on the physiology of the circulation, and in that work he realized, as Starling said of him, the necessity of avoiding, if possible, disturbing factors such as anaesthetics, pain, and discomfort in experimental work on the normal functions of the body. From 1888 to 1900 came his great work on digestion, particularly on the nervous control of digestion. From 1902 onwards Pavlov and his pupils dedicated themselves to the problems of the higher nervous processes in the brain. The whole subject of "conditioned reflexes" was developed by Pavlov during that period. His demonstration that intelligent behaviour in animals is built up largely of conditioned reflexes, just as skilled movement is the integration of simpler reflexes, although its consequences may often have been exaggerated by others, will remain one of the fundamental contributions to the physiology of the brain.

Pavlov remained an inspired and inspiring teacher to the end. A few weeks before he died he wrote a "Bequest to the Academic Youth of his Country", which gives vividly the philosophy of his experimental work: "Never attempt to screen an insufficiency of knowledge even by the most audacious surmise and hypothesis. Howsoever this soap-bubble will rejoice your eyes by its play, it inevitably will burst and you will have nothing except shame". "Perfect as is the wing of a bird it never could raise the bird up without resting on air. Facts are the air of a scientist. Without them you never can fly. Without them your theories are vain efforts". "Do not allow haughtiness to take you in possession. Due to that you will be obstinate where it is necessary to agree, you will refuse useful advice and friendly help, you will lose the standard of objectiveness". "Remember that science demands from a man all his life. If you had two lives that would be not enough for you. Be passionate in your work and your searchings".

With Pavlov died one of the greatest of our Foreign Members, one of the greatest teachers and investigators in physiology, and a very good and simple man.

Professor CONWY LLOYD MORGAN, who died at the age of 84, entered the School of Mines with a view to becoming an engineer: here he came into contact with T. H. Huxley, under whose stimulating influence he acquired a deep interest in biology. After occupying a post in South

Africa, he was appointed lecturer on geology and zoology at University College, Bristol, succeeding Sir William Ramsay as Principal of the College in 1887. He had long had a deep interest in psychology and philosophy, and his sound scientific training well fitted him to take a broad synoptic view of the problems of life and mind. His researches on comparative psychology, especially on birds and dogs, were directed particularly to the segregation of innate and acquired factors in early behaviour, and are of permanent value in the development of a truly scientific psychology, founded upon a sound biological basis. In his later years he built up a philosophy of Emergent Evolution.

GEORGE THURLAND PRIOR, distinguished as a mineral chemist and a well-known authority on meteorites, was elected a Fellow of the Society in 1912. He was born at Oxford in 1862, and, after a school and university education there, he entered the Mineral Department of the British Museum in January, 1887. There he did his life's work. In 1909 he succeeded Sir Lazarus Fletcher as Keeper of Minerals, and on reaching the Civil Service age-limit he retired in December, 1927, after over forty years of service.

In addition to his work as curator of large and growing collections and to the labour involved in determinations and reports on specimens submitted to the Museum, he made many investigations on minerals, rocks, and meteorites. Many new minerals were based on his careful analytical work, often done on very small amounts of material. He excelled in the difficult analyses of minerals containing niobium, tantalum, titanium, zirconium, and the rare-earths; and problems relating to these were often referred to him by workers in other countries. One of these minerals, a titano-niobate of yttrium and cerium earths from Swaziland, which he had analyzed, was named priorite after him by W. C. Brøgger, a Foreign Member of the Society. His petrographical work included descriptions of the rocks collected by the Antarctic expeditions of Ross (1839-43), Borchgrevink (1898-1900), and Scott (1901-04), and of alkali-rocks from Abyssinia and East Africa. In his work on meteorites he described many new falls and devised simpler methods for the partial analyses of others previously known. From his results he was able to show that "the richer in nickel is the nickel-iron, the richer in ferrous iron are the magnesium silicates". This may well be called Prior's Law. On it he based a new genetic classification of meteorites. His "Catalogue of Meteorites" is the standard work of reference. Dr. Prior was for eighteen years the General Secretary of the Mineralogical Society, and its President in 1927-30.

To the physiologist the name of JOHN SCOTT HALDANE will always be

associated with that masterly investigation of the respiration which was his outstanding contribution to pure physiology, for this has played a remarkable part in moulding the change of outlook in physiological thought which has been apparent since the beginning of the present century. Deeply interested in a philosophy of life which guided, and was in turn guided by, his own experimental researches, he has made clear by his work the exquisite and quantitative coordination of the different functions of the body on which the integrity of the living organism depends, and the delicate adaptive changes which are characteristic of life. By the introduction of new experimental methods and the design of special apparatus, he has shown how it is possible to use delicate methods of chemical and physical analysis to gain an insight into the physiology of the intact and normal human being. Far-seeing and original in his ideas and courageous in maintaining his views, his work ranged over a far wider field than academic physiology, for he drew no distinction between pure and applied science but found inspiration for his work in both alike. Much of his time and thought was devoted to investigations whose object was the reduction of the risks which the miner has to run in the course of his daily occupation, and the elimination of the diseases and discomforts associated with mining or with other occupations when men have to face foul air or extremes of temperature. By the application of strict scientific methods, he has rendered negligible the dangers which were formerly associated with deep diving and work in compressed air. Great as were his contributions to physiology his investigations in the field of general industrial hygiene were no less important and fruitful.

PERCY FRY KENDALL was born in London in 1856. He began his geological studies at evening classes, and in the early 'eighties took the full course at the Royal College of Science, South Kensington. He then went to Manchester as a Berkeley Fellow of Victoria University. His life's main work was the building up of the School of Geology at Leeds. Starting under difficult conditions as a part-time lecturer at the Yorkshire College in 1891, his teaching attracted students to his classes and brought prestige to the College, so that when Leeds University received its charter in 1906 he became the first occupant of the Chair of Geology.

Among geologists, Kendall will be remembered as the great protagonist of glaciation of Britain by land ice. He was the central figure in the organization of local workers who, through a British Association committee, made systematic records of the dispersion of glacial boulders. An outstanding contribution to natural knowledge is the demonstration of ice margin-retreat stages round the British hills, which was started

with his publication in 1902 on "The Glacial Lakes of Cleveland" in the *Quarterly Journal of the Geological Society*.

From about 1900, Kendall's attention was directed to the supply of underground water for Yorkshire towns and villages, and so to the problems of the coalfields. For the Royal Commission on Coalfields in 1905 he produced a masterly report, documenting the local application of the doctrine of posthumous folding, and estimating the unproved area of the Yorkshire, Nottinghamshire, and Derbyshire coalfield at 3885 square miles.

Professor Kendall was awarded the Lyall medal of the Geological Society in 1909. He retired from the Chair at Leeds in 1922 and was granted the title of Emeritus Professor. He was elected into this Society in 1924, and received the honorary degree of D Sc. at the coming of age of Leeds University in 1926. He died at Frinton-on-Sea in March, 1936.

By the death of Sir ARCHIBALD GARROD, the Society loses a Fellow who, while primarily an investigator, became famous as a practising physician and pathologist. He was trained in medicine at St. Bartholomew's Hospital. Early in his career he was attracted by the subject of urinary pigments, and published papers on haematoporphyrin, urochrome uroerythrin, and urobilin. His work on alkaptonuria was of primary importance: he saw in it, not a disease but an individual variation; these and other studies led to the publication of his book on "Inborn Errors of Metabolism" in 1909. His professional career absorbed much of his time, and left him little leisure for personal research, though his sympathies and interest were a direct stimulus to much valuable work while he was Regius Professor of Medicine at Oxford from 1920 to 1927. He was elected a Fellow in 1910 and was a Vice-President from 1926 to 1928.

Sir JOSEPH ERNEST PETAVEL was born in London in 1873, spent his early years at Lausanne where he studied engineering and returned to England in 1893 to continue the study of his subject for three years at University College, London. For the next three years he worked in the Davy Faraday Laboratory of the Royal Institution on the properties of matter at low temperatures, on the emission of light and heat from carbon and platinum with the object of obtaining a standard of light; there also he devised the well-known "Petavel gauge" for measuring the rate of rise of pressure in explosive reactions.

Proceeding to Manchester University in 1901, he lectured on mechanics and meteorology and applied his conspicuous gift for design to the evolution of a new technique for work at high pressures and temperatures. This had an important influence on the study of ballistics, and of com-

bustion, and on the industrial development of chemical reactions under the above conditions. He became Professor of Engineering there in 1909.

Through his interest in the problems of the upper air, he came into touch with aeronautics, and in the early days of the War supplied a definite stimulus to the study of aerodynamics, resulting in improvement in the stability of aeroplanes. His fertility in design was also employed in other work for the Admiralty and the War Office.

In 1919 Petavel succeeded Sir Richard Glazebrook as Director of the National Physical Laboratory and gave his undivided attention to the extension of its activities and especially to the increase of its usefulness to industry.

Petavel will be remembered not only for his achievements in pure science and in administration but also for his personal qualities, his courtesy, hospitality, and love of his house and gardens, for the upkeep of which he expressed a wish that a contribution should be made from his bequest to this Society.

Professor KARL PEARSON, Galton Professor of Eugenics at University College, London, from 1911 till his resignation in 1933 at the advanced age of 76, died suddenly on 27 April. Elected to the Goldsmid Professorship of Applied Mathematics at University College in 1884, he began the statistical work with which his name is chiefly associated about the year 1891, his first statistical memoir being printed in the 'Philosophical Transactions' of 1894. From then onwards there followed an ever-increasing mass of work at first largely in our 'Transactions' and 'Proceedings', later mainly in the journal 'Biometrika' which he founded in 1901, work which may well be said to mark a new epoch in the history of statistical method. Pearson was not only himself an indefatigable worker, but an outstanding teacher with a great capacity for rousing enthusiasm in others, and his pupils are scattered all over the world. But he was not only a statistician; he wrote on other branches of applied mathematics and in earlier years edited and completed Todhunter's "History of the Theory of Elasticity." This, the well-known "Grammar of Science," the "Life of Francis Galton," and several of the essays in "The Chances of Death and other Studies in Evolution," fall within the field of science. An early little book on the Veronica legend and portraits of Christ, and the essays of "The Ethic of Freethought" show the scholar, historian, and philosopher. Elected a Fellow in 1896, Pearson was awarded the Darwin medal in 1898, but never took any active part in the general work of the Society.

ALFRED CARDEW DIXON, who died on 4 May last at the age of 70, was

Senior Wrangler in 1886, Fellow of Trinity, and afterwards Professor of Mathematics successively in Queen's College, Galway, and the Queen's University of Belfast. Like most Cambridge mathematicians of what is now the older generation, his interests extended over a very wide domain in the science, and at different times he published original papers on geometry, analysis, dynamics, and the theory of elasticity. Among his best-known achievements may be mentioned his theory of the singular solutions of systems of differential equations of any order; his papers on the integration of partial differential equations; his great memoir of 1901 on matrices of infinite order—a subject in which he was a pioneer, and a subject now of great importance in the last decade on account of its applications in quantum mechanics—and the researches of his later years on the theory of integral equations and the problems of the elastic plate. As a teacher and administrator he was most highly regarded in the University of Belfast, which conferred on him the honorary Doctorate of Science. After retirement from his chair in 1930, he settled near London and took an active part in the affairs of the London Mathematical Society, of which he was President in 1932-33.

Sir GEORGE HADCOCK, a Fellow of the Royal Society since 1918, was a man of great charm of manner, and was much liked by all with whom he came in contact.

His extensive experimental work in connexion with the development of artillery in all its phases was largely responsible for the present position of the science of gunnery and ballistics; and his "Ballistic Tables," published in 1897, were for many years the official tables of the War Office to be used in conjunction with the "Text-book of Gunnery."

Hancock conducted experiments to determine the effect on the resistance of thick-walled cylinders to internal pressure, which were some of the first to be carried out in this country; and upon them our present knowledge of overstrain in metals is largely based.

He was the author of several books and many papers on Artillery and Ballistics, and wrote articles on these subjects for the "Encyclopaedia Britannica." He also contributed a paper, which was published in the 'Proceedings of the Royal Society,' on the "Longitudinal Strength of Cylinders, etc."

Professor WILLIAM ERNEST DALBY, Emeritus Professor of Engineering in the University of London, died on 25 June, 1936, at the age of 73. At the early age of 14 he commenced his practical training at the Stratford Works of the Great Eastern Railway. Then, having been awarded a Whitworth Scholarship, he went to the Crewe Works of the London and North-Western Railway. In 1891 he accepted an invitation from

Professor Ewing to act as his assistant and from that time onwards his career ran along academic lines.

After six years with Ewing, Dalby was appointed to a Professorship of Engineering at the Finsbury Technical College, where he remained from 1896 until 1904, when he was promoted to the Chair of Civil and Mechanical Engineering at the City and Guilds College at South Kensington. This Professorship of London University he retained until his retirement from academic work in 1931. Although Dalby in nowise neglected or belittled his duties as a teacher, his interests were mainly concentrated on research, particularly research of a practical variety. His researches were very varied and, with the exception of the electrical, dealt with almost every branch of engineering knowledge. When at Finsbury the research which monopolized his attention was concerned with "Balancing of Engines". On this subject he became recognized as the highest authority. It was his first love in research and it is the one with which his name will continue to be associated by future generations of engineers. Elected a Fellow in 1913, he served on the Council during the year 1924. Hard-working, conscientious, and conspicuously generous minded in his estimate of others, he leaves behind him the pleasing memory of a man who without motive invariably gave the best that was in him to the cause of engineering science and the betterment of engineering education.

RICHARD DIXON OLDHAM, who died on the 15 July, 1936, at the age of 78, spent 25 years of his active life of research as a member of the Geological Survey of India; and after his retirement from official work in 1904 he continued to carry on, with marked distinction, his studies of seismology and physical geography. His work in India was mainly devoted to the regional geology, and especially the stratigraphy of Baluchistan, the Himalayas, Northern Peninsular India, and the Andaman Islands. This wide range of field experience qualified him eminently for revising the official Manual of the Geology of India, which was published in 1893.

In a paper, published in 1906, analysing the seismographic records of fourteen world-shaking earthquakes, Oldham established the existence of two distinct sets of deep-seated waves, travelling at different speeds; and, from the way in which the waves of distortion were damped out in depth, he deduced the existence of a central core in the earth, four-tenths of the radius in thickness, which contrasted in physical properties with the external shells. In this way Oldham pointed to the pretty analogy between seismic waves as a source of information regarding intra-telluric conditions and those of light which, on analysis by the spectroscope, give information regarding the composition of the sun's atmosphere.

Oldham was elected a Fellow in 1911 and served on the Council of the Society in 1920-21. He was also elected President of the Geological Society of London in 1920, and in 1931 an Honorary Fellow of the Imperial College of Science in which he received his early training.

Sir HENRY WELLCOME, head of the great firm of Burroughs, Wellcome & Co., died in London on 25 July, at the age of 82. Famous throughout the world for his commercial achievements, he attained still greater renown for his lifelong interest in medical science, to the promotion of which, in one or other of its branches, he devoted most of his energies and practically all his wealth.

After an early training in pharmacy and chemistry in America, where he was born, he came to this country and founded with Burroughs, in 1880, the firm which later passed into his sole control.

In 1894 in the early days of serum therapy, he grasped the possibilities of protective and curative sera and founded the Physiological Research Laboratories with the twofold object of bringing serological and biological remedies within the reach of medical men and their patients and of carrying out researches into the fundamental problems of immunology and allied subjects. Two years later he founded the Chemical Research Laboratories, and then in 1913 the Bureau of Scientific Research to carry out researches in tropical medicine and coordinate the work of the various research laboratories and museums he had founded. The museums included the Museum of Medical Science depicting modern medicine in graphic form and the Historical Medical Museum illustrating, by a most extensive and priceless collection of instruments, objects, and books, the history of medicine from the earliest times to the present day.

He built the Wellcome Research Institution in the Euston Road, and established the Tropical Research Laboratories in Khartoum.

He made arrangements in his will for the continuance of his great business and of his various research laboratories and museums, all of which are now grouped under the name of the Wellcome Foundation. Over and above this, residuary profits are also to be devoted for the most part to the furtherance of scientific research.

Dr. BERNARD SMITH died on 19 August, having held for only ten months the Directorship of the Geological Survey of Great Britain and of the Museum of Practical Geology, London. He had served on the Council of the Royal Society for nearly a year and was chairman of a committee on Ordnance Survey Maps. For thirty years he had been a member of the Geological Survey. He had been since 1931 Assistant to the Director, and in charge of field work in England.

Smith was essentially a field geologist with a special bias to the study

of the relations of physiography to geology. This was well shown by his published text-book of Physical Geography, which is in its third edition. His principal contribution to British geological science was his interpretation of the Whitehaven coalfield. This difficult ground was entrusted to him, and a staff of geologists working under his direction, in 1920, and the maps and memoirs are now nearly all published. The work maintained a very high standard and solved many problems previously little understood. Almost equally important was his investigation of the iron-ore deposits of West Cumberland and Lancashire, the principal sources of British haematite.

Smith's early death cuts short a career of great promise. His ability was shown in all his investigations and his judgment was cautious, sound, and penetrating. With equal ease he handled a great variety of subjects and as a colleague and director he was universally esteemed. Gentle and unobtrusive in manner, he won the confidence of his colleagues and of the public, and, unspoiled by popularity and success, he exerted a stimulating influence on wide circles of British geologists.

HENRY LOUIS LE CHATELIER devoted almost the whole of a long and active life to physical chemistry in its applications to concrete problems, giving special attention in the later years to those of metallurgy. His early work on the dissociation of calcium carbonate led him to the enunciation of the "Le Chatelier principle", which indicates the influence of a change of external conditions on the state of a system in equilibrium. This principle has played a great part in the development of physical chemistry. His application of the theory of solutions to metallic alloys opened up a new field, which has proved very fertile. He was an excellent experimenter, and introduced several new instruments, the most important of which was the thermo-electric pyrometer, universally used in the study of alloys. By his foundation of the '*Revue de Métallurgie*' in 1904 he provided a medium for the publication of French researches in metallurgy, which has ever since retained its position as a leading technical journal. The esteem in which he was held by scientific men of many countries was shown by the celebration in Paris of his academic jubilee in 1922. A graduate of the *École des Mines*, and for many years one of its professors, he approached chemistry from the side of a mining engineer, and this fact determined his practical bias. Both by his teaching and through his important text-books he exerted a great influence on the development of chemistry and chemical industry in France. He was elected a Foreign Member of the Royal Society in 1913.

WILLIAM JOHNSON SOLLAS, who was elected a Fellow in 1889, died at the age of 87, retaining undiminished his remarkable energy and many-

sided interest in science. His researches not only illuminated his own special province of geology with mineralogy, but also included important contributions to zoology and anthropology, even, in his work on the Age of the Earth, venturing into the domain of physics. He was educated at the City of London School and the Royal School of Mines, and wrote, not many months ago, his memories of student days under the inspired teacher T. H. Huxley, and of the group of friends who, led by the late Dr. William Garnett, migrated to Cambridge. After many years of teaching his subject in Dublin, he became in 1897, and remained until his death, Professor of Geology at Oxford, where the arrangement and great development of the University collections and the deepening interest in geological study will be long remembered as the fruits of his occupancy of the Chair.

Sollas was formerly Fellow of St. John's College, Cambridge (elected 1882), and became Fellow of University College, Oxford, a few years after his election to the Professorship. His election last year to the honorary Fellowship of the Imperial College of Science gave him much pleasure. He was President of the Geological Society of London 1908-09, and was awarded a Royal Medal in 1914.

Professor GEORGE FORBES was a man of great versatility and was particularly interested in Physics, Astronomy, and Electrical Technology. He was born in 1848. After graduating at Cambridge he was appointed, 23 years of age, Professor of Natural Philosophy in Anderson's College, Glasgow, which post he held until 1880. One of his chief pieces of physical work was a determination of the velocity of light by a modified Fizeau method carried out in conjunction with Dr. T. Young and described in 'Philosophical Transactions' in 1882. The result obtained was a velocity of 301,382 kilometres per second. In 1874 he took charge of an expedition to Hawaii to observe a transit of Venus.

When incandescent electric lighting began commercially at about 1882, Forbes came to London to occupy a post in an electric manufacturing company and made improvements in arc lamps and electric meters. His chief contribution was the introduction of brushes for dynamo machines and motors made of hard graphite carbon; an improvement of general utility. When the great project of employing part of the water power of Niagara for generation of electric current was started, Forbes was appointed to superintend the work of the electric installation and plant erection at the site and acted as consulting engineer to the Cataract Company carrying out the work.

Forbes travelled extensively and was a correspondent of 'The Times' during the Russo-Turkish War. He invented a naval gunsight and a

military range-finder and was granted a Civil List Pension in 1931 for his services.

He was elected a Fellow in 1887 and was a Chevalier of the Legion of Honour of France and an Honorary Member of the Franklin Institute of America. He died at Worthing in October, 1936.

With the death of WILLIAM ARTHUR PARKS on 3 October, the Society loses a great Canadian and a great scientist. He was born at Hamilton and graduated at the University of Toronto, in which he was afterwards Professor of Palaeontology. He joined the geological staff of the University in 1893, and touched on nearly every aspect of geology during his career. His exploration of Northern Ontario broke new ground, and his report on the building and ornamental stones of Canada is well known. But his favourite subject was undoubtedly palaeontology, and to the world outside Canada he will be remembered chiefly for his classical work on dinosaurs. He became director of the Royal Ontario Museum of Palaeontology in 1913; in 1926 he became President of the Royal Society of Canada. He was elected to our Fellowship in 1934.

THOMAS MARTIN LOWRY, Professor of Physical Chemistry in the University of Cambridge, died on 2 November, 1936, at the age of 62. In his early days he was a pupil of, and an assistant to, Professor H. E. Armstrong and laid the foundation of his lifelong studies on optical rotatory power by discovering the mutarotation of nitrocamphor and the stereoisomerism of a number of halogen derivatives of camphor. He traced the mutarotation of nitro-*d*-camphor to the passage of equilibrium of two constitutionally different forms of the substance, and showed that the rate of change of the one form to the other could be influenced by the addition of traces of catalytic agents. By much careful work he established that the presence of an amphoteric agent is a factor in bringing about the isomeric change. Thus, whilst the mutarotation of tetra-methyl-*d*-glucose can be arrested in the hydroxylic solvent, cresol, and the basic solvent, pyridine, it proceeds very rapidly in a mixture of these two solvents. On the basis of this and much other work, Lowry founded his now well-known theory of *prototropy*, according to which the migration of a hydrogen ion, in compounds such as nitrocamphor and the sugars depends on the addition and removal of a proton at opposite poles of the molecule. It is largely due to Lowry's work that the conception of dynamic isomerism advanced by van Laar became generally accepted.

Concurrently with his chemical work on mutarotation, Lowry took up the study of optical rotatory dispersion which had been much neglected since the death of Biot in 1862 ; he demonstrated the validity of Drude's equation for simple substances and showed that it also covered the

anomalous rotatory dispersion of *d*-tartaric acid and the tartrates. This work formed the subject of the Bakerian Lecture given by Lowry and Austin in 1921. His later very precise determinations of the rotatory power of quartz in the visible and violet provided valuable data by which the validity of the Drude equation was further extended.

Lowry later extended his studies of the rotatory power of transparent media to that of absorbent media, namely of the Cotton effect, and was able to develop equations which are adequate to express the dispersion throughout the absorption band. Whilst occupied with the study of optical rotatory power, Lowry carried on parallel lines of research; his earlier verifications of Drude's equations were combined with corresponding measurements of magneto-rotatory dispersion and, in his search for possible relationships between diverse optical phenomena, he carried out a series of investigations on the refractive dispersion of organic compounds.

The Council's Report for the year is now in the hands of the Fellows. I propose to refer to one or two of its statements.

In the first place we are all happy to read in it the gracious letter which we have received from His Majesty the King, intimating his consent to become our Patron, and his pleasure in continuing the long-established connexion between the Crown and the Society.

It is also a source of gratification to the Society that His Majesty has promised to continue the annual grant of two Royal Medals.

Three magnificent gifts have been made during the last few months for the furtherance of research in this country. In May it was announced that Lord Austin had placed a quarter of a million sterling at the disposal of the University of Cambridge to be devoted to the work of the Cavendish Laboratory. More recently still Lord Nuffield has presented to the University of Oxford two millions for post-graduate research in medical science. This afternoon the Council of the Royal Society has accepted on behalf of the Society a principal share in the responsibility for the administration of a sum of £200,000 bequeathed by the late Mr. H. B. Gordon Warren. The interest of this money is to be applied to the encouragement of research in metallurgy, engineering, physics, and chemistry. The administering committee is to consist of eight members appointed by the Society and two by the Governors of Williams Deacon's Bank.

These great gifts are naturally a source of deep satisfaction to the Fellows of a Society which was founded for the purpose of "Improving Natural Knowledge". The givers are men who are or have been

engaged in industry: which fact is itself a source of gratification. It is good to see that practical affairs are in accord with the realization of the vital importance of research.

Lord Nuffield's gift recognizes the value of research for the prevention and cure of disease. The obvious success which has already been attained in this way is sure ground for the expectation of further benefits commensurate with the magnitude of the new effort. Lord Austin's gift is for the promotion of investigations which are at the time devoted mainly to the abstruse problems of the atomic nucleus. The terms of Mr. Gordon Warren's bequest suggest a more immediate contact with industry.

Thus these benefactions differ widely in respect to their immediate purposes: but they all acknowledge the same principle, that the improvement of Natural Knowledge is essential to the general welfare. As for our Society, it is the basis of its Charter and the reason for its existence.

The capital value of the funds administered by the Society, if we include in them the Warren bequest, is now more than a million sterling. In this amount is also included the bequest of about £40,000 by the late Sir Joseph Petavel, to which reference is made in the Report of the Council. By far the greater part of the money has been received within the last twenty years. In 1828 Dr. Wollaston founded the Donation Fund, the first fund of which the income was to be devoted to research; the amount was about £3400. By the beginning of this century there were several such funds, the combined income of which was £1375. In 1912 the total income had risen to a little over £2000 a year. Then in 1919 began a period of large donations. First came the Foulerton Gift and the Foulerton Bequest. The Messel bequest was received in 1921. The Yarrow and the Mond Funds came in 1923, the Medical Research Fund in 1924 and 1925. To these the Warren bequest has to be added. In all the Society now directs the expenditure of about £31,000 a year on research. The direction makes a considerable demand upon the time and energies of Fellows, and it is a pleasant duty to acknowledge their willing and able service on numerous committees.

The use to be made of these moneys is to a considerable extent limited by the terms of the respective trusts. Nevertheless, there is ample opportunity for a general policy at the discretion of the Society. It is natural and right that special emphasis is laid upon general or fundamental research, so far as donors' wishes allow; and indeed the terms in which the donors have expressed themselves are favourable to research of that kind.

It is to be observed that many other bodies possess funds which are

administered for similar purposes. In a list published by the Royal Commission for the Exhibition of 1851, the Commission itself takes place as one of the oldest, and the Leverhulme Trust as one of the newest. The list includes such well-known names as the Carnegie Trust, the Halley Stewart Trust, the Beit Memorial Fellowship Trust, and others. City companies are also to be found there. The Improvement of Natural Knowledge follows also on the activities of many bodies that have specific applications in view. Each branch of the Defence Services maintains its own research laboratories; so do the Medical Research Council, the Department of Scientific and Industrial Research, the Agricultural Research Council, the Post Office, and so on.

Still more closely concerned with the direct applications of Natural Knowledge are the laboratories of the country's industries. Many of these are of great and established reputation. On the whole, the industrial laboratory is some way from being as frequent a factor in industry as it ought to be, but undoubtedly progress has been made in recent years.

This brief enumeration of some of the agencies making for the improvement of natural knowledge will serve as a reminder that the sum total of the work done in this direction is very large. It may fall far short of what is to be hoped for, but it forms an agency which begins to acquire a certain coherence, something which can be viewed as a whole and considered in respect to its character and its effects. It is beginning to find itself, like Kipling's ship.

An immediate and obvious effect is the increase in the volume of published results. The publications of scientific societies have doubled and trebled in size; and their treasurers are in many cases hard put to it to meet the consequent additional expense. Numerous industrial publications also contain records of special investigations. There is every reason for satisfaction with the increase in natural knowledge which has followed on the encouragement of research.

In certain respects, at least, the application of the knowledge acquired is also satisfactory, though judgment on that point will vary according to the position of the observer in a very large field. There are obvious improvements in the health and general well-being of the nation, in its industries, in the strength of its trade, and in its powers of defence; and these are matters of primary importance. Though they may be no more than means to an end, they and the appropriate application of knowledge are a first consideration.

To such applications every kind of research may contribute; for even those who would have it that Science must be followed without thought of its usefulness must admit that it has to be very pure Science indeed

which only meets with its application, as a straight line meets its parallel, at infinity. In general the encounter may be expected to come so soon that its effect has a present importance, and must be taken into account. The individual member of the Society may keep his thoughts and his experiments within an isolated region, and so contribute what is due from him as a Fellow. But the Society as a whole must take the wider view, and watch constantly the relations between scientific advance and the people who are affected by it. It accepts these responsibilities when it undertakes to administer the great sums that have been entrusted to it. In the early days of the Society the Fellows recognized duties in these respects, as the records of their Transactions show. Many of the Founders occupied important positions in the State and their science bore directly on the needs of the nation. Throughout the three centuries of its existence, the same ideals have encouraged the activities of the Society. At some times they have been less effective than at others, but their general purpose has never been blurred. The whole of the work of the Society is therefore an important part of a general effort to improve natural knowledge in the expectation of resultant benefit.

Another consequence of that effort deserves especial consideration. The increase of knowledge and its applications are, each in its own way, worth working for. At the same time there should follow, and does follow, an increase in the quality and quantity of men who can add to knowledge and use it; also, it may be hoped, an increase in the number of those who realize its effectiveness. This is an exceedingly important point. It might seem unnecessary to observe that the resources which a nation possesses are of no use unless there are the foresight and the skill which are needed to make use of them. Yet a nation as a whole might fail to act on a principle to which its individuals would give a ready assent. The principle has to be stated plainly, so that it may be widely understood. One of the greatest assets of a nation is the presence within it of men who are quick to apply the knowledge of the time to the needs of the time. There are many varieties of such men. There are the handicraftsmen, whose skilled fingers are guided by intelligence; such skill is steadily increasing in this country, though the contrary is often asserted. There are those who can assemble and combine materials for a given purpose, and there are others who can seize upon the broad consequences of a new discovery and choose the right moment for setting the old to one side. History has shown many times how the fate of a nation may depend upon its capacity to use the knowledge and the materials at its disposal. One may be reluctant to draw examples from the catastrophe of the Great War, but in its heated atmosphere

developments came quickly to maturity. During its course engines and devices of all sorts came into being which, before the war began, had never been thought of seriously, if at all. Such were tanks, paravanes, sound ranging, wireless telephony, aeroplanes, and a thousand contrivances in every section of the war on the ground, under the ground, on the sea, under the sea, in the air. Their invention and development would not have been possible if there had not been the men for the work. It was fortunate that the nation also possessed a body of young men—chemists, physicists, engineers, biologists—trained in the laboratories of universities, technical schools, polytechnics, and so on, and in industrial workshops who were able to understand and work with the new devices. I doubt if the value of those trained young men has ever been fully realized. If, unfortunately, another great war broke out, the devices of to-day would surely be modified or superseded during its course, and the process of development would begin all over again. Provided that the defence withstood the first shocks, the men with knowledge of materials and skill in using them would be in demand as before.

Though war times may furnish the more obvious examples, the developments of peace follow the same road, at a slower pace. The major industries of this country have owed their advance in part to the national resources and to political relations, but largely also to the skill of the country's scientific and technological workers. The electrical trades depend largely on discoveries which these have made and been quick to use. The same may be said of her metallurgical work, of her shipping industry, of her business in textiles, of the dye industry in which she has now taken a position which might have been hers from the beginning. The battle for the health and the nutrition of the nation depends for its success upon the same qualities. This becomes continuously more so as natural knowledge increases, and its technical use requires a more intelligent craftsmanship.

Many a similar instance might be drawn from past history. But the past differs from the present in this, that the knowledge then to be drawn upon was scantier and far less abstruse. It was related to the technical skill of the workshop rather than, as now, to the science of the laboratory. The agencies of change were such as the discovery of cast iron, the invention of printing, the design of the ocean-going chronometer, the eighteenth-century additions to the loom, and so on. To-day great matters turn upon the complicated physical science of the wireless valve or the intricacies of the internal combustion engine, or the highly-skilled chemistry that brings assistance to medicine or the combination of physics and chemistry, biology, and engineering involved in the preservation of food.

From this point of view the suggestion sometimes made that scientific workers might take a holiday looks more ridiculous than ever. No nation could afford such an intellectual disarmament in the face of the world; nor could the world itself in face of the evils that are to be overcome.

The position of the men, and especially of the younger men, who are encouraged by these financial aids to devote the most ingenious years of their life to scientific research must be considered by those to whom the ordering of their lives is due. Some of the most brilliant young men in the Empire are selected for a specific purpose, which purpose they undoubtedly fulfil. Good work is done, and when it is finished a fine and most useful type of man is available for further service. In a great number of cases the satisfactory opportunity of further service presents itself. But it is not always so. It is possible to find a man living on income derived from one Research Trust after another until he ceases from age or other limitations to be eligible for further aid. His work may have been excellent, and his competence as great as ever, but he finds that he must look in some new direction for his living. Academic activities may be no use to him, nor he to them. His occupation has led him up a blind alley. I am told that there is a certain tendency for men who have been employed in industry as research workers to change over, when possible, to purely administrative work which is expected to be more lasting and in the end more remunerative. There is here a hint as to the true cause of the trouble. The blind alley should be a thoroughfare leading to occupations more suitable to the men and better fitted to get the best out of them. It is obvious what these occupations are. They are places of responsibility to which specialists in science are as yet but rarely admitted. There is an encouraging beginning, but it takes time to realize that the man who is in touch on one side with the growth of natural knowledge should be in close touch on the other side with the opportunities of its application. He should be an equal in the council chamber rather than a subordinate in the waiting-room. On the other hand, the scientific expert must himself help to take down the barricade that makes the alley blind. This requires that his education should be much more than sufficient to make him only a laboratory man: which brings us back again to the very important point that the man himself must be as much the care of those who give him research work to do as is the work which they set before him. Obviously, the more complete the equipment of the man, the better the chance that he will make his way, and the wider his final influence. The bodies that administer research funds are already beginning to consult each other for the sake of better efficiency in the choice

and direction of workers. As this becomes more general, there will surely be an effort to take a wider view of the responsibilities which the magnificent generosity of public men has placed upon them.

Reference is made in the Report to a plan of research on malaria in India. I think that I may well amplify the reference by describing rather more fully the proposals of Council in respect to Indian Medical Research, particularly as they involve the adoption of a special policy.

In 1924 the Royal Society received a legacy of £10,000, and in 1925 £28,108 19s. 6d., being part of the residue of an estate, for the prosecution of original research in medicine, for the prevention of disease and relief of suffering, with special reference to tropical diseases in British Possessions. There are particular reasons associated with the gift for connecting its use with India. Council decided at its meeting on 9 July that the whole income, together with the invested income, shall be employed for five years (*i.e.*, until 31 October, 1941) as follows :

A.—*Malaria research*—It decided to offer to Colonel Sinton, I.M.S., a stipend for five years to enable him to work at the Horton Centre on certain aspects of malaria. The Horton Centre will be under the control of the London School of Hygiene and Tropical Medicine, and unique opportunities will be available there for clinical study, for observations on the malaria parasite in man and *Anopheles*, for investigation of the serology and immunology of malaria, and for chemo-therapeutic testing and experimentation on the human subject. Colonel Sinton is now, and has been for many years, actively engaged in malaria work in India.

B.—*Experimental studies on the ecology of certain species of Anopheles*—Where the control of malaria is successful it is nearly always achieved by measures directed against *Anopheles*. A detailed plan has been suggested by the London School of Hygiene and Tropical Medicine, by which a young man experienced in modern experimental zoology should be given opportunity for 12 to 18 months, at that School, to learn about mosquitoes in general and the Oriental species of *Anopheles* in particular, and should undertake experimental work in the physiology and behaviour of *A. maculipennis*. He should then be sent for 2½ to 3 years to an appropriate centre in India to carry out a programme connecting malaria with the behaviour of *Anopheles*. Council was informed that for the tropical portion of the scheme part of the cost could probably be met by the London School of Hygiene and Tropical Medicine. Assuming that this is the case, it decided that a sum up to £3,750 be offered provisionally, over a period of five years, to finance the project. A suitable investigator has been appointed in Mr. Muirhead Thomson.

C.—*Nutrition in India*—The existence of widespread malnutrition in India is beyond dispute, but more detailed and intimate information is required as to its incidence and effects. Council decided that Dr. C. Wilson should be offered a research grant for one year in the first instance, with possible extension for two more years, to enable her to make a survey of the nutritional condition of Indian families and to draw up a report. A study of the incidence of malnutrition among school-children, an investigation of dietary habits, an assessment of the value of foods in common use, etc., would be made in collaboration with the Indian Research Funds Association and with Dr. Aykroyd, its Director of Nutrition Research. Dr. Wilson will be able, if necessary, to work for only part of the year in India, returning to England to carry out a statistical and experimental analysis of her results. One of her objects while in India will be to build up and train a small body of collaborators by which the work will be aided and perpetuated.

The total estimated cost of the three schemes, over a period of five years, is £8,550. The Council of the Royal Society believes that by a far-reaching plan of this character, involving work of three different kinds all bearing on health in India, its Medical Research Fund can be better employed than by small grants made from time to time for worthy but minor purposes. It could make good use of far more substantial funds on analogous lines.

Reference is made in the Report of Council to the decision in the matter of the Postal Ballot; this required the invocation of a curious provision contained in our ancient Charters. We were directed, in cases of a difference which we could not settle ourselves—and in this instance our legal advisers had been unable to settle it for us—to call in the services of certain High Officers of State. This we did, and the officers in question responded promptly, taking, I believe, no little interest in this ancient direction and its present application. We are greatly in their debt for their very kind assistance.

The great increase in the amount of material to be published has brought with it certain serious inconveniences. It has always been the practice of the Society to scrutinize with great care all papers submitted to it. Fellows have been ready to undertake this task, though, as we all know by experience, the labour involved is serious. Three times as many papers have now to be examined, as compared with a few years ago, and there has been no material increase in the number of those available as referees. It is not surprising that men who lead busy lives find it difficult to attend promptly to the work which they are asked to do, especially as the intricacies of modern science may make it necessary for

a referee to devote days to any one paper. If there is much delay, there is disappointment at the tardy publication of matter which the writer naturally thinks ought to appear at once.

The Council has considered this matter carefully, and has come to the conclusion that in the great majority of cases the summary of a paper might be set up in type and distributed within a very few weeks of its receipt, without waiting for the verdict of the referees on the paper as a whole. A Fellow who communicates a paper will, of course, take the responsibility for the summary. The reading of the paper and its publication will follow in due course, as the responsible committees advise, on receipt of the opinions of the referees.

Three years ago Sir Gowland Hopkins in his Presidential Address spoke with admiration of the work of the organic chemist and in particular of the "emergence of power to grasp the architecture of complex invisible entities such as organic molecules and the ability to construct them at will". He told how under modern methods of investigation the picture which the chemist had formed of the invisible molecule had actually taken shape. His picture-making had been amply justified. His stereometry was not, as some thinkers had maintained, to be swept away in favour of a mathematical symbolism.

This anticipation has been fully realized during the last few years, mainly through the remarkable increase in the accuracy with which the structure of molecules, molecular aggregates, and solid bodies in general can be determined. For this the methods of X-ray analysis of crystalline structure have been largely responsible. Moreover, other methods have been greatly strengthened by the example set by X-ray analysis and by its reactions upon themselves. Optical, electrical, magnetic, and other properties have been successfully studied with the same great purpose, viz., the correlation between the properties of a substance and the spatial arrangements of its components.

While the X-ray methods have been mainly useful in describing the arrangement of the atoms in assemblages surrounded by others of like nature and conditions, the methods of electron-diffraction are giving a remarkable insight into the modifications of arrangement that are to be found on surfaces. The extraordinary interest of such knowledge arises from the fact that natural processes so largely depend on surface actions.

For many years after its inception the X-ray analysis was, as might be expected, engaged in trying its own powers and learning how to apply them. It cleared up many structural problems on which older methods had little to say that was definite, as, for example, the distinction between

ionic, metallic, adamantine, and molecular compounds. Many crystal-line structures were determined, and the results, as is well known, have been serviceable in a wide field of scientific research, and in many industrial processes. The methods of analysis, the technique, and the interpretation of results have been greatly improved, as might be expected, by the researches of many hundreds of workers. The increase in accuracy is so great that new possibilities of usefulness come into view.

The improvement appears in two ways. In the first of the two, the measurements of the dimensions of the unit of pattern of a structure can now be made to one part in several thousand. Consequently, the determination of the electron charge  $e$ , made by the X-ray method, can stand beside the older determinations of the oil-drop method. There is a persistent discrepancy of about one part in two hundred, the former giving the value  $4.80 \times 10^{-10}$ , the latter  $4.77 \times 10^{-10}$ ; but it is clear that the larger value is at least as near the true value as the smaller. A full discussion of the X-ray method is given by Compton and Allison in their recent book on "X-rays", and a critical examination of some outstanding points is made by du Mond and Bollman ('Phys. Rev.', September, 1936).

Again, as has been observed by Bernal, the use of high-precision determinations of the lattice constants of metals will soon become the most reliable gauge of purity of a metallic element. Accuracy has here been pushed to one or two parts in forty thousand. Again, the phase boundaries of an alloy can be very closely and conveniently defined by observations of such a character. Accuracy has been of great importance to the well-known work of Hume Rothery on alloy structures, and to the curious and very important relations between order and disorder in alloys which have been specially studied at Manchester.

The accuracy with which the position of each atom in the unit cell can be measured is of quite a different order. Thanks in particular to the use of Fourier analyses by J. M. Robertson and others, the distances separating the atoms, centre to centre, can be found to about 1%, even when the complicated molecules of organic crystals are under examination. This is a great advance on the possibilities of even a few years ago, and it has important consequences. In particular, fresh light is thrown upon the problem of the chemical bond. At one time, single, double, and triple bonds were considered to be distinct and definite phenomena. The tetravalency of carbon, for example, was described as an assemblage of four equal powers of combination, of which one or more might be exercised in the same direction. When the diamond structure was found by the X-ray methods, it was no matter of surprise that the four separate

single bonds were displayed in the attachment of each carbon to four neighbours. In the structure assigned by the chemist to benzene, the fact that each atom had but three neighbours presented difficulties; various theories have been suggested in explanation, mostly little more than different ways of drawing diagrams, in which four single bonds were made to act somehow. In recent years, it has been more usual to propose that bonds may alternate between single and double, and that the tetravalency of carbon in the benzene ring is satisfied because three of the six links are double and three single, the two kinds alternating both in time and in order round the ring. The conception can be extended to cases much more complicated provided that the two forms between which alternation occurs do not differ much either in form or energy. The effect is described as one of "resonance", a term due to Hund but applied to organic chemistry mainly by Pauling and his collaborators. Its bearing on structural chemistry was discussed by Sidgwick a few months ago in a presidential address to the Chemical Society.

When substances in which this "resonance" is supposed to occur are examined by the X-rays, it is found that the actual centre to centre distance of two atoms connected by alternating a link between single and double is characteristic of neither of the two extremes. These last two are definite quantities, and the length of the varying link lies between them. An actual link is rarely a pure single or double or triple link. Pauling and Sidgwick both discuss a number of cases in which the centre to centre distances can be correlated with a probable or possible amount of resonance. An excellent example is furnished by oxalic acid which was examined by Zachariasen in 1934, but has just been remeasured by Robertson, using the powerful Fourier method of analysing the observations. The distance between the carbon atoms is 1.43 Å. The length of the single link of diamond is 1.54 Å. The length of a double bond is very nearly 1.33 Å. It might seem that in oxalic acid the link is actually more nearly double than single; but this is not so. A small proportion of double linking seems to shorten the distance considerably. For instance, each link in the hexagonal network of graphite must be two-thirds single and one-third double, yet its length is 1.41 Å. In benzene, the half-and-half arrangement (following Kékulé) is correlated with a length of 1.39 or 1.40 Å. Thus the actual length of a bond may prove to be a safe indication of its nature. Robertson points out that the oxalic acid molecule is always planar, which may be accounted for on the ground that rotation is restricted round a link which is even partially of a double character.

It has recently been shown by Bernal and Megaw ('Proc. Roy. Soc.,' A, vol. 151, p. 384 (1935)) that in all probability there are two types of

bond linking oxygen atoms through intermediary hydrogens. The one is the "hydrogen bond"; it is found, for example, in acids, and it corresponds to a separation distance, oxygen to oxygen, of 2.55 Å. The other is the hydroxyl bond; it is found in a number of hydroxides, and its length is about 2.8 Å. By the use of this conception it has been found possible to locate the positions of the hydrogen atoms in several hydroxide structures, particularly in the clayey mineral hydrargillite. The oxalic structure of Robertson seems to supply a new and interesting example of the difference between the two kinds of bond. One of the oxygens at each end of the oxalic acid molecule is bound to a water molecule in the crystal by a link 2.87 Å. the other by a link 2.52 Å.

It has been pointed out (Fricke, 'Koll. Z.', vol. 69, p. 312 (1934)) that the linking up of hydroxyl bonds explains the properties of the gels that are formed by neutral hydroxides.

These few examples may serve to show how improvements in the technique of X-ray analysis are sharpening a tool which has already been of assistance to research in many directions and now seems to be acquiring a new usefulness.

The chemist has already shown that the properties of the molecule depend on the internal disposition of its atoms. The characteristics of the solid state depend also on spatial relations, and in a manner which is even more complicated, much more complicated than in the case of the independent molecule. Accurate measurement of the spatial arrangements lays a firm foundation for the study of the properties of a substance in relation to its structure and its composition. The problems to be solved are, of course, extremely complex, but it is surprising how much can be done towards the examination of intricate molecular associations when the spatial relations between the most commonly occurring atoms are known. This applies, for example, to the study of the proteins which has already gone far; to the clays, and to the glasses and other extended structures. At one time it seemed hopeless to expect to learn much of the structure of bodies which were so irregular as to give no sign of crystallinity. But it is now possible to work from the regularity in occurrence of a few definite separation distances, even when regularity in orientation does not exist: and methods have been devised by which these distances can be determined by the X-ray methods.

It is clear, I think, that the stereometry which the chemist has developed so successfully is acquiring new powers which will have the widest applications.

---

*Awards of Medals, 1936*

Sir ARTHUR EVANS is awarded the COPLEY MEDAL. He is the leading British authority in classical archaeological studies: from his father he inherited a predilection for numismatics, a subject to which, in his earlier years, he made contributions of outstanding importance. His researches in Crete from 1893 onwards resulted in the discovery of the remains of a civilization which he named Minoan after the Sea-King, Minos. He traced the development of the Minoan civilization from approximately 3200 to 1400 B.C., from the late Neolithic through the Bronze Age. His Cretan work, published in six volumes—"The Palace of Minos"—has revolutionized our knowledge of the ancient history of the Near East.

The RUMFORD MEDAL is awarded to Professor ERNEST GEORGE COKER, who has devoted a lifetime to the investigation of stresses in solids by means of polarized light. The original effect was discovered by Brewster in 1815, and Brewster himself suggested that the effect might be used for the direct exploration of stress. But although many physicists since Brewster's time investigated the effect, no one, until Coker came, developed a practical method enabling stresses in a model to be actually traced. Coker not only applied to such researches a material, celluloid, not hitherto employed and capable of being cut to any shape, but he was the first to devise a reliable instrument (the lateral extensometer) for measuring at any point the sum of the principal stresses, which is not directly given by the optical results. In many other ways he made very important improvements in methods of observation, and he has, in fact, created a new technique and given the engineer a new instrument of discovery. His work is only now beginning to be recognized and taken up by the engineer; it is not too much to say that photo-elasticity will do for engineering what the application of spectroscopy has done for astronomy; the two cases are somewhat analogous, in each a previously known physical effect has been applied to explore a whole field of new facts.

Coker's first paper on this subject dated from 1910; since then he has published, either alone or with pupils and colleagues, some 50 or 60 papers, in which he has applied the method to almost every important engineering problem which can be approximated to on two-dimensional lines. In the course of this work not only has he cleared up a vast number of problems and difficulties, but he has rendered a great service

to applied mathematics, by demonstrating to the engineer the substantial accuracy of the results of the Mathematical Theory of Elasticity.

Coker's work fulfils admirably the condition laid down for the Rumford Medal which says that the discoveries for which it is awarded should be such as "tend most to promote the good of mankind". The results obtained by photoelasticity in such subjects as the stability of dams and the strength of aeroplane frameworks will certainly be the means of saving many lives.

Moreover, Coker has created a world-wide school: to his inspiration is largely due the modern development of photo-elastic laboratories in Japan, the United States, Belgium, Switzerland, and Russia, and many of the leading workers in these laboratories have started their researches under his auspices and have remained in touch with him ever since.

A ROYAL MEDAL is awarded to Professor RALPH HOWARD FOWLER. His general theory of statistical mechanics, his later applications of it to the equilibrium of mixed crystals and to a theory of semi-conductors are of outstanding importance. His paper on dense stellar matter contains the first working out of the properties of a degenerate electron gas, and those on the internal conversion of  $\gamma$ -rays and on thermionic emission and stray field emission of electrons from metals were fundamental. His work on the theory of the photo-electric effect, especially as a function of temperature, led to a rational means of analysing emission frequency curves, which enables one to determine the true threshold frequencies. His work on the quantum theory of energy exchange between gases and solids broke new ground. Further, he has made notable contributions to the theory of the photo-electric current in semi-conductors, and has made notable contributions in recent years by his adaptation of wave mechanics, as it has been developed, to the solution of problems actually under investigation by groups of experimentalists working in close association with him.

A ROYAL MEDAL is awarded to Professor EDWIN STEPHEN GOODRICH. He is distinguished for his long series of researches on the Comparative Anatomy, Embryology, and Palaeontology of Invertebrates and Vertebrates, which have thrown light on some of the most fundamental problems of Animal Morphology. His work on the excretory organs of Annelids and of *Amphioxus* resulted in a new conception of the nephridia and their relation to the coelom and coelomoducts. His memoirs on scales of fishes and on the median and paired fins threw fresh light on the classification and phylogeny of fishes and on the evolution of the verte-

brate skeleton. His contributions to our knowledge of the segmentation of the vertebrate head are recognized as of the first importance. His volume on Cyclostomes and Fishes in Ray Lankester's "Treatise on Zoology" and his more recent book, "Studies on the Structure and Development of Vertebrates," are masterly and original contributions to the subject of comparative anatomy. All his writings are distinguished by breadth of view, clarity of thought and expression, and mastery of technical methods. In the opinion of many he is the outstanding morphologist of our time.

The DAVY MEDAL is awarded to Professor WILLIAM ARTHUR BONE, who has had a wide and varied experience in the main branches of chemical science for a period of well over forty years and has by his masterly grasp of experimental technique made many discoveries and inventions of great scientific significance.

His early work on the alkyl substituted succinic acids and allied substances, which furnished a valuable chapter in synthetic organic chemistry, was speedily followed by more fundamental researches on the thermal decomposition of hydrocarbons and their oxidation products and by quantitative studies of hydrocarbon combustion. The latter researches, which occupied him for many years, were admirably summarized and illustrated experimentally in his Bakerian lecture of 1932. The evidence collected during these prolonged and systematic investigations, devised to include a great variety of experimental conditions of slow combustion and detonation, was overwhelmingly in favour of the hydroxylation theory of the combustion of hydrocarbons.

His study of the direct union of carbon and hydrogen led to a synthesis of methane from its elements. These researches on gaseous hydrocarbons and their oxidation products necessitated accurate gas analyses, and reference should be made to his improvements in the laboratory apparatus required in such determinations.

The closely related problem of flame movements in mixtures of burning or exploding gas has been submitted by him to exhaustive examination with improved methods, which made it possible to observe for the first time some striking characteristics of this phenomenon.

On the subject of catalysis, his contributions are of especial interest and importance. Thus he has recently demonstrated by a variety of convincing experiments that carbonic oxide and oxygen will unite in the gaseous phase in the absence of moisture. At an early stage in his career Bone adopted the now almost universally accepted view of the general

nature of contact catalysis to interpret experiments on the interaction of hydrogen and oxygen.

In collaboration with many colleagues and students, Bone has investigated the difficult problem of the chemistry of coal and has applied new physical and chemical methods of identifying the constituents of this complex material. The benzenoid constitution of coals of widely different geological ages and maturity was demonstrated by oxidation experiments which furnished a complete series of the polycarboxylic acids of benzene. In this field of chemical research, which is undoubtedly of the utmost importance to all coal producing countries, Bone will always be regarded as a pioneer.

The DARWIN MEDAL is awarded to Dr. EDGAR JAMES ALLEN, who for the past forty-two years has been Director of the Laboratory of the Marine Biological Association at Plymouth. Under his wise guidance the institution has risen from small beginnings to the premier position which it holds to-day.

Allen has made many notable additions to our knowledge of marine biology, dealing with such diverse subjects as the nervous system of the lobster, faunistic studies of estuarine and other areas, systematic work on the Polychaeta, the genetics of *Gammarus*, and contributions to fishery science. He initiated exact work on the association of bottom faunas with the nature of the deposits and has published valuable papers on the artificial culture of phytoplankton, in which he was one of the earliest to obtain successful results. Many years ago he followed the chain of events leading from sunshine and inorganic constituents of sea water, through phytoplankton and zooplankton to food fishes, making some of the first contributions to a subject which has since shown most striking developments.

When the International Fishery Investigations began, Allen undertook the English share of the work, which was then based on laboratories at Plymouth and Lowestoft. After the war the Lowestoft laboratory branched off and became the Government centre for economic fisheries investigations. He has been closely associated with the International Council for the Exploration of the Sea from its earliest beginnings. The organization of the work on water pollution, carried out by the River Tees Survey Committee, owes much to his initiative, and he is a member of the Committee dealing with similar problems in the River Mersey. He received the Hansen Memorial Medal and prize at Copenhagen in 1923 and was the Linnean Medallist in 1926.

Much of Allen's work has been directed to the study of evolution.

The Hooker lecture, which he delivered to the Linnean Society in 1929, deals with the origin of adaptations, and his presidential address to Section "D" of the British Association in 1922 is again concerned with the evolution of life in the sea.

Throughout his long term of office at Plymouth, he has been the inspiration of the workers at the laboratory, and the success of his labours is shown by the high quality of the research which has been carried out under his direction. Many discoveries of fundamental importance have been made and, one after another, new methods of oceanographic research have been worked out, to be adopted at once by fishery departments and marine biologists in all parts of the world.

The HUGHES MEDAL is awarded to Dr. WALTER SCHOTTKY of the Central Laboratory of Siemens & Halske, Berlin. He is best known by his contributions to the fundamental theory of thermionic emission. One of his investigations led in 1914 to the formulation of a theory of the effect of an electric field at the surface of a hot conductor upon the emission of electrons; another led to the discovery of the "Schrot" effect, which attributes certain variations in a thermionic discharge to random emission of individual electrons. He also discovered the so-called "temperature effect" in ordinary conductors of electricity, which he traced to the thermal agitation of the molecules. Further, in the early days of the subject, he made valuable contributions to the theory of space charge in vacuum tubes.

Apart from these mathematical contributions to our knowledge of principles, Schottky has added very greatly to engineering progress in most branches of wireless telegraphy. In particular, he invented the screening grid valve which has everywhere superseded the triode valve in the high frequency amplifiers employed in receiving broadcast signals. He is also the inventor of the method of superheterodyne reception wherein the currents of intermediate frequency are amplified. These are two of the most important wireless inventions of the past twenty years.

---



## INDEX TO VOLUME CLVII (A)

- Aldehydes, four, absorption spectra of (Kellner), 100  
Alpha-particles, velocity of (Briggs), 183.  
Asundi (R. K.), Jan-Khan (M.), and Samuel (R.) Spectra of  $\text{SeO}$  and  $\text{SeO}_2$ , 28  
Auger effect for the L level of xenon and krypton (Bower), 662  
Bagnold (R. A.) The movement of desert sand, 594  
Bone (W. A.) and Outridge (L. E.) Some influences of dilution on the explosive combustion of hydrocarbons, 234.  
Bower (J. C.) Auger effect for the L level of xenon and krypton, 662  
Bradley (A. J.) and Illingworth (J. W.) The crystal structure of  $\text{H}_3\text{PW}_{12}\text{O}_{40} \cdot 29\text{H}_2\text{O}$ , 113.  
Bragg (Sir William H.) Presidential address, 697.  
Browne (B. C.) See Kempton, Browne, and Maasdorp.  
Briggs (G. H.) A determination of the absolute velocity of the alpha-particles from Radium C', 183.  
Butler (J. A. V.) Hydrogen overvoltage and the reversible hydrogen electrode, 423  
Caesium vapour, absorption of light in (Ditchburn and Harding), 66  
Callow (R. K.) and Young (F. G.) Relations between optical rotatory power and constitution in the steroids, 194.  
Carbon suboxide, the spectrum and photochemistry of (Thompson and Healey), 331.  
Chang (W. Y.) See Waring and Chang.  
Chiong (Y. S.) Viscosity of liquid sodium and potassium, 264.  
Convection in air, effect of pressure upon (Saunders), 278.  
Copper, lattice spacings in silver and (Hume-Rothery, Lewin, and Reynolds), 167  
Copper-gold alloy  $\text{Cu}_3\text{Au}$ , atomic rearrangement process in (Sykes and Jones), 213.  
Cox (E. G.), Goodwin (T. H.), and Wagstaff (A. I.) The structure of isatin, I, 399  
 $\text{Cu}^+$ , self-consistent field, with exchange, for (Hartree and Hartree), 490  
Cylinder, circular, forces of, submerged in a uniform stream (Havelock), 526  
Cylinders, fluid friction between rotating (Taylor), 546.  
Deuterium, angular distributions of the protons and neutrons in, some transmutations of (Kempton, Browne, and Maasdorp), 386  
Deuterium, photosensitized exchange reactions of, with ammonia, methane, and water (Farkas and Melville), 625.  
Deuterons, transmutation of the lithium isotope of mass seven by (Kempton, Brown, and Maasdorp), 172.  
Diamond, further work on two types of (Robertson, Fox, and Martin), 579.  
Diffusion of gases through metals (Smithells and Ransley), 292.  
Ditchburn (R. W.) and Harding (J.) The absorption of light in caesium vapour in the presence of foreign gases, 66.  
Dymond (E. G.) The anomalous scattering of protons in light elements, 302.  
Electrode, reversible hydrogen and hydrogen overvoltages (Butler), 423.  
Electrolytes, univalent, in aqueous solution, dielectric capacity of (Shutt and Rogan), 359.

- Electro-kinetic effects in solution, a theory of (Moelwyn-Hughes), 621.  
 Electrons, relativistic interaction of (Swirles), 680.  
 Ethers, formation of, at high pressure (Newitt and Semerano), 348.  
 Ethylene, photochemical decomposition of (McDonald and Norrish), 480.  
 Explosives, high optical and physical effects of (Wood), 249
- Fairbrother (J. A. V.) A new method of investigating conduction phenomena in semi-conductors, 50.
- Farkas (A.) and Melville (H. W.) The mercury photosensitized exchange reactions of deuterium with ammonia, methane, and water, 625.
- Flow, turbulent, correlation measurements (Taylor), 537
- Fluorite region, photochemical reactions in (McDonald and Norrish), 480.
- Foord (S. G.) *See* Norrish and Foord
- Fox, (J. J.) *See* Robertson, Fox, and Martin
- Friction, fluid, between rotating cylinders (Taylor), 546
- Fuchs (K.) The elastic constants and specific heats of the alkali metals, 444.
- Gases, diffusion through metals (Smithells and Ransley), 292.
- Glückauf (E.) *See* Paneth, Glückauf, and Loleit
- Gollop (H.) *See* Harrison, Turney, Rowe, and Gollop
- Goodwin (T. H.) *See* Cox, Goodwin, and Wagstaff.
- Harding (J.) *See* Ditchburn and Harding
- Harrison (E. P.), Turney (G. L.), Rowe (H.), and Gollop (H.) The electrical properties of high permeability wires carrying alternating current, 451.
- Hartree (D. R.) and Hartree (W.) Self-consistent field, with exchange, for Cu<sup>+</sup>, 490.
- Hartree (W.) *See* Hartree and Hartree.
- Havelock (T. H.) The forces on a circular cylinder submerged in a uniform stream, 526
- Healey (H.) *See* Thompson and Healey.
- Helium, artificially produced, spectroscopic identification of (Paneth, Glückauf, and Loleit), 412.
- Hume-Rothery (W.), Lewin (G. F.), and Reynolds (P. W.) The lattice spacings of certain primary solid solutions in silver and copper, 167.
- Hydrocarbons, explosive combustion of (Bone and Outridge), 234.
- Hydrogen, energy balance, and energy efficiencies for the principal electron processes in (Lunt and Meek), 146.
- Hydrogen overvoltage and the reversible hydrogen electrode (Butler), 423.
- Illingworth (J. W.) *See* Bradley and Illingworth.
- Ionization, excitation, and chemical reaction in uniform electric fields (Lunt and Meek), 146
- Isatin, structure of (Cox, Goodwin, and Wagstaff), 399.
- Jan-Khan (M.) *See* Asundi, Jan-Khan, and Samuel.
- Jones (F. W.) *See* Sykes and Jones.
- Kellner (Miss L.) Absorption spectra of four aldehydes in the near infra-red, 100.
- Kempton (A. E.), Browne (B. C.), and Masadorp (R.) Angular distributions of the protons and neutrons emitted in some transmutations of deuterium, 386.

- Kempton (A. E.), Brown (B. C.), and Maasdorp (R.) Transmutation of the lithium isotope of mass seven by deuterons, 372.
- Krypton, Auger effect for the L level of (Bower), 662.
- Lewin, (G. F.) *See* Hume-Rothery, Lewin, and Reynolds
- Liquids, dielectric capacity of (Shuttle and Rogan), 359.
- Lithium isotope, transmutation of the, by deuterons (Kempton, Browne, and Maasdorp), 372.
- Loeit (H.) *See* Paneth, Glückauf, and Loeit.
- Lovell (A. C. B.) The electrical conductivity of thin metallic films. I—Rubidium on pyrex glass surfaces, 311.
- Lunt, (R. W.) and Meek (C. A.) Ionization, excitation, and chemical reaction in uniform electric fields II—The energy balance and energy efficiencies for the principal electron processes in hydrogen, 146
- Maasdorp (R.) *See* Kempton, Browne, and Maasdorp
- McDonald (R. D.) and Norrish (R. G. W.) Photochemical reactions in the fluorite region. I—Photochemical decomposition of ethylene, 480
- Magnetic field, distribution of, around simply and multiply connected supraconductors (Smith and Wilhelm), 132
- Martin (A. E.) *See* Robertson, Fox, and Martin
- Meek (C. A.) *See* Lunt and Meek.
- Metals, alkali, elastic constants, and specific heats of (Fuchs), 444.
- Melville (H. W.) A note on the quantum yield of the photosensitized decomposition of water and of ammonia, 621.
- Melville (H. W.) *See also* Farkas and Melville
- Metallic films, thin, the electrical conductivity of (Lovell), 311.
- Methane, kinetics of combustion of (Norrish and Foord), 667.
- Milner (S. R.) On wave matrices and some properties of the wave equation, I.
- Moelwyn-Hughes (E. A.) A theory of electro-kinetic effects in solution ; reactions between ions and polar molecules, 621.
- Newitt (D. M.) and Semerano (G.) The formation of ethers by the interaction of primary alcohols and olefines at high pressure, 348.
- Nickel, the diffusion of oxygen and hydrogen through (Smithells and Ransley), 292.
- Norrish (R. G. W.) and Foord (S. G.) The kinetics of the combustion of methane, 667.
- Norrish (R. G. W.) *See* McDonald and Norrish.
- Outridge (L. E.) *See* Bone and Outridge
- Oxygen and hydrogen, the diffusion of, through nickel (Smithells and Ransley), 292
- Paneth (F. A.), Glückauf (E.), and Loeit (H.) Spectroscopic identification and manometric measurement of artificially produced helium, 412.
- Phosphotungstic acid  $H_3PW_{12}O_{40} \cdot 29H_2O$ , crystal structure of (Bradley and Illingworth), 113.
- Photochemical reactions in the fluorite region (McDonald and Norrish), 480.
- Presidential address (Bragg), 697.
- Protons, the anomalous scattering of, in light elements (Dymond), 302.
- Quantum yield of the photosensitized decomposition of water and ammonia (Melville), 621.

- Radio-phosphorus, formation of (Waring and Chang), 652.  
 Ransley (C. E.) *See* Smithells and Ransley.  
 Relativity, integral electromagnetic theorems in (Synge), 434.  
 Resorcinol, structure of (Robertson), 79.  
 Reynolds (P. W.) *See* Hume-Rothery, Lewin, and Reynolds  
 Riemann zeta-function, the zeros of the (Titchmarsh), 261.  
 Robertson (J. M.) The structure of resorcinol. A quantitative X-ray investigation, 79.  
 Robertson (Sir Robert), Fox (J. J.), and Martin (A. E.) Further work on two types of diamond, 579.  
 Rogan (H) *See* Shutt and Rogan.  
 Rowe (H.) *See* Harrison, Turney, Rowe, and Gollop.  
 Rubidium, conductivity of film of, on pyrex glass surfaces (Lovell), 311.  
 Samuel (R.) *See* Asundi, Jan-Khan, and Samuel.  
 Sand, movement of desert (Bagnold), 594.  
 Saunders (O. A.) The effect of pressure upon natural convection in air, 278.  
 Selenium oxide, spectra of (Asundi, Jan-Khan, and Samuel), 28.  
 Self-consistent field method, relativistic interaction of two electrons in (Swirles), 680.  
 Self-consistent field, with exchange, for Cu<sup>+</sup> (Hartree and Hartree), 490.  
 Semerano (G.) *See* Newitt and Semerano.  
 Semi-conductors, conduction phenomena in (Fairbrother), 50.  
 Shutt (W. J.) and Rogan (H) A critical experimental investigation of the "Force" method of determining the dielectric capacity of conducting liquids at low frequencies : univalent electrolytes in aqueous solution, 359.  
 Silver and copper, lattice spacings in (Hume-Rothery, Lewin, and Reynolds), 167.  
 Smithells (C. J.) and Ransley (C. E.) The diffusion of gases through metals. IV—The diffusion of oxygen and hydrogen through nickel at very high pressures, 292.  
 Smith (H. G.) and Wilhelm (J. O.) Distribution of magnetic field around simply and multiply connected supraconductors, 132.  
 Sodium and potassium, viscosity of liquid (Chiong), 264.  
 Spectra absorption of four aldehydes (Kellner), 100.  
 Spectrum of carbon suboxide (Thomson and Healey), 331.  
 Steroids, relation between optical rotatory power and constitution (Callow and Young), 194.  
 Supraconductors, simply and multiply connected (Smith and Wilhelm), 132.  
 Swirles (Bertha) The relativistic interaction of two electrons in the self-consistent field method, 680.  
 Sykes (C.) and Jones (F. W.) The atomic rearrangement process in the copper-gold alloy Cu<sub>3</sub>Au, 213.  
 Synge (J. L.) Integral electromagnetic theorems in general relativity, 434.  
 Taylor (G. I.) Correlation measurements in a turbulent flow through a pipe, 537.  
 Taylor (G. I.) Fluid friction between rotating cylinders. I—Torque measurements. II—Distribution of velocity between concentric cylinders when outer one is rotating and inner one is at rest, 546, 565.  
 Thompson (H. W.) and Healey (H.) The spectrum and photochemistry of carbon suboxide, 331.

- Titchmarsh (E. C.) The Zeros of the Riemann zeta-function, 261.  
Turney (G. L.) *See* Harrison, Turney, Rowe and Gollop.  
Wagstaff (A. I.) *See* Cox, Goodwin, and Wagstaff.  
Waring (J. R. S.) and Chang (W. Y.) The formation of radio-phosphorus ( $P^{30}$ ), 652.  
Wave matrices and some properties of the wave equation (Milner), 1.  
Wilhelm (J. O.) *See* Smith and Wilhelm.  
Wires, high permeability, the electrical properties of (Harrison, Turney, Rowe, and  
Gollop), 451.  
Wood (R. W.) Optical and physical effects of high explosives, 249.  
Xenon, auger effect for the L level of (Bower), 662.  
Young (F. G.) *See* Callow and Young, 194.

END OF THE ONE HUNDRED AND FIFTY-SEVENTH VOLUME (SERIES A)

---



